LEABHARLANN CHOLÁISTE NA TRÍONÓIDE, BAILE ÁTHA CLIATH
Ollscoil Átha Cliath
TRINITY COLLEGE LIBRARY DUBLIN
The University of Dublin

Terms and Conditions of Use of Digitised Theses from Trinity College Library Dublin

Copyright statement

All material supplied by Trinity College Library is protected by copyright (under the Copyright and Related Rights Act, 2000 as amended) and other relevant Intellectual Property Rights. By accessing and using a Digitised Thesis from Trinity College Library you acknowledge that all Intellectual Property Rights in any Works supplied are the sole and exclusive property of the copyright and/or other IPR holder. Specific copyright holders may not be explicitly identified. Use of materials from other sources within a thesis should not be construed as a claim over them.

A non-exclusive, non-transferable licence is hereby granted to those using or reproducing, in whole or in part, the material for valid purposes, providing the copyright owners are acknowledged using the normal conventions. Where specific permission to use material is required, this is identified and such permission must be sought from the copyright holder or agency cited.

Liability statement

By using a Digitised Thesis, I accept that Trinity College Dublin bears no legal responsibility for the accuracy, legality or comprehensiveness of materials contained within the thesis, and that Trinity College Dublin accepts no liability for indirect, consequential, or incidental, damages or losses arising from use of the thesis for whatever reason. Information located in a thesis may be subject to specific use constraints, details of which may not be explicitly described. It is the responsibility of potential and actual users to be aware of such constraints and to abide by them. By making use of material from a digitised thesis, you accept these copyright and disclaimer provisions. Where it is brought to the attention of Trinity College Library that there may be a breach of copyright or other restraint, it is the policy to withdraw or take down access to a thesis while the issue is being resolved.

Access Agreement

By using a Digitised Thesis from Trinity College Library you are bound by the following Terms & Conditions. Please read them carefully.

I have read and I understand the following statement: All material supplied via a Digitised Thesis from Trinity College Library is protected by copyright and other intellectual property rights, and duplication or sale of all or part of any of a thesis is not permitted, except that material may be duplicated by you for your research use or for educational purposes in electronic or print form providing the copyright owners are acknowledged using the normal conventions. You must obtain permission for any other use. Electronic or print copies may not be offered, whether for sale or otherwise to anyone. This copy has been supplied on the understanding that it is copyright material and that no quotation from the thesis may be published without proper acknowledgement.

The Hydrology and Hydroecology of Turloughs

Bound By:
THE
THESIS CENTRE
65 Camden St. Lwr.,
Dublin 2. Ph: 475 3616
www.thesiscentre.com

The Hydrology and Hydroecology of Turloughs

Owen Naughton

Thesis submitted in fulfilment for the degree of Doctor of Philosophy to the University of Dublin, Trinity College

2011

TRINITY COLLEGE
2 3 AUG 2012
LIBRARY DUBLIN
Thesis 9497

Declaration

I hereby declare that:

a) The dissertation has not been submitted as an exercise for a degree at this or any other University

b) The dissertation is entirely my own work

c) I agree that the Library may lend or copy the dissertation upon request. This permission covers only single copies made for study purposes, subject to normal conditions of acknowledgement.

Signed: 

Summary

Turloughs are the characteristic feature of the Irish karst landscape, occurring predominantly on the well-bedded, pure limestone regions in the western third of Ireland and forming a significant part of this region's hydrological cycle. Turloughs are wetlands at the interface between groundwater and surface water, transient lakes resulting from a combination of high rainfall and accordingly high groundwater levels in topographic depressions in the karst limestone. The ephemeral nature of turlough hydrology gives rise to a characteristic ecology which has protected status under EU legislation.

Although turloughs are ephemeral lakes, they are essentially groundwater features and as such are classified as Groundwater Dependent Terrestrial Ecosystems (GWDTEs) under the Water Framework Directive (2000/60/EC), and as a Priority Habitat in Annex 1 of the EU Habitats Directive (92/43/EEC). Both EU directives necessitate the monitoring and management of these habitats to ensure that favourable conservation and groundwater status is achieved. In 2007, the turlough habitat was found to be of unfavourable conservation status. This was primarily due to insufficient knowledge of the linkages between hydrological and ecological variables that determine the habitat biological communities (Kimberley, 2007a). In order to address this deficiency, the National Parks and Wildlife Service (NPWS) commissioned a multidisciplinary project entitled "Assessing the Conservation Status of Turloughs".

The purpose of the NPWS project was to provide a greater understanding of the structures and functions of turloughs as GWDTEs, and to define and quantify linkages between hydrology and the characteristic ecology. This would provide a more comprehensive understanding of the pressures on these ecosystems. Characterising the intrinsic behaviour of turloughs both hydrologically and ecologically and identifying the linkages between various hydrological and ecological parameters will allow the risks posed to these protected habitats to be evaluated.

The research described in this thesis forms a part of this multidisciplinary project, and addresses the lack of detailed knowledge on the hydrological functioning of turloughs. An understanding of the fundamental hydrodynamics of turloughs was developed through the measurement of relevant hydrological parameters, the mapping of

topography within turlough basins, the analysis and interpretation of extensive hydrological datasets, and the hydrological modelling of turlough behaviour. Relevant hydrological and topographic data were collected for a set of 22 turloughs. Three years of hourly water-level data were collected for the twenty two study sites, and detailed topographic surveys were carried out. Digital terrain models were generated for each site from this topographic data and used to transform water level data into the corresponding volume and area time series. These datasets provided the first quantitative hydrological records upon which to base the characterisation of turlough hydrodynamic behaviour, and enabled the development of hydraulic models for the prediction of turlough water level response to rainfall. Relevant hydraulic and time series analysis techniques were used to develop a conceptual understanding of turlough hydrological response, operation and diversity.

Two general turlough models were developed for the prediction of water levels, flood-level duration and flood extent from rainfall and evapotranspiration records. The first model uses linear regression to predict turlough volume from aggregated rainfall over a defined charcteristic interval. This technique was applied to all monitored turloughs. The second model also predicts volume using rainfall as input, but uses a more refined version of the reservoir modelling technique. The basis of this approach was the identification of characteristic equations governing turlough inflow and outflow, based on rainfall and stage respectively. This method was used for a subset of turlough sites representing the range of recorded hydrological behaviours.

A further element of this research was to derive critical hydrological factors that influence biological diversity within and among turloughs. The "Assessing the Conservation Status of Turloughs" multidisciplinary project generated four ecological datasets: vegetation, aquatic invertebrates, hydrochemistry and phytoplankton, and soil nutrients. The nature and resolution of each ecological dataset was assessed to enable the identification of novel hydrological indicators representing the various aspects of turlough hydrological behaviour. A number of indicators were derived from water level, volume and area time series, while others emerged from the digital terrain and hydrological modelling processes.

Acknowledgements

In keeping with the style of my thesis, I've tried to keep this section concise. I'd like to acknowledge:

ACADEMIC	
Thesis:	
Paul Johnston	*Supervisor*
Laurence Gill	*Supervisor*
Pat Veale	*Field and technical assistance*
Funding:	
The National Parks and Wildlife Service	
Collaborating Project: "Assessing the Conservation Status of Turloughs"	
Sarah Kimberley	*Coordinator*
Nova Sharkey, Gwendolin Porst, Helder Pereira	*PhD students*
Project Team	
Steering Committee	
Colleagues and Peers:	
Paul Hynds, Niall O'Luannaigh, Shane Regan, Dave Morgan	
Support:	
Technical and administrative staff of the Department of Civil Engineering	
PERSONAL	
Family:	
Marie and Patrick Naughton	*Parents*
Julie and Donal Naughton	*Siblings*
Anne and Mick Battle	
Kevin and Mary Spain	
Friends:	
Peter Daynes, Mark O'Connor, Aoife Donnelly and Sarah Finnegan	
Wife:	
Christina Shannon	

Special Thanks:
I'd like to thank Paul Johnston for taking me on and passing on his lifelong passion for turloughs, and to Laurence Gill for his help and guidance throughout the project. Special thanks to Pat Veale, without whose boundless energy and flexible working hours I'd never have completed my fieldwork. Thank you to my parents for their constant support and guidance throughout my life, and for giving me the opportunity and confidence to pursue my goals. And finally a special thanks to my wife Christina. Thank you for your kindness, your patience and love. Especially your patience.

List of Contents

CHAPTER 1. INTRODUCTION 1
1.1. General 1
1.2. Objectives 2

CHAPTER 2. KARST HYDROLOGY 5
2.1. Karst 5
2.2. Karst Rock Types 5
2.3. The Conceptual Framework of Karst Aquifers 7
2.3.1. Karst Permeability 7
2.4. Recharge 10
2.4.1. Autogenic Recharge 10
2.4.2. Allogenic Recharge 13
2.5. Discharge 14
2.6. Carbonate Karst Chemistry and Development 15
2.7. Investigation of Karst Systems 18
2.7.1. General 18
2.7.2. Geomorphology and Speleology 19
2.7.3. Spring Hydrographs 20
2.7.4. Boreholes and Test Wells 23
2.7.5. Tracer Tests 24
2.7.6. Stable Isotope Analysis 25
2.7.7. Geophysical Methods 28
2.7.8. Karst Modelling 28
2.7.9. Polje Hydrology 33

CHAPTER 3. IRISH KARST, TURLOUGH GEOMORPHOLOGY AND HYDROLOGY 37
3.1. Irish Karst 37
3.1.1. Limestone Geology of Ireland 37
3.1.2. Irish Karstification 38
3.1.3. Lowland Irish Karst 41
3.2. Turloughs 42
3.2.1. Turlough Definition 42
3.2.2. Turlough Distribution 43
3.2.3. Turlough Hydrology 47

CHAPTER 4. TURLOUGH ECOLOGY AND CONSERVATION 53
4.1. Introduction 53
4.2. Flora 53
4.2.1. Vegetation Types 53
4.2.2. Vegetation Distribution 55
4.3. Fauna: Invertebrates 58
4.4. Fauna: Vertebrates 60
4.4.1. Birds 60
4.4.2. Mammals 60
4.4.3. Fish and Amphibians 61
4.5. Water Chemistry and Nutrient Status 63
4.6. Subsoil Type and Nutrient Status 65
4.7. Turlough Conservation 67

4.7.1. Drainage 67
4.7.2. Land-Use Practices 68
4.7.3. Nutrient Input 69
4.7.4. Assessing Turlough Conservation Status 69

CHAPTER 5. FIELD INVESTIGATION AND DATA COLLECTION 73
5.1. Site Selection and Description 73
5.2. Water Level Monitoring 76
5.3. Temperature Profiling 79
5.4. Precipitation 80
5.5. Evapotranspiration 83
5.6. Sea Level Monitoring 84
5.7. Visual Surveying 85
5.8. Stable Isotope and Hydro-chemical Sampling 85
5.9. Preliminary Turlough Catchment Areas 88

CHAPTER 6. SURVEYING AND DIGITAL TERRAIN MODELLING 91
6.1. Introduction 91
6.2. Global Positioning System Surveying 92
6.2.1. DGPS Field Surveying 93
6.2.2. Water Level Correction 97
6.3. Digital Terrain Modelling 98
6.3.1. Gridding Methods 100
6.3.2. Gridding Method and Grid Resolution Selection 103
6.3.3. Contour Maps 106
6.3.4. Stage Volume and Stage Area Curves 108

CHAPTER 7. HYDROLOGICAL ANALYSIS: FLOODING REGIME 111
7.1. Introduction 111
7.2. Water Level Profiles 111
7.3. Depth Volume Area Analysis 116
7.3.1. Depth 117
7.3.2. Volume 119
7.3.3. Area 122
7.4. Annual Temporal Variability 124

CHAPTER 8. HYDROLOGICAL ANALYSIS: FLOW DYNAMICS 127

8.1. General 127
8.2. Maximum Net Flows 128
8.3. Net Inflow Analysis 132
8.3.1. Flow Transition 135
8.3.2. Net Inflow and Rainfall 139
8.3.3. Cumulative Rainfall 142
8.4. Net Outflow Analysis 145
8.4.1. Stage-discharge Curve Derivation 153
8.4.2. Recession Approximation 156
8.5. Indirect Flow Estimation 160
8.5.1. Water Temperature 160
8.5.2. Stable Isotope Analysis 163

CHAPTER 9. TIME SERIES ANALYSIS 167
9.1. Simple Correlation Analysis 167
9.2. Autocorrelation 172
9.2.1. Stage Autocorrelation 173
9.2.2. Flow Autocorrelation 177
9.3. Cross Correlation 178
9.4. Time-lagged Correlation 182
9.4.1. Subset 1: Mayo 183
9.4.2. Subset 2: Williamstown 186
9.4.3. Subset 3: Roscommon 187
9.4.4. Subset 4: Burren 189
9.4.5. Conclusions 191
9.5. Frequency Analysis 192
9.5.1. Fast Fourier Transform (FFT) Analysis 192
9.5.2. Tidal Effects on Turlough Water Level 195

CHAPTER 10. MODELLING 199
10.1. Introduction 199
10.2. Model Efficiency 200
10.3. Soil Moisture Deficit Model 202
10.4. Aggregated Rainfall Model 205
10.4.1. Modelling Methodology 208
10.4.2. Model Results 212
10.4.3. Conclusion 219
10.5. Reservoir Modelling 221
10.5.1. Reservoir Outflow 222
10.5.2. Reservoir Inflow 223
10.5.3. Inflow Hydrograph 226
10.5.4. Volume-Stage Relationship 228
10.5.5. Modelling Results 230
10.5.6. Conclusions 240

CHAPTER 11. TURLOUGH HYDROECOLOGY 241
11.1. Introduction 241
11.2. Hydrological Indicators 242
11.2.1. Elevation 242
11.2.2. Flood Duration 244
11.2.3. Hydroperiod 246
11.2.4. Flood Frequency 247
11.3. Vegetation 249
11.3.1. Introduction 249
11.3.2. Hydroecological Indicators 250
11.3.3. Conclusions 253
11.4. Aquatic Invertebrates 258
11.4.1. Introduction 258
11.4.2. Hydroecological Indicators 258
11.4.3. Conclusions 263
11.5. Hydrochemistry and Phytoplankton 264
11.5.1. Introduction 264
11.5.2. Hydroecological Indicators 265
11.5.3. Conclusions 267
11.6. Soil Nutrients 270

11.6.1. Introduction 270
11.6.2. Hydroecological Indicators 270
11.6.3. Conclusions 272

CHAPTER 12. CONCLUSIONS 275
12.1. Turlough Hydrodynamics 275
12.2. Hydrological Modelling 279
12.3. Conceptual Model 280
12.3.1. Flow-Through Model 280
12.3.2. Surcharged Tank 282
12.4. Hydroecology 285
12.5. Recommendations 287
12.5.1. Further Investigations 287
12.5.2. Flood Risk Assessment 287
12.5.3. Continued Hydrological Monitoring 288
12.5.4. Indirect Flow Measurement 288

References 289

Appendix A: Surveying 303
Appendix B: Hydrological Plots 337
Appendix C: Correlation Analyses 359
Appendix D: Fourier Analyses 385
Appendix E: Aggregated Rainfall Model 399
Appendix F: Hydroecology 407

List of Tables

Table 2.1: Characteristics of the three components of the triple permeability model (from (White and White, 2005)) 8

Table 2.2: Matrix, fracture and channel porosity in four carbonate aquifers 9

Table 2.3: Principal flow and storage components in four carbonate aquifers 9

Table 4.1: Typical turlough invertebrate species 58

Table 4.2: Soil types present within turlough basins (Coxon, 1987b) 65

Table 5.1: Name, location and coordinates of 22 project study sites 74

Table 5.2: Geological summary of study sites 75

Table 5.3: Summary of water level monitoring periods for 22 study sites 78

Table 5.4: Met Eireann station types and description 82

Table 5.5: Met Eireann synoptic, climatic and rainfall stations from which meteorological data was obtained 82

Table 6.1: Sources of error in position calculation using GPS. (Maini and Agrawal, 2007) 92

Table 6.2: Summary of DGPS survey data 97

Table 6.3: Mean and standard deviation of residuals for a range of gridding methods and grid resolutions, Blackrock turlough, Co. Galway 104

Table 7.1: Summary statistics of maximum turlough flood depth, volume, area and average depth 117

Table 7.2: Ratio of highest to lowest yearly maxima for hydrological parameters of depth, volume and area (ranked by volume) 125

Table 8.1: Maximum average daily net inflow and outflows, inflow: outflow ratio and inflow and outflow as a percentage of maximum volume for study sites 129

Table 8.2: Maximum inflow, time-lagged correlation coefficients and lag for flow – rainfall analysis for main filling phase in 2007/2008 hydrological year 140

Table 8.3: Correlation coefficients between cumulative rainfall and volume and notional zone of contribution areas for inflow analysis subset 143

Table 8.4: Approximated drainage capacity and recession duration for study sites 159

Table 9.1: Maximum and minimum correlation coefficients 168

Table 9.2: Decorrelation lag times (in days) for stage and flow time series 176

Table 9.3: Results from cross-correlation analyses between net daily turlough flow and precipitation (all delays given in days) 180

Table 9.4: Geographically close site subsets 182

Table 9.5: Results of time-lagged correlation and manual comparison of maxima for Subset 1: Mayo 184

Table 9.6: Results of time-lagged correlation and manual comparison of maxima for Subset 2: Williamstown 187

Table 9.7: Results of time-lagged correlation and manual comparison of maxima for Subset 3: Roscommon 188

Table 9.8: Results of time-lagged correlation and manual comparison of maxima for Subset 4: Burren 1 190

Table 9.9: Results of FFT analysis on longest available stage time series for 19 turloughs 194

Table 10.1: Best-fit aggregated rainfall model results with corresponding maximum soil moisture deficit Hs_{max}, aggregation period T, storage capacity S and contributing area α 213

Table 10.2: Reservoir Modelling Results 230

Table 11.1: Spearman's rank correlations of environmental variables and species richness for Blackrock transect A (O'Rourke, 2009) 256

Table 11.2: Areal reduction rate information used in aquatic invertebrate analysis 260

Table 11.3: Flood velocities for aquatic sampling intervals on turlough subset 262

Table 11.4: Hydroperiod for the 2006/2007 flooding season for 22 monitoring sites (*2007/2008 value used due to hydrological data unavailability) 266

Table 11.5: Aggregation period for 19 monitored turloughs 267

Table 11.6: Mass balance calculations of the volume of water (as percentage of total final volume) that would need to enter a turlough as total nitrogen (TN) concentrations and water levels concomitantly decrease (adapted from Pereira 2010) 268

Table 11.7: Spearman Rank correlation matrix of R values with highlighted values significant at the $P \leq 0.001$ level 273

List of Figures

Figure 2.1: A conceptual model for drainage in a karst area (Gunn, 1986) 10

Figure 2.2: Subcutaneous storage, lateral sub-surface flow to zones of high permeability, and the evolution of solution dolines (Williams, 1983) 12

Figure 2.3: Types of springs encountered in karst, from Ford, D.C. and Williams, P.W. (2007) Karst Geomorphology and Hydrology 15

Figure 2.6: Geometrical Relationships and hydraulic conductivities at different scales (from Sauter, 1991) 24

Figure 2.7: Schematic diagram of linear systems analysis of karst conduit-type spring flow (Dreiss, 1989) 29

Figure 2.8: Conceptual model of Fontaine de Vacluse system (Fleury et al., 2007b) 31

Figure 2.9: Conduit network used to model flow in the downstream part of the Hölloch cave and sketch of the cave conduits (Jeannin 2001) 32

Figure 3.1: Distribution of Limestone in Ireland (Geological Survey of Ireland) 37

Figure 3.2: Geochronometric scale and chronostratigraphical divisions 38

Figure 3.3: Owenshree River sinking into riverbed during low flow conditions 42

Figure 3.4: (a) Aerial photograph of turlough #142, Mahony Dome, North-western Territories, Canada (D. Ford, pers. comm.) (b) Daily mean temperatures and daily precipitation at Norman Wells Airport for 1976 and water level in the south-eastern portion of depression No. 110 (Van Everdingen, 1981) 44

Figure 3.5: Distribution of turloughs in relation to limestone bedrock type (Sheehy Skeffington et al., 2006) 45

Figure 4.1: (a) Blackrock turlough following flood recession (b) Lack of vegetation on soil after flood recession (c) Sprouting of Silverweed (Potentilla anserina) from dormant rhizomes beneath the soil surface (photographs (b) and (c) courtesy of Nova Sharkey) 54

Figure 4.2: (a) Geranium sanguineum, Ballinderreen turlough, August 2007 and Ranunculus repens, Blackrock turlough, July 2007 (photographs courtesy of Nova Sharkey) 56

Figure 4.3: Pike specimen found in an estavelle in Garryland turlough, Co. Galway 62

Figure 4.4: Deposition of calcium carbonate on vegetation and turlough basin following flood recession in Lough Coy, Co. Galway 66

Figure 5.1: Locations of 22 study sites 74

Figure 5.2: (a) Diver platform, Rathnalulleagh, Co. Roscommon (b) downloading diver using Reading Unit, Garryland, Co. Galway 77

Figure 5.3 (a) Tipping bucket rain gauge at (a) Kilchreest and (b) Francis Gap, Co. Galway 81

Figure 5.4: Positioning of rain gauge away from any obstruction within 15^0 sight line 81

Figure 5.6: Variation in stage of Galway Port and Caherglassaun turlough, Co. Galway 84

Figure 5.7: (a) Estavelle in operation during turlough recession and (b) dry in Lough Coy, Co. Galway 85

Figure 5.8: Location of 2008 / 2009 stable isotope and water chemistry sampling points, Co. Galway 86

Figure 5.9: Water table map for area around Coolcam and Croaghill turloughs, Co. Galway 89

Figure 6.1: Flow chart for the turlough digital terrain modelling process 91

Figure 6.2: Conceptual operation of differential GPS surveying system ((Maini and Agrawal, 2007) 93

Figure 6.3: (a) Trimble 4700 GPS system and (b) Trimble R6 GPS system 94

Figure 6.4: (a) area of high point density and (b) area of gently undulating terrain with low point density, Blackrock turlough, Co. Galway 96

Figure 6.5: (a) GPS points and (b) Points with overlapping grid of evenly spaced rows and columns 99

Figure 6.6: (a) Voronoi Diagram for Set of 7 Nodes and x and (b) First and Second Order Voronoi Cells about x (Yanalak, 2003) 100

Figure 6.7: Delaunay triangulation of topographic points in Blackrock turlough, Co. Galway 102

Figure 6.8: Variation of residuals for a range of gridding methods and grid resolutions, Blackrock turlough, Co. Galway 105

Figure 6.9: Contour map of Termon at 1 metre grid resolution using (a) Multiquadric Interpolation and (b) Kriging 106

Figure 6.10: Contour map (top) and 3D terrain model (bottom) of Lough Gealain, Co. Clare 107

Figure 6.11: Solid used in volume calculation between surfaces for grid cell 108

Figure 6.12: Stage area and stage volume curve for Blackrock turlough, Co. Galway 109

Figure 7.1: (a) Daily Rainfall and evapotranspiration for monitoring period from 2006 to 2009, and water level time series plot for (b) Turloughmore, (c) Skealoghan and (d) Coolcam 113

Figure 7.2: Daily rainfall and corresponding peak water levels during the 2006/2007 inundation period for Turloughmore, Skealoghan and Coolcam turloughs 115

Figure 7.3: Maximum turlough flood depths recorded during the hydrological years 2006/2007, 2007/2008 and 2008/2009 118

Figure 7.4: Maximum turlough flood volumes recorded during the hydrological years 2006/2007, 2007/2008 and 2008/2009 119

Figure 7.5: Maximum turlough flood volumes under 1 million m^3 recorded during the hydrological years 2006/2007, 2007/2008 and 2008/2009 120

Figure 7.6: Plot of (a) Cumulative rainfall plot for Roscommon rainfall station and (b) corresponding water levels in Carrowreagh Turlough during major 2006/2007, 2007/2008 and 2008/2009 flooding events 121

Figure 7.7: Daily rainfall frequency distribution for Roscommon rainfall station during major 2006/2007, 2007/2008 and 2008/2009 flooding events 122

Figure 7.8: Maximum turlough flooded area recorded during the 2006/2007, 2007/2008 and 2008/2009 hydrological years 123

Figure 7.9: Ratio of highest to lowest yearly maximum for depth, volume and area for 21 study sites 125

Figure 8.1: Plot of maximum average daily inflow against estimated catchment area for 17 monitoring sites (excluding sites 11 to 14) 130

Figure 8.2: Ratio of maximum Inflow/ volume and maximum outflow/ volume for monitoring sites 131

Figure 8.3: Plot of net flow and rainfall for the filling phase of the volume hydrograph during 2007/2008 main flood event, Lough Gealain turlough, Co. Clare 133

Figure 8.4: Average daily flow for three turloughs following the onset of flooding in 2007 134

Figure 8.5: Average daily flow for Lough Coy, Turloughmore and Lough Gealain following the onset of flooding in 2007 135

Figure 8.6: Number of days of net inflow and net outflow for flow analysis subset during the period 1/12/2007 to 31/1/2008 136

Figure 8.7: Sum of daily net inflow and net outflow including inflow: outflow ratio for flow analysis subset during the period 1/12/2007 to 31/1/2008 137

Figure 8.8: Daily net flow and volume for Skealoghan and Ardkill turloughs, Co. Mayo 138

Figure 8.9: Plot of average daily flow and rainfall for filling phase of volume hydrograph during 2007/2008 main flood event for Ardkill, Co. Mayo 139

Figure 8.10: Correlation coefficient between inflow and average rainfall over varying averaging periods for Ardkill turlough, Co. Mayo 141

Figure 8.11: Plot of average daily flow and 6 day average rainfall (average rainfall over preceding 6 days) for Ardkill turlough, Co. Mayo 142

Figure 8.12: Plot of volume and cumulative rainfall for Ardkill turlough, Co. Mayo, for the period 23/11/2007 – 11/2/2008 143

Figure 8.13: Recession volume and flow for Brierfield turlough, Co. Roscommon 146

Figure 8.14: Plot of net outflow against stage with indicated stage – discharge curve for Ardkill turlough, Co. Mayo 147

Figure 8.15: (a) Continuous stage – discharge curve of Turloughmore, Co. Clare and (b) discontinuous curve for Skealoghan, Co. Mayo 148

Figure 8.16: Stage – discharge relationship indicating maximum outflow capacity and stage threshold for Brierfield turlough, Co. Roscommon 149

Figure 8.17: Illustration of proportion of flows in underground network during turlough recession for (a) case where system outflow capacity is reached during recession and (b) where system outflow capacity is not reached 151

Figure 8.18: Stage-discharge plot for Blackrock turlough, Co. Galway 152

Figure 8.19: Stage-discharge curve for Turloughmore, Co. Clare 154

Figure 8.20: Stage-discharge curve for Croaghill turlough, Co. Galway 155

Figure 8.21: Stage-discharge curve for Ardkill turlough, Co. Mayo 155

Figure 8.22: Linear approximation of volume recession, Ardkill turlough, Co. Mayo 157

Figure 8.23: Regression analysis of volume recessions for (a) Rathnalulleagh turlough and (b) Ardkill turlough 157

Figure 8.24: Approximated drainage capacity and notional recession duration for 21 monitored turloughs 158

Figure 8.25: Plot of Diver and Probe temperatures and corresponding rainfall during flood recession in Caranavoodaun turlough, Co. Galway 162

Figure 8.26: Plot of probe and air temperature time series during recession in Caranavoodaun turlough, Co. Galway 163

Figure 8.27: ^{18}O stable isotope results from turloughs and springs 164

Figure 8.28: Plot of water levels for Blackrock, Lough Coy and Caherglassaun turloughs with average of turlough $\delta^{18}O$ values 165

Figure 9.1: Normalised depth plot for Coolcam and Termon turloughs, Co. Galway 169

Figure 9.2: Comparison of stage depth hydrographs for Coolcam turlough, Co. Galway and Lough Aleenaun, Co. Clare 170

Figure 9.3: A plot of correlation with Lough Aleenaun versus the corresponding correlation with Coolcam for each turlough for the 2006/2007 and 2007/2008 hydrological years 171

Figure 9.4: Autocorrelation functions for (a) Lough Coy (b) Lough Coy for 2007/2008 hydrological year, (c) Termon (d) Turloughmore 174

Figure 9.5: (a) Autocorrelation function for Lough Aleenaun using 2007/2008 stage data and (b) plot of 0.2 lag time against 0.4 lag time for autocorrelation analyses carried out using 2007/2008 stage data 177

Figure 9.6: Autocorrelation functions for (a) Lisduff and (b) Blackrock using daily flow data 178

Figure 9.7: Cross-correlation functions using daily net flow and precipitation data from 2007/2008 hydrological year for (a) Lisduff, (b) Knockaunroe, (c) Skealoghan and (d) Turloughmore 181

Figure 9.8: Plot of water levels as mAOD, rainfall and computed maxima for Subset 1: Mayo 184

Figure 9.9: Time-lagged correlations for Skealoghan vs. Ardkill and Kilglassaun vs. Skealoghan (hydrological year) 185

Figure 9.10: Plot of water levels as mAOD, rainfall and computed maxima for Subset 2: Williamstown 186

Figure 9.11: Plot of water levels as mAOD and computed maxima for Subset 3: Roscommon 188

Figure 9.12: Plot of water levels as mAOD and computed maxima for Subset 4: Burren 1 190

Figure 9.13: FFT results for (a) Ardkill and (b) Lough Aleenaun analysed over entire monitoring period 193

Figure 9.14: Comparison of water level in Caherglassaun turlough and tide level in Galway Bay 196

Figure 9.15: FFT data for Caherglassaun recession data for (a) for 2 – 2.5 mAOD flood depth and (b) 6 – 6.5 mAOD flood depth 197

Figure 9.16: Comparison of water level in Garryland turlough and tide level in Galway Bay 198

Figure 10.1: Conceptual SMD reservoir model 203

Figure 10.2: Operation of the soil reservoir under (a) soil moisture deficit and (b) field capacity conditions 204

Figure 10.3: (a) Linear relationship between rainfall and volume and (b) the principles of instantaneous inflow and superposition used in the rainfall aggregation model 207

Figure 10.4 Aggregated rainfall model for (a) Lough Gealain, (b) Caranavoodaun, (c) Skealoghan and (d) Lough Aleenaun 210

Figure 10.5: Aggregated rainfall model for Caranavoodaun using (a) rainfall and (b) effective rainfall as input 211

Figure 10.6: Aggregated rainfall model results for Coolcam turlough, Co. Galway 214

Figure 10.7: Aggregated rainfall model results for Skealoghan turlough, Co. Galway 215

Figure 10.8: Aggregated rainfall model for (a) Lough Aleenaun, Co. Clare and (b) Turloughmore, Co. Clare 216

Figure 10.9: Arcing channel within Lough Aleenaun, Co. Clare 218

Figure 10.10: Flow chart for reservoir modelling methodology 221

Figure 10.11: Stage-discharge curve for Lough Gealain, Co. Clare 222

Figure 10.12: (a) Stage time series and (b) associated stage-discharge plot for Caranavoodaun turlough, Co. Galway 223

Figure 10.13: Plot of net flow, hypothetical outflow and inflow for Ardkill turlough, Co. Mayo 224

Figure 10.14: (a) Plot of cumulative infiltration and cumulative inflow for the 2008/2009 flooding period and (b) plot of cumulative infiltration versus cumulative inflow for Lisduff turlough, Co. Roscommon 226

Figure 10.15: Unit hydrographs associated with routing of instantaneous flow through series of linear reservoirs (Shaw, 1994) 228

Figure 10.16: Volume – stage curve for Coolcam turlough, Co. Galway 229

Figure 10.17: Inflow, outflow and net flow time series during the main 2007/2008 flooding period for Lough Gealain, Co. Clare 232

Figure 10.18: Plot of recorded and modelled volume for Lough Gealain, Co. Clare 233

Figure 10.19: Plot of recorded and modelled stage for Lough Gealain, Co. Clare 233

Figure 10.20: Plot of recorded and modelled volume for Lough Aleenaun, Co. Clare 234

Figure 10.21: Plot of recorded and modelled volume for Turloughmore turlough, Co. Clare 236

Figure 10.22: Plot of recorded and modelled volume (a) without overflow and (b) with overflow for Lisduff turlough, Co. Roscommon 237

Figure 10.23: Plot of recorded and modelled volume for Ardkill, Co. Mayo 238

Figure 10.24: Plot of recorded and modelled volume for Coolcam turlough, Co. Galway 239

Figure 11.1: Contour map and elevation profile used in the derivation of sample point elevation in Ardkill turlough, Co. Mayo 243

Figure 11.2: Duration curve for Rathnalulleagh, Lough Aleenaun and Lisduff turloughs for the 2007/2008 hydrological year 245

Figure 11.3: Example of different definitions of hydroperiod for Skealoghan turlough, Co. Mayo, during the 2007/2008 hydrological year 246

Figure 11.4: (a) Stage hydrograph and (b) associated flood frequencies at 0.5 m intervals for Caranavoodaun turlough, Co. Galway over monitoring period from September 2006 to July 2009 248

Figure 11.5: Location of vegetation transects together with the elevation profiles of each transect in Blackrock turlough, Co. Galway 251

Figure 11.6: Flood duration distribution of relevé points for 2007 and 2008 calendar years 252

Figure 11.7: Median duration and frequency of relevé points for each of 28 turlough vegetation communities 255

Figure 11.8: The change in vegetation composition and species richness along transect Blackrock transect B (O'Rourke, 2009) 257

Figure 11.9: (a) Contour map of Blackrock turlough including invertebrate sampling transect, (b) Elevation profile of transect and (c) calculations of flood velocity between sampling events 261

Figure 11.10: Transect elevation profile and aquatic invertebrate sampling locations for Caranavoodaun turlough, Co. Galway 262

Figure 11.11: Distribution of flood duration of soil sample locations for the 2007 and 2008 calendar years 271

Figure 11.12: Distribution of flood frequencies of soil sample locations for the 2007 and 2008 calendar years 272

Figure 11.13: Scatterplots of associations between (a) total phosphorus (TP) and flooding frequency (FF) and (b) total phosphorus (TP) and average inundation duration (AD) 274

Figure 12.2: Conceptual model for the flow-through turlough system 281

Figure 12.3: Conceptual model for turlough operation as a surcharged tank 283

CHAPTER 1. INTRODUCTION

1.1. General

Turloughs are the characteristic feature of the Irish karst landscape, occurring predominantly on the well-bedded, pure limestone regions in the western third of Ireland and forming a significant part of this region's hydrological cycle. Turloughs are wetlands at the interface between groundwater and surface water, transient lakes resulting from a combination of high rainfall and accordingly high groundwater levels in topographic depressions in the karst. The ephemeral nature of turlough hydrology gives rise to a characteristic ecology which has protected status under EU legislation.

Although turloughs are ephemeral lakes, they are essentially groundwater features and as such are classified as Groundwater Dependent Terrestrial Ecosystems (GWDTEs) under the Water Framework Directive (2000/60/EC), and as a Priority Habitat in Annex 1 of the EU Habitats Directive (92/43/EEC). Both EU directives necessitate the monitoring and management of these habitats to ensure that favourable conservation and groundwater status is achieved. In 2007, the turlough habitat was found to be of unfavourable conservation status. This was primarily due to insufficient knowledge of the linkages between hydrological and ecological variables that determine the habitat biological communities (Kimberley, 2007a). In order to address this defficiency, the National Parks and Wildlife Service (NPWS) commissioned a multidisciplinary project entitled "Assessing the Conservation Status of Turloughs".

The purpose of the NPWS project was to provide a greater understanding of the structures and functions of turloughs as GWDTEs, and to define and quantify linkages between hydrology and the characteristic ecology. This would provide a more comprehensive understanding of the pressures on these ecosystems. Characterising the intrinsic behaviour of turloughs both hydrologically and ecologically and the identifying linkages between various hydrological and ecological parameters will allow the risks posed to these protected habitats to be evaluated.

The research described in this thesis forms a part of this multidisciplinary project, and addresses the lack of detailed knowledge on the hydrological functioning of turloughs.

An understanding of the fundamental hydrodynamics of turloughs is developed through the measurement of relevant hydrological parameters, the mapping of topography within turlough basins, and the analysis and interpretation of extensive hydrological datasets. Relevant hydraulic and time series analysis techniques are used to develop a conceptual understanding of turlough hydrological response, operation and diversity. In addition, two general turlough models are developed for the prediction of water levels, flood-level duration and flood extent from rainfall and evapotranspiration records.

A further element of this research is to derive critical hydrological factors that influence biological diversity within and among turloughs. The "Assessing the Conservation Status of Turloughs" multidisciplinary project generated four ecological datasets: vegetation, aquatic invertebrates, hydrochemistry and phytoplankton, and soil nutrients. The nature and resolution of each ecological dataset is assessed to enable the identification of novel hydrological indicators representing the various aspects of turlough hydrological behaviour. A number of indicators are derived from water level, volume and area time series, while others emerged from the digital terrain and hydrological modelling processes.

1.2. Objectives

The primary aim of this study is to characterise the hydrodynamic behaviour and hydrological regime of a broad set of turloughs chosen as representative of turlough geographical distribution and hydrological behaviour. The secondary aim is to apply this new found understanding of turlough hydrology, through the use of hydroecological indicators, in order to explain aspects of the characteristic ecology associated with turlough flooding. To achieve this outcome, the project objectives are follows:

1. To collect relevant hydrological data for a set of 22 turloughs chosen to represent the hydrological and ecological diversity of the turlough habitat
2. To carry out detailed topographic surveys on the study sites to enable the quantification of flood areas, volumes and associated flow rates

3. To develop a conceptual understanding of the hydrodynamics of these karst systems, or how turloughs function hydrologically, using appropriate hydraulic and time series analysis techniques

4. To quantify and develop a hydrological modelling methodology for predicting turlough water levels, flood duration and extent from historic rainfall and evapotranspiration records. Emphasis is on the need for practical data requirements and ready applicability to ungauged sites

5. To derive critical hydrological factors influencing biological diversity within and among turloughs

CHAPTER 2. KARST HYDROLOGY

2.1. Karst

Karst can be defined as a "terrain with distinctive hydrology and landforms that arise from a combination of high rock solubility and well developed secondary porosity" (Ford and Williams, 2007). The surface and near surface outcrops of the principal karst rocks are estimated to cover approximately 20% of the planet's dry ice-free land, with carbonate karst occurring across 10 to 15% of the continental area (Ford and Williams, 2007). The defining feature of karst terrains is the dominance of solution as a geomorphic agent, with solution and solutional transport the dominant process in the development and formation of karst (White, 1988). It is these solutional processes which produce the secondary porosity, in the form of dissolution conduits, which provide a low resistance pathway for groundwater flow and interact with the granular and fracture permeability of the karst rock (White, 2002).

2.2. Karst Rock Types

A relatively high degree of solubility is a prerequisite for karstification, and so only rock groups which display this characteristic are classified as karst rocks. Based upon this criterion, the principal karst rock types are silicates, evaporites and carbonates (Gunn, 1986). Silicate rocks can develop dissolutional karst landforms on a small and intermediate scale, but the development of secondary porosity within silicates is inhibited by products of the weathering process, namely insoluble clays and hydroxides, which can restrict or seal the solutional flow paths (Ford and Williams, 2007; Gunn, 1986).

Evaporites, such as halite, gypsum and anhydrite, are highly soluble in pure water and so are susceptible to the process of karstification (Gunn, 1986). Areas of extensive evaporite karst include regions of the United States (Black, 1997), Canada (Ford, 1997), Germany (Goldscheider and Bechtel, 2009), as well as parts of the Ukraine and Russia (Klimchouk, 1992). As a result of the high solution rates of evaporite rocks, surface features are rapidly destroyed and so are restricted to arid and semi-arid climatic regions with relatively low rainfall (Gunn, 1986; White, 1988). This is

particularly the case with halite, which is the most soluble of the evaporites and so rarely exposed at the surface (Gunn, 1986). The main evaporite rock type associated with karst development is that of gypsum. Gypsum bedrock exposures, with a slower rate of dissolution, commonly exhibit similar landforms as are seen on carbonate pavement karst such as karren, dolines and sinking streams (White, 1988).

When anhydrite comes into contact with water it is converted into gypsum, resulting in a volumetric increase of between 30 and 67% and the generation of pressures of 5 - 10 MN/m^2 (Ford and Williams, 2007; Goldscheider and Bechtel, 2009). Sufficiently strong and thick overburden can prevent the hydration process from occurring, thus maintaining the long term stability of the anhydrite formation (Gunn, 1986). Contact between groundwater and anhydrite may occur during geotechnical and infrastructural projects and can have catastrophic effects. Such an event occurred in Staufen, Germany, in 2007 when geothermal boreholes were drilled up to 140m deep into anhydrite formations. The resulting introduction of water into the anhydrite resulted in an uplift rate in excess of 1 cm/month and massive resultant damage to over a hundred properties (Goldscheider and Bechtel, 2009). This volumetric expansion of anhydrite limits karstification as any joints or fissures penetrating the anhydrite are likely to close up, inhibiting the passage of water further into the rock.

The dominant karst rocks are the carbonates, which cover approximately 10% of the ice-free continental areas (Ford and Williams, 2007). However, not all carbonates are susceptible to karstification with numerous factors influencing the degree of karst development such as the presence of impurities, lithology, structural features and position within gross stratigraphy (Gunn, 1986). The two pure mineral end-members involved in the solutional processes of carbonate rock types are limestone and dolomite, with limestones being the most widespread and significant (Ford and Williams, 2007). The main chemical component of limestone, calcium carbonate ($CaCO_3$), can exist in the form of the minerals calcite, aragonite and vaterite. Due the instability of vaterite and the common recrystallization of aragonite over time into calcite, the most common form is that of calcite (Gunn, 1986).

2.3. The Conceptual Framework of Karst Aquifers

According to Bakalowitz (2005), karst rocks must be considered as aquifers as they generally contain sufficient groundwater to be used for water supply. However, the use of the term "aquifer" has led to some debate as the common definition where the aquifer acts "as a single body of groundwater in which water moves down a hydraulic gradient towards a specific surface outlet" is not generally applicable, and these conditions rarely apply in karst rock sequences due to the development by dissolution of channel networks (Gunn, 2010). The highly heterogeneous, anisotropic nature of karstification within carbonate rocks means that while significant storage may be held within the matrix permeability of the rock formation, it may not be exploitable. Instead, exploitable water supplies may only be available from limited, highly karstified areas within the rock body and so whether the entire karst system can be considered an aquifer is debatable. However, in the context of this study, the term karst aquifer will be used as a general term to describe the karstified limestone rock formations prevalent in Ireland.

2.3.1. Karst Permeability

The permeability of a karst aquifer is comprised of a number of elements. The primary porosity is associated with intergranular permeability of the unfractured rock, while secondary porosity is caused by rock folding, fracturing and dissolution pathways, which themselves vary in size, carrying capacity and interconnectivity (Ford and Williams, 2007). Conceptually, karstic aquifers can be described using the triple permeability or triple porosity model, which is composed of matrix, fracture and conduit permeability (White, 2002):

Matrix Permeability – The intergranular permeability of the unfractured rock
Fracture Permeability – The permeability of joints, fractures and bedding plane partings, solutionally enlarged or otherwise
Conduit Permeability – Pipe-like openings with an aperture size greater than 1 cm

This tripartite of permeabilities occupy different roles within the karst aquifer, with differing aperture sizes, distributions, flow mechanisms defined for each type. A summary of the characteristics of each is given in Table 2.1 (White and White, 2005).

Permeability	Aperture Size	Travel Time	Flow Mechanism	Guiding Equation	Distribution
Matrix	μm to mm	Long	Darcian flow field; Laminar	$h_f = \frac{\eta v L}{\rho g (N d^2)}$	Continuous medium
Fracture	10 μm to 10mm	Intermediate	Cube Law; Mostly laminar; may be non-linear components	$\frac{Q}{h} = \frac{C}{f} b^3$	Localised but statistically distributed
Conduit	10mm to 10m	Short	Darcy-Weisbach; Turbulent; Open channel and pipe flow	$h_f = \frac{f L v^2}{4 g r}$	Localised

Table 2.1: Characteristics of the three components of the triple permeability model (from (White and White, 2005))

Matrix porosity is composed of the individual pores within the carbonate rock, and is characterised by high storage but low groundwater velocities and laminar flow conditions (Cheng and Chen, 2005). Fractures normally have apertures in the range 50-500 μm but can be up to 0.01m, and typically have a laminar flow regime but may have non-linear components (White and White, 2005). At the point where fractures exceed an aperture size of 0.01 m they are reclassified as conduits. Although some fractures can have apertures in excess of 0.01 m, they may not be continuous at this size and so are not considered to be conduits (White and White, 2005). Conduits are solutionally enlarged flow paths through the karst aquifer. Conduit permeability is characterised by localised distribution, low storage and high groundwater velocities (Sauter and Liedl, 2000). Worthington *et al* (2000) examined the relative proportions of storage (Table 2.2) and flow fraction (Table 2.3) for four karst aquifers in Ontario (Canada), Kentucky (USA), the Cretaceous Chalk (England) and Nohoch Nah Chich (Mexico). This study

identified that while almost all of the storage was within the rock matrix, the conduit system accommodated the vast majority of flow within the karst aquifer.

Area	Proportion of Storage (%)		
	Matrix	Fracture	Conduit
Smithville, Ontario, Canada	99.7	0.3	0.05
Mammoth Cave, Kentucky	96.4	1.2	2.4
Cretaceous Chalk, England	99.9	0.03	0.07
Nohoch Nah Chich, Mexico	96.6	0.6	2.8

Table 2.2: Matrix, fracture and channel porosity in four carbonate aquifers

Area	Fraction of storage in the matrix (%)	Fraction of flow in conduits (%)
Smithville, Ontario	99.7	97
Mammoth Cave, Kentucky	96.4	99.7
Cretaceous Chalk, England	99.9	94
Nohoch Nah Chich, Mexico	96.6	99.7

Table 2.3: Principal flow and storage components in four carbonate aquifers

Karst aquifers are composed of a combination of matrix, fracture and conduit permeability, with the relative contribution of each to regional groundwater flow dependent upon the properties of the carbonate rock itself and the degree of karstification. As a result of this complexity the effective permeability of a karstic aquifer is highly scale-dependent. Standard tests for determining permeability may only elucidate a small element of the overall permeability of the aquifer (Sauter, 1992). For example, the permeability determined from cores in the laboratory may have little effect on the overall groundwater movement within a conduit dominated karst aquifer (White, 2002). Similarly, field tests such as pumping tests carried out on test wells, are highly site specific and the results potentially only representative of the fracture permeability in the vicinity of the borehole. As highlighted by Worthington (2003) and shown in Table 2.3, the vast majority of groundwater flow may be dominated by and contained within the conduit system, yet the conduits may only make up a minute

percentage of the aquifer volume. Overflow conduit systems may also exist within the aquifer whose operation is intermittent and dependent upon prevailing hydrological conditions, thus adding a temporal variability to the already highly heterogeneous spatial nature of karst permeability (Ray, 1997).

2.4. Recharge

Recharge derived from precipitation may enter a karst aquifer in a variety of forms. The range of recharge forms and pathways are shown in Figure 2.1 (Gunn, 1986). Recharge can be divided into those sources which originate within the karst body (autogenic) and those that originate from outside the karst aquifer (allogenic).

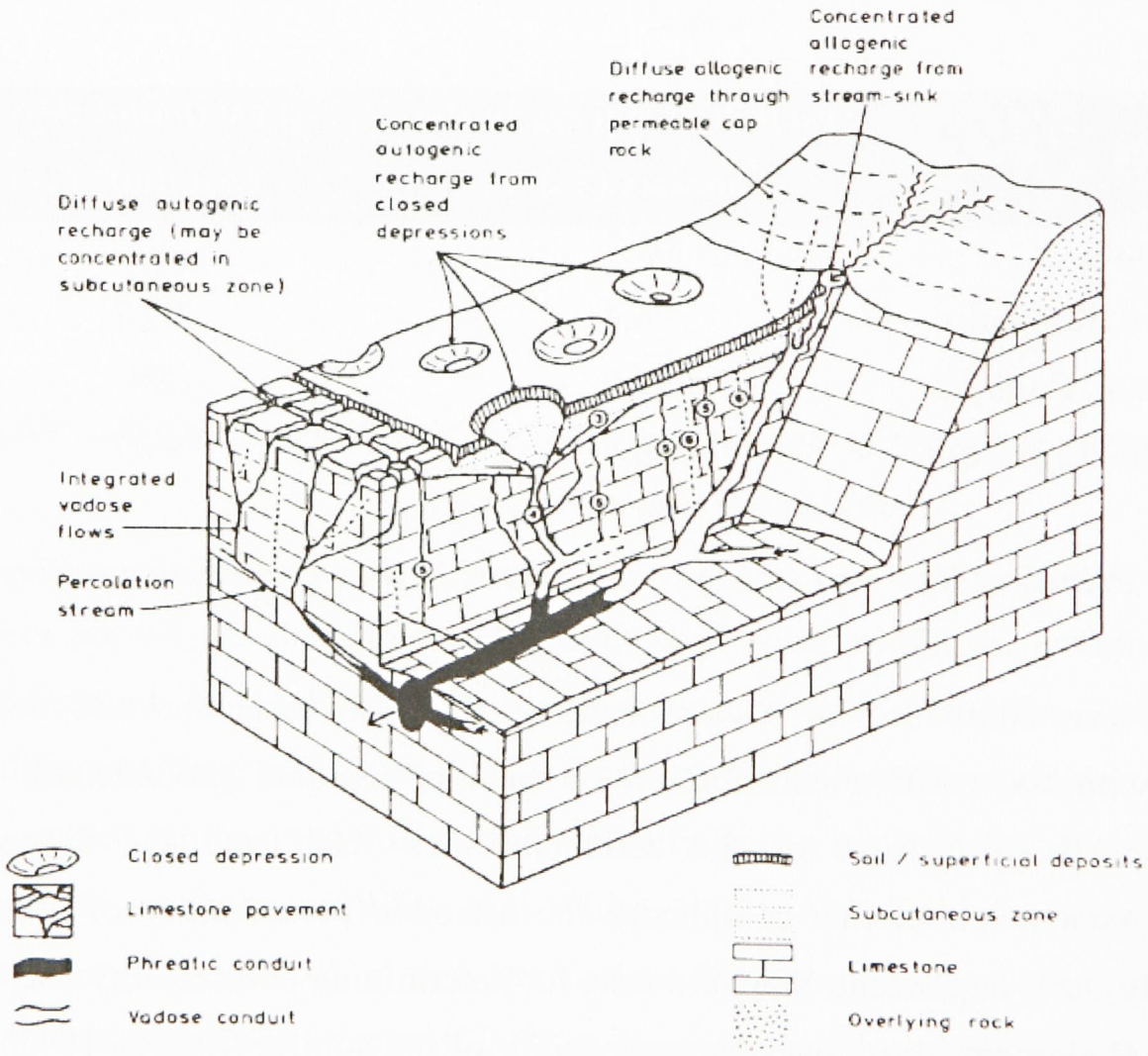


Figure 2.1: A conceptual model for drainage in a karst area (Gunn, 1986)

2.4.1. Autogenic Recharge

Autogenic recharge is derived solely from precipitation falling directly onto the karst body, and can take the form of both point and diffuse recharge (Ford and Williams, 2007). Diffuse (or dispersed) infiltration consists of precipitation directly onto the karst surface. Where soil cover is present, this infiltration is governed by the same soil

moisture processes as occur in non karstic aquifers. Rainfall exceeding the soil moisture capacity percolates downwards until it reaches the phreatic zone of the aquifer. In addition to the controls on recharge imposed by soil cover, karst recharge is further governed by the subcutaneous (or epikarst) zone.

The uppermost section of the karst bedrock, known as epikarst, can impact upon the rate and quantity of recharge entering the saturated karst aquifer. Epikarst is a term used to describe the zone of carbonate rock near the upper surface where significant weathering, fracturing, solutional enlargement and storage may occur (Ford and Williams, 2007; Zhou, 2007). The epikarst is typically 3 to 10 m deep, often highly irregular and fractured with high secondary permeability due to the considerable chemical solution in the zone (Ford and Williams, 2007). Fracture widths reduce with depth before eventually giving way to the largely unweathered rock below (Figure 2.2) (Ford and Williams, 2007; White, 2002; Williams, 1983). An example of this can clearly be seen in the Burren, Co. Clare, where the surface fractures are clearly visibly on the exposed limestone pavements. A close inspection of the extensive solutionally widened joints shows the reduction in dissolution with depth, as the fractures close to hairline cracks within a few metres of the surface (Williams, 1983).

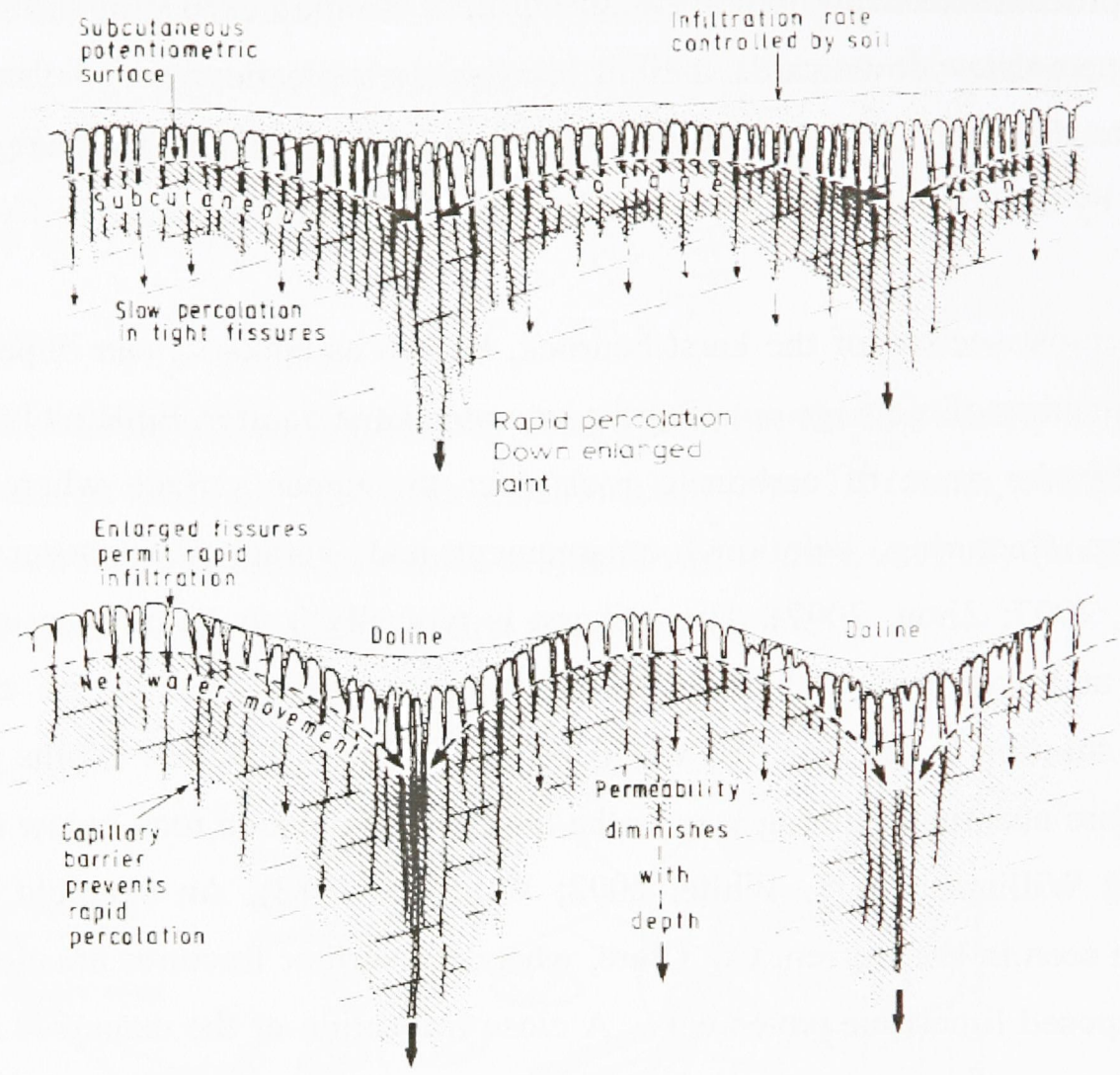


Figure 2.2: Subcutaneous storage, lateral sub-surface flow to zones of high permeability, and the evolution of solution dolines (Williams, 1983)

The link between epikarst and the underlying regional water table is often limited to sporadic subcutaneous drains and vadose shafts (Quinlan, 1989). Due to the heterogeneous nature of karstification within the epikarstic zone, and the consequent reduction in permeability with depth, recharge is unable to percolate down directly into the phreatic zone (Williams, 1983). Because of this, the epikarst zone can operate as an important groundwater store with the development of a perched potentiometric surface. The potentiometric surface generates a gradient towards areas of high vertical permeability, inducing a major lateral flow component within the epikarst (Williams, 1983). In this way the transmission of diffuse recharge to the phreatic zone is concentrated within this subcutaneous zone. As a result, epikarst can act as a buffer between recharge events and the corresponding response within the phreatic zone, with the residence time of water ranging anywhere between a few hours to weeks reach the water table (White, 2002).

The presence of an epikarst zone can also influence the development of the karst flow network beneath(Worthington and Ford, 2009). The dissolution rate of limestone is a function of the concentration of calcium carbonate ($CaCO_3$) with respect to saturation levels in recharge waters (dissolution rate reduces when water approaches saturation of $CaCO_3$, see section 2.6). When recharge must first percolate through an epikarst zone, rather than, for example, concentrated into streamflow on non-carbonate rocks first, the recharge at the base of the epikarst zone is close to saturation and so most dissolution occurs close to the surface (Ford and Williams, 2007). This leads to less selective fracture enlargement and the development of a large number of small channels within the karst (Worthington and Ford, 2009).

Point autogenic recharge occurs where precipitation is concentrated into internal runoff, generated when rainfall exceeds a given threshold and results in surface runoff (Gunn, 1983). This internal runoff is analogous to normal overland flow and enters the aquifer rapidly via surface depressions or dolines (White, 2002).

2.4.2. Allogenic Recharge

Allogenic recharge is derived from an adjacent non-carbonate catchment area and flows onto the karst body at a geological boundary (Ford and Williams, 2007). Precipitation is first concentrated into surface flow paths with then flow across the boundary onto an adjacent carbonate aquifer. Where this occurs, the stream or river can often sink abruptly via a doline or swallow hole, or be lost more gradually via a series of smaller swallow holes along the flow path. The quantity of allogenic recharge is obviously dependent upon the size and nature of the adjoining catchment. Chemically aggressive waters derived from non-carbonate catchment areas can often rapidly advance the development of substantial karst flow systems. An example of this can be seen in the Gort lowlands, Co. Galway, Ireland, where the acidic allogenic waters derived from the peat catchment of the Slieve Aughty Mountains has led to the development of a complex network of sinking streams, conduits and surface storages (turloughs).

The ability of the karst aquifer to accommodate concentrated recharge is dependent upon the level connection between surface and subsurface flow systems, and the drainage capacity of the underlying conduit flow system. Where the conduit system is

capable of accommodating the full allogenic recharge, no surface flow will be seen. However, where the capacity of the swallow hole is inadequate to accommodate the full point recharge, excess flow may continue as surface overflow or result in surface ponding around the surface water – groundwater interface, such as poljes and turloughs (White, 2002). Similarly, where the drainage capacity of the conduit flow path is reduced, either by physical constriction, sedimentation or human activity, comparable surface flooding can occur (Zhou, 2007).

2.5. Discharge

Karst aquifers generally discharge to springs, which represent the termination of the subterranean karst systems and account for the runoff from the entire karst catchment area (Ford and Williams, 2007; White, 2002). The rate of discharge, temperature and chemical composition from springs can vary substantially depending upon the supplying flow system. Discharge from conduit-driven springs can vary by many orders of magnitude, whereas the flow rate and hydrochemistry of springs derived from solutionally widened fracture swarms can remain constant irrespective of recharge events (White, 2002).

There are a number of spring types and configurations depending upon the topographic and structural context of the spring (Ford and Williams, 2007). Examples of free-draining, dammed and confined spring types are shown in Figure 2.3. In free-draining springs (Fig 2.3 (a) and (b)) the open conduit is drained freely under gravity in the direction of the slope of the karst bedrock. Dammed springs form when a barrier, such as glacial material or alleviated sediment causes the groundwater discharge to emerge, and are the most common type of spring (White, 2002). Such springs can have multiple outputs at different elevations, with the lowest permanently in operation while higher springs activate in response to high levels of recharge (Ford and Williams, 2007).

Submarine springs have been recorded discharging both fresh and brackish water from some coastal karst aquifers (Figure 2.3 (e)). Fleury *et al.* (2007a) proposed a classification system for coastal karst aquifers which is composed of three types; systems with poorly developed karstification (type 1), systems with well-developed karstification below sea level and open to the sea (type 2), and systems with well-

developed karstification below sea level but partially or totally closed to the sea (type 3). The Gort lowlands conduit system is an example of a type 2 system, where the periodic sea level fluctuations have an effect upon the behaviour of springs at Kinvarra as well as exerting an influence over turloughs as much as 10 km inland (see Chapter 8). Springs showing a rhythmic element have also been recorded, where the conduits act as a siphon periodically draining storage within the aquifer (Bonacci and Bojanic, 1991).

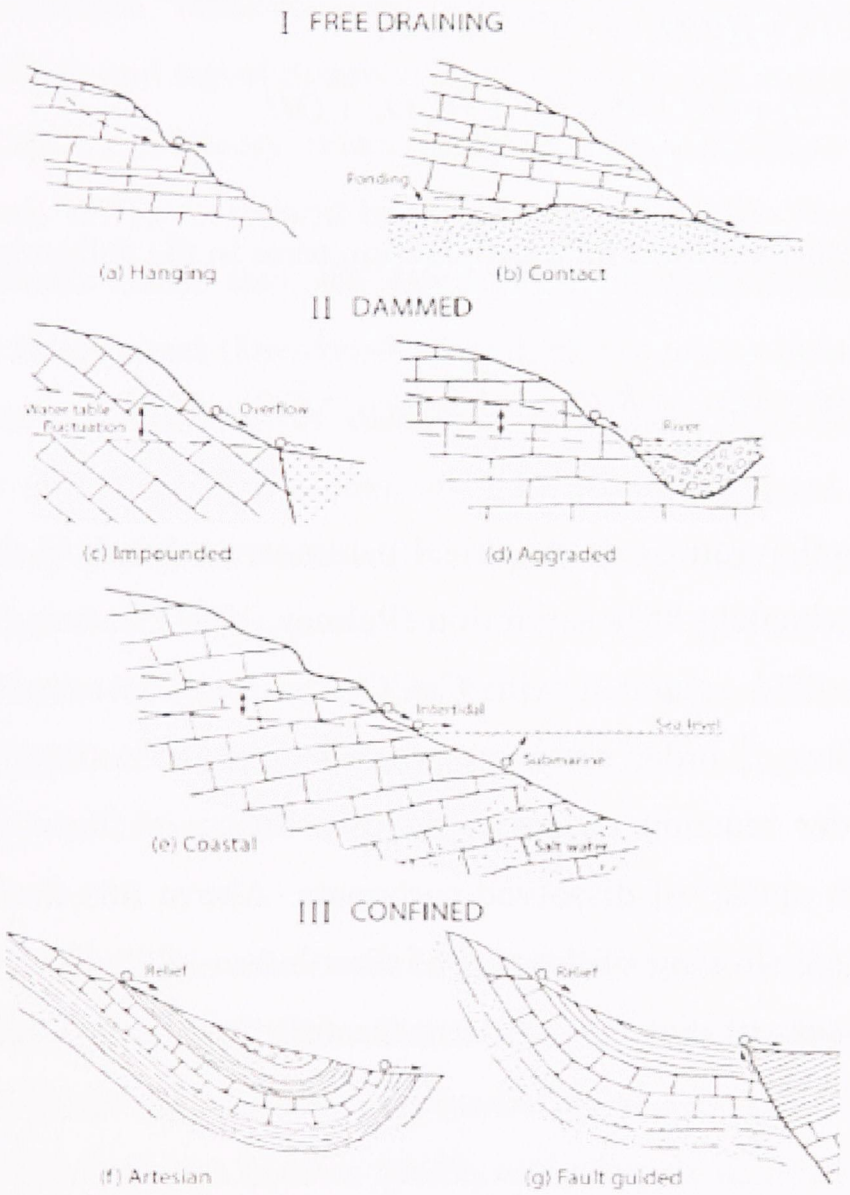


Figure 2.3: Types of springs encountered in karst, from Ford, D.C. and Williams, P.W. (2007) Karst Geomorphology and Hydrology

2.6. Carbonate Karst Chemistry and Development

Calcite is an ionic salt which dissociates into its constituent ions when exposed to pure water (Gunn, 1986). The development of secondary karst permeability is linked to the dissolution of the carbonate rock by acidic waters. The solvent action of meteoric waters on carbonate rocks is dependent upon the acid content, in particular carbonic

acid from dissolved carbon dioxide (Gunn, 1986). The chemistry governing calcite dissolution was successfully formulated in the 1980s with the establishment of interpretative parameters of hardness, saturation index and CO_2 partial pressure and the publication of reliable values for equilibrium constants by Plumer and Busenberg (1982) (White, 2002). The reactions involved in this process are:

$$CaCO_3 + H^+ \Rightarrow Ca^{2+} + HCO_3^- \qquad \textit{Equation 2.1}$$

$$CaCO_3 + H_2CO_3 \Rightarrow Ca^{2+} + 2HCO_3^- \qquad \textit{Equation 2.2}$$

$$CaCO_3 + H_2O \Rightarrow Ca^{2+} + HCO_3^- + OH^- \qquad \textit{Equation 2.3}$$

Each reaction is described for a forward reaction term in the following rate equation:

$$Rate = k_1 a_{H^+} + k_2 a_{H_2CO_3} + k_3 a_{H_2O} - k_4 a_{Ca^{2+}} a_{HCO_3^-} \qquad \textit{Equation 2.4}$$

By treating the reaction rate as an empirical parameter, a break in the reaction rate was identified at approximately 85% saturation (Palmer, 1991). It was found that when the water is less than 85% saturated with $CaCO_3$ the reaction rate is approximately 1st order, but approaches 4th order when saturation reaches 85% (Svenson and Dreybrodt, 1992). The 1st order reaction causes rapid dissolution of the carbonate rock and a corresponding high uptake of dissolved carbonate. Above this threshold, the 4th order reaction rate means a slowing of the rate of dissolution with slightly unsaturated water continuing the process of dissolution along the full flow path, albeit at a much slower rate.

As the fracture size slowly increases, a threshold value is reached above which the fracture becomes sufficiently large to allow the penetration of water with less than 85% saturation along the entire flow path. This critical point is known as the "breakthrough point". Once a fracture has reached this aperture size the rate of dissolution along the flow path greatly increases, leading to the development of conduits. Dreybrodt calculated the time to breakthrough to be in the range of 10,000 years for wide initial fractures and short travel distances under common natural hydraulic gradients, but can be as short as 100 years in special cases of large initial fracture size, high hydraulic gradient and short path length (Dreybrodt, 1992; Dreybrodt, 1996). The aperture size at

which breakthrough occurs is 0.01 m, which corresponds to the threshold size for the onset of turbulent flow, a shift from fourth order to linear kinetics, and the transport threshold where aperture size and flow velocities become sufficient to carry clastic material (White, 2002). The higher permeability of this "breakthrough" flow route means that it acts as a preferential flow path, accommodating a greater component of recharge which further accelerates its development.

The specific path in which "breakthrough" occurs is dependent upon the initial aperture size, hydraulic gradient and travel distance between input and output points, with initial enlargement occurring selectively under laminar flow conditions (Dreybrodt, 1990; Groves and Howard, 1994). In natural karst systems, where the lengths of the fractures are large and hydraulic heads low, the development is determined by the dissolution rates at the exit of the channel (Dreybrodt, 1996). In the case where the initial fractures are uniform in size, the majority of enlargement occurs along the most direct route between recharge and discharge points, as this offers the least resistance to flow (Groves and Howard, 1994). In reality, the initial fracture size is rarely uniform. Since flow rates in laminar flow are proportional to the fourth power of diameter, but only linearly proportional to hydraulic gradient, the path offering the least flow resistance may not be the most direct route, and so the preferentially enlarged set of fractures may follow an indirect path (Groves and Howard, 1994).

The breakthrough path itself is often a function of the structure and stratigraphy within the karst bedrock, with the orientation and position of conduit development occurring along horizons which are particularly susceptible to dissolution. These horizons have been termed inception horizons (Lowe, 2000), and are part of a rock succession that is particularly susceptible for the development of karst conduits because of physical, lithological or chemical deviation from the predominant carbonate facies within the limestone sequence (Filipponi et al., 2009). The inception horizon may take the form of bedding planes, joints or faults and may be discrete (most penetrable joints and faults terminate in comparatively short distances) or more continuous and propagate for large distances through the bedrock (Ford and Williams, 2007). A recent study of detailed geological 3D models and cave surveys from 18 large cave systems around the world confirmed that the development of karst conduits under phreatic conditions is strongly related to a restricted number of inception horizons (Filipponi et al., 2009).

The occurrence of breakthrough along a flow path or channel leads to the development of self-organised permeability in the carbonate aquifer (Worthington and Ford, 2009). The increase in permeability associated with the rapid enlargement along a flow path or channel following the occurrence of "breakthrough" causes a local drop in head (Dreybrodt, 1990). Rather than following the regional gradient as occurred prior to breakthrough (Fig. 2.4(a)), this local drop in head causes a reorganisation of the flow field so that flow is towards the channel (Fig. 2.4(b)). Similarly, as the karst aquifer continues to develop breakthrough occurs along secondary or tributary flow channels, further modifying the flow field (Fig. 2.4(c)). As this process continues the aquifer permeability thus becomes dominated by dendritic, self-organised system of channels (Worthington and Ford, 2009).

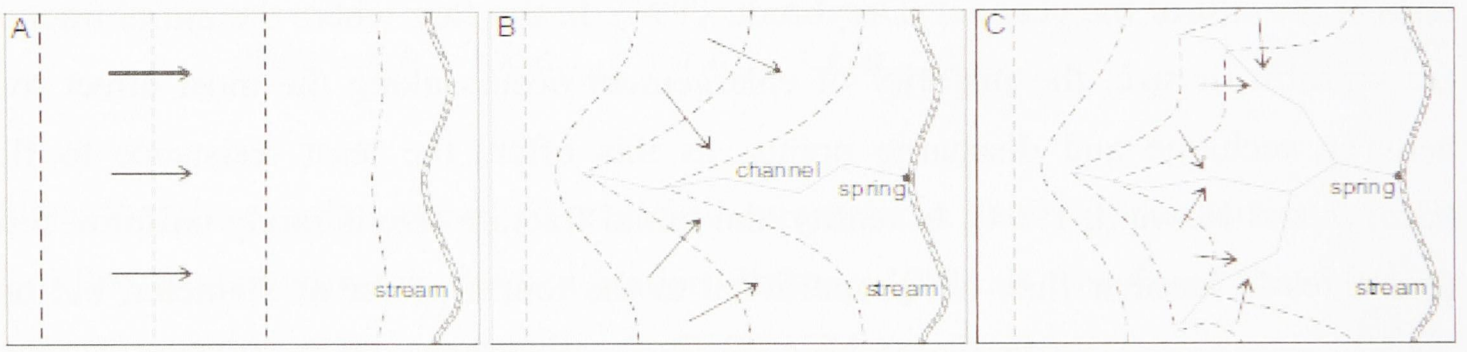


Figure 2.4: Development of self-organized permeability in carbonate aquifers, showing (A) the initial flow field, (B) the modified flow field after one channel has achieved breakthrough, and (C) after tributary channels have achieved breakthrough. Arrows represent flow lines and dashed lines represent equipotentials (Worthington and Ford, 2009)

2.7. Investigation of Karst Systems

2.7.1. General

The extreme heterogeneity and complexity of groundwater flow of karst aquifers lead to obvious problems in the determination of karst system structure and functioning (Einsiedl, 2005; Field, 1993). As a result, a wide variety of investigation techniques are utilised in the investigation of karst systems. These include conventional techniques from water resource surveys as well as special techniques developed with karst systems in mind (Ford and Williams, 2007). Brief descriptions of some of the main methods

used are given here, but for a thorough explanation see Goldscheider and Drew (2007) and Ford and Williams (2007).

2.7.2. Geomorphology and Speleology

An understanding of the nature of karst geological formations; their stratigraphy, lithology, fracturing and faulting, is necessary when studying karst groundwater systems as the geological setting can determine the nature of the karst aquifer (Goldscheider and Andreo, 2007). In Ireland, for example, it is the well bedded, pure Carboniferous limestones which have undergone significant karstification (Drew and Daly, 1993). However the degree of karstification is not spatially homogeneous, but varies with limestone purity and, in some areas such as the Gort lowlands, evolved under lithographic control whereby cherty beds within the limestone exerted a strong influence (Johnston and Peach, 1999). Identification of such lithographic features is therefore useful in evaluating the likelihood of the presence of significant conduit flow paths within the karst formation.

The evaluation of karst features in the context of their geologic setting can aid in the understanding of groundwater flow in karst aquifers (Sasowsky, 2000). The presence and spatial orientation of karst landforms, such as dolines, are often indicative of the geometry of the underlying conduit network (Goldscheider and Andreo, 2007). Such a pattern was noted by Hickey (2003) during a karst mapping programme in Co. Roscommon, Ireland. Linear assemblages of collapse features at the bottom of dry valleys in the Castlerea area suggested a highly developed, possibly conduit dominated, underground drainage system (Hickey, 2003). During this research, karst features identified within turlough basins, such as swallow-holes and estevelles, provided evidence of the strong role played by active conduit networks in determining the hydrological regime of individual turloughs.

Detailed geomorphological mapping has also proven valuable in the hydrological modelling of karst flow systems. On a local scale, the presence and location of active karst features has been used to delineate zones of groundwater flow within a polje basin (Zibret and Simunic, 1976). A set of characteristic flow equations were derived for each zone allowing the accurate prediction of flow rates through the polje based upon piezometric measurements in adjacent boreholes. On a regional scale, a study of the

Gempen plateau in Switzerland used mapping of aquifer and aquitard geometry along with fault delineation to generate a 3D geological model (Butscher and Huggenberger, 2007). Through the application of a conceptual karst model approximating flow in shallow karst systems to open surface flow on the top of the uppermost aquitard or aquifer base, this model has been used to delineate spring catchment areas and identify flow processes in mature, shallow karst regions (Butscher and Huggenberger, 2007).

The presence of large conduits or caves allow the direct observation of karst conduits, thus giving access to major flow paths for sampling and measurement (Jeannin et al., 2007). Cave mapping using a combination of GPS, underwater compass, dive computers, digital depth gauges, and detailed surveys of active cave systems can define the actual pathways of groundwater through the karst formation. Cave geometry provides information on cave genesis and the formation processes controlling cave morphology and micromorphology (Jeannin et al., 2007). For example, the cross-sections of dissolution scallops have been used to estimate flow velocities and discharges in conduit systems (Gale, 1984; Jeannin, 2001).

2.7.3. Spring Hydrographs

One of the most important and distinctive aspects of karst hydrogeology is the temporal variation in spring discharge, as expressed by the spring hydrograph. The spring hydrograph represents the cumulative effects of all recharge and flow processes within the contributing karst formation, and provides an insight into the storage and flow characteristics of the catchment area (Groves, 2007). In this way the karst system acts as a transfer function, transforming the input function (precipitation) into the output function (spring discharge).

Spring hydrographs can show a range of response behaviours to storm events with many factors affect the timing of the response, such as the relative quantities and nature of allogenic and autogenic recharge (diffuse or point), the internal structure of the conduit system, and the size of spring's contributing area (White, 2002). A fast response time will result in a series of clear peaks and recessions in the spring hydrograph representing the effects of individual storm pulses, and is generally associated with systems containing well-developed conduit networks and dominated by allogenic recharge (White, 1988). Karst springs with a slower response time show a

smoother, less structured hydrograph, and is often indicative of a catchment dominated by diffuse recharge with a poorly developed conduit system (White, 1988). The linkage between response time, recharge type and level of conduit development is not, however, universal as a fast response could be as a result of concentrated recharge close to the spring outlet (Quinlan et al., 1991). Equally, a slow response time could occur in a well-developed conduit network which is mainly fed by diffuse infiltration (White, 2002).

Quantitative analysis of spring hydrograph recessions was founded on the equations formulated by Boussinesq and Maillet in the early 20th century, based on the premise that spring discharge is a function of the volume of water held in storage within the aquifer (Ford and Williams, 2007). Boussinesq (1904) expressed the decrease in flow in a karstic spring in quadratic form using the equation:

$$Q_t = \frac{Q_0}{(1+\alpha t)^2} \qquad \textit{Equation 2.5}$$

Where:

$$Q_0 = \frac{1.724 K h_m{}^2 l}{L} \qquad \textit{Equation 2.6}$$

And:

$$\alpha = \frac{1.115 K h_m}{n_e L^2} \qquad \textit{Equation 2.7}$$

Where Q_t is the discharge at time t, Q_0 is the discharge at time 0, K is aquifer hydraulic conductivity, n_e is the effective porosity, l is the aquifer width perpendicular to its length L, h_m is the initial hydraulic head at a distance L (Ford and Williams, 2007). The dimensionless parameter α is the recession coefficient or coefficient of discharge, which is a function of the aquifer's transmissivity and specific yield (Kresic and Bonacci, 2009). A study by Drogue (1972) applied the modified form of this equation:

$$Q_t = \frac{Q_0}{(1+\alpha t)^n} \qquad \textit{Equation 2.8}$$

where n had the values of ½, 3/2 and 2 according to the difference between the initial and final discharges (Drogue, 1972). When applied to 100 discharges, 73 were satisfactorily represented using this equation. Maillet (1905) described the recessional limb of the hydrograph with an exponential response of the form:

$$Q_t = Q_0 e^{-\alpha t}$$ *Equation 2.9*

When this exponential behaviour holds for the entire recession duration, a semi-log plot of time versus spring discharge for the recession period yields a single straight line with slope α. However, it is common for springs to diverge from this exponential behaviour, shown by two or more straight line segments on semi-log plots of recession limbs (Kresic and Bonacci, 2009). Figure 2.5 shows such a case, where the semi log plot of time versus discharge for a spring recession shows three distinct straight lines. Each line can be approximated by a corresponding exponential function with a recession coefficient, and these three functions combined to form the complete spring recession.

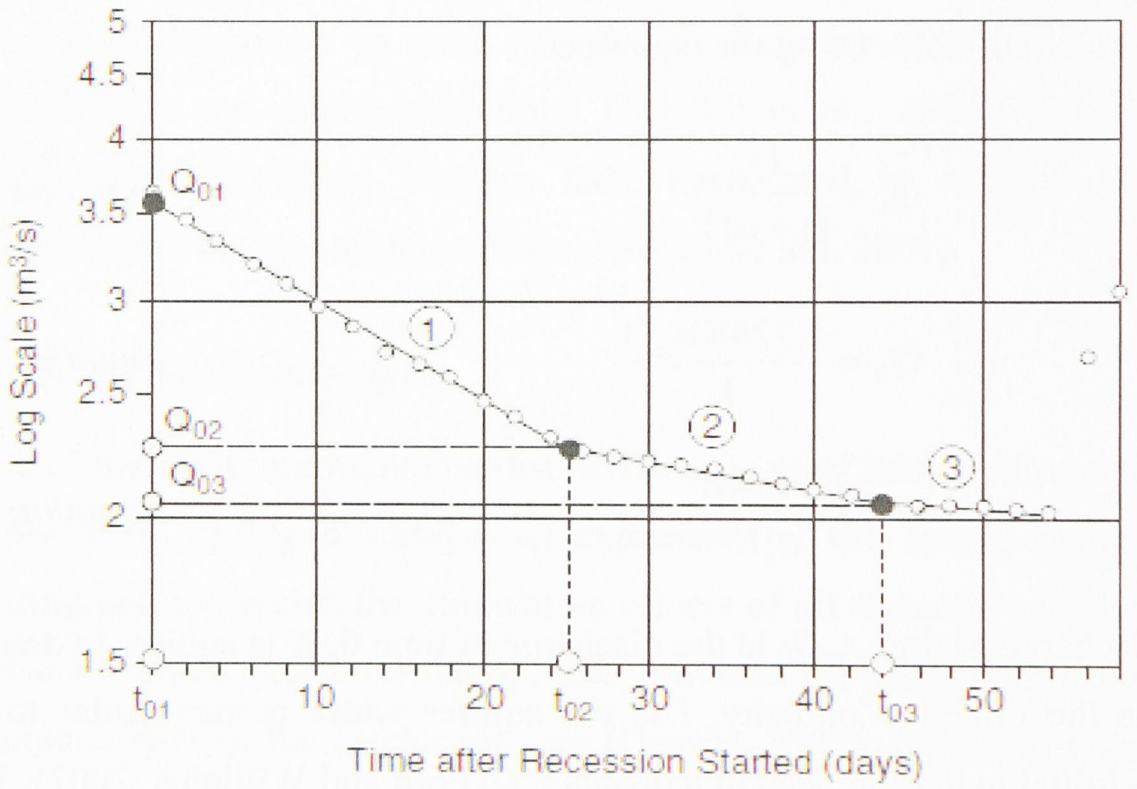


Figure 2.5: Semi-log graph of time versus discharge for a spring recession period showing three distinct recession slopes (from Kresic and Bonacci, 2009)

The coefficients defined by the slope of such lines can yield information on aquifer and conduit hydraulic characteristics (Kovacs et al., 2005). Atkinson (1977) divided the response into "quickflow" and "slowflow", where "quickflow" is a response to the portion of the catchment which drains quickly via conduit flow, while the "slowflow" or "baseflow" represents the purely Darcian response of the draining from the matrix of a conduit system (Halihan and Wicks, 1998). However, a number of alternative mechanisms have been proposed that would produce the multiple limbs commonly

present in hydrograph recessions, for example purely Darcian models (Eisenlohr et al., 1997) or reservoir constriction models (Halihan and Wicks, 1998). For example, changes in the spring drainage area of effective porosity of the karst aquifer with falling head would result in breakpoints in the recession curve (Bonacci, 1993). While less common, the slope of the recession curve may even increase (the recession coefficient increases with time) due to, for example, the effects of flooded caves or poljes up gradient of the spring (Kresic and Bonacci, 2009). Complementary hydrochemistry and spring chemograph data can help to identify the most appropriate interpretation of spring recession behaviour (Grasso et al., 2003).

2.7.4. Boreholes and Test Wells

Given the highly heterogeneous nature of groundwater flow, and the scale-dependency of hydraulic conductivities in karst formations (Figure 2.6), the use of boreholes and the associated monitoring, potentiometric mapping and hydraulic tests require specific adaptations for use in karst aquifers (Field, 1993; Sauter, 1991). Given that the chance of a borehole penetrating a main conduit system is understandably low, found to be 0.4 to 3% on the central Kentucky karst (Worthington et al., 2000), a clear understanding of the underlying hydrogeology is required when interpreting borehole hydraulic data (Kresic, 2007).

Despite the limitations, boreholes can provide useful hydraulic parameters applicable on a range of scales to various aspects of the karst system (Sauter, 1991). On a micro scale, laboratory tests on cores can help determine the matrix porosity of the rock itself. Packer and injection tests can be used to evaluate the hydraulic conductivity on a sub-local scale and at discrete intervals along the borehole depth, while the use of downhole video cameras can help identify active flow areas such as open conduits and fracture zones (Kresic, 2007; Sauter, 1991; White, 2002). Pump tests can also provide information on the hydraulic conductivity of the fracture systems intercepted by the borehole but, as mentioned earlier, such data must be interpreted carefully as the fracture systems themselves can often be discontinuous dissolution features and not representative of the regional flow system (Halihan et al., 2000; White, 2002).

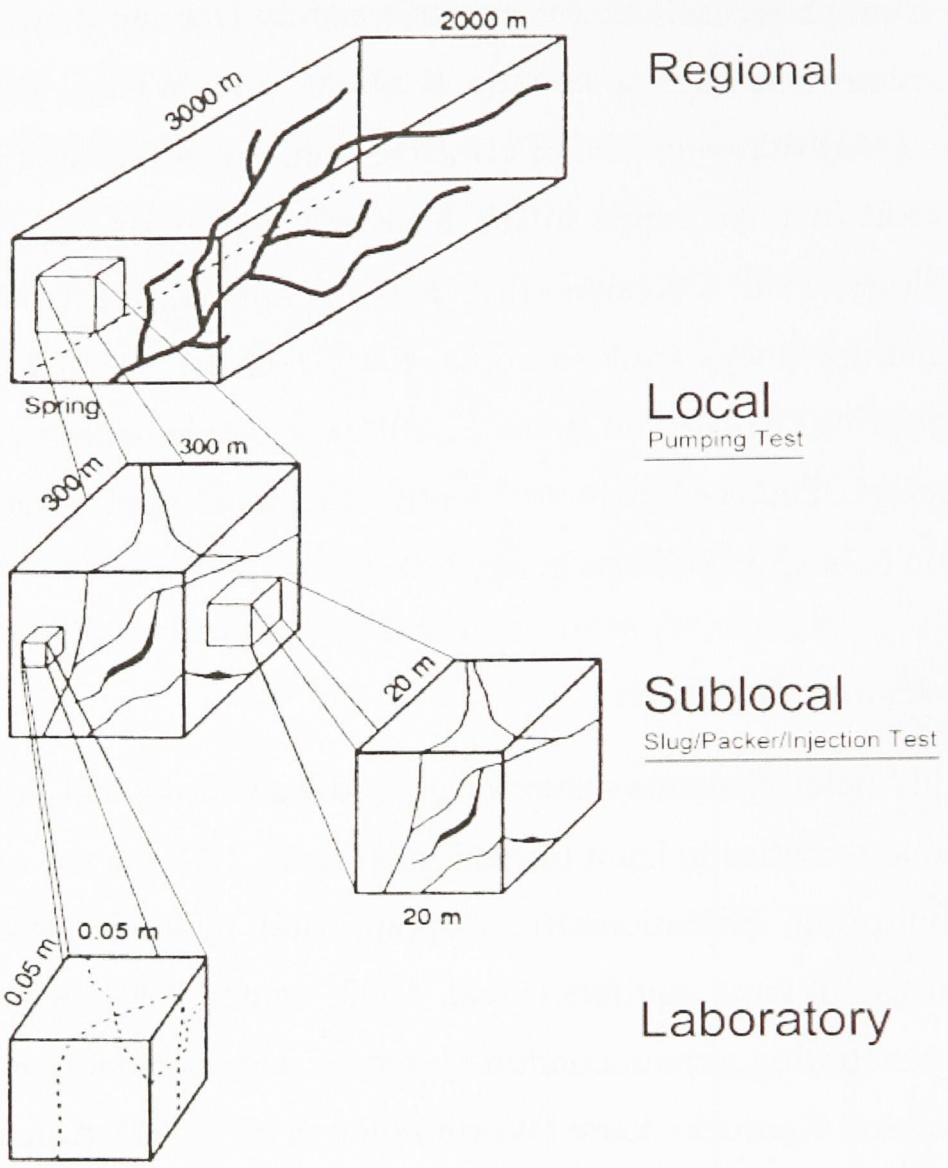


Figure 2.6: Geometrical Relationships and hydraulic conductivities at different scales (from Sauter, 1991)

2.7.5. Tracer Tests

Tracer tests are the primary method used to delineate catchment areas, identify hydraulic connections between points, and provide information on the flow dynamics and transport within the system (Benischke et al., 2007; Morales et al., 2007). Tracer studies can also yield information on the geometric and hydraulic properties of conduit systems (Atkinson et al., 1973; Birk et al., 2004). Tracing involves introducing conservative substances at input point(s), such as a swallow hole or sinking stream, and measuring the presence and/or concentration at output points, principally springs. Qualitative tracing involves simply trying to establish a connection between input and output points, whereby a tracer is injected into a stream or swallow-hole and then monitored for at a downstream location. Quantitative tests, whereby the tracer concentration is regularly or continuously recorded at the output point, allow more detailed information to be obtained. The change in concentration of tracer recorded at

the spring, as defined by the concentration breakthrough curve, categorises the mean transit time through the system while the dispersivity within the system can provide an estimate for the catchment area of the spring (Einsiedl, 2005). Often both qualitative and quantitative tracing studies are carried out simultaneously, such as was carried out in the Beech Creek karst aquifer in Indiana using Rhodamine WT and ionic bromide where a conduit velocity of 286m/hr was recorded (Baedke and Krothe, 2000).

Fluorescent dyes are widely used in tracing studies given their excellent properties as groundwater tracers; they are water-soluble, non-toxic, widely absent in natural waters, and have a low detection limit (Benischke et al., 2007). The concentration of fluorescent dyes are also easily measureable either directly at the output point or in the laboratory using fluorescence spectroscopy (Benischke et al., 2007). The most common fluorescent substances used include fluorescein, rhodamine and optical brightener, and there are numerous examples of the successful use of such tracers to elucidate the characteristics of karst aquifers (Atkinson et al., 1973; Banks et al., 1996; Dreiss, 1982). In the Irish context, tracer experiments used to estimate groundwater flow and delineate spring zones of contribution have identified groundwater velocities in the range of between 5 and 250 m/h recorded in lowland areas and velocities between 20-300 m/h in upland areas (Drew, 2008). Other tracer substances which have been used include salts such as bromide (Einsiedl, 2005), and particulates such as Lycopodium clavatum spores (Atkinson et al., 1973).

2.7.6. Stable Isotope Analysis

Oxygen has three stable isotopes, ^{16}O, ^{17}O and ^{18}O, with relative abundances in the environment of 99.76, 0.035 and 0.2% respectively (Nier, 1950). As the ^{18}O isotope is more abundant and therefore more accurately measurable than ^{17}O, it is the ratio of $^{18}O/^{16}O$ that is generally used in hydrological studies (Mook, 2000). Isotopic concentrations of ^{18}O, as a ratio of $^{18}O/^{16}O$, are conventionally given in delta (δ) units, which are parts per thousand (per mil) deviations from the standard and given by:

$$\delta‰ = \left(\frac{R_{sample} - R_{standard}}{R_{standard}} \right) \times 1000 \qquad \textit{Equation 2.10}$$

Where R is the ratio of heavier (^{18}O) to lighter (^{16}O) isotopes (Ford and Williams, 2007). The standard $^{18}O/^{16}O$ ratio is that of Vienna Standard Mean Ocean Water (VSMOW) which has an absolute ratio of $(2005.2 \pm 0.45)*10^{6}$ (Baertschi, 1976). Thus a positive $\delta^{18}O$ values indicates enrichment of ^{18}O isotopes relative to VSMOW, while a negative value indicates ^{18}O depletion.

When water evaporates from the surface of an open water body, such as a turlough, the vapour leaving the surface is depleted in heavy isotopes (^{2}H, ^{18}O), as they have slightly lower saturation vapour pressures than the ordinary molecules (^{1}H, ^{16}O). This process which leads to the enrichment of heavy isotope molecules in the remaining water, is called kinetic isotope fractionation (Mayr et al., 2007). The kinetic isotope fractionation (ε_k) is given by:

$$\varepsilon_k = (1 - h) * C_k \qquad \textit{Equation 2.11}$$

Where h is humidity and C_k is an empirically derived coefficient of 12.5 for hydrogen and 14.2 for oxygen (Gonfiantini, 1986). Processes other than evaporation, such as chemical and biological reactions, can also alter the ratio of stable isotopes within a given phase. The enrichment of heavy molecules also involves equilibrium isotope effects, where the equilibrium isotope fractionation (ε^*) is a dependent on temperature and is given by (Clark and Fritz, 1997):

$$\varepsilon^* = \left(\frac{R_{WATER}}{R_{VAPOUR}} - 1 \right) * 10^{3} \qquad \textit{Equation 2.12}$$

ε^* values for hydrogen and oxygen differ by a factor of 8, with this factor remaining constant throughout the range of temperatures at which precipitation normally forms (Mayr et al., 2007). Therefore a plot of $\delta^{2}H$ against $\delta^{18}O$ will give a straight line with a gradient of 8, known as the Global Meteoric Water Line (GMWL) (Craig, 1961). If water samples analysed for both δH^{2} (deuterium δD) and $\delta^{18}O$ are plotted on such a graph and lie below the line (i.e. a relative increase in $\delta^{18}O$ with respect to δH^{2}), in a hydrological setting such as the west of Ireland this generally indicates the water has undergone evaporation (Diefendorf and Patterson, 2005).

The relevant theory here is that in the course of evaporation, the remaining water of a desiccating water body will become gradually enriched with heavy isotope molecules until an equilibrium condition is reached and no further fractionation will occur (Gat, 1995; Mayr et al., 2007). Therefore an increase in $\delta\ ^{18}O$, the ratio of heavier ^{18}O to lighter ^{16}O, would imply enrichment of the heavier isotope due to evaporation. This was demonstrated in a study by Mayr *et al.* (2007), which used stable isotope analyses to investigate and compare two deep crater lakes against more ephemeral water bodies. This study showed that the highest isotopic enrichment occurred towards the end of the dry season, and that isotopic enrichment of lake waters largely dependent on the lake type, with different area/volume ratios affecting isotopic composition. The study was also able to identify the flow through nature of the two deep lakes.

2.7.7. Geophysical Methods

Given the spatial heterogeneity of flow paths within karst hydrogeological systems, geophysical methods can help in the siting of boreholes, the determination of soil thickness, and the detection and characterisation of water-bearing fractures and conduits (Bechtel et al., 2007). Common methods such as electrical resistivity surveys, ground penetrating radar (GPR) and microgravity have all proved valuable in obtaining information on the aquifer structure including the epikarst, bedding planes, fractured and karstified zones, conduits and other typical karst landforms (Al-fares et al., 2002; Ford and Williams, 2007; McGrath et al., 2002). Down–borehole geophysics has also extended the scope of geophysical methods into areas inaccessible to humans. These methods can be used to map subsurface features and, together with an accompanying conceptual model, can be used to estimate the physical characteristics of subsurface karst flow systems (Ford and Williams, 2007; Rodriguez, 1995). However, care should be taken in the selection of the appropriate geophysical technique based upon the expected physical property of the feature of interest and its contrast with the surrounding formation, and often a combination of methods will achieve the greatest level of success (Bechtel et al., 2007; Mochales et al., 2008).

2.7.8. Karst Modelling

The highly heterogeneous nature of karst groundwater flow has led to the development of specially adapted hydrological modelling methodologies (Kovacs and Sauter, 2007). The most important step in the modelling procedure is the development of a conceptual model of the aquifer (Ford and Williams, 2007). The conceptual model is a theoretical representation of the real system being studied, and consists of physically representative parameters such as aquifer geometry, flow equations, initial and boundary conditions (Kovacs and Sauter, 2007). There are two fundamental approaches to the mathematical modelling of karst hydrogeological systems; global models and distributive models. The form of the conceptual model determines which of these modelling approaches is taken to achieve the desired goals. Global (or lumped parameter) models concentrate on mathematically deriving a relationship between input and output, where the input is usually a precipitation event and output the spring discharge time series. In contrast, distributive models use theoretical concepts such as

aquifer structure and hydrodynamic flow equations to simulate the hydraulic behaviour of karst aquifers (Ford and Williams, 2007).

2.7.8.1. Global Models

Global models consider the karst aquifer as a transfer function which transforms the storm input signal into the output spring hydrograph signal, which is taken to represent the overall (or global) hydrogeological response of the karst aquifer to storm events (Kovacs and Sauter, 2007). An example of this is schematically shown in Figure 2.7, where a transfer or kernel function is used to transform the infiltration into storm-derived spring flow (Dreiss, 1989). The transfer function itself can be represented by a single mathematical function or a time series, and is an example of a single event model (Long and Derickson, 1999). Single event models quantify the response of karst systems to individual storm events based on physical laws derived from reservoir models, and in doing so can provide information on the hydraulic properties of the karst aquifer (Kovacs and Sauter, 2007).

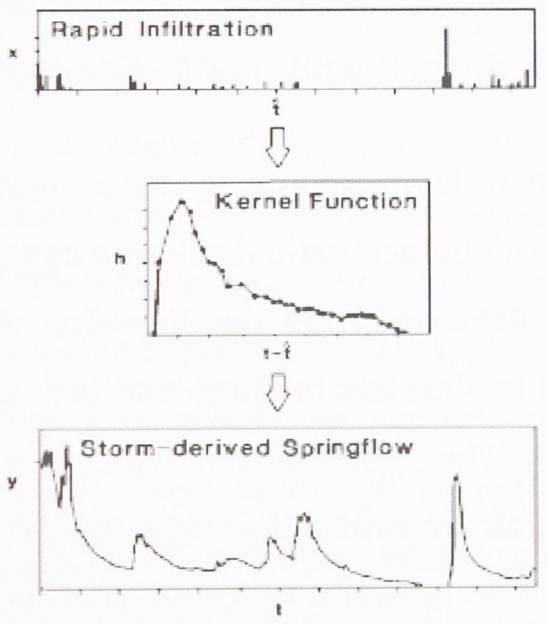


Figure 2.7: Schematic diagram of linear systems analysis of karst conduit-type spring flow (Dreiss, 1989)

The relationship between input and output for a linear, time-invariant system is described by the convolution equation:

$$y(t) = \int_0^t h(t - t')x(t')dt' \qquad \textit{Equation 2.13}$$

Where y(t) is the system output time series, h(t-t') is the transfer function, x(t') is the system input time series and (t-t') represents the delay between input and output (Long and Derickson, 1999). Therefore, if both the input and output functions are known the transfer function can be derived using deconvolution methods such as linear programming (Dreiss, 1989; Neuman and De Marsily, 1976) or time series analysis techniques (Labat et al., 2000a; Labat et al., 2000b; Labat et al., 2002).

Given the inherent non-linearity of karst systems, linear time-invariant transfer functions were found to produce unstable oscillatory functions which had difficulty in simulating spring discharge during long recession periods (Denic-Jukic and Jukic, 2003; Dreiss, 1982). To address this problem, composite transfer functions have been developed which use the superposition of two transfer functions adapted for the quick flow and the slow flow hydrograph components (Denic-Jukic and Jukic, 2003). Non-linear kernel functions have also been derived from the time-invariant and non-anticipatory Volterra series (Jukic and Denic-Jukic, 2005). More recently, Padilla and Pulido-Bosch (2008) derived three transfer functions, one each for the surface zone, the unsaturated zone and the saturated zone to simulate the discharge of a spring from the Torcal de Antequera aquifer, Spain (Padilla and Pulido-Bosch, 2008).

Global models have also been developed using conceptual linked reservoirs with each reservoir governed by a set of characteristic discharge equations. A good example is the empirical reservoir model developed for the Fontaine de Vaucluse aquifer, France which used three reservoirs to simulate the high and low spring discharge rates (Figure 2.8) (Fleury et al., 2007b). The first soil reservoir uses a simple water balance to calculate the effective rainfall or infiltration into the system at each time step. The infiltration was then partitioned between two flow-routing reservoirs, one representing the slow flow and the other the fast flow portion of the spring discharge. Together these reservoirs represent the transfer function. The discharge from each reservoir was proportional to the water level within the reservoir. The outflow coefficient for the slow discharge reservoir was derived using hydrodynamic analysis of the spring hydrograph, while the rapid discharge reservoir coefficient was a fitted parameter (Fleury et al., 2007b).

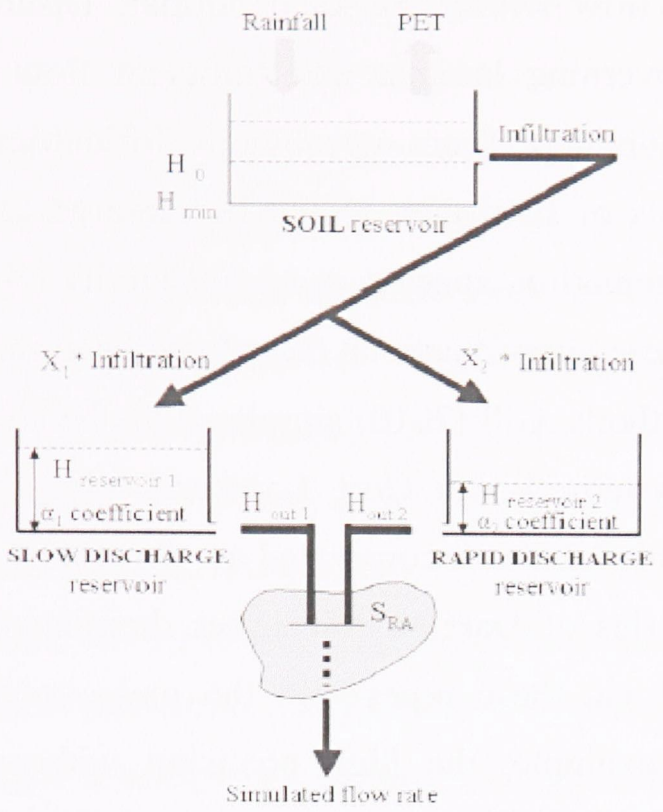


Figure 2.8: Conceptual model of Fontaine de Vacluse system (Fleury et al., 2007b)

2.7.8.2. Distributive Models

As described earlier, distributive models use theoretical concepts such as simplified aquifer geometry and hydrodynamic flow equations to simulate the hydraulic behaviour of karst aquifers (Kovacs and Sauter, 2007). Distributive karst aquifer models can consist of a single continuum representing the effective overall parameters of the aquifer, or a discrete set of fractures and conduits with flow only within those discrete flow paths considered (Kovacs and Sauter, 2007). Equivalent porous medium (EPM) models largely ignore conduit flow within the aquifer, instead it is assumed that the flow conditions at a sufficiently large scale can be approximated as Darcian. Such models which treat the aquifer as an isotropic, homogeneous medium clearly do not reflect the complexities of groundwater flow within karst aquifers and have been shown to produce fundamentally different temporal hydraulic behaviour from karstified media (Kovacs et al., 2005; Kovacs and Sauter, 2007). A study by Scanlon *et al.* (2003) on the Barton Springs Edwards aquifer, USA showed that EPM models were limited to simulating spring flow, but were incapable of simulating groundwater flow rate and direction or delineating contributing areas.

Discrete fracture network (DFN) and discrete channel network (DCN) models have a similar conceptual basis to EPM models, in that one form of permeability is assumed to

dominate groundwater flow within the karst aquifer. Discrete network models use hydraulic equations governing laminar and turbulent flow to model the discharge through fractures and conduits. There are obvious difficulties in constructing discrete models, as vast amounts of field data would be required to accurately replicate the fracture and conduit orientation, spacing and connectivity (Kovacs and Sauter, 2007). However, using geometric simplifications there have been many successful modelling attempts using such methods. Gill (2010) simulated the behaviour of turloughs along a major conduit flow system in the Gort Lowlands using a conduit network with surcharged tanks. This model also incorporated an element of diffuse contribution from the epikarst using a series of Darcian soil stores draining to permeable pipes. This recharge was then fed via these pipes into the main conduit network linking the turloughs. In another example, the high precision with which the hydrodynamic behaviour of the Hölloch cave network in Switzerland (Figure 2.9) could be measured allowed the development of DCN model which accurately simulated the turbulent flow in the variably saturated, conduit flow-dominated karst system (Jeannin, 2001).

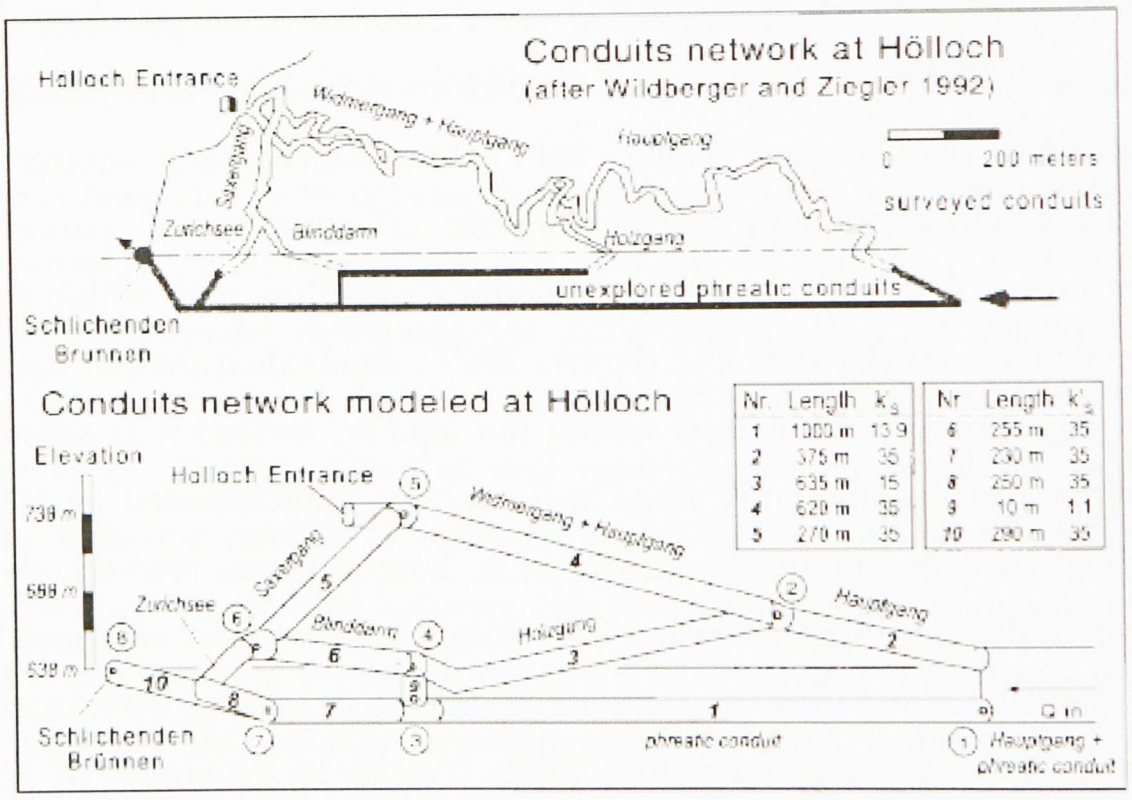


Figure 2.9: Conduit network used to model flow in the downstream part of the Hölloch cave and sketch of the cave conduits (Jeannin 2001)

2.7.9. Polje Hydrology

Studies of polje hydrology are significant to the research in this thesis as there are many parallels between polje and turlough hydrology. Polje are large, flat-floored depressions in karst with interior karst drainage, and are subsystems of water retention in the karst system (Avdagic, 1976; Ford and Williams, 2007). Hydrologically polje are similar to turloughs, as both display periodic inundation and lacustrine sediment deposition. They also have the common problem of difficulties in measuring inflows and outflows and in defining the associated water budget parameters. Polje flooding occurs when the sum of the various inflows exceed the outflows, with the excess retained within the polje as surface storage (Ford and Williams, 2007). Inflow may come from surface streams, springs or estevelles, while drainage can occur via swallow-holes (ponors) or surface outflow points. A schematic representation showing a series of polje within a karst system is shown in figure 2.10 (Bonacci, 1982). This figure shows the different connections polje can have with the underlying karst flow system, with the nature of inflow and outflow to the polje dependent upon its location within the system and the nature of the hydraulic connections.

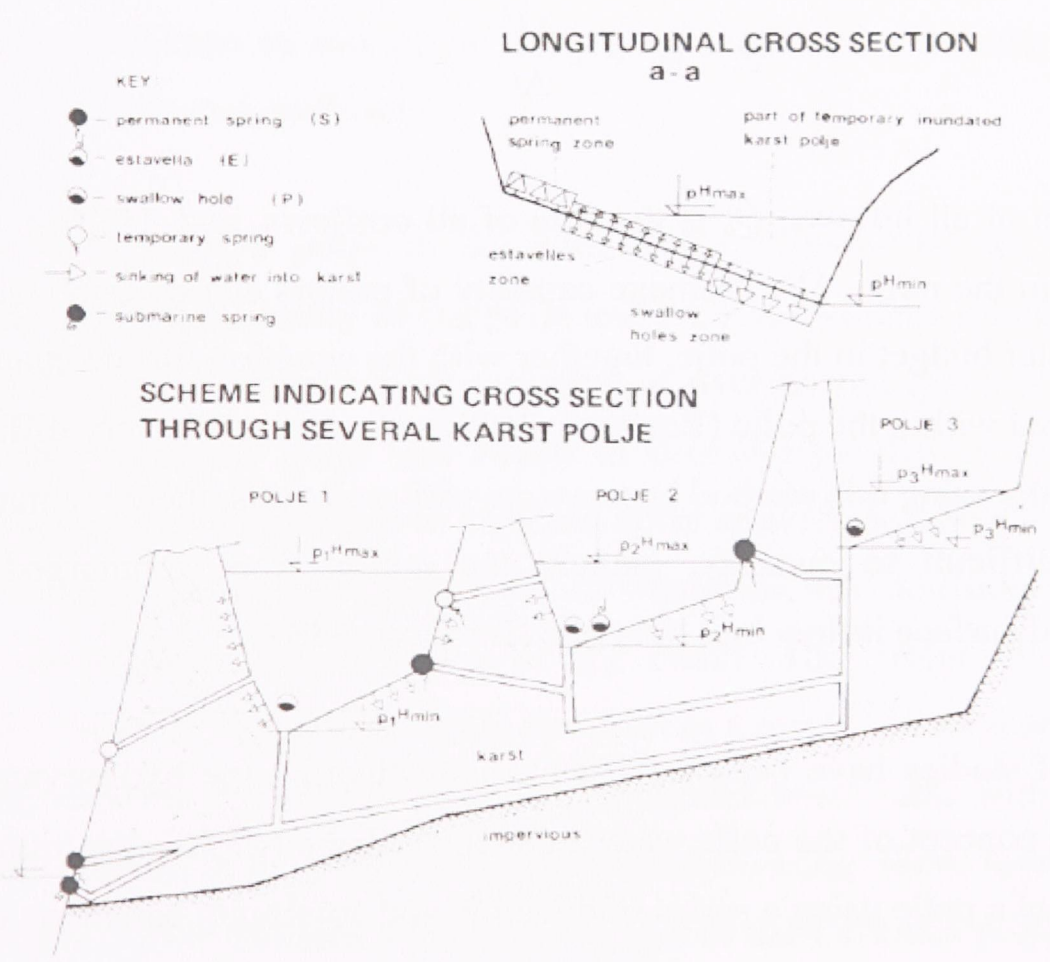


Figure 2.10: Schematic presentation of outflows in karst poljes (Bonacci, 1982)

The general equation describing a polje's water budget, which can also be used to describe a turlough's water budget, is given by (Bonacci, 1987):

$$\sum_{i=1}^{3} Qi_i - \sum_{j=1}^{3} Qo_j = \sum_{k=1}^{2} (\Delta V_k / \Delta t) \qquad \textit{Equation 2.14}$$

Where:

Qi₁: inflow to the polje from areas not belonging to its own topographic catchment

Qi₂: inflow from the polje topographic catchment

Qi₃: inflow from other catchments via hydrotechnical structures

Qo₁: outflow through ponors

Qo₂: water losses by evapotranspiration from topographic catchment area of the polje

Qo₃: outflow through the hydrotechnical structures

ΔV₁: variation in the volume of water storage in the polje

ΔV₂: changes in the volume of groundwater in the topographic catchment of the polje

In practice many of these terms are not applicable (such as inflow and outflow via hydrotechnical structures) or are difficult or impossible to determine (such as inflow from topographic catchment or ponor outflow) and so a simplified version of the water budget equation is used (Kovacic, 2010):

$$Q_i - Q_o = \pm \frac{\Delta V}{\Delta t} \qquad \textit{Equation 2.15}$$

Where:

Q_i is the sum of all inflows, Q_o is the sum of all outflows, and $\Delta V/\Delta t$ is the change in storage within the polje. The drainage capacity of ponors can be established indirectly using the water budget in the polje, together with the equation for the change in volume of water stored within the polje (Bonacci, 1982). However, it is very difficult to obtain accurate results using this method because, as with turloughs, there are many unknowns which are difficult to quantify, namely the output from submerged springs and estevelles and surface inflow into the polje (Bonacci, 1987) .

A number of studies have been carried out investigating the hydrodynamics of polje based on the concept of the polje water budget. Avdagic (1976) determined the inflow and outflow of a polje using a series of dynamic and continuity equations of the form:

$$\sum_{i=1}^{n} k_i \Delta H_{j,i}^{\ a_i} = \left(\frac{\Delta W}{\Delta t} \right)_j \qquad \textit{Equation 2.16}$$

Where n is the number of zones or channels, k_i and a_i are constants for certain flow conditions and $\Delta W/\Delta t$ is change in storage within the polje. The flow was determined using differences in level between the water within the polje and a level or pressure measuring point within a conveyance channel (as represented by the head measured in a piezometer). Four systems of flow equations were determined representing flow from different zones within the polje. The coefficients depended on the mean elevation of each zone, the water level in the polje and the water level or pressure in the piezometer. Avdagic (1976) also identified a constant outflow capacity for some parts of the polje subsystem during flood conditions. Zibret and Simunic (1976) demonstrated a method of estimating the swallow-hole drainage capacity (Q_o) based on the assumption that outflow depended on the preceding precipitations, the water level within the polje and the month of the year. The model developed consisted of a multiple linear regression equation of the form:

$$Qo = A_o + A_1 H + A_2 M + A_3 I_{pp} \qquad \textit{Equation 2.17}$$

Where $\boldsymbol{H}$ is the water level in the polje, $\boldsymbol{M}$ represents the month of the year and $\boldsymbol{I_{pp}}$ is an index of previous precipitation. Zibret and Simunic (1976) also highlighted the approximations necessary in approaching water budget calculations of enclosed karst plains given the problems of solving an equation (in this case the water budget) with two unknowns (inflow and outflow).

A study of the Zafarraya polje in southern Spain (Lopez-Chicano et al., 2002) determined the drainage capacity of the polje using a stage-volume relationship for the polje basin and recorded inflows from a number of riverine and ephemeral inputs. The infiltration capacity of the polje was found to decrease parallel to the decrease in flooded surface area, as the number of swallow holes actively draining water decreased while at the same time the permeable area of limestone and dolostones in the karst aquifer also decreased (Lopez-Chicano et al., 2002). The extent of flooding was exacerbated by the high water table within the karst as a result of two years of relatively heavy rainfall, with the intersection of the karst aquifer water table with the height of the main swallow holes in the polje causing sustained flooding. More recently, a similar study by Kovacic (2010) examined the water budget of the Cerknica polje based on the water fluctuations in the polje and rainfall and spring discharges recorded in the surrounding areas. This study provided values for the maximum inflow and outflow

rates during the 1975 hydrological year, and estimated the mean runoff capacity of the ponors at the bottom of the polje at $8m^3/s$. While there are large differences in scale between turloughs and the studied poljes (Cerknica Polje, for example, has a floor area of $70km^2$ and a catchment of $470km^2$), the comparable nature of polje flooding suggests the water budget method may have similarly successful applications to turlough hydrology.

CHAPTER 3. IRISH KARST, TURLOUGH GEOMORPHOLOGY AND HYDROLOGY

3.1. Irish Karst

3.1.1. Limestone Geology of Ireland

Carboniferous limestones are the most common rock type in Ireland underlying over 30,000 km^2, or almost half the land surface of the Republic of Ireland, making it the primary aquifer in the country (Figure 3.1) (Karst Working Group, 2000).



Figure 3.1: Distribution of Limestone in Ireland (Geological Survey of Ireland)

The main Irish Limestones were formed during the Lower Carboniferous or Dinantian age (Drew et al., 1996). A transgression (rising of sea levels) during the Tournaisian resulted in the flooding of sections of the Old Red Sandstone continent, including much of Ireland (Guion et al., 2000). As this Lower Carboniferous sea progressed northwards there was a change from a coastal to marine environment, with areas of the country lying under a shallow sea with local deeper water basins (Sevastopulo and Wyse Jackson, 2001). Shallow water sandstones and mudstones were deposited over the Old Red Sandstone, followed by muddy limestones and calcareous shales when waters became deeper and no longer disturbed by wave action (Pracht et al., 2004). The progression of the sea northwards led to the deposition of carbonate Waulsortian mudmounds over much of south and central Ireland. "Waulsortian" refers to a type of mudmound formed by the in situ production of carbonate mud by algal bacterial communities (Guion et al., 2000).

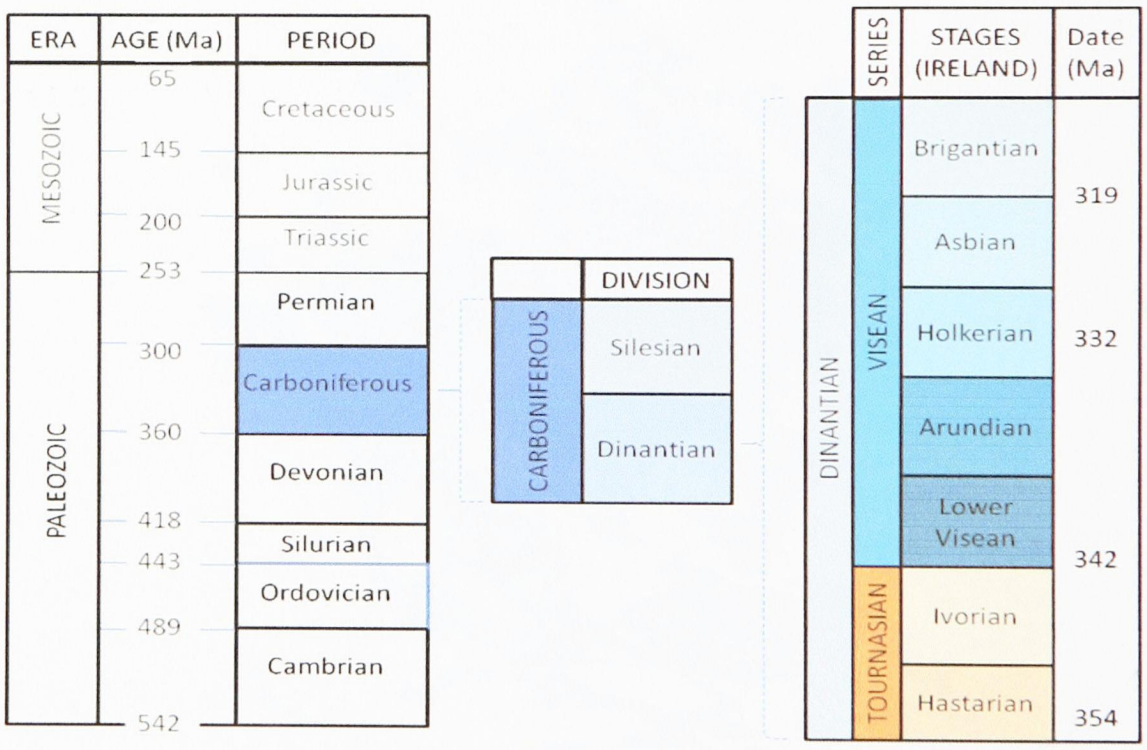


Figure 3.2: Geochronometric scale and chronostratigraphical divisions

3.1.2. Irish Karstification

As described in Chapter 1, karst may be defined as "*terrain with distinctive hydrology and landforms that arise from a combination of high rock solubility and well developed secondary porosity*" (Ford and Williams, 2007). Many carbonate based rocks such as limestone, marble and gypsum are susceptible to dissolution; in the Irish context it is the Carboniferous Limestone which has undergone significant karstification. As a

result, karst landforms and karst drainage form an important part of the Irish landscape. Characteristic Irish karst features include dolines, bare rock exposures, turloughs, sinking and intermittent streams, dry valleys, springs and caves (Drew and Daly, 1993). Karst features have been documented in 80 – 85% of limestone outcrops implying that most if not all Carboniferous limestones have some degree of karstification (Drew et al., 1996).

The Irish Carboniferous Limestone has undergone karstification many times since the beginning of the Dinantian, with the most significant period being that of the Tertiary (65 to 2 Ma) (Drew, 1990; Williams, 1970). In addition to Tertiary karstification, more recent dissolution processes have occurred during the Holocene (10 ka to present). This resulted in the development of a weathered zone of limestone near the bedrock surface known as epikarst, as well as active karst features such as stream caves in the Burren (Drew, 2008; Drew and Jones, 2000; White, 1988). Table 3.1 shows different periods of karstification and the location of some associated karst features. The periods of karstification associated with turlough formation are dealt with separately in section 3.2.1.

<table>
<tr><th>ERA</th><th>PERIOD</th><th>EPOCH</th><th>SOUTH-EAST
(after Keeley 1996)</th><th>AGE OF DEPOSIT
* = marine</th><th>MIDLANDS
(after Naylor 1992)</th><th>ULSTER
BASIN</th></tr>
<tr><td rowspan="7">CENOZOIC</td><td rowspan="2">Quat-
ernary</td><td>Holocene</td><td>karstification</td><td>west Burren caves</td><td>karstification</td><td>karstification</td></tr>
<tr><td>Pleistocene</td><td>cold climate</td><td>cave bones dated >45ka
cave calcite dated >350ka</td><td>cold climate</td><td>cold climate</td></tr>
<tr><td rowspan="5">Tertiary
Neo-
gene
Palæo
-gene</td><td>Pliocene</td><td rowspan="4">erosion >0.5km uplift</td><td>Galmoy, Pollnahalia</td><td>erosion</td><td rowspan="4">L. Neagh clays &
lignites
igneous activity &
interbasaltic soils</td></tr>
<tr><td>Miocene</td><td>Cormackstown, Hollymount,
Lisheen, Tynagh</td><td>/ karstification</td></tr>
<tr><td>Oligocene</td><td>Aughinish Loughshinny
Ballygiblin Ballymacadam</td><td>/ mantling</td></tr>
<tr><td>Eocene</td><td></td><td></td></tr>
<tr><td>Palæocene</td><td>erosion >1km uplift</td><td>Garron Point</td><td>erosion / karstification</td><td>erosion /
karstification</td></tr>
<tr><td rowspan="4">MESOZOIC</td><td rowspan="2">Creta-
ceous</td><td>Upper</td><td>sedimentation >0.5km</td><td>Ballydeenlea *</td><td>sedimentation variable
around islands/ in valleys?</td><td>sedimentation <3km</td></tr>
<tr><td>Lower</td><td rowspan="2">sedimentation <0.5km</td><td rowspan="2">Piltown (*)</td><td>erosion</td><td></td></tr>
<tr><td rowspan="2">Jurassic</td><td rowspan="2"></td><td>erosion</td><td></td></tr>
<tr><td>erosion/ karstification
>1.5km uplift</td><td>Cloyne</td><td>sedimentation
around islands?</td><td>sedimentation
>0.25km</td></tr>
<tr><td rowspan="3">PALAEOZOIC
Upper pars</td><td>Triassic</td><td></td><td rowspan="2">sedimentation >1km</td><td rowspan="2"></td><td>Topography Established
erosion</td><td>sedimentation <3km</td></tr>
<tr><td rowspan="2">Permian</td><td>Upper</td><td></td><td></td></tr>
<tr><td>Lower</td><td>erosion >2km uplift</td><td></td><td></td><td></td></tr>
<tr><td rowspan="2">Carbon-
iferous</td><td>Silesian</td><td>sedimentation ~2km</td><td></td><td>sedimentation</td><td></td></tr>
<tr><td>Dinantian</td><td colspan="4">erosion will include the karstification of limestones</td></tr>
</table>

Shaded areas indicate probable karstification

Table 3.1: Post-carboniferous karst history of Ireland (Drew and Jones, 2000)

The degree of karstification is not spatially homogeneous but varies depending on the relative purity of the limestone. In some areas, such as the Gort lowlands, the presence of impurities within the limestone, in this case cherty (silica rich) beds, controlled the degree and distribution of karstification (Johnston and Peach, 1999). The Gort lowland itself is the product of a combination of solution planation during the Tertiary period followed by scouring of the surface by glacial action during the Pleistocene (Ford and Williams, 2007). Karst features are sparse or absent across large areas of limestone in the Midlands and the east of the country, where the dominant landforms are those of glacial and fluvioglacial deposition (Coxon, 1986). These areas have developed normal surface drainage systems with little interaction with the underlying karst aquifer. This is thought to be due to the relative impurity of the limestone in this area rendering them less susceptible to dissolution processes. The purer limestones are present predominantly to the west of the Shannon with the greatest density of surface karst features in counties Galway, Clare, Roscommon and Mayo. These areas display greater levels of karstification, as reflected in the large number of karst features recorded in the GSI karst database (GSI, 2011).

The level and extent of karstification of Irish Limestone has proved difficult to map accurately due to the large subsoil cover in the central regions of the country (Drew et al., 1996). Glacial action during the Quaternary period covered much of the limestone of Ireland with Pleistocene and Holocene subsoil deposits (Drew and Daly, 1993; Mitchell and Ryan, 1998). Detritus deposited as till or boulder clay during the greatest extent of the last ice age (18 ka) has resulted in large tracts of the Irish landscape being covered in this glacial drift, meaning the karstification of these areas of limestone is relatively unknown (Drew, 2008). It has also led to the infilling and/or destruction of many surface karst features such as dolines, swallow holes and conduits that formed earlier. This infilling of subsurface depressions with glacial and fluvioglacial deposits may have rendered the karst features inoperative or hydrologically separate from the contemporary system. Such systems are referred to as palaeokarst structures/features. These Palaeokarst environments may still form significant parts of the Irish groundwater flow systems, as groundwater flows can erode the sediments in the infilled karst features thereby reactivating the conduits, resulting in the reintegration of palaeokarst into the active system. Drew and Daly (1993) suggest that the groundwater flow systems in the Gort lowland karst areas today may be a combination of newer,

shallow epikarst systems developed during the Holocene and older reactivated palaeokarstic systems.

3.1.3. Lowland Irish Karst

Over 90 percent of karst in Ireland is located in lowland areas of less than 150 mAOD (Drew, 2008). Upland karst is restricted to the plateaux in the Burren, Co. Clare and the north-west of the country. Lowland karst in Ireland exhibits relatively low hydraulic gradients, estimated at 0.01 – 0.001, with groundwater flow velocities of between 5 and 250 m/h recorded. The hydraulic gradients in the plateau karst are typically an order of magnitude higher (Drew, 2008). These higher plateau gradients, however, do not produce correspondingly higher flow velocities and have been measured at between 20-300 m/h (Drew, 2008).

Lowland karst areas are characterised by a high level of interaction between ground and surface waters. Subterranean karst flow systems coexist with surface drainage leading to complex hydrological interactions (Coxon and Drew, 1998). Water is lost to and gained from groundwater sources via swallow holes, estavelles and springs depending on the prevailing hydrological conditions. An example of such an interaction is shown in Figure 3.3. During dry periods the entire flow of the Owenshree River, Co. Galway, sinks into the riverbed and passes beneath the nearby Blackrock turlough, while at higher flows the river feeds directly into the turlough. Such complex and extensive interactions between surface and groundwater can make it extremely difficult to delineate the boundaries of contributing areas or accurately quantify recharge for karst groundwater bodies (Drew, 2008). Contributing areas can vary greatly in areal extent depending upon prevailing hydrological conditions. Coupled with this, the heterogeneous nature of karst flow paths mean that aquifer vulnerability can vary substantially within a contributing area making it difficult to assign viable protection areas to springs and water supplies (Deakin, 2000).



Figure 3.3: Owenshree River sinking into riverbed during low flow conditions

3.2. Turloughs

3.2.1. Turlough Definition

Turloughs are one of the characteristic features of the Irish karst landscape. They are transient lakes resulting from a combination of high rainfall and accordingly high groundwater levels in topographic depressions in the karst. A turlough is effectively a hydrogeological feature defined as "A topographic depression in karst which is intermittently inundated on an annual basis, mainly from groundwater, and which has a substrate and/or ecological communities characteristic of wetlands" (p9, Tynan et al., 2007).

Hydrologically, turloughs have been compared to poljes, as both are periodically flooded karst basins with interior drainage and lacustrine sediment deposition. Geomorphologically, however, the two karst features differ greatly (Coxon, 1986). Turloughs are of smaller dimension and possess gentler side slopes, while poljes have a clearer topographic boundary with the side slopes rising steeply. Also, unlike turloughs, tectonic movement played a role in polje location and formation.

The origin of turloughs has not yet been firmly established (Coxon et al., 2005). Turloughs were originally considered hollows in glacial drift with underlying karst drainage systems (Williams, 1964). However, Drew (1976) asserted that turloughs invariably lie in bedrock hollows and were solutional features requiring a far longer period to develop than has passed since the last glaciation. Given that sufficient time

has not passed since the last glaciation for a well-developed network of karst depressions to develop, this places the likely origin of turloughs in pre-glacial time (Coxon et al., 2005). This was supported by Coxon (1986), who found in a study of 90 turloughs that in most cases, where it was possible to determine, bedrock hollows appeared to be present with bedrock close to or at the surface. Coxon (1986) suggested that while glacial deposition may have an influence on the shape and area of turloughs, solutional rather than glacial processes may be the determining factor in turlough formation. Evidence from the Pollnahallia townland, Co. Galway, further supported the idea of a pre-glacial influence on turlough origin, where dating of organic sediments in both deep and shallow depressions to the late Pliocene implied a limestone land surface of Pliocene or pre-Pliocene age (Coxon et al., 2005). The lines of high permeability associated with turloughs may thus represent the re-use of remnants of karst drainage systems created during Tertiary dissolution but partially blocked by glacial drift, rather than post-glacial dissolution pathways.

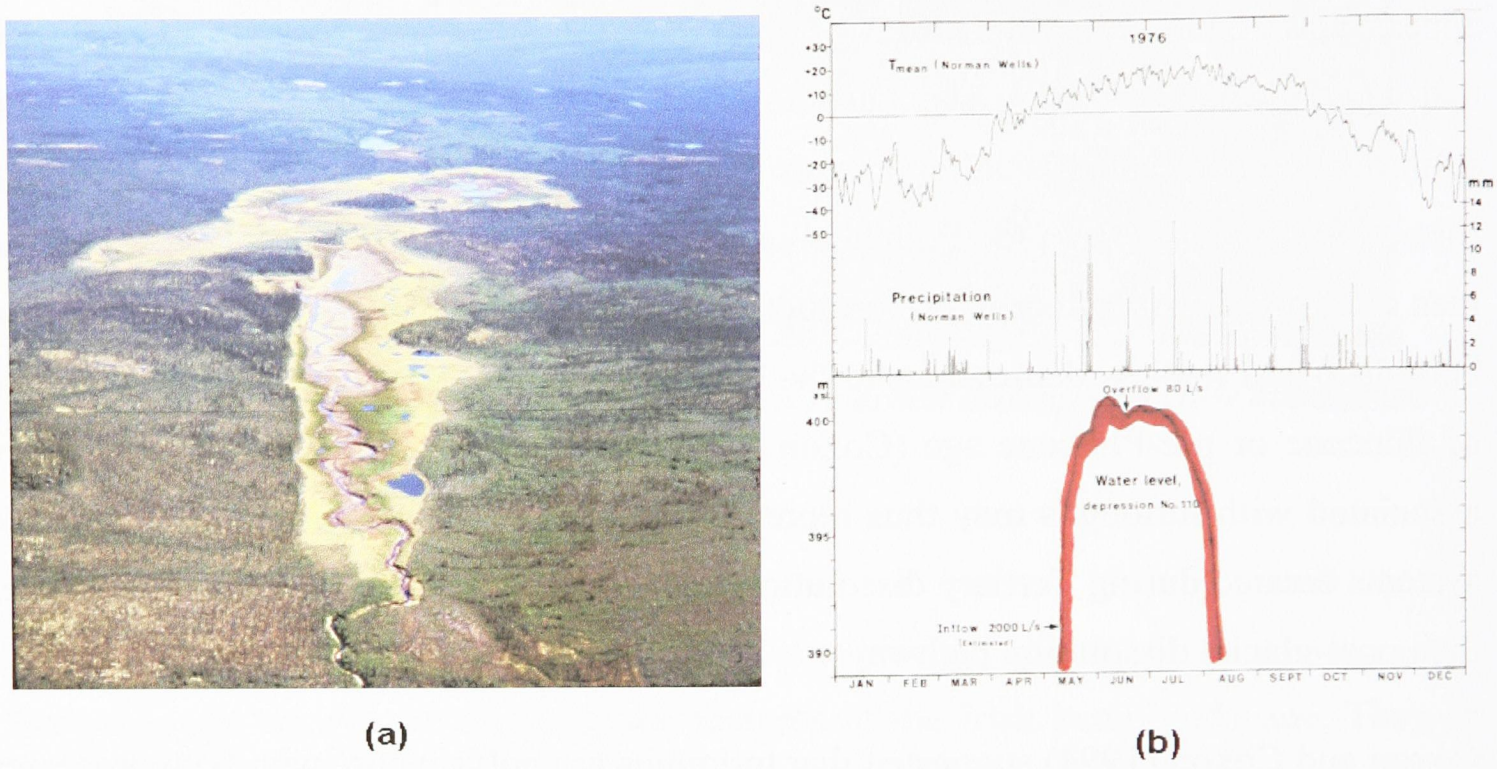
Coxon and Coxon (1994) suggested that turloughs are polygenetic, with both processes playing a part in their formation, with the orientation of the turlough basins themselves a result of the glacial processes in the area. Recognizing the polygenetic origins of turloughs, Coxon (1986) suggested three models to explain the origin of turloughs and the presence of high permeability zones required for turlough formation. The model proposes that turloughs are:

- Glacial hollows with flow paths developed post-glacially
- Glacial hollows which developed along the line of existing pre-glacial flow routes
- Pre-glacial karst features with associated flow paths which have been modified by glaciation

3.2.2. Turlough Distribution

Turloughs are often referred to as a uniquely Irish karst feature due to the combination high rainfall and low lying karst topography. However, examples of similar karst features have been reported in Wales, Slovenia, Spain and Canada (Blackstock et al., 1993; Goodwillie and Reynolds, 2003; Hardwick and Gunn, 1995; Sheehy Skeffington and Scott, 2008). The seasonal behaviour of turloughs reported in the North-western

Territories of Canada is quite different to their Irish counterparts, as flooding occurs during spring and summer due to the spring thaw rather than the excess winter precipitation (Figure 3.4) (Van Everdingen, 1981).



(a) (b)

Figure 3.4: (a) Aerial photograph of turlough #142, Mahony Dome, North-western Territories, Canada (D. Ford, pers. comm.) (b) Daily mean temperatures and daily precipitation at Norman Wells Airport for 1976 and water level in the south-eastern portion of depression No. 110 (Van Everdingen, 1981)

To date there are over 300 recorded turloughs within the GSI karst database, although not all have been verified as such (Sheehy Skeffington et al., 2006). The sites are distributed across over 12 counties with the highest concentrations occurring in counties Galway, Clare, Mayo and Roscommon (Figure 3.5) (Fossitt, 2000). Turloughmore, the largest recorded turlough, was some 400ha in area and lay in the Clare River catchment, Co. Galway, before being drained in 1847 (D'Arcy, 1983). Nowadays the largest single turlough is in Rahasane, Co. Galway measuring approximately 260 ha at maximum inundation (Sheehy Skeffington et al., 2006). During extreme rainfall events, water levels can rise above normal turlough boundaries and connect bordering turloughs to form open water bodies with areas far in excess of 260 ha. The most comprehensive survey of turloughs was carried out by Coxon (1986) who explored the distribution of turloughs based on geology, topography and drift

cover. Ninety sites of area greater than 10 ha were identified using mainly the 1:10560 Ordnance Survey maps of areas underlain by Carboniferous limestone.

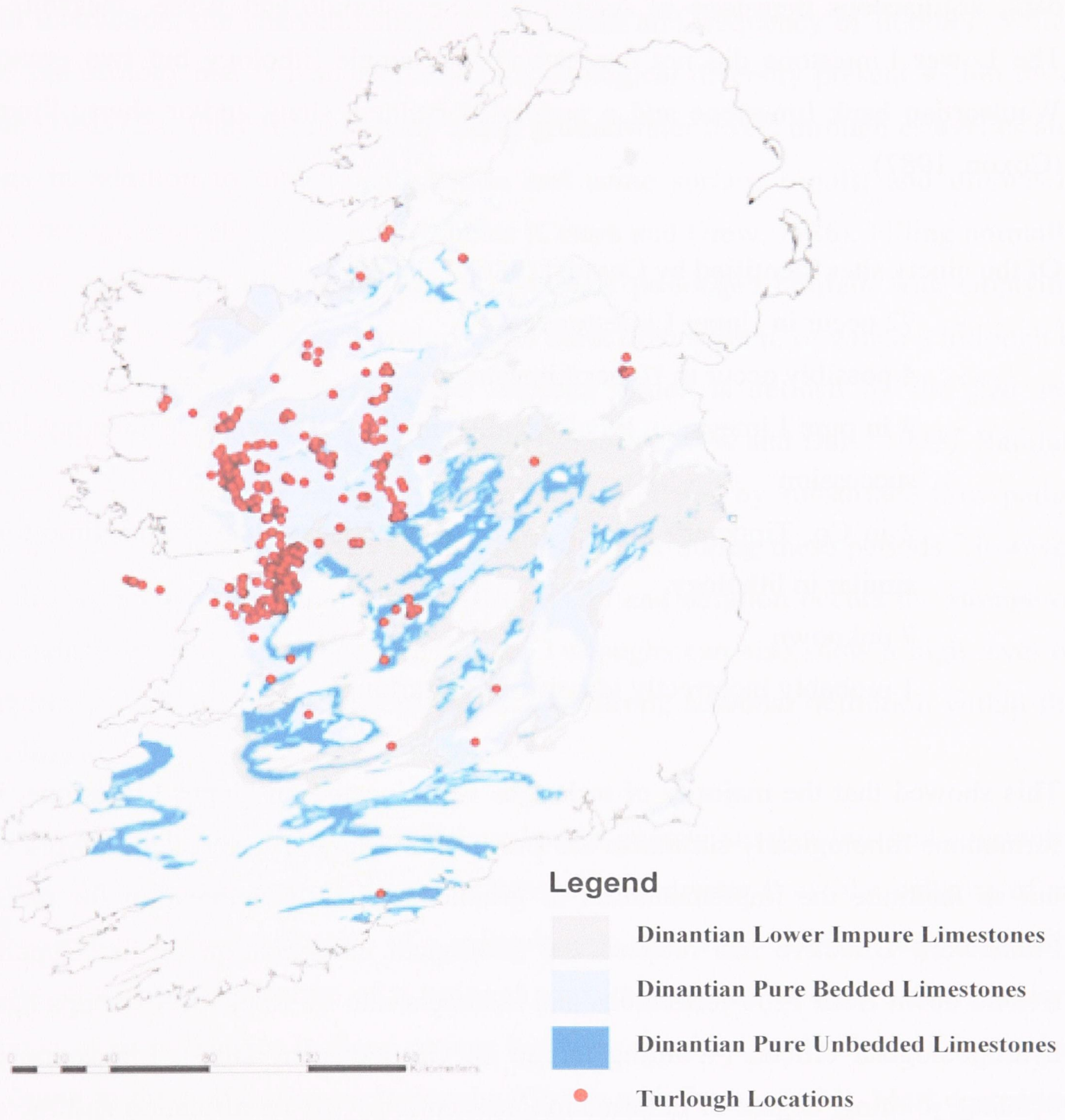


Figure 3.5: Distribution of turloughs in relation to limestone bedrock type (Sheehy Skeffington et al., 2006)

At the time of Coxon's study there was no consistent bedrock mapping available for the limestone areas west of the Shannon. Geological mapping carried out by the Geological Survey between 1856 and 1890 divided the Carboniferous Limestone into Lower, Middle and Upper Limestone (Coxon, 1987). While stratigraphically this division did not hold true on a regional scale, the three divisions retained their lithological characteristics and formed the basis for Coxon's analysis of turlough spatial

distribution. The Upper Limestone corresponded to limestones lithologically similar to the Burren limestone, while the Middle Limestone corresponded to Calp Limestone, a dark, argillaceous limestone of Asbian age (Sevastopulo and Wyse Jackson, 2001). The Lower Limestone did not correspond to a single lithology but two groups, the Waulsortian bank limestone and a variety of bedded, shaly and/or cherty limestones (Coxon, 1987).

Of the ninety sites identified by Coxon (1986):

- 72 occur in Upper Limestone
- 4 possibly occur in Upper Limestone
- 4 in pure Limestone, lithologically similar to Burren limestone but lower in succession
- 2 in Co. Tipperary in rock lower in the Visean than Burren limestone but similar in lithology
- 7 unknown
- 1 probably incorrectly identified as a turlough

This showed that the majority of turloughs were located on Upper Limestone, i.e. on formations lithologically similar to the Burren Limestone. More recently, work carried out to facilitate the implementation of groundwater body delineation for the Water Framework Directive has reduced the geological classification of the Republic of Ireland down from 1200 formations and members into 27 Rock Unit Groups based on hydrogeological criteria (Working Group on Groundwater, 2005). Limestone purity, bedding, jointing, degree of deformation, susceptibility to karstification and the effects these had on groundwater flow properties were all considered during the Rock Unit Group definition. When the distribution of Coxon's original sites was cross referenced with the new Rock Groups all 90 were found to lie on Rock Unit Group 11, Dinantian pure bedded limestone (Figure 3.5) (Tynan et al., 2007). The presence of turloughs on this Rock Unit Group is thought to be due to its greater purity, rendering it more soluble and so susceptible to a high degree of karstification. Its well bedded and well jointed nature is also considered important as this provides the initial pathways along which bedrock dissolution can occur and groundwater flow paths develop. This new classification validates Coxon's assumption that turloughs occur on lithologically similar bedrock with comparable bedding characteristics (Tynan et al., 2007).

3.2.3. Turlough Hydrology

Turloughs are at the interface between groundwater and surface water. It is the nature of this interaction, the characteristic depth, duration and frequency of flooding, which drives the ecology and is responsible for the ecological diversity present within these unique GWDTEs. They fill mainly by rising groundwater levels through estavelles and springs in addition to direct precipitation and some surface runoff; and ultimately empty through estavelles and swallow holes (Coxon and Drew, 1986). Filling normally occurs in late autumn due to periods of intense or prolonged rainfall, with emptying typically occurring from March onwards. The karst flow system, of which a turlough is a surface expression, possesses a flow capacity which is defined by the size and connectivity of the flow paths present within the rock (Drew and Daly, 1993). Rainfall of insufficient duration or intensity can be accommodated by subsurface flow paths; hence no surface flooding occurs in the turlough basin during these periods. However once the required combination of rainfall intensity and duration occurs the storage of the system is exceeded and flooding begins. Turloughs can also show a high level of variability from year to year due to the lack of strong seasonal definition within the Irish climate.

The karst hydrological systems in which turloughs operate are dynamic and constantly changing. Due to the localised nature of karstic groundwater flow, the collapse of an active conduit or the reactivation of a palaeokarstic system can rapidly and drastically alter the characteristic regime of a turlough and its response to excess precipitation. Evidence of such changes in flood regime has been provided in the form of lacustrine marl found in the basin of many turloughs (Coxon and Coxon, 1994). Marl deposition implies a permanent water body, whereas the present day hydrological regime of such turloughs does not facilitate the deposition of lacustrine marl. This implies that a fundamental shift has occurred in their hydrological operation from a permanent to ephemeral lake. Possible reasons for such a shift include the natural enlargement of drainage paths due to dissolution, or the reactivation of a previously sediment-filled conduit flow paths.

Turloughs in Ireland have been the continuing focus of research interest mainly due to the unique flora and fauna in this type of aquatic environment but, from a more anthropogenic point of view, due to the risks of localised flooding. The present day

drainage network in many of the karstic areas of western Ireland has been systematically modified by arterial drainage schemes designed to compensate for the lack of extensive surface drainage and reduce flooding in the area (Coxon and Drew, 1986). What has often been poorly understood is the key role turloughs play as flood attenuation devices in the regional hydrological regime. Turlough inundation has often been seen as part of the problem, rather than a beneficial natural flood attenuation system. Areas in which turloughs occur are characterised by little or no surface drainage, and so all effective rainfall in the area must be accommodated by subsurface karstic flow systems. These systems have finite flow capacities and turloughs are utilised to store the excess during periods of high and prolonged rainfall. When the system has drained sufficiently and head levels have dropped enough the temporary storage is fed back into the system.

Due to the localised nature of groundwater flow through karst aquifers they are particularly sensitive to activities which may interfere with these flow paths, such as artificial drainage, disturbance of estavelles and quarrying. While drainage activities may benefit stakeholders on a local scale by extending the availability of pasture land within turloughs, on a regional scale these activities could have a negative effect by intensifying flooding in more economically or socially important areas. The absence of natural channels to act as outlets to drainage schemes, drainage activities in upland areas tend to just prolong and exacerbate flooding down gradient.

The hydrology of turloughs has been identified as particularly under-researched with detailed studies of turlough hydrology and their mechanisms of flooding a rarity (Sheehy Skeffington et al., 2006). To date, the description of turlough hydrology has been mainly qualitative and consistent long term hydrological records are either sparse or absent, with previous investigations tending to comprise of a small number of measurements taken in isolation. As discussed previously, the first general study of the hydrology and geomorphology of turloughs was carried out by Coxon (1986). This study investigated the distribution of turloughs based on geology, topography and drift cover. 90 sites of area greater than 10 ha were identified. Of these, 30 had previously been drained by artificial drainage works completed between the mid 19th and mid 20th century carried out to reduce the extent of flooding during the winter period and provide more arable land for agriculture (Coxon and Drew, 1986). The general

geomorphologic and hydrological characteristics were also qualitatively documented using descriptors such as depth, area, shape factor, deposits and duration. Many of the results from this study detailing turlough formation, distribution and morphology have already been mentioned in previous sections and so will not be reiterated here.

In the context of turlough hydrology, the hydrological variables generated by Coxon were derived indirectly, rather than through continuous water level measurement. Flood depth and duration was inferred from the extent of the moss *Cinclidotus fontinaloides*, while turlough areal extent was taken from Ordnance Survey maps. In order to be classified as a turlough, a site had to satisfy the following (Coxon, 1987b):

- The area must flood seasonally to a minimum depth of 0.5 m, meaning that it must consist of open water for part of the year, and must be dry (except for any small residual pools) for part of the year
- the turlough must show evidence of emptying to groundwater, generally meaning that there must be no surface water outlet

Coxon also identified the prevalence and importance of swallow holes, estavelles and temporary springs in the operation of turloughs as hydrological entities. Of the 90 sites surveyed, 80 were found to contain swallow holes and/or estavelles which were generally located around the edge of the basin where bedrock is at or close to the surface. Also tracer and borehole monitoring studies carried out in the area around Kilmaine, Co. Mayo identified the link between a changing water table and turlough water level.

The most extensive investigation of turlough hydrology where quantitative data on turlough flooding were collected was carried out in the Gort lowland region in the years following 1995 by a consortium led by Southern Water Global (Southern Water Global, 1998). This report was commissioned after a series of major flood events between 1990 and 1995 which caused extensive disruption and damage to property and infrastructure in the area around Gort. The primary aim of the Gort Flood Study was to produce a hydrological model of the area which could be used to determine the potential effectiveness of flood alleviation works. The Gort Flood Studyutilised multiple investigation techniques including drilling, tracer studies, geophysics, water table mapping, as well as geological and topographic modelling. The water levels in a

number of turloughs in the area were monitored continuously to provide the first detailed turlough hydrological records. Borehole water levels were monitored to establish regional flow gradients and tracer studies established flow routes and groundwater velocities in the area, with flow velocities ranging from 60-1000 m/h and flow rates up to 15 m^3/s recorded in the Coole area. From this data catchment areas and groundwater divides were established.

The study identified three types of groundwater flow in the Gort Ardrahan area, dividing the flow regimes into epikarstic flow systems, deep karst flow systems and distributed groundwater flow systems. Epikarstic systems are characterised by fluted clint and grike structures, solution opened fissures and joints in the upper 2 to 5 m of limestone as well as major conduits supporting very large flows in the upper 10 to 15 m of limestone (Peach et al., 1997). These systems were considered to have developed relatively recently and are likely be post glacial. The deep karst flow systems consisted of major conduits, often several metres in diameter, and fracture/ conduit systems with a range of flow capacities. These were much older systems that had developed in response to different hydrogeological conditions. The third type identified were distributed groundwater flow systems, composed the older, slow responding, relatively impermeable carboniferous limestone and superficial deposits such as sandy till.

The heterogeneous nature of groundwater flow described above meant that traditional porous media models were unsuitable for representing flow in the fractured karst aquifer. Instead a pipe-flow network model of the area was created by Southern Water Global using *Hydroworks*© (a sewer network model), where fracture and conduit systems were modelled as single conduit pipes connecting nodal storages representing turloughs. While the model itself was site specific and not applicable as a generic turlough hydrological model, it did show it was possible that turloughs act as storage tanks within the karst system and that fracture and conduit flow systems in this area may be conceptually represented using single conduits.

A more recent attempt to model turloughs using the pipe network and tank approach was completed by Gill (2010). A model of five turloughs in the Gort lowlands area (Blackrock, Lough Coy, Coole, Garryland and Caherglassaun) was developed using the InfoWorks software package. As with the Gort Flood Study model, the karst conduit flow system was represented by a pipe network while turloughs were represented as

storage tanks with depth-volume characteristics derived from detailed topographic surveys. River flows from the Slieve Aughty Mountains and precipitation were used as inputs for the system. This model provided a good simulation for all the turloughs, further supporting that the system operates on the basis of a significant conduit system with surcharged tanks.

Given the lack of quantitative hydrological data characterising turlough flooding, and the local emphasis on turloughs in the Gort area of both the study by Gill (2010) and the Gort Flood Study (1998), there is still a clear gap in knowledge in relation to general turlough hydrodynamic behaviour. The research described in this thesis address this lack of knowledge.

CHAPTER 4. TURLOUGH ECOLOGY AND CONSERVATION

4.1. Introduction

The behaviour of a turlough as a wetland is fundamentally driven by its hydrology, with the hydrological regime resulting in a characteristic ecology associated with the pattern of groundwater inundation. As such, turloughs provide a habitat for many floral and faunal species of national and international importance, including species listed in the Irish Red Data Book such as Mudwort (*Limosella aquatica*), Fen Violet (*Viola persicifolia*) and Northern Yellow-cress (*Rorippa islandica*) (Regan et al., 2007). In this chapter an outline of the characteristic ecological communities and habitat structures present within turloughs is given, together with the role hydrology plays in determining their composition. The main pressures are outlined, and hydrological indicators required to elucidate hydro-ecological relationships and determine the effect changes in pressures will have on the turlough habitat are described.

4.2. Flora

4.2.1. Vegetation Types

Many factors influence the pattern and diversity of turlough plant communities. These include subsoil type, grazing regime, nutrient quality in water and substrates, and the presence or absence of non-vegetated areas (MacGowran, 1985). The depth, duration and frequency of inundation strongly influences the vegetation communities present within turloughs with flood duration primarily controlling plant species survival (Casanova and Brock, 2000; Sheehy Skeffington et al., 2006). Flooding disrupts the ecosystem by changing the physical environment and resources available to species, such as oxygen and light, and so is a type of disturbance (O'Rourke, 2009; White and Pickett, 1985). Adaptation to the periodic inundations and associated oxygen starvation is necessary for plant survival. Species are partitioned into two groups; those that can survive the flooding in situ and those that colonise quickly following flood recession, namely ruderal species and other annuals. As a result there is lower species diversity present within turloughs when compared to marshes or limestone grassland, with the composition of vegetation communities constantly changing as species adapt to the variable hydrological conditions from year to year (Goodwillie, 2003).

The variability and unpredictability of flooding within turlough basins has led to the development of specialised plant communities adapted to the frequent interruption of gaseous exchange (Tynan et al., 2007). These adaptations take many forms and are demonstrated by annual, biennial and perennial species. Annuals utilise avoidance as dormant rhizomes or stolons (silverweed *Potentilla anserina*) or as seed, with germination delayed until suitable conditions occur (*Persicaria* spp) (Tynan et al., 2007). Following flood recession, annuals can grow quickly to colonise recently exposed areas. The surface rhizomes, stolons or buds allow the species to avoid the worst effects of anaerobic conditions within the soil and survive even when the roots have died off (Goodwillie, 2003). Figure 4.1(a) and (b) shows the characteristic absence of vegetation in Blackrock turlough, Co. Galway directly following flood recession. Figure 4.1 c) shows the Silverweed (*Potentilla anserina*) just sprouting from flood tolerant rhizomes lying dormant beneath the soil.

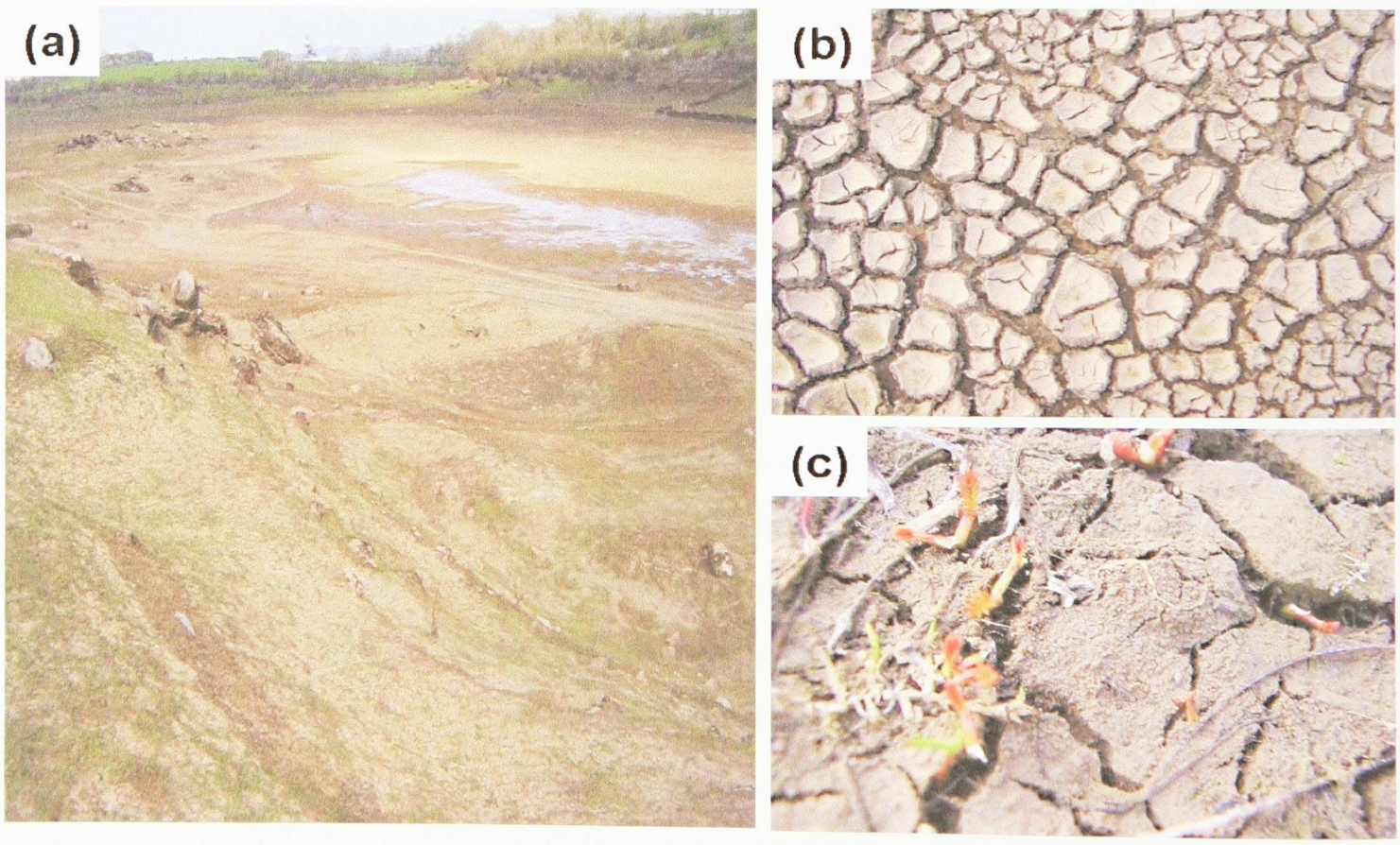


Figure 4.1: (a) Blackrock turlough following flood recession (b) Lack of vegetation on soil after flood recession (c) Sprouting of Silverweed (Potentilla anserina) from dormant rhizomes beneath the soil surface (photographs (b) and (c) courtesy of Nova Sharkey)

Perennials may develop a full physiological tolerance of submergence and alternate from aerobic to anaerobic respiration during inundation, for example the buttercup *Ranunculus repens* (Lynn and Waldren, 2001; Lynn and Waldren, 2003). *Ranunculus repens* has even been known to develop elongated stems up to four metres in length to the water surface during periods of inundation (Goodwillie, 2003; Sheehy Skeffington et al., 2006). Some aquatic species such as the reed *Phragmites australis* maintain a direct connection to the water surface during winter allowing oxygen to reach the roots through the dead stems of the plant.

4.2.2. Vegetation Distribution

The most extensive survey of turlough vegetation was carried out by Goodwillie (1992). 61 turloughs were examined and from the plant species recorded 24 principal plant communities were described (Goodwillie, 2003; Sheehy Skeffington and Gormally, 2007). The 24 can be classified into two major phytosociological classes: the *Scheuzerio-Caricetea fuscae* and the *Plantaginetea majori*. *Scheuzerio-Caricetea fuscae* is characterised by sedge-dominated communities associated with higher soil moisture and peat formation, while *Plantaginetea majoris* generally consists of grasses connected with more mineral soils (Sheehy Skeffington and Gormally, 2007). The dominance of these groups can vary along a contour within the same turlough where different land use and grazing regimes are present, implying that some vegetation differences are due to the local land-use practises (Ni Bhriain et al., 2002). Turloughs have long been valued as summer grazing sites resulting in the removal of larger species, thus eliminating the control on smaller species allowing them to flourish. Consequently, adjacent fields with identical hydrological regimes but with differing land management practises and grazing regimes can exhibit contrasting vegetation communities.

Some species are present throughout the turlough basin, such as the buttercup *Ranunculus repens*, silverweed *Potentilla anserina* and the sedge *Carex panacea* (Goodwillie, 2003). The characteristic black moss *Cinclidotus fontinaloides* is prevalent on surfaces within the range of flooding, leading Coxon (1986) to use the distribution of *Cinclidotus* as the indicator of flooding extent in the study of 60 undrained turloughs. In more aquatic parts of the basin *Cinclidotus* is out-competed by the vigorous

Fontinalis antipyretica moss and so the relative distributions of these species give an insight into a turlough's hydrological regime. The presence of *Fontinalis* indicates semi-permanent water while *Cinclidotus* in the base of a turlough implies shorter flood duration conditions (Allott, 1976).

Turlough vegetation displays a regular zonation with the relative abundance of species varying along the flooding gradient according to their survival abilities. Praeger (1932) was the first to document this zonation pattern from dry species at the outer edge of the turlough to wetland and aquatic species deeper in the basins. The fringes of the flooding area generally consist of either dry ash / hazel woodland, limestone heath, grassland or bogs (Goodwillie, 1992). Typical woodland and shrubby species include Hazel (*Corylus avellana*), Ash (*Fraxinus excelsior*), Holly (*Ilex aquifolium*), Blackthorn (*Prunus spinosa*), Buckthorn (*Rhamnus catharticus*), Alder buckthorn (*Frangula alnus*) and Shrubby Cinquefoil (*Potentilla fruticosa*), the latter two being listed Irish Red Data Book species (Goodwillie, 1992). Limestone heaths and dry calcareous grasslands, such as those found in the Burren, possess a rich flora with species such as Bloody Cranesbill (*Geranium sanguineum,* Figure 4.2*(a)*), Wild Thyme (*Thymus praecox*) and Juniper (*Juniperus communis*) common as well as orchids such as the Lesser Butterfly Orchid (*Platanthera bifolia*) and Dense-flowered Orchid (*Neotinea maculata*). Trees and shrubs are absent from the main basin due to the controlling factors of grazing and duration of flooding (Goodwillie, 1992; 2003). Exceptionally high flood levels can cause total leaf fall or even death of bordering flood intolerant species such as Holly, Buckthorn and Blackthorn, resulting in the highest flood level visible as a dark contour in the vegetation.



Figure 4.2: (a) Geranium sanguineum, Ballinderreen turlough, August 2007 and Ranunculus repens, Blackrock turlough, July 2007 (photographs courtesy of Nova Sharkey)

Further into the turlough basin bordering the woody and shrub species, large grasses such as the tall fescue (*Festuca arundinacea*) and tufted hair-grass (*Deschampsia caespitosa*) can be found in grazed, nutrient poor sites. In ungrazed sites tall herbs such as meadowsweet (*Filipendula ulmaria*) and the reed canary-grass (*Phalaris arundinaceae*) are often present (Goodwillie, 2003). Within the main basin there are two distinct vegetation groups; those associated with nutrient-rich sites and those with nutrient-poor sites. Nutrient-poor sites are characterised by sedge-dominated communities generally linked to higher soil moisture and low total P and N, such as the tawny (*Carex hostiana*) and carnation sedge (*Carex panacea*) (Visser et al., 2006). Plant communities associated with grazed, nutrient-poor sites with good drainage include heath-grass (*Danthonia decumbens*) and purple moor-grass (*Molinia caerulea*). Grass communities favour lower soil moisture conditions with deeper mineral deposits, with an increased nutrient availability (Visser et al., 2006). Relatively more nutrient-rich sites are dominated by the common sedge (*Carex nigra*), ribwort (*Plantago lanceolata*) and silverweed (*Potentilla anserina*) (Goodwillie, 2003).

In turloughs with longer flood duration, the grass- or sedge-dominated vegetation grades into wetland communities and fully aquatic species (Sheehy Skeffington et al., 2006). Turloughs with semi- or permanent water bodies support a range of fully aquatic species such as Amphibious Bistort (*Polygonum amphibium*), Water Mudwort (*Limosella aquatica*) and Rigid Hornwort (*Ceratophyllum demersum*) (Sheehy Skeffington et al., 2006). In areas that dry out irregularly few perennial plants can survive, with a small number of exceptions such as shoreweed (*Litorella uniflora*). Instead the mudflats are colonised by annuals such as mudwort (*Limosella aquatica*), cudweed (*Gnaphalium uliginosum*) and the bur marigold (*Bidens trifoliata*) (Goodwillie, 2003). Mudwort has been described as possibly the most specialised turlough plant species, requiring exposed mud that remains wet throughout the growing season (Goodwillie, 1992). The conditions at Caherglassaun turlough, Co. Galway, are particularly suitable for mudwort as the mud flat at the base of the turlough is kept wet during dry periods by periodic low level flood events caused by tidal fluctuations.

4.3. Fauna: Invertebrates

The variable hydrological conditions that lead to characteristic plant communities also result in largely specialised aquatic invertebrate communities, with flooding regime exerting significant influence over the composition and abundance of invertebrate species in turloughs (Porst, 2009; Williams, 2006). Most aquatic invertebrates found in turloughs are common in other habitats, but there are some rare species such as the periglacial crustaceans *Eurycercus glacialis* and *Diaptomas castor*, as well as the only recorded Irish example of the freshwater anostracan *Tanymastix stagnalis* (Duigan and Frey, 1987; Reynolds, 1997; Reynolds et al., 2004). The ephemeral nature of turlough flooding is likely to be responsible for the success of such species as the absence of permanent water commonly precludes larger predatory species such as fish.

The dominant taxa within turloughs consist of three insect groups: true bugs, beetles and midges, alongside microcrustaceans and mites (Williams, 2006). Typical species present include flatworms, gastropod molluscs, cladocerans, copepods, ostracods, mayfly nymphs and beetles (Sheehy Skeffington et al., 2006). Communities are dominated by detritivores and, where suitable low disturbance pressures occur, populations of herbivores and predatory species may appear (Porst and Irvine, 2009a; Reynolds, 2003). A list of typical turlough invertebrate species is given in Table 4.1:

Group	Taxon
Mollusca	*Lymnaea palustris, Lymnaea peregra, Bithynia tentaculata*
Insecta	*Cloeon simile, Agonum lugens, Agonum livens, Badister meridionalis, Blethnisa multipunctata, Pelophila borealis*
Crustacea	*Tanymastix stagnalis, Eurycercus glacialis, Diaptomus castor, Diaptomus cyaneus, Diaptomus gracilis, Gammarus duebeni*

Table 4.1: Typical turlough invertebrate species

The dry phase of an ephemeral wetland can be defined as an ecological disturbance for its aquatic fauna (Porst et al., 2009). Aquatic invertebrates present in turloughs are required to adapt to the effects of disturbance and have developed a number of survival and colonisation strategies (Jocque et al., 2007). These include the production of resting stages resistant to desiccation, migration of adult to permanent water bodies, or an amphibious lifestyle (Sheehy Skeffington et al., 2006). Some species such as snails and crustaceans use passive dispersion, where resting stages hatch when suitable flood conditions occur. Alternatively permanent aquatic environments like drainage ditches, swallow holes or even damp mud serve as a refuge for species during dry periods with rapid occupation of the littoral zone occurring following flooding. Active dispersion is characterised by rapid larval development and comprises most insects (Jocque et al., 2007; Porst, 2009).

As aquatic invertebrates must mature, reproduce and/or disperse before flood recession, the prevailing flooding regime is critical in determining community composition. Turloughs that display a multimodal flooding regime tend to have lower species diversity as invertebrate occurrence and diversity is dependent upon the availability of species at the time of flooding (Porst, 2009). If the required life stage does not coincide with the onset of flooding, for example an aerial adult insect, colonisation cannot occur (Reynolds, 2003). This unpredictability leads to substantial variation in communities between years and even within the flooding season. In contrast, sites with long flood duration and lower flood frequencies support higher species diversity as they offer a more stable aquatic habitat enabling continuous colonization of invertebrates (Porst, 2009).

The turlough habitat also provides a refuge for many rare and protected terrestrial invertebrate species. The terrestrial invertebrate fauna of turloughs includes several rare species of coleopterans such as the rare rove beetle *Philonthus furcifer*, and the ground beetles *Platynus livens*, *Badister meridionalis*, and *Badister peltatus* (Lott and Foster, 1990; Speight, 1977). A study carried out as part of the Gort Flood Study Report identified a total of 115 beetle species present in turloughs, while a parallel survey of lepidoptera (butterflies and moths) in the same area identified 240 species (Bond, 1997; Good, 1997; Southern Water Global, 1998).

4.4. Fauna: Vertebrates

4.4.1. Birds

Turloughs have long provided good sites for over-wintering wildfowl. The vegetation-covered basins offer abundant feeding grounds for a diversity of dabblers and grazers such as whooper swan, whimbrel, widgeon and teal, as well as diving duck such as tufted duck and pochard (Sheehy Skeffington et al., 2006). The two largest turlough complexes, Coole-Garryland and Rahasane, are of international importance for their populations of wildfowl and waders. Rahasane supports an internationally important population of black-tailed godwit as well as nationally important populations of widgeon, pintail, shoveler, golden plover and teal (Boland et al., 2008). Rahasane is also the only major inland over-wintering site in both Ireland and the United Kingdom for Dunlin (Sheppard, 1993). The Coole-Garryland complex once supported an internationally important population of whooper swans but, with a recent decline in numbers, the population is now of national importance (Boland et al., 2008; Madden and Heery, 1997).

The characteristic hydrological regimes and geomorphology of individual turloughs determine their suitability as feeding and breeding grounds for bird populations. Slow-responding turloughs with wide, shallow basins provide ideal feeding grounds for bird species as the low water levels result in plentiful marginal feeding areas (Madden and Heery, 1997). Birds frequently move between such sites to take advantage of local flood conditions, with birds favouring low to moderate flood levels (Madden and Heery, 1997). Where turloughs slowly recede or retain water throughout the summer and are not heavily grazed, populations of nesting waders such as Snipe, Lapwing, Redshank, and Dunlin are present (Madden and Heery, 1996). In contrast highly variable flooding or deep, steep-sided turloughs are less likely to support significant bird populations.

4.4.2. Mammals

Turloughs and the surrounding areas provide a habitat for many native Irish mammals including the Hare (*Lepus timidus hibernicus*) and Pine Marten (*Martes martes*), as well as the non-native Brown Rat (*Rattus norvegicus*) (Sheehy Skeffington et al.,

2006). Otters (*Lutra lutra*) have previously been found in turloughs such as the Coole – Garryland complex in Co. Galway but the most recent study in 2000 did not find any evidence for the presence of otters (Springer, 2002). Otters may only reside in turloughs during specific times of the year when favoured prey such as eels and frogs are present and easily caught (Sheehy Skeffington et al., 2006). Bat species such as the Natterer's Bat (*Myotis nattereri*) and Lesser Horseshoe Bat (*Rhinolophus hipposideros*) have been recorded roosting in the vicinity of a number of turlough sites, with the latter species classified as a priority species under Annex II of the Habitats Directive. Other species such as Leisler's bat (*Nyctalus leisleri*) and Daubenton's bat (*Myotis daubentoni*) may also use the turlough habitat for foraging (O'Mahony, 1998).

4.4.3. Fish and Amphibians

The presence of long-lived fish species is rare in turloughs due to their ephemeral nature. However, stickleback species *Gasterosteus aculeatus* and *Pungitius pungitius* have been recorded in turloughs unconnected to surface water sources, indicating that some turloughs act as long term refuges for such species or that migration is possible through the karst flow system (Williams et al., 2006). Pike (*Esox lucius*) and eels (*Anguilla anguilla*) have previously been documented in turloughs, with eels particularly abundant in turloughs within the Dunkellin catchment, Co. Galway (Reynolds, 1997; Sheehy Skeffington et al., 2006). Pike currently inhabit at least two turloughs in the Gort – Kinvarra chain of turloughs, namely Caherglassaun and Garryland, as witnessed during this study (Figure 4.3). Here small permanent water bodies located in estavelles are used as refuges for fish species during times of low water level.



Figure 4.3: Pike specimen found in an estavelle in Garryland turlough, Co. Galway

As a result of the widespread absence of predatory fish, amphibians are relatively common in turloughs. During spring there is extensive use of turloughs as spawning sites by frogs (*Rana temporaria*) (Marnell, 1999). The rarer smooth newts (*Triturus vulgaris*) also use turloughs as breeding sites with turlough habitat making up approximately 6% of national newt breeding sites (Marnell, 1998). Newts require water throughout the summer as newt tadpoles are confined to aquatic habitats until late July and August, and so only breed in turloughs with slow recessions or permanent water bodies (Sheehy Skeffington et al., 2006).

4.5. Water Chemistry and Nutrient Status

The nature of groundwater flow in karst and the close connection of turloughs with the karst groundwater bodies render them particularly susceptible to anthropogenic pressures (Coxon and Drew, 2000; Kilroy et al., 2001). High groundwater velocities, surface – groundwater interactions and point recharge such as sinking streams all enable nutrient transfer through the groundwater body. The typically high pH and alkalinity of turlough waters affects nutrient status, with the high alkalinity due to $CaCO_3$ from the dissolution of limestone reducing the availability of nutrients (Tynan et al., 2007). Highly calcareous waters can immobilise soluble phosphate and so reduce the availability of nutrients in a form usable to vegetation leading to oligotrophic or ultra-oligotrophic conditions (Southern Water Global, 1998). Other water attributes, such as colour and turbidity, can affect aspects of turlough ecology. A study by Pereira (2010) carried out as part of the NPWS "Assessing the conservation status of turloughs" project found a general linear relationship between phosphorus and algal biomass in 18 of the 22 sites studied, the exception being: Blackrock, Lough Coy, Garryland and Caherglassaun. These turloughs form part of the Gort – Kinvarra system which receives significant allogenic recharge in the form of highly coloured, peaty waters fed from the Slieve Aughty Mountains. The reason suggested for the relatively low algal biomass at these sites is that despite high phosphorus concentrations algal growth is limited due to light suppression caused by the highly peaty water (Pereira et al., 2009).

The nature of the hydrological connection between turlough and karst groundwater bodies and the hydrological operation of individual turloughs are influential in shaping turlough water chemistry. Flood depth, frequency, duration, and residence time define the period and conditions under which waterborne and subsoil nutrients interact. For example, turloughs showing a high frequency, short duration flooding regime may have a different nutrient signature than less hydrologically active turloughs due to lower residence times. Hydro-chemical parameters themselves can give an insight into turlough operation, such as the high alkalinity shown at the onset of flooding due to the ingress of waters which have had long exposure to the limestone and the associated higher concentrations of $CaCO_3$.

Waterborne nutrients in turloughs can be derived from two main sources: the catchment and the turlough basin itself. Land use within turlough catchments is predominantly agricultural which contributes nutrients to groundwater, which in turn can cause the eutrophication of associated groundwater dependent surface water bodies (Kilroy et al., 2001; Pereira et al., 2009). Agricultural practises within the turlough basin itself such as grazing and the application of fertilisers can lead to enrichment of turlough soils, with the possibility of nutrients being released into the water column following the onset of flooding.

The nutrient status of turloughs plays a key role in determining species composition, abundance and productivity, as well as being an important controlling factor on the turlough phytoplankton (Working Group on Groundwater, 2004). The trophic status of turloughs is dependent upon both water and substrate nutrient levels (Tynan et al., 2007). The interaction of these elements and the interchange of nutrients between soil and water are poorly understood, and which dominates turlough trophic status is unknown (Goodwillie and Reynolds, 2003). Previous studies have based turlough trophic status upon the Ellenberg N indicator values for vegetation species present within a turlough basin. Ellenberg indicator values are based upon the tolerance of plant species to certain environmental variables, such as degree of N enrichment, and so the occurrence of certain species indicates the available nutrient level. However, recent research has shown P to be the limiting nutrient which throws the effectiveness of Ellenberg indices into doubt as they are based on the level of N present (Kimberley, 2007a; Pereira et al., 2009). The same work has shown that the trophic status of turloughs can change depending upon the criteria used (Pereira et al., 2009). A classification based upon the maximum Chlorophyll a levels showed 6 sites as oligotrophic and 12 as mesotrophic, whereas the classification of the same sites based upon mean Total Phosphorus (TP) and mean Chlorophyll a had 4 sites as oligotrophic and 8 as mesotrophic.

4.6. Subsoil Type and Nutrient Status

The diversity of the turlough habitat is reflected in the high variability in type, thickness, distribution and origin of soils within and between turlough basins (MacGowran, 1985). Typical turlough soils consist of inorganic gleys, peaty gleys, peats and thick marl deposits (Kimberley, 2007a). As with turlough vegetation a zonation pattern has been identified in turlough soil type with different soils located in the upper, middle and lower zones of turloughs corresponding to increasing duration and frequency of flooding (Goodwillie, 1992; Kimberley, 2007a; MacGowran, 1985). A comprehensive study of turlough soils carried out by MacGowran (1985) found gleys and gleyed rendzinas to be the most common soil type. A gley is a soil type typical of wetlands which is caused by periodic inundation and the associated anaerobic conditions. Coxon (1987b) identified five main unconsolidated sediment types occurring within turlough basins (Table 4.2), and noted that an individual turlough basin can contain several of these types. It was further suggested that a link existed between deposit type and flood duration. Deposits of marl and peat seemed to be linked to longer duration flooding while silt/clay, sand/silt and diamicton sediments were associated with a shorter inundation periods. However, the results were unclear whether flooding regime was the cause or result of soil type.

Soil Type	Description
Marl	Calcium carbonate rich silt containing > 80% $CaCO_3$, white to light grey in colour
Peat	Organic material ranging from slightly humified, fibrous, reddish brown peat to very humified, dark brown or black peat. The most common type within turlough basins is the latter very humified fen-type peat
Silt/Clay	Sediments in the silt / clay (<0.06mm particle size) range of unknown origin, possibly containing high levels of $CaCO_3$
Sand/Silt	Sediments in the particle size range of 0.002 to 2mm, generally of unknown origins with highly variable characteristics
Diamicton	Unsorted deposits of clay and gravel of glacial origin

Table 4.2: Soil types present within turlough basins (Coxon, 1987b)

One characteristic feature of turlough soils is the presence of marl, a calcium-carbonate rich silt. Marl forms as a result of the precipitation of $CaCO_3$ from groundwater high in CO_2 and $CaCO_3$ concentrations resulting from the dissolution of carbonate limestone

rock. Upon exposure to the atmosphere excess CO_2 diffuses out leaving the water supersaturated in $CaCO_3$, which in turn causes precipitation (Coxon and Coxon, 1994). Following the recession of flood waters the layer of calcium carbonate crystals can be seen coating vegetation and rock surfaces (Figure 4.4). Often peat layers are found overlaying marl which raises the possibility of marl deposits acting as a drainage restriction, thus allowing permanent water to remain year round and provide suitable conditions for peat formation. Other variations of soil composition with depth signifying past changes in hydrological behaviour have been found in turloughs, such as the presence of lacustrine deposits indicating a previous permanent water body.



Figure 4.4: Deposition of calcium carbonate on vegetation and turlough basin following flood recession in Lough Coy, Co. Galway

Soil nutrient status of soils has been shown to vary significantly along flooding gradients within turlough basins as well as between turloughs (Kimberley, 2007b). This variation has led to the establishment of different vegetation communities depending upon nutrient availability and soil drainage properties. The highly calcareous nature of some turloughs may reduce the availability of phosphorous, a limiting nutrient in vegetation development, leading to nutrient deficient conditions and very different vegetation communities than are present in meso- and eutrophic turloughs (Kimberley, 2007b).

4.7. Turlough Conservation

Due to the intimate connection between turloughs and karst groundwater bodies, turloughs are classified as Groundwater Dependent Terrestrial Ecosystems (GWDTEs) under the Water Framework Directive (2000/60/EC) and as a Priority Habitat in Annex 1 of the EU Habitats Directive (92/43/EEC). Both EU directives necessitate the monitoring and management of these habitats to ensure favourable conservation and groundwater status is achieved. In particular, the Water Framework Directive requires a good understanding of the hydrological linkage between the turlough wetland, its ecological functioning and the connected groundwater body. Under the Water Framework Directive all water bodies must achieve "Good" status by the end of 2015. Central to the achievement of this goal is the definition of "damage". The notion of "damage" within a turlough is a complex one, and does not conform to the classifications of other surface water bodies. Turloughs display a great ecological diversity from the pristine oligotrophic environments of the Burren turloughs to nutrient rich eutrophic turloughs of the Gort – Kinvarra chain. Therefore it is overly simplistic to assume that eutrophic is damaged and oligotrophic is undamaged. Turlough ecologies as they exist today are at least partially a product of long term anthropogenic effects, such as agricultural practices within turlough basins.

The three principle threats to the conservation status of turloughs are drainage, land use practises and nutrient input.

4.7.1. Drainage

By modifying the hydrological regime, drainage permanently alters the structure of characteristic turlough communities. Extensive artificial drainage works were carried out in the 19th and parts of the 20th century to reduce the extent of flooding during the winter period and provide more arable land for agriculture. Through the creation of the Clare River, Co. Galway, a number of turloughs including the largest, Turloughmore, were permanently destroyed. Such works has had an irreversible impact on approximately a third of turloughs over 10 hectares, reducing the total flooded area by at least 50% (Coxon, 1986; Drew and Coxon, 1988). It has also resulted in the permanent drying of some turloughs, loss of recharge to the karst system, lowering of water tables, alteration of underground flow routes and periodic groundwater

contamination (Drew and Coxon, 1988; Kimberley, 2007a). The drainage of many turloughs was also found to have a detrimental effect on the quality of turlough basins as agricultural land, as the shallow soils were liable to poaching and fertilisers were required (D'Arcy, 1983; Kimberley, 2007a).

Recent groundwater flooding in November 2009 has renewed the calls for flood alleviation work to be carried out, posing a further risk to groundwater dependent turlough habitats. While further large scale drainage works are unlikely due to their prohibitive costs and limited benefit, smaller scale activities such as overflow channels, surrounding drainage and swallow-hole alteration still pose a threat. Channels designed to limit the maximum level of flooding will obviously damage any flood dependent communities present about the imposed limit, as well as potentially increasing the rate of flood recession. In 1992, the clearance of part of the Dunkellin River channel flowing through Rahasane turlough, Co. Galway, removed much of the wetland vegetation habitat available during the summer months (Reynolds, 1996b). Drainage activities can also prolong flooding such as occurred recently due to the unauthorized reactivation of a stretch of drainage channel feeding into Croaghill turlough SAC near Williamstown, Co. Galway. According to local landowners this has delayed flood recession within the basin and therefore potentially altered the composition of ecological communities by altering the characteristic hydrological regime.

4.7.2. Land-Use Practices

Turlough ecologies as they exist today are at least partially a product of long term anthropogenic effects, such as agricultural practices within turlough basins. Part of their diversity, and therefore ecological merit, is dependent upon maintaining these practices. The primary land use type within turloughs is grazing pasture, with turloughs being commonly used for grazing livestock such as cattle, sheep and horses during dry periods (Goodwillie, 1992; Ní Bhriain et al., 2003). Grazing plays a major role in determining the composition of vegetation and invertebrate communities within turlough basins by limiting shrub growth and vegetation height, and also preferentially removing many of the palatable species thus allowing less favourable species to spread (Goodwillie, 1992; Ni Bhriain et al., 2002; Ryder et al., 2005). Over-grazing can also have a negatively impact on soil quality with the presence of heavier livestock such as

cattle promoting soil compaction which can lead to prolonged flooding (Kimberley, 2007a). Poaching and soil erosion can occur when livestock are allowed graze before vegetation has had time to regenerate following flood recession (Ni Bhriain et al., 2002). If widespread this may seriously disturb the soil surface and encourage the proliferation of weedy species (Goodwillie, 2001). Under-grazing also poses a significant risk to vegetation diversity. The abandonment of sites as grazing land can prove harmful to diversity as certain grazing intensities can have a positive impact on vegetation species diversity (Kimberley, 2007a; Tynan et al., 2007).

4.7.3. Nutrient Input

The dependence of turloughs upon the quality and quantity of groundwater from the karst systems of which they form a part makes them highly susceptible to anthropogenic pressures. The nature of groundwater flow within karst systems and the connection between groundwater body and turlough is such that a relatively small stress such as a change in nutrient loading can cause a disproportionately large response (Drew and Hotzl, 1999; Tynan et al., 2007). A combination of shallow subsoils and relatively rapid flow rates result in limited time for attenuation of nutrients or pollutants within karst systems, and the high level of interaction between surface water and groundwater also provide a direct pathway for nutrients to enter the groundwater body. Nutrient sources within both the catchment and the turlough basin itself, such as slurry spreading, silage effluent and septic tank percolation areas can affect turlough nutrient status.

4.7.4. Assessing Turlough Conservation Status

In order to determine if a turlough is damaged an un-impacted baseline condition is required but, prior to the work carried out under the NPWS "Assessing the Conservation Status of Turloughs" research project, no such observational data were available for turloughs with which to define such a baseline. This is further complicated by the natural variation of turlough hydrological regime caused by changeable seasonal rainfall patterns, with population abundances shifting considerably under such natural conditions. In order to gain an understanding of how changes in turlough pressures will impact on turlough ecosystems, a quantitative link between hydrological and ecological parameters needs to be defined. Turlough hydrology can affect ecological communities

both directly and indirectly. The direct effect is caused by the nature of the flooding itself, such as the duration, frequency and timing of inundation. Hydrology also indirectly affects turlough ecological communities by influencing the environmental variables of water chemistry, soil type and nutrient status. Thus understanding the linkages between turlough ecological parameters and hydrology is vital in the assessment of future risk to the turlough habitat.

A recent study carried out by Tynan *et al.* (2007) attempted to classify turloughs in relation to their flooding regime, geomorphology and trophic status. Under the Environmental RTDI Programme this work was tasked with developing a methodology for the characterisation of turloughs as karstic groundwater dependent bodies based upon linkages between hydrological and ecological parameters. Data sources relating to turlough hydrogeology were collated, and potential relationships between hydrological and ecological variables were investigated. For example, stage duration curves were generated for a limited subset of sites and compared against the elevation of plant communities derived from vegetation mapping. It was recommended that this methodology be extended to other turloughs to elucidate this relationship and investigate whether the approach could be used generically across all turloughs. If so, it could potentially provide significant insights into the relationship between flood regime and vegetation ecology. However, while the study by Tynan et.al. (2007) found tentative linkages between hydrological ecological parameters; it also highlighted the need for further research on these linkages. The report identified the need for a comprehensive study into the hydrological regime of turloughs. Such a study would be necessary to develop a greater understanding of the hydrological processes involved in such complex systems, as it is vital to ensuring the sustainability of water resources and groundwater dependent ecologies in the future. Tynan et al. (2007) identified the main data limitations in assessing the conservation status of turloughs:

- Lack of long-term and consistent hydrological data
- Absence of water chemistry data
- Sporadic invertebrate population data
- Lack of temporally and spatially coincident data on multidisciplinary turlough characteristics

One of the aims of the "Assessing the conservation status of turloughs" project is to address these limitations and define a baseline condition for turloughs and quantify the links between hydrology and ecological variables so the potential impacts of changes can be accurately assessed. While a characteristic turlough ecology may not exist, by collating temporally and spatially coincident multidisciplinary data for a wide group of turloughs, and elucidating the processes shaping individual habitats it becomes possible to assess and ensure the conservation status of turloughs. This will be achieved through the definition of hydroecological indicators for use in the interpretation of various ecological datasets, namely vegetation, aquatic invertebrates, water chemistry, phytoplankton and soil nutrients.

CHAPTER 5. FIELD INVESTIGATION AND DATA COLLECTION

5.1. Site Selection and Description

As hydrology is considered the main driver in the establishment and maintenance of wetland processes, the main criterion for the selection of sites was hydrological. Sites were selected from the list of 90 turloughs of area greater than 10ha identified by Coxon (1986) with emphasis on those already designated as candidate Special Areas of Conservation (SACs). Of these 90, 30 were discounted as they had undergone significant drainage works in the past and so were not thought to give a true representation of turlough behaviour. Hydrological and ecological data, of varying forms and standards, were collated for the remaining 60 undrained sites (Tynan et al., 2007; Southern Water Global, 1998; Goodwillie, 1992; Coxon, 1986). Where reliable hydrological data were available, turloughs were characterised based on the Karstic Flow System hypothesis, which proposed that ecological characteristics within turlough basins are associated with the karstic flow system type (shallow epikarst, conduit) surrounding the turlough (Tynan et al., 2007; Southern Water Global, 1998; Drew, 1990). Where no hydrological data were available, surrogates such as the distribution of the aquatic mosses *Cinclidotus fontinaloides* and *Fontinalis antipyretica* of were used to characterise the depth and duration of turlough flooding (Coxon, 1986).

22 turloughs were chosen using the best available hydrological criteria to represent a geo-hydrological spectrum and a broad but practical geographical distribution at the same time as covering the range of conservation states (oligotrophic to eutrophic). The site selection process was driven by the research group and steering committee members of the project "Assessing the Conservation Status of Turloughs", of which I was a member. The locations of the chosen 22 turloughs are shown in Figure 5.1, while the turlough name and location is given in Table 5.1. All sites are located on well bedded, pure limestone, and a summary of site specific geology is given in Table 5.2. With the exception of three sites in Roscommon (Rathnalulleagh, Carrowreagh and Brierfield), all of the selected study sites have been designated as candidate Special Areas of Conservation (SAC).

Site Name	ID	County	Easting	Northing
Skealoghan	1	Mayo	124800	262940
Ardkill	2	Mayo	127300	262270
Kilglassaun	3	Mayo	127710	265000
Coolcam	4	Galway	157700	270800
Croaghill	5	Galway	159490	270860
Rathnalulleagh	6	Roscommon	177960	273650
Carrowreagh	7	Roscommon	178570	275230
Brierfield	8	Roscommon	181870	277070
Lisduff	9	Roscommon	184300	255700
Caranavoodaun	10	Galway	145380	215460
Blackrock	11	Galway	149870	207920
Lough Coy	12	Galway	148890	207460
Garryland	13	Galway	141720	206390
Caherglassaun	14	Galway	141500	203900
Termon	15	Galway	141200	197150
Roo West	16	Galway	138540	202200
Turloughmore	17	Clare	134640	199340
Lough Gealain	18	Clare	131260	194610
Knockaunroe	19	Clare	131450	194200
Lough Aleenaun	20	Clare	124980	195470
Ballinderreen	21	Galway	139660	215590
Tullynafrankagh	22	Galway	143120	215340

Table 5.1: Name, location and coordinates of 22 project study sites

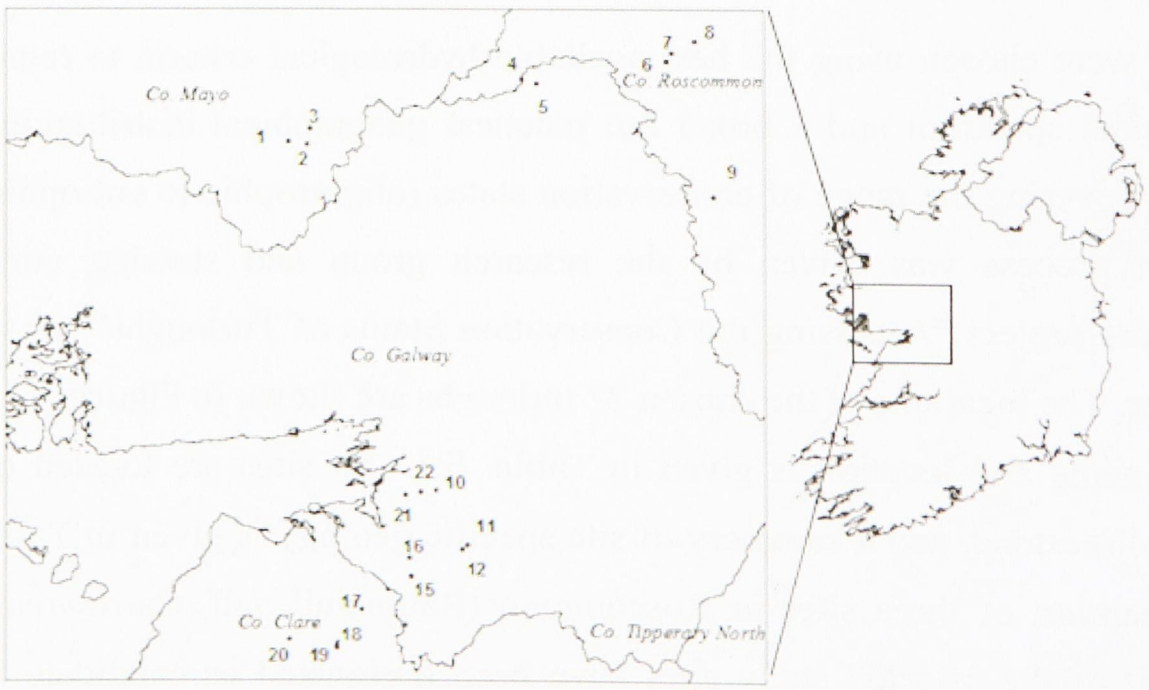


Figure 5.1: Locations of 22 study sites

Site Name	*Formation Name*	*Member Name*	*Stratigraphic Code*	*Description*	*Additional Details*
Skealoghan	Cong Limestone		CO	Thick bedded pure limestone	
Ardkill	Cong Limestone		CO	Thick bedded pure limestone	
Kilglassaun	Cong Limestone		CO	Thick bedded pure limestone	
Coolcam	Oakport Limestone		OK	Pale grey massive limestone	Lies in WNW - ESE syncline. Major faulting to the south with trend in NE direction
Croaghill	Oakport Limestone		OK	Pale grey massive limestone	
Rathnalulleagh	Visean Limestone (undifferentiated)		VIS	Undifferentiated limestone	
Carrowreagh	Visean Limestone (undifferentiated)		VIS	Undifferentiated limestone	
Brierfield	Visean Limestone (undifferentiated)		VIS	Undifferentiated limestone	
Lisduff	Visean Limestone (undifferentiated)		VIS	Undifferentiated limestone	
Caranavoodaun	Tubber	Castlequarter	TU cq	Monotonous limestone sparsely fossiliferous	
Blackrock	Tubber	Newtown	TU nt	Cherty limestone	On eastern limb of shallow syncline broadly dipping NW
Lough Coy	Tubber	Newtown	TU nt	Cherty limestone	
Garryland	Burren	Hawkhill	BU hh	Peloidal limestone with chert	
Caherglassaun	Burren	Hawkhill	BU hh	Peloidal limestone with chert	On SE limb of SW - NE trending syncline
Termon	Tubber		TU	Crinoidal and cherty limestone and dolomite	
Roo West	Burren	Maumcaha	BU mc	Massive limestone sparsely fossiliferous	
Turloughmore	Burren	Maumcaha	BU mc	Sparsely fossiliferouos massive limestone	Lies along SW - NE anticline axis
Lough Gealain	Burren	Maumcaha member[1] Aillwee member[2] (lower)	BU mc[1], BU al[2]	[1]sparsely fossiliferous massive limestone. [2]Bedded and massive fossiliferous limestone	
Knockaunroe	Burren	Maumcaha member[1] Aillwee member[2] (lower)	BU mc[1], BU al[2]	[1]sparsely fossiliferous massive limestone. [2]Bedded and massive fossiliferous limestone	Centred on small anticline with axis running SW - NE
Lough Aleenaun	Slievenaglasha	Fahee North	SLfh	Cherty limestone, crinoidal intervals	Northern limb of anticline
Ballinderreen	Tubber	Castlequarter	TU cq	Monotonous limestone sparsely fossiliferous	
Tullynafrankagh	Tubber	Castlequarter	TU cq	Monotonous limestone sparsely fossiliferous	Southern limb of shallow anticline

Table 5.2: Geological summary of study sites

5.2. Water Level Monitoring

Sites were instrumented between September 2006 and January 2007 with monitoring continuing until July 2009. Water levels were recorded at hourly intervals using a variety of Schlumberger Divers® (Marton Geotechnical Ltd, Suffolk, UK) placed at or near the lowest point in each turlough. Divers measure the pressure of the water and air column above them, and from this the depth of water can be calculated. A Diver consists of a ceramic (Al_2O_3) pressure sensor housed within a sealed steel casing. It is capable of taking measurements to an accuracy of 1 cm H_2O within the temperature compensated range of 0 to 40°C. The Diver is hermetically sealed to ensure that measurements will be unaffected by moisture. Divers typically have a memory of between sixteen and twenty-four thousand measurements and so can accommodate up to three years of water level data logged at hourly intervals.

The majority of Divers used were Schlumberger Mini-Diver® models DL501 and DL502. The Mini-Diver® DI501 has a range of 10 m of water with an accuracy of 0.5 cm and resolution of 0.2 cm. For sites where the flooding range exceeded 10 m the Mini-Diver® DI502 was used, which has a range of 20 m of water, an accuracy of 1 cm and a resolution of 0.4 cm. Nineteen of the twenty two Divers used were equipped with temperature probes which recorded ambient water temperature at hourly intervals to an accuracy of 0.1°C. A CTD Diver was installed in Blackrock turlough which, in addition to depth and temperature sensors, has a conductivity sensor with a range of 0 to 80 mS/cm and so recorded conductivity on an hourly basis.

A concrete platform or paving slab was used to anchor the Divers in place (Figure 5.2 *(a)*). A thirty centimetre length of pipe was bolted to the platform to house the Diver® and protect it from direct sunlight during dry periods. A hole was drilled in the centre of the platform through which a length of rope was threaded and a secure knot tied beneath the platform. A buoy was attached to the other end of the rope to mark the position of the platform and enable recovery during inundation periods. However, in most cases the divers were left in position until the turloughs had receded enough to allow recovery on foot. Divers were downloaded roughly every six to nine months using a Reading Unit into which the end of the diver was inserted having removed the

mounting cap (Figure 5.2 (b)). The Reading Unit was connected to a laptop and the data downloaded using Schlumberger LoggerDataManager® software. The data was then imported into an Excel® spreadsheet format for further processing.



Figure 5.2: (a) Diver platform, Rathnalulleagh, Co. Roscommon (b) downloading diver using Reading Unit, Garryland, Co. Galway

A summary of the water level monitoring periods for the twenty two study sites is given in Table 5.3. Five equipment failures occurred during the monitoring program in Ardkill, Ballinderreen, Kilglassaun, Lough Aleenaun and Roo West with a resultant loss in water level records. Failure in Roo West was caused by the puncturing of the pressure transducer membrane leading to inaccurate readings. All other failures were associated with faulty sealing 'O' rings and/or batteries. Notes on missing records are also given in Table 5.3.

Site ID	Site Name	Start	End	Days Recorded	Failure
1	Skealoghan	06/11/2006	08/07/2009	975	
2	Ardkill	05/11/2006	13/10/2008	708	13/10/2008 onwards
3	Kilglassaun	04/02/2007	21/08/2008	564	21/08/2008 onwards
4	Coolcam	04/11/2006	06/08/2009	1006	
5	Croaghill	04/11/2006	06/08/2009	1006	
6	Rathnalulleagh	04/11/2006	08/07/2009	977	
7	Carrowreagh	04/11/2006	08/07/2009	977	
8	Brierfield	04/11/2006	08/07/2009	977	
9	Lisduff	05/11/2006	08/07/2009	976	
10	Caranavoodaun	24/09/2006	04/08/2009	1045	
11	Blackrock	05/11/2006	23/06/2009	961	
12	Lough Coy	24/09/2006	05/08/2009	1046	
13	Garryland	10/01/2007	23/06/2009	895	
14	Caherglassaun	24/09/2006	05/08/2009	1046	
15	Termon	05/11/2006	05/08/2009	1004	
16	Roo West	27/09/2007	05/08/2009	678	Before 27/9/2007
17	Turloughmore	06/11/2006	24/06/2009	961	
18	Lough Gealain	11/01/2007	05/08/2009	937	
19	Knockaunroe	05/11/2006	05/08/2009	1004	
20	Lough Aleenaun	06/11/2006	19/02/2009	836	19/02/2009 onwards
21	Ballinderreen	05/11/2006	05/08/2009	557 + 294	From 15/5/2008 to 15/10/2008
22	Tullynafrankagh	01/10/2006	04/08/2009	1038	

Table 5.3: Summary of water level monitoring periods for 22 study sites

In order to determine the water level accurately, compensation for the variation in prevailing air pressure was made by means of a combination of BaroDiver® (DI500) and Met Eireann synoptic station data. The air pressure readings were converted into equivalent water head and then taken away from the water levels recorded by the Divers. As air pressure varies exponentially with height according to equation 5.1 the barometric data was adjusted prior to compensation to allow for the difference in elevation between the BaroDiver or Met station elevation and that of the Diver on site.

$$P_H = P_0 e^{-\frac{MgH}{RT}} \qquad \textit{Equation 5.1}$$

Where:

P_H = air pressure at height H (cm H_2O)

P_0 = air pressure at reference height (cm H_2O)

M = $28.8 \cdot 10^{-3}$ kg/mol (molecular mass of air)

g = acceleration due to gravity (9.81 m/s^2)

H = height (m)

R = gas constant (8.314 J/mol/K)

T = temperature (°K)

Diver and BaroDiver® elevations relative to ordnance datum Malin Head (mAOD) were obtained using differential GPS surveying techniques. In certain cases the diver level could not be surveyed directly as the platform lay in excessively deep water. In these instances the elevation of the water surface in mAOD was taken and the time noted. The elevation of the diver was then back calculated based on the water depth recorded at the time of the GPS measurement.

In addition to the adjustment of barometric data for differences in site elevations, each Diver record had to be adjusted for differences in the Diver calibration itself. While all Divers accurately measure changes in pressure, the absolute value recorded varies between Divers. This can lead to an individual Diver reading either a slightly positive or negative value after compensation when in fact it should be reading zero. The correction factor for this was derived in two different ways. If a Diver remained dry for a significant period the difference from zero recorded by the Diver was used as a correction factor. If the Diver remained inundated for most or all of the monitoring period the stage was recorded using GPS surveying equipment and used to back calculate the diver correction factor. It was also noticed that there was a low level of drift over time for some Divers, particularly those that had to be exposed to the air for extended periods. During dry periods the rate of drift could be measured directly and applied to the time series. If a change in zero level occurred over the inundation period drift was assumed to have occurred linearly and a linear regression equation was used to calculate the drift correction for each individual reading.

5.3. Temperature Profiling

Further to the integrated temperature probes housed within the Divers, a vertical array of temperature probes was installed in an estavelle in Caranavoodaun turlough, Co. Galway to measure the temporal variation in temperature with depth. The aim of the temperature array was to allow comparison of water temperature at the estavelle with the temperature record of the Diver further out into the turlough. In theory, by

comparing the temperature record from a known operational estavelle with the record from the main turlough water body, an indication of the periods during which the estavelle operated as an inflow point could be ascertained. Caranavoodaun turlough was chosen as a trial site for this investigation technique as preliminary site investigations identified a single, clearly active doline on the site which provided a good location for the instrumentation. A 1.5 m length of plastic pipe was attached vertically to a 75 kg concrete base. Five Campbell Scientific 109-L temperature probes were affixed at 0.25 m intervals inside the pipe using cable ties. The 109-L probe uses a thermistor to record ambient air and water temperature within the range of -10°C to 70°C with a maximum error of ±0.2°C. The probes were connected to a Campbell Scientific CR200 multi-channel data logger attached to a nearby tree above the maximum flood level.

5.4. Precipitation

Three ARG100 tipping bucket rain gauges (Environmental Measurement Ltd) were installed in Kilchreest (Figure 5.3 *(a)*) Francis Gap (Figure 5.3 *(b)*) Co. Galway as well as Ballintober, Co. Roscommon. Their purpose was to provide detailed rainfall records and to supplement existing Irish Meteorological Service (Met Eireann) rainfall and synoptic stations. The ARG100 tipping bucket rain gauge consists of an hourglass shaped plastic funnel with funnel diameter of 254 mm and funnel height of 340 mm, aerodynamically designed to minimise wind effect errors. Precipitation is collected by the funnel and passed through to one of a pair of buckets on a balance arm within the gauge. When the bucket is full the balance arm tips, empties the bucket, and passes a magnet across a reed switch. This in turn generates a small current which is registered by the logger. Each tip represents approximately 0.2 mm of rainfall, the exact amount being determined for each individual rain gauge during calibration carried out by the manufacturer. Precipitation was recorded at intervals of fifteen minutes as errors increase significantly at intervals less than this (Habib et al., 2001). The data were then aggregated into hourly totals and daily totals from 0900 UTC to 0900 UTC (coordinated universal time) and so are consistent with Met Eireann rainfall station records.

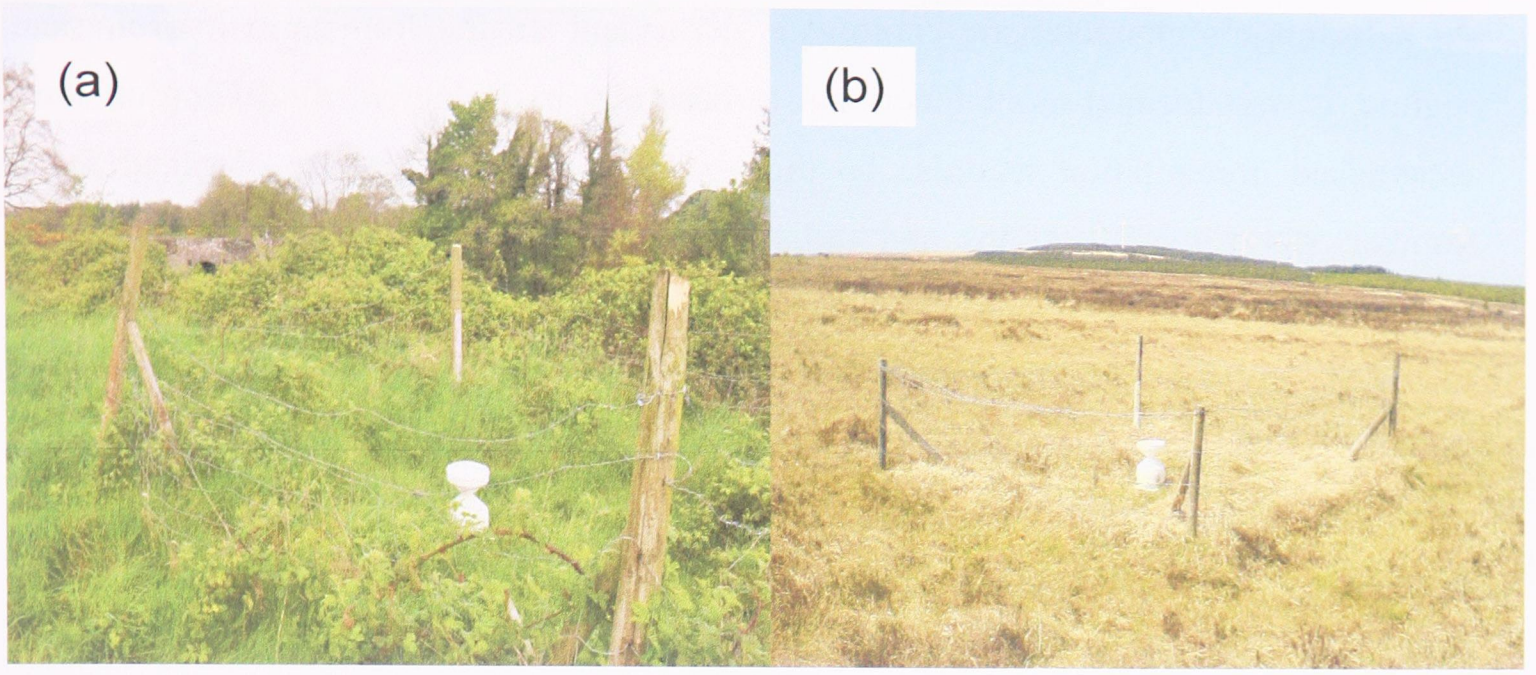


Figure 5.3 (a) Tipping bucket rain gauge at (a) Kilchreest and (b) Francis Gap, Co. Galway

The gauges were positioned away from any interference or obstruction within a maximum of 15° sight line (Figure 5.4) and also not in an over-exposed area (Shaw, 1994). The gauge was attached to a metal base plate and bolted securely to a concrete slab. The gauge was then levelled using the adjustment screws and integrated bubble level. A fence was erected around each gauge to prevent interference and damage from livestock. Rainfall records were downloaded every four to six months.

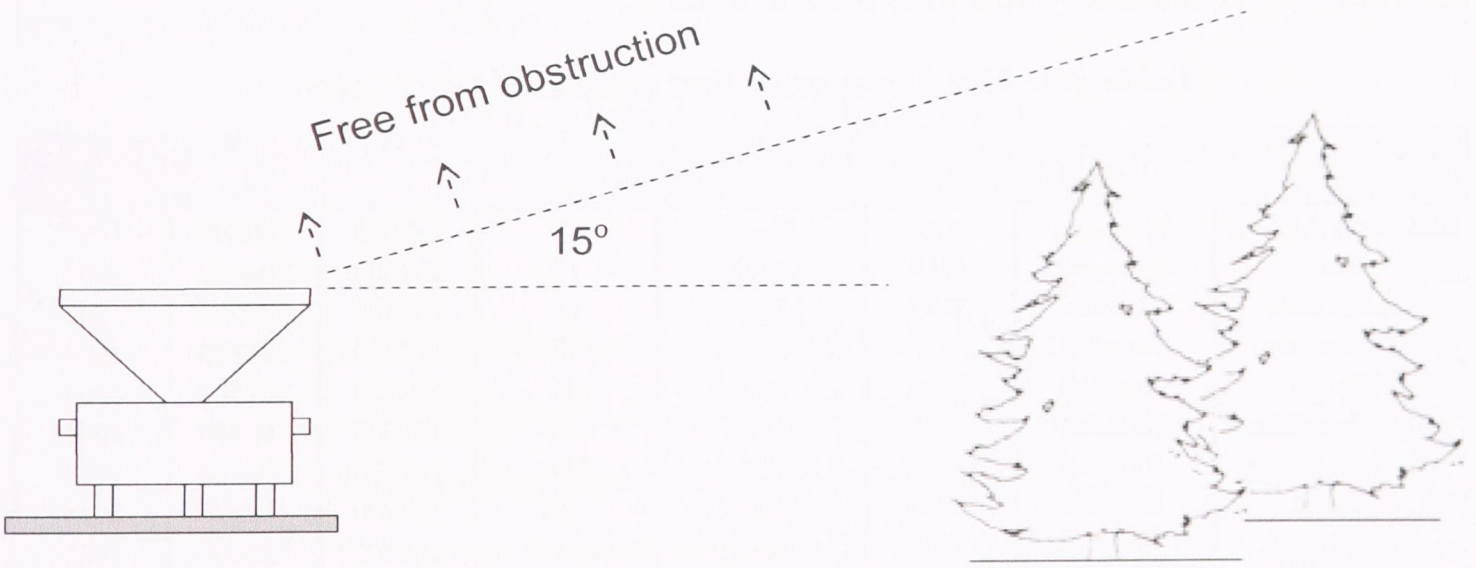


Figure 5.4: Positioning of rain gauge away from any obstruction within 15^0 sight line

As a turlough's characteristic ecology is dependent on the long term hydrological regime, it was deemed more functional to base any hydrological modelling on long established precipitation records. To this end long term data were obtained for a number Met Eireann stations and utilised in the modelling process. Met Eireann operates three different station types: synoptic; climatic and rainfall (Table 5.4). A list of the Met Eireann stations from which meteorological data was obtained is given in Table 5.5. Standard techniques (e.g. Theisson polygons) were considered for the calculation of areal rainfall but given the wide distribution of rain gauges, and the lack of clearly defined catchment areas, the rainfall record from the nearest Met Eireann rain gauge was used as an estimate of areal rainfall. As a number of rainfall stations approximately equidistant from the Ballintober turloughs, the Ballintober raingauge record was used to select the most appropriate Met Eireann record.

Station Type	Recorded Parameters
Synoptic	Meteorological elements such as rainfall, air temperature, wind speed, wind direction and atmospheric pressure on an hourly basis and the calculated parameters of evaporation, evapotranspiration and soil moisture deficit on a daily basis
Climatic	Meteorological elements on a daily basis, such as rainfall, air pressure and temperatures. Some elements available on an hourly basis at select stations
Rainfall	Rainfall only on a daily basis at 0900utc

Table 5.4: Met Eireann station types and description

Location	Station Type	Station Number	County	Elevation (mAOD)	Easting	Northing	Year Open
Shannon Airport	Synoptic	518	Clare	6	137900	160300	1937
Birr	Synoptic	4919	Offaly	73	207400	204400	1954
Claremorris	Climatic	2727	Mayo	71	134500	273900	1943
Balllinagare	Rainfall	7129	Roscommon	87	174700	287700	2003
Ballygar	Rainfall	2228	Galway	61	178400	252500	1969
Ballyvaughan	Rainfall	2321	Clare	23	121500	208300	1984
Carheeny Beg	Rainfall	2018	Galway	49	144400	194300	1993
Carron	Rainfall	1718	Clare	134	127700	198200	1974
Craughwell	Rainfall	2521	Galway	27	149800	220000	1985
Glenamaddy	Rainfall	3127	Galway	84	162900	261600	1944
Gort	Rainfall	2121	Galway	155	159700	201900	1982
Kilkeeran	Rainfall	5127	Mayo	27	116400	272800	1994
Loughrea	Rainfall	2721	Galway	76	160100	218100	1998
Milltown	Rainfall	3027	Galway	50	141000	262800	1944
Roscommon	Rainfall	5829	Roscommon	58	186700	264100	1984
Strokestown	Rainfall	6329	Roscommon	52	192800	278200	1987

Table 5.5: Met Eireann synoptic, climatic and rainfall stations from which meteorological data was obtained

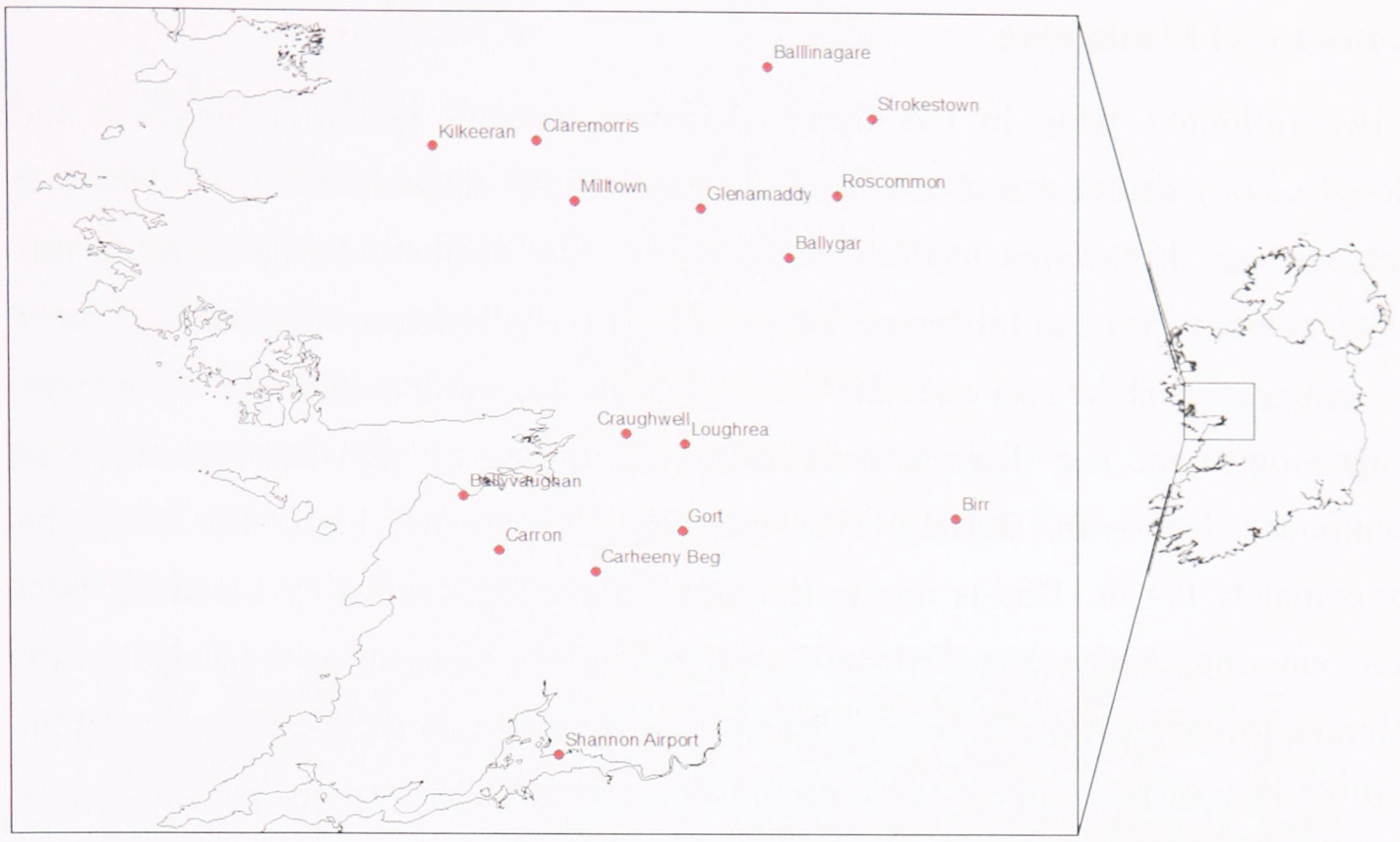


Figure 5.5: Met Eireann station locations

5.5. Evapotranspiration

Daily evapotranspiration data were obtained from Met Eireann synoptic stations located in Shannon Airport (Co. Clare), Knock Airport (Co. Mayo), and Birr (Co. Offaly). Met Eireann calculates potential evapotranspiration using the FAO Penman – Monteith equation as given by:

$$ET_0 = \frac{0.408\Delta(R_n - G) + \gamma \frac{900}{T+273} u_2 (e_s - e_a)}{\Delta + \gamma(1 + 0.34u_{2)}} \qquad \textit{Equation 5.2}$$

Where:

ET_0 = Potential evapotranspiration (mm d^{-1})

R_n = Net radiation at the crop surface (MJ m^{-2} d^{-1})

G = Ground heat flux density (MJ m-2 d-1)

Γ = Psychrometric constant (kPa $°C^{-1}$)

T = Air temperature at 2 m height (°C)

u_2 = Wind speed at 2 m height (m s^{-1})

e_s = Saturation vapour pressure (kPa)

e_a = Actual vapour pressure (kPa)

Δ = Slope of the vapour pressure curve (kPa $°C^{-1}$)

5.6. Sea Level Monitoring

As two turloughs lying in the Gort – Kinvarra conduit system (Garryland and Caherglassaun) demonstrated a tidal influence at low stages, tide level data was obtained from the Marine Institute for analysis. The nearest Marine Institute tide gauges, Galway Port and Inishmore, consist of OTT Hydrometry CBS Bubbler water level gauges which record accurate tide levels at six minute intervals in mAOD. Comparison of the two datasets showed that the timing of high and low tide was synchronous but with Galway Port showing the greater high tide level by approximately 0.4 m. This is due to the tidal bore effect caused by incoming tidal waters entering Galway bay. Galway Port tide levels were used in the analysis with Inishmore levels used to compensate for any missing data points, suitably adjusted for the difference in maximum level. The tide level time series was reduced to hourly readings to allow comparison with hourly water level time series for Caherglassaun and Garryland. A plot of stage for Galway Port and Caherglassaun turlough for May and June 2008 is shown in Figure 5.6. The variation in tide level maxima with spring and neap tides is clearly visible as well as the corresponding effect on water levels within the turlough.

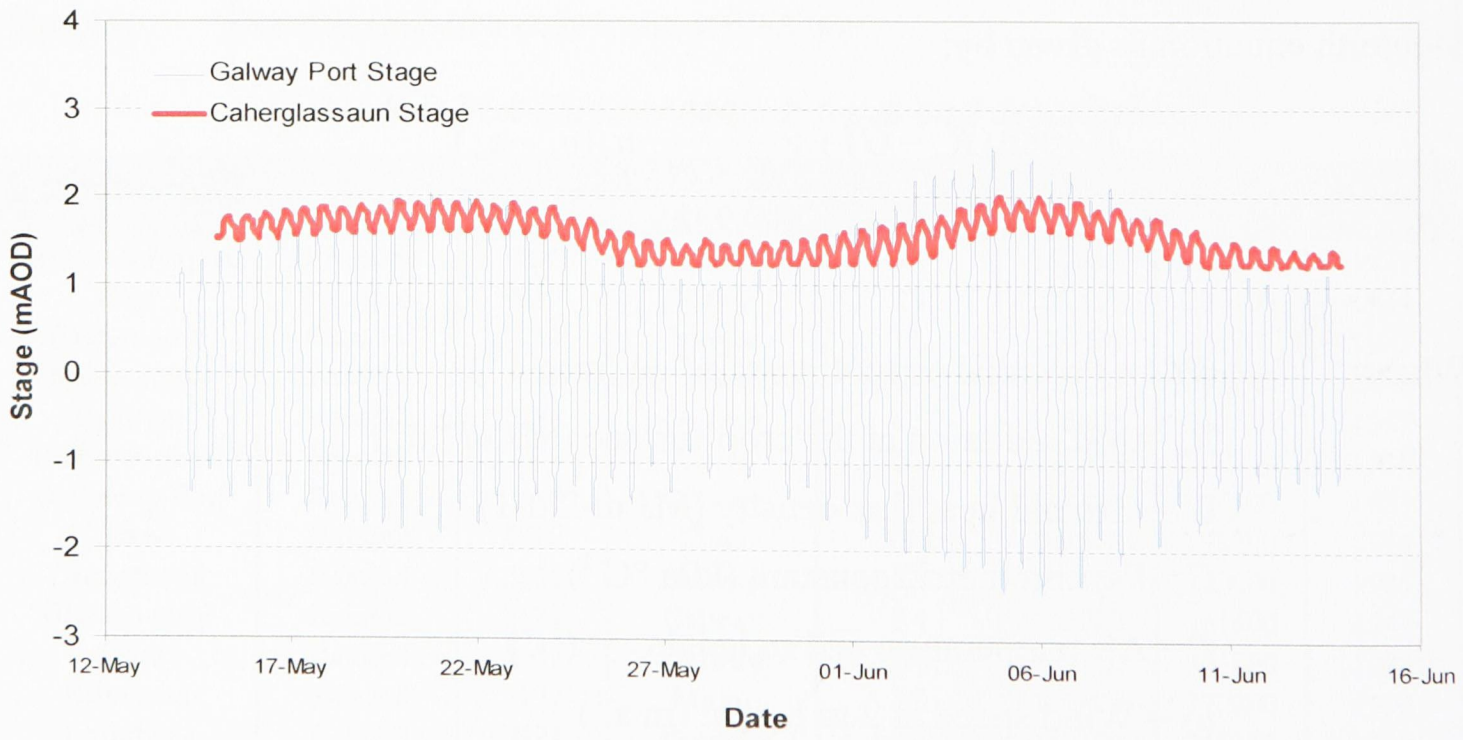


Figure 5.6: Variation in stage of Galway Port and Caherglassaun turlough, Co. Galway

5.7. Visual Surveying

A great deal of insight into the hydrological regime and hydrogeology of each site was gained during the DGPS surveying process (see chapter 6). Specific active hydrological features such as estavelles (Figure 5.7 *(a)* and *(b)*), springs and swallow holes were identified at a number of sites. In total the location and nature of over one hundred previously undocumented karst features were identified and their position accurately surveyed. These features have been submitted for inclusion within the GSI karst database.

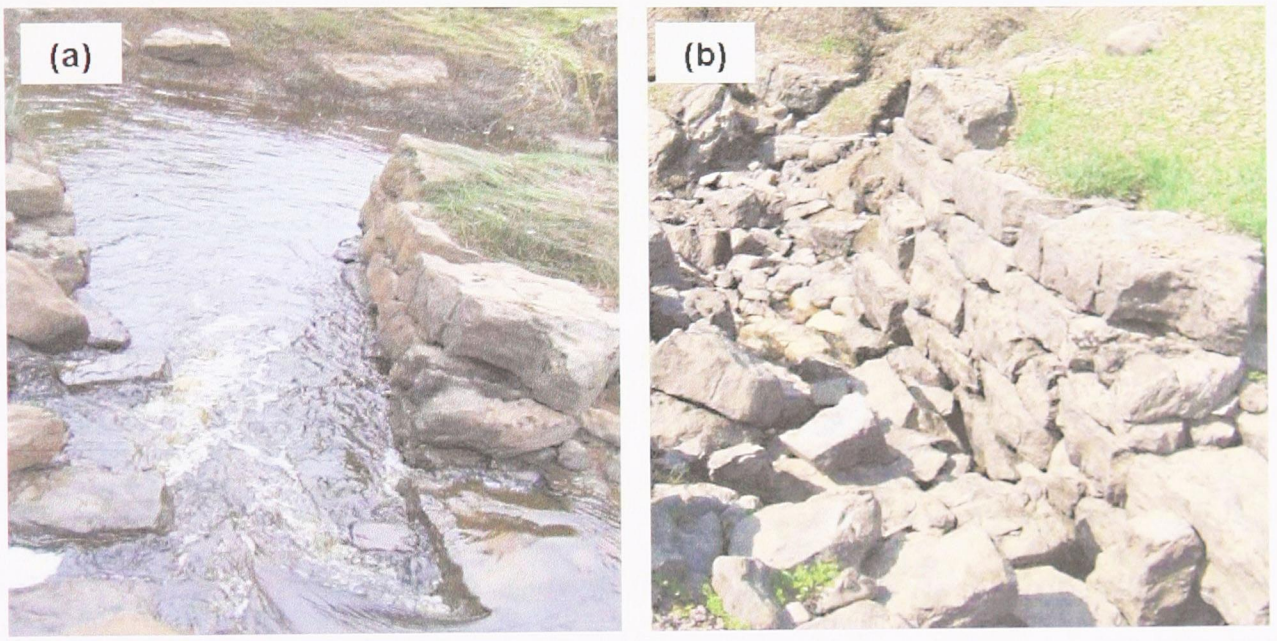


Figure 5.7: (a) Estavelle in operation during turlough recession and (b) dry in Lough Coy, Co. Galway

5.8. Stable Isotope and Hydro-chemical Sampling

Water samples were collected between December 2008 and June 2009 for stable isotope and chemical analysis. Five turloughs lying along a major conduit system in Co. Galway were chosen for sampling, namely Blackrock, Lough Coy, Coole, Garryland and Caherglassaun. Three contributing rivers were also sampled, the Owenshree, Ballycahalan and Beagh, along with two springs at the main system outlet in the coastal village of Kinvarra, County Galway (Figure 5.8). Duplicate samples were taken in 200 ml glass jars on each sampling occasion. The samples were flooded and sealed under water to minimise trapped air and refrigerated until analysis.

Conductivity and temperature was measured on site in the turlough and river water using an electrical conductivity (EC) meter (WTW® Cond.197i).

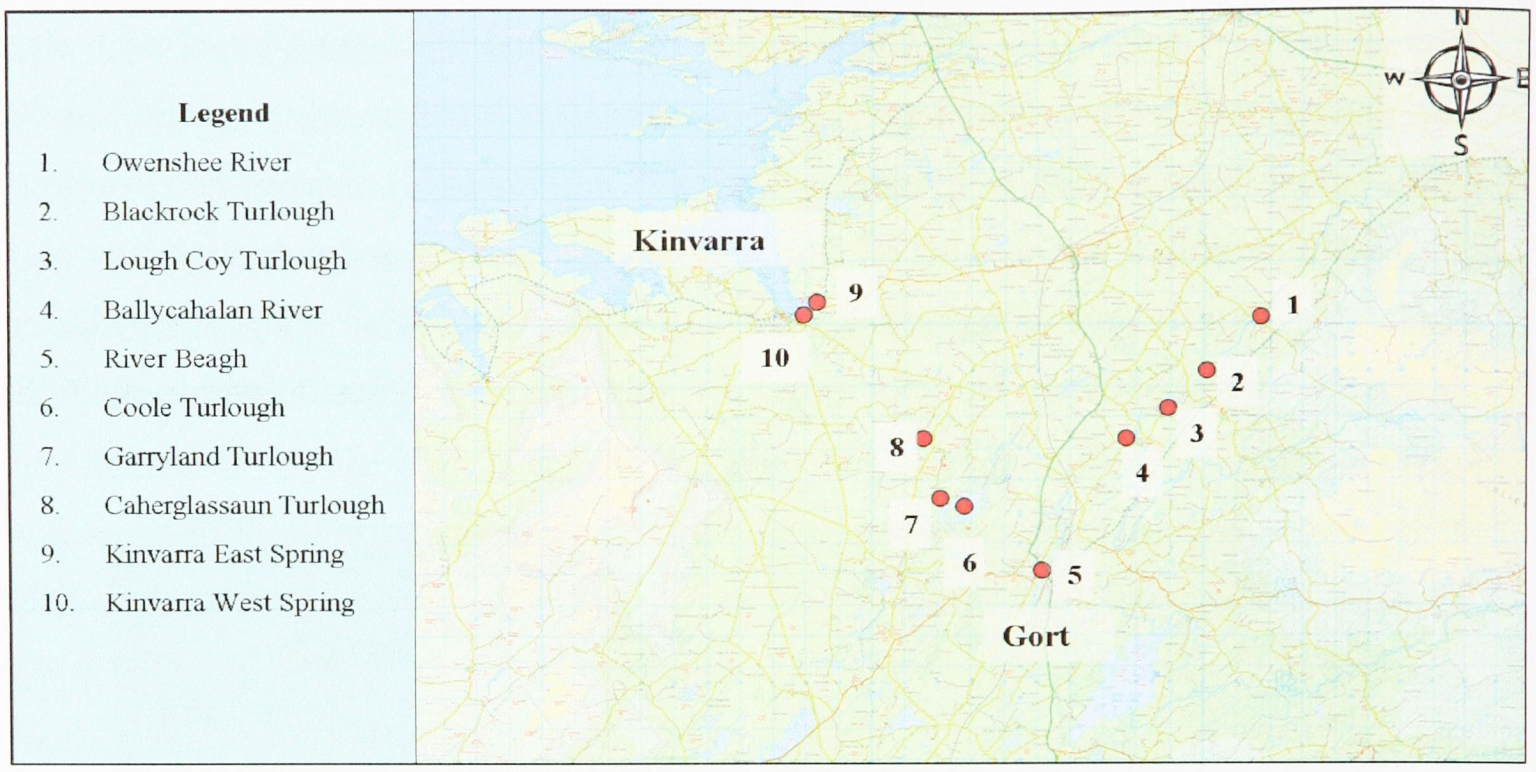


Figure 5.8: Location of 2008 / 2009 stable isotope and water chemistry sampling points, Co. Galway

The samples were analysed in the laboratory using a continuous flow-isotope ratio mass spectrometry (Thermo Deltaplus CF-IRMS) to determine the $^{18}O/^{16}O$ ratio. Nitrogen and total organic carbon (TOC) analysis was carried out using a *vario TOC cube* (Elementar, Germany) which operates on the principle of thermo-catalytic oxidation and subsequent infrared analysis of the oxidation products. Phosphorous and multi-element analysis was carried out using a Varian Liberty AX Series II ICP-AES (induce coupled plasma – atomic emission spectroscopy). Prior to analysis samples were prepared by filtering 10 ml of sample through a 1.2 µm Whatman glass microfibre filter and then the sample was acidified by adding 1 ml of nitric acid to ensure element stability. The samples were refrigerated until analysis was carried out.

Standards were prepared for each element included in the analysis. 10 ml standards for total phosphorous were made up using AccuStandard (AccuTrace Reference Standard Phosphorous 1000 µg/ml) to 0.25, 0.5, 1, 2, 5 and 10 mg/l by dilution with deionised water and then acidified using 1ml of nitric acid. 10 ml standards for multi-element were made up using AccuStandard Custom (AccuTrace Reference Standard Al, Cu, Fe, Mg, Mn 5 µg/ml, and K 50 µg/ml) to 0.25, 0.5, 1 and 2 mg/l for Al, Cu,

Fe, Mg and Mn. A blank was also prepared using only deionised water and nitric acid. The principle of operation of an ICP –AES is as follows. A stream of argon gas is ionised by passing it through a high-frequency electromagnetic field, causing intense heating of the gas and creating argon plasma. The sample is then injected as a mist into the plasma, vaporising the sample and breaking down any compounds into their individual atoms. The atoms then absorb energy and emit light at a characteristic wavelength depending on the element. The light is passed via a polychromator to a photoelectric multiplier which measures the intensity of the spectral emission. During calibration the relationship between this measured intensity and element concentration is defined using the standards of known concentration. Calibration was carried out with a maximum percentage error of 10%. The concentration of each element was then measured using Plasma 96 Version 1.12 software and displayed in spreadsheet form.

The stable isotope $^{18}O/^{16}O$ ratio was determined using continuous flow-isotope ratio mass spectrometry (Thermo Delta^{plus} CF-IRMS). The sample preparation to find the $\delta^{18}O$ of water by equilibration was as follows:

- 0.5 mL of water was pipetted into a 12 mL exetainer and capped with a rubber septum
- The exetainer was flushed with a 0.3% CO_2 in helium for 800 seconds
- The exetainer was allowed to equilibrate in the sample block for >20 hours. Two equilibrations occur:

  (1) $CO_2(g) <=> CO_2\ (aq)$

  where CO_2 is exchanged between the gaseous and aqueous phase

  (2) $CO_2\ (aq) + H_2O <=> H_2CO_3$

  where dissolved CO_2 reacts with water to form carbonic acid
- Samples were run with standard method (5 reference CO_2 peaks, 10 sample peaks and 2 reference CO_2 peaks). The middle 8 sample peaks were then averaged to give the $\delta^{18}O$ value

Corrections to the standard were made and the Standard Deviation was reported as 1SD for all standards run with unknowns.

5.9. Preliminary Turlough Catchment Areas

Estimates of catchment areas or zones of contribution were required for each turlough under the "Assessing the Conservation Status of Turloughs" project in order to investigate relationships between catchment wide parameters, such as land-use and stocking density, with within-site parameters like nutrient status, under the premise that the catchment areas are related to potential sources of pollution. However, given the low level of certainty associated with many of these areas, the uncertainty surrounding the nature of the interaction between turloughs and their zones of contribution, and the lack of sufficient time or resources to validate them during this project, these catchment areas are only used for a general comparison with recorded net inflow rates and not in any of the hydrological analyses, water balances or modelling carried out as part of this thesis.

Of the 22 study sites, 16 estimates of catchment areas were generated by members of the research project "Assessing the Conservation Status of Turloughs" from relevant hydrological research (Coxon, 1986; Coxon and Drew, 1986; Hickey, 2009; Southern Water Global, 1998), as well as more recent work carried out under the Water Framework Directive (WFD) risk assessment. The remaining six (Coolcam, Croaghill, Turloughmore, Lough Gealain, Knockaunroe and Lough Aleenaun) were derived as part of this thesis. These six catchments were derived topographically using interpolated 10m resolution Ordnance Survey Discovery series maps. To aid in the process of catchment estimation, limited water table mapping was carried out as part of this PhD research in the area surrounding Coolcam and Croaghill turloughs in north Co. Galway (Figure 5.9). Spot water level measurements were taken (in mAOD) of any turloughs, surface water bodies and rivers in the area surrounding the study sites using a Trimble R6 Differential GPS. Water table maps were then generated using Surfer 8©. This work provided information on regional gradients in this area and helped to refine the possible catchment boundaries given the low resolution of topographic data available.

All catchment estimates were reassessed by the research team utilising individual experience, relevant hydrological research, topographic data, tracer studies and

guidance documents used for the delineation of groundwater bodies (Working Group on Groundwater, 2005). The areas for all 22 estimated catchments are given in table 5.6, with overlapping catchments highlighted in the same colour.

Site ID	Turlough	Catchment Area (km^2)	Site ID	Turlough	Catchment Area (km^2)
1	Skealoghan	8.9	12	Lough Coy	83.3
2	Ardkill	3.1	13	Garryland	393
3	Kilglassaun	15.1	14	Caherglassaun	398
4	Coolcam	5.7	15	Termon	6.3
5	Croaghill	9.7	16	Roo West	14.8
6	Rathnalulleagh	18.8	17	Turloughmore	4.5
7	Carrowreagh	18.8	18	Lough Gealain	13.5
8	Brierfield	3.8	19	Knockaunroe	16.9
9	Lisduff	10.5	20	Lough Aleenaun	4.6
10	Caranavoodaun	9.3	21	Ballindereen	1.7
11	Blackrock	80.9	22	Tullynafrankagh	0.9

*Overlapping catchments in same colours

Table 5.6: Preliminary catchment area estimates

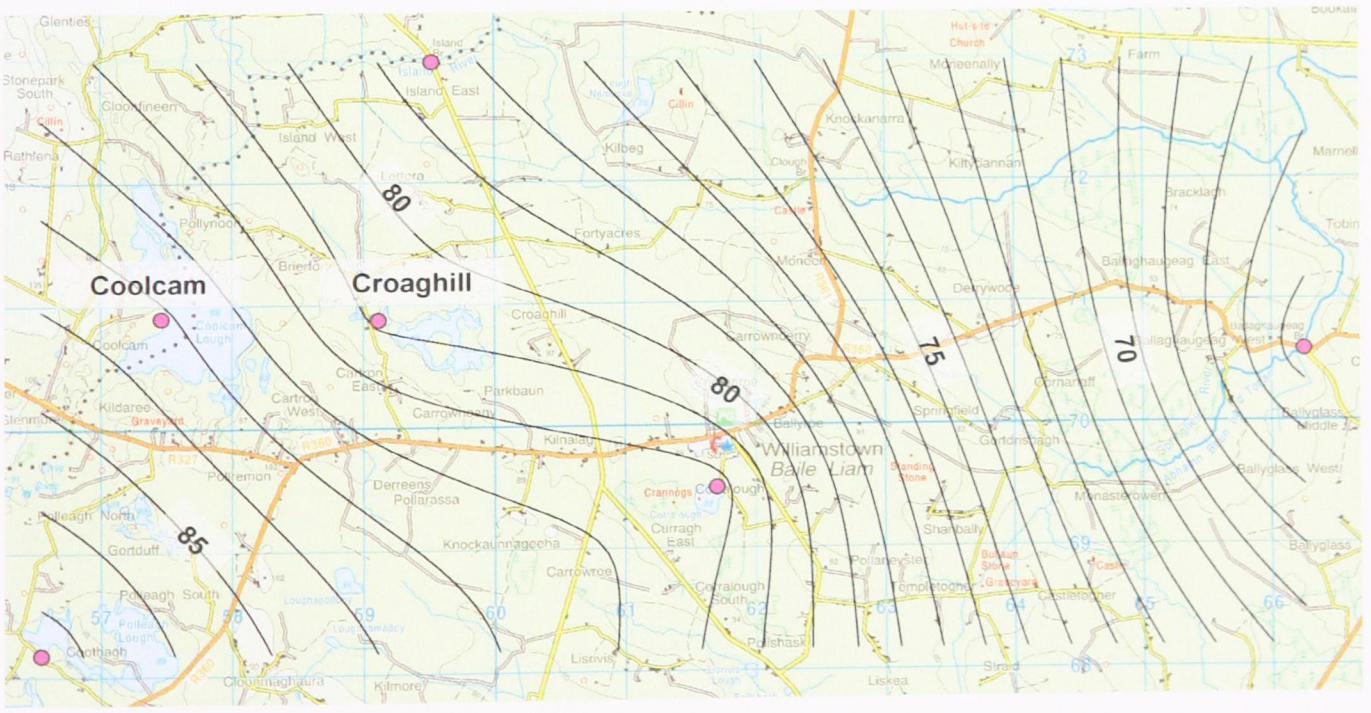


Figure 5.9: Water table map for area around Coolcam and Croaghill turloughs, Co. Galway

CHAPTER 6. SURVEYING AND DIGITAL TERRAIN MODELLING

6.1. Introduction

GPS surveys were carried out on 21 monitoring sites in order to develop digital terrain models (DTMs) from which stage / volume / surface area relationships could be defined. The theory behind differential GPS surveys is outlined and the field method for collecting topographic data is detailed. The various methods for generating digital terrain models from GPS field data are assessed using relevant statistical methods and the most suitable interpolation method selected. Contour maps, stage – volume and stage – surface area relationships are produced from the turlough DTMs. The steps involved in the DTM process are shown in the Figure 6.1 flow chart.

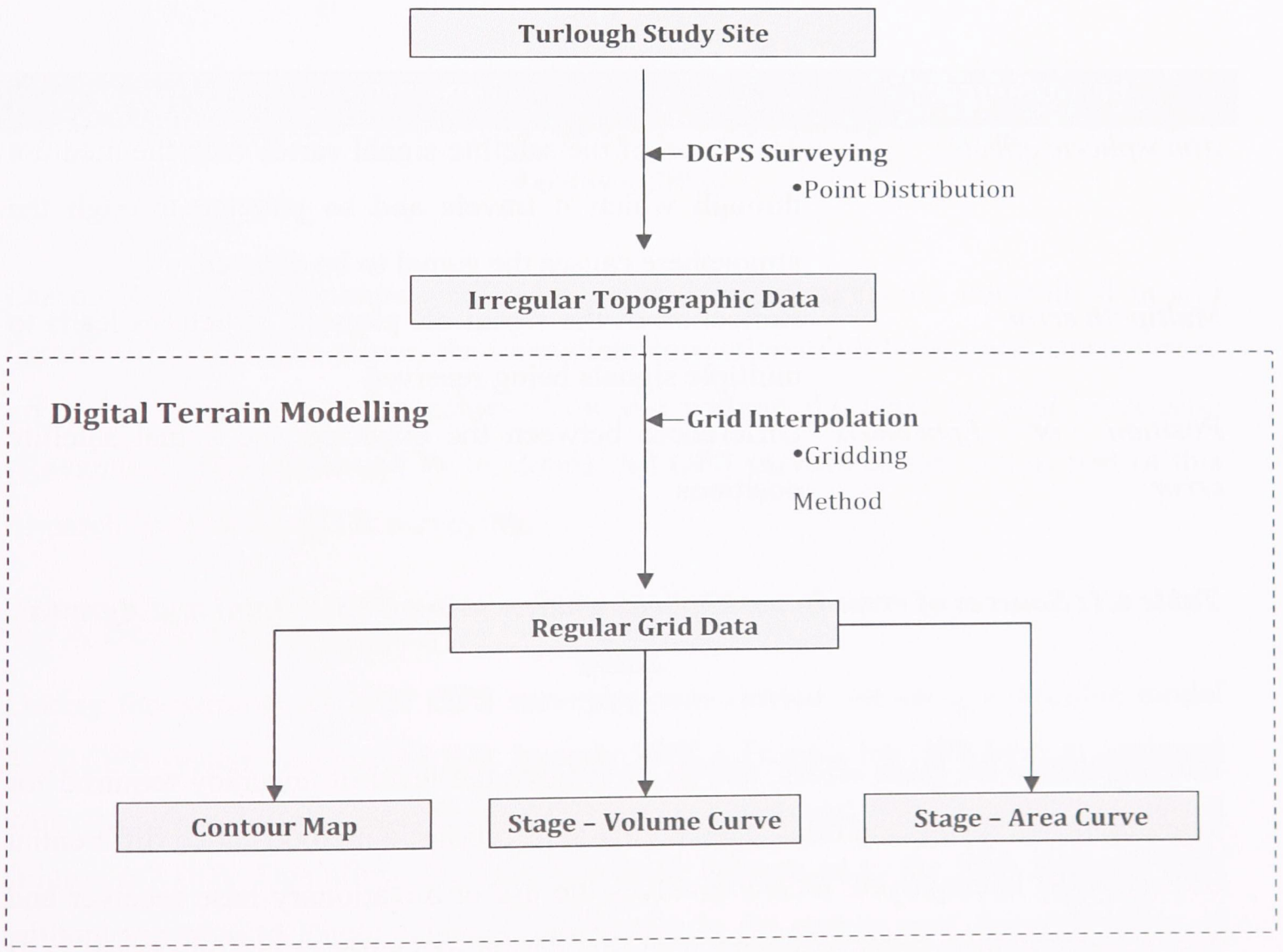


Figure 6.1: Flow chart for the turlough digital terrain modelling process

6.2. Global Positioning System Surveying

The Global Positioning System, or GPS, is the global navigation satellite system developed and maintained by the U.S. It originally comprised twenty four satellites and five ground stations that continuously transmit radio signals of time and distance (Kavanagh, 2009). GPS receivers use the satellite signals to pinpoint their coordinates on the earth's surface to within a few metres and, then, with the use of further methods such as differential GPS, down to centimetre accuracy. The position of the GPS receiver is calculated using triangulation. By analysing the travel time of the signal between the receiver and satellite the distance between them can be calculated. Repeating this process with a number of satellites simultaneously allows the receiver position to be determined. Mathematically just four satellites are required for this but, due to various sources of error, in practise more are needed for accuracy (McCormac, 2004). The main sources of error as described by Maini and Agrawal (2007) are summarised in Table 6.1:

Error Source	Description
Atmospheric effects	The speed of the satellite signal varies with the medium through which it travels and so passage through the atmosphere causes the signal to be delayed
Multipath error	Reflection of the signal off physical structures leads to multiple signals being received
Position or Ephemeris error	Differences between the expected and actual satellite positions

Table 6.1: Sources of error in position calculation using GPS. (Maini and Agrawal, 2007)

To compensate for these errors, and so to achieve the level of accuracy required for topographic surveying and other engineering applications, a method called differential GPS (DGPS) is employed. DGPS involves the use of a stationary base receiver and one or more mobile rover receivers. The foundation of DGPS is that the location of the base receiver is precisely known. The base measures the timing errors for each satellite at this receiver using its known coordinates and from the accumulated errors

a correction signal is generated. This signal is transmitted to the rover receiver thus allowing the rover position to be measured to a high degree of accuracy (Figure 6.2).

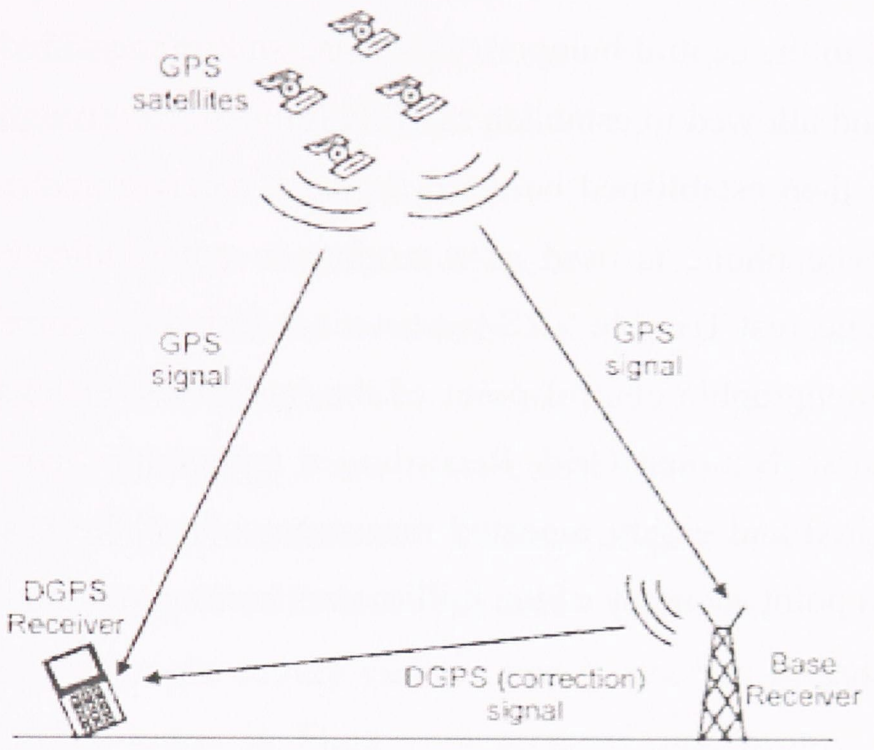


Figure 6.2: Conceptual operation of differential GPS surveying system ((Maini and Agrawal, 2007)

During Real Time Kinematic (RTK) surveys the corrections are transmitted in real time to the rover. This allows the immediate correction of GPS data and accuracies of up to one centimetre to be achieved on site without the need for post processing (Kavanagh, 2009; Uren and Price, 2006). All GPS surveys carried out as part of this research used DGPS RTK surveying.

6.2.1. DGPS Field Surveying

During the summer of 2007 GPS surveying was carried out using a Trimble model 4700 GPS system (*Figure 6.3* (a)). In early 2008 a Trimble R6 GPS System equipped with the Virtual Reference Station (VRS) hardware and software was purchased (Figure 6.3 (b)). This allowed all surveys to be referenced to the Irish National Grid without the need to locate existing benchmarks in the survey area. A combination of the R6 and 4700 GPS systems were used to carry out subsequent surveys. Both systems have identical levels of accuracy and so results obtained with each system were compatible.

The procedure to carry out a GPS survey is outlined below. Initially the base station is set up at a high point within the turlough basin and clear of any obstructions such as trees or bushes. The base receiver is placed on top of the tripod, levelled and distance from the ground to the central bumper of the base station measured. The base receiver is powered up and allowed to establish satellite links to get a rough fix on its position. A connection is then established between the base receiver and a Bluetooth enabled mobile phone. The phone is used as a modem to communicate between the base receiver and the nearest Trimble VRS base station. Using the correcting data from the VRS station a topographic control point of the base receiver location is determined relative to the Irish National Grid. Recording a topographic control point involves taking one hundred and eighty repeated measurements of the base receiver location until a minimum point accuracy of ten millimetres horizontally and fifteen millimetres vertically is achieved.



Figure 6.3: (a) Trimble 4700 GPS system and (b) Trimble R6 GPS system

Once this has been completed, the external radio is connected to the base receiver and a new RTK survey started. The location of the base receiver is entered as determined during the VRS survey and the transmission of error corrections by the base station started. The connection between the base station and rover receiver is then initialised. The rover is located on top of an adjustable surveying staff with which topographic

survey points are taken. The height of the rover is read from the staff, generally two metres, and inputted into the controller. At each point required on the survey the rover was held vertically by means of a bubble level and the point taken. The recording of a point involved the taking of five readings and once the root mean squared (RMS) error between these readings does not exceed a predetermined limit the point is stored. If this limit is exceeded the point must be retaken. The RMS error corresponded to a horizontal accuracy of at least twenty millimetres and twenty five millimetres vertically, but with accuracies down to fifteen millimetres regularly achieved. To obtain this generally required contact with seven satellites or more. Point density depended on the terrain variability. Points were taken at approximately ten to fifteen metre intervals in areas of gentle undulation. In areas of greater topographic variation (such as estavelles) a spacing of as little as one metre was used. An example of point density for Blackrock turlough, county Galway can be seen in Figure 6.4. Note how point spacing was much lower in Figure 6.4 area (a) than in area (b) as area (a) contained a steep sided channel entering the turlough whereas area (b) consisted of gently undulating terrain.

A temporary benchmark (TBM) was established at each site above the highest recorded water level. As the survey of each site normally took a number of days to complete, the TBMs were surveyed at the start and end of every day to ensure stability during the day. As the process of setting up the base receiver had to be repeated on each day of surveying, the TBM also ensured consistency between datasets collected on different days. Points were taken on average every fifteen to twenty metres but depended on the topography; the higher the variability the greater the point resolution. The upper boundary of the survey was defined by the maximum water level recorded during the monitoring period.

Often natural barriers such as woodland or impassable marl deposits were present within the boundary of the turlough, which prevented an area being surveyed in detail. Areas of open water shallower than 1.5 metres were surveyed using chest waders or a wetsuit if necessary. A canoe was used to take a limited number of points in areas of deeper water. When encountering woodland, points were taken at breaks in the canopy within the woodland, or transects in clear ground beyond it taken and used to define the upper bound. Upon completion the topographic dataset was downloaded

from the controller in .CSV file format for further processing. In total over twenty thousand topographic points were taken with an average of over one thousand points per turlough. A summary of the surveys is given in Table 6.2.

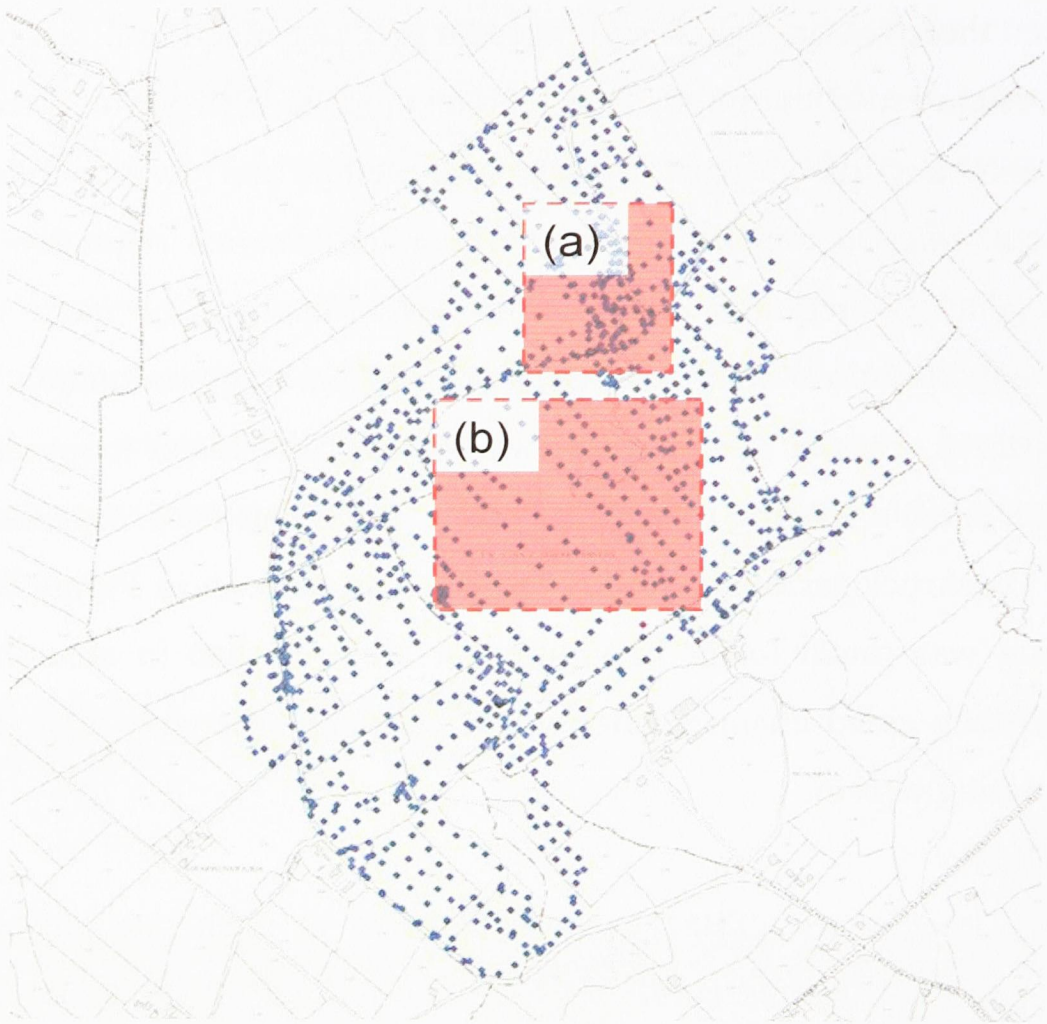


Figure 6.4: (a) area of high point density and (b) area of gently undulating terrain with low point density, Blackrock turlough, Co. Galway

ID	Site Name	Max Stage (mAOD)	No. of Points	Range (m)			Spacing	
				X	Y	Z	Mean (m)	Standard Deviation (m)
2	Ardkill	39.78	960	580.0	730.6	12.6	10.6	6.6
21	Ballinderreen	14.66	1571	1380.9	1208.3	9.3	12.8	8.5
11	Blackrock	26.40	1323	915.3	1344.2	19.9	12.2	8.2
8	Brierfield	92.53	1056	1269.0	1362.9	8.7	14.0	8.1
14	Caherglassaun	10.51	1554	1686.2	1077.1	19.4	11.3	7.4
10	Caranavoodaun	24.53	1043	1190.5	636.7	10.6	10.6	6.6
7	Carrowreagh	86.89	739	1436.5	814.5	12.9	15.5	8.4
4	Coolcam	84.94	630	1064.3	1424.9	9.2	12.2	7.3
5	Croaghill	81.16	1091	1167.0	982.8	9.2	13.0	7.5
13	Garryland		645	669.3	666.8	7.1	10.8	7.8
3	Kilglassaun	35.27	1028	1004.8	1785.0	12.1	13.3	8.0
19	Knockaunroe	30.46	1663	1540.1	1412.8	14.1	12.4	8.2
9	Lisduff	50.00	740	977.7	1326.1	4.8	17.2	8.7
20	Lough Aleenaun	78.32	880	909.2	427.0	16.5	9.1	6.4
12	Lough Coy	18.36	1011	635.9	815.3	16.6	8.5	6.0
18	Lough Gealain	30.90	1020	964.0	982.9	9.9	11.8	8.9
6	Rathnalulleagh	81.40	654	1125.3	713.1	12.0	12.5	8.0
16	Roo West	15.38	945	1124.8	863.5	11.3	12.7	7.3
1	Skealoghan	34.10	690	933.8	753.7	8.3	13.5	7.0
15	Termon	22.60	831	1115.5	992.5	10.2	13.7	6.9
17	Turloughmore	30.16	937	766.3	1399.1	10.1	12.0	7.6

Table 6.2: Summary of DGPS survey data

6.2.2. Water Level Correction

The elevation of each Diver was surveyed to ensure accurate barometric compensation and adjustment of water level time series data to ordnance datum. Diver elevations during the 2006 / 2007 flooding period were tied in to the TBM at each site using the Trimble 4700. The TBMs were later adjusted to mAOD using a Trimble R6

VRS survey. When a Diver was recovered during an inundation period the water level was recorded with the Trimble R6 to allow the alignment of the time series before and after recovery as it was impossible to replace the diver in the exact position.

6.3. Digital Terrain Modelling

Digital terrain modelling is defined as a "form of computer surface modelling which deals with the specific problems of numerically representing the surface of the earth" (Kennie and Petrie, 1990). Digital terrain modelling is a way to represent topography and has a wide variety of applications across the fields of hydrology, geomorphology and biology (Davis, 1990; Moore et al., 1991; Moran et al., 2008). It allows useful quantities such as slope, volume, planar and surface area to be derived. In the context of this research project, digital terrain models (DTM) are required for a variety of purposes. Hydrologically, DTMs provide a way to transform water level data into flooded areas, volumes and the associated flow rates. Ecologically, DTMs aid in the determination and representation of depth, duration and frequency of flooding, factors shown to be of great importance to the diversity and characteristic ecology of wetlands (Reynolds et al., 1998; Sheehy Skeffington et al., 2006; White, 1984) .

The elements required for a DTM are a finite number of reference points such as GPS points. Interpolation or "gridding" is then used to predict or extrapolate the elevation at unobserved locations based on known elevations at a set of reference points. The process of gridding involves producing a regularly spaced, rectangular array of elevation values from irregularly spaced field data. Gridding allows the extrapolation and interpolation of elevation (z) values for points at which no field data exists. A grid consists of evenly spaced rows and columns with each intersection of row and column known as a grid node (Figure 6.5). Rows contain nodes with equal Y coordinates while columns contain nodes with equal X coordinates. The rows and columns themselves are known as gridlines. The distance between gridlines is known as the grid density or grid resolution.

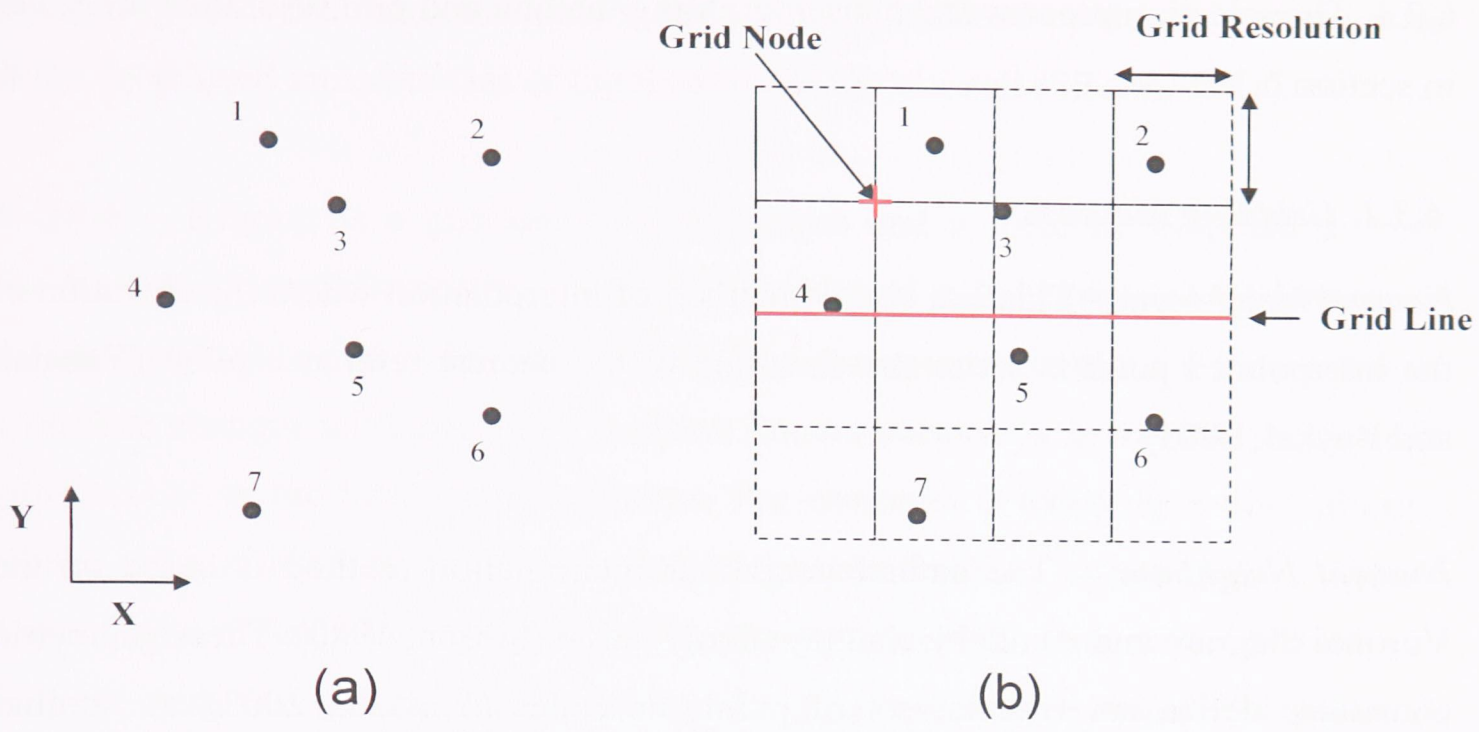


Figure 6.5: (a) GPS points and (b) Points with overlapping grid of evenly spaced rows and columns

Gridding methods can be roughly partitioned into two classes, exact interpolators and smoothing interpolators. If a point coincides exactly with a grid node an exact interpolator will assign the z value of the point to the node. In other words, in the interpolation process the coincident point will have a weight of 1.0 while all other points have a weight of 0. By increasing the grid resolution the likelihood of points and grid nodes coinciding is greater. Smoothing interpolators do not assign weights of 1.0 to any point, even if that point coincides exactly with the grid node being interpolated; instead they assign weights to produce a smoother, more natural surface.

Three factors have been shown to affect the accuracy of DTMs: point distribution gridding method and grid resolution (Heesom and Mahdjoubi, 2001; Thompson et al., 2001; Yanalak, 2003). Point distribution is dependent on the density of points taken during the GPS surveying (section 6.2). A wide variety of interpolation algorithms exist for interpolation of DTMs. To determine the most appropriate for use in modelling turloughs, eight common methods (nearest neighbour, natural neighbour, kriging, multiquadric, triangulation with linear regression, polynomial regression, local polynomial and minimum curvature) were tested using the Surfer® version 8.6 software. A brief description of the theory behind each method is given in section

6.3.1. The selection process and chosen gridding method and grid resolution are given in section 6.3.2.

6.3.1. Gridding Methods

Nearest Neighbour – This is a simple method of interpolation where the elevation of the interpolated point is set to the elevation of the nearest reference point (Yanalak and Baykal, 2003).

Natural Neighbour – The natural neighbour interpolation method is based on the Voronoi diagram and its dual Delaunay triangulation (Sibson, 1980). These geometric constructs define an irregular set of points or nodes (Yanalak, 2003). A familiar practical application of this can be found in the Thiessen polygon method used in the spatial analysis of rainfall data (Shaw, 1994).

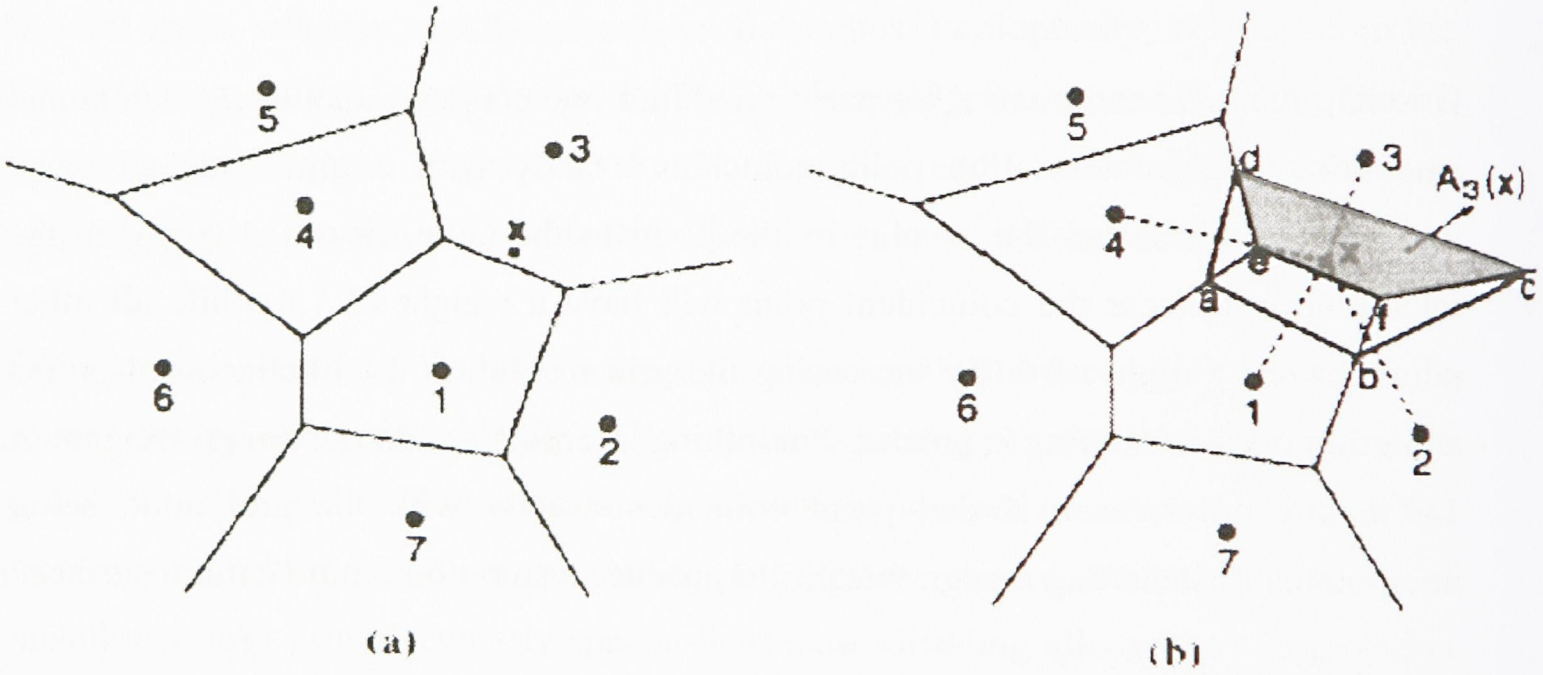


Figure 6.6: (a) Voronoi Diagram for Set of 7 Nodes and x and (b) First and Second Order Voronoi Cells about x (Yanalak, 2003)

Figure 6.6 (a) shows the Voronoi diagram generated from a set of 7 nodes (numbered 1 – 7). The boundaries of the Voronoi cells are defined by the bisectors of the lines joining adjacent nodes. If the point *x* is introduced and the procedure repeated a new first order Voronoi cell (polygon *abcd*) is created which is a composite of second order Voronoi cells (polygons *abef*, *bcf*, *cdef* and *aed*) (*Figure 6.6 (b)*). The area of the second order cells are known as "borrowed areas" as they already formed part of

an existing cell. The value assigned to the point x is defined by the ratio of the areas of the "borrowed areas" to that of the first order Voronoi cell (Sibson, 1981).

Kriging – Kriging is a geo-statistical technique and a form of weighted average estimator (Golden Software Inc, 2002). The principal tool in kriging interpolation is the variogram (Lloyd and Atkinson, 2001). The variogram provides a measure of how a variable changes with direction. It allows known anisotropy in the data to be taken into account in the interpolation process. For example, if mapping a vertical cross section of stratified rock the data might be weighted to favour points aligned horizontally rather than vertically. The variogram itself is a three dimensional function with two independent variables (the direction θ, the separation distance h) and one dependent variable (the variogram value $\gamma(\theta,h)$) (Golden Software Inc, 2002). A mathematical model is fitted to the variogram and the coefficients of the model are used to assign the optimal interpolation weights (Lloyd and Atkinson, 2001). All kriging interpolation was carried using point kriging and the default Surfer® linear variogram. A derivation and detailed discussion of this method is outlined in Cressie (1991).

Multiquadric Interpolation – The multiquadric interpolation method falls within the range of radial basis functions, a range of complex mathematical interpolation methods. First a trend surface is fitted to the data points, normally a 1^{st} or 2^{nd} order polynomial (Yanalak and Baykal, 2003). The residuals for this trend surface are then calculated. The basis kernel functions define the weights applied to the data points when interpolating a grid node, and are comparable to the variogram used in kriging (Golden Software Inc, 2002). The multiquadric basis kernel function takes the form:

$$B(h) = \sqrt{h^2 + R^2} \qquad \textit{Equation 6.1}$$

Where h is the anisotropically rescaled, relative distance from the point to the node and R^2 is the predefined smoothing factor. Refer to Hardy (1990) for a complete discussion of the multiquadric method.

Triangulation with Linear Regression – This interpolation method creates a net of triangles by joining up the GPS points using the Delaunay optimal triangulation algorithm to make non-overlapping triangles. An example of triangulation for Blackrock turlough, Co. Galway is shown in Figure 6.7.

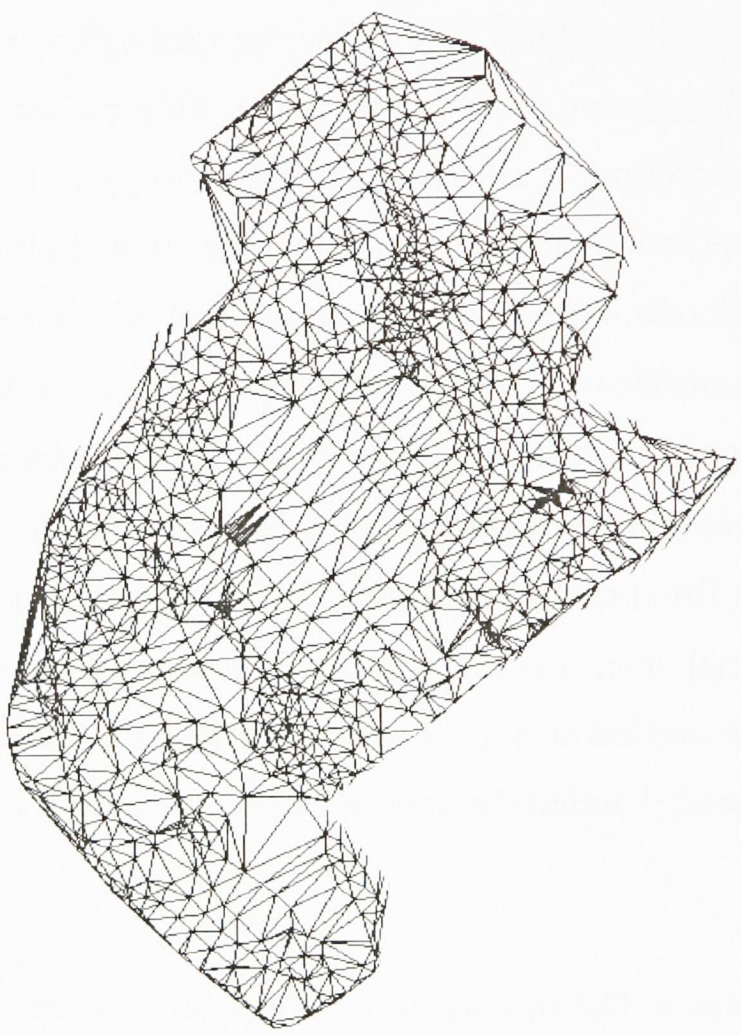


Figure 6.7: Delaunay triangulation of topographic points in Blackrock turlough, Co. Galway

The vertices of each triangle define a plane z given by:

$$z = a_{00} + a_{01}x + a_{10}y \qquad \textit{Equation 6.2}$$

Where the coefficients a_{00}, a_{01} and a_{10} are calculated using the vertices values (Yanalak, 2003). The elevation of any point (or grid node) lying within the triangle can be found using this linear regression formula.

Polynomial Regression – Polynomial regression is useful in identifying general patterns and trends in the data but is of limited use as an interpolator (Draper and Smith, 1981). Polynomial regression represents the surface using a single n^{th} order polynomial. The elevation f(x, y) at any point on the surface is given by:

$$f(x,y) = \sum_{k=0}^{n} \sum_{\substack{i=0 \\ j=k-i}}^{k} a_{ij} x^i y^j \qquad \textit{Equation 6.3}$$

Surfer® allows the generation of up to third degree polynomials, with the polynomial coefficients a_{ij} fitted by minimising the residuals using the least squares method.

Local Polynomial – This interpolation method has the same theoretical basis as polynomial regression, except instead of fitting n^{th} order polynomial to the entire dataset it only uses data points located within the search ellipse of the grid node. The search ellipse defines an area surrounding the grid node, the default in Surfer® 8 being a circle. If a data point lies within the ellipse it is included in the polynomial calculation. Weights assigned to data points are higher the closer they are to the grid node.

Minimum Curvature – The minimum curvature interpolating method is based on the minimisation of the curvature of a surface at the grid points (Yanalak and Baykal, 2003). Surfer® uses an iterative procedure as described by Smith and Wessel (1990). First a planar model of the form:

$$Z(X,Y) = aX + bY + C \qquad \textit{Equation 6.4}$$

is fitted to the data using least squares regression. The differences or residuals between the regression plane and the original data values are calculated. An iterative procedure of interpolating the residuals using the minimum curvature algorithm (Briggs, 1974; Smith and Wessel, 1990) is used to interpolate the residuals at the grid nodes. The iterations are continued until the difference between two consecutive iterations is less than a predefined maximum residual. The iterated residuals are then added to the original regression plane to construct the interpolated final surface.

6.3.2. Gridding Method and Grid Resolution Selection

An initial evaluation of the eight various gridding methods was carried out using the Blackrock topographic coordinate dataset. A grid and associated contour map was

generated using each method (Appendix A). While five methods produced visually similar and realistic contour maps, three methods (nearest neighbour, local polynomial and polynomial regression) produced physically unrealistic, over-simplified surfaces and so were disregarded for further analysis. Statistical methods from relevant literature (Heesom and Mahdjoubi, 2001; Li, 1992; Yanalak, 2003; Yanalak and Baykal, 2003) were used to further assess accuracy of the various gridding methods. Using the Blackrock dataset, grids were generated for the five remaining methods at a range of grid resolutions: 13.5 m, 5 m and 2 m. The absolute residual mean and standard deviation were calculated for each gridding method at each grid resolution (Table 6.3).

Gridding Method	Residual Mean (m)			Residual Standard Deviation (m)		
	2	5	13.5	2	5	13.5
Natural Neighbour	0.039	0.089	0.203	0.063	0.143	0.306
Kriging	0.030	0.073	0.185	0.048	0.117	0.288
Multiquadric	0.006	0.034	0.193	0.015	0.091	0.461
Triangulation	0.033	0.081	0.198	0.054	0.133	0.302
Minimum Curvature	0.044	0.103	0.246	0.074	0.159	0.356

Table 6.3: Mean and standard deviation of residuals for a range of gridding methods and grid resolutions, Blackrock turlough, Co. Galway

A significant improvement was found by increasing the resolution from 13.5 m down to 2 m. Kriging and multiquadric interpolation consistently showed the lowest mean residuals, with multiquadric showing the lowest overall at high grid resolution (*Figure 6.8*). A direct comparison of kriging and multiquadric interpolation was then carried out.

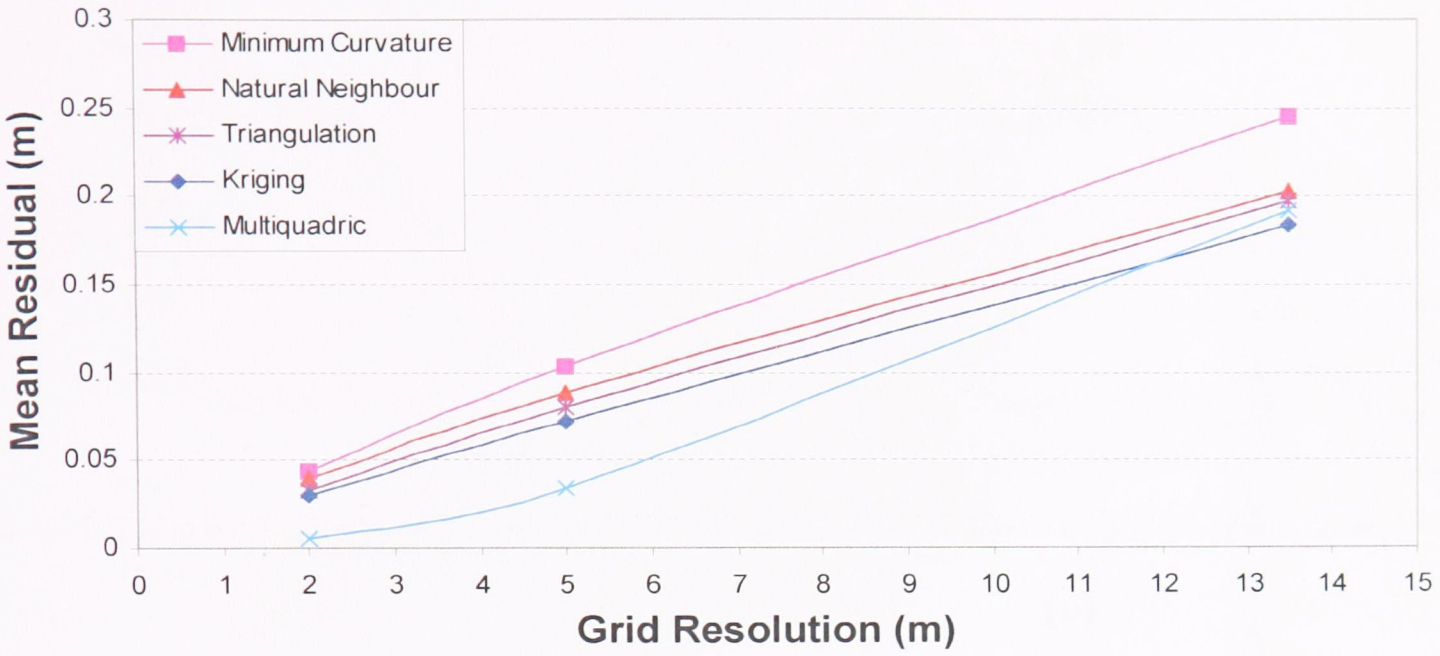


Figure 6.8: Variation of residuals for a range of gridding methods and grid resolutions, Blackrock turlough, Co. Galway

Grids with 1, 2, 4, 6 and 10 m grid resolution were created using topographic datasets for Termon, Turloughmore, Caranavoodaun and Rathnalulleagh. A significant improvement was found from 10 m down to 2 m grid resolution after which the improvement was minimal. While the multiquadric method showed a lower residual mean and standard deviation, upon visual inspection of the contour maps it generated unrealistic physical features and contours at higher grid resolution (Figure 6.9). In contrast, kriging produced low residual mean and standard deviation as well as realistic topographic maps at high grid resolution, and so kriging at 2 m grid resolution was chosen for all DTM work.

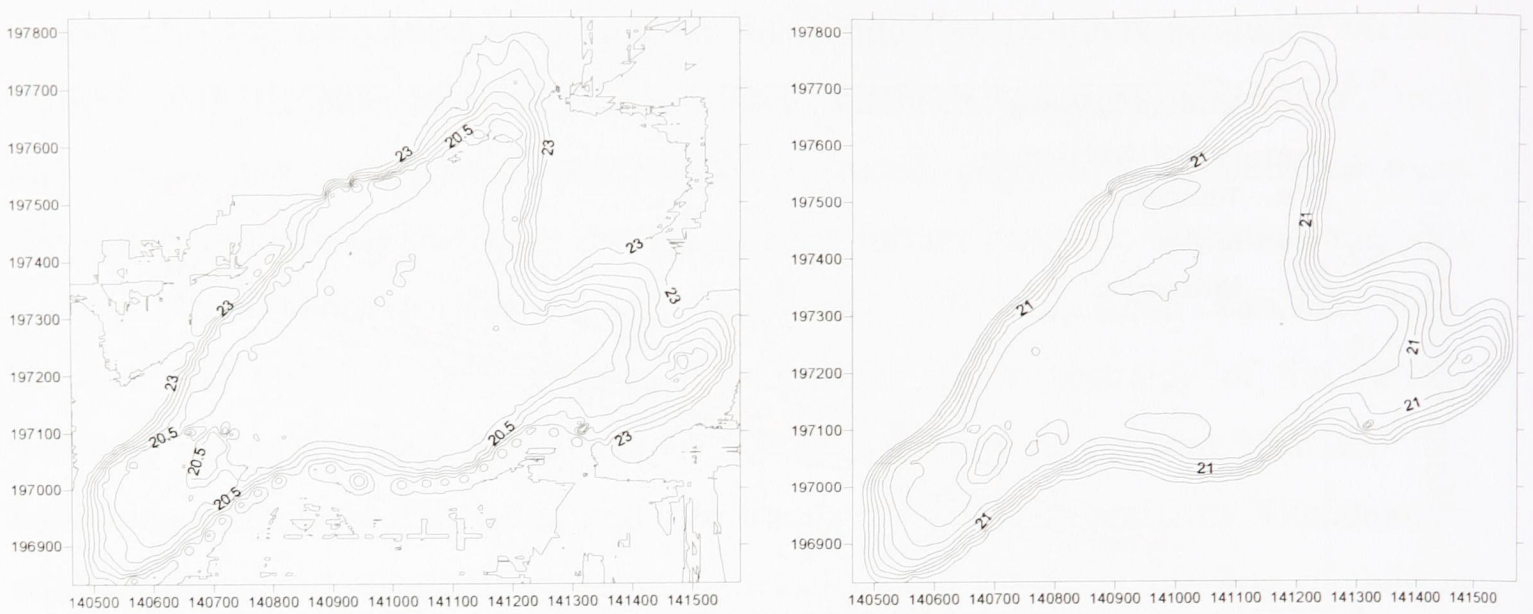


Figure 6.9: Contour map of Termon at 1 metre grid resolution using (a) Multiquadric Interpolation and (b) Kriging

6.3.3. Contour Maps

Once the surface has been computed the software was used to produce contour maps, as shown for Lough Gealain turlough in Figure 6.10. These were also combined with a wireframe plot to give a 3-D representation of each turlough (Figure 6.10). The duration and frequency flooding for each contour can be calculated from water level time series and combined to give duration and frequency maps. The contour plots and 3-D surfaces of all of the turloughs are given in Appendix A.

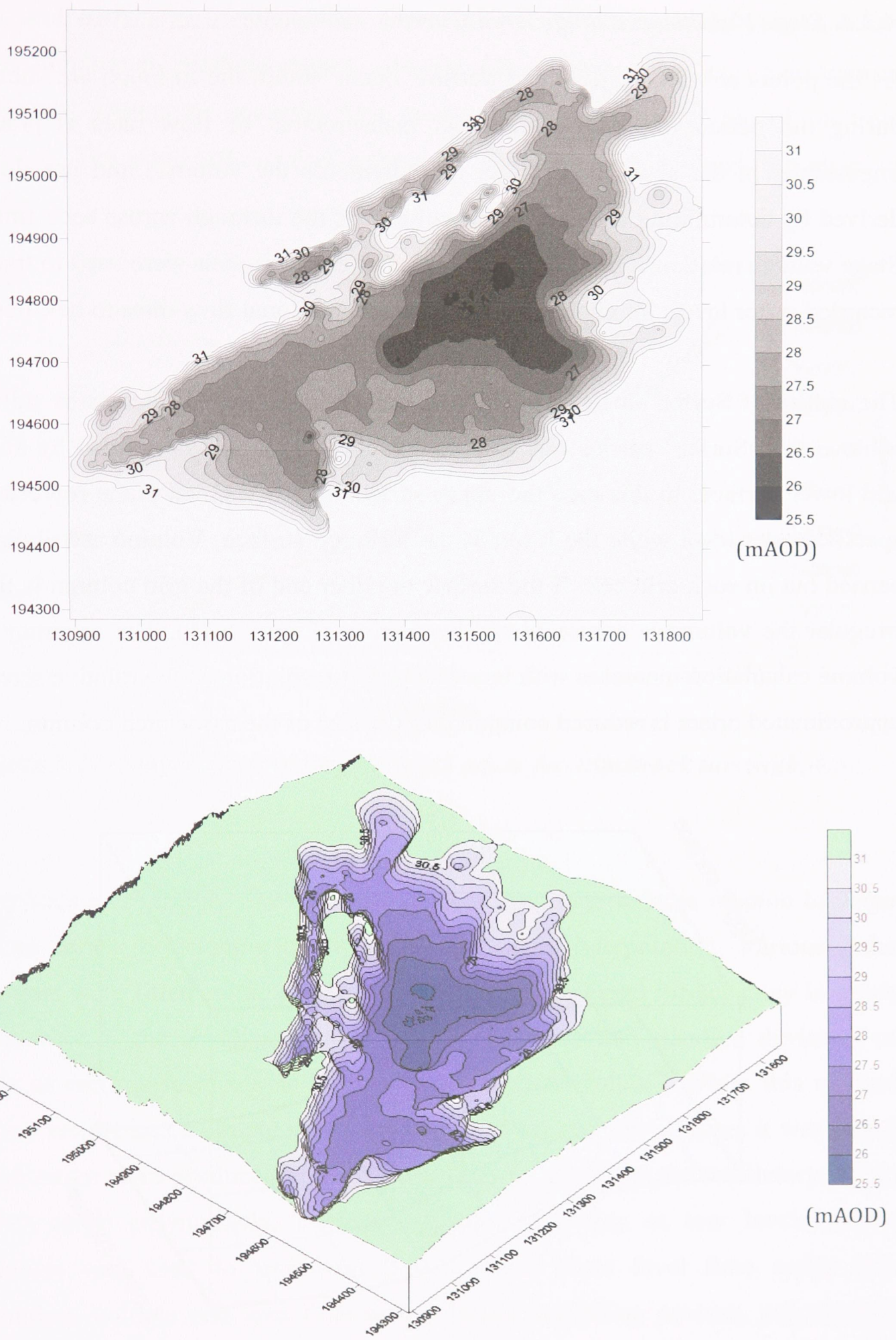


Figure 6.10: Contour map (top) and 3D terrain model (bottom) of Lough Gealain, Co. Clare

6.3.4. Stage Volume and Stage Area Curves

As the points at which inflow and outflow occur within the turlough are submerged during the period of inundation, direct measurement of flow rates is practically impossible. In the absence of direct measurements the volumes and net flows are derived by determining the changes in volume of the turlough across each time step. Stage volume relationships derived from digital terrain models were used to transform recorded water levels into volumes, thus allowing notional flow rates to be calculated.

The ability of Surfer® 8 to compute volumes between two surfaces was utilised to achieve this. Surfer® carries out volume calculations on solids defined by an upper and lower surface. In this case the upper surface is a horizontal plane representing a specific water level while the lower is the turlough surface. Volume calculations are carried out on each grid cell. If the surface at either end of the grid column is tilted or irregular the volume is approximated by a prism (Figure 6.11). The accuracy of the volume calculation increases with increasing grid resolution as the relative size of the approximated prism is reduced compared to the size of the associated column.

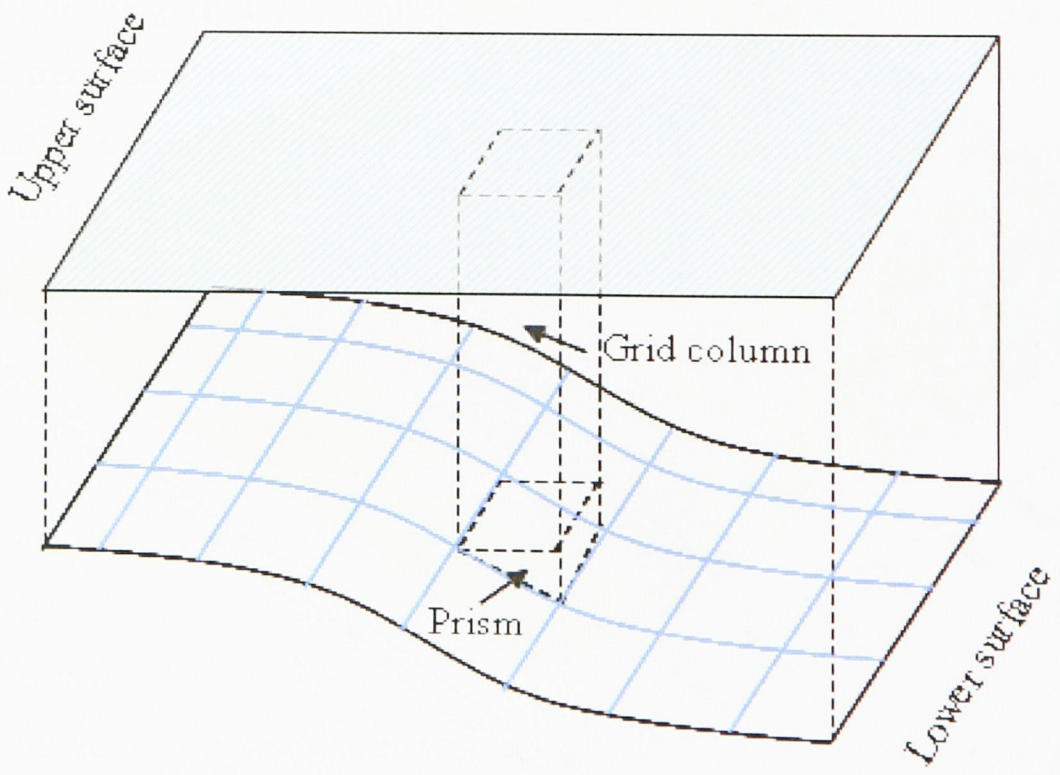


Figure 6.11: Solid used in volume calculation between surfaces for grid cell

Volume and surface area calculations were carried out at 2cm intervals across the range of flooding to produce stage – volume curves (Figure 6.12). A SurferScript program was written to automate this process and perform and record multiple calculations. The stage volume and stage area curves for each turlough are given in Appendix A.

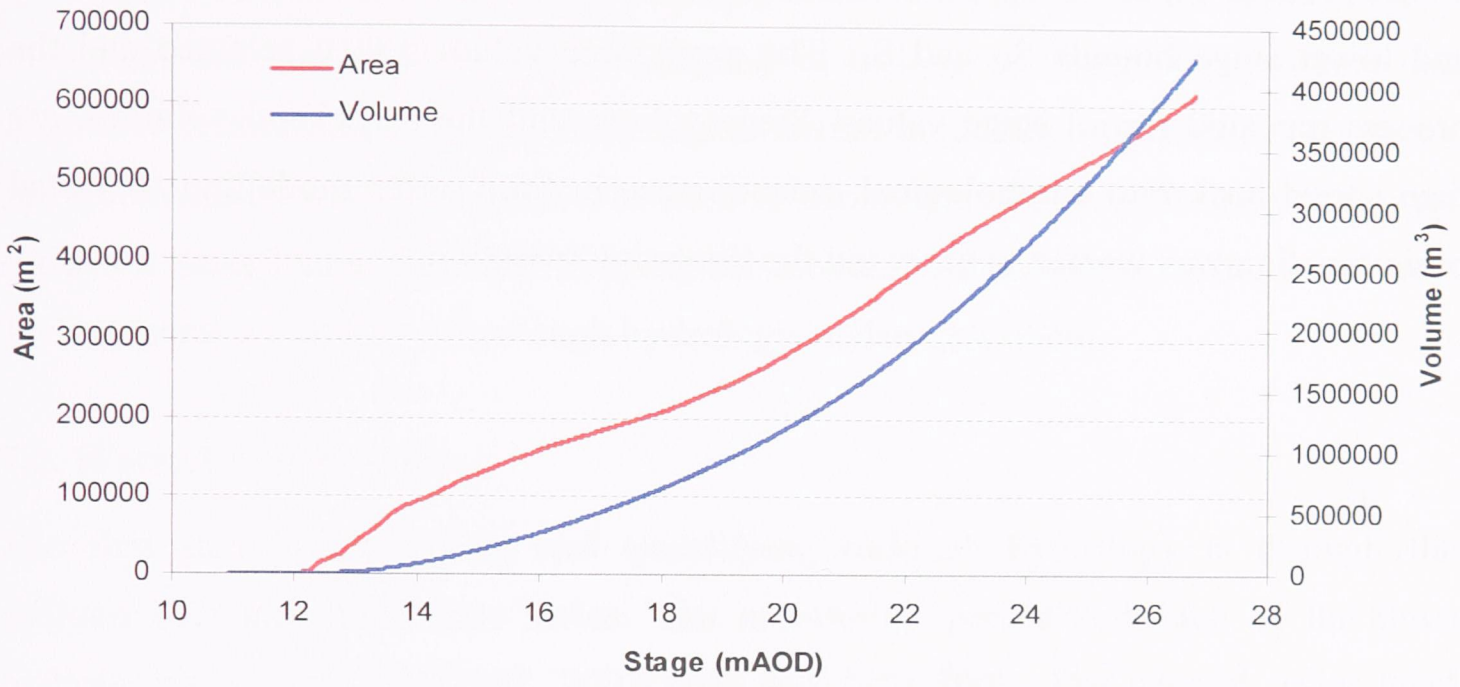


Figure 6.12: Stage area and stage volume curve for Blackrock turlough, Co. Galway

Two methods were trialled for the application of the stage volume relation to water level time series: polynomial curve fitting and linear interpolation. Various order polynomials were fitted to the depth-volume data and assessed for accuracy in much the same way as the gridding methods, using the mean and standard deviation of residuals as well as residuals as a percentage of actual volume. While this method gave good results and a simple way to transform from stage to volume, it was found that large errors were produced at the lowest water levels due to the oscillatory nature of higher order polynomials. Because of this inaccuracy at low levels, linear interpolation was used to transform the recorded water level time series into corresponding volume and area time series. In the modelling process, polynomials were used to convert volume back into stage due to their ease of use.

The linear interpolation process is as follows. First the data was sorted in order of ascending stage values. Next the interval within which the stage value to be

transformed (S) was defined by the upper stage bound S_U and lower bound S_L. These bounds were found by stepping through the stage – volume dataset until S lay between S_U and S_L. The volume V corresponding to stage S is given by:

$$V = V_L + (S - S_L)\frac{V_U - V_L}{S_U - S_L} \qquad \textit{Equation 6.5}$$

Where V_L and V_U are the upper and lower volume bound corresponding to the upper and lower stage bounds S_U and S_L. The next stage value is then selected and the process repeated for all stage values. Stage values, and the associated volumes, are then sorted back into chronological order for use in time series modelling. A visual basic function was written to carry out the linear interpolation.

CHAPTER 7. HYDROLOGICAL ANALYSIS: FLOODING REGIME

7.1. Introduction

Water level time series collected for 21 study sites are compared and analysed to gain an insight into the hydrological functioning of turloughs. Using stage-volume and stage-area relationships derived from digital terrain modelling, time series of volume and flooded area were generated. The diverse behaviour of turloughs as hydrological entities is described and quantified using the metrics of flood depth, volume and area. The temporal variability of turlough hydrology is also described.

7.2. Water Level Profiles

The first step in classifying and quantifying turlough hydrology is through the analysis of water level time series. The monitoring period consisted of the three hydrological years: 2006/2007, 2007/2008 and 2008/2009. The general water level profile recorded during the 2006/2007 and 2007/2008 hydrological years demonstrated what is often considered typical turlough flooding behaviour. In 2006, water levels began to rise in mid-September, reaching a peak in December and another towards the end of January, with emptying occurring from April onwards. The highest water level recorded in the more flashy turloughs such as Lough Aleenaun, Turloughmore and Blackrock coincided with the first mid December peak, while the majority of the other sites displayed a seasonal maximum during late January. A low level flood event took place in July / August 2007 in a number of turloughs due to unusually high rainfall for the period, with floodwaters persisting until mid-September 2007. The subsequent dry period caused a later onset of flooding in the 2007/2008 hydrological year whereby inundation began across all study sites at the end of November. Thereafter, flooding followed the typical pattern as in 2006/2007 year with most peak water levels taking place in February. In contrast, the 2008/2009 hydrological year showed a distinct pattern with low level, long duration flooding consisting of several filling and emptying events taking place throughout the year.

While the maximum flood level over the entire monitoring period occurred during the 2006/2007 year in the majority of sites, others showed the highest overall level during 2007/2008. Turloughs located in the north of the study area, in counties Mayo, Roscommon and north Galway, as well as those in the Gort area, all recorded maximum levels in the 2006/2007 hydrological year. In contrast, turloughs in Co. Clare and around the Ardrahan area in Co. Galway showed maxima in 2007/2008. All sites showed the lowest yearly level of flooding in the 2008/2009 hydrological year.

Within the broadly similar flooding patterns there are some stark contrasts between turloughs. A plot of water level time series from 2006 to 2009, illustrating the general seasonal pattern of flooding, can be seen in Figure 7.1 (b) to (d). The water level hydrographs shown demonstrate the range of flooding regimes observed across the monitored turloughs. Hydrographs for all other sites are included in appendix B. Representative rainfall and evapotranspiration records for the period shown in Figure 7.1 (a). At one end of the flooding regime continuum is Turloughmore, Co. Clare (Figure 7.1(b)), which displays a multimodal flooding pattern consisting of a series of rapid filling and emptying events. At the other end of the flooding spectrum are sites such as Coolcam, Co. Galway, which show a single long duration flood event with an extended recession within each hydrological year (Figure 7.1(d)). The regimes of Skealoghan and many others lie somewhere in between these extremes, and possess a wide variety of depth, duration and frequency characteristics.

Some turlough pairs display practically identical water level profiles, such as Garryland and Caherglassaun, Lough Gealain and Knockaunroe, and Rathnalulleagh and Carrowreagh. The sites that show the greatest level of similarity are geographically close to each other suggesting the possibility of hydraulic connections between them allowing simultaneous responses to occur. Other sites within close proximity, such as Ardkill and Skealoghan, have substantially different regimes with Ardkill showing deeper flooding and markedly longer recession characteristics than Skealoghan.

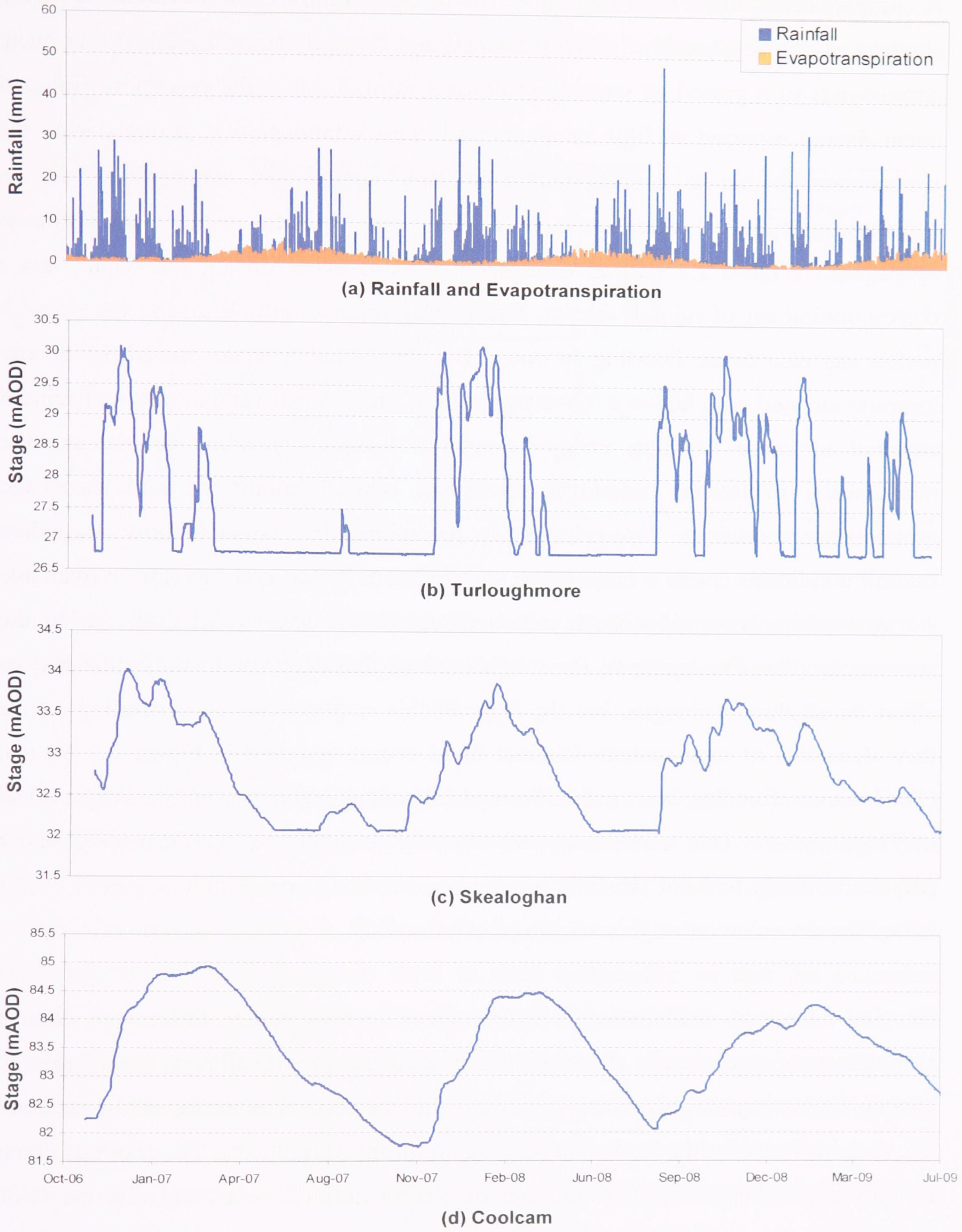


Figure 7.1: (a) Daily Rainfall and evapotranspiration for monitoring period from 2006 to 2009, and water level time series plot for (b) Turloughmore, (c) Skealoghan and (d) Coolcam

A comparison of water level hydrographs with the rainfall record of the same period shows a strong relationship between rainfall and flood dynamics. Each filling event corresponds to a period of intense, prolonged rainfall while the recession limbs all occur during a period of little or no rainfall. This relationship is strong during the winter months due to a combination of high rainfall and lower losses due to evapotranspiration. A clear example of this can be seen in the Turloughmore hydrograph (Figure 7.1 (b)) as each distinct flood event during the winter has a corresponding set of rainfall events. Sufficiently intense rainfall during the summer period can also cause flooding to occur, but on a smaller scale due to the greater losses associated with higher evapotranspiration. The intensity and duration of rainfall required to cause flooding varies between turloughs depending on the specific mechanisms controlling flooding, antecedent rainfall conditions and associated groundwater conditions. This relationship is explored in chapter 8. Low antecedent rainfall conditions create a cumulative soil moisture deficit and increase in available storage within the aquifer itself, which dampens the effect of rainfall during the summer months. For example, the rainfall events that occurred in mid 2007 had an effect on all three turloughs, but the form of this response varied depending on the flow dynamics of each system. Distinct flood events occurred in Figure 7.1 (b) and (c). However, flooding occurred earlier and had a longer duration in Skealoghan than in Turloughmore. Due to the long recession characteristics of Coolcam (Figure 7.1 (d)) the turlough had not yet fully emptied and so the corresponding rainfall events halted the recession rather than causing fresh flooding.

Despite the clear differences in hydrological regime across the study sites, a comparison of peak levels shows similarities in the timing of response to rainfall events. Following the cessation of rainfall the net flow direction quickly becomes negative in flashy turloughs, leading to a rapid fall in water levels. The result of this is a hydrograph characterised by number of clearly defined peaks and discrete flood events. This reversal of flow direction is a much slower process in turloughs like Coolcam. The lower recession rate means that sustained rainfall has a greater cumulative effect on the water level hydrograph in these sites. During a period of little or no rainfall, the level in the turlough drops at a much slower rate than is witnessed in flashy turloughs, leaving the turlough at a relatively high level when rainfall resumes. Thus, while the timing of peak flood levels may be similar across a wide set

of turloughs, the magnitude of the peaks themselves can differ greatly. A demonstration of this is shown using the peak periods 1, 2 and 3 in the 2006/2007 hydrological year (Figure 7.2).

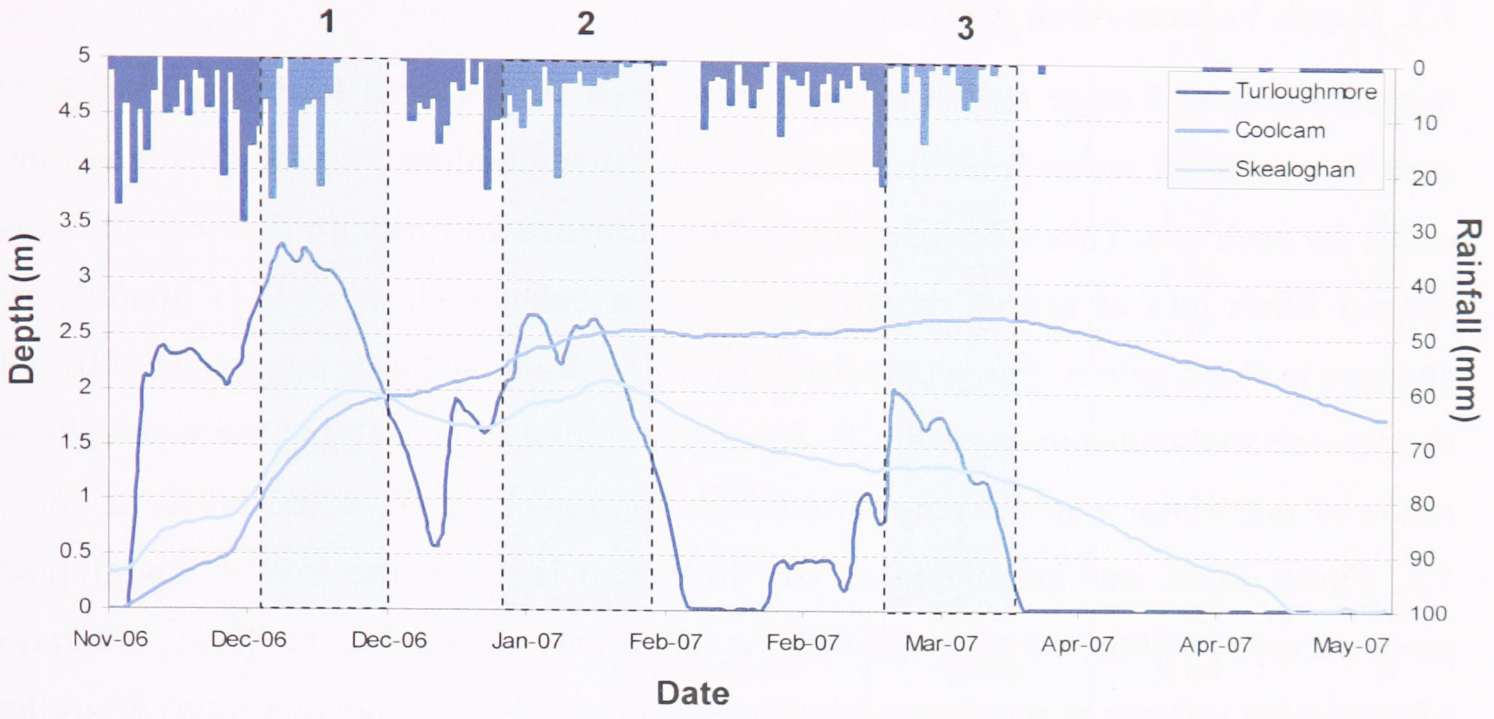


Figure 7.2: Daily rainfall and corresponding peak water levels during the 2006/2007 inundation period for Turloughmore, Skealoghan and Coolcam turloughs

While a peak or significant change in slope occurred in all turloughs during periods 1, 2 and 3, the relative magnitude of each peak was different for each turlough; the annual maximum level occurs in Turloughmore in period 1, in Skealoghan in period 2 and in Coolcam in period 3. Following peak 1 the higher drainage capacity of Turloughmore allowed the water level to drop sufficiently so that the causative rainfall for peak 2 resulted in a lower overall level. While the water level in Skealoghan also fell following peak 1, it was at a slower rate than that of Turloughmore and so when rainfall resumed it caused the highest recorded level in peak 2. Due to the slow recession rate of Coolcam, the water level scarcely dropped following both peaks 1 and 2, and so the cumulative effect of this led to the highest water level occurring during peak 3. This contemporaneous behaviour of peaks has implications for the nature of turlough flow systems. This behaviour generally implies the system is dominated by a confined (pressurised) flow system where changes in pressure are rapidly felt throughout, rather than a phreatic (at atmospheric pressure) system where a lag dependent upon the position of the turlough within the system

would be expected. The relative timing of peak water levels is further investigated in Chapter 8.

7.3. Depth Volume Area Analysis

Stage volume and stage area relationships derived from digital terrain models were used to transform water level time series into corresponding volume and area time series for each site. This allowed a detailed examination of turlough flow dynamics as the net flows into or out of the turlough can be calculated, as well as quantifying changes in flood extent. The plots of water level, volume and area are provided for all twenty one study sites in appendix B. Summary statistics quantifying the turloughs in terms of maximum water depth, volume, area and average depth are given in Table 7.1. Flood depth was calculated as the difference between the lowest topographic point surveyed within the turlough and the maximum recorded water level. The ratio of maximum volume to maximum area (referred to as the volume/area ratio) gives the average depth of water in the turlough basin at the time of the highest recorded water level. The average depth is the average depth recorded at the Diver site across the monitoring period.

The large range of flooding in terms of depth, volume and area demonstrates the great diversity in the characteristics of turloughs as hydrological entities. At one end of the scale lie shallow expansive basins such as Ballinderreen, where the volume/area ratio was only 0.85 metres across an area of almost 60 hectares. At the other extreme lie turloughs occupying steep sided depressions with substantial depths of flooding, such as Lough Coy. Covering only 25 hectares, Lough Coy was one of the smallest turloughs monitored in terms of area but showed one of the highest volumes and volume/area ratios, approximately 1.5 million m^3 and 5.8 m respectively, figures far in excess of those in Ballinderreen and many others.

Site ID	Site Name	Max Depth (m)	Max Volume ('000 m^3)	Max Area ('000 m^2)	Volume / Area (m)	Average Depth (m)
1	Skealoghan	3.2	382.2	326.8	1.17	1.95
2	Ardkill	7.7	652.6	233.4	2.8	4.24
3	Kilglassaun	4.9	809.6	510.4	1.59	3.49
4	Coolcam	4.5	1570.2	781.2	2.01	2.98
5	Croaghill	4.4	636	386.1	1.65	2.92
6	Rathnalulleagh	8.2	877.9	294.6	2.98	2.89
7	Carrowreagh	8.1	546.2	282.5	1.93	3.21
8	Brierfield	4.2	933.5	541	1.73	2.36
9	Lisduff	3.0	771.3	537.4	1.44	1.88
10	Caranavoodaun	3.8	498.5	345.5	1.44	2.25
11	Blackrock	15.4	4008.1	592.9	6.76	6.06
12	Lough Coy	10.6	1479.1	252.6	5.86	5.79
13	Garryland	10.9	2330.4	420.8	5.54	3.28
14	Caherglassaun	9.4	2998.9	626.1	4.79	4.28
15	Termon South	3.7	956	420	2.28	2.39
16	Roo West	5.5	1077.3	409.9	2.63	2.28
17	Turloughmore	3.5	416.5	307.9	1.35	1.03
18	Lough Gealain	4.9	919.9	357.9	2.57	2.84
19	Knockaunroe	5.8	1841.6	788.2	2.34	3.6
20	Lough Aleenaun	5.9	355.6	137.1	2.59	2.55
21	Ballinderreen	4.3	592.6	695.2	0.85	2.95
Range		(3.0 – 15.4)	(355.6 – 4008.1)	(137.1 – 788.2)	(0.85 – 6.76)	(1.03 – 6.06)

Table 7.1: Summary statistics of maximum turlough flood depth, volume, area and average depth

7.3.1. Depth

Water level can either be given in terms of stage (mAOD) or depth (m). Stage is measured in metres above the mean sea level at Malin head, whereas depth is measured above an arbitrary point within the turlough basin. In this case, depth was measured above the lowest measured topographic point within the basin. Stage is a useful measure when comparing water levels between sites, for example to calculate hydraulic gradients, as it is measured above a common datum. However, depth can be

a more useful measure as it allows the comparison of sites by quantifying the within site variations in water level.

Maximum depth of flooding varied substantially between monitored turloughs, reflecting the differences in characteristic flood regime and geomorphology of each site (Figure 7.3). Not all turloughs completely dried up, with some sites containing standing water in low lying areas throughout the year. Flood depths ranged from 3.0 to 15.4 metres with Blackrock turlough, Co. Galway, displaying the greatest fluctuation and Lisduff, Co. Roscommon, showing the least. Broadly speaking the variation in flood depth reflects the topography of the flood basin. Sites showing a low range of flooding tended to be shallow extensive depressions with gentle side slopes, whereas turloughs with a greater flood depth were formed in steeper sided basins. The four highest flood depths were displayed by turloughs forming part of the Gort – Kinvarra chain, a conduit karst system running from the foot of the Slieve Aughty Mountains in the east to springs discharging into Kinvarra Bay in the west. This system combines large quantities of allogenic recharge, extensive catchment area, a high capacity conduit system and relatively deep surface depressions created the conditions for such a high flood range. As mentioned before and can be seen in Figure 7.3 below, the year containing the highest overall flood level varied between turloughs, with the majority of sites recording a maximum in 2006/2007. All sites showed the lowest level of flooding in the 2008/2009 hydrological year.

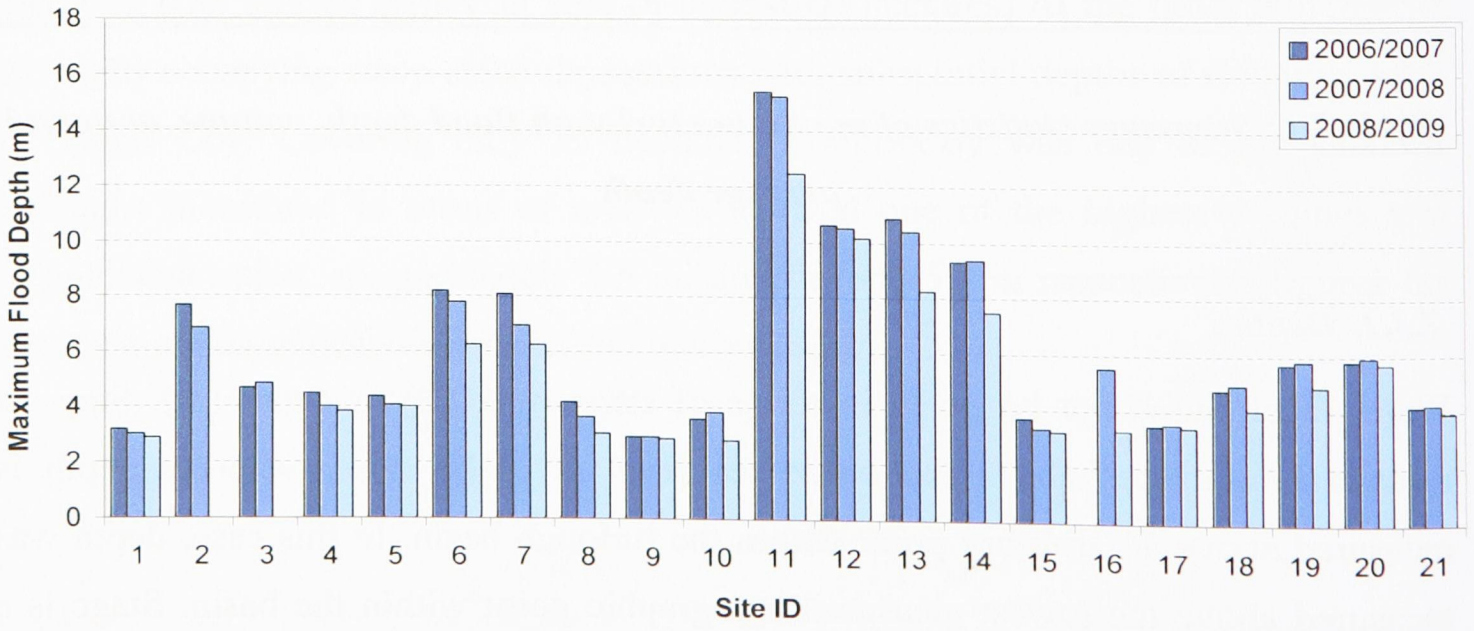


Figure 7.3: Maximum turlough flood depths recorded during the hydrological years 2006/2007, 2007/2008 and 2008/2009

7.3.2. Volume

The maximum recorded volume of each turlough for the 2006/2007, 2007/2008 and 2008/2009 hydrological years is shown in Figure 7.4. There was a greater degree of variation in volume between the study sites than was witnessed between corresponding turlough depths. An order of magnitude difference existed between the largest and smallest sites volumetrically, with Lough Aleenaun filling to around 350,000m^3 compared to the 4 million m^3 of Blackrock. As with the depth data, the turloughs of the Gort – Kinvarra chain showed the highest maxima, with total volumes ranging from 1.5 million to 4 million m^3. The fluctuations in level and volume of Blackrock dwarf those of most other turloughs. In a three day period the water levels rose by approximately six metres with a corresponding inflow of 1.6 million m^3, equating to an average flow rate of 6m^3/s sustained for the entire 3 day period. As the range of volumes is so great, a second plot comparing turloughs whose mean volume was less than 1 million m^3 is given in Figure 7.5.

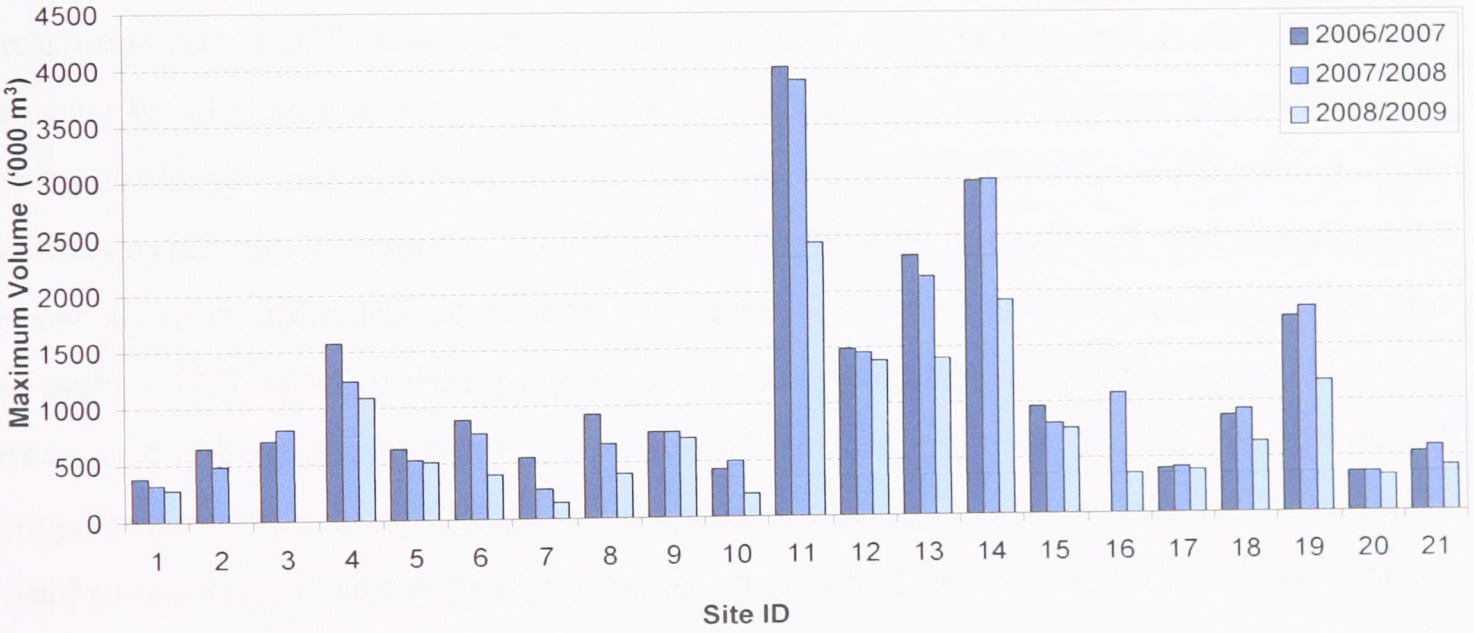


Figure 7.4: Maximum turlough flood volumes recorded during the hydrological years 2006/2007, 2007/2008 and 2008/2009

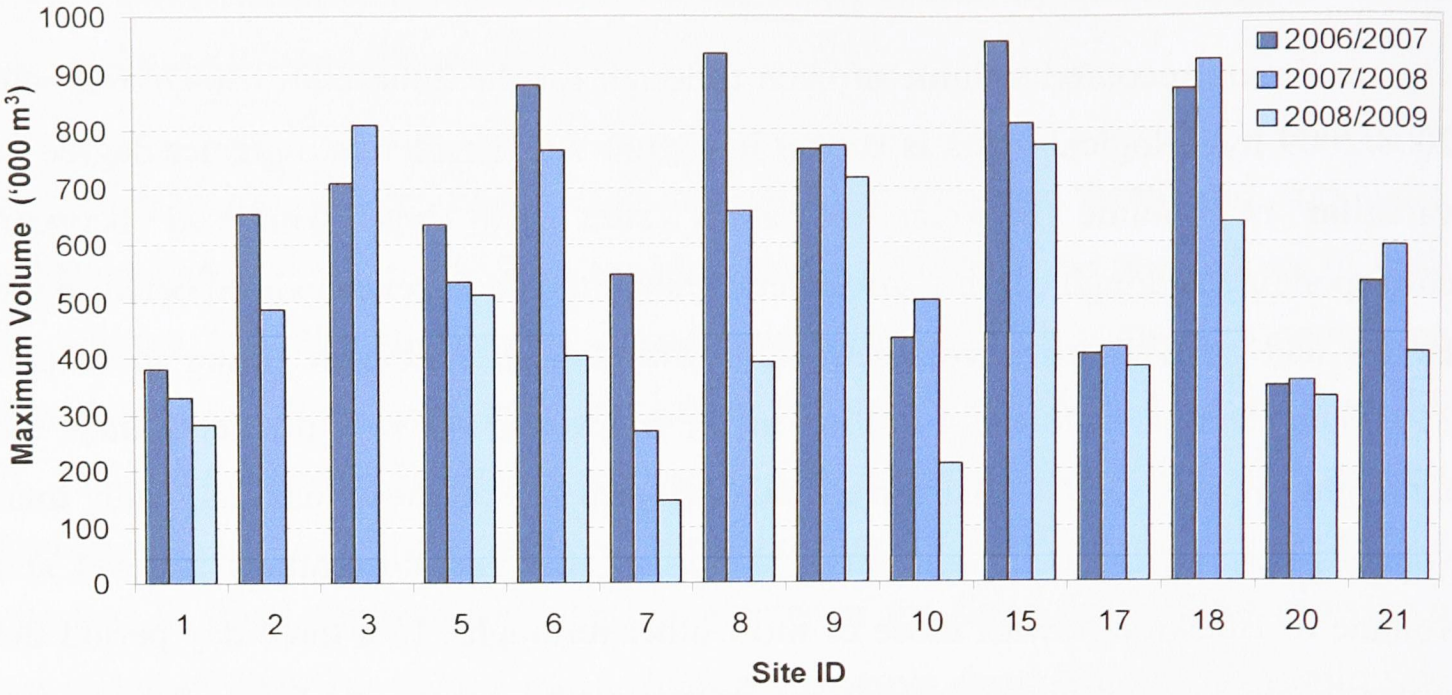
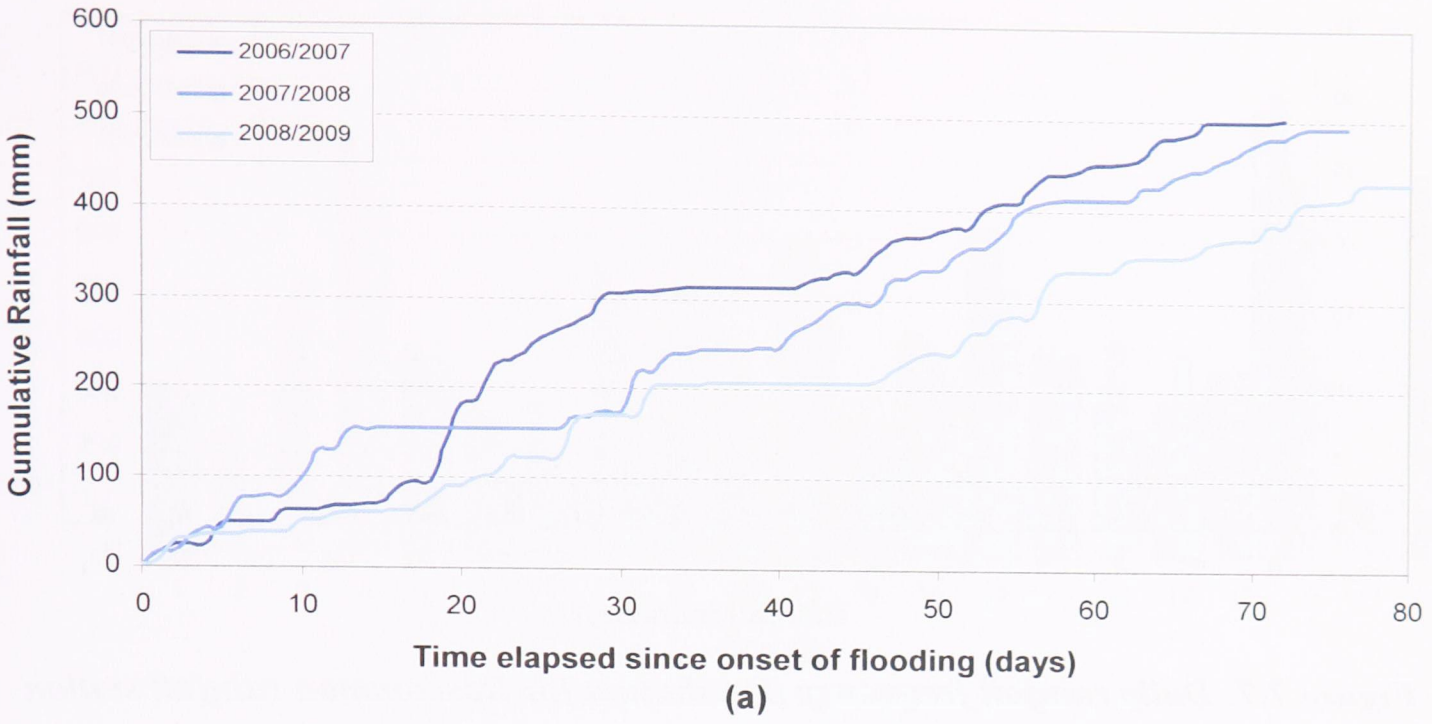


Figure 7.5: Maximum turlough flood volumes under 1 million m^3 recorded during the hydrological years 2006/2007, 2007/2008 and 2008/2009

The most noticeable yearly variation in maximum volume occurred in sites 6, 7 and 8, all sites within a 3km radius of each other in Co. Roscommon. The yearly reduction was particularly acute in site 7, Carrowreagh, with the volume almost halving year on year. A comparison of cumulative rainfall from the Roscommon rainfall station gives some insight into the cause of this decline in maximum volumes. Cumulative rainfall was calculated starting just before the onset of flooding to just after the peak water level. The reason for the lowest flood volume occurring during 2008/2009 is clear as the cumulative rainfall over the period is significantly lower than the other two years (Figure 7.6 (a)). It shows a high frequency of days with little or no rainfall (Figure 7.7) where the turloughs had sufficient time to partially empty and for storage to build up within the system, thus lessening the effects of subsequent rainfall. While the 2006/2007 cumulative rainfall total of 500mm was only marginally higher than that of 2007/2008, the rate at which this was reached was significantly faster occurring a full week earlier in 2006/2007 than 2007/2008. While all years followed the characteristic J-distribution for daily rainfall frequencies, the 2007/2008 hydrological year showed the highest frequency of days with no rainfall (Figure 7.7). These dry periods, represented by horizontal sections within the cumulative rainfall plot, would have facilitated draining of the catchment storage and even partial outflow from the turlough itself, thereby dampening the effect of subsequent rainfall events.



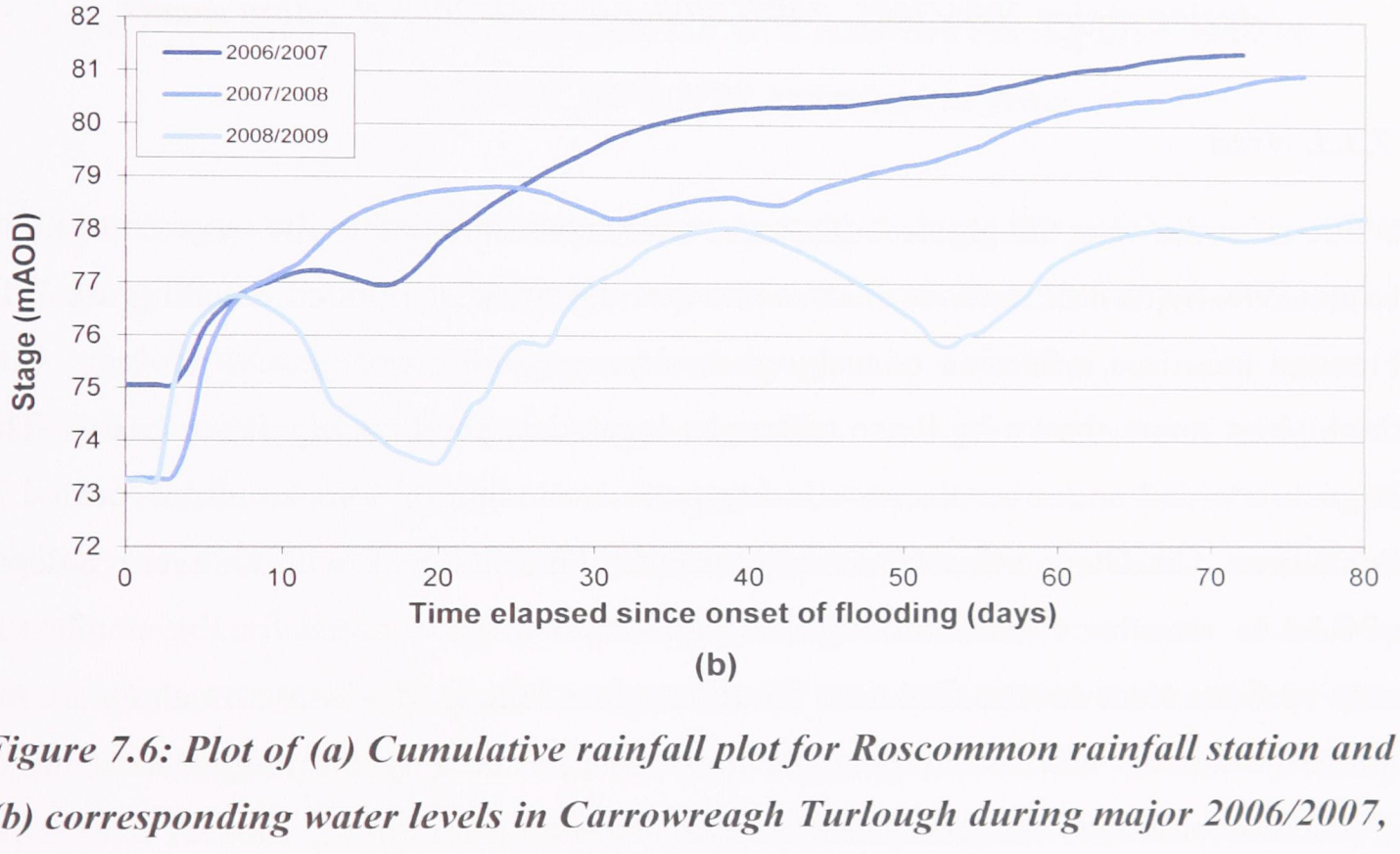


Figure 7.6: Plot of (a) Cumulative rainfall plot for Roscommon rainfall station and (b) corresponding water levels in Carrowreagh Turlough during major 2006/2007, 2007/2008 and 2008/2009 flooding events

Another contributing factor to relative levels in 2006/2007 and 2007/2008 was the antecedent flood conditions. The flood event resulting in the 2006/2007 maximum immediately followed a lesser flood event in September 2006. As a result of this previous event the system would have been close to saturation, with little storage available to dampen the effects of subsequent rainfall events. In contrast, the 2007/2008 flood event followed an extended dry period and so the drainage capacity of the flow systems would not necessarily have been operating at full capacity, and a portion of effective recharge would have been taken up as storage within the system.

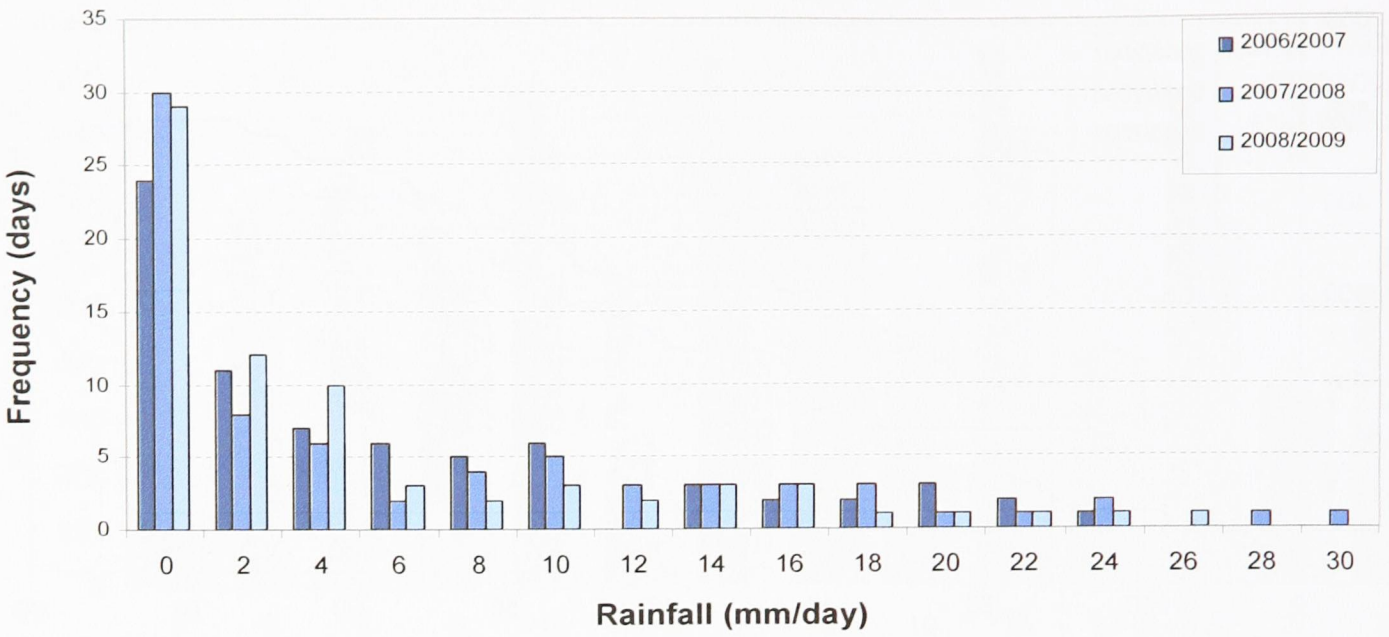


Figure 7.7: Daily rainfall frequency distribution for Roscommon rainfall station during major 2006/2007, 2007/2008 and 2008/2009 flooding events

7.3.3. Area

While sites showing the greatest depth generally corresponded to the largest turloughs volumetrically, a different set of sites showed the greatest flooded area (Figure 7.8). Flooded area is a reflection of turlough basin topography and geomorphology, with the highest areas shown by those turloughs located in shallow expansive basins. The largest recorded area over the monitoring period was that of Knockaunroe, located in the Burren, Co. Clare, which covered almost 80 ha at its peak with an average depth of 2.34 m. Another Burren turlough, Lough Aleenaun, accounted for the smallest at only 13.7 ha. Here for the first time the turloughs of the Gort – Kinvarra chain are not the extreme case with Blackrock, the turlough considerably the largest in terms of depth and volume, ranking only fifth in terms of area.

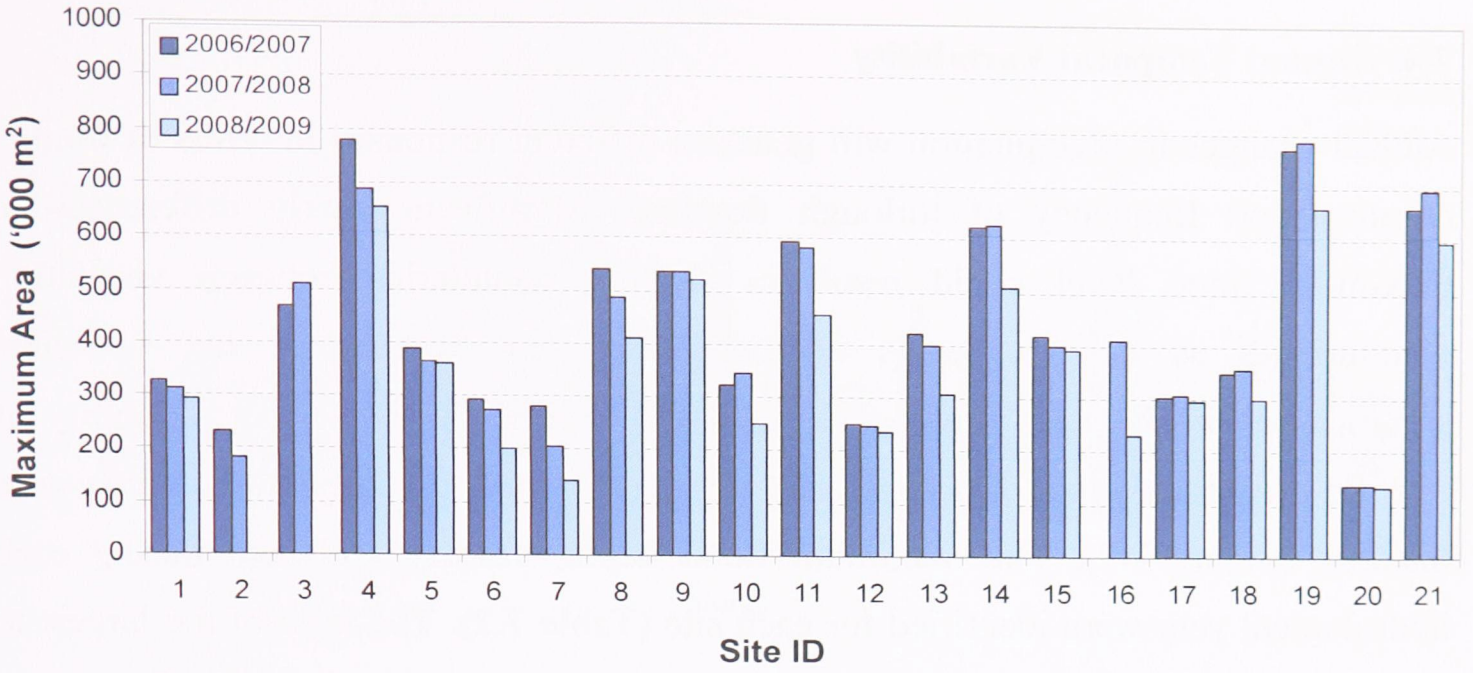


Figure 7.8: Maximum turlough flooded area recorded during the 2006/2007, 2007/2008 and 2008/2009 hydrological years

While area may seem the least important of the hydrological variables, it can be a controlling factor in terms of mixing, evaporation, direct rainfall, nutrient release and ecological disturbance. Shallow expansive turloughs are more likely to be completely mixed than smaller, deeper sites as a greater surface area per unit volume is exposed to wind, which induces turbulence in the water column as it drags across the water surface. A greater area potentially means higher levels of evaporation and direct rainfall, both important in the interpretation of stable isotope and water chemistry data. Turloughs covering large areas may also be more susceptible to nutrient release from subsoils, particularly those with a low average depth. The rate at which flooding expands or recedes is important for ecological communities. This can be a controlling factor for aquatic invertebrates as some species are not mobile enough to adapt to rapidly fluctuating conditions, and so the rate of areal change can be a limiting factor in community composition.

7.4. Annual Temporal Variability

Annual changes in precipitation will generate different responses in terms of timing, duration and frequency of turlough flooding. Significant yearly differences in maximum flood level could result in shifting boundaries between vegetation communities as variable levels of disturbance are experienced by ecological communities in the upper reaches of turlough basins. The temporal variability of hydrological parameters was compared using the ratio of highest to lowest yearly maxima (Figure 7.9). The maximum flood depth, volume and area during each hydrological year were identified for each site (Table 7.2). The ratio of the largest to smallest yearly maximum was then calculated. Volume was found to show the greatest variation between years with an average ratio of 1.67, meaning the highest recorded volume was 1.67 times greater than the lowest.

The three Roscommon turloughs, Rathnalulleagh, Carrowreagh and Brierfield, showed the greatest degree of yearly variation, with the volume in Carrowreagh turlough reducing by a factor of over 3.5 between the inundation periods of 2006/2007 and 2008/2009. The mean area variability ratio was 1.26, while depth of flooding was the most stable parameter across the monitoring period with a mean ratio of 1.2. When the geomorphology and topography of turlough basins is considered, depth would intuitively be the least variable parameter. As depth of flooding increases the volume of water (and associated rainfall) required for each incremental rise in depth becomes greater, as shown in the stage / volume / area relationships (appendix B). Therefore while the difference in maximum flood levels may be small in terms of the overall flood depth, the increase in volume associated with this difference is proportionally much greater.

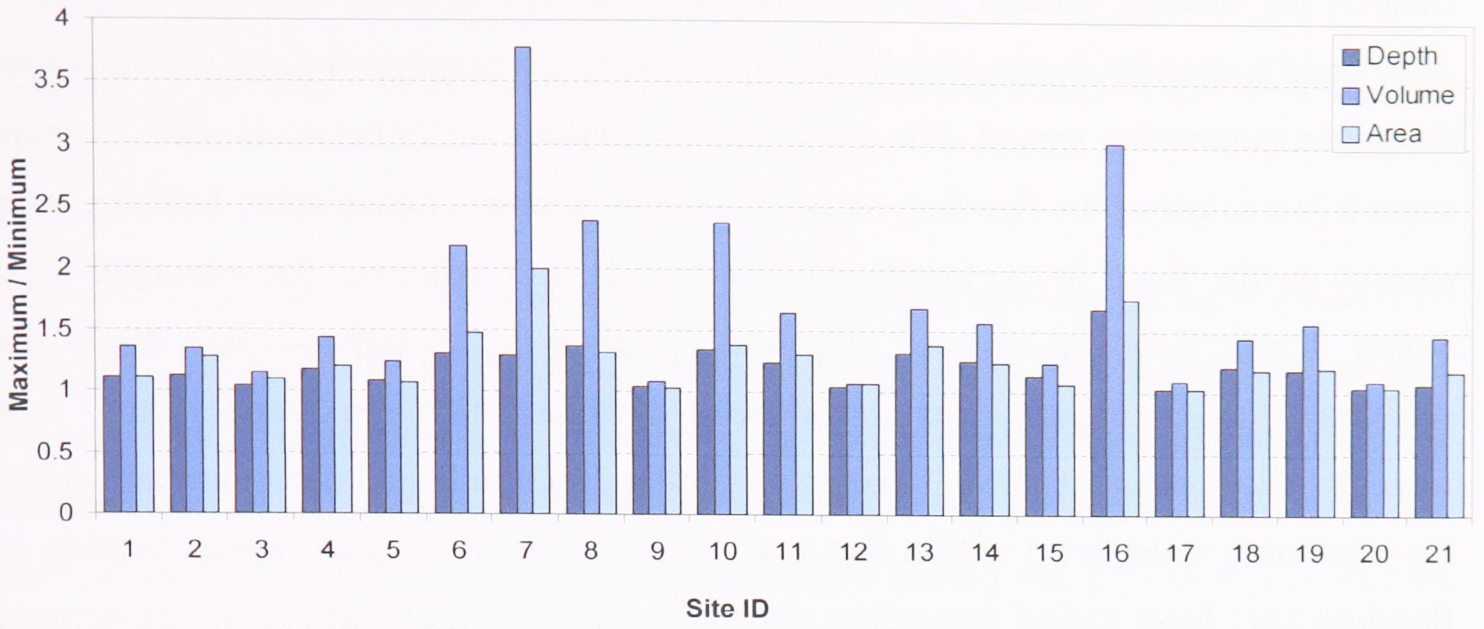


Figure 7.9: Ratio of highest to lowest yearly maximum for depth, volume and area for 21 study sites

Site ID	Site Name	Depth	Volume	Area
7	Carrowreagh	1.29	3.77	1.99
16	Roo West	1.68	3.02	1.76
8	Brierfield	1.37	2.38	1.32
10	Caranavoodaun	1.35	2.37	1.38
6	Rathnalulleagh	1.31	2.17	1.47
13	Garryland	1.31	1.68	1.37
11	Blackrock	1.24	1.64	1.3
19	Knockaunroe	1.19	1.56	1.19
14	Caherglassaun	1.26	1.56	1.23
21	Ballinderreen	1.07	1.46	1.17
18	Lough Gealain	1.21	1.45	1.19
4	Coolcam	1.17	1.44	1.2
1	Skealoghan	1.11	1.36	1.11
2	Ardkill	1.12	1.34	1.28
5	Croaghill	1.08	1.24	1.07
15	Termon South	1.14	1.24	1.07
3	Kilglassaun	1.05	1.14	1.1
17	Turloughmore	1.03	1.09	1.03
20	Lough Aleenaun	1.04	1.09	1.04
9	Lisduff	1.04	1.08	1.03
12	Lough Coy	1.04	1.07	1.06

Table 7.2: Ratio of highest to lowest yearly maxima for hydrological parameters of depth, volume and area (ranked by volume)

Despite the distinct rainfall patterns that occurred within each hydrological year a number of turloughs displayed a remarkably consistent maximum flood extent across the entire monitoring period. The cause of this stability varies between sites. In some cases it is a result of the flooding regime, whereas in others topographic features exert control on the flood level. Lough Aleenaun and Turloughmore, for example, have highly flashy flooding regimes responding rapidly to rainfall events. While the seasonal rainfall pattern may have been different between years, each year incorporated a series of rainfall events of similar magnitude and duration that caused the maximum water level within that year. Thus, while the frequency and duration of flooding may have varied depending upon the overall rainfall pattern, the maximum level remained steady. In the case of Lough Coy and Ballinderreen, maximum flood levels are limited, artificially via a drainage channel in the case of Ballinderreen and naturally via a connection to an adjoining depression in Lough Coy. The reason for such consistency in Lisduff is unclear, but possibly the presence of an overflow connection to a neighbouring bog serves as a control at high water levels. Alternatively, perhaps at higher levels the flood waters interact with a distinct flow system which can accommodate the excess. The elevation of well-established roads and farm buildings bordering the turlough supports the idea of a stable long term maximum flood level and an associated limiting factor to flood extent, as they are only slightly above the recorded maximum level.

CHAPTER 8. HYDROLOGICAL ANALYSIS: FLOW DYNAMICS

8.1. General

Through the analysis of net flows entering and exiting a turlough an insight into their hydrological operation can be gained. While ideally actual inflow and outflow time series would be available for analysis, as mentioned previously direct flow measurement in turloughs is practically impossible as the points at which inflow and outflow occur within the turlough are submerged during the period of inundation. Therefore the first step in quantifying the hydrological operation of turloughs must be through the analysis of net flow time series. Depending upon the hydrological configuration of a turlough, the net flow time series may represent the combined effect of all the processes supplying and draining water from the turlough with both inflow and outflow occurring simultaneously (flow-through). Alternatively, if the turlough behaves as a surcharged tank, the net flow time series may predominantly represent the actual flow time series (with some additional inflow such as direct rainfall). Nevertheless, relationships derived from analysing net flows, such as quantifying the link between turlough and rainfall or between water level and net outflow, provide an insight into turlough hydrological operation which has so far been lacking in turlough research.

In the absence of direct measurements, net flows are derived by determining the changes in storage (volume) of the turlough across each time step. Daily net flow was calculated as the average change in volume from hourly volume time series. This chapter provides a detailed study of these time series. Firstly, the maximum net flows recorded in each site are calculated and compared (section 8.2). Next is an investigation of temporal inflow patterns and the relationship between net inflow and rainfall (section 8.3), followed by a detailed study of the recession behaviour of turloughs (section 8.4). Finally, methods which may be used to identify periods of inflow are described (section 8.5).

8.2. Maximum Net Flows

Initially the highest recorded average daily net inflow and outflow values were calculated for each site (Table 8.1). The inflow magnitude is indicative of the properties of a turlough's catchment area and flow capacity, while outflow is a function of the drainage capacity of the system. The relative magnitude of inflow and outflow values shows that all turloughs have the ability to fill significantly faster than they empty, with a maximum average daily inflow / outflow ratio of 2.91. As it is thought to be a lack of capacity or constriction within the system that causes turlough flooding, it is intuitive that maximum inflow values would exceed outflow. Water fed to the turlough via direct rainfall, overland flow and shallow groundwater flow would also serve to further increase the divergence between the recorded flow maxima.

Blackrock turlough showed the greatest average daily inflow of over $10m^3/s$ which equates to an increase in volume of around $886000m^3$ in a single day, a figure greater than the maximum volume recorded in the majority of the other study sites. This inflow is also approximately 8 times higher than the maximum inflow in neighbouring Lough Coy. The main reason for this difference is the form of the connection between turlough and karst system. Blackrock and Lough Coy lie along the same conduit system which is fed by the predominantly allogenic Owenshree River running off the relatively impermeable sandstone bedrock of the Slieve Aughty Mountains. At high flow rates the capacity of the conduit system flowing beneath Blackrock is exceeded causing the Owenshree River to discharge directly into the turlough. This does not occur in Lough Coy, which is isolated from any surface water inputs and solely fed via an estavelle linked to the underlying conduit system. Therefore flow from the river which cannot be accommodated within the conduit, and thus cannot fill Lough Coy, can enter Blackrock directly causing the extremely high volume increase shown. A comparison of inflow/outflow ratio supports this, with Blackrock showing a ratio of over 5 while the Lough Coy ratio is only 1.58 as in Coy most flood waters enter and exit via connections to the conduit system.

Site Name	Site ID	Average Daily Inflow (m^3/s)	Average Daily Outflow (m^3/s)	Inflow / Outflow	Daily Inflow / Volume (%)	Daily Outflow / Volume (%)
Skealoghan	1	0.500	-0.166	3.0	11.3	3.7
Ardkill	2	0.439	-0.086	5.1	5.8	1.1
Kilglassaun	3	1.626	-0.488	3.3	17.4	5.2
Coolcam	4	0.684	-0.193	3.6	3.7	1.1
Croaghill	5	0.496	-0.117	4.3	6.7	1.6
Rathnalulleagh	6	0.461	-0.325	1.4	4.5	3.2
Carrowreagh	7	0.523	-0.214	2.4	8.3	3.4
Brierfield	8	0.380	-0.134	2.8	3.5	1.2
Lisduff	9	0.341	-0.157	2.2	3.8	1.8
Caranavoodaun	10	0.309	-0.162	1.9	5.4	2.8
Blackrock	11	10.253	-2.018	5.1	22.1	4.4
Lough Coy	12	1.331	-0.842	1.6	7.8	4.9
Garryland	13	1.832	-0.626	2.9	6.8	2.3
Caherglassaun	14	2.496	-1.192	2.1	7.2	3.4
Termon South	15	0.254	-0.149	1.7	2.3	1.4
Roo West	16	0.995	-0.275	3.6	8	2.2
Turloughmore	17	1.746	-0.585	3.0	36.2	12.1
Lough Gealain	18	0.844	-0.222	3.8	7.9	2.1
Knockaunroe	19	1.333	-0.582	2.3	6.3	2.8
Lough Aleenaun	20	1.548	-0.555	2.8	37.6	13.5
Ballinderreen	21	0.594	-0.271	2.2	8.7	3.9
Mean				***2.91***	***10.5***	***3.7***
Standard Deviation				***1.05***	***9.9***	***3.3***

Table 8.1: Maximum average daily net inflow and outflows, inflow: outflow ratio and inflow and outflow as a percentage of maximum volume for study sites

In a comparison of preliminary estimated catchment area against maximum net inflow (excluding the sites in the Gort chain), there is a general pattern of increasing maximum inflow rate with increasing estimated catchment (Figure 8.1). While it is difficult to draw any firm conclusions given the substantial uncertainties associated with the preliminary catchment areas (see section 5.9), it is worth looking at the two main sets of outliers that deviate substantially from the approximately linear pattern. Sites 6 and 7 (Rathnalulleagh and Carrowreagh), are located in Roscommon and are relatively close to site 8 (Brierfield). The outlying nature of these sites may point to a

possible error in the catchment estimate, as it was assumed that the catchments of these study sites included that of the nearby Brierfield turlough (Site 8). If this were reduced it would bring these values roughly in line with the majority of other study sites. Alternatively, given the presence of other substantial ephemeral water bodies and an apparent sinking stream in the area, this deviation may indicate a more complex flow configuration for these sites, such as the conduit bypass which exists in Lough Coy, albeit on a much smaller scale.

Turloughs 17 and 20, Turloughmore and Lough Aleenaun respectively, show the most rapidly fluctuating water levels of all the study sites, and their deviation from the general linear pattern may be more indicative of a different hydrological operation than of a catchment area estimation error. Both turloughs are located in the Burren, an area of thin or absent soil cover which allows rainfall to enter the karst system almost immediately. In addition, both sites lie at the foot of a steep hill which provides a high hydraulic gradient, allowing rapid flow into the turloughs. The relative capacity of the outflow systems are also extremely high, resulting in a hydrological regime characterised by frequent, distinct flood events.

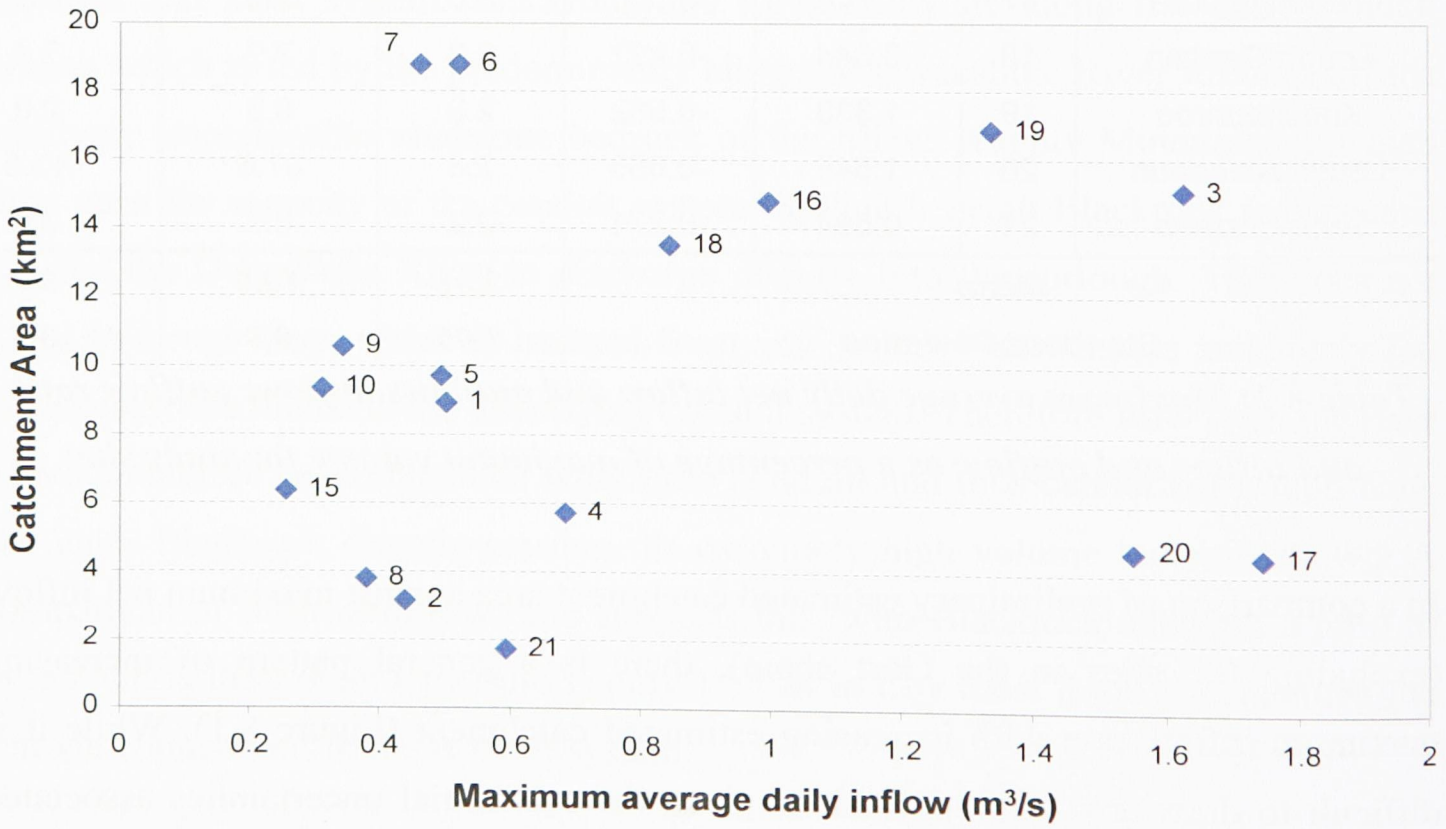


Figure 8.1: Plot of maximum average daily inflow against estimated catchment area for 17 monitoring sites (excluding sites 11 to 14)

To illustrate the relative scale of turlough flows, the maximum inflow and outflow values were calculated as a percentage of highest recorded volume over the monitoring period (Table 8.1, Figure 8.2). Inflow ratios range from 2.3 to 37.6% while outflows were 1.1 to 13.5%. The ratios further demonstrate the continuum of temporal flooding behaviour from slow to fast. The lowest ratios are shown by those sites characterised by low frequency, long duration flooding with ratios increasing through intermediately responsive sites up to the flashy multimodal flooding regime of Lough Aleenaun.

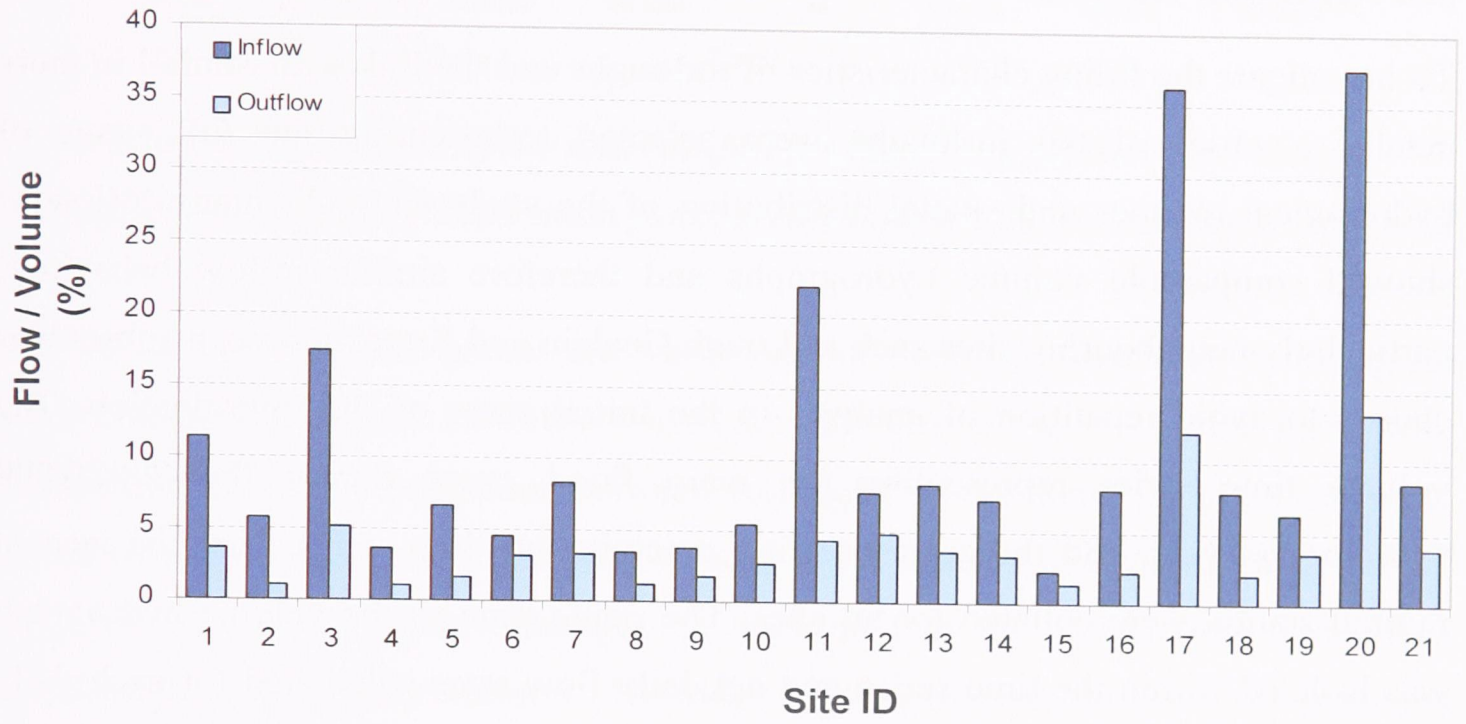


Figure 8.2: Ratio of maximum Inflow/ volume and maximum outflow/ volume for monitoring sites

The lowest inflow ratio was shown by Termon turlough, Co. Galway. The hydrograph of Termon reflects this with a longer than average filling period and maximum water level between 35 to 55 days later than the average across the study sites. The characteristic extended recession of Termon is also represented here with a low outflow/maximum volume percentage of 1.4%, which signifies that, even at maximum recorded outflow capacity, it would take 75 days for the turlough to empty. The hydrographs of other turloughs with similarly low outflow / volume percentages, such as Coolcam and Brierfield, also show lengthy recession limbs and corresponding long duration of flooding.

The inflow and outflow figures of Turloughmore (site 17) and Lough Aleenaun (site 20) are the most significant in terms of overall maximum volume. The highest daily

increases of 150780m^3 in Turloughmore and 133747m^3 in Lough Aleenaun represent 36.2% and 37.6% of the total maximum recorded volume in each turlough. The corresponding outflow percentages of 12.1% and 13.5% are also the highest recorded within the study sites. As a result of this behaviour both sites show a highly fluctuating regime with numerous filling and emptying events. Lough Aleenaun was the archetypal example of this with 16 distinct flood events (water levels rising from empty, peaking and then completely receding) recorded during the monitoring period.

8.3. Net Inflow Analysis

To investigate the filling characteristics of turloughs and the link with rainfall in more detail, a subset of ten turloughs were selected representing the full range of hydrological regimes and spatial distribution of the study sites. As many turloughs showed comparable volume hydrographs and therefore similar inflow behaviour, particularly neighbouring sites such as Lough Gealain and Knockaunroe, a subset was chosen to avoid repetition of analysis in the initial stage of the investigation. The volume time series representing the main flood event during the 2007/2008 hydrological year, and the corresponding precipitation time series from the nearest rainfall station were collated for all sites. The rising limb of the volume hydrograph was isolated within the time series and net daily flow rates calculated for each daily time step. A plot of flow and rainfall for the period from the onset of flooding until the highest volume recorded during the 2007/2008 hydrological year shows the general turlough flow behaviour and response to rainfall (Figure 8.3).

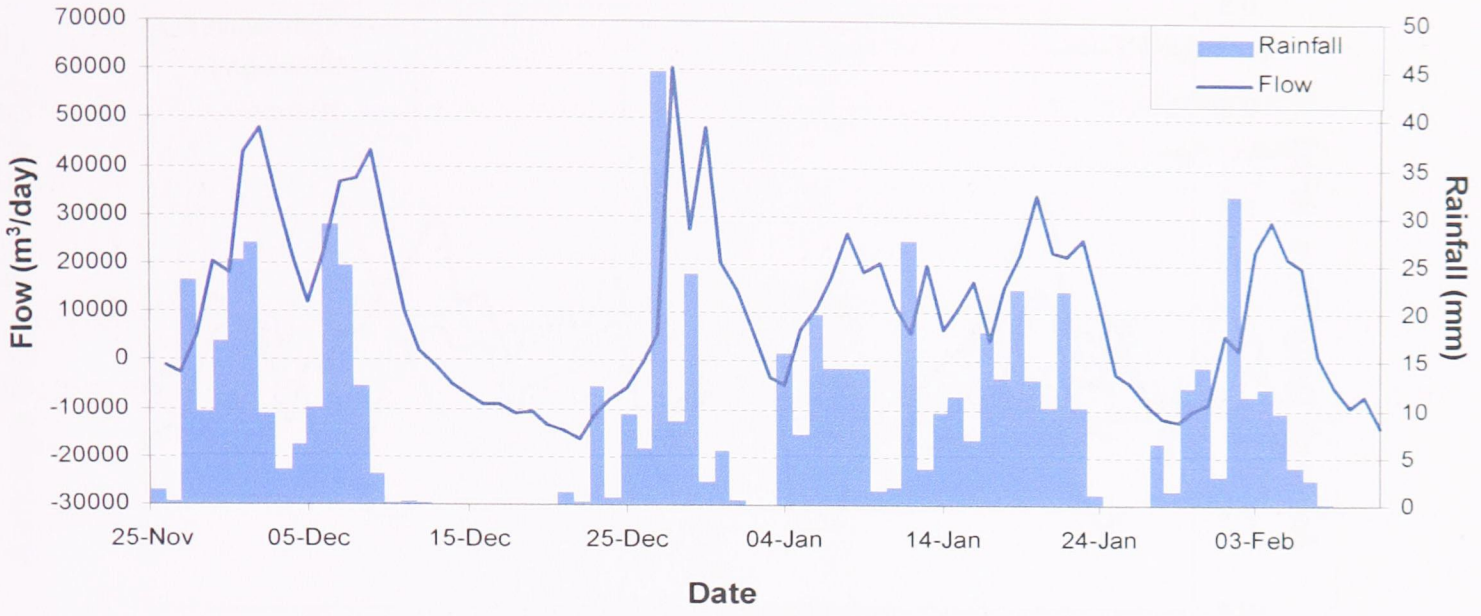


Figure 8.3: Plot of net flow and rainfall for the filling phase of the volume hydrograph during 2007/2008 main flood event, Lough Gealain turlough, Co. Clare

As would be expected given the variations in turlough size and hydrological behaviour, the magnitude of inflow varied substantially (Figure 8.4), but there were similarities in inflow behaviour between turloughs in the same geographical area. Seven of the sites showed maximum average daily inflows of a similar scale in the range of 0.24 to 0.42m^3/s, although the duration that the higher flow rates were sustained for was highly variable. No clear relationship existed between estimated catchment area and maximum net inflow, illustrating the dependence of inflow on properties other than the catchment area such as catchment gradient, flow system type, degree of karstification, and the nature of the connection between flow system and turlough.

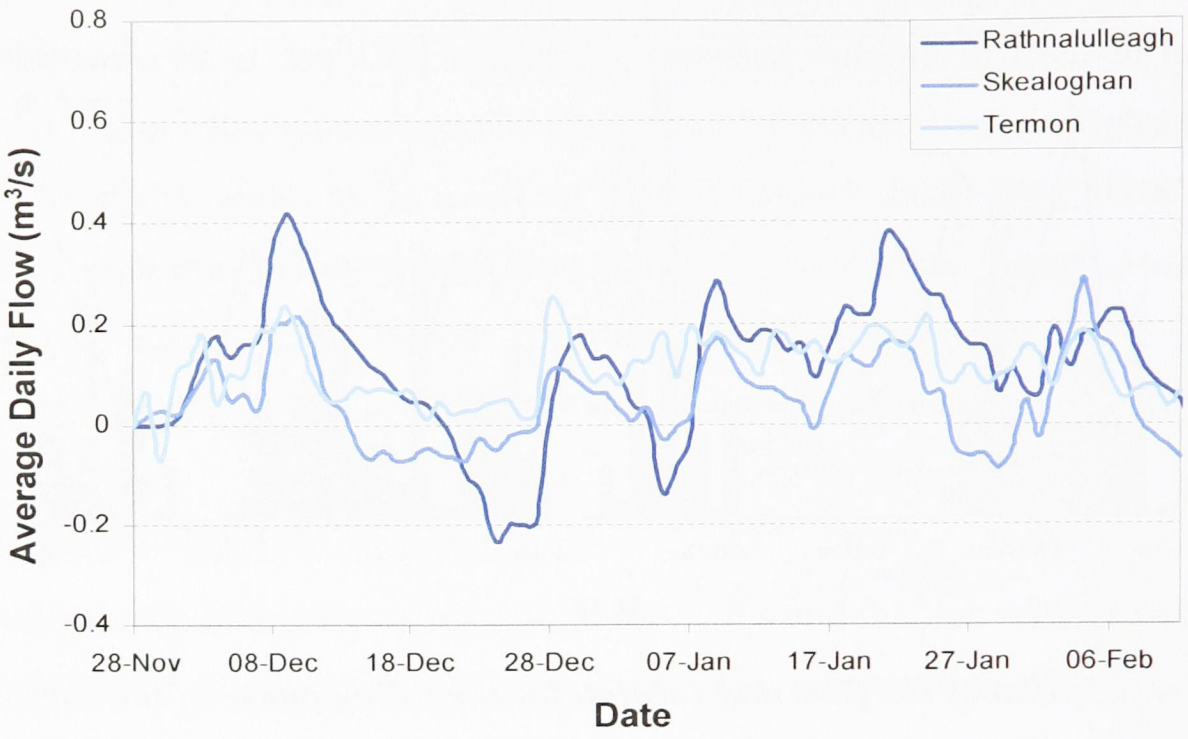


Figure 8.4: Average daily flow for three turloughs following the onset of flooding in 2007

The remaining three sites, Lough Coy, Turloughmore and Lough Gealain, showed larger flow rates of up to 1.74m^3/s (Figure 8.5). Turloughmore shows the highest net inflows but these were sustained only for a very short period. Of these three sites it has by far the smallest estimated catchment, so there is a smaller area from which to derive recharge compared to the other two sites. However, the steepness of the catchment may allow a recharge and runoff rate sufficiently high enough to produce flows of comparable scale, which take the form of pulses of rainfall passing quickly through the system temporarily routed through the turlough. In comparison, Lough Coy does not reach the same maximum values but is able to maintain high inflows for a longer duration due to the greater catchment area drained by the karstic conduit system to which the turlough is linked.

An inconsistency can be seen after the 5th of January in Lough Coy where little or no flow appears to occur, compared to the highly fluctuating flows of the other two sites. This discrepancy is due to the interaction of Lough Coy with an adjoining basin at high stages. When the turlough reaches a threshold level it overflows across into an adjacent depression, limiting the maximum water level and causing an apparent flow cessation in the hydrological record.

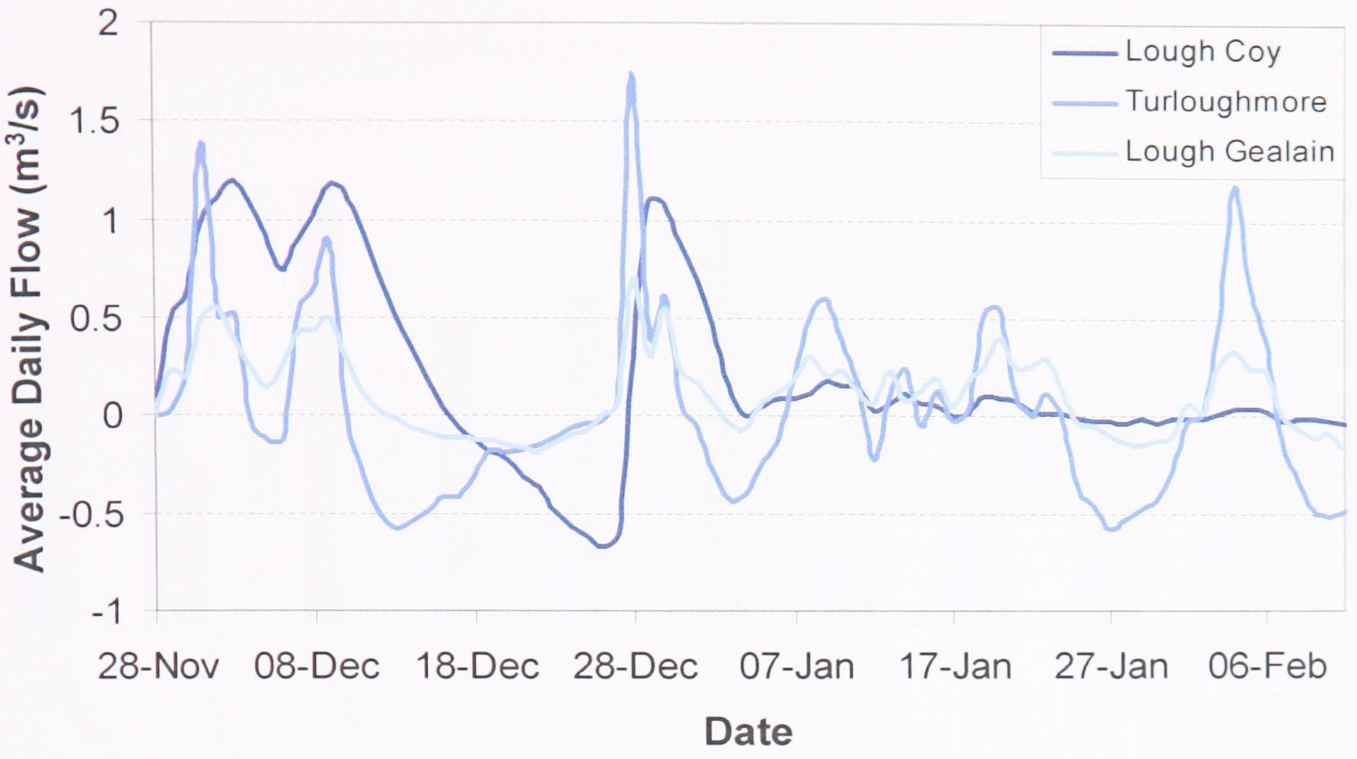


Figure 8.5: Average daily flow for Lough Coy, Turloughmore and Lough Gealain following the onset of flooding in 2007

8.3.1. Flow Transition

The turloughs within the analysis subset were highly variable in terms of their temporal flow behaviour. The time between the cessation of rainfall and the occurrence of flow transition or change in flow direction is indicative of the nature of the underlying karst flow system and was found to have a strong role in determining the characteristic hydrological regime of a turlough. While a few maintained a net inflow for most or all of the monitoring period, most sites fluctuated from net inflow to net outflow on a number of occasions in response to the prevailing rainfall conditions. The number of days of net inflow and net outflow recorded at the sites for the period 1/12/2007 to 31/1/2008 is shown in Figure 8.6. This interval was chosen as it covered the major net inflow period between the flooding onset and maximum water levels for all sites, and so allowed the comparison of filling behaviour across a range of sites and in response to the same general rainfall signal. Taking into account local differences in rainfall, this reveals the general trend in transition time from net inflow to outflow. Sites where this occurs quickly, such as Turloughmore and Skealoghan, have a higher frequency of flooding and the capacity of the flow system is high relative to the volume stored within the turlough. Sites where this occurred at a

slower rate, such as Lisduff and Termon, were characterised by much longer duration, low frequency flooding and so represented a lower disturbance environment.

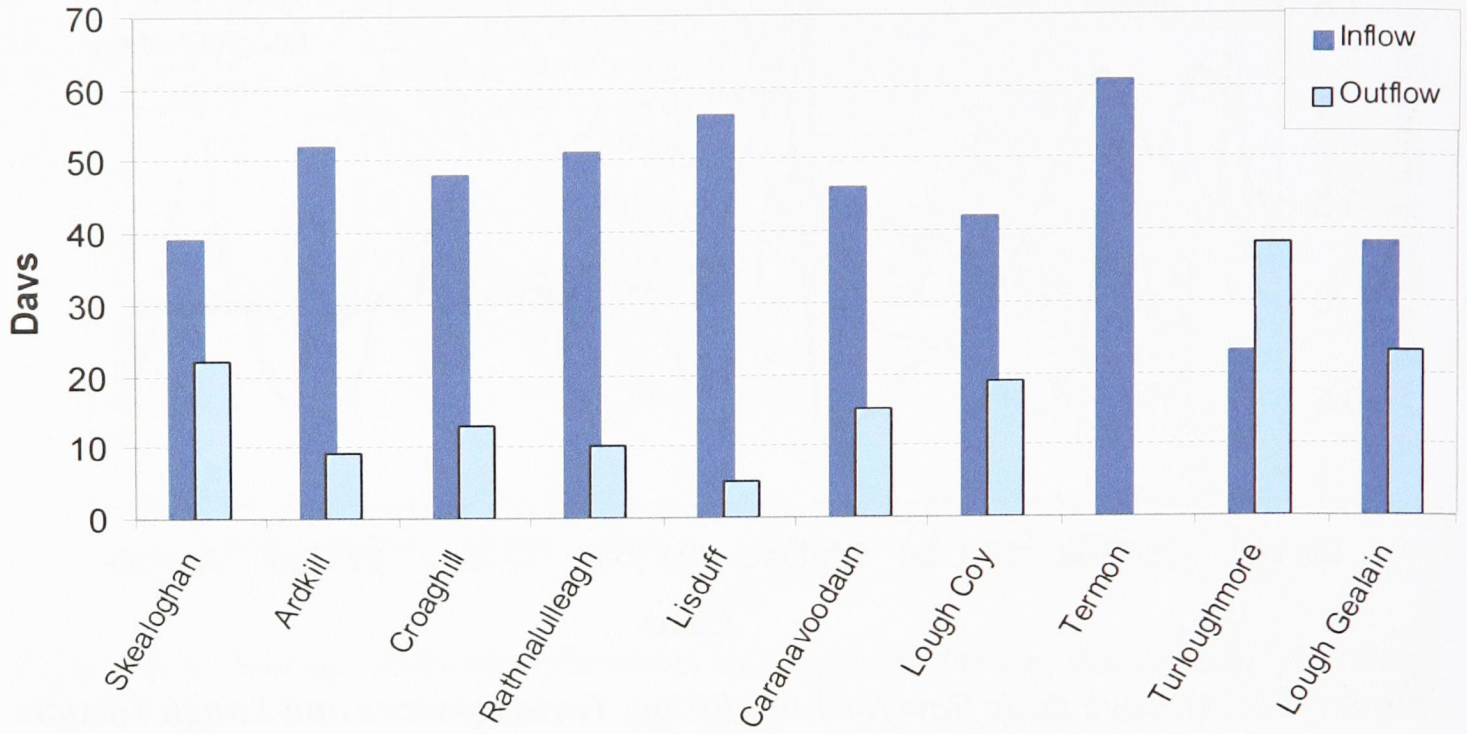


Figure 8.6: Number of days of net inflow and net outflow for flow analysis subset during the period 1/12/2007 to 31/1/2008

However, the duration of each net flow type does not fully reflect the overall flow behaviour, as there was a disparity between number of outflow days and the relative magnitude of the outflow during the analysis period, with some sites reaching far greater net outflows than others, as demonstrated by the inflow to outflow ratios (Figure 8.7). Despite Turloughmore experiencing a net outflow for 15 days more than a net inflow, the cumulative volumes over this period are approximately equal with a ratio of 1:1. Both Ardkill and Rathnalulleagh showed the same inflow and outflow durations, but the greater outflow capacity of Rathnalulleagh results in a ratio of 6:1 compared to only 18:1 in Ardkill.

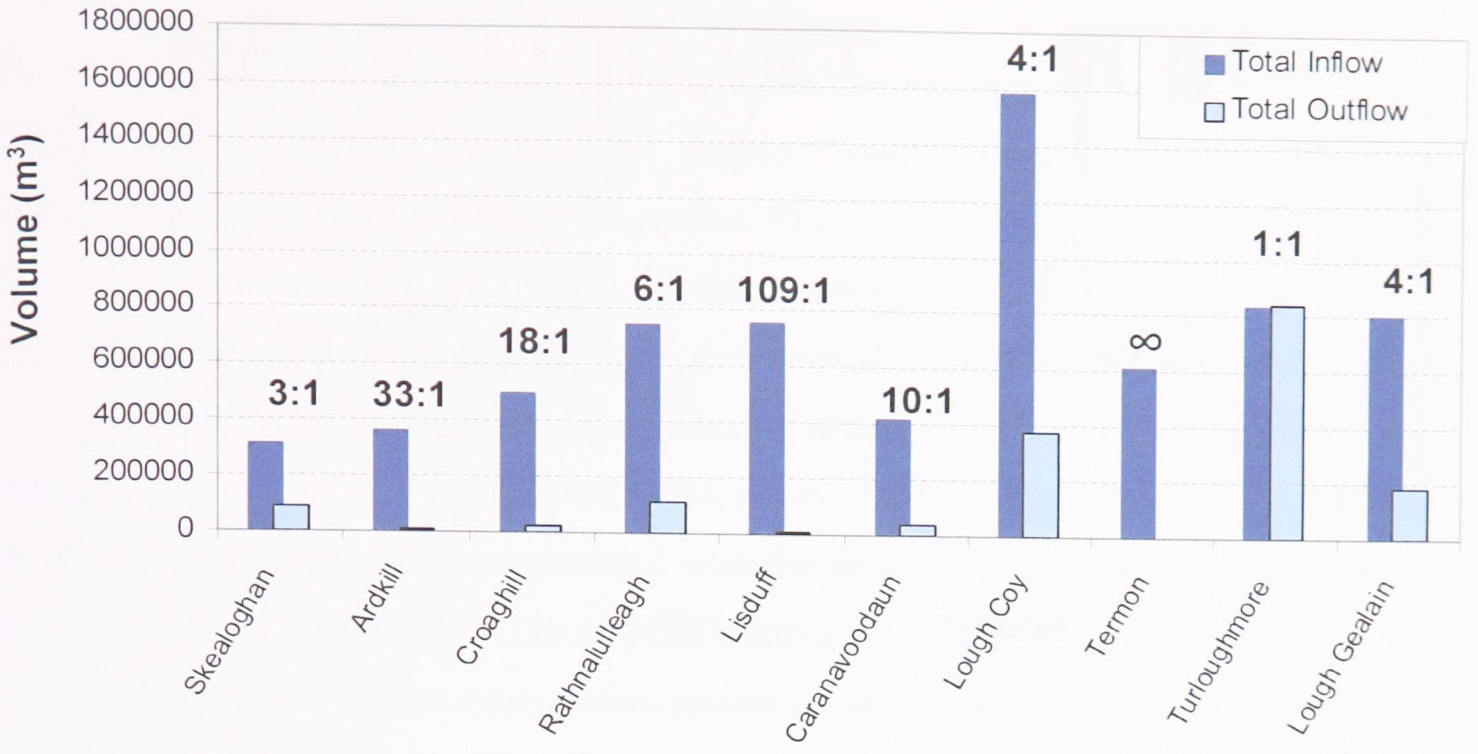


Figure 8.7: Sum of daily net inflow and net outflow including inflow: outflow ratio for flow analysis subset during the period 1/12/2007 to 31/1/2008

The effect of differences in flow behaviour is clearly demonstrated by comparing the net flows in the geographically close turloughs of Skealoghan and Ardkill (Figure 8.8). Despite the estimated zone of contribution for Skealoghan being twice that of Ardkill, the two turloughs show remarkably similar inflow characteristics in terms of quantity and timing with coincident net inflow peaks occurring in both series. The major difference in flow behaviour occurs following the cessation of rainfall and the subsequent transition to net outflow. Skealoghan shows a much shorter transition time and displays a net outflow for 25 days of the analysis period, reaching a maximum average net outflow of approximately $0.087m^3/s$. This compares with only 12 days of net outflow in Ardkill, and a maximum outflow of $0.027m^3/day$. This equates to less than a third of that shown in Skealoghan. The cumulative effect of this, as shown in the lower plot, is a volume approximately $150000m^3$ greater in Ardkill than in Skealoghan at the end of the analysis period. This "easier" drainage for Skealoghan makes sense as it helps to offset the effect of a larger catchment area, i.e. if its drainage characteristics were similar to Ardkill, then the inflow characteristics would presumably not be so similar.

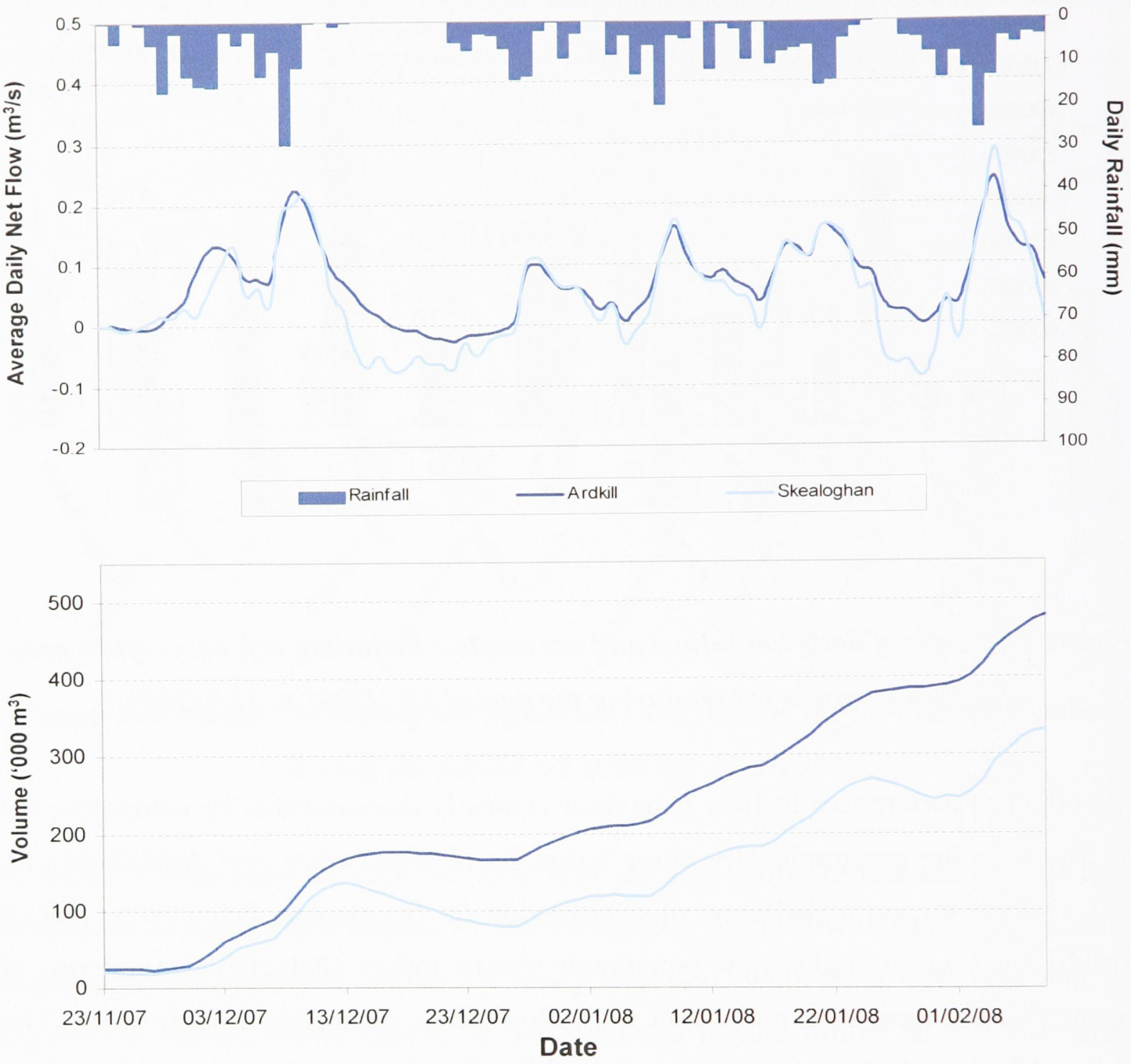


Figure 8.8: Daily net flow and volume for Skealoghan and Ardkill turloughs, Co. Mayo

Another interesting feature of the flow hydrograph is the behaviour of Skealoghan during the significant recession period in mid December 2007. Following the cessation of rainfall the net flow rate decreased, eventually reversing direction and becoming a net outflow. The net outflow rate then appears to plateau at approximately -0.07m^3/s. This behaviour was repeated in other turloughs that experienced significant recessions during the analysis period, and potentially points to a characteristic maximum outflow capacity limiting the recession and is further investigated in section 8.4.

8.3.2. Net Inflow and Rainfall

The inflow time series and corresponding precipitation time series from the nearest rainfall station during the analysis period (main filling phase in 2007/2008 hydrological year) were collated for all sites. Plots of net inflow clearly show a strong relationship between net inflow and rainfall, with peaks in the inflow time series in evidence after each major rainfall event in winter (Figure 8.9). When rainfall ceased, the net inflow dropped eventually transitioning to a net outflow following sufficiently long dry spells. The time for this transition to occur differed greatly between the sites. Generally the highest inflows coincided with the greatest magnitude rainfall event, but this was not always the case. The rainfall–inflow relationship displayed a cumulative effect where high inflow rates were generated by a series of consecutive lower intensity rainfall events. Another factor affecting the association between rainfall and inflow was the preceding flow conditions. The flow response shown by turloughs to similar magnitude rainfall events was less following a recession period than following a prolonged filling period. It was also apparent that the length of the recession had an effect upon the level of inflow, with longer recessions further damping the inflow response.

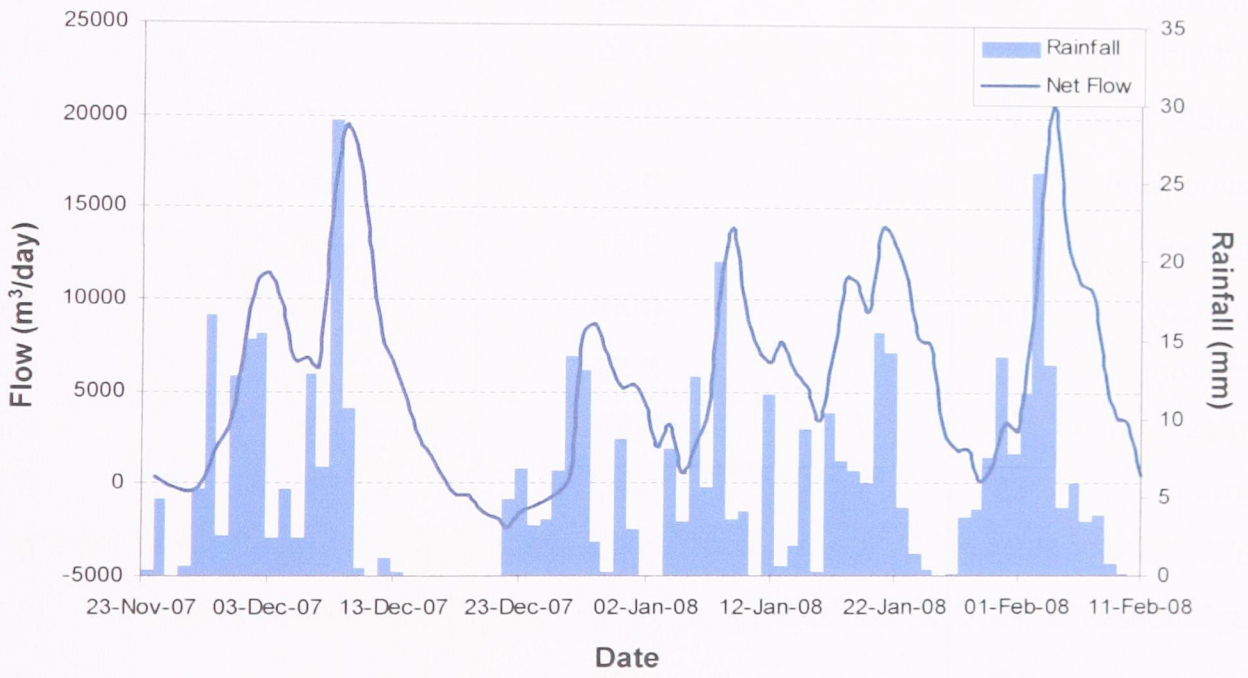


Figure 8.9: Plot of average daily flow and rainfall for filling phase of volume hydrograph during 2007/2008 main flood event for Ardkill, Co. Mayo

A clear delay can be seen between the rainfall event itself and the corresponding maximum inflow. This would be expected as it would take some time for rainfall-derived recharge to enter the karst system and thereafter the turlough. Time-lagged

correlation was used to quantify the length of this delay for each turlough, whereby net flow values were correlated with rainfall offset by varying intervals; the lag corresponding to the maximum correlation coefficient was thus identified (Table 8.2). A number of individual lags were also checked manually and found to match those indicated by those of the time-lagged correlation. The delay, ranging from 1 to 3 days, showed little difference between sites and was not related to overall turlough hydrological regime, as turloughs with radically different flood durations and frequencies showed identical lag.

Site Name	Site ID	Lag (days)	Lag Correlation	Averaging Interval n (days)	Interval Correlation
Skealoghan	1	2	0.64	5	0.84
Ardkill	2	2	0.62	6	0.87
Kilglassaun	3	1	0.41	6	0.59
Coolcam	4	3	0.51	7	0.74
Croaghill	5	2	0.65	6	0.80
Rathnalulleagh	6	2	0.43	9	0.73
Carrowreagh	7	2	0.49	4	0.71
Brierfield	8	2	0.46	7	0.76
Lisduff	9	2	0.34	7	0.75
Caranavoodaun	10	3	0.56	9	0.67
Blackrock	11	1	0.67	3	0.74
Lough Coy	12	2	0.36	8	0.76
Garryland	13	3	0.56	8	0.79
Caherglassaun	14	1	0.59	6	0.72
Termon	15	1	0.67	7	0.73
Roo West	16	3	0.59	6	0.74
Turloughmore	17	1	0.76	4	0.79
Lough Gealain	18	1	0.78	5	0.89
Knockaunroe	19	3	0.69	7	0.88
Lough Aleenaun	20	1	0.80	3	0.77
Ballinderreen	21	1	0.54	3	0.67

Table 8.2: Maximum inflow, time-lagged correlation coefficients and lag for flow – rainfall analysis for main filling phase in 2007/2008 hydrological year

The level of correlation could be improved by using average rather than time-lagged rainfall (Table 8.2). Average rainfall at time t, $\boldsymbol{AR_t}$, is given by:

$$AR_t = \frac{\sum_{i=0}^{n} R_{t-i}}{n}$$

Where R is rainfall and $\boldsymbol{n}$ is the averaging interval, i.e. the number of preceding days rainfall is averaged over. Correlation was found to increase to a maximum after between four and nine days and then drop off, as shown for example in Ardkill turlough (Figure 8.10). The averaging intervals corresponding to maximum correlation are given in Table 8.2. The process of averaging rainfall is in effect applying an instantaneous unit hydrograph to the rainfall data, where the length of the unit hydrograph is defined by the interval with the highest correlation coefficient and an equal weight of 1/interval is applied to each ordinate of the hydrograph. The applicability of unit hydrographs for generating inflow from rainfall records shown here is further developed in the turlough modelling process (Chapter 9).

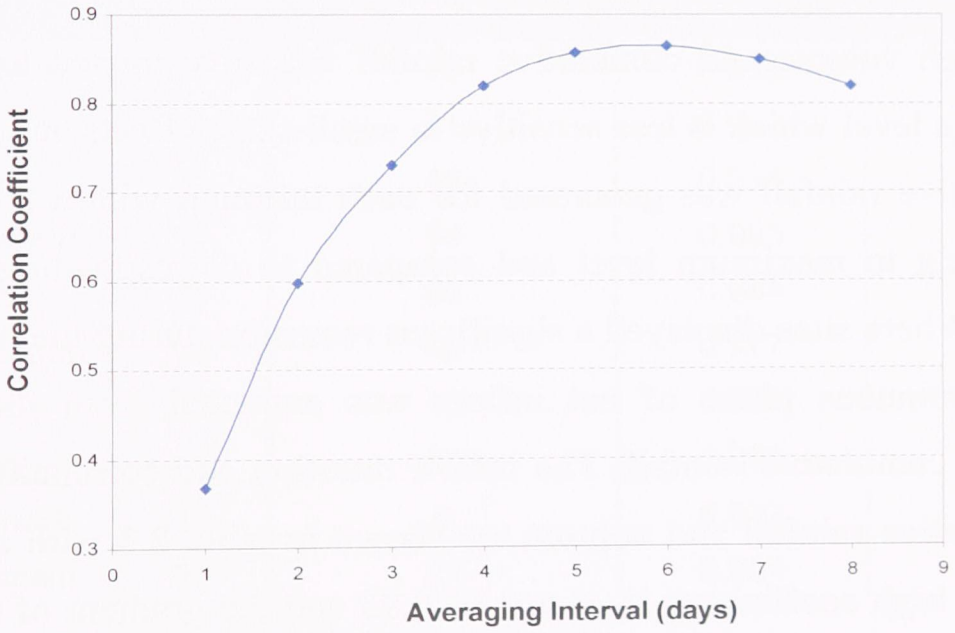


Figure 8.10: Correlation coefficient between inflow and average rainfall over varying averaging periods for Ardkill turlough, Co. Mayo

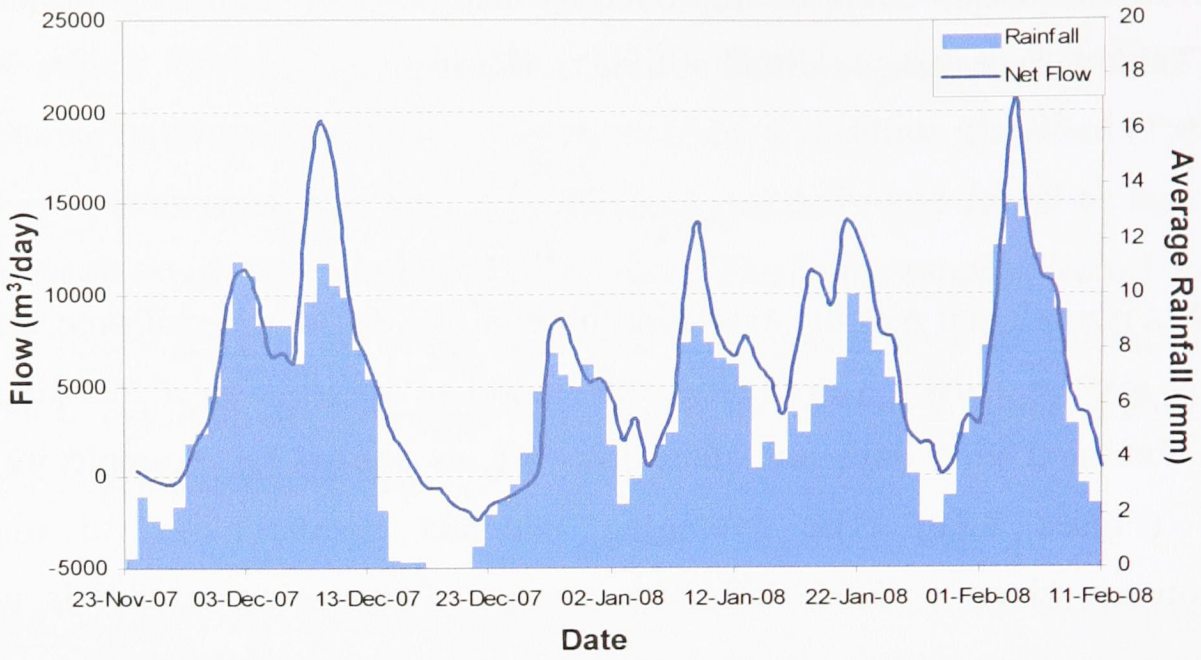


Figure 8.11: Plot of average daily flow and 6 day average rainfall (average rainfall over preceding 6 days) for Ardkill turlough, Co. Mayo

8.3.3. Cumulative Rainfall

Given the high correlation identified between rainfall and net inflow, the connection between turlough volume and cumulative rainfall was investigated to quantify this relationship on a level which is less sensitive to small-scale effects and data errors. A plot of cumulative rainfall was generated for each turlough within the subset from onset of flooding to maximum level and compared to corresponding volume data (Figure 8.12). Where sites displayed a significant recession during the analysis period the longest continuous phase of net inflow was extracted from the dataset and correlated with cumulative rainfall. The inflow duration and correlation coefficients between cumulative rainfall and volume are shown in table 8.3 with all sites in the subset showing high coefficients in excess of 0.95 and the gradient of the regression line denoted as the notional area.

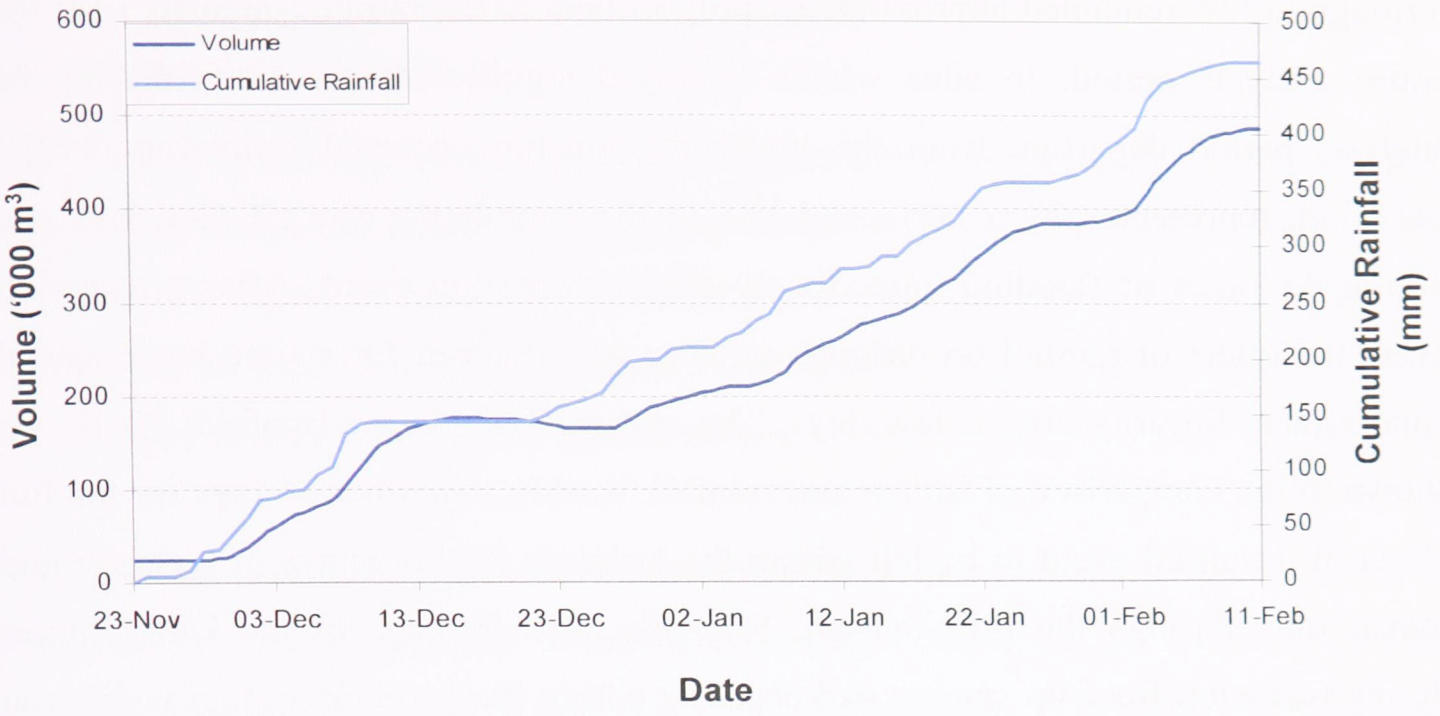


Figure 8.12: Plot of volume and cumulative rainfall for Ardkill turlough, Co. Mayo, for the period 23/11/2007 – 11/2/2008

Site Name	Site ID	Inflow Duration (days)	Correlation Coefficient	Notional Area (km^2)
Skealoghan	1	19	0.996	1.230
Ardkill	2	81	0.992	1.010
Croaghill	5	48	0.991	1.431
Rathnalulleagh	6	36	0.985	2.412
Lisduff	9	58	0.984	2.643
Caranavoodaun	10	48	0.977	1.383
Lough Coy	12	18	0.954	9.437
Termon	15	81	0.996	1.357
Turloughmore	17	6	0.952	4.603
Lough Gealain	18	21	0.984	1.351

Table 8.3: Correlation coefficients between cumulative rainfall and volume and notional zone of contribution areas for inflow analysis subset

Strong relationships for the longest duration were shown by those sites which maintained a net inflow throughout the analysis period, principally because there was insufficient time between rainfall events to allow flow transition to occur. For example, the plot for Ardkill turlough demonstrates the close match found between time series, with a Pearson correlation coefficient of 0.992 (Figure 8.12). In these sites, characterised by long transition times associated with low outflow capacity,

turlough inflow remained approximately proportional to the rainfall intensity over the entire analysis period. In sites which displayed significant recessions during the analysis period departure from the linear relationship occurred following rainfall cessation, represented by a horizontal line in the cumulative rainfall plot, and also during the onset of flooding immediately after a recession event. After a recession event the effect of rainfall on turlough volume was reduced for a time but regained approximate linearity after a few days. The reasons for this are twofold. Firstly, as shown in the comparison of inflow and rainfall, it takes a number of days for the full effect of a rainfall event to be felt within the turlough due to delays in recharge and transit time through the flow system. Secondly, the drainage of the karst aquifer during recession frees up storage and capacity within the bedrock system which can accommodate a component of subsequent rainfall thus lessening the amount of water passing to storage within the turlough.

One implication of the linear relationship identified between cumulative rainfall and volume is that during inflow periods a unit of rainfall causes a unit increase in turlough volume. While the mechanisms and processes involved are inherently non-linear, the high correlations found show that it can be approximated as such for inflow periods. The constant of proportionality between rainfall and volume represents a notional catchment or contributing area. This constant is essentially the product of a mass balance and gives the absolute minimum area required to account for the recorded volume in the turlough. The actual catchment area is likely to be substantially greater than this, as losses such as evapotranspiration are not accounted for. Also, considering the heterogeneous nature of karst systems, the actual contributing area may vary with changing hydrological conditions both within the catchment and the turlough itself. The strong relationship between cumulative rainfall and volume is expanded upon in the modelling processes detailed in Chapter 9.

8.4. Net Outflow Analysis

The analysis of turlough hydrology during draining or recession periods can yield key information about the nature and capacity of the underlying karst flow system. To elucidate this aspect of turlough behaviour major recession events for each site were studied and all recession information (in the form of days showing an overall average net outflow) collated and plotted against corresponding stage.

Stage, rather than depth, was used throughout these net outflow analyses. Depth is measured relative to a point within the turlough basin, for example the lowest recorded topographic point. If this point lies, for example, at the base of a 2 metre deep doline, the volume contained within the doline is insignificant compared to the rest of the turlough and therefore including the depth of the doline in any discharge relationships would be unnecessary. Thus measurements in terms of the absolute stage (mAOD) are more appropriate.

A common temporal pattern was identified whereby the rate of net outflow increased during the initial phase of recession (Figure 8.13). A negative net flow indicates a period of net outflow, i.e. a fall in the water level hydrograph. In the absence of rainfall, net outflow continued to rise to a maximum value, the magnitude of which depended upon the capacity of the individual drainage system.

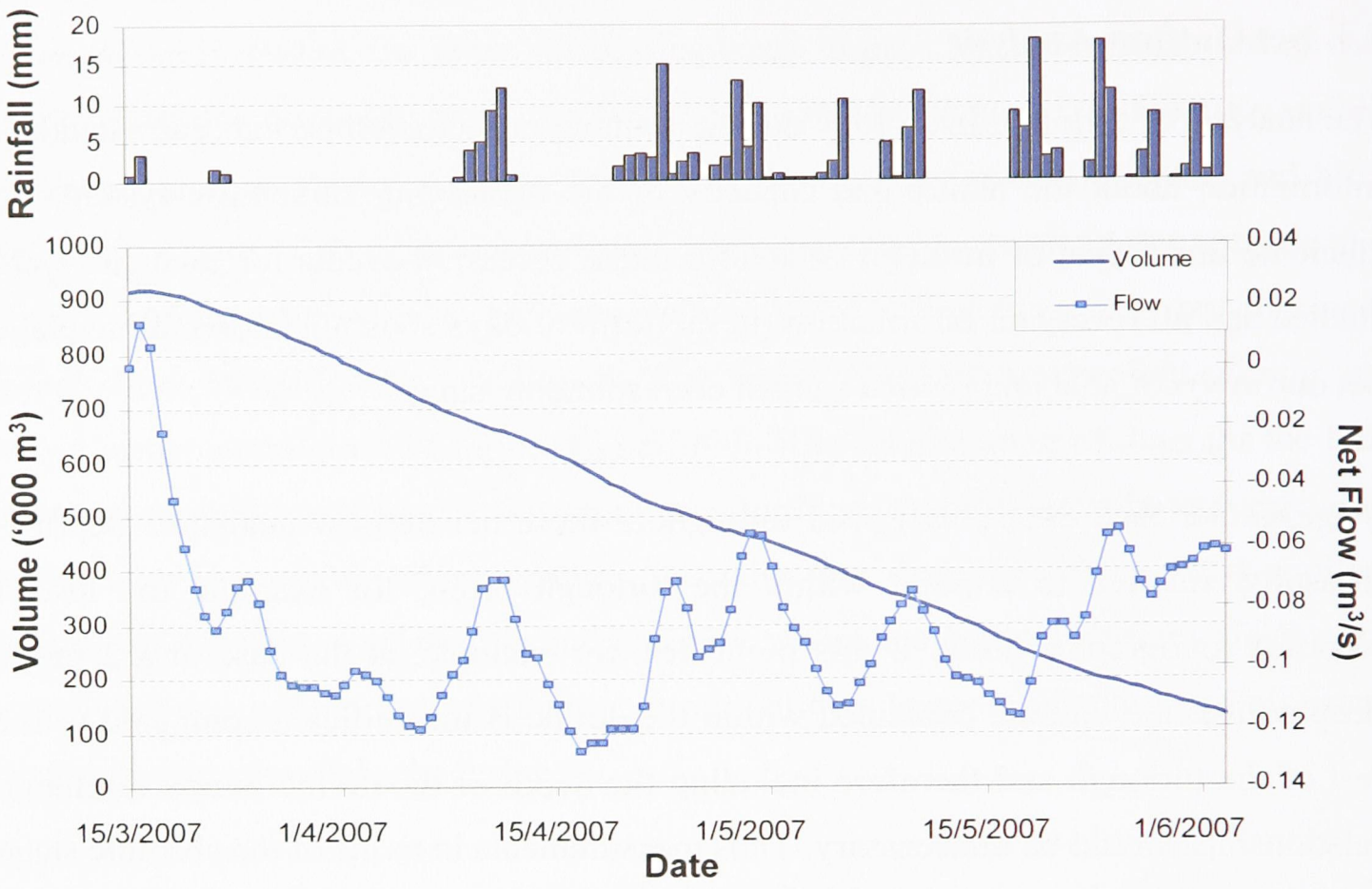


Figure 8.13: Recession volume and flow for Brierfield turlough, Co. Roscommon

The time taken to reach the maximum outflow varied depending upon system outflow capacity and rainfall conditions. Peak outflow was quickly reached in some sites within the first few days of recession which thus enabled the rapid drainage of floodwaters. Other slower responding sites took far longer to reach the maximum discharge. Generally it was found that the higher the outflow capacity, the shorter the delay between onset of recession and peak outflow. Rainfall during the recession period reduces the outflow rate and so delays the onset of maximum outflow. Rainfall events in Figure 8.13 can be seen to clearly correspond with a decrease in net outflow. Significant rainfall reduces the outflow rate by raising the head within the underlying flow system, where the outflow from the turlough is reduced due to a higher proportion of the total drainage capacity of the system being taken up with contribution from the underlying system. The net outflow rate also falls due to inflow entering the turlough directly via rainfall onto the turlough surface and runoff from the immediate surroundings. The relative importance of each element varies between turloughs and is dependent upon the hydrological operation of the turlough, and the nature of the connection between turlough and underlying system.

The nature of the relationship between stage and outflow was derived from stage-discharge plots generated for each site. It was shown that a stage-discharge curve defining a turlough's maximum drainage capacity was formed by the maximum outflow values across the flooding range (Figure 8.14). This curve defines the characteristic relationship between stage and turlough discharge at peak outflow conditions. During the initial recession phase, turlough outflow increases until it reaches a maximum value on the stage-discharge curve ("Recession Events" Figure 8.14). Thereafter outflow decreases with falling water level, as would be expected in a reservoir. The underlying assumption here is that points on the stage-discharge curve represent the actual outflow from the turlough. In other words, there is no inflow occurring at this time and so net outflow and actual outflow are one and the same at these points.

The majority of net outflow values fall short of the maximum as defined by this curve, as shown by the wide scattering of points above the curve in the outflow plots (Figure 8.14). These points are made up of outflows during two scenarios:

a) Increasing net outflows during the initial recession period when flow is in a state of transition
b) Reduction in net outflow caused by rainfall events during the recession

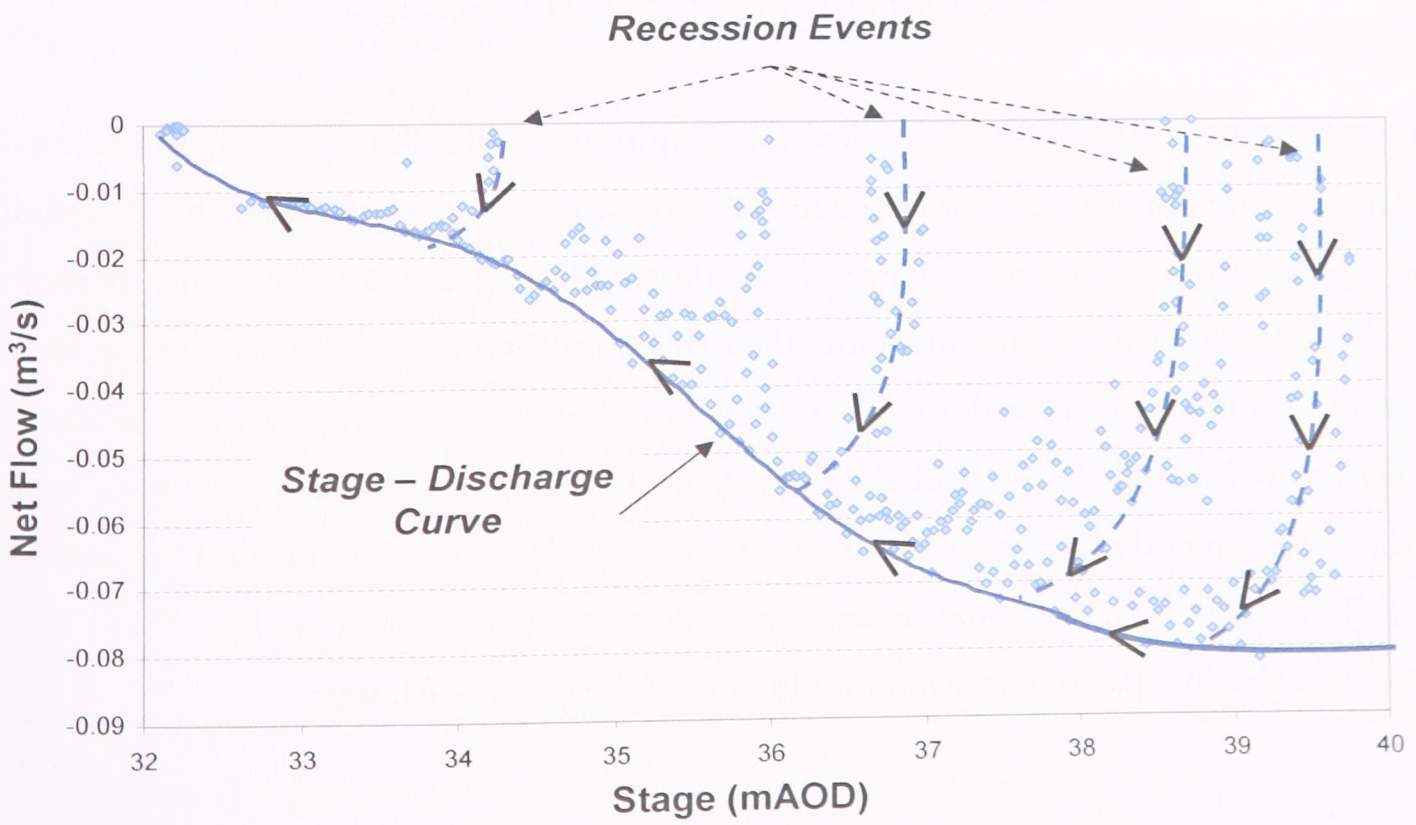


Figure 8.14: Plot of net outflow against stage with indicated stage – discharge curve for Ardkill turlough, Co. Mayo

The stage-discharge curves of studied turloughs took an array of forms. Many sites showed a continuous smooth curve across most or all of the flood range, such as Turloughmore, Co. Clare (Figure 8.15 (a)). Others, such as Skealoghan, Co. Mayo, had a number of discontinuities in the stage-discharge relationship, with distinctive discharge curves applying within different flood ranges (Figure 8.15 (b)). This discontinuous behaviour may represent the operation of distinct systems within the turlough basin, with additional outflow capacity available at higher flood levels.

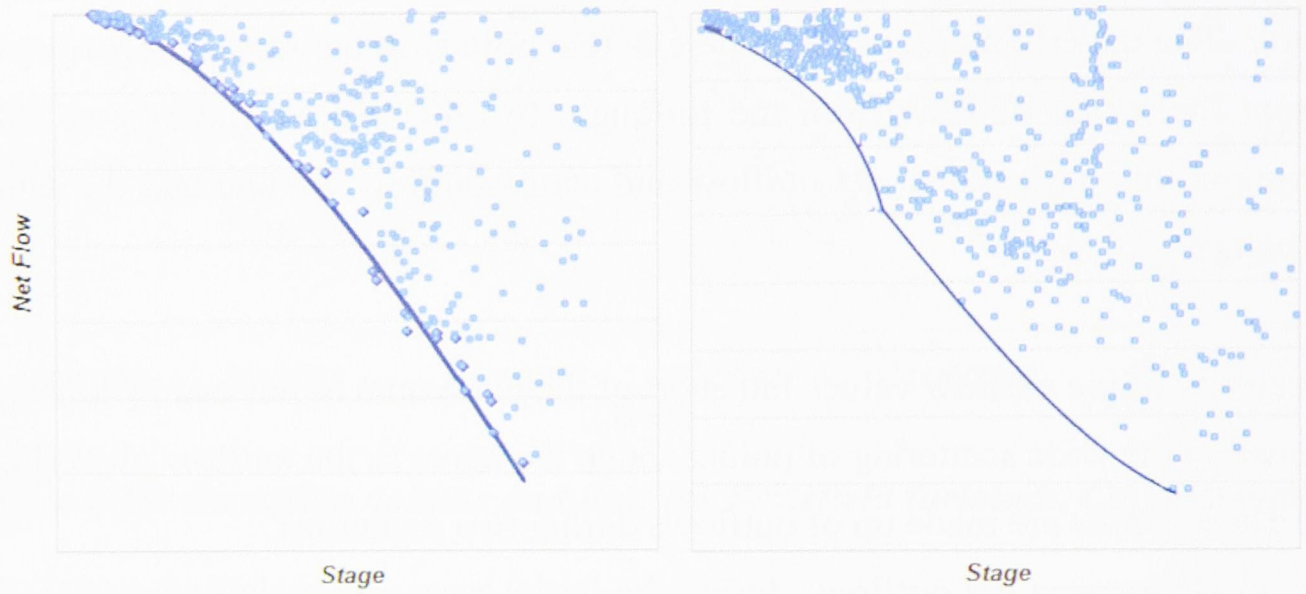


Figure 8.15: (a) Continuous stage – discharge curve of Turloughmore, Co. Clare and (b) discontinuous curve for Skealoghan, Co. Mayo

In such cases a threshold water level is required within the turlough to maintain outflow at the upper maximum capacity. As the water levels fall below this threshold the upper system becomes inaccessible, thus reducing the total outflow capacity available to the turlough and dropping the overall outflow capacity to that of the lower system. Similar behaviour definitely occurs in many turloughs at low water levels, as sinks located above the base of the depression become isolated from the main water body. Consequently, the estavelles cease to operate as outflow points and the outflow rate drops severely. In some cases, outflow effectively ceases at low flood level leaving a shallow permanent water body at the base of the turlough.

A number of sites showed an apparent maximum outflow capacity independent of water level in the upper range of flooding. Rather than a reduction in outflow with falling head within the turlough, as would be expected in a raised tank draining out through an orifice into the underlying system, the outflow is limited by a single maximum value across a range of stages (Figure 8.16). This trait is prevalent in turloughs characterised by long duration, low frequency flooding such as Brierfield, Termon and Coolcam.

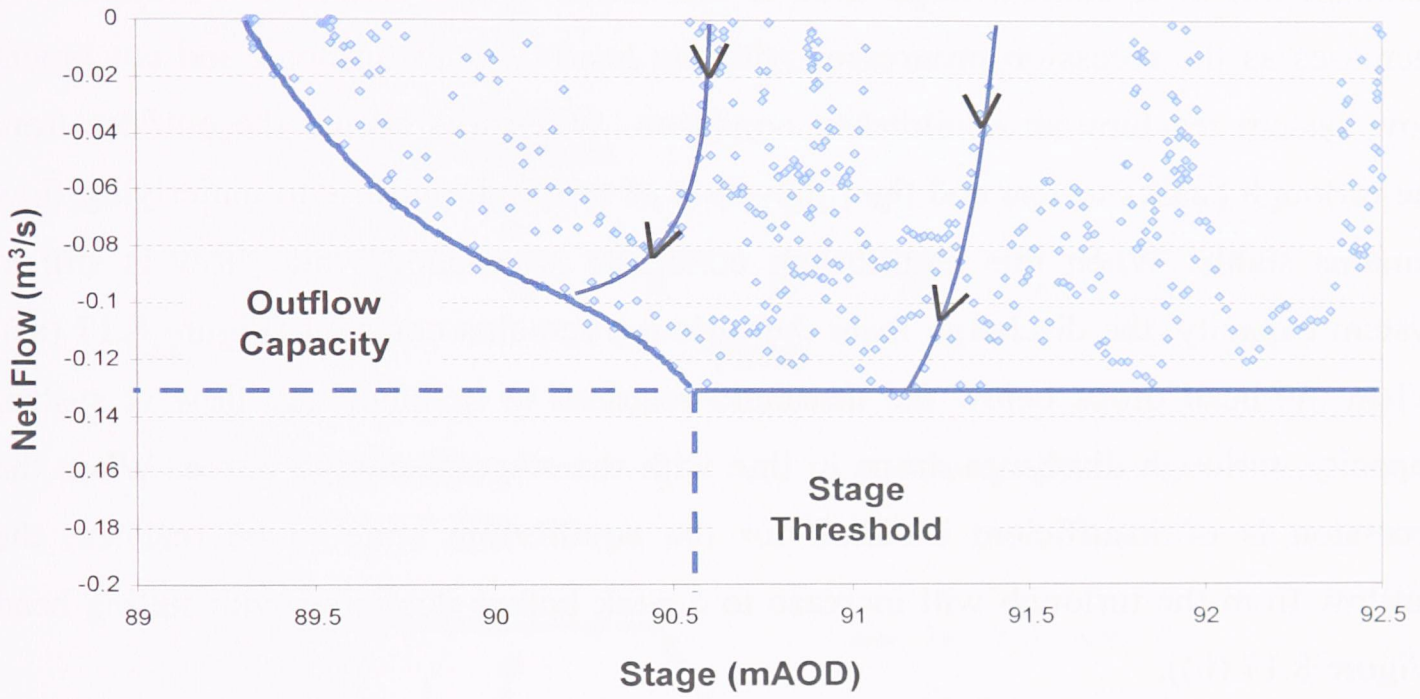
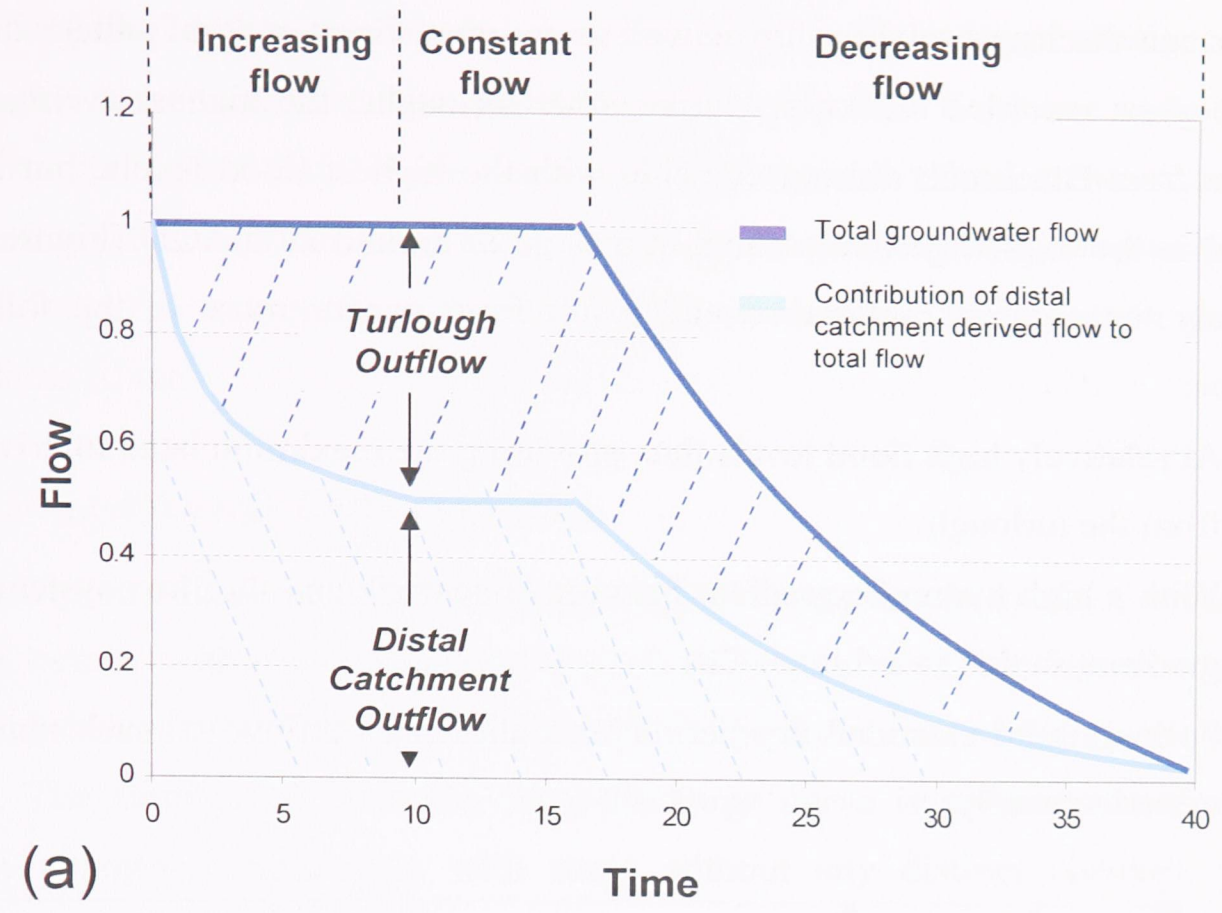


Figure 8.16: Stage – discharge relationship indicating maximum outflow capacity and stage threshold for Brierfield turlough, Co. Roscommon

This constant outflow rate may represent the maximum drainage capacity of the system in equilibrium conditions. When levels fall below the threshold required to maintain outflow at maximum capacity, the controlling factor on discharge becomes water level and the turlough is draining more or less freely, where outflow is regulated by the system's discharge capacity. These slower turloughs can be seen to take significantly longer to reach maximum outflow for a given stage, and in many cases there is insufficient time between rainfall events for outflow capacity to be reached. Consequently, turlough outflow operates below capacity for substantial periods of the recession resulting in prolonged flood duration.

In this interpretation, the total capacity of the karst flow system is composed of two elements: flow derived from water held in storage within the turlough itself (turlough flow) and flow derived from a distal catchment which does not necessarily enter the turlough. The floodwater which enters the turlough during the main filling phase may be composed of both waters derived from local (proximal) sources, such as the topographic catchment, and waters derived from the distal catchment. The proportion of each element within this total is controlled by their relative heads. During the initial recession phase the underlying catchment flow is preferentially accommodated with a resultant fall in catchment head. Due to this drop, the proportion of turlough flow increases as the recession progresses with the head of both turlough and catchment flow system reaching an equilibrium condition. When this occurs the outflow from the turlough ceases to rise and the proportion of turlough outflow to underlying flow remains stable. When this equilibrium condition is reached while flow is still at system capacity, the discharge from the turlough remains constant (Figure 8.17 (a)). When the head drops below the threshold required to maintain the flow at system capacity, turlough discharge drops in line with the stage-discharge curve. When the recession is of insufficient duration for the equilibrium state to be reached, the outflow from the turlough will increase to a peak before declining with falling head (Figure 8.17 (b)).

Alternatively, the constant net outflow rate may represent the maximum possible discharge after the cessation of any inflow into the turlough. In this scenario, both inflow and outflow occurs simultaneously and there is no water derived from a distal catchment. Here, the turlough is continuously discharging at maximum capacity, and the difference between net outflow and maximum capacity gives the inflow time series. When a sufficient amount of time has elapsed after the cessation of rainfall inflow into the turlough ceases, and the net outflow reaches the maximum outflow capacity.



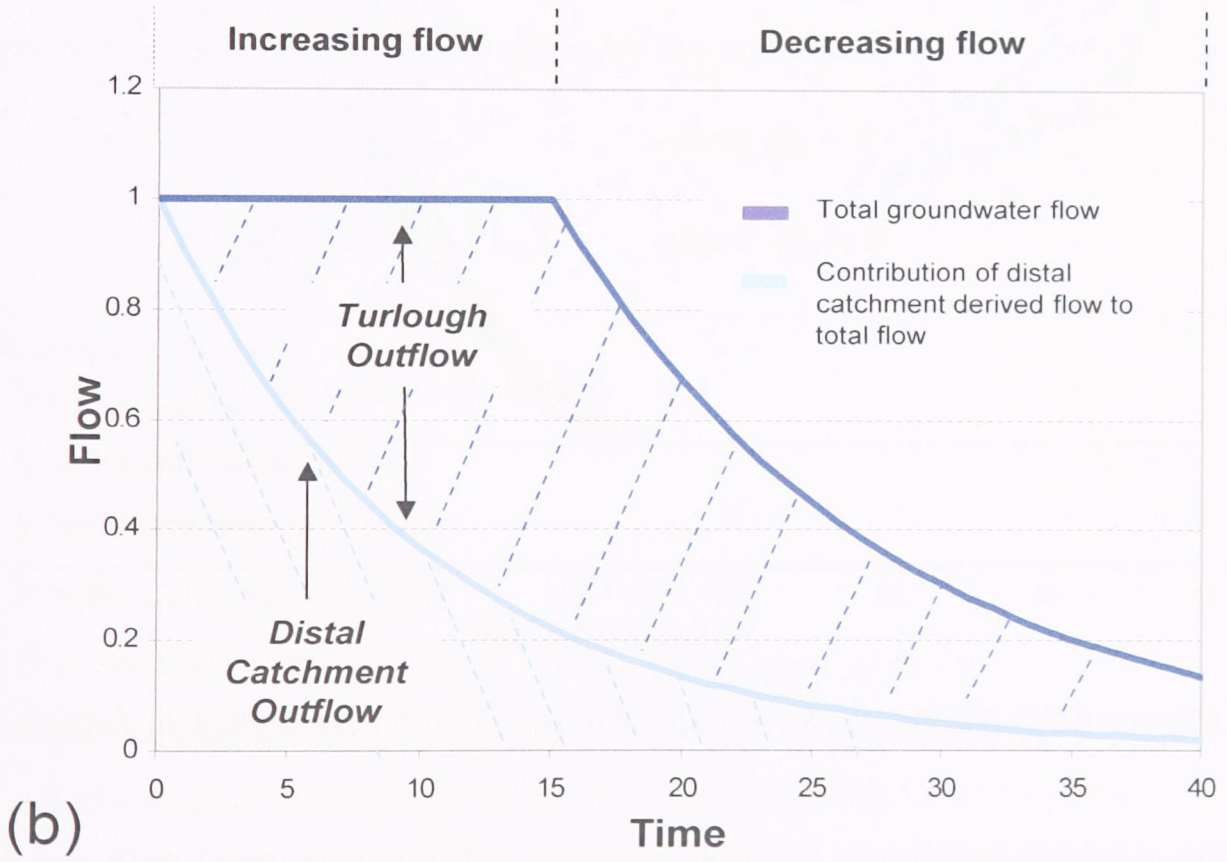


Figure 8.17: Illustration of proportion of flows in underground network during turlough recession for (a) case where system outflow capacity is reached during recession and (b) where system outflow capacity is not reached

The outflow rates of Blackrock turlough, the largest site volumetrically, show a unique stage-discharge relationship as well as an interesting temporal pattern in terms of the highest recorded outflows. Unlike other turloughs, the highest average daily outflows from Blackrock did not coincide with the highest flood levels, but instead occurred in the mid-range of flooding, at a stage of around 20 mAOD (Figure 8.18). Intuitively the greatest outflows would result from one or more of the following scenarios:

- At relatively high flood levels thus providing the maximum head to drive flow from the turlough
- With a high hydraulic gradient between Blackrock and the flow system down gradient, in this case Lough Coy
- Following an extended dry period thus allowing outflow to reach maximum system capacity

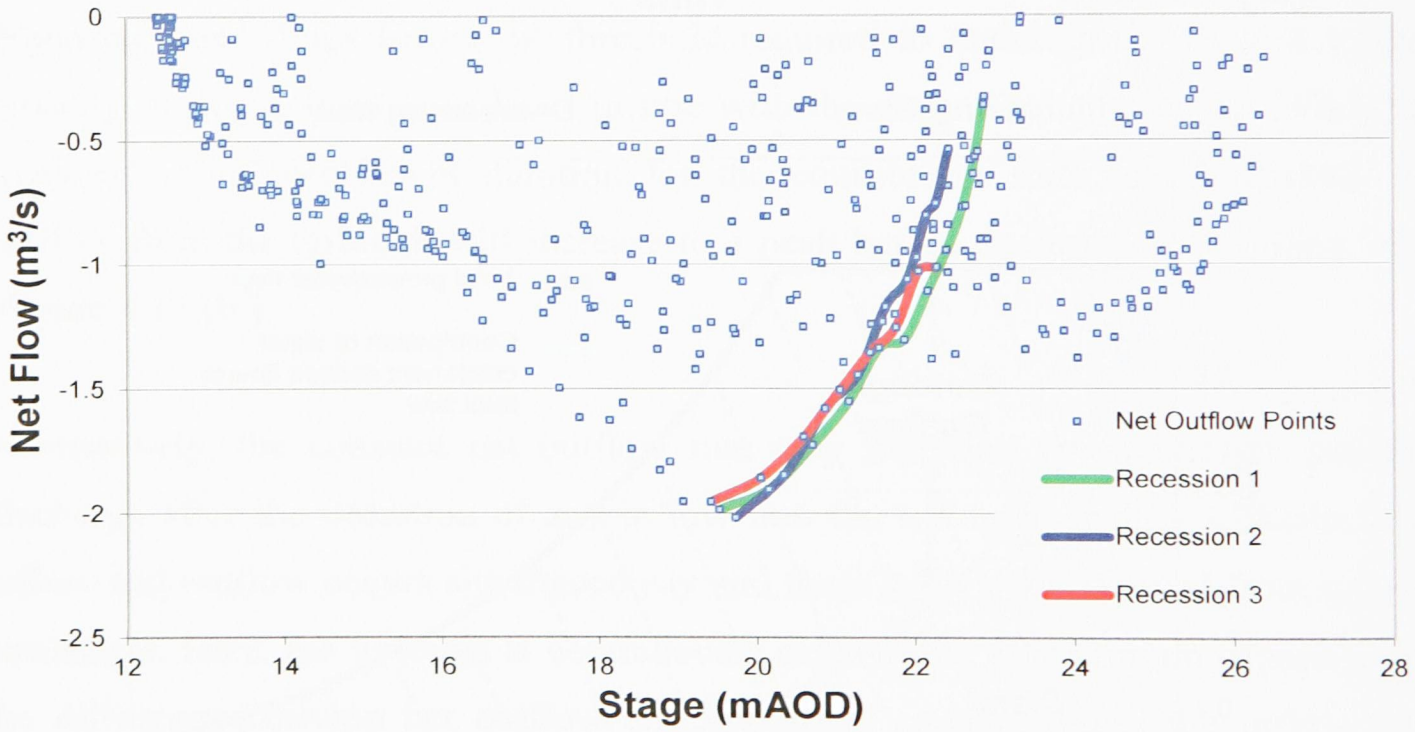


Figure 8.18: Stage-discharge plot for Blackrock turlough, Co. Galway

The stage at which maximum outflow occurred did not correspond with any of these scenarios. Instead the common trait across the three recessions containing the highest recorded outflows is that they follow periods of low or absent levels of flooding. One possible explanation for this is that in the early phase of flooding, significant storage exists lower down the system which is able to accommodate higher outflow quantities from Blackrock. Later in the season, when the system has reached equilibrium, the outflow from Blackrock is limited and does not exceed the threshold of around

1.4m^3/s. The riverine nature of Blackrock must also be highly influential in determining flow behaviour. Blackrock is the only riverine turlough within the study group with the Owenshree River discharging directly into the basin at high flood levels. As the highest flood levels coincide with the greatest flow in the river, it may be that the actual outflow from Blackrock is much greater at higher stages than is indicated by the net outflow figures due to continuous, direct inflow from the Owenshree River.

8.4.1. Stage-discharge Curve Derivation

The derivation of a stage-discharge relationship is complicated by the occurrence of rainfall events within the recession period. The maximum outflow events were extracted from the outflow dataset and used in the derivation of the stage-discharge curves. The simplest form of the stage-discharge curve is present where turlough outflow changes continuously with stage without any distinct changes in flow behaviour (Figure 8.19). In this case the stage-discharge relation is comprised of a single curve where the outflow ***Q*** is given by the equations:

$$Q = a(H - H_0)^b \qquad \textit{where } Q_0 = 0$$

$$Q = q + a(H - H_0)^b \qquad \textit{where } Q_0 > 0$$

Where:

Q_0 is the outflow at stage H_0 (m^3/s)

Q is the outflow (m^3/s)

a is the scaling coefficient

b is the orifice coefficient

H is turlough stage (mAOD)

H_0 is turlough base level (mAOD)

q is the outflow rate at lowest recorded stage (m^3/s)

The additional flow term ***q*** is required where the Diver was located slightly above the lowest level within the turlough. In this case there would still be outflow at stage ***H_0***, and therefore the stage-discharge curve must to be offset by an amount ***q*** during derivation. The parameters a and b are derived using the least squares estimation method.

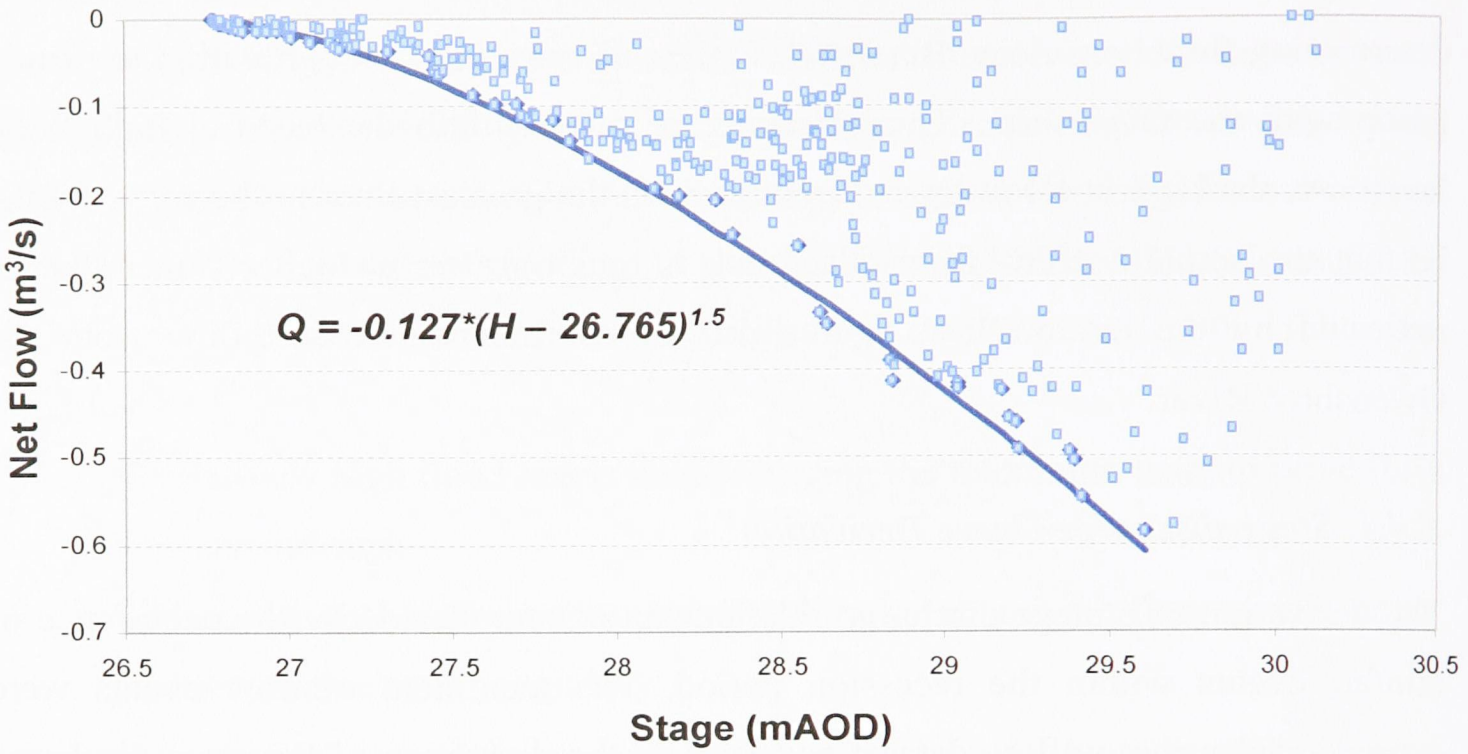


Figure 8.19: Stage-discharge curve for Turloughmore, Co. Clare

The second variation on the stage-discharge relationship is for those sites which display a maximum outflow capacity above a certain stage threshold, but below this have a consistent stage-discharge relationship (Figure 8.20). Here the stage-discharge relationship consists of two parts covering constant and varying outflow, and the outflow Q is given by:

$$\textit{For } H < H_t \quad : \quad \begin{cases} Q = a(H - H_0)^b \\ Q = q + a(H - H_0)^b \end{cases}$$

$$\textit{For } H \geq H_t \quad : \quad Q = Q_{max}$$

Where:

H_t is the threshold stage above which outflow is at maximum capacity (mAOD)

Q_{max} is the maximum outflow capacity

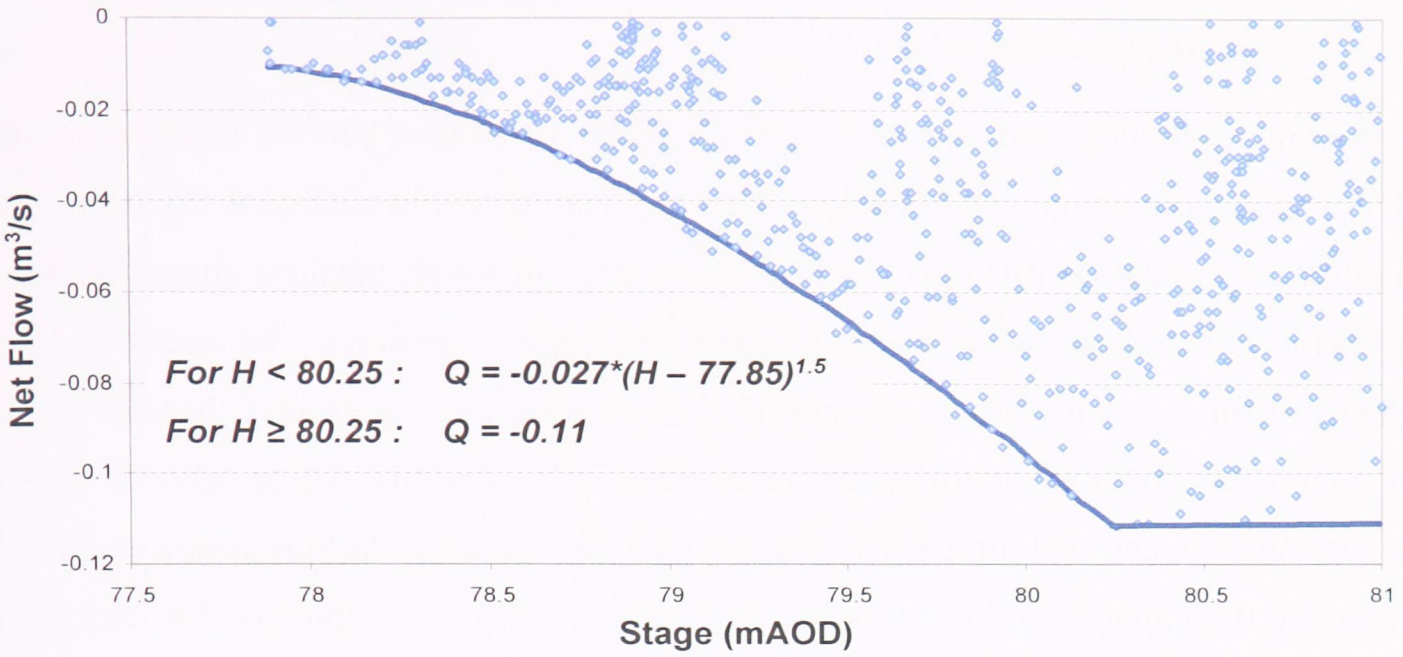


Figure 8.20: Stage-discharge curve for Croaghill turlough, Co. Galway

The final stage-discharge type is for those turloughs which demonstrated differing outflow behaviours with changing stage, either due to the complex interaction and operation of distinct flow systems at different levels within the basin, or the lack of sufficient outflow data to clearly define a continuous relation. In such cases, a number of individual curves were fitted to represent all identifiable outflow behaviours accurately (Figure 8.21).

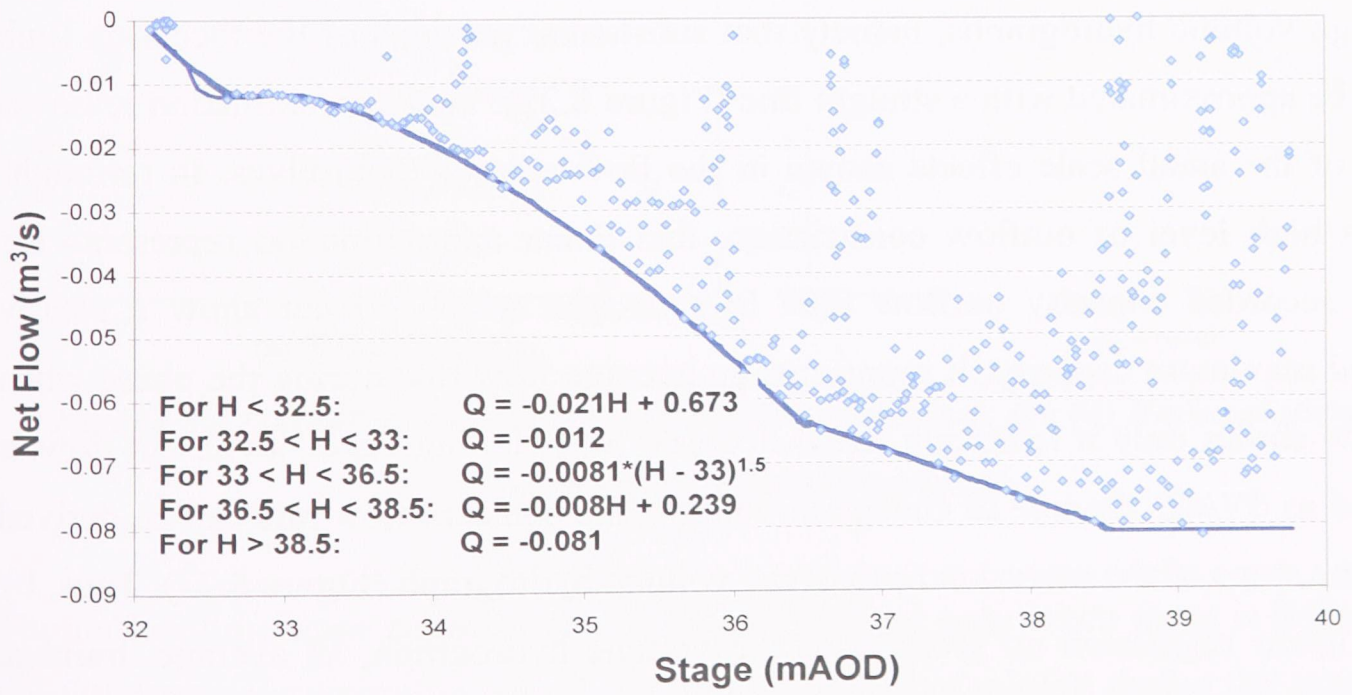


Figure 8.21: Stage-discharge curve for Ardkill turlough, Co. Mayo

8.4.2. Recession Approximation

As shown previously, the recession behaviour of turloughs can be complex, with different stage-discharge relationships often applicable within different flood ranges. This diversity makes it difficult to directly compare turlough outflow characteristics, or generate a standard metric for quantifying turlough recessions. The most obvious solution to this is to use the maximum drainage capacity or a variant thereof which was identified for the majority of turloughs. The capacity value allows direct comparison between turlough flow systems and, by dividing the maximum recorded volume by the capacity value, it also provides a hydrological indicator for recession duration. This figure represents a notional minimum time it would take for the turlough to drain from full. While this time will obviously be less than the actual recession duration, as flow rates drop at lower stages, it does provide an indicative hydrological indicator for turlough recession for use in the interpretation of ecological data.

To ensure consistency in analysis, and to compensate for the lack of a clearly defined outflow capacity in a number of turloughs, a standard method for deriving a constant turlough recession rate was devised. This method utilised a common feature of turlough volume hydrographs, namely that substantial portions of the recession limb could be approximated with a straight line (Figure 8.22). This approximation removes many of the small scale effects shown in the flow records themselves. In turloughs with a high level of outflow constriction, this linear approximation represents the actual recorded capacity outflow rate. In turloughs which do not show a clearly defined maximum capacity, it represents an average flow rate during the phase when outflow shows only a relatively small decrease with falling water level. As flow is defined as dV/dT, the rate of change in volume, the constant flow rate can be derived from the slope of the recession limb of the volume hydrograph (Figure 8.23). Thus, by using linear regression on sections of the volume hydrograph, an average drainage capacity was derived for each turlough.

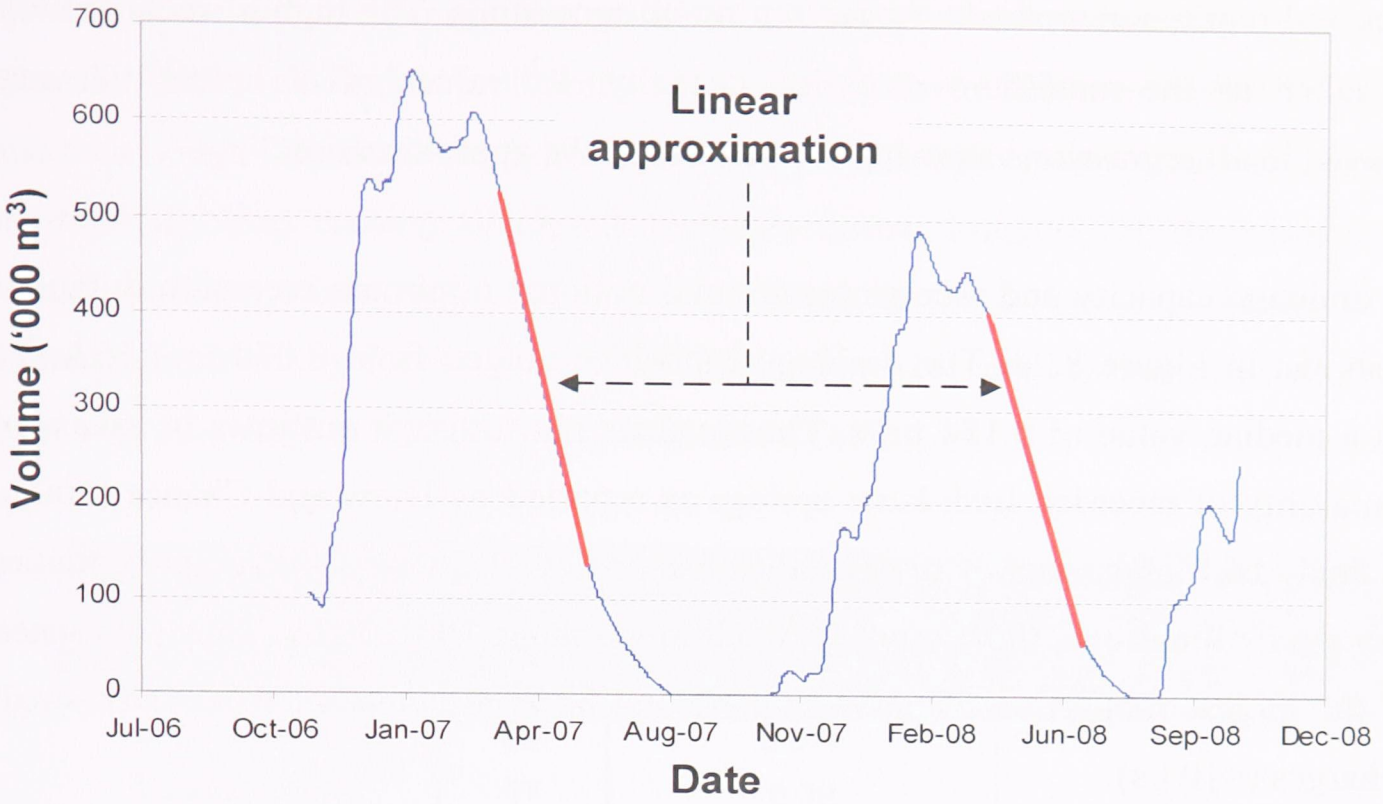


Figure 8.22: Linear approximation of volume recession, Ardkill turlough, Co. Mayo

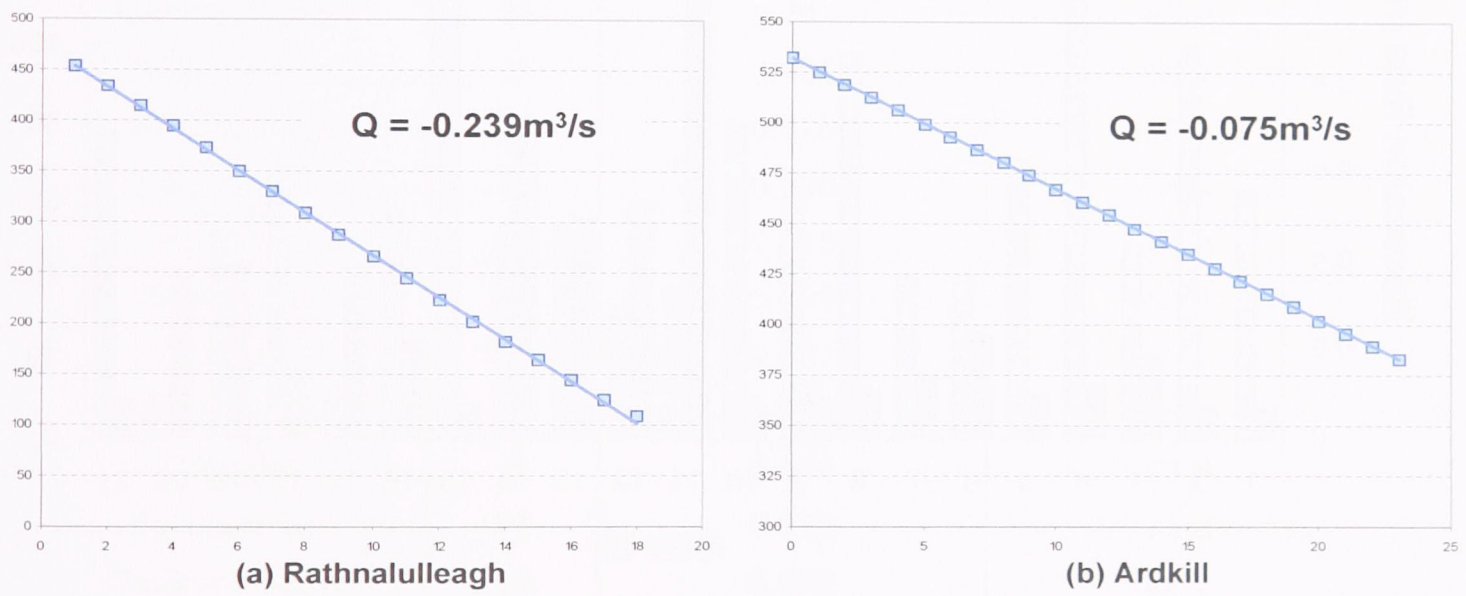


Figure 8.23: Regression analysis of volume recessions for (a) Rathnalulleagh turlough and (b) Ardkill turlough

The notional drainage capacity can be clearly defined only when there is little or no rainfall during the recession period. To limit the effect of rainfall during the recession, regression analysis was carried out on data from mid-March to late April 2007, a period where little or no rainfall fell across all study sites. A few fast responding turloughs such as Turloughmore and Lough Aleenaun had fully receded prior this period. In these cases multiple recession events were isolated from the volume time

series and regression analysis carried out on all recessions. The highest recorded rate was taken as the maximum recession capacity. R^2 values of at least 0.98 were achieved in all regressions showing the validity of the approximation.

The drainage capacity and recession rates and notional minimum recession durations are shown in Figure 8.24. The drainage capacities ranged from 0.070 to 1.152m^3/s, with a median value of 0.154 m^3/s. These values put turlough outflows in excess of the majority of recorded Irish karst springs as reported by Drew and Chance (2007). In a study of Irish springs with discharges exceeding 10 l/s in eight sample counties underlain by limestone, they found 66% fell in the range 10 - 100 l/s. They also stated that the largest proportion of springs in Ireland is represented by those with small discharges (<10 l/s).

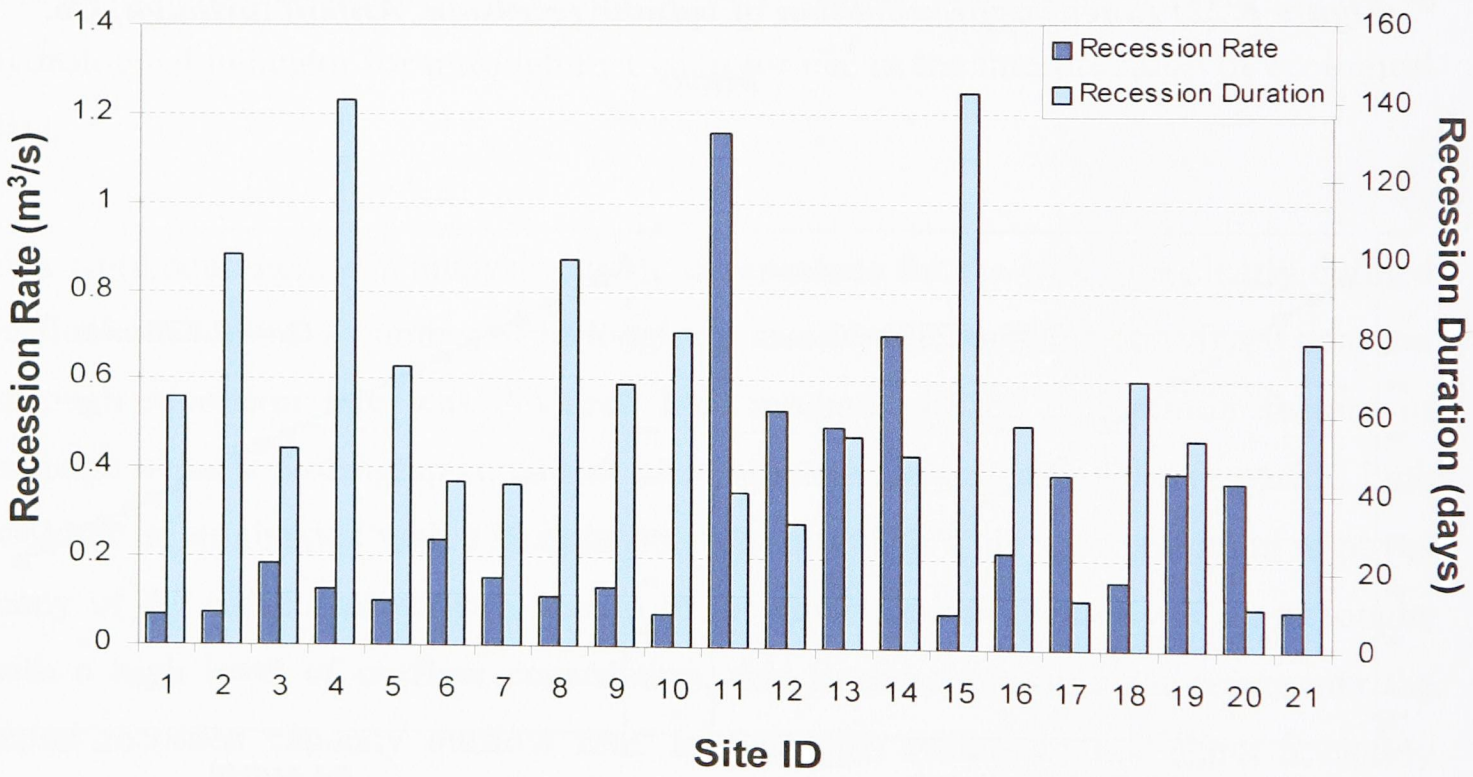


Figure 8.24: Approximated drainage capacity and notional recession duration for 21 monitored turloughs

As found in earlier analysis, the turloughs of the Gort-Kinvarra chain (sites 11 to 14) showed the greatest outflow capacity, accounting for the four highest values. This is thought to be due to a well-developed conduit system and its ability to accommodate large flows. Interestingly, Lough Coy displayed lower notional recession duration than Blackrock, despite the fact that Blackrock consistently empties before Lough Coy. This anomaly can be explained by considering the configuration of the flow

system, where due to their relative gradients and connection to the underlying conduit system, Blackrock drains preferentially to Lough Coy. This preferential drainage prevents Lough Coy from emptying at a high rate until Blackrock has already dropped significantly, thus causing Blackrock to empty before Lough Coy. As a fraction of overall volume, however, the drainage capacities of Lough Aleenaun and Turloughmore are by far the greatest. This is reflected in the low recession durations of 11 and 12.4 days respectively for these sites (Table 8.4).

Site Name	Site ID	Approximated Drainage Capacity (m^3/s)	Minimum Recession Duration (days)
Lough Aleenaun	20	0.374	11
Turloughmore	17	0.39	12.4
Lough Coy	12	0.535	32
Blackrock	11	1.156	40.1
Carrowreagh	7	0.152	41.6
Rathnalulleagh	6	0.239	42.4
Caherglassaun	14	0.701	49.5
Kilglassaun	3	0.185	50.7
Knockaunroe	19	0.396	53.8
Garryland	13	0.496	54.4
Roo West	16	0.218	57.3
Skealoghan	1	0.069	64.1
Lisduff	9	0.132	67.5
Lough Gealain	18	0.154	69.1
Croaghill	5	0.103	71.8
Ballinderreen	21	0.088	78.3
Caranavoodaun	10	0.072	80.7
Brierfield	8	0.109	99.4
Ardkill	2	0.075	100.6
Coolcam	4	0.129	140.9
Termon	15	0.078	142.5

Table 8.4: Approximated drainage capacity and recession duration for study sites

8.5. Indirect Flow Estimation

Flows calculated based on volume time series give the net flow rates rather than actual flows, although depending upon the modus operandi of the flow system these may be one and the same. The direct measurement of flow within turloughs is an extremely difficult task, as the points at which inflow and outflow occur within the turlough are not well confined (such as within a channel) and are submerged during the period of inundation. However, the identification of inflow periods would provide a greater understanding of turlough hydrological operation, as well as elucidate the relationship between net flow and actual flow. In order to achieve this, a number of potential methods to identify the presence of inflow were considered.

Direct flow measurement using electromagnetic current sensors and specialised loggers could provide an in-situ means of velocity measurement, but were found to be prohibitively expensive for this project. The use of thermal imaging or thermography could potentially identify the locations of inflow points due to differences in water temperature between surface and groundwater (Bogle and Loy, 1995). Ideally two sets of images would be taken during both the filling and emptying phases, and if possible during cold weather maximising the temperature differential. This too was prohibitively expensive and outside the scope of the project. However, as a surrogate for thermal imaging, an array of temperature probes was installed in an estavelle in Caranavoodaun, Co. Galway.

8.5.1. Water Temperature

The aim of the temperature array was to allow comparison of water temperature at the estavelle with the temperature record of the Diver further out into the turlough. The water temperature at an operational estavelle would reflect groundwater temperatures during inflow periods and the ambient temperature of the turlough water body during outflow periods. Evidence from spatial sampling of a turlough basin (Gill, 2010) indicated that turloughs are well mixed, and so the Diver temperature was assumed to be representative of the water temperature throughout the turlough water body. In theory, by comparing the temperature record from a known operational estavelle with the record from the main turlough water body an indication of the periods during

which the estavelle operated as an inflow point could be ascertained. Multiple probes were also set at 0.25 m height intervals to record changes in temperature within the water column itself. Insignificant differences were seen between the probes in the array during full submersion. However, as the water level began to drop, the upper probes were exposed to air temperatures and thus ceased to give a useful indicator of water temperature. As a result, the probe closest to the base of the estavelle was used for comparison with the Diver record.

A plot of hourly water temperatures recorded by the Diver and probe is shown in Figure 8.25, together with the stage time series showing the flood recession. The rainfall during the same period is also shown in the upper graph. It is clear that there is little to distinguish the two temperature series during the initial part of the recession with both signals matching each other closely. This is despite the substantial rainfall events which occurred during the recession. These would have been sufficient to produce inflow into the turlough in the flow-through scenario, and so a difference would be expected between the temperature records during this period. The lack of difference indicates that both locations experienced similar hydrological conditions, thus implying the estavelle was draining water from the main water body throughout this period. Alternatively, it is possible that the swallow hole is not an estevelle, and there is another location in the turlough through which the majority of recharge enters the turlough.



Figure 8.25: Plot of Diver and Probe temperatures and corresponding rainfall during flood recession in Caranavoodaun turlough, Co. Galway

The water temperatures showed a substantially damped response to air temperatures in the initial recession phase, but as water levels drop the response becomes more pronounced. This is particularly evident in the probe temperature record (Figure 8.26). Later in the recession, the temperature records begin to diverge with the daily fluctuations in the probe temperature readings become more pronounced as the water level drops. Despite the estavelle being at a lower elevation than the Diver, the estavelle completely dried out towards the end of the recession, thus responding more rapidly to air temperature. In contrast, the Diver remained submerged under more than 0.5 m throughout and so showed a more stable temperature reading (Figure 8.25). The greater outflow capacity of the estavelle facilitated complete emptying, whereas the central pond in which the Diver was located appears to be perched.

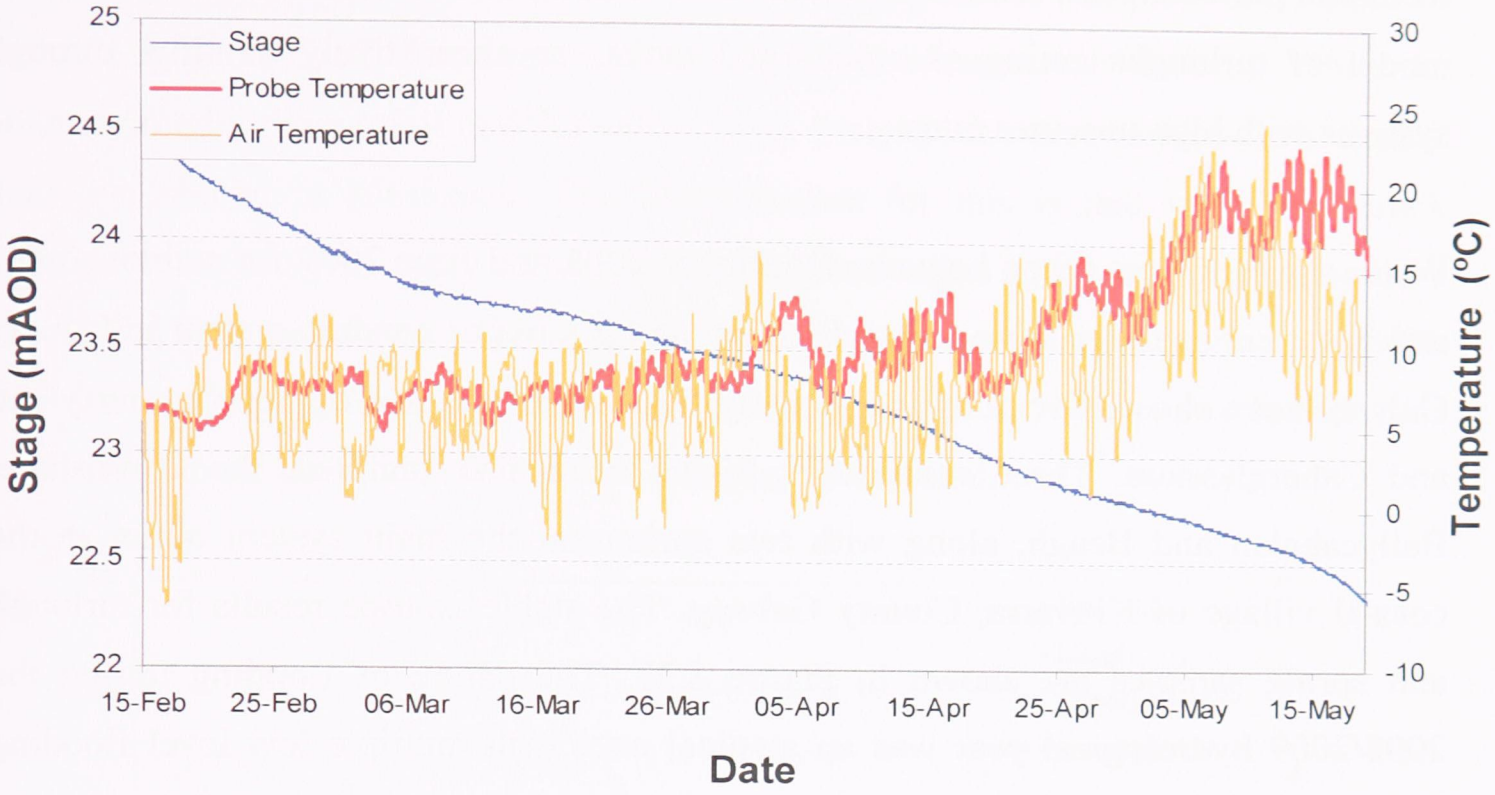


Figure 8.26: Plot of probe and air temperature time series during recession in Caranavoodaun turlough, Co. Galway

In summary, this trial provided some tentative support for the idea that turloughs do not experience significant groundwater inflows during the recession period. However, the results were not conclusive as all possible inflow and outflow sites across the turlough would have to be instrumented to provide a more definitive picture of turlough operation. In this case, inflow into the main turlough basin was witnessed from a depression located in the eastern end of the turlough. This could potentially have been in operation during the recession period, and so would have to be instrumented to clarify. However, this method showed promise and a full scale instrumentation of a site, particularly if in conjunction with the continuous measurement of an indicative hydrochemical parameter of groundwater flow such as conductivity, would give a better understanding of turlough flow behaviour.

8.5.2. Stable Isotope Analysis

The technique of stable isotope analysis was also investigated to see if it could provide an insight into the hydrological operation of turloughs. Through the sampling of waters from turloughs and contributing rivers within the Gort area and examining the spatial and temporal changes in their isotopic composition, it was hoped that it might be possible to identify whether or not significant inflows were occurring during

recession periods. This, in turn, would then provide evidence for either the conceptual model of turloughs acting as surcharged tanks, or alternatively as flow through systems with high turnover rates.

Water samples were taken between December 2008 and June 2009 for stable isotope and chemical analysis. Five turloughs lying along a major conduit system in County Galway were chosen for sampling, namely Blackrock, Lough Coy, Coole, Garryland and Caherglassaun. Three contributing rivers were also sampled, the Owenshree, Ballycahalan and Beagh, along with two springs at the main system outlet in the coastal village of Kinvarra, County Galway. The stable isotope results for turlough and spring samples are shown in Figure 8.27. The nature of flooding during the 2008/2009 hydrological year was an atypical one, with multiple low level flooding events from August 2008 onwards. The short timescale at which filling and emptying occurred throughout the season made it difficult to ascertain the true $\delta^{18}O$ behaviour during filling and recession periods.

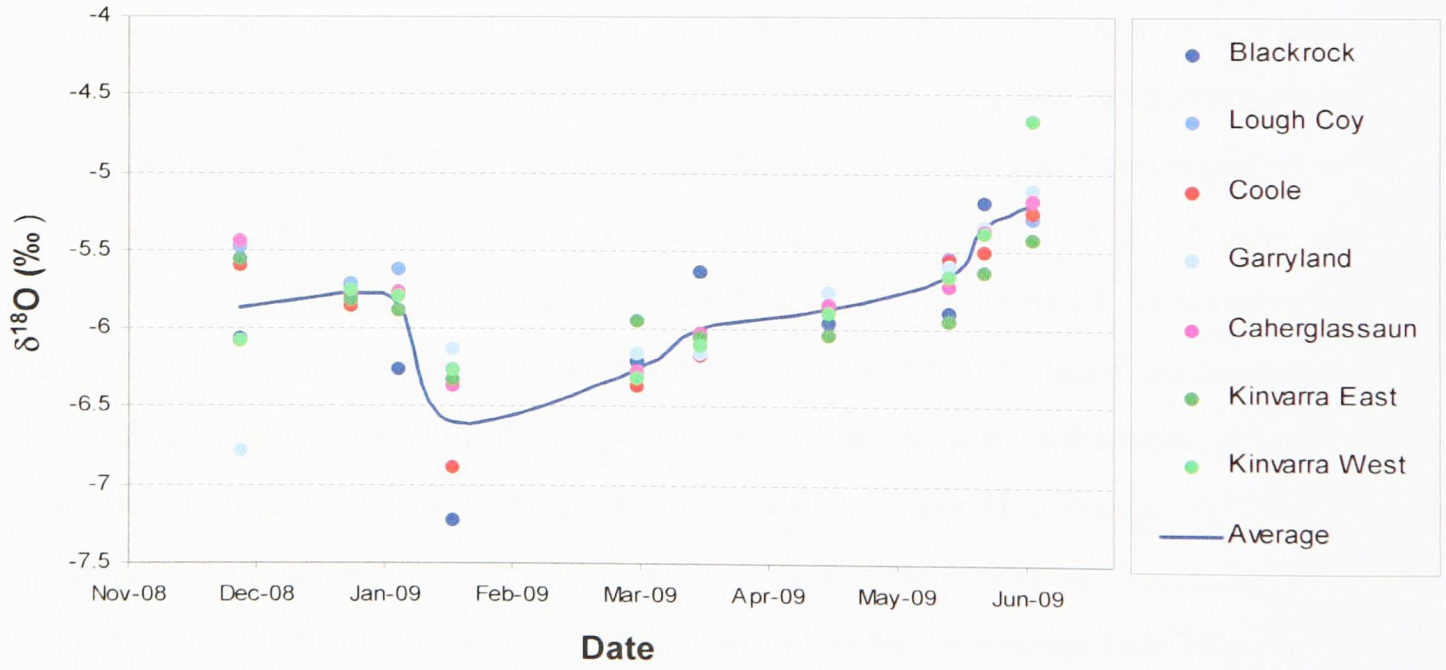


Figure 8.27: ^{18}O stable isotope results from turloughs and springs

The general trend in $\delta^{18}O$ values shows a slight enrichment from February onwards. The fall in $\delta^{18}O$ values occurring between January and February coincides with renewed flooding within the turlough basins (Figure 8.28). The incoming floodwater would have a lighter isotopic signature than the existing water within the turloughs, thus causing a fall in $\delta^{18}O$. The lowest level of turlough enrichment during this sampling event was shown by Blackrock in February 2009, with a $\delta^{18}O$ of -7.22‰.

This sample was taken from a flood event which followed a complete drying out of the turlough, and so all floodwaters within the basin where newly derived. While the other turloughs show a fall in $\delta^{18}O$ values from January, the decrease is much smaller than that shown in Blackrock. The likely reason for this is that while Blackrock emptied completely in early January, the other turloughs did not and maintained a substantial volume of water throughout. The new floodwater would have mixed with this existing slightly enriched water body, thus giving a net $\delta^{18}O$ value higher than otherwise would have been if they had completely emptied.

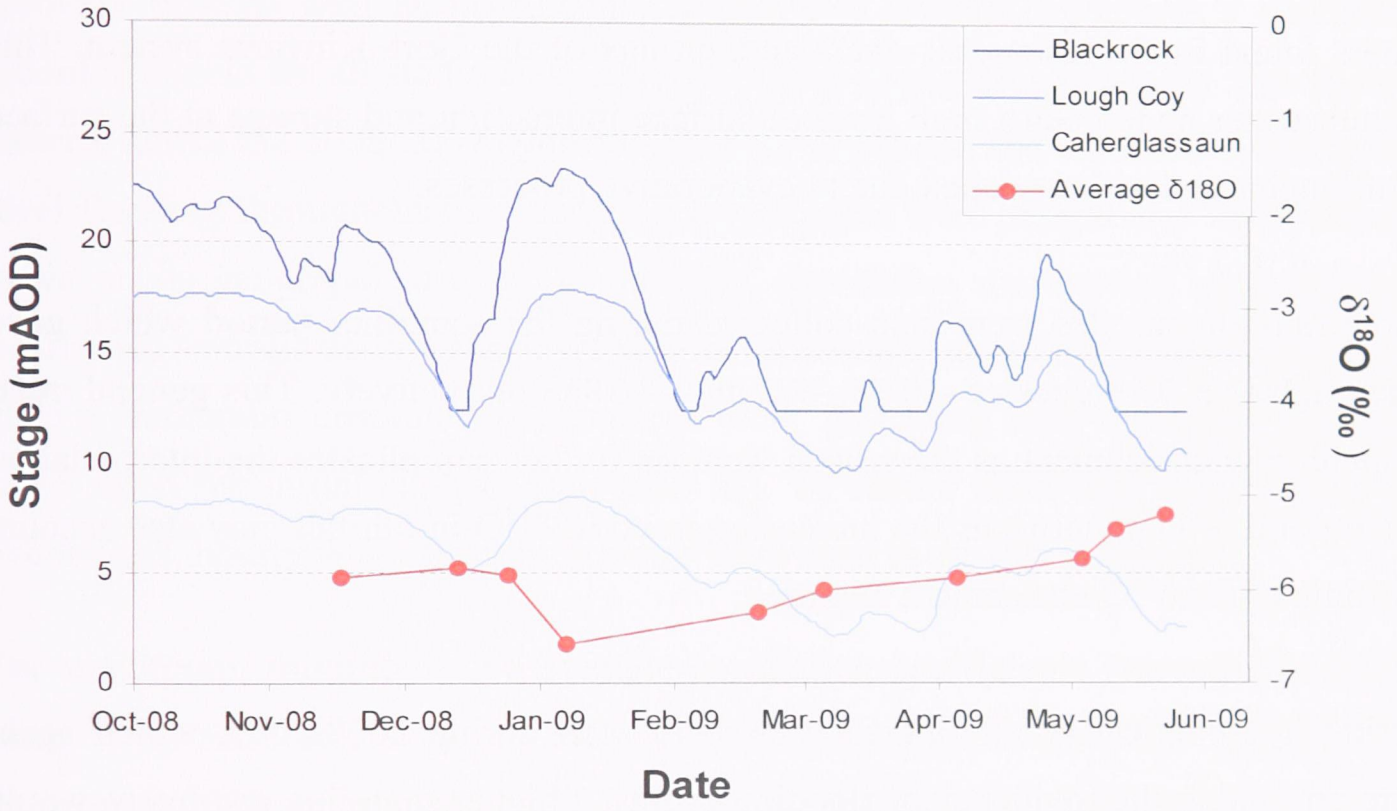


Figure 8.28: Plot of water levels for Blackrock, Lough Coy and Caherglassaun turloughs with average of turlough $\delta^{18}O$ values

Following this flood event, there is a trend of $\delta^{18}O$ enrichment during recession periods and generally as the season progresses. The rate of $\delta^{18}O$ enrichment is greater between 17/3/2009 and 1/4/2009 than it is earlier in the recession between 2/2/2009 and 17/3/2009. There are a number of potential causes for this pattern. Firstly, the rate of evaporation may have increased due to rising temperatures and longer days. Alternatively, the latter recession occurred at lower flood levels, where the turloughs have a higher volume to surface area ratio and so are susceptible to higher rates of evaporation per unit volume. Finally, just before the sampling in March 2009 there was a rise in turlough water levels, signifying an inflow of water (Figure 8.28). This inflow would have been recently derived from rainfall and so be characterised by

lower levels of enrichment. This could have masked the true scale of enrichment during this period.

Two boreholes were also sampled in the area, giving $\delta^{18}O$ values of -7.78 and -8.39‰. Both show a level of enrichment lower than that of any turlough, river or spring sampled. This would be expected as rainfall recharge infiltrates directly into the karst aquifer, and so spends little time at the surface exposed to fractionation processes such as evaporation. These values may represent the isotopic signature of groundwater derived from matrix and fracture porosity rather than the conduit derived waters found in the turloughs, rivers and springs of the Gort–Kinvarra system. This conduit water undergoes a high level of surface interaction and storage at the surface in turloughs, and so is enriched due to evaporative processes.

Three rainfall samples were also collected during the sampling period which gave much lighter $\delta^{18}O$ values of -10.78, -9.2 and -8.38‰ respectively. This general trend of increasing enrichment as the season went on further complicates the interpretation of temporal $\delta^{18}O$ patterns, as the increasing trend in $\delta^{18}O$ in rainfall may also account for some of the $\delta^{18}O$ enrichment recorded.

During hydrological conditions such as were seen during 2008/2009, which again were unusual in the frequency of flooding events, a higher sampling resolution would be required to accurately record turlough isotopic behaviour. A future study could be carried out with a more frequent sampling regime of turlough water and rainfall, as well as the isotopic values of air vapour. Water samples could be taken from suspected estavelles throughout the flooding season to see if any discernable differences can be picked up in the isotopic signature of incoming water and water in the main turlough body. Such a study, if carried out concurrently with intensive spatial temperature monitoring, would provide a valuable insight into turlough operation and potentially bring clarity to the issue of turlough hydrological operation. Also the testing of samples for stable hydrogen isotopes, which was unavailable during this project, would provide added information on the level of evaporation occurring during the turlough flooding season.

CHAPTER 9. TIME SERIES ANALYSIS

9.1. Simple Correlation Analysis

To examine initial similarities between different turlough water level profiles, correlation analysis was carried out on water level time series. The hydrological year from October 1st 2007 to the 30th September 2008 was chosen as the analysis period as it represented a full flooding cycle. Also due to variations in installation and recovery time as well as instrument failures, this interval represents a continuous record available for all study sites. 2007/2008 also displayed a relatively typical flood pattern, unlike the 2008/2009 hydrological year which showed extended duration, low level flooding throughout the year. Site ID numbers were assigned to each turlough based on its geographical location. Initially, correlation was carried out using both hourly and average daily water level records. A comparison of correlation coefficients gave a maximum absolute difference of 0.04, indicating data resolution had little effect upon the initial analysis (appendix C). To ensure short-term effects were not overlooked, hourly water level time series were used in the initial analysis.

The maximum, minimum, and average correlation coefficients between the hourly water level time series for all turloughs for the period October 1st 2007 to 30th September 2008 are shown in Table 9.1, with the full correlation matrix given in appendix C. The range of coefficients, from 0.996 to 0.048, shows the diversity of hydrological regimes and the continuum that exist across turlough ecosystems. Generally there is a good level of correlation between time series with high average coefficients, indicating a broadly similar flooding regime across the study sites corresponding to the seasonal inundation pattern. Some sites showed an extremely high level of correlation, with values approaching 1 derived for several turlough pairs: 0.995 between Garryland and Caherglassaun, and 0.996 between Lough Gealain and Knockaunroe. These pairs are geographically adjacent, with hydrograph comparisons showing them to be almost identical in terms of level and response time, with virtually simultaneous changes in water levels. Such close correlations would be expected if direct, relatively unrestricted connections existed between the water bodies or, in the absence of a direct linkage, a connection to a common groundwater flow system with both sites responding similarly to changing hydrological conditions.

Alternatively, given that adjacent turloughs receive identical rainfall inputs, a similar modus operandi could result in highly correlated hydrological regimes even if each site operated in isolation. The relationships between geographically bordering, possibly hydraulically linked sites are further investigated in Section 9.4.

Site ID	Site Name	Maximum Correlation		Minimum Correlation		
		Value	Corresponding Site ID	Value	Corresponding Site ID	Average Correlation
1	Skealoghan	0.972	10	0.548	4	0.846
2	Ardkill	0.975	5	0.303	20	0.758
3	Kilglassaun	0.950	14	0.538	4	0.839
4	Coolcam	0.990	15	0.048	20	0.608
5	Croaghill	0.975	2	0.303	20	0.785
6	Rathnalulleagh	0.978	7	0.537	20	0.846
7	Carrowreagh	0.978	6	0.516	20	0.820
8	Brierfield	0.946	5	0.213	20	0.721
9	Lisduff	0.952	16	0.413	20	0.838
10	Caranavoodaun	0.988	16	0.516	20	0.857
11	Blackrock	0.952	12	0.292	4	0.757
12	Lough Coy	0.973	14	0.325	4	0.770
13	Garryland	0.995	14	0.502	4	0.844
14	Caherglassaun	0.995	13	0.465	4	0.833
15	Termon	0.990	4	0.096	20	0.649
16	Roo West	0.988	10	0.541	20	0.867
17	Turloughmore	0.863	20	0.101	4	0.602
18	Lough Gealain	0.996	19	0.603	4	0.866
19	Knockaunroe	0.996	18	0.611	4	0.862
20	Lough Aleenaun	0.863	17	0.048	4	0.531

Table 9.1: Maximum and minimum correlation coefficients

Some of the highest values correspond to sites which occur in completely different regions of the study area. Termon shows a high correlation of 0.99 with Coolcam, which is located approximately 70km to the north. The similarities between the flooding characteristics are clearly demonstrated in the plot of water levels normalised with respect to maximum depth (Figure 9.1). In contrast, Termon has a relatively low correlation of around 0.5 with nearby sites Garryland and Caherglassaun, again emphasising the spatial heterogeneity that can exist in flow properties within karst systems.

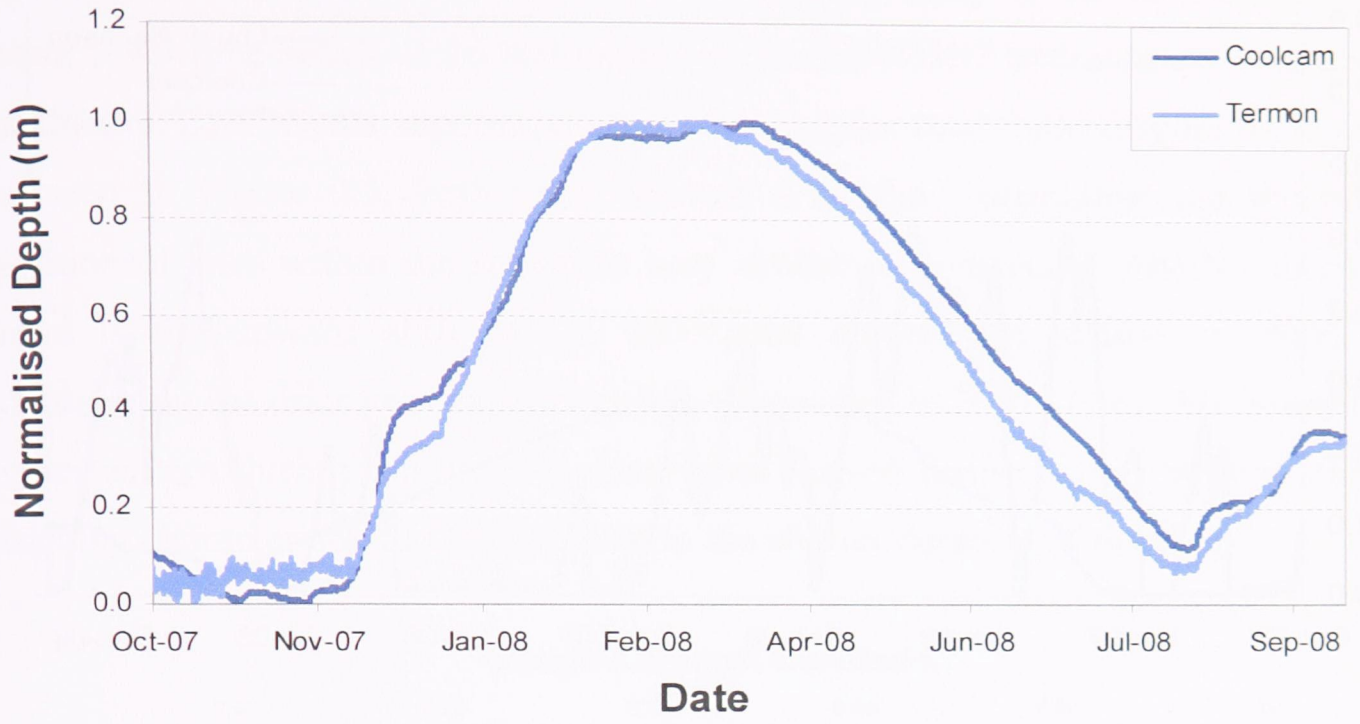


Figure 9.1: Normalised depth plot for Coolcam and Termon turloughs, Co. Galway

While there is a wide spatial variation in the sites corresponding to maximum correlation, it is interesting to note that only two sites account for all of the lowest correlations evaluated: Coolcam (site 4) and Lough Aleenaun (Site 20). As identified in previous analyses, these turloughs represent the extremes of turlough hydrological behaviour. Coolcam's regime consists of a single long duration flood event with gentle rising and recession hydrograph limbs, resulting in a low level of ecological disturbance. Lough Aleenaun displays a multimodal flooding regime with seven distinct flooding events within the same period (*Figure 9.2*). In contrast to Coolcam, the rapid responses to rainfall events and highly fluctuating water levels throughout the year represent a high level of disturbance.

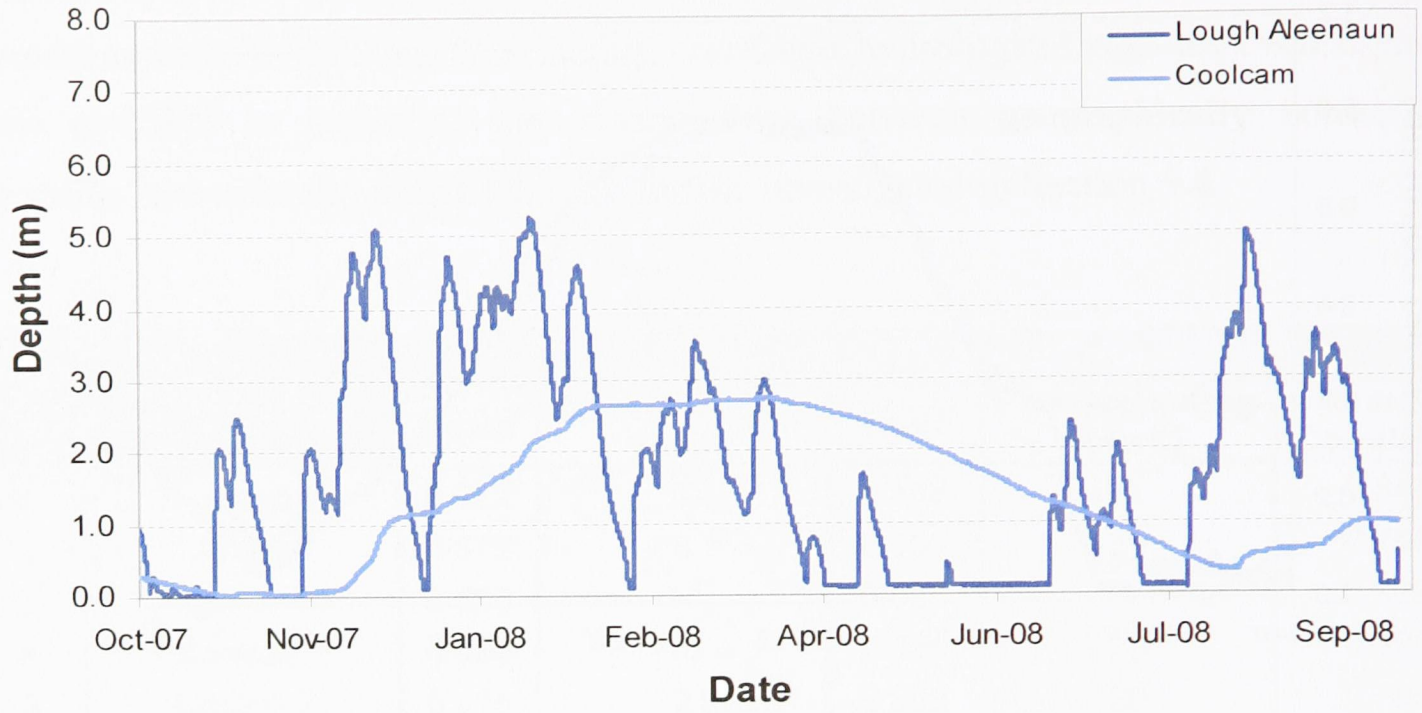


Figure 9.2: Comparison of stage depth hydrographs for Coolcam turlough, Co. Galway and Lough Aleenaun, Co. Clare

By using the behaviour of Coolcam and Aleenaun as benchmarks, an indication as to the nature of a turlough's hydrological regime and the scale of disturbance (frequency and duration of flood events) it represents can be established. A minimum correlation with Coolcam implies a higher level of disturbance with faster and more responsive flooding, whereas a minimum correlation with Aleenaun is indicative of a unimodal flood regime with low disturbance. The minimum correlation ID specifies which end of the disturbance spectrum a site tends towards, with Coolcam signifying a higher level and Aleenaun a lower level. The value of the minimum correlation coefficient itself indicates how far along the spectrum the turlough is, with lower values implying a more extreme regime and vice versa.

A plot of correlation coefficient with Coolcam versus the corresponding Aleenaun coefficient for each turlough shows the relative distribution of disturbance (Figure 9.3). Sites plotted in the lower left corner (Coolcam, Termon, Brierfield, Ardkill and Croaghill) represent the slower responding turloughs with lower levels of disturbance while those in the upper right corner (Lough Aleenaun and Turloughmore) correspond to those sites with highly fluctuating levels and high disturbance. The wide distribution of points from low to high disturbance clearly represents the range of hydrological behaviours that exist within the study sites and across turlough habitats as a whole. It is this variability which results in the high level of habitat and

ecological diversity found between sites. Correlation analysis was then carried out on water level time series of 16 turloughs for the 2006/2007 hydrological year and the correlation coefficients superimposed on the plot for 2007/2008 (Figure 9.3). As can be seen in Figure 9.3, both years showed a similar distribution and the relative position of sites within the spectrum very similar in both years. Another interesting trend is the upward shift of the 2007/2008 distribution relative to 2006/2007, highlighting the drier year experienced by many sites in 2007/2008. This upward shift indicates that during this period, many sites moved further from the long duration flooding characteristic of Coolcam due to the shorter duration of flooding.

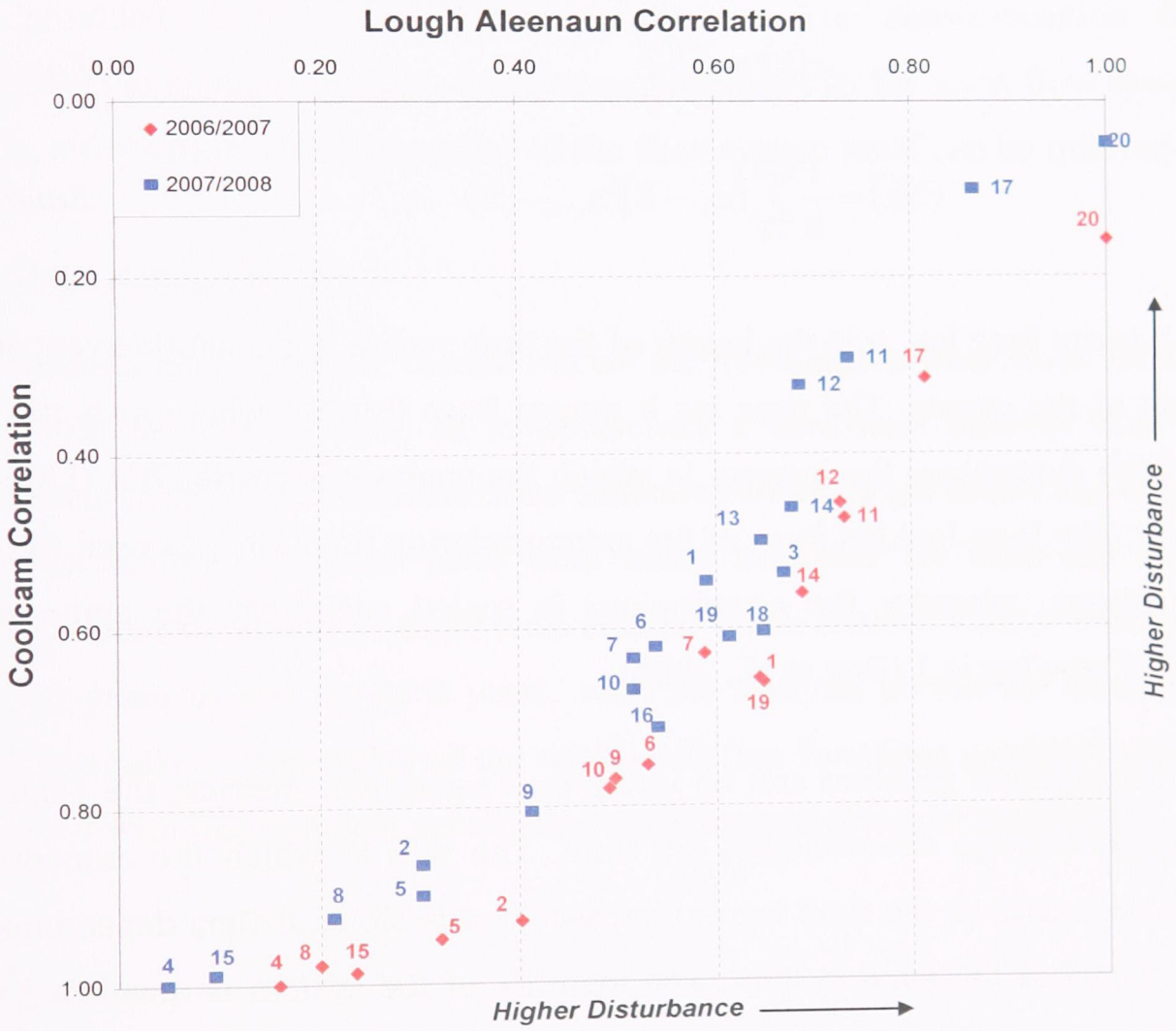


Figure 9.3: A plot of correlation with Lough Aleenaun versus the corresponding correlation with Coolcam for each turlough for the 2006/2007 and 2007/2008 hydrological years

9.2. Autocorrelation

Autocorrelation is a widely used method for analysing time series data used in the time domain. The autocorrelation function provides a normalized measure of the linear dependence of successive values within a time series, and allows the quantification of the memory effect in the system (Box et al., 2008; Padilla and Pulido-Bosch, 1995). In the analysis of karst systems, the correlogram provides information on the level of karstification and storage within the aquifer (Bailly-Comte et al., 2008; Labat et al., 2000a; Panagopoulos and Lambrakis, 2006). The autocorrelation function itself, r (k), is given by:

$$r(k) = \frac{C(k)}{C(0)} \qquad \textit{Equation 9.1}$$

$$C(k) = \frac{1}{n}\sum_{t=1}^{n-k}(x_t - \bar{x})(x_{t+k} - \bar{x}) \qquad \textit{Equation 9.2}$$

Where ***k*** is the time lag, ***n*** is the length of the time series, ***x*** is a single event and $\bar{x}$ is the mean of the events. The time lag k ranges from 0 to m, where m is the cutting point which determines the interval in which the analysis is carried out (Larocque et al., 1998). The Box-Jenkins form of the autocorrelation function was used throughout these analyses, whereby the correlogram is scaled such that the autocorrelation function at zero lag is 1 (Box et al., 2008).

The autocorrelation function can be interpreted using two metrics; the slope of the correlogram and the decorrelation lag time. The rate at which the autocorrelation function decreases as the time lag is increased, or its slope, differs depending on the characteristics of the karst system. The memory of the system is quantified using a parameter known as the decorrelation lag time. This is defined as the lag at which the autocorrelation function has fallen a predetermined value (Panagopoulos and Lambrakis, 2006). The exact magnitude of this value is somewhat arbitrary, but is usually between 0.1 and 0.2 as below this the memory effect of the system is adjudged to be indistinguishable from signal noise (Valdes et al., 2007). Where the karst system is poorly developed and has major groundwater storage, the correlogram will have a relatively gentle slope and consequently a high decorrelation lag time (Larocque et al., 1998; Padilla and Pulido-Bosch, 1995). Where the system

demonstrates more rapid drainage characteristics the correlogram will have a much steeper slope and correspondingly lower decorrelation lag time.

The majority of previous studies using time series analysis techniques have been carried out on spring discharge records. However, it has also been demonstrated that water level records and piezometric heads can also be used as they provide information on the system dynamics (Larocque et al., 1998; Lee and Lee, 2000; Panagopoulos and Lambrakis, 2006). While classically the storage within a karst aquifer is considered to consist of groundwater held within the matrix, fractures and conduit permeability, in the case of lowland Irish karst systems there is additional storage provided in the form of turlough basins. The autocorrelation function characterises the manner in which this storage is utilised by the karst flow system and from this, information about the nature of the flow system itself can be inferred.

9.2.1. Stage Autocorrelation

Autocorrelation analyses were carried out on the hydrological year from 1st October 2007 to 30th September 2008, as it represented a consistent interval with similar rainfall inputs over which autocorrelation functions could be generated and compared. The longest continuous water level time series available for each site was also analysed to identify potential longer term effects. These records varied in length from around 1.5 years to just under 3 years, with the analysis period for each turlough given in appendix C. Examples of the autocorrelation functions produced are shown in Figure 9.4 with the complete set of stage correlograms given in appendix C.

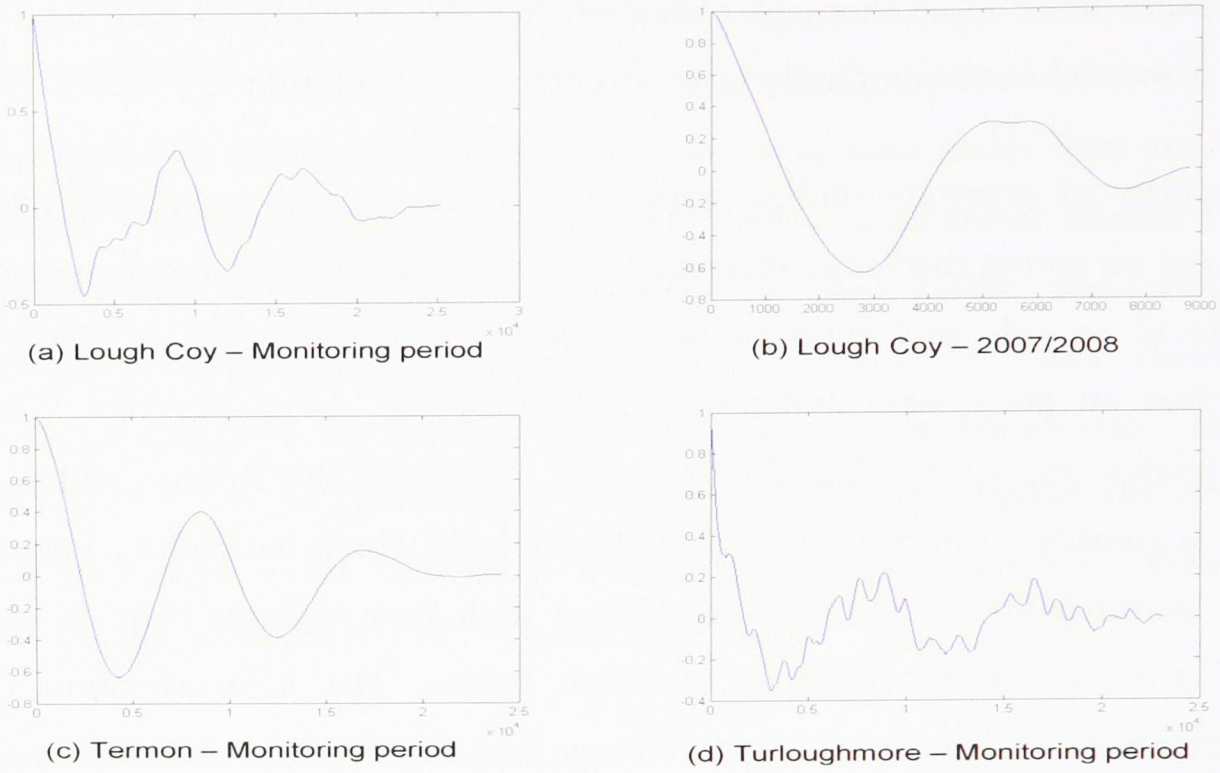


Figure 9.4: Autocorrelation functions for (a) Lough Coy (b) Lough Coy for 2007/2008 hydrological year, (c) Termon (d) Turloughmore

(Time in hours on x axis, correlation coefficient on y axis)

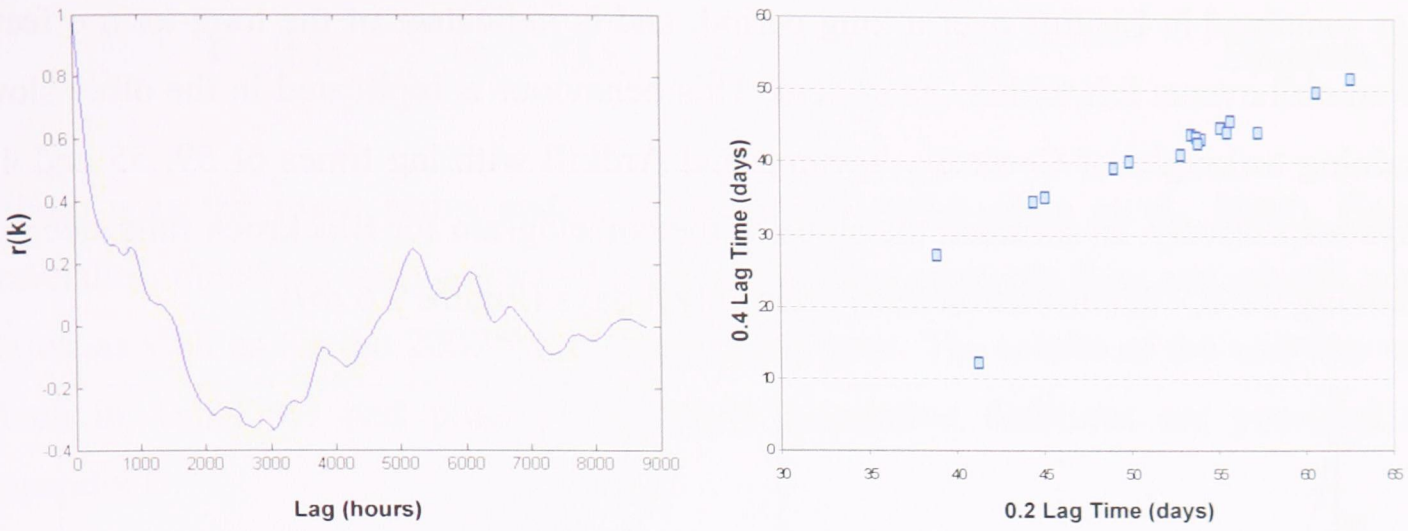
A cursory look at the correlograms reveals that the seasonality of turlough flooding associated with the annual recharge cycle of the aquifer is clearly visible, with positive r(k) peaks occurring at lags roughly coinciding with flooding events during the winters of 2007/2008 and 2008/2009 (Figure 9.4 (a)). The smoothest correlograms with the slowest slope changes are shown by sites characterised by long duration, low frequency flooding such as Brierfield, Coolcam and Termon (Figure 9.4 *(c)*). The slope changes of more responsive turloughs show far more variability and changes in autocorrelation slope, such as Lough Aleenaun and Turloughmore (Figure 9.4 (d)). Between these lay a continuum of behaviours such as that shown by Lough Coy (Figure 9.4 (a) and (b)) with increasing regularity of the autocorrelation function implying greater temporal stability in water levels. Decorrelation lag times were initially identified for all sites using a decorrelation level of 0.2 (Table 9.2). As expected a range of lag times was identified, with the lower values representing turloughs with highly fluctuating regimes, while higher values signified sites with more slowly responding regimes. The continuum of flooding behaviour was repeated here. There was a relatively low range of lag times, with standard deviations of 6.6 and 9.4 days for the two analysis period showing the similarity between many of the turlough flooding regimes. Interestingly, despite showing the steepest initial slope on

the correlogram Lough Aleenaun does not show the lowest decorrelation lag. Instead, it is Turloughmore with the lowest lag time at 38.9 days, compared to 41.3 days for Lough Aleenaun. This anomalous result is due to the chosen decorrelation level of 0.2. A visual inspection of the Lough Aleenaun correlogram confirms this, with a clear change in slope of the autocorrelation function at r(k) values around 0.25 (Figure 9.5 (a)). Lough Aleenaun fills and empties far more frequently compared to Turloughmore. While the two sites show similar regimes during the winter months, Turloughmore shows a damped response to summer rainfall events and thus has a lower frequency of flooding. This may be due to the additional storage available within the Turloughmore karst system compare to that of Lough Aleenaun. This extra storage is able to accommodate flows generated by precipitation events during the summer months without the onset of turlough flooding, whereas the low storage capacity of the Aleenaun system results in the onset of flooding in response to rainfall throughout the year.

Analysis Period	Stage Autocorrelation			Flow Autocorrelation	
	2007/2008	2007/2008	Full	2007/2008	Full
Decor. Level	0.2	0.4	0.2	0.2	0.2
Turloughmore	38.9	27.2	55.9	3	3
Lough Aleenaun	41.3	12.2	46.5	3	2
Blackrock	44.4	34.5	59.3	4	5
Lough Coy	45.1	35.1	59.6	10	8
Caherglassaun	49	39.2	65.3	11	10
Garryland	49.9	40	61.3	9	10
Ardkill	52.8	41	80.2	45	46
Knockaunroe	53.4	43.9	67.5	11	10
Lough Gealain	53.7	43.6	63.6	8	7
Skealoghan	53.8	42.5	71.8	6	7
Croaghill	54	43.1	73.1	30	20
Lisduff	55.1	44.9	73.1	40	33
Rathnalulleagh	55.5	44	62.4	19	13
Caranavoodaun	55.5	44.6	69.8	13	14
Roo West	55.7	45.6	56.2	8	6
Carrowreagh	57.3	44.3	72.8	7	12
Brierfield	60.6	49.8	78.1	33	22
Coolcam	62.5	51.5	75.5	59	58
Termon	62.5	51.7	82.4	55	61
Mean	***52.7***	***41***	***67.1***	***19.7***	***18.3***
Standard Deviation	***6.6***	***9.1***	***9.4***	***18.2***	***18.1***

Table 9.2: Decorrelation lag times (in days) for stage and flow time series

To assess the sensitivity of lag time to decorrelation level, and how it affected the interpretation of stage time series, lag times were recalculated for decorrelation level of 0.4 and plotted against 0.2 lag time (Figure 9.5 (b)). This showed an approximately linear relationship between the two lag times with one exception: Lough Aleenaun. Generally the correlograms showed a smooth, continuous decrease in r(k) with increasing lag but, in the correlogram for Lough Aleenaun, the autocorrelation function levels out for lags between 25 and 40 days before falling off thereafter. Therefore it is important to consider the shape of the autocorrelation function and any distinct changes in slope when interpreting turlough correlograms.



(a) (b)

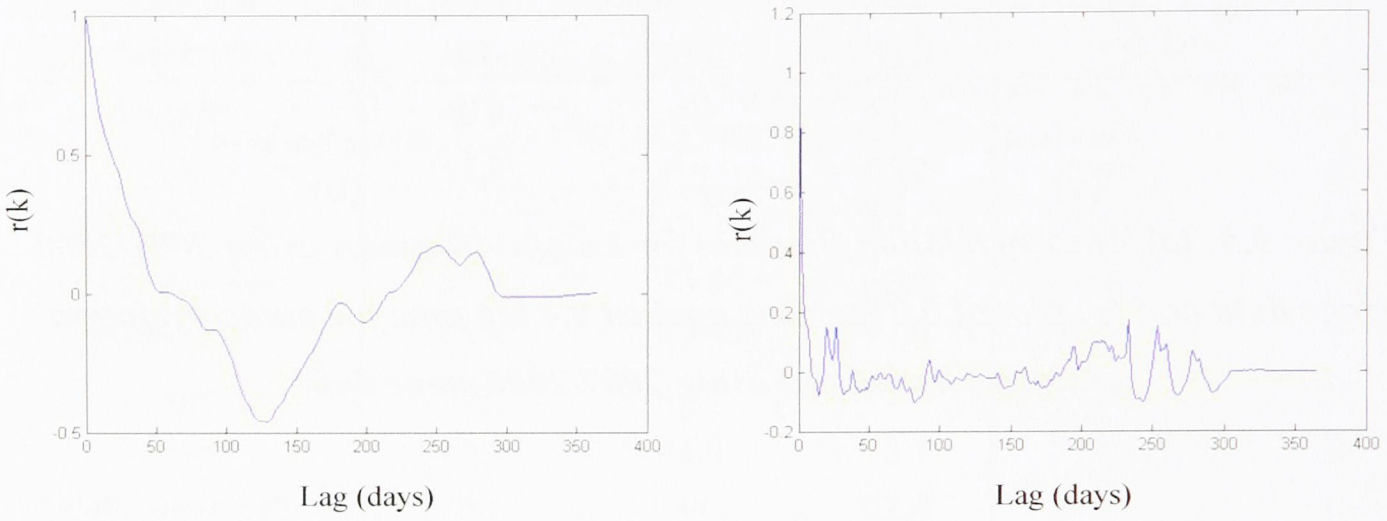
Figure 9.5: (a) Autocorrelation function for Lough Aleenaun using 2007/2008 stage data and (b) plot of 0.2 lag time against 0.4 lag time for autocorrelation analyses carried out using 2007/2008 stage data

9.2.2. Flow Autocorrelation

Autocorrelation was also carried out on net daily flow rate time series. As with the stage time series, analyses was carried out using data from the 2007/2008 hydrological year as well as the longest available record. The flow correlograms are provided in appendix C and the decorrelation lag times for the flow time series are shown in Table 9.2. There was a greater distinction between flow correlograms and corresponding lag times compared to that found during the stage analyses. The lag times varied by order of magnitude, from 3 days for Lough Aleenaun to 59 days for Coolcam, while the standard deviation of 18.2 days for 2007/2008 hydrological year is also far higher than the figure of 6.6 days for stage correlograms over the same period. It is also relatively high when compared to the mean lag time across the study sites of 19.7 days. This would be expected, since turlough flows are a response to the shorter-term events, namely precipitation, whereas the turlough water level represents a more long term response of the aquifer to the excess recharge during the winter period.

An example of the differences in flow behaviour is clearly demonstrated in Figure 9.6 (a) shows the correlogram for Lisduff. Here, the correlogram shows a gentle slope with the 0.2 lag time of 40 days is far above the mean of 19 days. This links in well with the direct analyses of flow rates carried out in Chapter 7 where a net inflow rate

was sustained in Lisduff over a long period, and is indicative of the long-term effects of rainfall events felt within the system. This behaviour is replicated in the other slow draining turloughs of Coolcam, Termon and Ardkill with lag times of 59, 55 and 45 days respectively. In contrast, the slope of the correlogram for Blackrock falls steeply, reaching the 0.2 decorrelation level after only 4 days (Figure 9.6 *(b)*).



(a) Lisduff (b) Blackrock

Figure 9.6: Autocorrelation functions for (a) Lisduff and (b) Blackrock using daily flow data

9.3. Cross Correlation

The flow behaviour was further investigated using cross correlation with precipitation records. Cross correlation is used to establish a link between input and output time series and provides information on the causal and non-causal relationships between input and output time series (Larocque et al., 1998; Lee and Lee, 2000). Where the input series is a random process, the cross correlation function provides information on the response of the system to a unitary impulse, in this case the flow response to precipitation events (Larocque et al., 1998; Padilla and Pulido-Bosch, 1995). In preparation, autocorrelation was carried out on all rainfall records used in this study (appendix C). The rapid decrease in the autocorrelation function demonstrates that rainfall is an uncorrelated process, a prerequisite for cross correlation. The cross correlation function itself is given by:

$$r_{xy}(k) = \frac{C_{xy}(k)}{\sigma_x \sigma_y} \qquad \textit{Equation 9.3}$$

$$C_{xy}(k) = \frac{1}{n}\sum_{t=1}^{n-k}(x_t - \bar{x})(y_{t+k} - \bar{y}) \qquad \textit{Equation 9.4}$$

Where x_t is the input series and y_t is the output series (Box et al., 2008). Cross correlation functions were generated using the longest available flow and rainfall time series, as well as for the 2007/2008 hydrological year. The results of the analyses are given in Table 9.3 and plots of the cross correlation functions are provided in appendix C.

The time delay, defined as the lag at which the maximum value of the cross correlation function $r_{xy}(k)$ occurs, indicates the level of development or karstification of the system (Padilla and Pulido-Bosch, 1995). The direction of the relationship is given by the sign of the delay, with a positive delay indicating that the output y_t shows a response to the input signal x_t. A shorter delay represents a more rapid transfer of the input through the system, and in studies of karst springs is generally associated with well-developed flow systems (Panagopoulos and Lambrakis, 2006). As can be seen in Table 9.3 all flow delays were positive, showing the intuitive relationship that turlough flow reacts to precipitation events. However, the delay is fairly constant across the study sites and shows a very low range of between 1 and 4 days, thus provides little information on the relative operations of the systems. Part of the reason for this ambiguousness can be ascribed to features of a turlough flow time series and the role turloughs occupy within karst systems compared to that occupied by springs.

Site Name	2007/2008			Full		
	Max R	Delay	R=0 Delay	Max R	Delay	R=0 Delay
Lough Aleenaun	0.56	1	4	0.56	1	4
Turloughmore	0.44	1	6	0.44	1	6
Blackrock	0.5	2	11	0.5	2	12
Skealoghan	0.43	2	14	0.43	2	13
Carrowreagh	0.33	2	16	0.33	2	17
Knockaunroe	0.51	3	16	0.51	2	16
Lough Gealain	0.61	1	16	0.61	1	12
Lough Coy	0.44	2	17	0.44	2	14
Caherglassaun	0.48	1	18	0.48	1	15
Rathnalulleagh	0.28	3	18	0.28	3	20
Garryland	0.45	2	19	0.45	2	14
Caranavoodaun	0.41	2	30	0.41	1	26
Roo West	0.42	1	30	0.42	1	23
Brierfield	0.34	2	49	0.34	2	52
Lisduff	0.39	4	51	0.39	3	31
Croaghill	0.47	2	59	0.47	1	32
Ardkill	0.46	2	70	0.46	1	48
Termon	0.4	1	70	0.4	1	67
Coolcam	0.35	1	73	0.35	1	58
Average	***0.44***	***1.8***	***30.9***	***0.44***	***1.6***	***25.3***
Standard Deviation	***0.08***	***0.8***	***23.2***	***0.08***	***0.7***	***18.3***

Table 9.3: Results from cross-correlation analyses between net daily turlough flow and precipitation (all delays given in days)

A karst spring represents the output from the karst system; the cross correlation function is the product of all processes which transform precipitation within the aquifer including storage effects. In contrast, a turlough forms an integral part of the storage within a karst system rather than a system output. The turlough net flow cross correlation function represents an element of the internal processes which transforms precipitation within the karst system, including the contribution of direct rainfall onto the turlough surface. Turlough flow is a function of both the input signal (precipitation) and also state of the system, i.e. the relative heads within the turlough itself and the underlying aquifer. In addition to the contributing factors of flow path development and degree of karstification, the hydrological state of the overall system

determines the effect rainfall will have on turlough flow. It may cause a positive flow into the turlough, or alternatively just decrease the rate of net outflow if the turlough is in recession. If fact, during dryer periods it may have no effect at all on the turlough as the flow system is able to accommodate the recharge completely without utilising turlough storage.

A useful indicator generated from the cross correlation function is the delay between a lag of zero and the time at which $r_{xy}(k)$ drops to 0. This metric gives a general indication as to the period during which a precipitation event has a positive effect on net flow. This variable ranged from a low of just 4 days for Lough Aleenaun to 73 in Coolcam during the 2007/2008 hydrological year. This variation is reflected visually in the cross correlation functions and the number and degree of slope change shown, with an increasing irregularity indicating a shorter rainfall effect (*Figure 9.7 (a) to (d)*).



Figure 9.7: Cross-correlation functions using daily net flow and precipitation data from 2007/2008 hydrological year for (a) Lisduff, (b) Knockaunroe, (c) Skealoghan and (d) Turloughmore

9.4. Time-lagged Correlation

In order to investigate turlough dynamics and provide relevant information concerning the nature of site interconnectivity, time-lagged correlation was performed on turlough water level time series. Time-lagged correlation involves offsetting one time series relative to the other and identifying the time lag at which the maximum correlation occurs. The direction of the lag between two sites indicates which reacts more readily to rainfall, while the value of the lag quantifies the temporal difference in response time. Four subsets of study sites were defined based on the criteria of geographical location and proximity, denoted subset 1 to 4 (Table 9.4). These criteria were used for two reasons. Firstly, sites in close proximity have the same input signal (rainfall). Therefore, differences in the timing of response would be due to differences in hydrological operation rather than spatial variation in rainfall patterns. Secondly, this methodology can provide information on the nature of potential hydrological connections between turloughs in close proximity. For example, a turlough consistently peaking earlier than a neighbouring down gradient turlough would imply a connection. Within each subset, time-lagged correlation was carried out using both the entire 2007/2008 hydrological year dataset and the shortest continuous period of inundation of any site within the subset.

Subset 1: Mayo	Subset 2: Williamstown
Skealoghan	Coolcam
Ardkill	Croaghill
Kilglassaun	
Subset 3: Roscommon	**Subset 4: Burren**
Rathnalulleagh	Lough Gealain
Carrowreagh	Knockaunroe
Brierfield	

Table 9.4: Geographically close site subsets

During the analysis process it was observed that, while differences in recession duration were correctly identified, in many cases the shorter lag time between actual water level peaks was overestimated. When comparing sites with similar duration flooding regimes, such as in the Burren subset, the delay between peak water levels was accurately represented. However where sites exhibited comparable filling patterns but distinctive recession durations, such as in the Roscommon subset,

similarities in the maxima were masked by large disparities in recession duration. In order to ascertain the relative timing of peaks, clearly defined maxima in the water level time series were manually isolated within each subset and the lag measured. A positive lag in *site A vs. site B* implies the peak level occurred in *site A* earlier than *site B*. A negative lag implies the reverse, with the *site B* maxima preceding that of *site A*. Each maximum represents a point at which the flow direction changes from net inflow to net outflow. As sites in the same geographical location are subject to common rainfall patterns and events, a comparison of peak water level across each subset can give an insight into the temporal dynamics of the flow systems. Through the interpretation of these relative delays together with local hydraulic gradients, the determining factors affecting turlough hydrology on a local level can be explored.

9.4.1. Subset 1: Mayo

The Mayo subset consists of the three turloughs Skealoghan, Ardkill and Kilglassaun and is located approximately 8km east of Ballinrobe. Morphologically, Ardkill is located in a deep depression while the other two sites have much flatter topographies consisting of shallow basins surrounded by gentle side slopes. The water level hydrographs for each site are shown in Figure 9.8. As can be seen from the plot, the bases of Skealoghan and Ardkill lie at approximately the same level with that of Kilglassaun around a metre higher. Visually the hydrographs of Skealoghan and Kilglassaun show a similar flooding pattern with maximum flood depths of 1.9 and 2.2 m respectively, but with a slower recession in Skealoghan. Ardkill displays a far greater range of flooding with a maximum recorded depth of close to 7 m, and a recession limb far in excess of that shown by either Skealoghan or Kilglassaun. This divergence in recession behaviour was identified earlier, with Ardkill showing one of the lowest lag times 45 days compared to only 6 for Skealoghan.

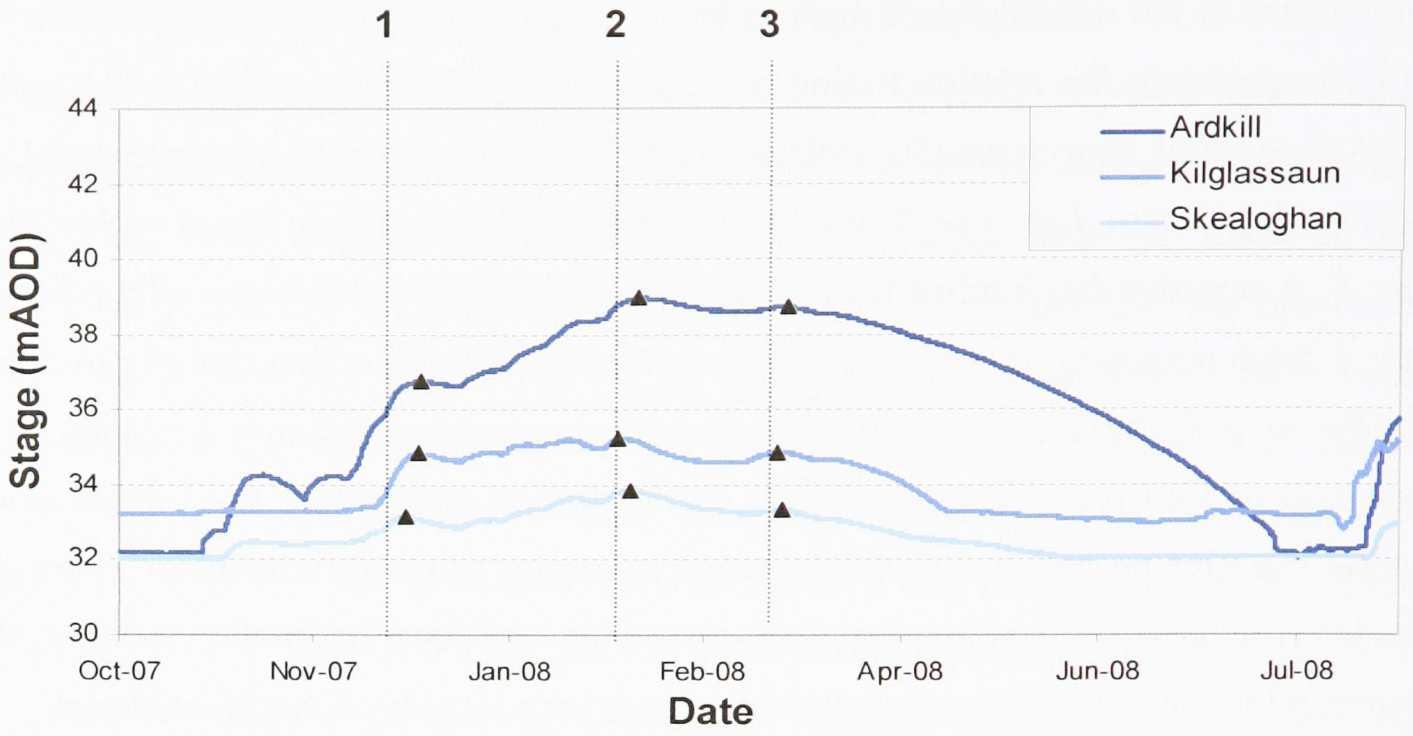


Figure 9.8: Plot of water levels as mAOD, rainfall and computed maxima for Subset 1: Mayo

The differences in recession duration are clearly picked up in the time-lagged correlation. The maximum correlation between Skealoghan and Ardkill occurred with a positive lag of 689 hours or 29.7 days (Table 9.5, Figure 9.9). When assessed over the inundation period this dropped to 418 hours (17.5 days), but with Ardkill still lagging considerably behind Skealoghan. Skealoghan in turn was found to lag behind Kilglassaun, but on a smaller scale with a negative lag of 108 hours across the hydrological year. This reflects the extended recession of Skealoghan compared to that of Kilglassaun.

	Hydrological Year		Inundation Period		Peak 1	Peak 2	Peak 3
Correlated Sites	**Lag (hrs)**	**Correlation**	**Lag (hrs)**	**Correlation**	**Lag (hrs)**	**Lag (hrs)**	**Lag (hrs)**
Skealoghan vs. Ardkill	689	0.908	418	0.760	94	53	43
Skealoghan vs. Kilglassaun	-108	0.937	-28	0.832	73	-69	-27
Ardkill vs. Kilglassaun	-723	0.871	-675	0.664	-21	-122	-70

Table 9.5: Results of time-lagged correlation and manual comparison of maxima for Subset 1: Mayo

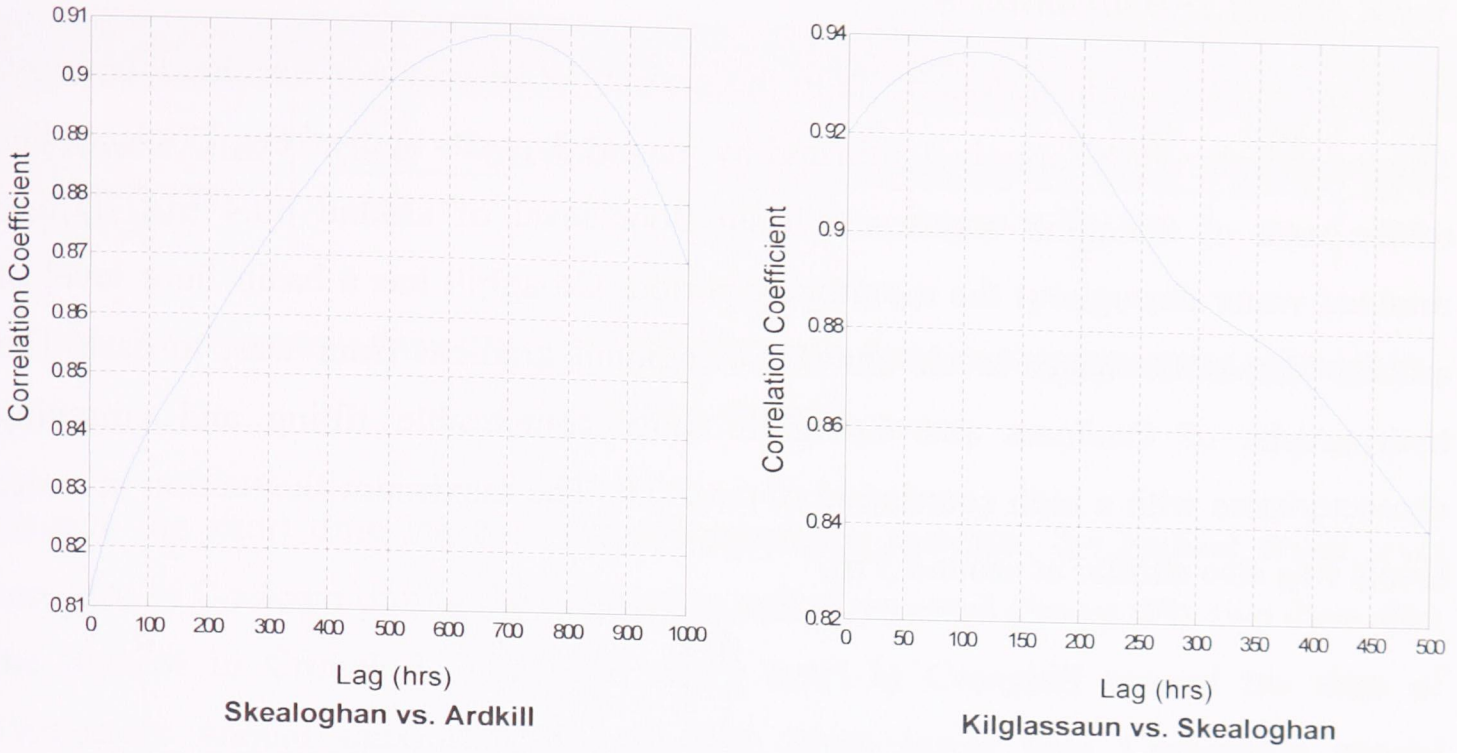


Figure 9.9: Time-lagged correlations for Skealoghan vs. Ardkill and Kilglassaun vs. Skealoghan (hydrological year)

Three water level maxima were identified, labelled 1 to 3, and the relative time delays between them determined. Despite the large variation in flood duration, depth and recession characteristics present within the subset, the water level maxima all occurred within a relatively short interval. The initial maxima in Skealoghan preceded that of Kilglassaun by almost 3 days, but later in the season this pattern was reversed with Kilglassaun peaking first. While the peak in Ardkill water levels consistently occurred after that of the other two sites, the delay of between 2 to 4 days was far shorter than what might be expected given the contrasting hydrological regimes.

When the maximum water level events are compared with the rainfall record, as expected they all follow periods of little or no rainfall. This is to be expected as rainfall is the driver that causes water levels to rise, and so when this driver ceases the water within the turlough will eventually start to drain. It is interesting to note that despite the differences in net flow rates and recession duration, the time it takes for this process to begin is remarkably consistent across the sites within the subset. If the controlling factor governing turlough hydrology was the filling process, a far greater difference would be expected between sites within subset 1.

9.4.2. Subset 2: Williamstown

Coolcam and Croaghill turloughs lie to the west of Williamstown, north Co. Galway. The topography of the area is dominated by glacial deposits and eskers. Coolcam lies to the west of Croaghill and has a basin floor level of around 80.4 mAOD and retained water throughout the monitoring period. Croaghill has a basin floor level of around 78mAOD. Water levels showed a regional gradient from west to east. The hydrographs of Coolcam and Croaghill show comparable filling and emptying characteristics with a high correlation of over 0.9. The maximum fluctuation in water levels was also similar at around 3 m.

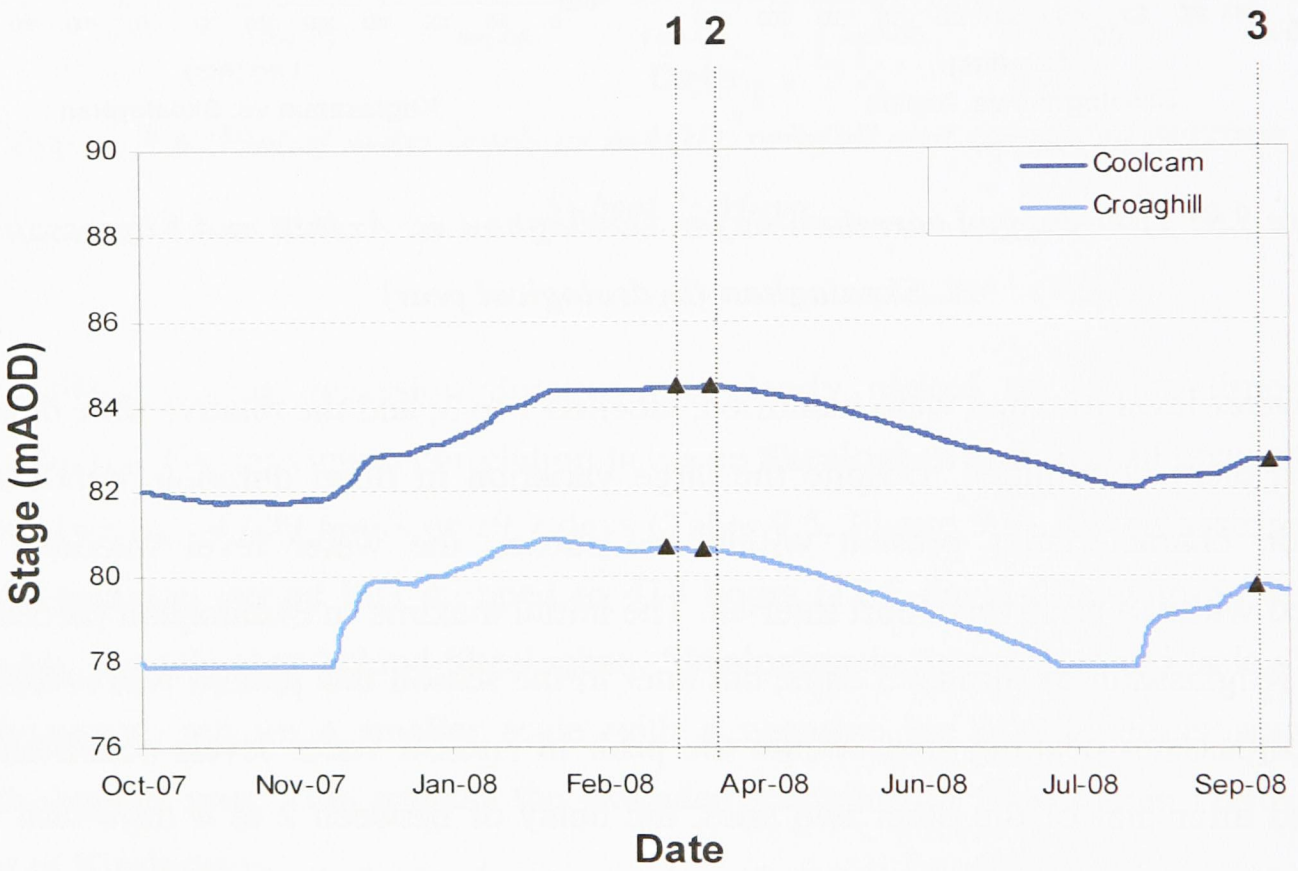


Figure 9.10: Plot of water levels as mAOD, rainfall and computed maxima for Subset 2: Williamstown

The time-lagged correlation results indicate Coolcam lagging behind Croaghill by 17 days (Table 9.6) across the hydrological year, a similar lag as that found between Skealoghan and Ardkill in subset 1. Again this reflects the relative difference in recession durations, as Croaghill emptied on the 18th June whereas the water levels in Coolcam were still receding 20 days later when water levels began to rise. A comparison of water level maxima shows a lag in Coolcam with respect to Croaghill in the order of 3 days. Again, as with subset 1, this is a considerably shorter period than was indicated by the time-lagged correlation.

	Hydrological Year		Inundation Period		Peak 1	Peak 2	Peak 3
Correlated Sites	Lag (hrs)	Correlation	Lag (hrs)	Correlation	Lag (hrs)	Lag (hrs)	Lag (hrs)
Coolcam vs. Croaghill	-406	0.963	-463	0.968	-94	-91	-64

Table 9.6: Results of time-lagged correlation and manual comparison of maxima for Subset 2: Williamstown

Despite the short time lag between corresponding maxima, the highest water level recorded in Coolcam during the inundation period occurred almost fifty two days after the highest in Croaghill. The peak water level in Croaghill around the time of Coolcam's annual maximum was in fact 26cm lower than Croaghill's annual maximum. The disparity between these two values can be explained by a greater level of restriction or lower capacity of the outflow from Coolcam than is present in Croaghill. During an extended period of low or no rainfall, the greater drainage capacity of Croaghill allows its water level to drop significantly more than that which occurs in Coolcam during the same period. This difference in drainage capacity has a cumulative effect across the flooding period, with the result that the renewed flooding begins from a relatively higher level in Coolcam than it does in Croaghill when rainfall recommences. Thus while there are corresponding peaks in both time series their relative levels within the series can be different.

9.4.3. Subset 3: Roscommon

The Roscommon subset, located 3km to the southeast of Castleplunket, contains the turloughs Rathnalulleagh, Carrowreagh and Brierfield. In terms of elevation Brierfield is the uppermost turlough, followed by Carrowreagh with Rathnalulleagh the lowest (Figure 9.11). An initial examination of the hydrographs shows some level of similarity between all sites within the subset, with a simultaneous onset of flooding across the sites and peak water levels occurring at approximately the same time. There is a strong resemblance between Rathnalulleagh and Carrowreagh with parallel filling and emptying characteristics in evidence, as would be expected given the correlation of 0.978. Brierfield, in contrast, displays a longer period of inundation with a recession far in excess of that demonstrated by either Carrowreagh or Rathnalulleagh. At 3.6 m the maximum flooded depth of Brierfield is also significantly less than that

of either Rathnalulleagh or Carrowreagh, which have maximum depths of 7.8 and 7 m respectively.

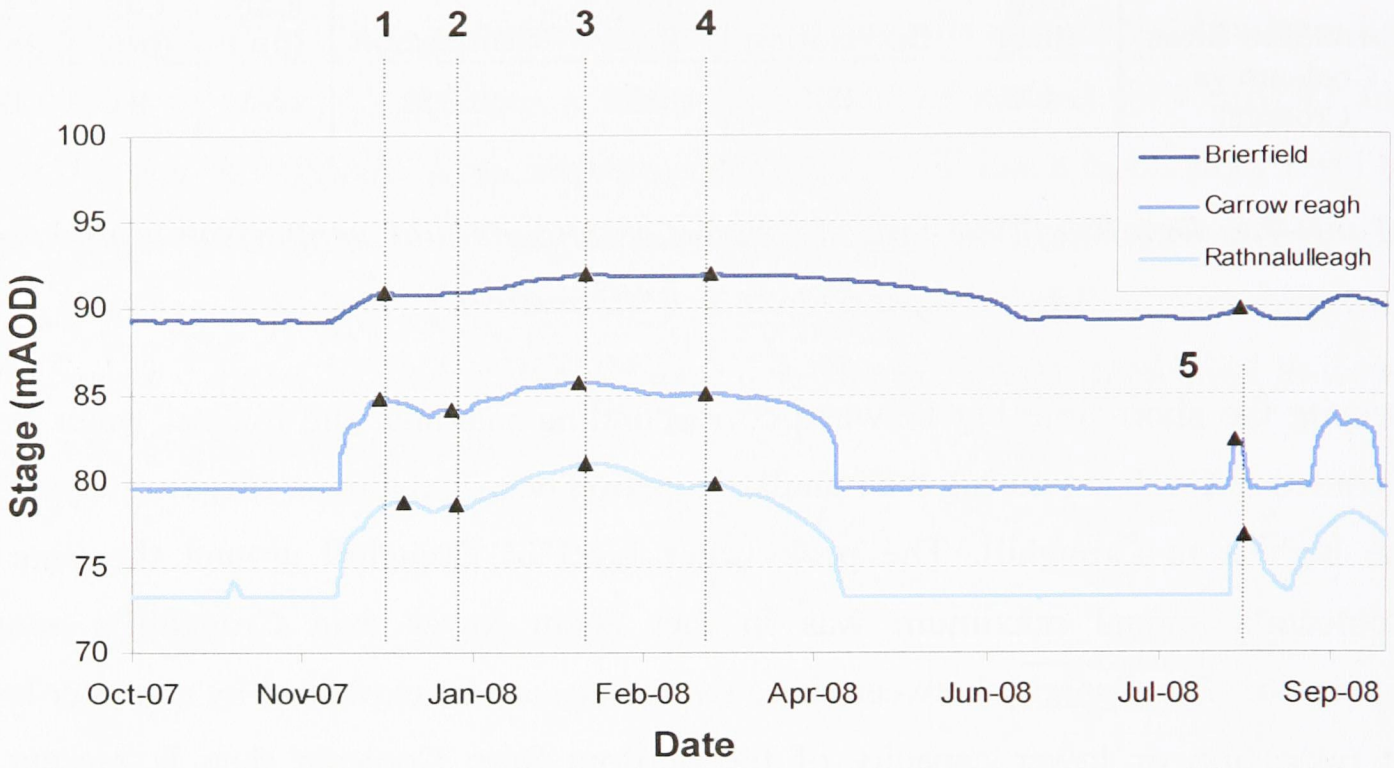


Figure 9.11: Plot of water levels as mAOD and computed maxima for Subset 3: Roscommon

	Hydrological Year		Inundation Period	
Correlated Sites	**Lag (hrs)**	**Correlation**	**Lag (hrs)**	**Correlation**
Rathnalulleagh vs. Carrowreagh	-16	0.979	-4	0.992
Rathnalulleagh vs. Brierfield	707	0.901	904	0.925
Carrowreagh vs. Brierfield	728	0.892	938	0.916

	Peak 1	Peak 2	Peak 3	Peak 4	Peak 5
Correlated Sites	**Lag (hrs)**	**Lag (hrs)**	**Lag (hrs)**	**Lag (hrs)**	**Lag (hrs)**
Rathnalulleagh vs. Carrowreagh	-168	-43	-63	-63	-66
Rathnalulleagh vs. Brierfield	-145	-	-9	-37	-30
Carrowreagh vs. Brierfield	23	128	54	26	36

Table 9.7: Results of time-lagged correlation and manual comparison of maxima for Subset 3: Roscommon

The turloughs of subset 3 follow a similar pattern as that identified in subset 1 and 2. The disparity in flood duration between the sites is clearly identified using the time-lagged correlation method, in this case with Brierfield showing a maximum correlation when lagged by 707 hours (29 days) behind Rathnalulleagh (Table 9.7). The difference in final emptying dates between these sites was greater still at just over 50 days. Rathnalulleagh was found to marginally lag behind Carrowreagh with less than a day offset required to maximise correlation, further highlighting the

contemporaneous behaviours of these sites. The timing of flood maxima followed the same trend identified in subsets 1 and 2, with peak levels in all sites occurring in a short interval irrespective of the relative lengths of the recession. In this case Rathnalulleagh was preceded by both Carrowreagh and Brierfield with the lag remaining fairly constant for peaks 2 to 4, but showing a noticeably longer delay of a full week during peak 1. This could be due to the relative positions of each turlough within their particular flow system. The probable hydrological configuration of these sites has Rathnalulleagh and Carrowreagh forming part of the same flow system, with Carrowreagh at the upper end of the catchment, while Brierfield forms part of a separate system. This would explain the similar peak times between Brierfield and Carrowreagh, while the delay experienced in Rathnalulleagh is caused by the damping effect of Carrowreagh located up gradient in the system.

9.4.4. Subset 4: Burren

The sites of subset 4, Lough Gealain and Knockaunroe, border each other on the limestone pavement at the foot of Mullaghmore. If a purely flow-through turlough system existed it would be in this locale that one would expect it, as the bare rock outcrops which characterise the area would present ideal conditions for the distributed flow system throughout the epikarst. Despite this there are still obvious swallow holes present in both turlough basins, with water clearly draining to a depression in Lough Gealain witnessed during this study. It appears that the deposition of marl within the basins have formed low permeability barriers covering much of the epikarst, thus promoting the development of larger flow systems.

The correlation and lag time remained consistent across the periods of analysis, with Knockaunroe consistently lagging behind Lough Gealain by approximately 24 hours. The manual analyses uncovered a slightly greater delay between maximum water levels, but with Lough Gealain still preceding Knockaunroe. The main flood events themselves during the year, peaks 3 and 4, showed a similar lag of 77 and 61 hours respectively (Table 9.8). This is similar to the relationship identified between Carrowreagh and Rathnalulleagh in Subset 3. The upper turlough (Lough Gealain) has a damping effect on the impulse response to recharge, causing a delay to be felt in the lower turlough (Knockaunroe) further down the system. The preferential drainage of

the upper turlough also helps to maintain a positive gradient into lower turlough, thus causing a lag in peak time.

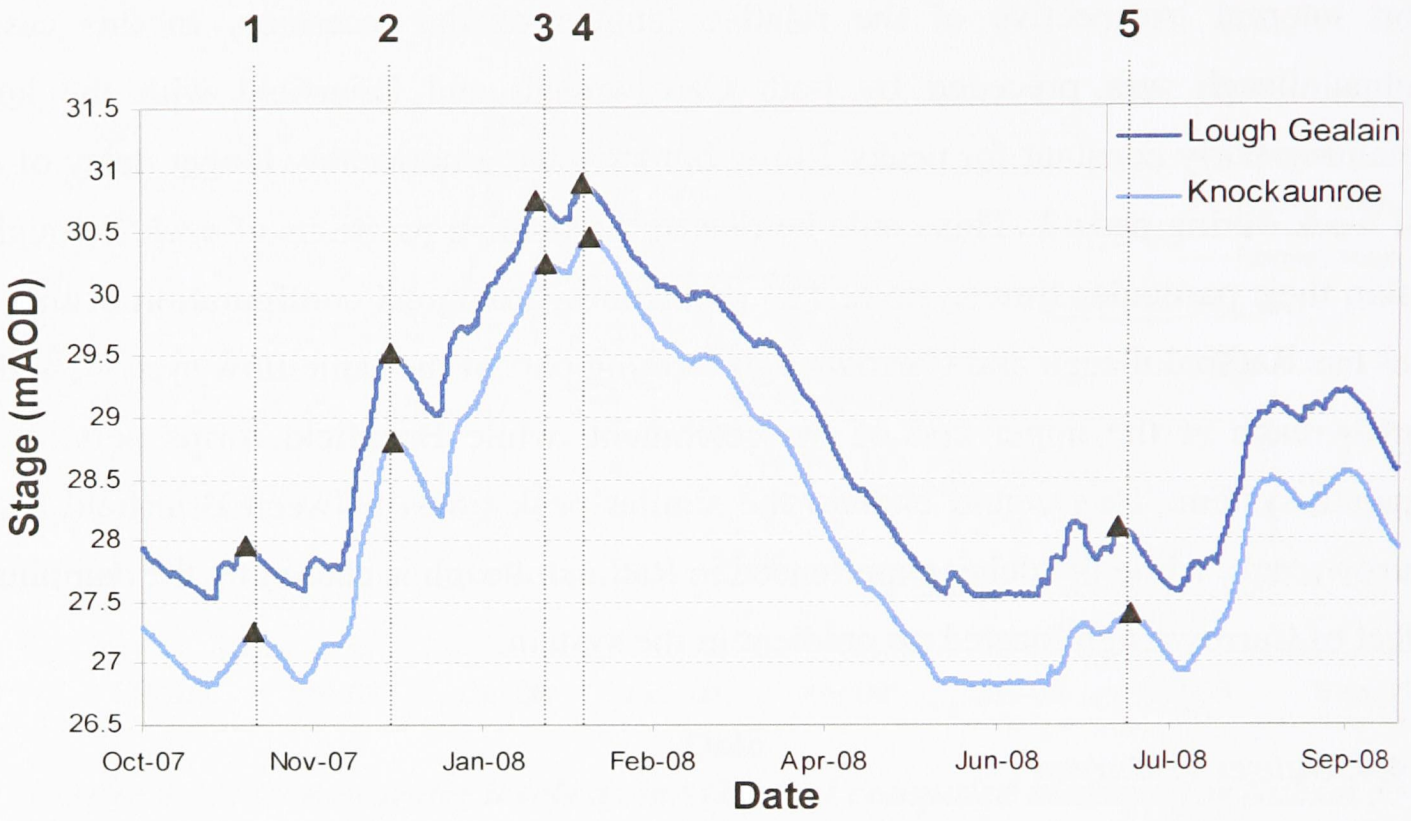


Figure 9.12: Plot of water levels as mAOD and computed maxima for Subset 4: Burren 1

	Hydrological Year		Inundation Period	
Correlated Sites	**Lag (hrs)**	**Correlation**	**Lag (hrs)**	**Correlation**
Lough Gealain vs. Knockaunroe	23	0.997	26	0.997

	Peak 1	Peak 2	Peak 3	Peak 4	Peak 5
Correlated Sites	**Lag (hrs)**	**Lag (hrs)**	**Lag (hrs)**	**Lag (hrs)**	**Lag (hrs)**
Lough Gealain vs. Knockaunroe	48	7	77	61	90

Table 9.8: Results of time-lagged correlation and manual comparison of maxima for Subset 4: Burren 1

9.4.5. Conclusions

Time lagged correlation has been shown to provide a standard method for quantifying differences in turlough recession behaviour. Across all the subsets, the sites which showed longer recessions consistently lagged behind other sites in close proximity. The magnitude of the lag was found to be indicative of the relative difference in recession duration, with longer lag times indicating a greater delay. The time-lagged correlation lag times did not, however, give an accurate comparison of the relative timing of peak water levels. Direct comparison of clearly defined maxima within the water level time series generally showed shorter lag times than the time-lagged correlation, with all peaks within each subset occurring within a few days of each other. This indicates that the mechanisms controlling the drainage of turloughs exert a dominant control on their functioning and associated characteristic hydrological regime.

Interestingly, the peaks in turloughs with the longest recession were close to and did not always follow those which drained more quickly. For example, in subset 3 Brierfield had by far the longest recession but consistently reached peak water level before Rathnalulleagh. Elevation was not the determining factor either as the peak levels in Coolcam, despite being at a higher elevation than Croaghill, consistently lagged behind Croaghill. While these turloughs may be part of the same groundwater system, this shows that these turloughs are not simply connected in series, with storm pulses moving from the top of the groundwater system. However, the turloughs which were very close to each other and most likely directly connected (Carrowreagh and Rathnalulleagh, Lough Gealain and Knockaunroe) did consistently show the turlough up gradient peaking and emptying before the down gradient turlough. Thus the relative difference in timing of peaks may indicate the level of connection between turloughs in close proximity.

9.5. Frequency Analysis

9.5.1. Fast Fourier Transform (FFT) Analysis

To complement the analysis of data in the time domain, stage and flow time series were also analysed in the frequency domain using the technique of Fourier analysis. The basic principle of Fourier analysis is that every signal can be expressed as the sum of weighted frequency functions or sinusoids of varying frequency, amplitude and phase (Chatfield, 1989). The Fourier transform of a time series shows how the energy is distributed across the frequency spectrum (Box et al., 2008). Frequency analyses were carried out using the Fast Fourier Transform (FFT), an efficient algorithm for the calculation of the Discrete Fourier Transform (DFT), which is given by Cooley and Tukey (1965):

$$F(\omega) = \int_{-\infty}^{\infty} f(t) e^{-j\omega t} dt \qquad \textit{Equation 9.5}$$

$$X(k) = \sum_{j=1}^{N} x(j) \omega_N^{(j-1)(k-1)} \qquad \textit{Equation 9.6}$$

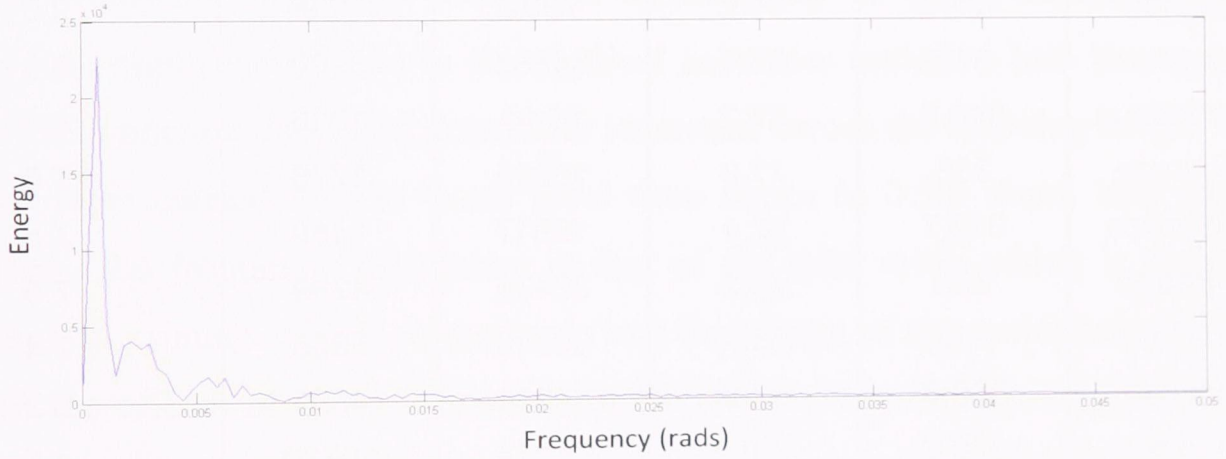
$$\omega_N = e^{(-2\pi i)/N} \qquad \textit{Equation 9.7}$$

Stage time series datasets comprising the longest continuous monitoring period for each turlough were analysed using FFT in the MatLab software package (version r2008a). The data was detrended to remove any long term drift and then transformed into the frequency domain using the FFT. The first ten peaks were extracted from the FFT results. Peaks corresponding to the length of the analysed dataset were then discarded, and the remaining peaks sorted in descending order of energy. The frequencies ω were converted into time period T using the relation $T = 2\pi/\omega$ (appendix D).

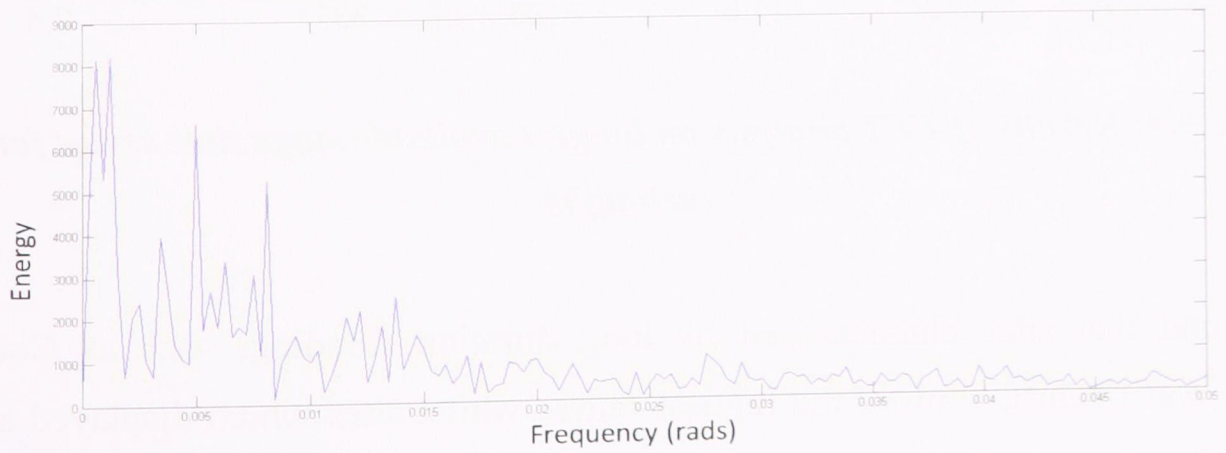
The annual pattern of inundation was identified in the FFT analysis of the full monitoring period, with the highest energy for each turlough corresponding to frequencies ranging from 312 to 355 days (Table 9.9). The one exception to this was Lough Aleenaun, which showed the greatest energy at 209 days. This demonstrates

the less significant impact the annual recharge cycle has on the flooding regime of Lough Aleenaun. This turlough regularly floods in response to heavy rainfall events throughout the year, and so the flooding regime is more sensitive to short term rainfall patterns and the effect of the annual recharge cycle is less pronounced.

In turloughs with unimodal flooding regimes, such as Ardkill, Coolcam and Termon, the dominant frequency is that of the annual flooding pattern (Figure 9.13 *(a)*). In such cases the vast majority of signal energy is associated with lower frequencies representing the seasonal flooding pattern, and as the frequency is increased the peaks become poorly defined and greatly reduced in magnitude. In contrast, turloughs showing multimodal flooding regimes such as Lough Aleenaun had a more even distribution of energy across the frequency spectrum, with clearly defined peaked of comparable magnitude (Figure 9.13 *(b)*). This reflects the greater frequency of flooding driven by higher flow capacities and lower transmission time within the aquifer.



(a) Ardkill



(b) Lough Aleenaun

Figure 9.13: FFT results for (a) Ardkill and (b) Lough Aleenaun analysed over entire monitoring period

The largest energy peaks were shown by those sites which experienced the greatest range of flooding, such as Blackrock, Caherglassaun and Lough Coy, whereas shallower turloughs tended to have lower energy more evenly distributed across a range of frequencies. In order to quantify and compare the energy distribution across frequencies, the ratio of energy between the first and fifth peak was calculated. Table 9.9 shows the study sites arranged in order of descending energy ratio.

Site Name	Period (days)		Energy		Ratio of Energy 1^{st} : 5^{th}
	1^{st} Order	5^{th} Order	1^{st} Order	5^{th} Order	
Termon	335	77.3	11316	568	19.9
Coolcam	335.9	53	12839	732	17.5
Lisduff	325.7	54.3	9607	559	17.2
Croaghill	335.6	91.5	13246	905	14.6
Ardkill	354.6	41.7	22704	1632	13.9
Brierfield	326	139.7	13368	1198	11.2
Roo West	339.5	45.3	9746	993	9.8
Rathnalulleagh	326	61.1	34638	3609	9.6
Skealoghan	325.3	54.2	7302	789	9.3
Caherglassaun	349	65.4	34885	3900	8.9
Caranavoodaun	348.9	87.2	8244	1016	8.1
Knockaunroe	335	77.3	13295	1776	7.5
Lough Gealain	312.7	52.1	10917	1459	7.5
Carrowreagh	326	75.2	32431	4299	7.5
Lough Coy	349	65.4	39749	5355	7.4
Garryland	298.3	63.9	30391	4865	6.2
Blackrock	320.6	120.2	48214	10720	4.5
Turloughmore	320.6	120.2	9762	2546	3.8
Lough Aleenaun	209.2	41.8	8193	3371	2.4

Table 9.9: Results of FFT analysis on longest available stage time series for 19 turloughs

This found that sites characterised by long duration flooding, such as Coolcam, Termon and Lisduff, showed the highest ratios, whilst sites which displayed a more disturbed regime, such as Lough Aleenaun and Turloughmore, the energy was more evenly distributed and so the ratio was substantially lower. This is as would be expected as in unimodal flooding regimes; the majority of energy is contained at low

frequencies as the dominant flooding pattern is that of seasonal increase in recharge. In contrast, when the flood regime consists of more frequent flood events, the energy within the signal is understandably distributed across a greater range of flood frequencies. The ranking of sites using this ratio also corresponds well to the correlation analysis carried out in section 9.1, where the correlation coefficients for Lough Aleenaun and Coolcam were used to plot the relative distribution of disturbance. Here, the rate at which energy dissipates at higher frequencies, given in the form of the ratio of 1st to 5th peak, provides a similar indicator of disturbance.

9.5.2. Tidal Effects on Turlough Water Level

The stage records of two turloughs in the Gort-Kinvarra chain, Garryland and Caherglassaun, displayed a clear tidal response at lower water levels (Figure 9.14). This tidal effect does not represent direct flow of seawater into the turlough, but rather a decrease in the hydraulic gradient in the system with the tide level even exceeding the turlough stage for brief periods. This was picked up in some of the springs in Kinvarra following high tide where the conductivity of water emerging from the springs rose significantly due to the cyclical saltwater intrusion into the system. To quantify this phenomenon and determine its extent across the flooding range, specific analyses were carried out on water level time series in 0.5m depth intervals using FFT. Here, the frequency of interest is that of the tidal cycle which is typically 12 hours and 26 minutes which corresponds to a frequency of approximately 0.5 rads/hr. To limit the effects of noise caused by rainfall-induced recharge impulses travelling down the system, sections of the recession curve were extracted representing different ranges of flooding and analysed using FFT.

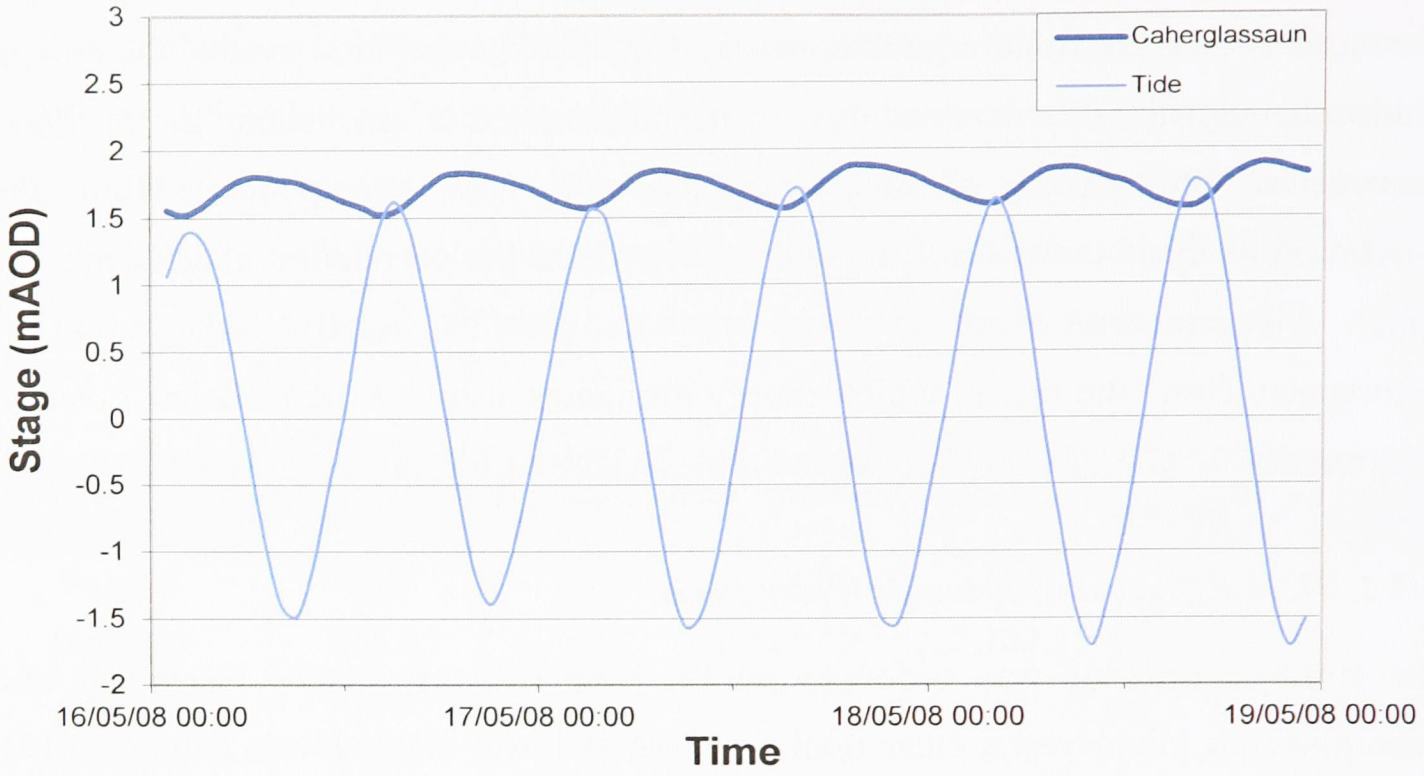
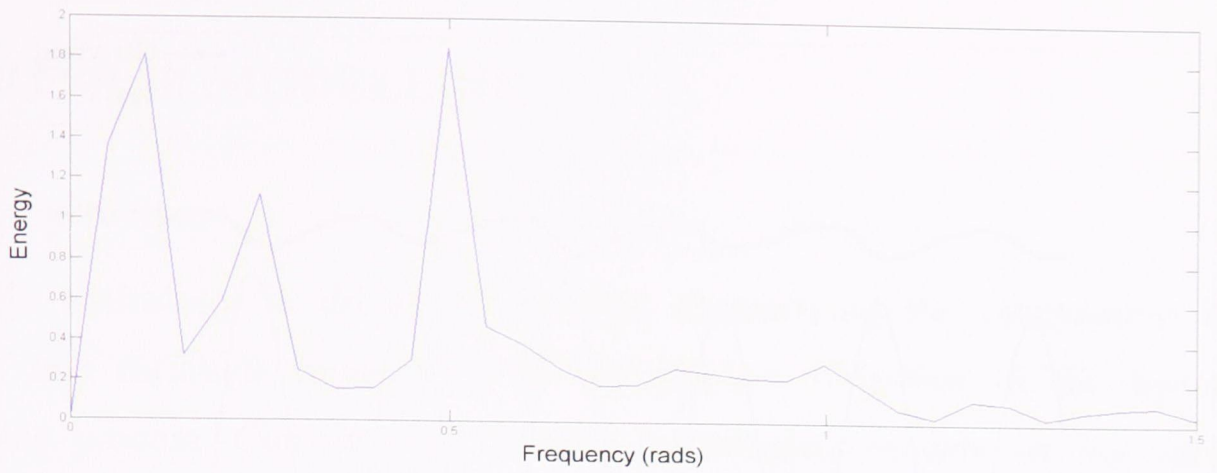
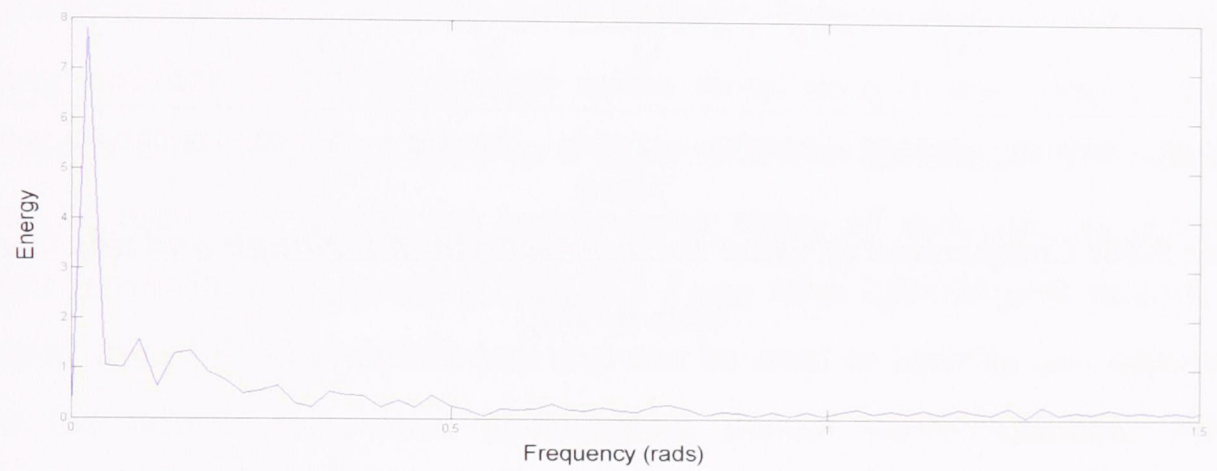


Figure 9.14: Comparison of water level in Caherglassaun turlough and tide level in Galway Bay

Caherglassaun itself is located 8 km inland. Here, the power of the tidal frequency drops with increasing flood depth, representing the lessening effect tidal fluctuations have on turlough water level. A peak in the FFT plot at the tidal frequency of 0.5 rads/hr is clear in the lower range of depths, such as 2 to 2.5 mAOD (Figure 9.15 (a)). At flood levels of above 6 mAOD the tidal effect is not clearly identified and so this was taken as the upper extent of tidal influence (Figure 9.15 (b)). To determine the lag between the tidal cycles and water fluctuations within the turloughs themselves, time-lagged correlation was carried out between water level and tide time series using the sections of the time series where the tidal effect was most clear, namely the shallower flood depths. The maximum correlation coincided with a lag time of 5 hours, indicating the level of attenuation by the conduit system.



(a) 2 – 2.5 mAOD



(b) 6 – 6.5 mAOD

Figure 9.15: FFT data for Caherglassaun recession data for (a) for 2 – 2.5 mAOD flood depth and (b) 6 – 6.5 mAOD flood depth

Garryland is located up gradient of Caherglassaun and approximately 10km away from Kinvarra, but also shows a marked tidal effect at low water levels (Figure 9.16). FFT analyses on depth intervals revealed the upper limit on tidal effects to be approximately 6 mAOD, as was found for Caherglassaun. A greater time lag was identified for Garryland than in Caherglassaun, with the water level signal lagging behind the tide by 8 hours. This increase in lag time represents the extra degree of attenuation caused by the conduit system between Caherglassaun and Garryland.

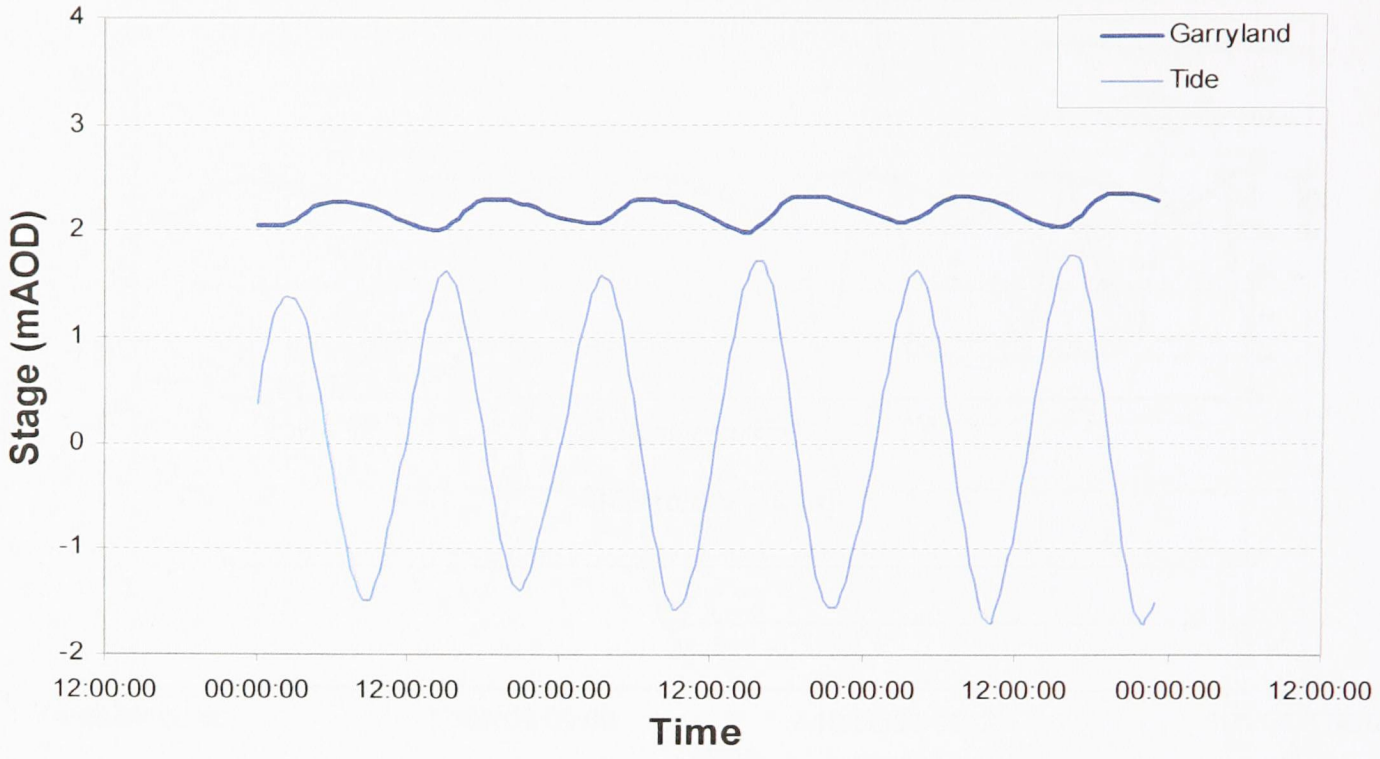


Figure 9.16: Comparison of water level in Garryland turlough and tide level in Galway Bay

CHAPTER 10. MODELLING

10.1. Introduction

Turlough hydrology is driven by rainfall. Quantifying the relationship between rainfall and turlough water level is the primary objective of the hydrological modelling process. Conventional riverine hydrological models are not appropriate given the nature of the turlough response to rainfall. The aim of the modelling aspect of this research was therefore to devise an appropriate hydrological model, capable of generating turlough water level time series from rainfall and evapotranspiration records. Such a model, when used in conjunction with ecological and management data, can be used to evaluate the conservation status of turloughs as groundwater dependent terrestrial ecosystems (GWDTE). Long term hydrological records can be synthesised from historic rainfall data and can be used to identify and quantitatively describe the critical long term hydrological factors which influence biological diversity within and among turloughs. By inference this allows ecological 'damage' or risk to be assessed. The models developed also have applications in flood risk assessment in karst areas,

Of necessity a decisive factor for any turlough hydrological model are the minimal data requirements. Long term monitoring of turlough hydrology is limited to a group of turloughs around the Gort area, and even amongst this group continuous, consistent records are scarce. In general, there are little or no existing data for use in the generation or calibration of any long term hydrological model. Therefore the approach was to devise a conceptual model of turlough functioning based on data collected during this research and to use this as a basis for the generic model formulation. Firstly, a simple soil moisture deficit (SMD) model was developed to simulate the soil reservoir and evapotranspiration effects. Following this, two modelling techniques were devised to predict turlough water level using the output from the SMD model and parameters based upon field data and analysis: the *aggregated rainfall* model and the *general reservoir* model.

10.2. Model Efficiency

The specific criterion used to determine model efficiency or measures of fit, is dependent upon the requirements of the model in question. For example, the focus of the model may be to predict the peak, the duration of flooding or the recession behaviour. A number of performance statistics exist for assessing the goodness of fit of a hydrological model. Most of these measures are based upon the sum of squared errors or error variance (σ_ε^2) as summarised by Beven (Beven, 2000):

$$\sigma_\varepsilon^2 = \frac{1}{n-1}\sum_{t=1}^{n}(y_t - \hat{y}_t)^2 \qquad \textit{Equation 10.1}$$

where $\hat{y}_t$ is the predicted value of variable y at time step t = 1, 2..., n. The first measure, the coefficient of determination or R^2, is defined as the square of the Pearson correlation coefficient and is given by:

$$R^2 = \left(\frac{\sum_{t=1}^{n}(y_t - \bar{y})(\hat{y}_t - \bar{\hat{y}})}{\sqrt{\sum_{t=1}^{n}(y_t - \bar{y})^2}\sqrt{\sum_{t=1}^{n}(\hat{y}_t - \bar{\hat{y}})^2}} \right)^2 \qquad \textit{Equation 10.2}$$

R^2 varies from 1 to 0 with 1 indicating that the dispersion of the prediction is equal to that of the observation, and 0 indicating no correlation (Krause et al., 2005). Another similar criterion used in hydrological modelling is the Nash-Sutcliffe modelling efficiency (E), given by:

$$E = 1 - \frac{\sum_{t=1}^{n}(y_t - \hat{y}_t)^2}{\sum_{t=1}^{n}(y_t - \bar{y})^2} \qquad \textit{Equation 10.3}$$

where $\bar{y}$ is the mean of the observed variables and the range of E is from 1 (perfect fit) to $-\infty$. Due to the use of sum of squares in its calculation, model efficiency has a number of limitations (Beven, 2000). Firstly, as the errors are squared the largest residuals tend to be found near the peaks. This gives greater weight to the prediction of peak than to lower values, although when using a model for flood prediction this is not necessarily a disadvantage. Secondly, model efficiency may be sensitive to timing errors so even if a model is predicting the magnitudes correctly there could be large

residuals if the timing was not precise. Finally, it is assumed that the errors at successive time steps are independent whereas this is often not the case. For example, if modelling the storage of water in a reservoir, the error in each time step can have a cumulative effect over the modelling period.

A number of modified forms of E exist to compensate for these limitations. E can be calculated using logarithmic values of y and $\hat{y}$. This decreases the influence of peak values and increases low value influence thus increasing the sensitivity to model over- or under-prediction (Krause et al., 2005).

$$\log E = 1 - \frac{\sum\left(\log(y_t + \varepsilon) - \log(\hat{y}_t + \varepsilon)\right)^2}{\sum\left(\log(y_t + \varepsilon) - \overline{\log(y_t + \varepsilon)}\right)^2} \qquad \textit{Equation 10.4}$$

Alternatively, inv E can be used which gives more weight to low flows:

$$invE = 1 - \frac{\sum\left(\frac{1}{y_t + \varepsilon} - \frac{1}{\hat{y}_t + \varepsilon}\right)^2}{\sum\left(\frac{1}{y_t + \varepsilon} - \overline{\frac{1}{y_t + \varepsilon}}\right)^2} \qquad \textit{Equation 10.5}$$

Bias gives the overall error in volume (in m^3/year) and can be calculated as:

$$Bias = \frac{\sum_{t=1}^{n}\left(V_t - \overline{V}_t\right)}{n} \qquad \textit{Equation 10.6}$$

A combination of efficiency measures in combination with an additional assessment of absolute or relative volume criteria should be used, with the method selection carried out in the context of the modelled quantities relevant to the study in question (Jannsen and Heuberger, 1995; Krause et al., 2005). As the primary purpose of the modelling carried out as part of this research is to produce a reasonably good fit across the full range of flooding, rather than say the high water levels as would be used in flood risk assessment, the main model performance indicator used in this research is the Nash – Sutcliffe criterion for efficiency.

10.3. Soil Moisture Deficit Model

Soil cover within a catchment controls the quantity and rate at which infiltration occurs into the karst aquifer system. Water is contributed to the system in the form of precipitation, and is lost through a combination of evaporation and transpiration by vegetation cover known as evapotranspiration (E_t). The soil itself can retain a certain amount of water under gravity, known as its field capacity. When the water supplied to the soil exceeds the field capacity the soil becomes saturated, with excess precipitation converted into overland flow or percolation. If there is insufficient rainfall to replenish the soil moisture lost over time through E_t, a deficit develops within the soil. This is known as soil moisture deficit (SMD) and is defined as the amount of rainfall required to restore the soil to field capacity (Shaw, 1994).

Evapotranspiration (E_t) does not always occur at the potential rate but decreases with increasing SMD. As the moisture level in the soil drops it is no longer available to plants with shallower root systems and so the rate of E_t reduces accordingly. Penman (1950) introduced the idea of a root constant which defined the amount of moisture that could be extracted without difficulty by a given vegetation type (Shaw, 1994). Different vegetation types were assigned root constants based on root depth and their ability to easily extract soil moisture. For example, permanent grassland has a root constant of 75mm while woodland, with its associated deeper root systems, has a root constant of 200mm. It is assumed that E_t occurs at the potential rate for a given vegetation type while the SMD is less than the root constant plus 25mm. As the SMD increases it becomes more difficult for vegetation to obtain water from the soil leading to actual ET eventually dropping to zero. If SMD reaches a critical value, known as the permanent wilting point, the vegetation wilts and dies.

An SMD reservoir model provides a simple way to represent the differences in soil moisture conditions throughout the year and to calculate percolation to groundwater (Fleury et al., 2007b). This is conceptually represented as a linear reservoir with the fluctuation in levels dependent on the reservoir inputs and outputs, namely rainfall as input and potential evapotranspiration and percolation as outputs. A level of zero corresponds to the base of the reservoir (Figure 10.1). The reservoir has a maximum

level which is defined by the soil field capacity parameter Hs_{max}. Hs_{max} is regarded as a characteristic of the catchment and varies with overburden thickness, soil and vegetation type. For example in areas where rock outcrop is close to or at the surface, such as in the Burren, the value of Hs_{max} would be close to zero as the soil would have very little capacity for storing moisture, and so a high percentage of rainfall percolates throughout the year. If the level in the reservoir exceeds the soil capacity ($Hs_t > Hs_{max}$), the amount by which it is exceeded equates to the percolation. As the lower limit of the soil reservoir is zero, Hs_{max} also limits the maximum soil moisture deficit that may exist, thus preventing the reservoir from becoming excessively under-saturated.

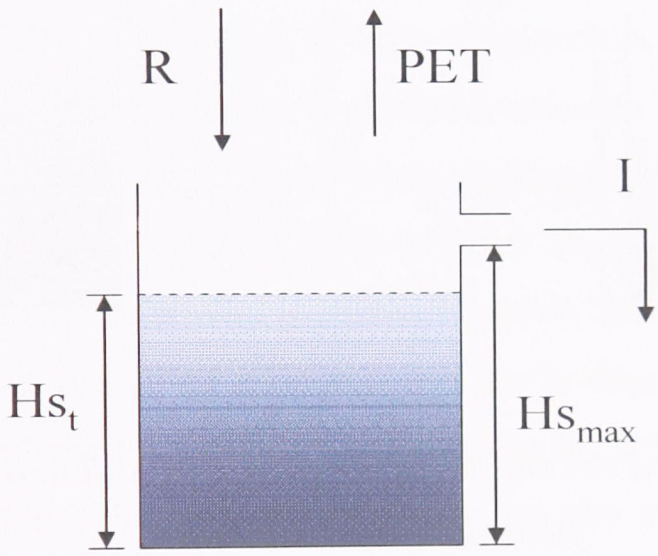


Figure 10.1: Conceptual SMD reservoir model

Where:

Hs_t is the level in the reservoir at time t (mm)

Hs_{max} is the soil field capacity (mm)

R is rainfall (mm)

PET is potential evapotranspiration (mm)

I is infiltration/percolation (mm)

The reservoir level at time t (Hs_t) is calculated by a mass balance for each time step and given by:

$$Hs_t = Hs_{t-1} + R - PET - I \qquad \textit{Equation 10.7}$$

The operation of the soil reservoir is demonstrated in the scenarios shown in Figure 10.2 (a) and (b). In Figure 10.2 (a), the reservoir level Hs_{t-1} at 50mm is below field capacity. Given rainfall and PET during the time step are 20mm and 5mm respectively, the change in level ΔHs_t is +15mm. As the new level is still less than Hs_{max} infiltration is zero. In Figure 10.2 (b) the reservoir level Hs_{t-1} is equal to Hs_{max} at the beginning of the time step. Again, the change in level is +15mm. As this would exceed the upper limit of the reservoir, the excess becomes an infiltration, or percolation to groundwater, of 15mm.

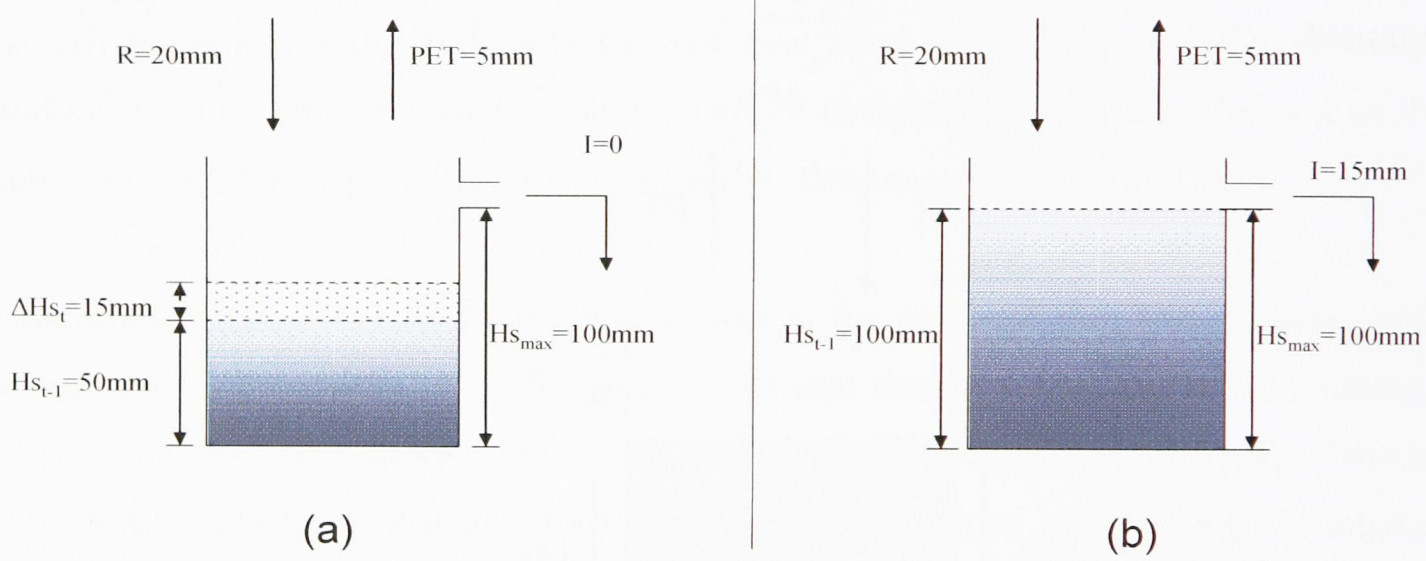


Figure 10.2: Operation of the soil reservoir under (a) soil moisture deficit and (b) field capacity conditions

Once the soil reservoir is near capacity, typically during the winter months in temperate climates, the value of Hs_{max} has little impact on the net infiltration. Where Hs_{max} has a greater effect is during dry periods. A low value for Hs_{max} can result in the model predicting more numerous low level flood events, as relatively little rainfall is required to produce infiltration which in turn causes flooding. Similarly, the onset of flooding would be predicted to occur earlier in the turlough basin for lower Hs_{max} as less rainfall is required to bring the soil reservoir up to field capacity. Hs_{max} has little or no buffering during the inundation period as dry periods are too short and PET too low for the deficit to become significant. The value of Hs_{max} for each turlough which produced effective runoff coincident with the onset of flooding, and also gave the highest model efficiency, was used throughout the modelling process.

Daily potential evapotranspiration (PET) data calculated using the FAO Penman-Monteith equation was obtained from Met Eireann synoptic stations located in Shannon Airport (Co. Clare), Knock Airport (Co. Mayo), and Birr (Co. Offaly). Knock data was taken to be representative of evapotranspiration conditions for the northern turloughs while Birr PET data was used for turloughs located in counties Galway and Clare. A program to simulate the operation of the SMD model was written in MATLAB.

10.4. Aggregated Rainfall Model

Previous analysis has shown a strong relationship between cumulative rainfall and volume during the filling period, with Pearson Product Moment correlations of >0.95 established (Chapter 8). Consequent to this relationship, the possibility of using cumulative rainfall as the basis for a generic turlough hydrological model was explored. While this relationship was strong during the filling phase, cumulative rainfall continuously increases and so a method was required to incorporate a recession element into the cumulative rainfall model. The methodology devised is based on the idea that the filled turlough volume is dependent on the cumulative rainfall over a defined period, hereafter referred as to as the aggregation period ***T***. Thus, the aggregated rainfall model is founded on the notion that volume in the turlough at time ***t*** is a function of the cumulative rainfall over the preceding ***T*** days.

The modelling methodology consists of summing rainfall over successive consecutive intervals, and correlating the subsequent time series with volume. The period over which the rainfall is summed is the aggregation period ***T***. It was found that the correlation coefficient increased with increasing ***T*** towards a maximum value, and then decreased for higher values of ***T***. A linear regression between the aggregated rainfall and turlough volume time series gives a linear equation of the form:

$$V = S + \alpha * AR \qquad \textit{Equation 10.8}$$

Where:

V is modelled volume (m^3)

S is karst storage capacity (m^3)

α is contributing area (m^2)

AR is aggregated daily rainfall (m)

Where

$$AR = \sum_{t=1}^{T} R_t \qquad \textit{Equation 10.9}$$

This methodology produces three characteristic parameters for each turlough:

***Aggregation period T*:** An indicator of the memory of the system, or how long water is retained within the turlough, and so provides an indirect measure of flood duration. A large aggregation period implies long flood duration with a lengthy recession, while a smaller value indicates a hydrological regime with rapid filling and emptying.

***Storage capacity S*:** This is the volume of water required to have built up in the karst flow system before flooding occurs in the turlough basin. The storage capacity represents both the storage and the flow capacity of the underlying flow system, and is a characteristic of the karst aquifer in which the turlough is located as well as being indicative of the hydrological operation of the turlough. A high storage capacity implies that significant quantities of rain falling within the turlough contributing area do not actually enter the turlough, but are taken up by storage or accommodated by the karst flow system. The reverse of this, a low storage capacity value, implies that the vast majority of rainfall within the contributing area passes directly through the turlough. In this scenario the turlough would operate like a surface reservoir, with discrete input and output points whose operation are dependent upon the prevailing hydrological conditions such as rainfall and water level within the turlough.

Contributing area α*:** The contributing area ***α defines the minimum magnitude of the zone of contribution and so provides a lower limit for the required catchment area. This is the minimum topographic area required to supply the recorded water volume within the turlough. The actual scale of the catchment area could be much greater than that specified by the contributing area ***α***, as it is assumed that all effective rainfall within this area enters the turlough. It is a fitted parameter of the model. This may not be the case, as some recharge could be retained in storage within the matrix and fracture porosity of the karst bedrock. Depending upon the hydrological operation of the turlough and the associated karst flow system, the groundwater entering the

turlough may only represent a fraction of the total recharge with the remainder potentially bypassing the turlough basin altogether.

A number of simplifying assumptions are made to assist in the application of this modelling methodology. The first is that of linearity; it is assumed that a direct proportional relationship exists between rainfall and volume, i.e. that 1 mm of rainfall at time ***t*** results in an increase in volume of α m^3 (0.001 x α) irrespective of existing hydraulic conditions. Similarly at time ***t*** + ***T*** the volume decreases by α m^3 (*Figure 10.3 (a)*).

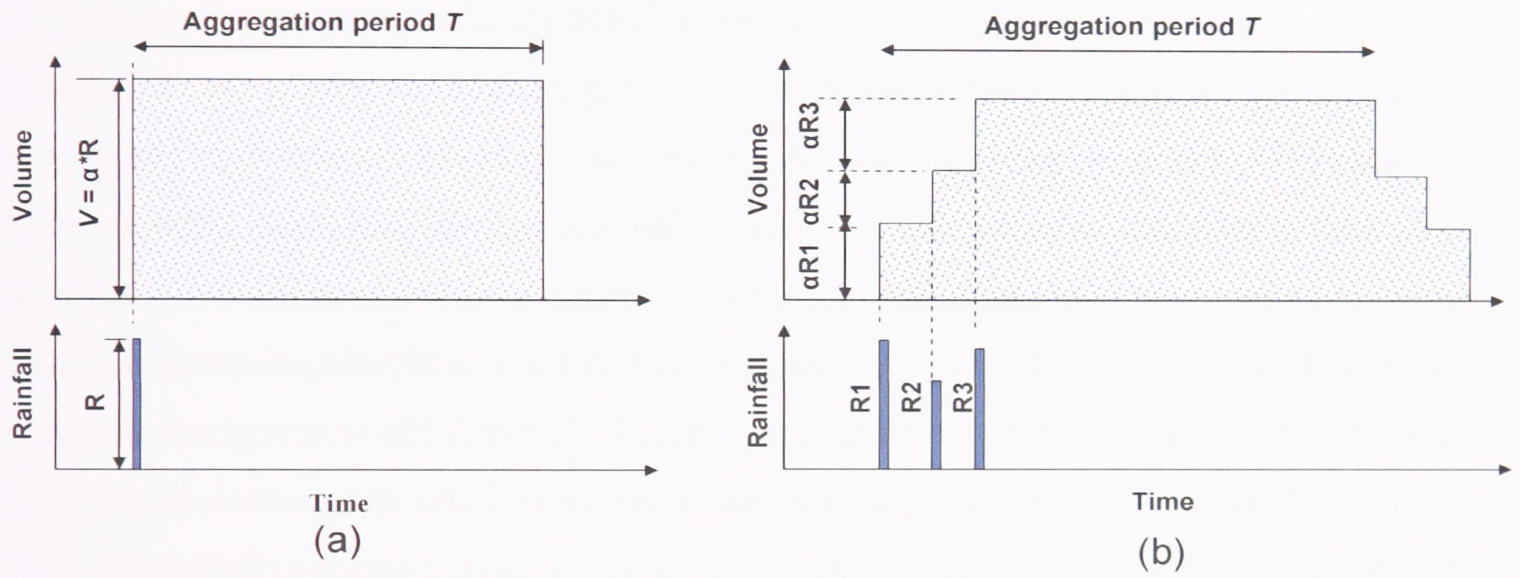


Figure 10.3: (a) Linear relationship between rainfall and volume and (b) the principles of instantaneous inflow and superposition used in the rainfall aggregation model

The second assumption is that of instantaneous inflow, where 100% of rainfall enters the turlough during the time step in which it occurred. This means that the rising limb of the hydrograph increases in a series of steps, with the magnitude of each volume step proportional to the magnitude of the associated rainfall event (Figure 10.3 (b)). Due to the heterogeneous nature of karst aquifers, rainfall will infiltrate much faster in highly karstified areas than in adjacent, perhaps less karstified areas. The result of this characteristic is a lag between a rainfall event and its full extent being realised within the turloughs, shown in the delay between a rainfall event and the associated peak water level. The parallel assumption for the recession limb means that once a rainfall event is no longer within the aggregation period, it is not included in the regression.

As a result, the recession limb of the volume hydrograph drops in a series of discrete steps as the aggregation period for each rainfall event elapses (Figure 10.3 (b)).

The third simplifying assumption is that the contributing area remains the same for all hydrological conditions, and that once the karst storage capacity has been reached, 100% of effective rainfall in the contributing area enters the turlough. Catchment areas in karst regions may vary significantly with changing hydrological conditions, as various flow systems may only be operational within a certain range of water levels. This situation may often be the case within karst aquifers, with multiple groundwater flow systems operating and interacting during different hydrological conditions, and even may include the amalgamation of adjacent catchment areas during periods of high groundwater levels. This may also occur within the basin itself; an example being estavelles located above the base of a turlough no longer functioning as sinks once the water level recedes below their threshold. Also, where a flow system exists beneath the turlough a significant proportion of the flow potentially bypasses the turlough altogether, and so the contributing area represents a fraction of the area from which total floodwater is derived. However, given the good results achieved using this simplifying assumption and the difficulties involved in quantifying the variability without extensive local site investigations, the contributing area was held constant for all hydrological conditions.

10.4.1. Modelling Methodology

Initial trials of this modelling technique were carried out for all turlough topographies using daily rainfall data as the input. The modelling methodology used was as follows:

i) For values of ***T*** frin1 to 250 days, the total rainfall over the preceding ***T*** days was calculated at each time step to give the aggregated rainfall time series.

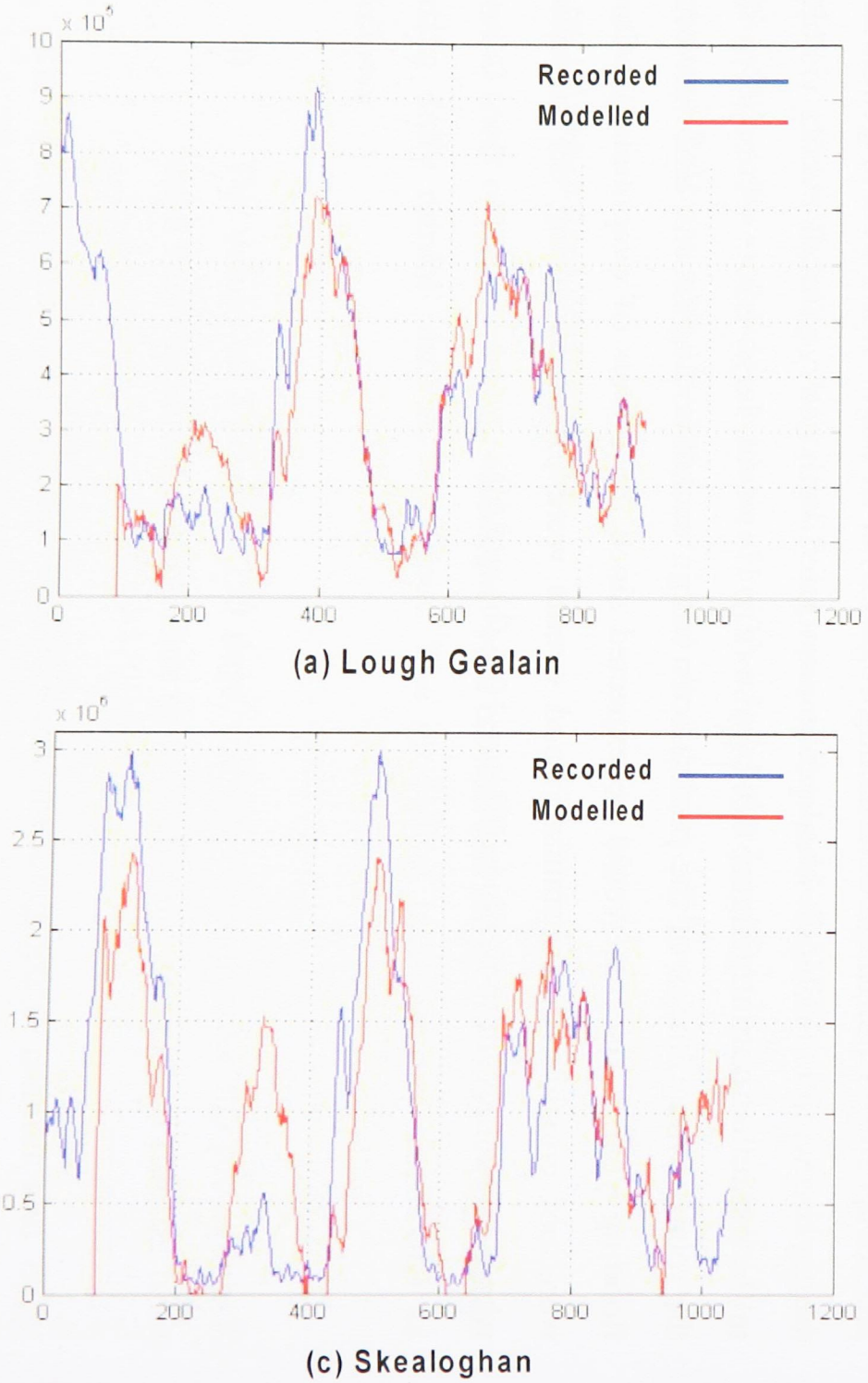
ii) Correlation was carried out between the aggregated rainfall and daily turlough volume time series, with a record kept of the correlation coefficient and associated aggregation period ***T***.

iii) The aggregation period corresponding to the highest correlation was selected, and the aggregation time series for this period recalculated.

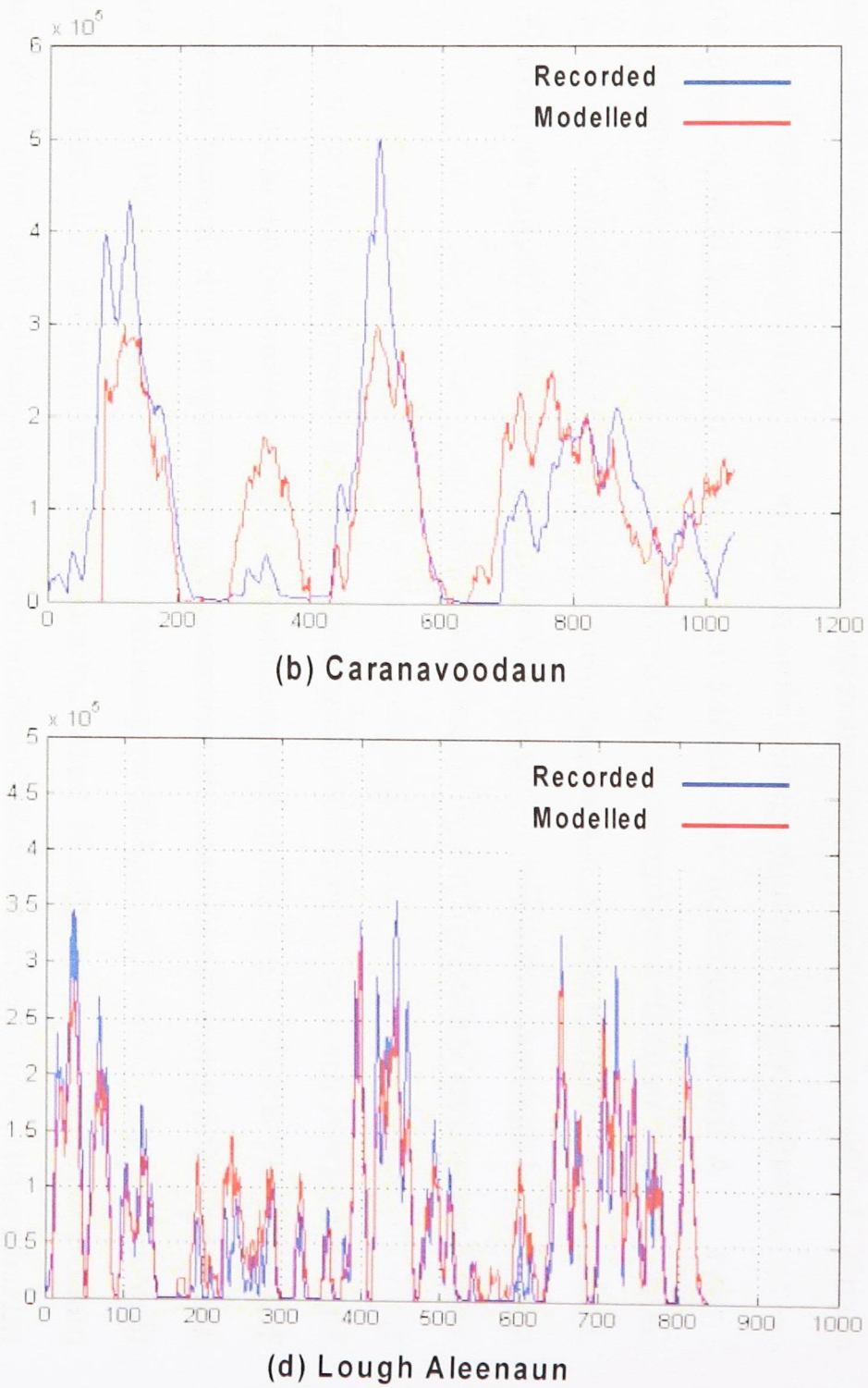
iv) A linear regression was carried out ($V = AR^* \alpha + S$) and used to generate the modelled volume as the dependent variable, along with the fitted model parameters of storage capacity ***S*** and contributing area ***α***.

v) The Nash-Sutcliffe efficiency criterion was calculated using the recorded and modelled volume time series.

The first model run was carried out using rainfall data as the input for all study sites. This run gave an average maximum correlation of 0.78 and standard deviation of 0.1. The range of aggregation period values showed the diversity in hydrological regimes, from a low of 12 days for rapidly responding Lough Aleenaun up to 203 days for much slower Termon Lough. In terms of modelling performance, this run yielded mixed results, with Nash – Sutcliffe efficiencies varying greatly from only 32% for Brierfield, Co. Roscommon, to 81.9% for Lough Aleenaun, Co. Clare (Figure 10.4 (d)). Despite these low efficiency values, the general seasonal pattern of flooding was picked up across the range of flooding regimes, with major flood events generated during the winters and individual peaks associated with heavy rainfall events visible in the modelled output (Figure 10.4 (a) to (d)). However, large errors were shown in the relative magnitudes of the peaks, both within each flooding season and between flooding years. Also, as would be expected since the effects of evapotranspiration were not considered, substantial flood events were predicted during the summer where no such event took place (Figure 10.4 (b) and (c)).



(a) Lough Gealain



(b) Caranavoodaun

(c) Skealoghan

(d) Lough Aleenaun

Figure 10.4 Aggregated rainfall model for (a) Lough Gealain, (b) Caranavoodaun, (c) Skealoghan and (d) Lough Aleenaun

The modelling process was then repeated using effective rainfall (rainfall – potential evapotranspiration) as the model input. This resulted in an average model efficiency increase of approximately 16%, up to a mean of 77.7%. In the case of Coolcam and Croaghill, the increases were as much as 43% and 37% respectively. The inclusion of evapotranspiration effects served to damp the response to rainfall during the warmer months, and so reduced the appearance of anomalous flood events during the summer. As this also increased the magnitude of the higher peaks relative to the lower ones, the peak volume error following regression was also reduced. This can be seen in the example shown for Caranavoodaun turlough, Co. Galway (Figure 10.5 (a) and (b)). A large over-prediction error can be seen in the model using rainfall as input due to the predicted summer flood event after approximately 300 days on the graph (Figure 10.5 (a)). The error associated with the same event is greatly reduced when effective rainfall is used as input (Figure 10.5 (b)). Improvements can also been seen in both peak volume and timing estimation.

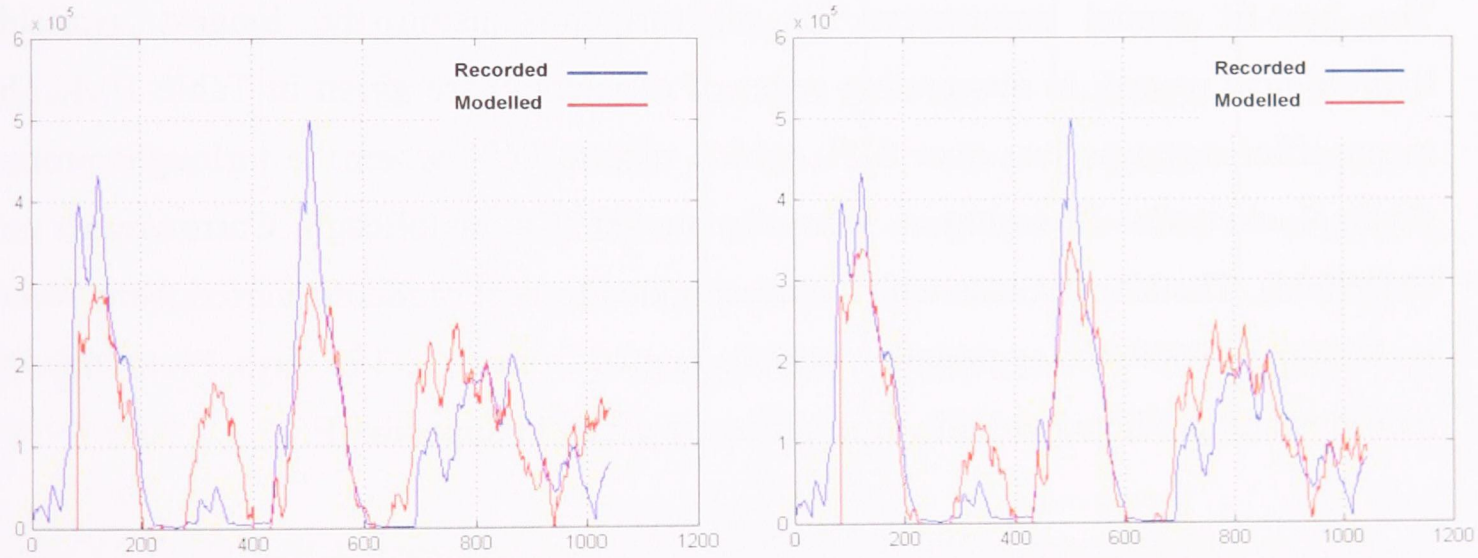


Figure 10.5: Aggregated rainfall model for Caranavoodaun using (a) rainfall and (b) effective rainfall as input

Next, infiltration time series were generated for each turlough using the SMD model for Hs_{max} values from 10 up to 60mm, in increments of 10mm. The revised form of the modelling equation thus becomes:

$$V = S + \alpha * AI_{Hs\,max} \qquad \textit{Equation 10.10}$$

where ***AI*** is the aggregated infiltration generated using a maximum allowable SMD of Hs_{max}. It was unnecessary to test values above 60mm as deficits rarely if ever reached this level using the SMD model. Also, with Hs_{max} below 10mm the SMD reservoir output rapidly approaches effective rainfall which had already been used. The variation in Hs_{max} had little impact on the turlough behaviour during the winter months, as high rainfall and low evapotranspiration meant that only a minimal soil moisture deficit build up during this period and rarely reached the defined maximum. The main changes in flooding behaviour were shown during the summer months. Lower values of Hs_{max} caused a slightly higher flooding frequency, but the increase in storage capacity generated during the regression tended to partially counteract this. It is also clear that the role of evapotranspiration in turlough response decreases with the more rapid response to rainfall.

10.4.2. Model Results

The best-fit model parameters for all turloughs using the longest available hydrological record, in descending order of efficiency, are given in Table 10.1. The mean efficiency was just over 81%, which rose to 86% when the turloughs around Castleplunket, Co. Roscommon were discounted (Rathnalulleagh, Carrowreagh and Brierfield). The Hs_{max} values which corresponded to best model fit varied from 10mm up to 60mm, while the aggregation periods ranged from 10 to 173 days. Plots showing recorded and predicted volume time series are given in appendix E.

Site Name	Max Correlation Coefficient	Max Efficiency (%)	Hs_{max} (mm)	T (days)	S (m^3)	α (m^2)
Coolcam	0.97	93.4	40	163	-267581	3113
Ardkill	0.96	92.6	10	135	-135397	1075
Croaghill	0.95	91.4	50	120	-79572	1481
Knockaunroe	0.94	89.7	20	82	-286320	2720
Lough Gealain	0.94	89.2	10	81	-53264	1297
Lisduff	0.94	89	60	90	-45514	2013
Skealoghan	0.93	88.6	10	73	-57898	827
Lough Aleenaun	0.94	88.6	30	10	-6972	2070
Caranavoodaun	0.93	87.9	60	80	-63696	767
Caherglassaun	0.93	87.7	20	66	-425394	6849
Termon	0.94	87.7	60	176	-219354	1342
Garryland	0.91	83.9	20	67	-336211	4542
Lough Coy	0.91	82.2	60	44	-19709	5215
Blackrock	0.88	79.9	10	38	-677436	13127
Turloughmore	0.85	75.9	30	15	-36222	1620
Roo West	0.85	73.6	30	82	-148322	1197
Rathnalulleagh	0.80	66	20	85	-154359	1399
Brierfield	0.74	54.2	50	144	-182895	1616
Carrowreagh	0.70	49.3	10	108	-69695	470

Table 10.1: Best-fit aggregated rainfall model results with corresponding maximum soil moisture deficit Hs_{max}, aggregation period T, storage capacity S and contributing area α

The aggregated rainfall model showed some good results for every type of turlough flooding regime. The highest efficiency was shown by Coolcam, Co. Galway, a turlough with one of the longest flood durations of any site (Figure 10.6). The modelled volume hydrograph shows a good general fit for as well as picking up the timing and magnitude of volume peaks in all three hydrological years.

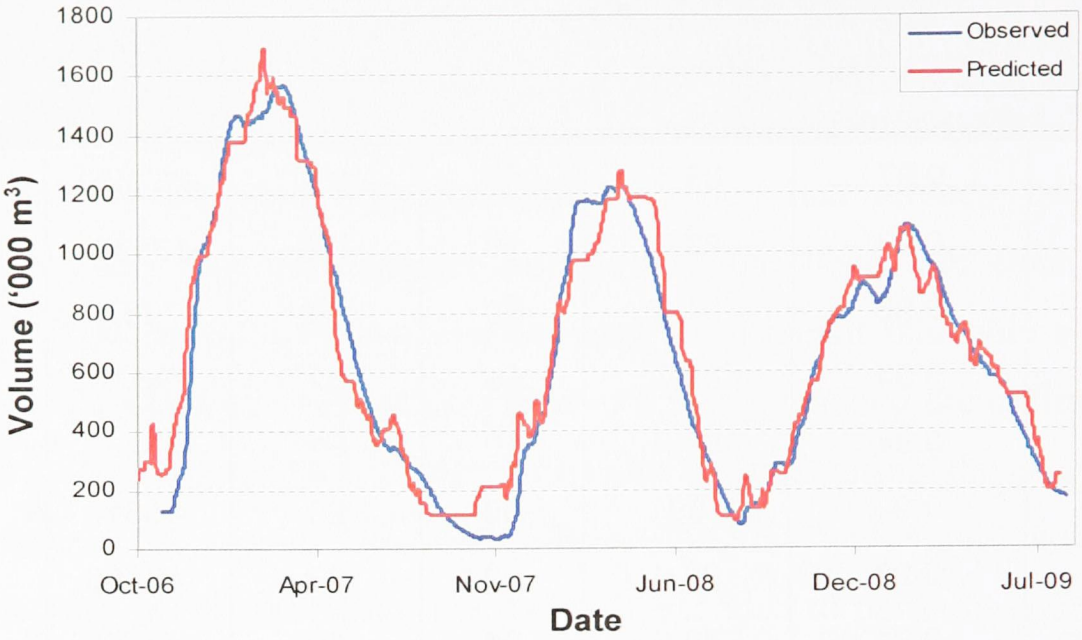


Figure 10.6: Aggregated rainfall model results for Coolcam turlough, Co. Galway

Skealoghan turlough, Co. Mayo, has a flooding regime somewhere in the mid-range of frequency and duration. The efficiency of 88.6% shows the general pattern of flooding was clearly picked up (Figure 10.7). However, the length of the best-fit aggregation period, at 73 days, meant that the modelling procedure was unable to accurately represent the short term level fluctuations shown by the turlough. While peaks do exist within the modelled time series which correspond to the recorded peaks, the lack of sensitivity means that the model underestimates the rate of recession following the maxima. The effect is less prominent during the main recession, but did lead to substantially smaller predicted peaks in 2006/2007 and 2008/2009. In effect the model may be over – simplifying the recharge process in this case.

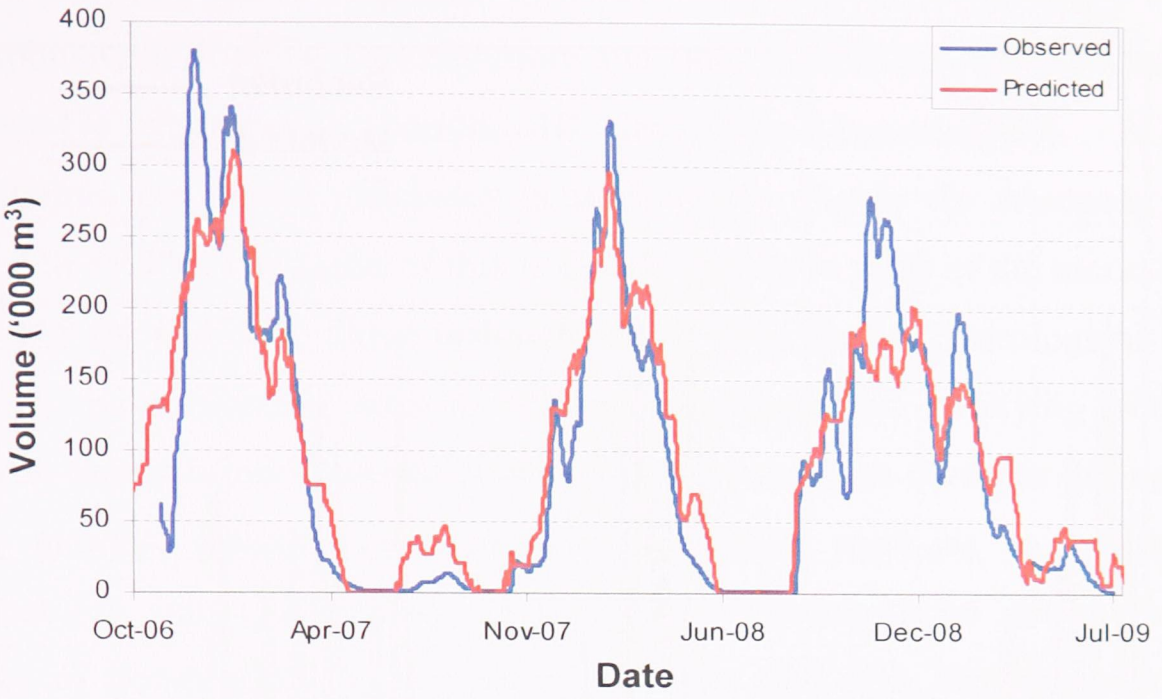


Figure 10.7: Aggregated rainfall model results for Skealoghan turlough, Co. Galway

As the aggregation period was further reduced for the more responsive sites, the predicted response was able to pick up short term fluctuations in volume. The best example of this is shown by Lough Aleenaun, Co. Clare. Here, the low aggregation period of 10 days allows the high frequency flooding events to be represented within the predicted hydrograph (Figure 10.8 (a)). It also showed the low memory of the system which is indicative of low residence times within the turlough basin.

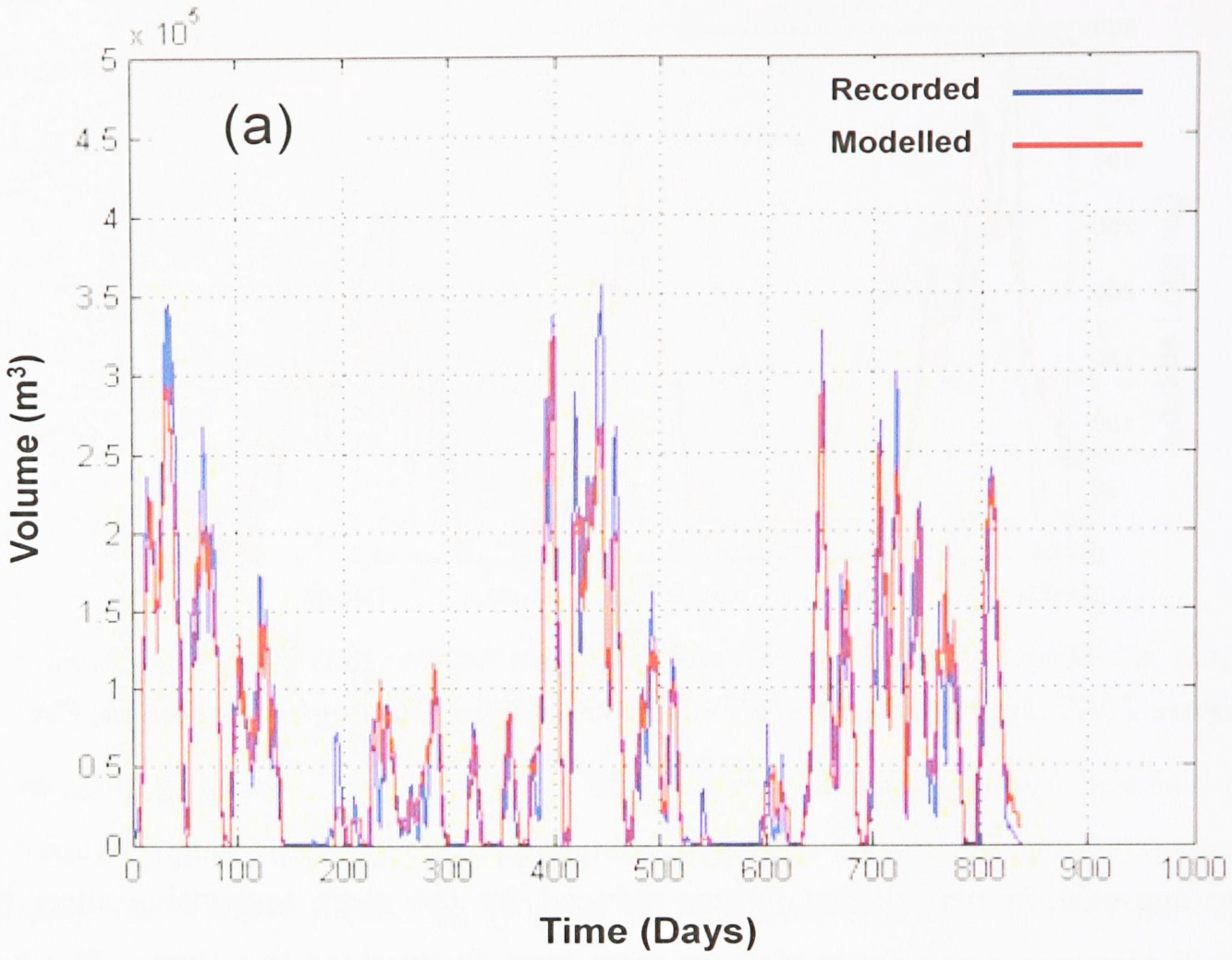


Figure 10.8: Aggregated rainfall model for (a) Lough Aleenaun, Co. Clare and (b) Turloughmore, Co. Clare

The modelling process has highlighted a key difference in the operation of the two most responsive turloughs, Turloughmore and Lough Aleenaun. Both turloughs show a comparable aggregation period, 10 days for Aleenaun and 15 days for Turloughmore, but model efficiency is substantially higher for Aleenaun at 88.6% compared to 75.9%. The cause of this is clearly visible in plots of the modelled results (Figure 10.8 (a) and (b)). These turloughs show very similar hydrological behaviour during the main flooding season, with rapid filling and emptying occurring in response to heavy rainfall events. However, their behaviour diverges during the drier summer months. Lough Aleenaun shows a flood response to rainfall events throughout the year (Figure 10.8 (a)); whereas Turloughmore has a much lower frequency of flooding during dry periods (Figure 10.8 (b)). The magnitudes of the higher volume peaks are also substantially under-predicted while flood frequency is over-predicted in the case of Turloughmore.

This distinction in behaviour points to a difference in the flow capacity of the respective systems underlying each turlough. The response of Lough Aleenaun to all major rainfall events suggests an extremely low bypass flow capacity, or even its operation as a reservoir with distinct inputs and outputs. The flow system containing Turloughmore, in contrast, is able to accommodate considerable flow before Turloughmore becomes flooded. The presence of additional storage within the Turloughmore system is demonstrated by the higher storage capacity value of 36222 m^3, compared to only 6972 m^3 for Lough Aleenaun. This is supported by physical features observed within and surrounding each turlough. In Lough Aleenaun, a channel fed by a permanent spring runs in an arc from the eastern side of a central rocky outcrop, before sinking at the western end of the outcrop (Figure 10.9). When flooding occurs it expands out from this channel until the entire basin is inundated. This channel is also the last area to drain, and often retains a small amount of water throughout the year.



Figure 10.9: Arcing channel within Lough Aleenaun, Co. Clare

In Turloughmore, there are no such features indicating a continuous inflow of water into or through the turlough during dry periods. The behaviour of a turlough directly beside Turloughmore, which has a lower base elevation, gives an insight into the groundwater flow conditions in the vicinity of the turlough. Flooding has been observed in the adjoining depression both in the summer, when no flooding occurred in Turloughmore, and during the winter after complete recession has occurred in Turloughmore. The summer flooding demonstrates the existence of a flow path which bypasses Turloughmore and feeds directly into this depression during lower flow periods. This depression acts as additional storage within the system, offsetting the effects of rainfall and limiting the occurrence of flooding within Turloughmore. During the winter, the depression damps the effects of rainfall during the initial filling phase, but when it reaches capacity later it ceases to damp the inflow signal and so the flow response into Turloughmore increases. Therefore, as the aggregated rainfall model represents the behaviour of the turlough using a single linear relationship, the overall effect of the neighbouring depression is to over-predict flood events and under-predict inflow at higher volumes. In Lough Aleenaun there is no such storage capacity, and so flooding occurs more frequently and the linear relationship between rainfall and inflow provides a better approximation throughout the year.

Clearly, the worst results achieved were shown by the subset of turloughs located near Ballintober, Co. Roscommon. As all three used data from the same rain gauge, the data integrity of the rainfall record was first checked to ensure this was not the cause of the errors. The rainfall time series used was from a rain gauge installed as part of this project, located only 3 km away from the sites. This was compared to data from the Met Eireann station in nearby Roscommon Town, and both showed extremely similar rainfall patterns and intensities so that data error did not explain the poor model performance. The Roscommon subset showed among the highest levels of temporal variation in volume. Carrowreagh, for example, showed a 50% reduction in maximum volume year on year during the monitoring period. The yearly decrease in depth was relatively much less, with only a 14% decrease from 2006/2007 to 2007/2008 and 10% from 2007/2008 to 2008/2009.

A possible explanation here is that the water level in the turloughs, and associated volumes of water, are responses to the head within the subsurface flow systems and the interactions between the turloughs. In order for a turlough to fill, there must be a hydraulic gradient towards the turlough. The rate at which the turlough fills, and the level to which it rises, is dependent upon the interaction and the head. If this were the case, a smaller decrease in head would cause a proportionally much greater change in volume due to the depth-volume characteristics of each turlough. The water entering from the underlying system would depend upon the relative levels of the two. But the consequential effect is a massively lower volume within the turlough, as draining occurs.

10.4.3. Conclusion

Given the relatively high recharge rates, the aggregated rainfall model showed that reasonable results could be obtained using a simple generic model based upon the correlation between turlough volume and rainfall. This model showed that 32.5% to 81.9% of the variability in daily turlough volume could be predicted from rainfall data, with mean and median efficiencies of 62% and 64.3% respectively. This increased to between 49.3 and 93.4% when soil moisture deficit effects were included (mean 81.6%, median 87.7%). Despite its limitations, it provided a good estimate of turlough water volume, and associated stage, based upon rainfall and

evapotranspiration records. It also demonstrated that, at least during the rising limb of the volume hydrograph, the interaction between effective rainfall and volume could be relatively successfully modelled using a linear relationship.

The methodology also generated a set of characteristic hydrological parameters for each turlough. These descriptors for the first time allow the comparison of turlough hydrological behaviour based on quantitative recorded data rather than qualitative descriptions. The low data requirements and simplicity of use of this model also makes it suitable for use as a classification system for turlough hydrology. Moreover, the model demonstrates the strong correlation between net rainfall and water level response confirming the relatively rapid recharge as a characteristic feature of turlough hydrology. Simple though it is, the model also encapsulates and supports the basic conceptualisation of a turlough as a reservoir.

10.5. Reservoir Modelling

Using the insights gained during the hydrological analysis process, a more refined version of the reservoir modelling technique was utilised for a subset of turlough sites. Reservoir ("storage-release") modelling is particularly well suited to the modelling of turloughs, as they physically act as reservoirs for excess recharge during the winter months. This approach conceptualises the turlough as a reservoir with the same physical characteristics as the turlough being modelled (stage-volume-area relationships), and where the hydrological signature of the turlough is controlled by the nature and functioning of the reservoir inflows and outflows. The objective of this modelling approach is to identify the characteristic equations governing the flow rates, and therefore the volume and stage, and to enumerate the relationship these have with rainfall in order to accurately predict turlough hydrological regimes. Figure 10.10 outlines the elements of the modelling process:

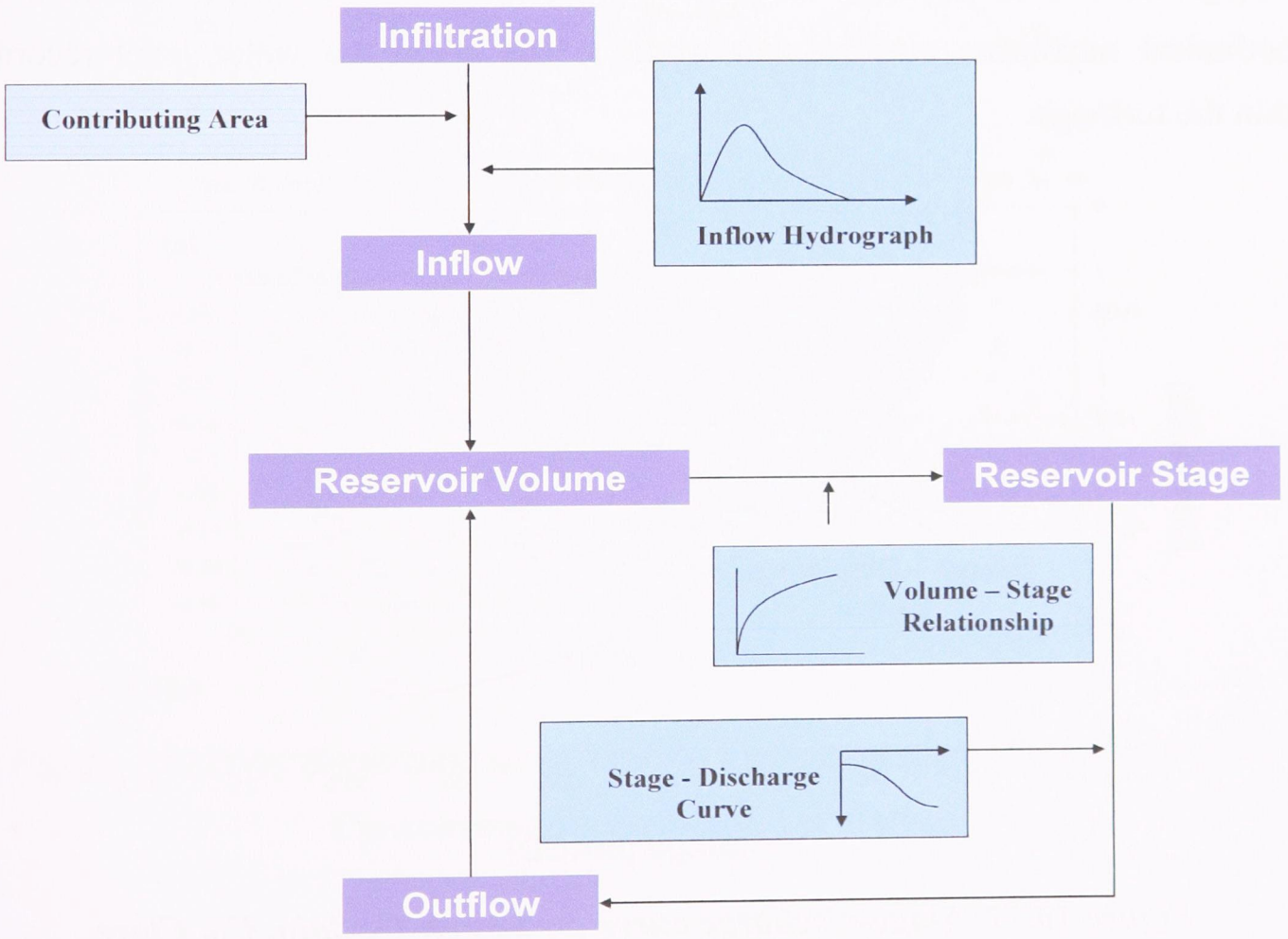


Figure 10.10: Flow chart for reservoir modelling methodology

The light blue boxes in Figure 10.10 highlight the parameters that control the operation of the reservoir at each time step. The contributing area and inflow hydrograph transform infiltration or groundwater recharge into reservoir inflow.

Reservoir outflow is a function of stage, and so a volume – stage relationship is required to transform volume into stage. The outflow itself is then calculated using the stage – discharge curve, and used to calculate the volume at the next time step. The derivation of these parameters begins with reservoir outflow and the stage – discharge curve.

10.5.1. Reservoir Outflow

The first step in the modelling process was the identification of the equations governing reservoir drainage or outflow. This was based upon the outflow analyses carried out in chapter 7, where it was shown that a stage - discharge curve defining a turlough's maximum drainage capacity was formed by the maximum outflow values across the flooding range. This curve defines the characteristic relationship between stage and turlough discharge at peak outflow conditions (Figure 10.11). Using this relationship, a potential outflow time series was calculated by applying the stage - discharge relation to the stage time series. This outflow time series represents the hypothetical maximum outflow that would occur given the water level recorded within the turlough.

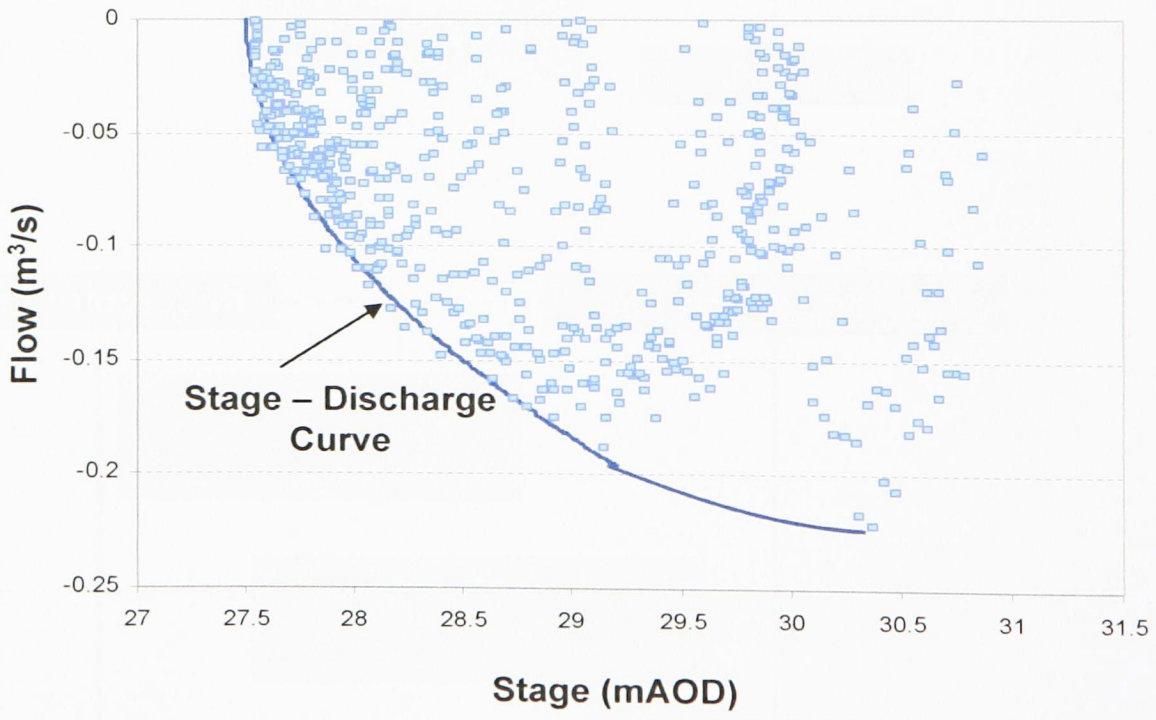


Figure 10.11: Stage-discharge curve for Lough Gealain, Co. Clare

As described in chapter 8, the complexity of stage - discharge curves varied significantly between turloughs. The form of the curve itself also varied, with some showing a convex (stage power less than 1) and others a concave (stage power greater

than 1) curve. Some sites, such as Lough Gealain and Ardkill, showed a smooth, well defined stage-discharge curve across the full range of flooding. Other turloughs had a number of discontinuities in the curve, with distinctive discharge curves applying within different flood ranges. These discontinuities are possibly indicative of multiple zones of groundwater flow in operation at different levels within the turlough basin, for example where a swallow hole ceases to operate at lower water levels when it becomes disconnected from the main water body. Another cause of discontinuities in the curve is a lack of data at certain intervals within the range of flooding. An example of this can be seen in Caranavoodaun (Figure 10.12 (a) and (b)). During both the 2006/2007 and 2007/2008 hydrological years, rainfall events disrupted the recession in the stage interval centred around 23.5 mAOD (Figure 10.12 (a)). This resulted in a lack of definition in the stage-discharge curve at (Figure 10.12 (b)).

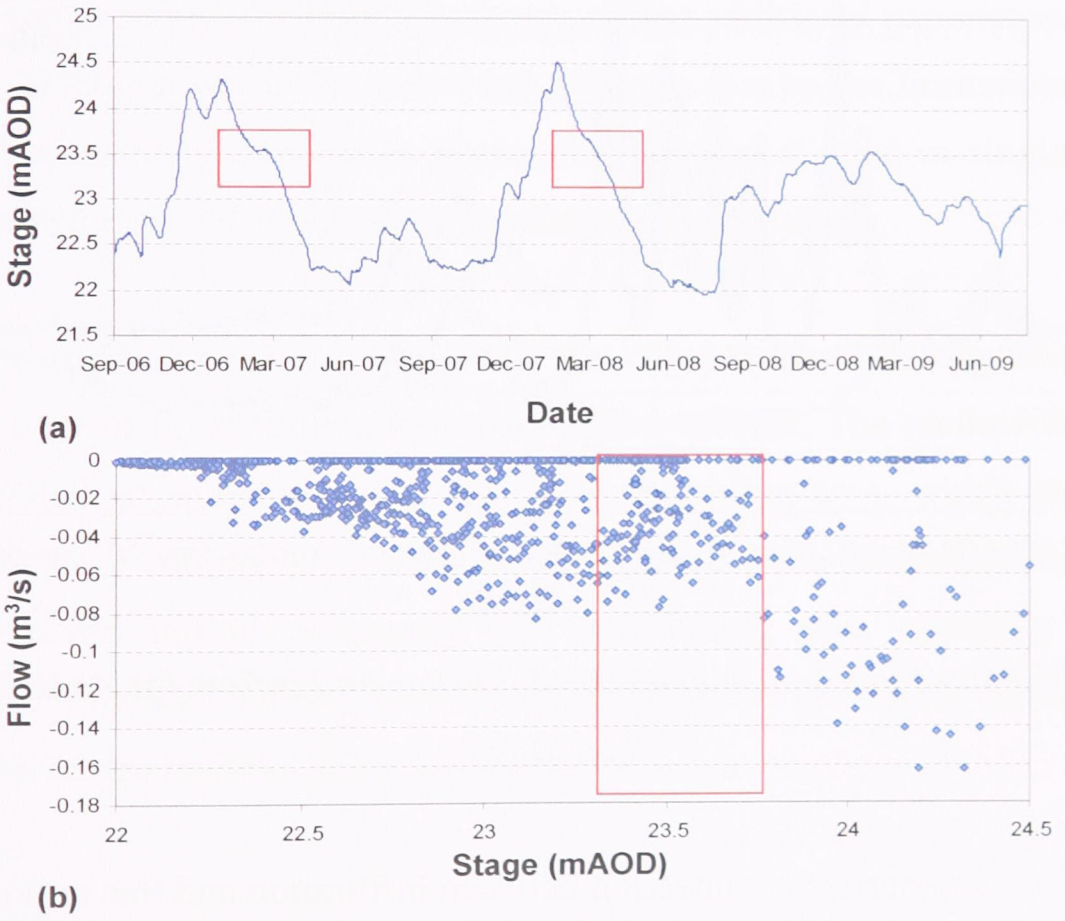


Figure 10.12: (a) Stage time series and (b) associated stage-discharge plot for Caranavoodaun turlough, Co. Galway

10.5.2. Reservoir Inflow

The next step in the reservoir modelling process was the derivation of a relationship between effective rainfall or infiltration and turlough inflow. The basic principle on which this step is based is that the volume response recorded in the turlough is the

resultant of a combination of inflow and outflow signals. It follows then, that since the net change in volume (ΔV) at each time step (Δt) is the sum of inflow (Q_{in}) and outflow (Q_{out}) during that step, and with the stage-discharge curve defining the maximum possible outflow at each time step, then inflow is given by:

$$\frac{\Delta V}{\Delta t} + Q_{out} = Q_{in} \qquad \textit{Equation 10.11}$$

As is clear from the above equation and can be seen in Figure 10.13, the inflow signal follows closely that of the net flow signal, but is offset upwards at each time step by the magnitude of the outflow.

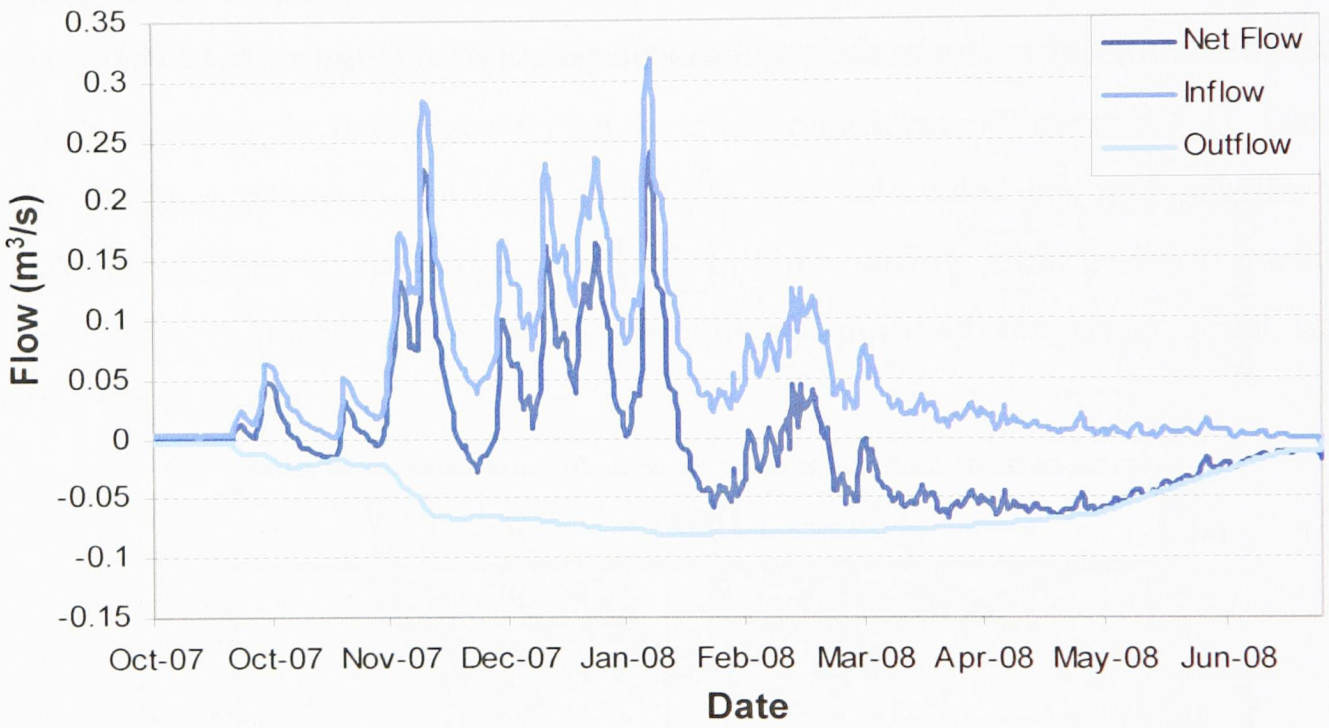


Figure 10.13: Plot of net flow, hypothetical outflow and inflow for Ardkill turlough, Co. Mayo

The next step was to derive a connection between infiltration and this notional inflow. To achieve this, a development on the strong correlation between cumulative rainfall and net inflow identified in chapter 7 was utilised. Rather than using gross rainfall as an input, the SMD reservoir model was once again employed here since, as well as providing a more realistic representation of infiltration, it was shown to greatly improve the results from previous hydrological analyses and modelling outcomes. The same SMD parameters were used for each turlough as were identified in the aggregated rainfall modelling procedure (*section 10.4.1*).

First, the cumulative inflow and SMD infiltration was calculated over the calibration period (Figure 10.14 *(a)*). Next, a linear regression was carried out between cumulative infiltration and inflow (Figure 10.14 *(b)*), with the slope of the regression line giving the contributing area. This contributing area, measured in $m^2 * 10^3$ where infiltration is in mm, represents the area required to generate sufficient infiltration for hypothetical inflow over the corresponding period. It is similar to the contributing area defined in the aggregated rainfall model, except that it defines the relationship between infiltration and flow rather than infiltration and volume.

This method of inflow prediction is a lumped parameter method, in that it represents all inflow processes with a single parameter and does not differentiate between the different sources of inflow such as direct rainfall versus conduit flow, or matrix versus conduit driven groundwater flow. However, adding additional parameters to represent the relative fractions would be somewhat arbitrary due to the limitations of the data available, but could be a possible future development if used in single site studies where more detailed hydrological information were available.

During the modelling process it was found that using the contributing area often led to significant over or under estimation of modelled volume. The methodology outlined above provided an initial estimate for the contributing area, which then could be altered during the calibration process to give the best overall result. The calibration process involved initially changing the contributing area manually to improve performance, followed by an iterative optimisation to maximise model efficiency using the Solver tool within Microsoft Excel.

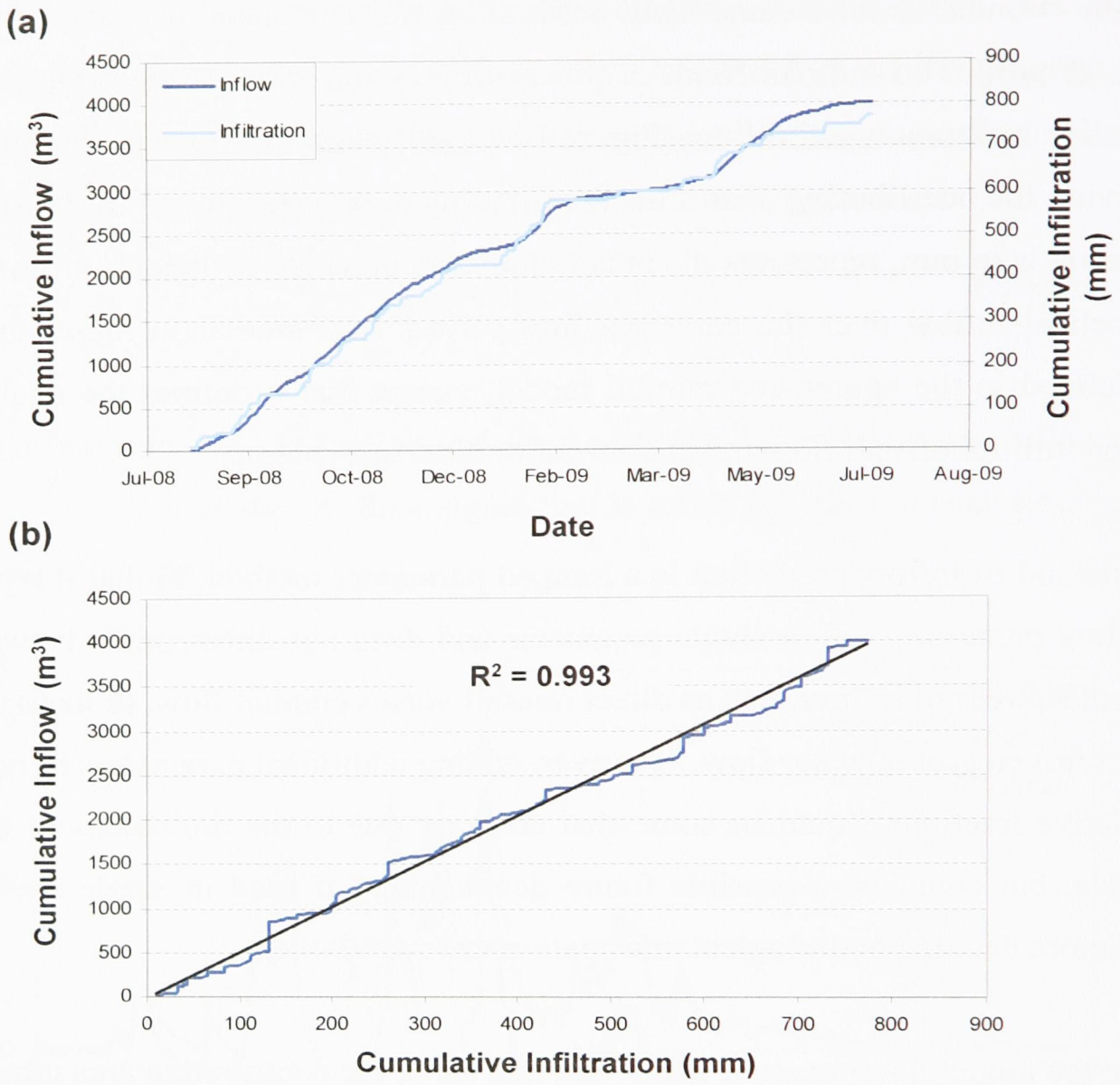


Figure 10.14: (a) Plot of cumulative infiltration and cumulative inflow for the 2008/2009 flooding period and (b) plot of cumulative infiltration versus cumulative inflow for Lisduff turlough, Co. Roscommon

10.5.3. Inflow Hydrograph

Earlier investigations as part of this PhD research (section 8.2) found that significant improvements in relationships between rainfall and net inflow could be achieved simply by averaging the rainfall over increasing intervals, and selecting the interval which showed the best match. A development on this process is the use of a unit hydrograph or transfer function. One widely used model for the generation of unit hydrographs in surface water modelling is the Nash cascade (Beven, 2000).

The Nash model transforms effective rainfall into surface runoff by routing the rainfall through a series of linear reservoirs or storages, with the relationship between the storage in each reservoir (S) and the outflow (Q) given by:

$$S = KQ \qquad \textit{Equation 10.12}$$

where K is a time constant or mean residence time for the reservoir (Nash, 1959; Shaw, 1994). When a number N of these linear reservoirs are combined in series, the unit hydrograph ($h(t)$) produced due to a unit input into the first reservoir is of the form:

$$h(t) = \left(\frac{t}{K}\right)^{N-1} \frac{e^{(-t/K)}}{K(N-1)!} \qquad \textit{Equation 10.13}$$

Mathematically the value of N does not have to be an integer but can be fractional, and so (N-1)! is replaced by $\Gamma(N)$, the tabulated gamma function, to give:

$$h(t) = \left(\frac{t}{K}\right)^{N-1} \frac{e^{(-t/K)}}{K\Gamma(N)} \qquad \textit{Equation 10.14}$$

The advantage of this model is its flexibility, with different values of the parameters N and K combining to give a wide range of unit hydrograph shapes (Figure 10.15). In the context of this study, the Nash reservoirs are used to transform effective rainfall into recharge, with the conceptual reservoirs representing storage present within the epikarst and underlying karst flow system. The flexibility of the Nash model allows the inflowing water entering the turlough derived from a combination of sources (storages) to be combined into a single inflow hydrograph. The hydrograph parameters are N and K together with the number of intervals or length (duration) of the hydrograph. Varying lengths of hydrograph were trialled during the modelling process. As no significant improvement was seen in model performance for lengths greater than 14 days, this figure was used for all modelled turloughs. This does not impact on those sites with a shorter response time as all coefficients after the response time would be set to zero in the parameter fitting process. The coefficients N and K were optimised using the Least Squares method under the restriction that the sum of all coefficients was unity.

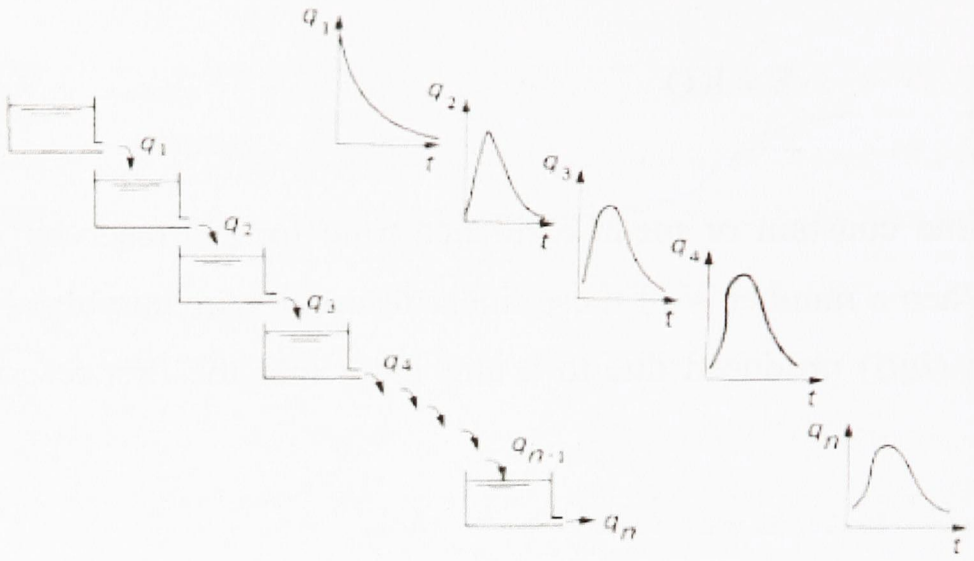


Figure 10.15: Unit hydrographs associated with routing of instantaneous flow through series of linear reservoirs (Shaw, 1994)

There are a number of assumptions associated with unit hydrograph theory: linearity, superposition and invariance (Shaw, 1994). Linearity supposes that there is a direct proportional relationship between input and output, in this case infiltration and inflow, so that a unit input produces a unit output. The second assumption, namely superposition, states that the combined output from a series of inputs is the sum of the component hydrographs. The third assumption is that the relationship between input and output does not alter with time. The apparently linear response of turlough water level to cumulative rainfall provided strong support for the application of the linear reservoir modelling approach. Given the complexities and inherent non-linearity of karst flow systems it is unlikely that all of these assumptions hold true. However, the unit hydrograph does provide a relatively simple tool for simulating the complex natural processes involved in catchment hydrology and, given the data limitations involved in model was selected as the appropriate method.

10.5.4. Volume-Stage Relationship

The purpose of the reservoir modelling process is to accurately predict the volume, rather than stage, response in the reservoir to a given precipitation input. The reservoir water level can then be ascertained using the depth volume characteristics of the turlough basin in question. However, as outflow is a function of stage (i.e. hydraulic head), there was a requirement to transform the predicted volume into stage continuously at each time step. This can be achieved using the stage – volume data derived from the digital terrain modelling in chapter 6.

In the initial data processing phase, stage was transformed into volume using linear interpolation of data points at 0.02 m intervals. While interpolation could be used to represent this transformation, the method is cumbersome and difficult to code. Instead, polynomials were used as a tool to perform this transformation. Polynomials were generated and fitted covering the range of flooding experienced by the turlough, thus facilitating easy conversion. Due to discontinuities in the relationship, curves were broken up into intervals and polynomials of 2nd and 5th order were generated for each interval (Figure 10.16). The polynomials were fitted using the Least Squares method in MATLAB (R2008a). The maximum error in the conversion process was set at 2 cm, in line with instrumentation accuracy, and the order of the polynomial adjusted on a trial and error basis until an acceptable fit was achieved. For each site, between two and four volume – stage polynomials were required to give an accurate conversion across the full range of flooding.

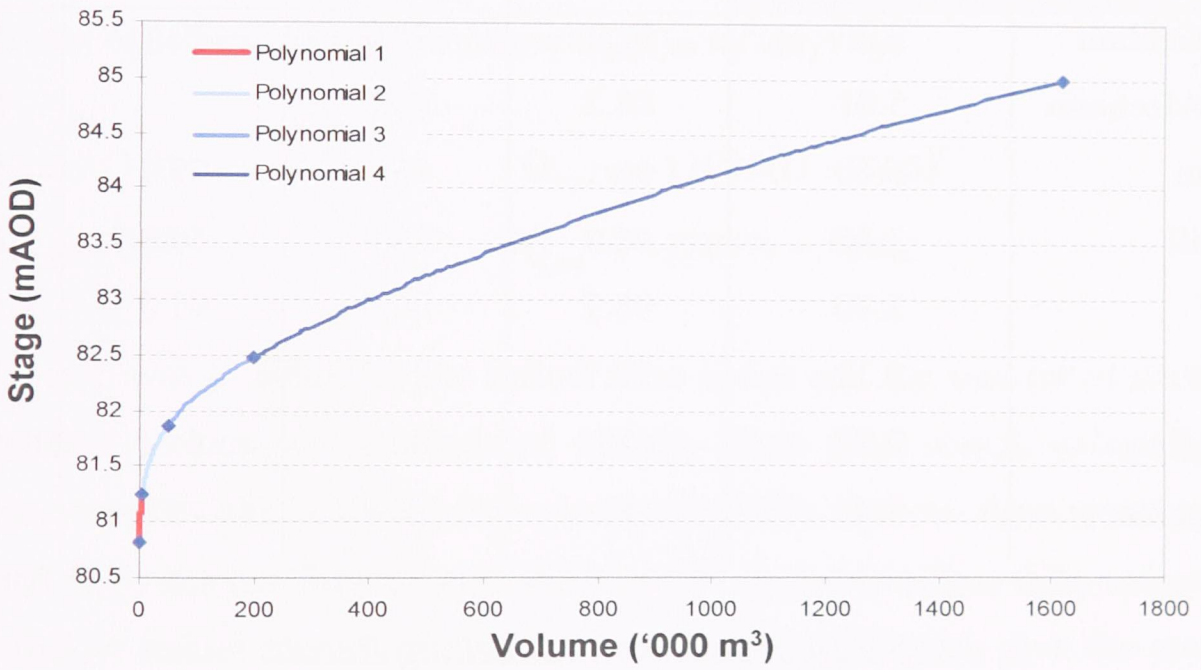


Figure 10.16: Volume – stage curve for Coolcam turlough, Co. Galway

Care had to be taken when defining the relationship for the upper extremes of flooding. In some cases the oscillatory nature of the polynomials resulted in unrealistic predicted behaviour, such as a decrease in stage with increasing volume. To prevent this, each volume – stage curve was generated using data above the highest recorded water level. This additional data came directly from the DTM, as the level to which the turloughs was surveyed was substantially above the highest recorded water level. However, if the models were to be used for the prediction of

extreme flood levels, details of the basin topography would have to be extended upwards. This could be achieved with additional GPS surveying or, on a larger scale, by utilising contours from GIS/DTM datasets such as those maintained by the Ordnance Survey.

10.5.5. Modelling Results

Reservoir modelling was carried out on eight turloughs with reasonably well defined stage – discharge curves and representing the spectrum of turlough hydrological behaviours. The subset consisted of Lough Gealain, Lough Aleenaun, Turloughmore, Lisduff, Ardkill, Coolcam, Croaghill, and Skealoghan, with Table 10.2 summarising the results for each site. The specific performance of this technique and notable aspects of the modelling procedure are detailed for each site in the following sections.

Site Name	Contributing Area (km^2)	Model Efficiency (%)			
		2006/2007	2007/2008	2008/2009	Overall
Lough Gealain	3.25	97.6	98.6	89.7	96.7
Lough Aleenaun	5.01	88.2	92.8	-	90.5
Coolcam	6.40	96.1	95.1	69.6	92.7
Croaghill	3.40	93.9	93.9	56.9	86.9
Lisduff	5.70	98.7	96.3	91.5	96.7
Ardkill	2.12	97.7	97.2	-	96.6
Skealoghan	2.78	96	80.6	91.4	90.7
Turloughmore	5.41	86.7	85.6	75.8	83.9

Table 10.2: Reservoir Modelling Results

10.5.5.1. Lough Gealain

Lough Gealain was selected as the first suitable candidate for this modelling approach for a variety of reasons. Firstly, it is located at the upper end of its catchment in the Burren, an area of thin or absent subsoils. As such there are no substantial water bodies, extensive flow systems, or significant depths of overburden adding complexity to the system and affecting the rainfall response. Another decisive factor was the presence of a major spring in the northern end of the turlough, which was identified during field investigations. Based on observations of the spring flows it was

deemed possible that the majority of the recharge entering the turlough was from this source. This would match well with the simplest interpretation of the reservoir, with unconnected inflow and outflow points. This is supported by diving carried out by Byrne and Reynolds (1982), where no evidence of conduits or water movement apart a small, shallow, debris filled trench were identified within the basin. The stage – discharge curve of the turlough was also well defined across the flood range and so the outflow calculations could be carried out with some degree of certainty. The final reason for this site selection was the good performance of the turlough's aggregated rainfall model. As the aggregated rainfall technique is a more simplistic version of the reservoir modelling attempted here, the high efficiency shown indicates good promise for more detailed modelling.

As described in the modelling methodology, the first step involved the derivation of the stage – discharge curve. Two different relations were defined within the Lough Gealain curve, one for those stages above 29.2 mAOD and second for those below. The relevant equations gave the outflow Q_{out} (in m^3/day) by:

$H < 29.2$ mAOD: $\quad Q_{out} = -13000(H - 27.5)^{0.5}$

$H \geq 29.2$ mAOD: $\quad Q_{out} = -2289H + 50482$

The next step was to calculate the inflow time series and the associated contributing area. Outflow values were calculated for the stage time series, using the above equations, for the 2007/2008 hydrological year. This outflow time series was then subtracted from the net flow to give the required notional inflow time series (Figure 10.17). Inflow values were added over the calibration period to give the cumulative inflow time series. Linear regression of the inflow and cumulative infiltration time series gave an initial contributing area of 3.7km^2. It is interesting that this area is far smaller than the preliminary estimated catchment area of over 13km^2.

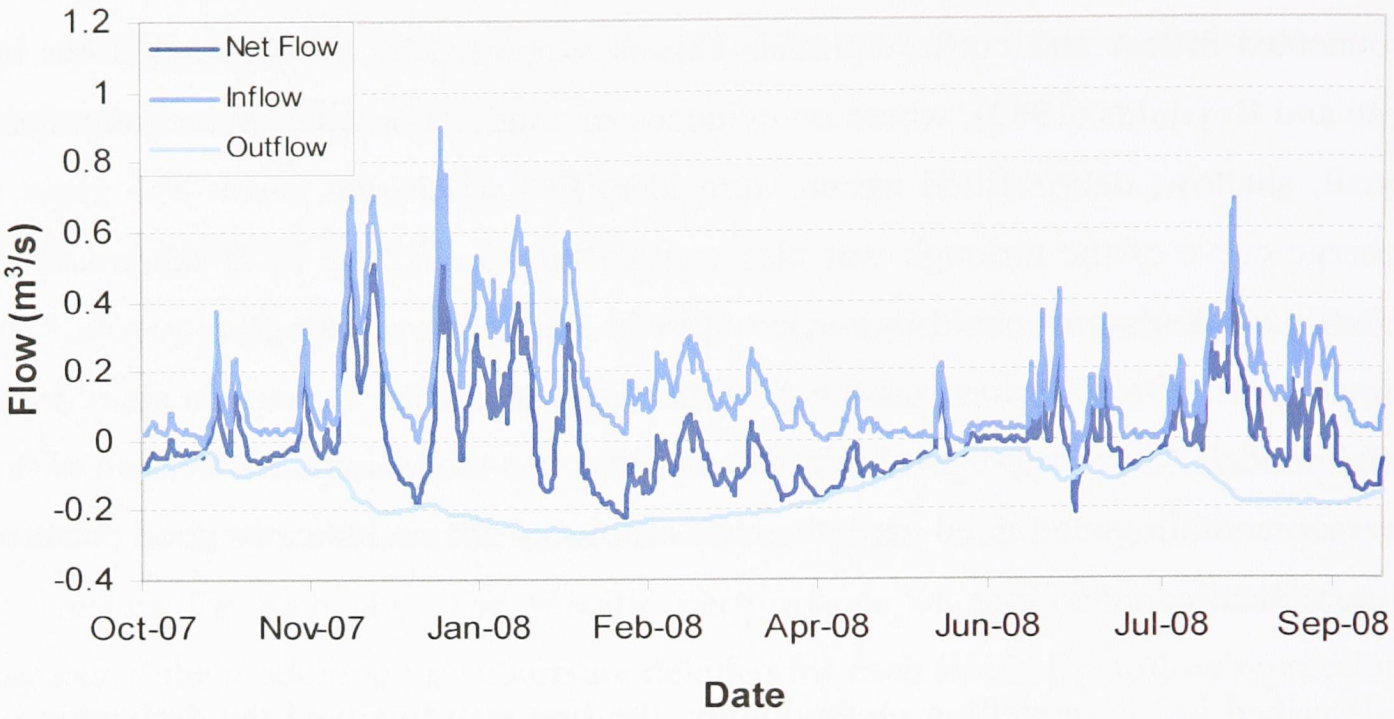


Figure 10.17: Inflow, outflow and net flow time series during the main 2007/2008 flooding period for Lough Gealain, Co. Clare

Next, the volume–stage relationship was derived from the turlough's DTM data. Two 2nd order polynomials were required to accurately transform volumes across the full flooding range, one for volumes below 75000 m^3 and a second for those above. All the relevant parameters were then entered into the modelling spreadsheet.

Rainfall and evapotranspiration records beginning in January 2006 were input into the SMD model to produce the infiltration time series for the model input. During the calibration process it was found that a contributing area of 3.7 km^2 produced excessive inflow into the turlough, and so this was reduced down to 3.2 km^2 to produce a better fit. The model showed an excellent performance during both filling and recession phases, with predicted peak magnitudes and times corresponding very closely with recorded values (Figure 10.18). This is reflected in the model performance statistics, with the overall efficiency coming in at 96.7%.

The greatest deviations between model and recorded time series were found in the 2008/2009 year, which showed an efficiency of 89.7%, compared to almost 98% for the 2006/2007 and 2007/2008 hydrological years. One reason for this is the nature of the flooding pattern during this period. The flooding season was far longer in the

2008/2009 year than in previous years, with a greater number of filling and recession events. Small errors over this phase had a cumulative effect. The higher recession rate of the model during February 2009 leading to a downward offset of the model volume for the remaining monitoring period, with a greater degree of storage occurring within the turlough basin than was predicted.

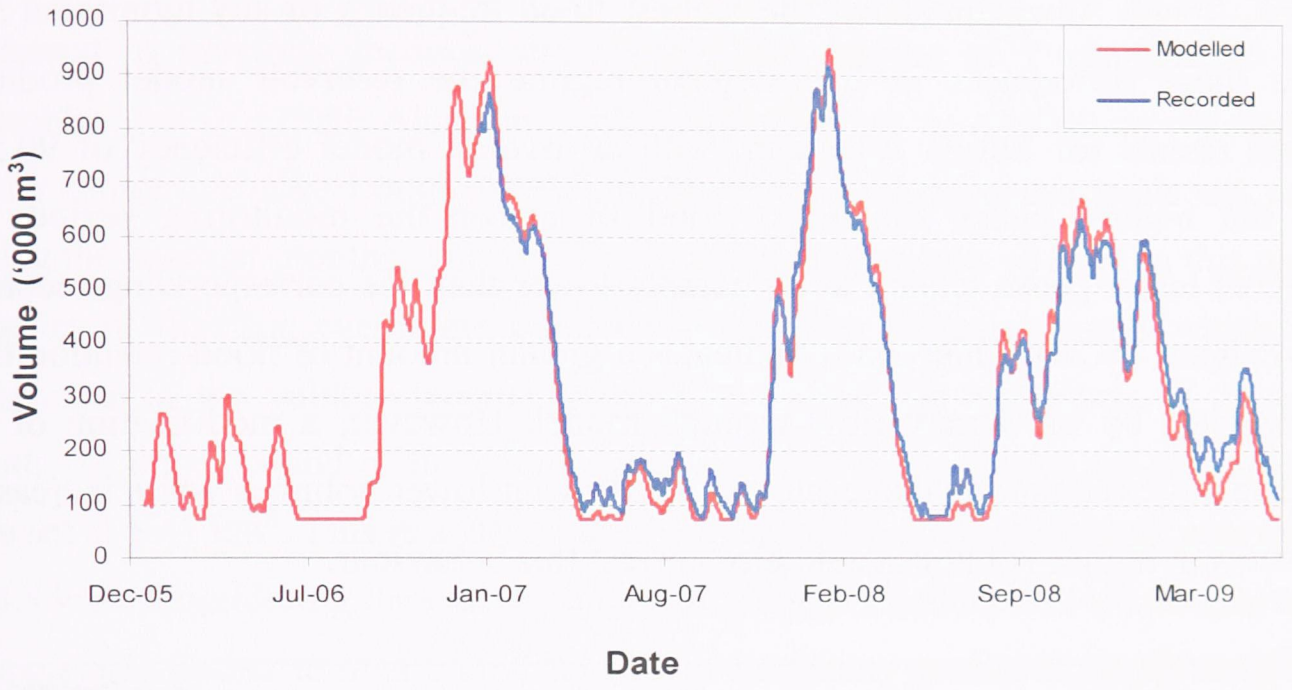


Figure 10.18: Plot of recorded and modelled volume for Lough Gealain, Co. Clare

A comparison of recorded versus modelled stage also yields a good fit for all years (Figure 10.19). As it is stage, rather than volume, which is used in the derivation of hydroecological variables such as duration and frequency of inundation this shows the applicability of this modelling technique for the long term characterisation of Lough Gealain's hydrological regime.

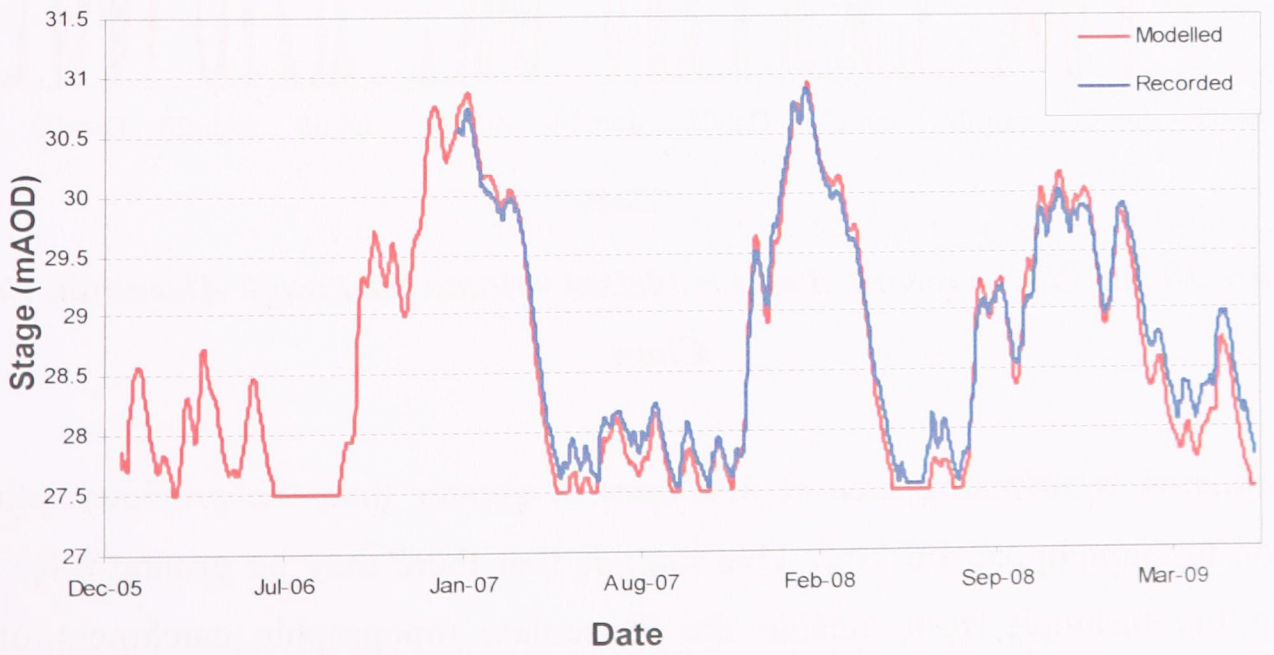


Figure 10.19: Plot of recorded and modelled stage for Lough Gealain, Co. Clare

10.5.5.2. Lough Aleenaun

Like Lough Gealain, Lough Aleenaun is a promising turlough for reservoir modelling due to its location in the Burren plateau, its potential flow through operation and also the good performance of the aggregated rainfall method *(Section 10.4.2)*. However unlike Lough Gealain, which would be in the mid-range in terms of flooding response, Lough Aleenaun shows the highest flood frequency of any monitored site. Despite these differences in hydrological regime the reservoir model produced excellent results for Lough Aleenaun, with an overall model efficiency of 90.5%. While the highest peaks showed a good fit across the monitoring period, the subsequent lesser peaks tended to be notably lower than the corresponding recorded values (Figure 10.20). This, again, indicates a greater amount of flood retention than was predicted by the purely flow through model. However, a modification of the stage-discharge relation by decreasing the outflow at lower volumes while increasing the outflow at higher volumes could also correct this behaviour.

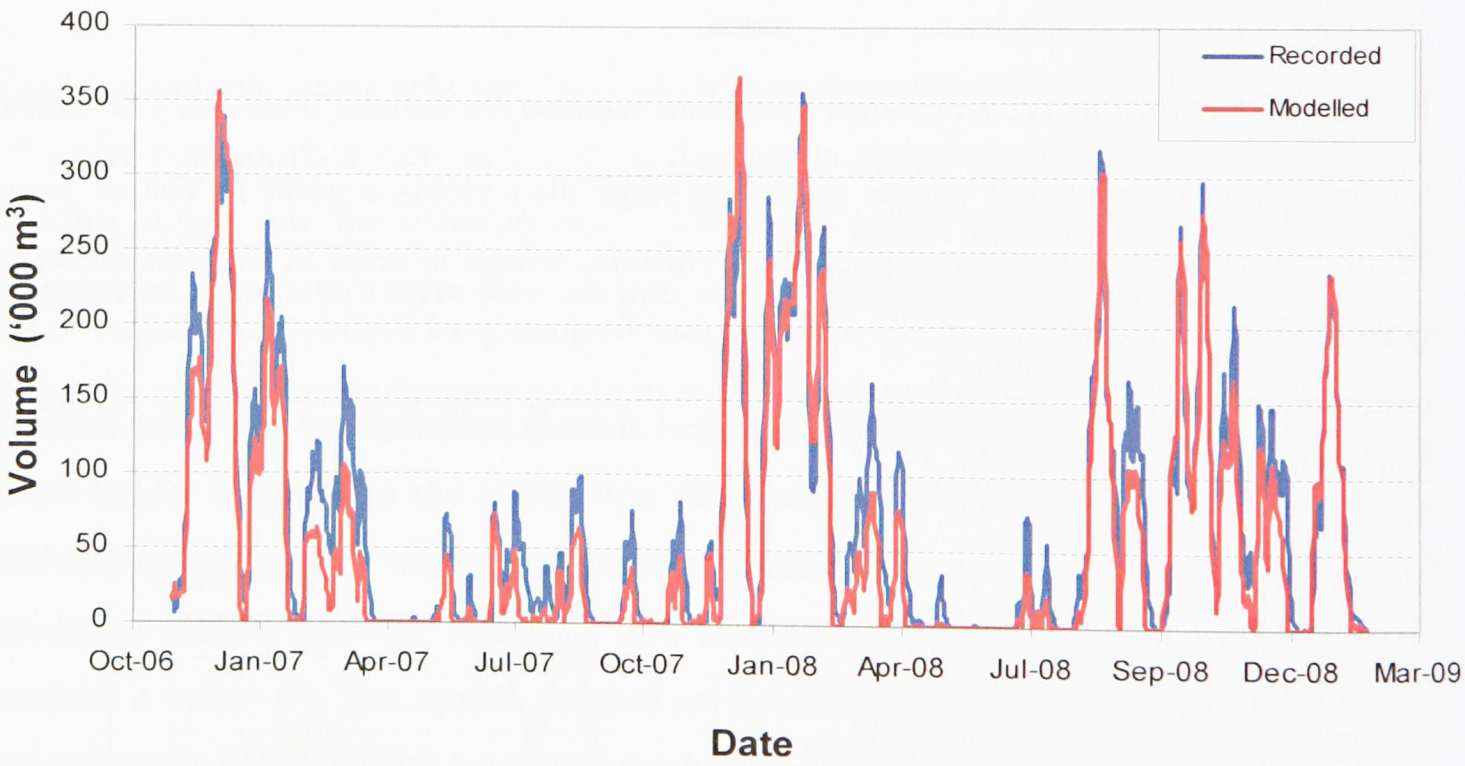


Figure 10.20: Plot of recorded and modelled volume for Lough Aleenaun, Co. Clare

The estimated contributing area at 5.01 km^2 is greater than the previous estimate based on topography of 4.6 km^2. This implies that there may be groundwater flow entering the turlough from outside the immediate topographic catchment of the turlough. This supports a hypothesis suggested by Drew (*Pers. Comm.*), which stated

that when groundwater conditions are high, Lough Aleenaun may receive groundwater recharge from an adjacent catchment to the north.

10.5.5.3. Turloughmore

The reservoir model predicted with reasonable accuracy the volume response of Turloughmore, giving an overall efficiency of 83.9% (Figure 10.21). As has been discussed in previous sections, the hydrological regime of Turloughmore closely resembles that of Lough Aleenaun with a fast response to rainfall events during the winter months. Unlike Lough Aleenaun, however, Turloughmore tends not to flood during the summer months. This difference is the main source of error in this instance. A series of flooding events are predicted during the summer months which do not materialise in the volume record. In order to control the magnitude of these flood events the upper bound of the contributing area was limited, with the area parameter here set at 5.41 km^2. This is a 20% increase over the previous catchment area estimate of 4.5 km^2. Considering the current stage – discharge relation, this would also have to be increased further to over 6 km^2 in order to accurately predict the peak water levels. Given that this model assumes that 100% of effective recharge enters the turlough, the actual catchment area would then have to be factored up further still. This highlights one of the shortcomings of this reservoir model configuration; it does not facilitate the bypass of flow beneath the turlough. This mode of groundwater flow is highly probable in Turloughmore, given the behaviour of the adjoining, lower depression described in *Section 10.4.2*.

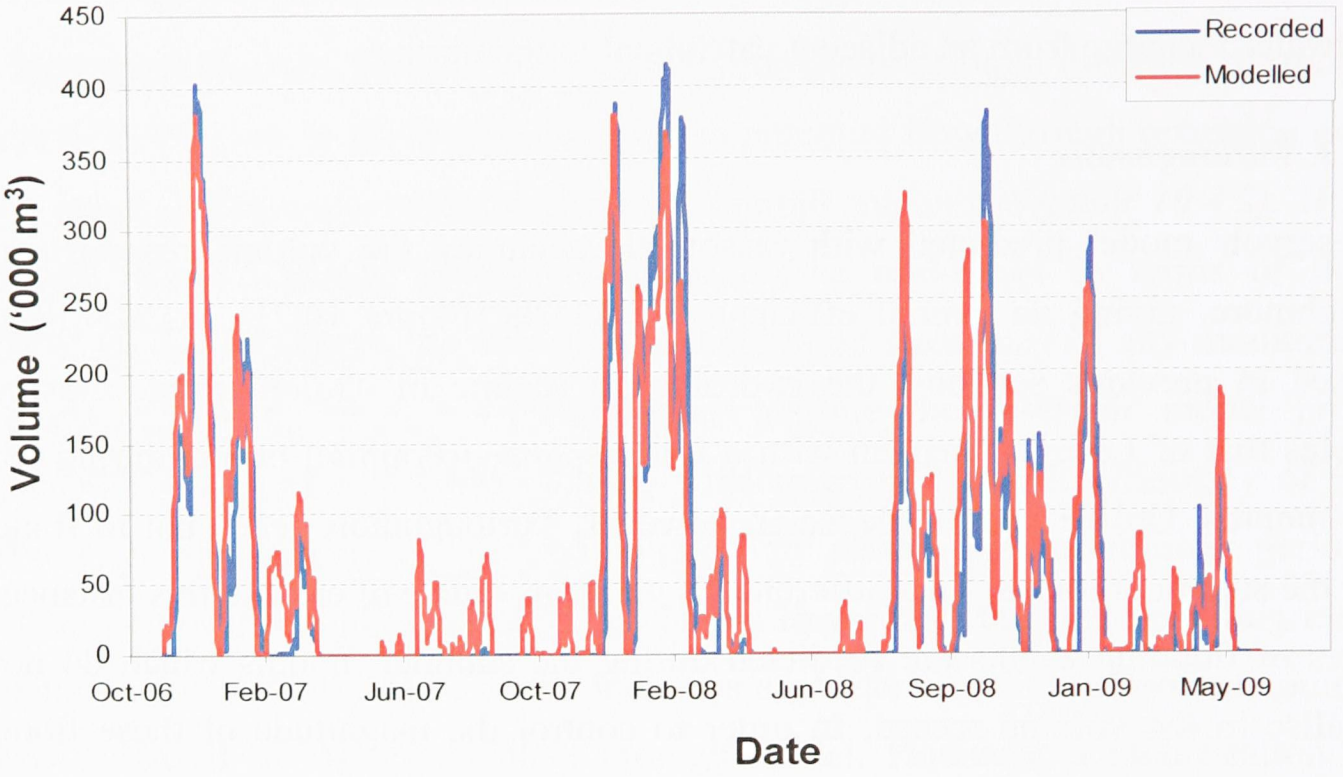


Figure 10.21: Plot of recorded and modelled volume for Turloughmore turlough, Co. Clare

10.5.5.4. Lisduff

During the initial model trial for Lisduff, it was found that while the time to peak was fairly well matched across the monitoring period the volume was substantially over predicted in 2006/2007 and 2007/2008, while at the same time substantially under predicting 2008/2009 volumes (Figure 10.22 (a)). The annual stability of Lisduff's maximum water level had previously been identified in chapter 6 where, despite the variability in annual rainfall patterns, Lisduff turlough showed little variation in terms of maximum stage levels reached. One suggested explanation for this was the presence of an unidentified overflow at the upper reaches of the turlough basin. A high level overflow such as this would change the hydrological behaviour by artificially lowering the flow response at the upper end of flooding. In order to test if such an outlet would produce a better modelling result, an outflow with a capacity of 0.5 m^3/s was added at 49.9 mAOD. This allowed the volume in 2008/2009 to be significantly raised relative to the previous two years (Figure 10.22 (b)).

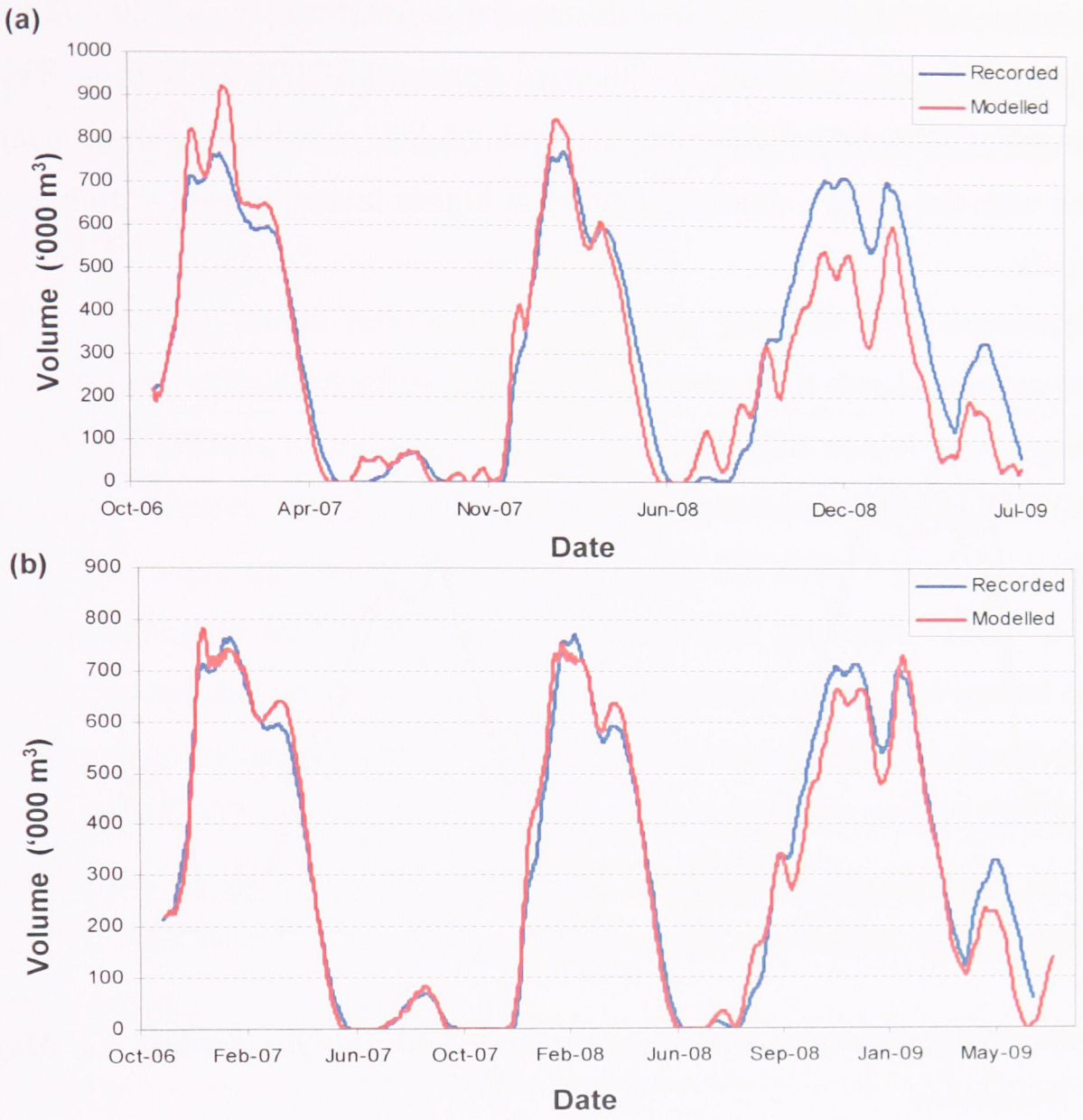


Figure 10.22: Plot of recorded and modelled volume (a) without overflow and (b) with overflow for Lisduff turlough, Co. Roscommon

As can be seen from a comparison of Figure 10.22 (a) and (b) the high level overflow resulted in a significant improvement by considerably decreasing the magnitude of inflow at higher flood levels. As with Lough Gealain, the main inaccuracies in the Lisduff model were shown during the 2008/2009 hydrological year. The predicted volume falls short of the first major peak of the flooding season, and also under predicts the final peak following the main recession in May 2009.

10.5.5.5. Ardkill

The model follows the turlough behaviour extremely well during both recorded recession periods (Figure 10.23), indicating that the mode of drainage is similar to that of a tank draining through an orifice. The required contributing area, at 2.12 km^2, also tallies well with catchment area of Ardkill, previously estimated at only 3.1 km^2.

The maximum level is well matched during the calibration year of 2007/2008 but is underestimated by approximately 60,000 m^3 during the 2006/2007 year. This under prediction translates into difference in level of 0.3 m which, given uncertainties associated with the stage – discharge curve at higher levels, is well within acceptable error bounds.

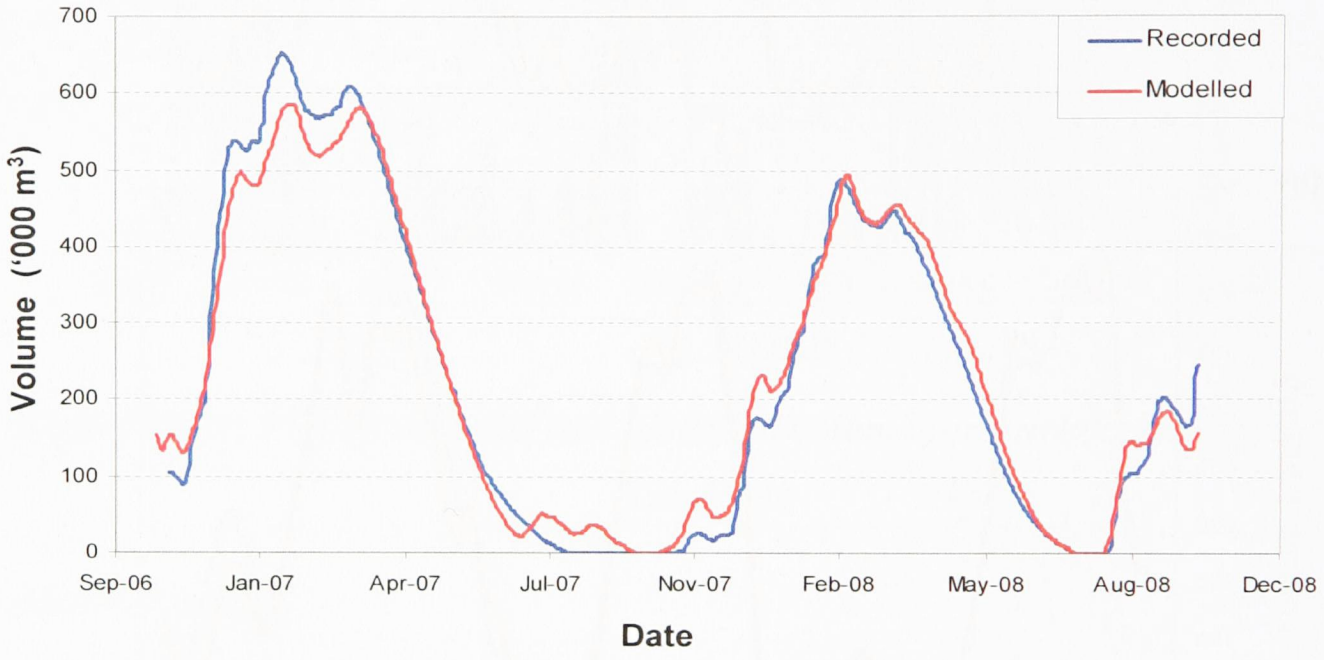


Figure 10.23: Plot of recorded and modelled volume for Ardkill, Co. Mayo

The apparent overfilling which occurs during July at the end of the first main recession event may not be an error associated with the model, but rather due to deficient monitoring data over this period. In the first monitoring year, the Diver was located a little above the base of the turlough and so did not record water level fluctuations at low water levels. Based on records from nearby turloughs, it is likely that Ardkill experienced some renewed flooding in July 2007, and so the renewed flooding predicted during July 2007 may in fact have occurred.

Some over filling was predicted during the initial flooding phase of the 2007/2008 hydrological year. This was shown by some of the other turloughs modelled using this technique (see Coolcam and Croaghill). The presence of additional storage within the karst system could account for this deviation. While the SMD model accounts for some storage which may build up due to evapotranspiration effects, it is very likely that the karst system itself possesses additional storage in the form of matrix and fracture porosity. During periods of heavy rainfall following relatively dry conditions,

some of the recharge may be taken into storage. This would have the effect of reducing the recharge entering the turlough. Once this storage reached capacity, it would have little impact upon the mechanisms controlling turlough flooding.

10.5.5.6. Coolcam

Overall the reservoir model produced a reasonably good fit for Coolcam turlough, showing an overall efficiency of 92.7%, although visually it doesn't appear to give as good a fit as this statistic would suggest (Figure 10.24). The model gave a good fit for both the peak volumes and the general recession behaviour during 2006/2007 and 2007/2008. However, significant errors arose in the 2008/2009 year, with efficiency falling substantially to 69.6%. As was seen in Ardkill turlough, reservoir volumes were overestimated during the initial phases of flooding. Also, the model showed a greater response to recharge events during recession periods. This is particularly clear in the main 2006/2007 recession, where the calculated inflow caused filling to occur in the model during August 2007. The actual response of the turlough to the same event was far less where a decrease in outflow was shown but the overall volume continued to recede.

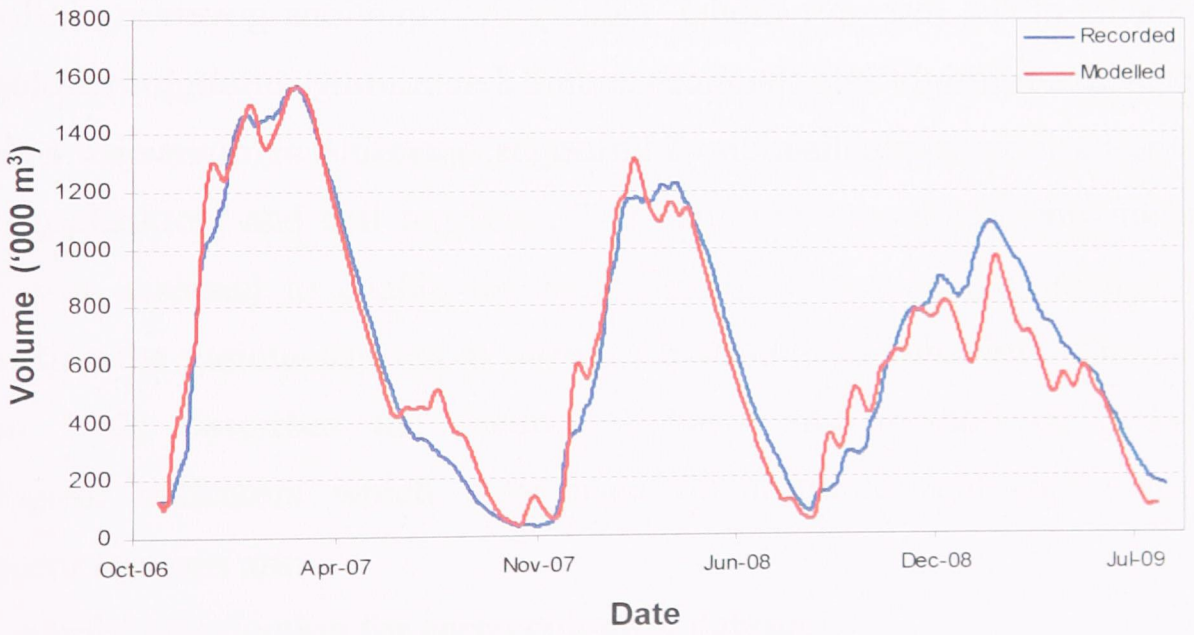


Figure 10.24: Plot of recorded and modelled volume for Coolcam turlough, Co. Galway

Given these discrepancies, it is possible that additional storage plays an important role in the Coolcam flow system. If this storage drained concurrently with the turlough, it could provide the dampening that would be required to remove the tendency towards

overfilling in the initial filling and recession phases. It could also go some way to correct the relative magnitude of the annual maxima. The flooding in 2008/2009 occurred over a longer period than either of the previous two years. It also contained more recession events. If turlough recession is taken as an indicator of a more general drainage of storage within the system, then the higher recession frequency in 2008/2009 would represent a greater degree of activity of catchment storage. This activity would serve to decrease the inflow reaching the turlough during such periods. Such a modus operandi would also reduce the impact of rainfall during recession events, as a portion of the generated recharge would be taken up by the catchment storage.

10.5.6. Conclusions

The quantitative numerical modelling methodology developed here was found to accurately predict the water levels of a subset of turloughs spread across the continuum of turlough hydrological regimes. The model outputs well represented the recorded water levels and showed an average efficiency of 91%, an improvement of 4% over the same sites modelled using the aggregated rainfall method. The nature of the components of the reservoir model, namely the equations governing inflow and outflow, provide an insight into the mechanisms determining turlough hydrology and validated the basic conceptualisation of turloughs operating as reservoirs within the karst flow network.

CHAPTER 11. TURLOUGH HYDROECOLOGY

11.1. Introduction

The research described in this thesis forms part of the broader study "Assessing the Conservation Status of Turloughs" carried out on behalf of the National Parks and Wildlife Service of the Department of the Environment. The aim of this broader study is to assess and establish the conservation status of turloughs as wetland habitats protected under the Habitats Directive through the integration of data representing different characteristics of turlough hydrology and ecology with a view to identifying the critical factors which influence biological diversity within and among turloughs. The research described in this thesis has been focused solely on developing an understanding of the hydrodynamics of turloughs, through the use of appropriate hydraulic and time series analysis techniques and the development of hydrological modelling methodologies. In this latter chapter, the emphasis is shifted from interpreting the hydrodynamics of turloughs in a hydrological context to an ecological one, with the objective of deriving the critical hydrological indicators influencing biological diversity within and among turloughs.

The "Assessing the Conservation Status of Turloughs" multidisciplinary project generated four ecological datasets: vegetation, aquatic invertebrates, hydrochemistry and phytoplankton, and soil nutrients. The nature and resolution of each ecological dataset was assessed to enable the identification of novel hydrological indicators representing the various aspects of turlough hydrological behaviour. The first section (section 11.2) describes the theoretical basis and method of derivation for hydrological indicators which were used for multiple ecological datasets. The subsequent sections are:

i) a brief introduction for each ecological dataset;

ii) the relevant hydrological indicators identified and derived as part of this research thesis;

iii) A short summary to put into context the effects of hydrology on each ecological parameter.

11.2. Hydrological Indicators

From water level, volume and area time series a number of potential indicators were derived, each tailored to fit with the nature and resolution of the ecological dataset with which it was to be integrated. The hypothesis behind the hydrological indicators used in the interpretation of multiple ecological datasets (namely flood duration, frequency and hydroperiod) will be described here. Further indicators used in the interpretation of a particular ecological dataset are detailed in the relevant section.

11.2.1. Elevation

For the majority of hydrological indicators derived in this research, the critical parameter is the elevation of the sampling site. Once the elevation is known, the pattern of inundation for an exact location can be characterised and so relevant hydrological indicators for that point derived. During ecological fieldwork, carried out as separate tasks within the turlough conservation project, the position of sample points were recorded using a handheld GPS. This logged the (X, Y) coordinates of each point, but not the elevation. Thus the elevation of sample points, such as vegetation relevés and soil samples, had to be derived indirectly using the digital terrain models (DTM) created as part of the hydrological research. The elevation of each sample point was determined by identifying the elevation of the corresponding coordinate on the surface of the DTM. A visual representation of this process is shown for Ardkill turlough in Figure 11.1. In practice, this was evaluated by calculating the difference or residual between a plane at zero elevation and the turlough ground surface at each (X, Y) point using Surfer version 8.6 (Golden Software Inc.).

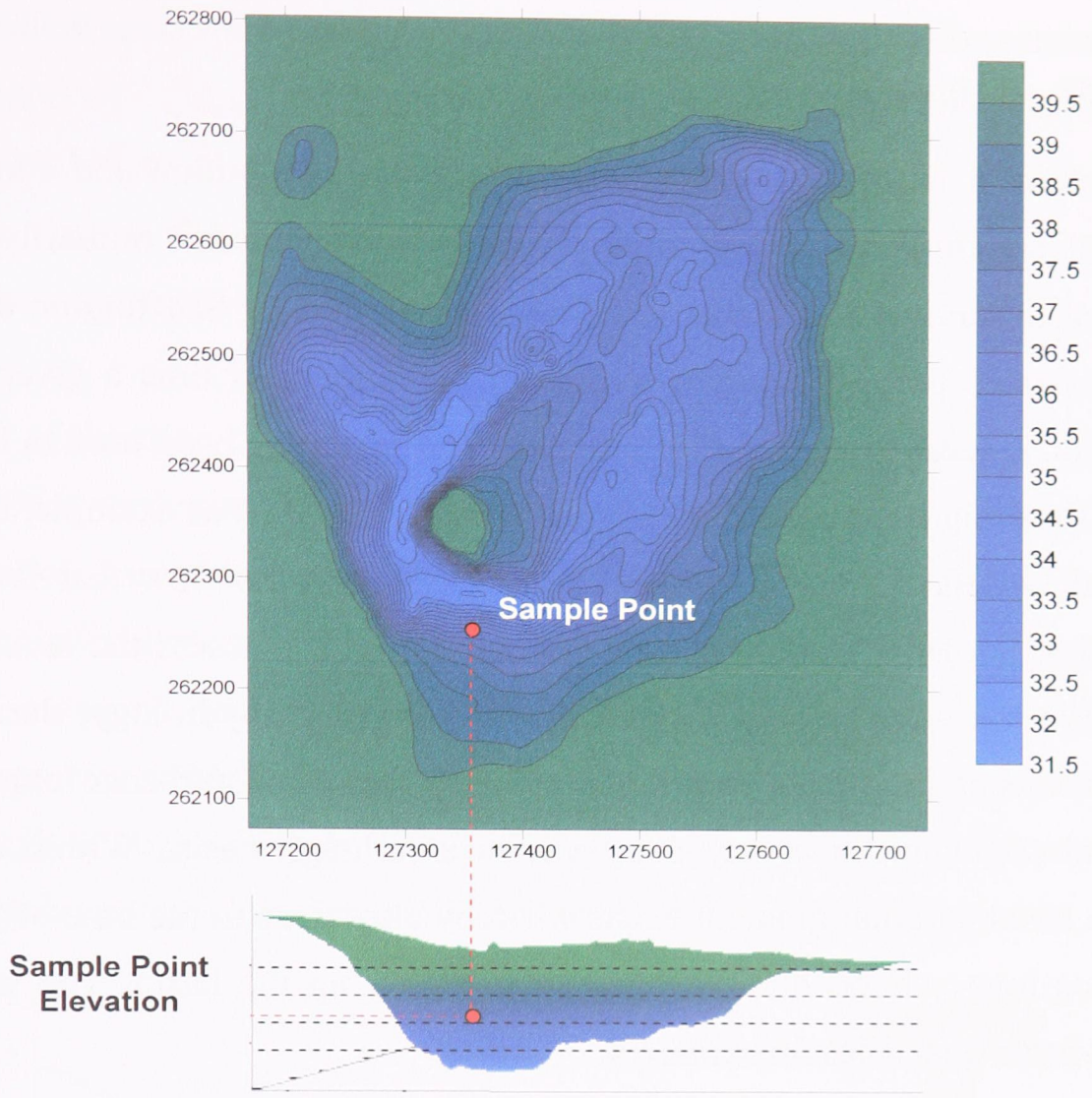


Figure 11.1: Contour map and elevation profile used in the derivation of sample point elevation in Ardkill turlough, Co. Mayo

11.2.2. Flood Duration

The duration of inundation strongly influences the distribution and composition of ecological communities within turloughs with flood duration primarily controlling plant species survival (Casanova and Brock, 2000; Sheehy Skeffington et al., 2006). Duration curves provide a way to represent the amount of time a given quantity is equalled or exceeded over a defined interval and have long been used in hydrological analysis for design and regulatory purposes (Fetter, 2001). For example, in river flow it is used to define the 95th percentile flow, which is the flow that is equalled or exceeded 95% of the time, a statistic commonly used to assess the level of dilution available in the water course. In the context of turlough hydrology, duration curves present a means of quantifying the flooding effect or disturbance experienced by ecological communities at any point within a turlough basin. Within any defined period, a flood duration gradient exists whereby elevations at the base of the turlough experience longer flood duration that those higher up the basin. The water level - duration curve quantifies this gradient.

The procedure for generating a duration curve, as outlined in Fetter (2001), is as follows:

- The level data is first sorted in descending order, from highest to lowest
- A rank m is assigned to each value from 1 to n, n being the length of the data set
- The probability P of a given level being equalled or exceeded within the period n is given by:

$$P = 100\frac{m}{n+1} \qquad \textit{Equation 11.1}$$

- A plot of probability P against stage (the so-called duration curve) shows the percentage of time each level is equalled or exceeded

Duration curves can be generated over any defined period such as calendar year, hydrological year, inundation period or entire monitoring record, depending upon the application. Invertebrate communities (e.g. population densities) in a given year are

highly dependent upon the hydrological regime of that year and so short term duration curves are applicable. In contrast, many vegetation communities respond to long term changes in hydrological regime, and so a particularly wet or dry year may not significantly change the communities present within a turlough. Therefore, longer term duration curves would be more relevant.

An example of duration curves for Rathnalulleagh, Lough Aleenaun and Lisduff for the 2007/2008 hydrological year is shown in Figure 11.2. The primary use of flooding depth - duration curves in the context of this research is to quantify the duration of inundation at individual sampling points based upon their respective elevation. So, for example, if a sample point was located at a height of 4 m above the base of the turlough, from Figure 11.2 it can be seen that the duration of flooding at that point in Rathnalulleagh is approximately 40% and around 10% in Lough Aleenaun, while in Lisduff the point at this elevation would not have flooded during this period.

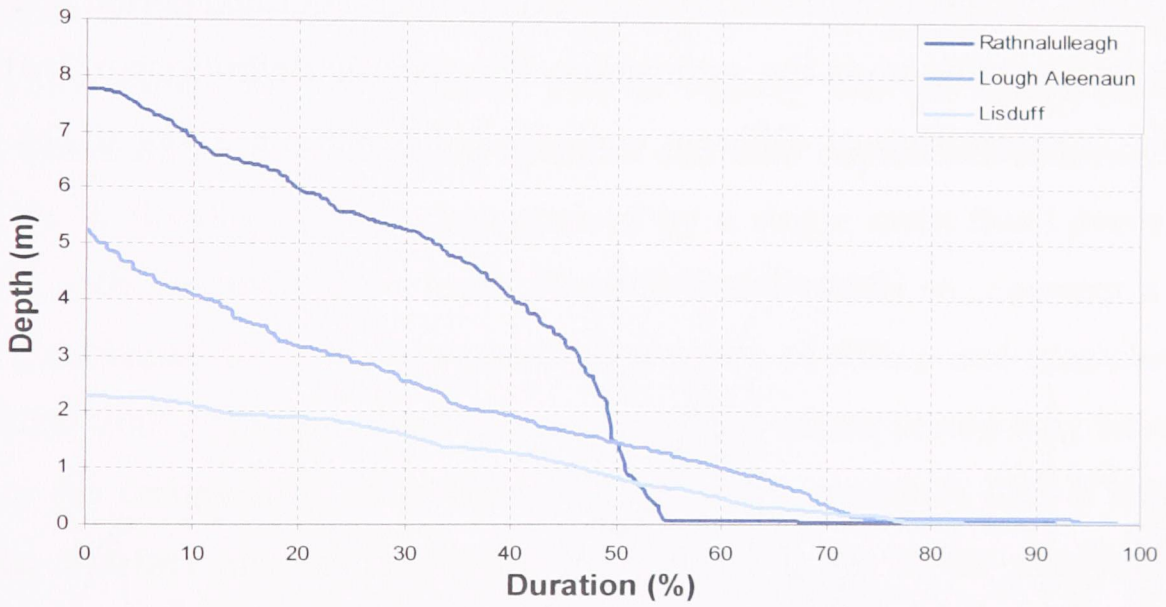


Figure 11.2: Duration curve for Rathnalulleagh, Lough Aleenaun and Lisduff turloughs for the 2007/2008 hydrological year

Flooding depth - duration gives the cumulative time a given elevation is inundated during a defined period. It may not, however, fully quantify the level of disturbance experienced within the turlough basin. This is clearly demonstrated through the comparison of duration curves for Lough Aleenaun and Lisduff in Figure 11.2. Lough Aleenaun is the most highly responsive of the study sites, with multiple short-duration flooding events occurring throughout the year. In contrast, the hydrological behaviour of Lisduff is characterised by a single main flood event during the year. Therefore in

Lough Aleenaun the total duration, as represented by the duration curve, is split into a number of distinct flooding events whereas in Lisduff it predominantly represents a single flood event. This difference in behaviour is not clear from the duration plots alone, hence there is a need for additional hydrological indicators describing the frequency of flooding.

11.2.3. Hydroperiod

A variation on the idea of flood duration is the hydroperiod. This is a widely used variable in ecological studies but can often have vague or very different definitions depending upon the application. The hydroperiod does not differentiate between different elevations within the turlough basin, but instead uses a single variable intended to characterise the flooding duration for each turlough. This variable may take the form of the duration of flooding prior to sampling (Figure 11.3 (1)), the longest continuous inundation period during which sampling took place (Figure 11.3 (2)), or the sum of the durations of all flood events over a defined period (Figure 11.3 (2) and (3)), depending upon the application. The specific definitions of hydroperiod used in the interpretation of different ecological datasets are given in the relevant section.

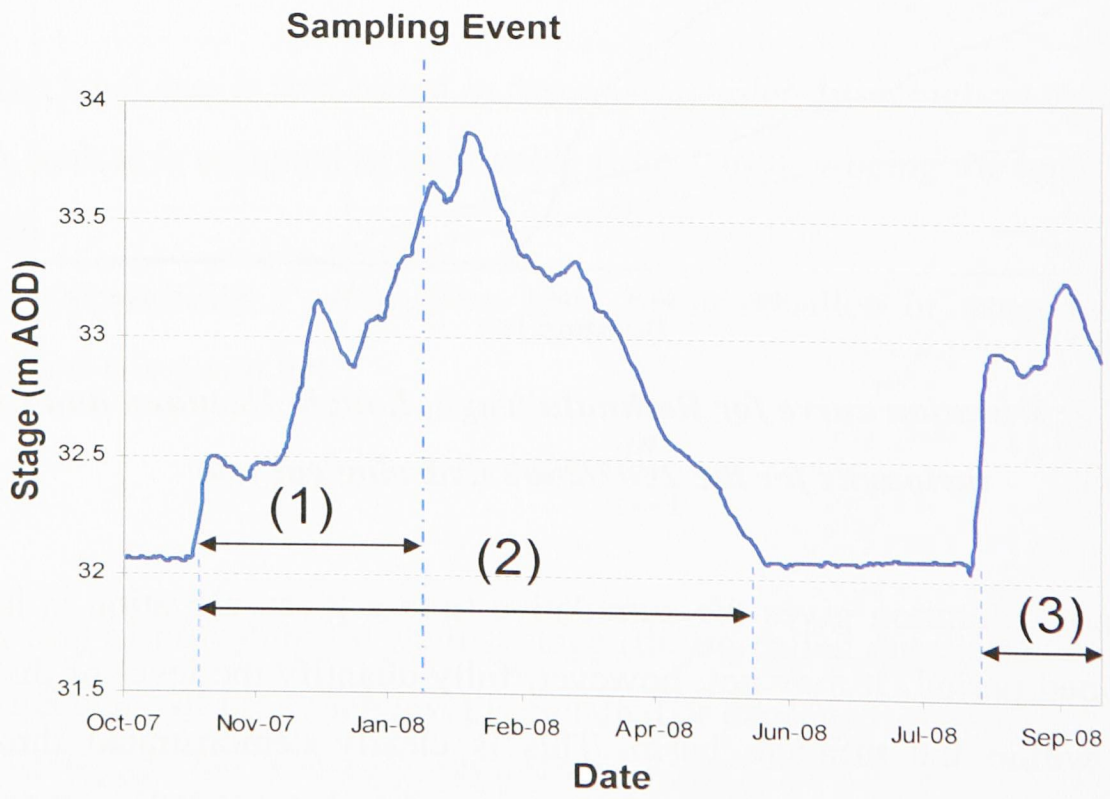


Figure 11.3: Example of different definitions of hydroperiod for Skealoghan turlough, Co. Mayo, during the 2007/2008 hydrological year

11.2.4. Flood Frequency

Flood frequency is defined as the number of times a given water level is equalled or exceeded over a given interval, and is thus dependent upon the specific flood pattern over the analysis period. Like flood duration, frequency can be generated over any defined period depending upon the application. Unlike flood duration, a frequency gradient does not exhibit a simple pattern from the base of the turlough upwards (Figure 11.4). Instead, the lowest flood frequencies tend to be shown by zones at the extremes of the flooding range, i.e. the highest and lowest flood levels, with zones in the intermediate range of flooding experience the highest flood frequency.

A flood event represents a disturbance to terrestrial turlough ecological communities as floodwaters change conditions from dry to wet, or aerobic to anaerobic. This transition, and the frequency at which it occurs, plays a major role in determining species composition within such ephemeral water bodies as turloughs. Ecological communities which experience a high frequency of flooding must be able to quickly adapt to this change in environment. This is equally true for communities within different zones of a turlough basin, as these can also experience different flooding frequencies. A flooding season characterised by a single main flood event, such as 2006/2007, will generally show lower flood frequencies and so represent a different level of disturbance than one composed of a series of filling and recession events, such as 2008/2009. Multiple flood events during the winter period may have a lesser impact on the composition of turlough ecological communities than a single event during the summer and so flooding seasonality also has to be considered in the interpretation of flood frequency data.

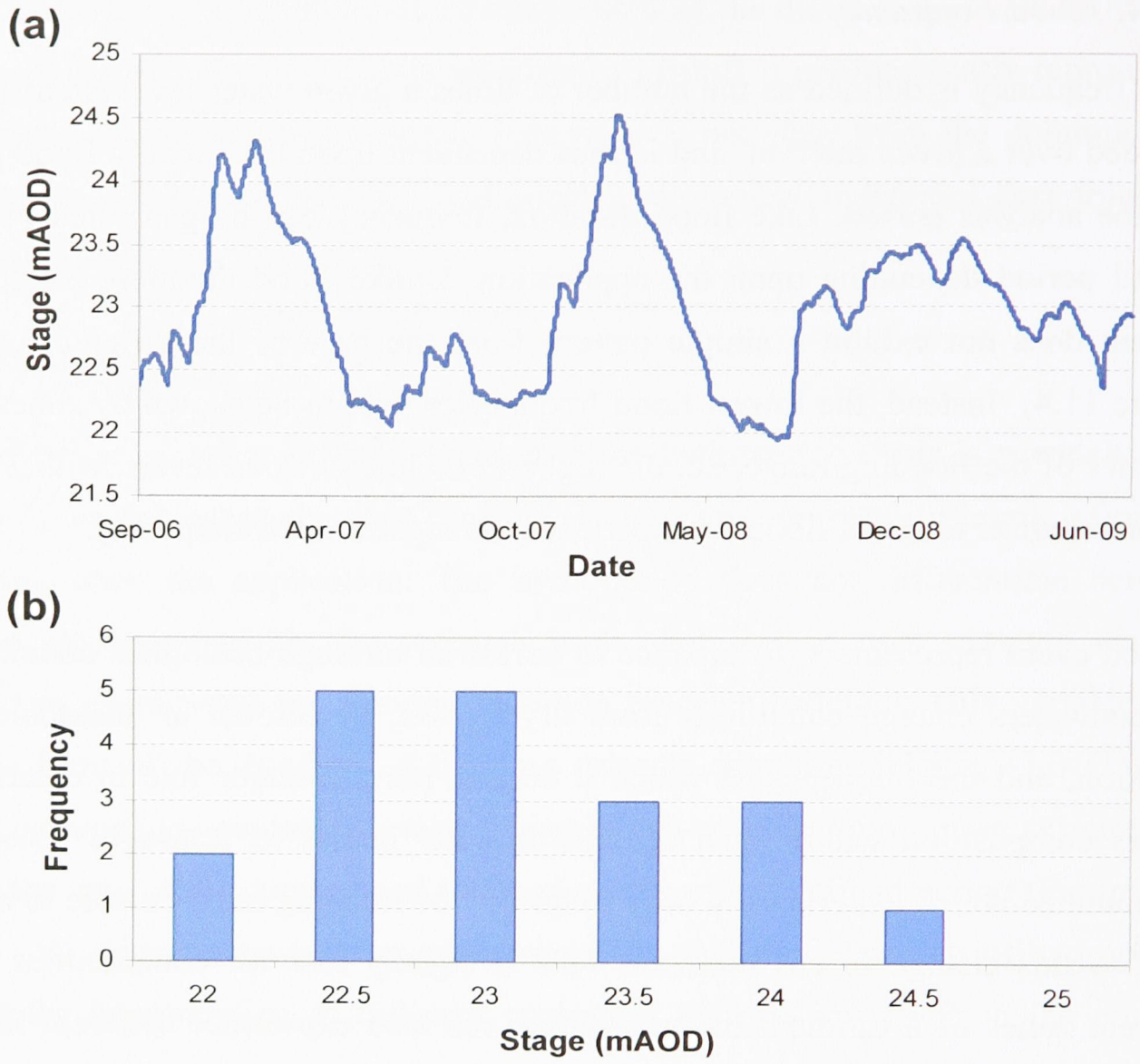


Figure 11.4: (a) Stage hydrograph and (b) associated flood frequencies at 0.5 m intervals for Caranavoodaun turlough, Co. Galway over monitoring period from September 2006 to July 2009

11.3. Vegetation

11.3.1. Introduction

Hydrological data were used in the interpretation of two main vegetation datasets. The primary vegetation study was carried out as part of a separate research study by Nova Sharkey, while a second smaller study was carried out by Aoife O'Rourke as part of a MSc in Biodiversity and Conservation (O'Rourke, 2009). The primary vegetation fieldwork completed by Nova Sharkey was conducted over three field seasons, 2006, 2007 and 2008, with a total of 685 relevés recorded. An additional 25 relevés were recorded in May 2009. The dataset was supplemented by the inclusion of relevés from a previous study on two turloughs within the group (Feeney, 2007); 100 relevés were included from this study. Sample points for two turloughs, Kilglassaun and Tullynafrankagh, were discounted due to a lack of sufficient hydrological data in the case of Kilglassaun, and the lack of a topographic survey in Tullynafrankagh. This brought the total number of relevés included in the hydrological integration to 750. Each turlough was walked over to determine the range of vegetation types present. Within each relevé, the vascular plant species present and their cover-abundance were recorded. The location of each relevé was recorded using a hand held Garmin Etrex GPS receiver.

The secondary vegetation fieldwork, carried out by Aoife O'Rourke, involved the collection of vegetation data from four transects, two in each of Blackrock and Caranavoodaun turloughs, Co. Galway. The aim of this work was to identify the effect of disturbance, in the form of flood duration and frequency, on the diversity of turlough plant species. Each transect covered the flooding gradient from high to low water level, and comprised of between 45 and 60 1 m^2 relevés. Cluster analysis, NMS ordination and indicator species analysis (ISA) was used in the analysis of vegetation data, and four vegetation communities were identified (O'Rourke, 2009).

11.3.2. Hydroecological Indicators

11.3.2.1. Topographic Data

To allow the integration of hydrological and vegetation data, the elevations of the relevés was a precursor. These were derived from the digital terrain models for each turlough, using the method outlined in *Section 11.2.1*. Elevation values were calculated for all 750 quadrats across 20 turloughs.

For the secondary vegetation research study, the individual quadrats of the four vegetation transects were surveyed in using the Trimble R6 DGPS. Topographic points were taken at 1 m intervals along each transect, defining the endpoints of each quadrat. Using the XYZ coordinates of the endpoints for each quadrat along the transect, the topographic slope S_Q was then determined using:

$$S_Q = \frac{\Delta H}{\Delta L} \qquad \textit{Equation 11.2}$$

with:

$$\Delta L = \sqrt{(X_2 - X_1)^2 + (Y_2 - Y_1)^2} \qquad \textit{Equation 11.3}$$

and:

$$\Delta H = (Z_2 - Z_1) \qquad \textit{Equation 11.4}$$

The location of the Blackrock transects and their elevation profiles are shown in Figure 11.5.

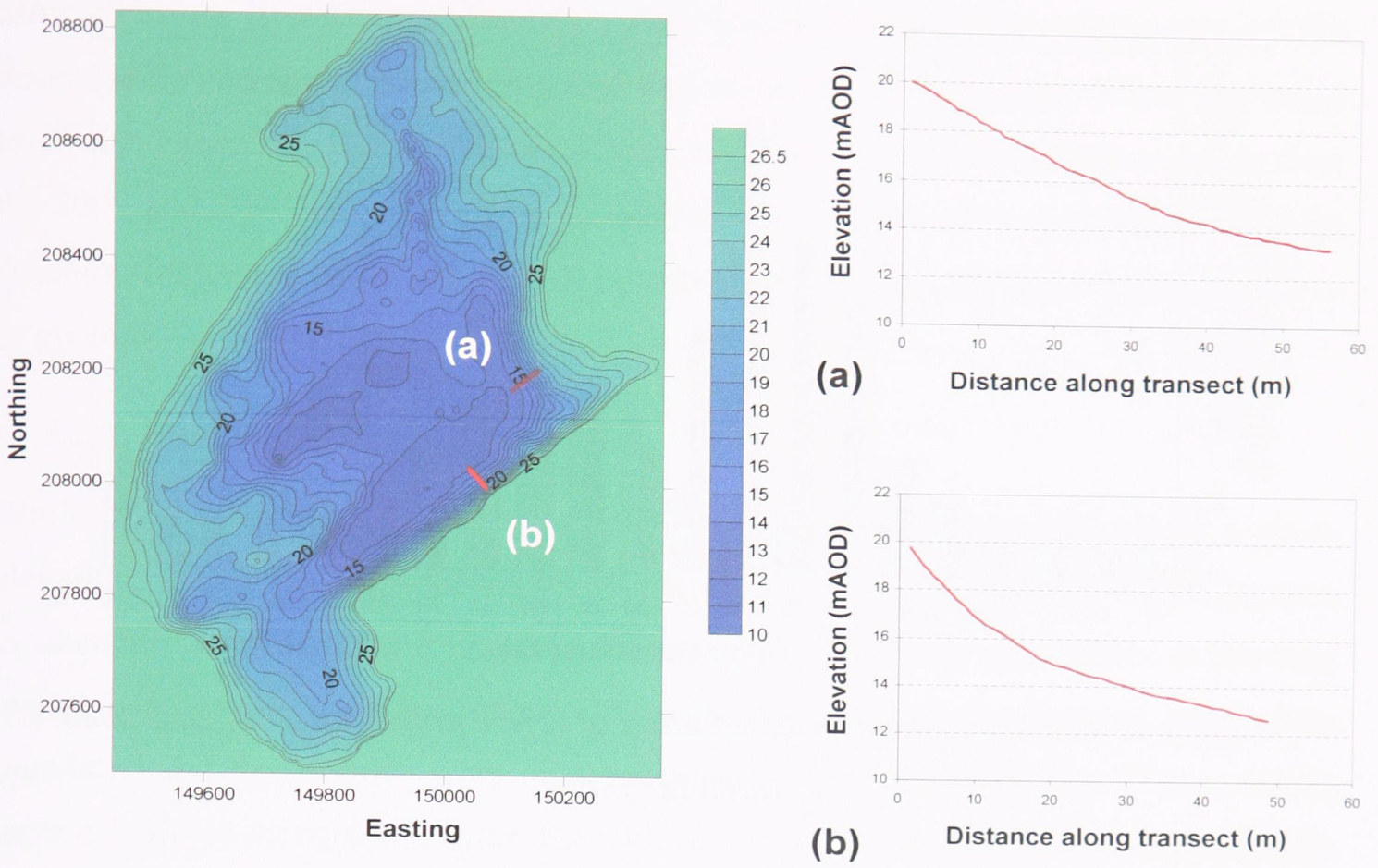


Figure 11.5: Location of vegetation transects together with the elevation profiles of each transect in Blackrock turlough, Co. Galway

11.3.2.2. Duration of Inundation

Duration data were derived for each soil sample point using daily average water levels from the 2007 and 2008 calendar years. Calendar years, rather than hydrological years, were used as this provided the longest parallel hydrological records for as many turloughs as possible. Duration curves were generated for each turlough, using the method outlined in *Section 11.2.2*, for both individual years and the combined two year period. Next, the specific duration corresponding to each relevé elevation was derived from the duration curve. Thus, the flood durations were calculated for all 750 vegetation relevés. The distribution of relevé flood duration, as shown in Figure 11.6, varied significantly between years. This was predominantly due to the relatively late onset of flooding in late 2007 compared to 2008. To minimise the effect of this inter annual variability in hydrological regime, the duration over the combined two year period was used in vegetation community analyses.

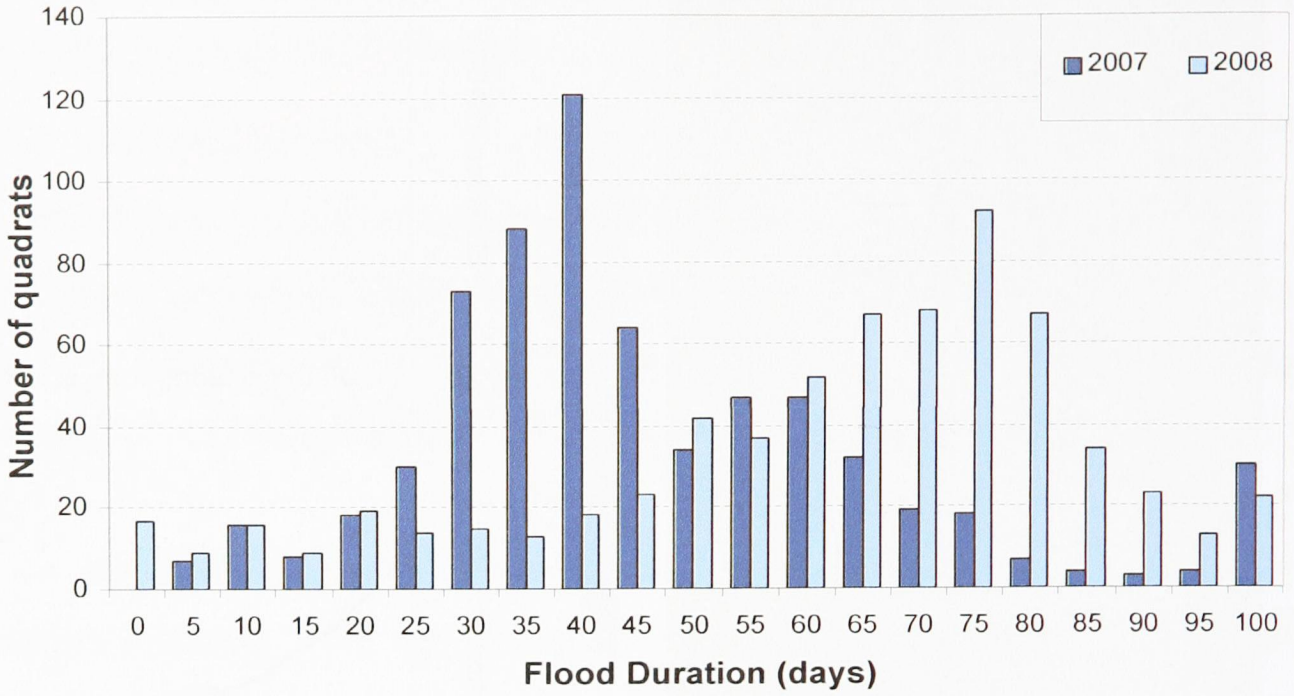


Figure 11.6: Flood duration distribution of relevé points for 2007 and 2008 calendar years

To further explore the role hydrological regime plays in determining vegetation composition for the relevé data, the length of time each relevé was submerged by at least 0.5 m was also calculated. The figure of 0.5 m was chosen by Nova Sharkey as it represented the depth at which the vast majority of species would be completely submerged, and so would no longer have access to atmospheric oxygen. For the second vegetation dataset, consisting of two transects in both Blackrock and Caranavoodaun, the duration was similarly calculated for the mean elevation of each quadrat.

11.3.2.3. Frequency

A flooding event disturbs terrestrial vegetation species by changing the physical environment and available resources, with more frequent flooding events representing a greater level of disturbance (O'Rourke, 2009; White and Pickett, 1985). Flood frequency, together with duration, provides a metric for quantifying this disturbance. As outlined in *section 11.2.4*, flood frequency is defined as the number of times a given water level is equalled or exceeded over a given interval. Here, the flood frequency was calculated over the interval of the 2007 and 2008 calendar years as well as the combined 2007/2008 period. Flood frequency was calculated for each point by counting the number of times that the sample elevation became inundated during the interval in question. This process was carried out for all vegetation samples

using a custom Visual Basic function within Excel. The function stepped through the water level time series, identifying any two consecutive time steps where the water level was exceeded. Flood frequency was calculated for all 750 quadrat points over the 2007 and 2008 calendar years, as well as over the two years combined. As with duration, frequency calculations were repeated for all points for flood depths of 0.5 m or greater.

11.3.2.4. Wet/Dry Periods

While flood frequency quantifies the number of flood events experienced by a given elevation, it does not consider the relative lengths of each flood event. When duration is taken into consideration this goes some way to highlight the distinctions in flooding regime. However, to allow more thorough comparison, the longest continuous inundated and dry periods were also calculated for all relevé points. These periods were calculated using the longest available water level record rather than on a yearly basis, as the longest flooded period tended to cross over years. The wet/dry start date was recorded along with the period length, both in days and as a percentage of the water record length.

These additional parameters further distinguish the different hydrological regimes experienced by vegetation communities within turlough ecosystems. For example, a point showing a short dry period and a long wet period would imply a slow, unimodal flooding regime like that of Coolcam, Co. Galway. In contrast, a short dry period combined with a short wet period would indicate a highly responsive regime with frequent short duration flood events such as Lough Aleenaun as discussed earlier.

11.3.3. Conclusions

Hierarchical, polythetic, agglomerative cluster analysis was used to group the species data into vegetation communities. This procedure calculates a distance matrix by measuring the dissimilarity or similarity between each pair of samples in the data matrix, with the most similar samples being grouped together. In total, 28 vegetation communities were categorised encompassing all vegetation types currently found within the turlough habitat (appendix F), and the spatial distribution of the 28 communities was then mapped for all turloughs within the study group.

The process of integrating vegetation and hydrological data is currently on-going. However, preliminary results point towards a strong relationship between the distribution of vegetation communities and derived hydrological indicators. The first indications of this were encountered during the vegetation mapping phase. The zonation of vegetation commonly identified within the turlough habitat was found to correspond to topographic zones within individual turlough basins, with boundaries between adjacent communities closely following the topographic contours derived from DTMs. As these boundaries were not directly linked with spatial variation in other environmental factors such land use or soil composition, it is likely they are due to characteristic hydrological measures.

The focus of the continuing research undertaken by Sharkey, using the hydrological data is to quantify the links between the 28 communities and specific hydrological control levels. Initial results from that study are presented here. A comparison of the median duration of flooding of relevé points for each of 28 turlough vegetation communities shows a continuum from wet to dry (Figure 11.7), or from the amphibious and fully aquatic species of communities 14 and 24 (*Persicaria amphibia, Mentha aquatica, Schoenoplectus lacustris*) to the relatively flood intolerant species of community 10 (*Lolium perenne, Trifolium repens*). The frequency parameter quantifies the level of temporal disturbance experienced by communities, and so helps to differentiate between communities showing similar duration levels. Nevertheless, the hydrological indicators as presented here, are clear drivers for the characteristic vegetation communities found in turloughs, as might be expected for this unique type of wetland.

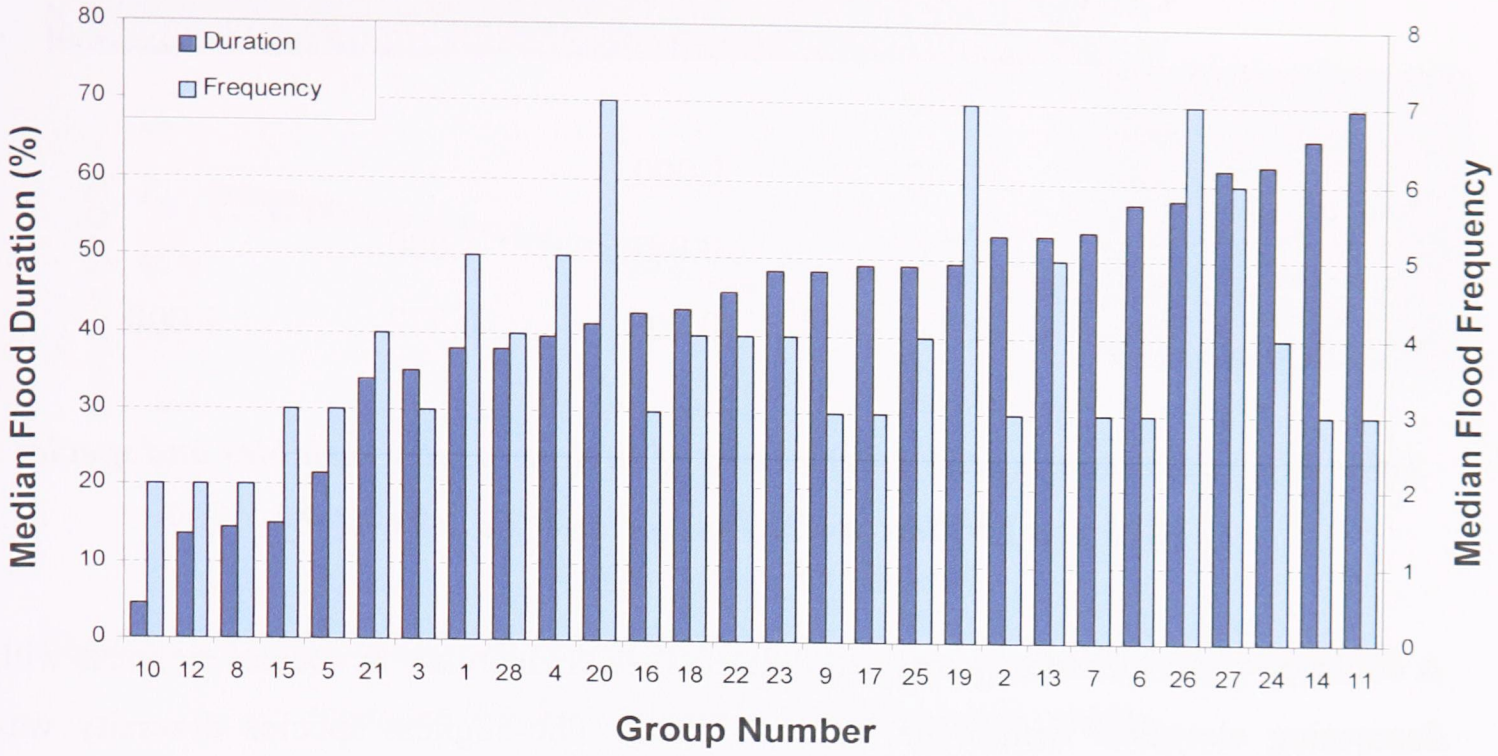


Figure 11.7: Median duration and frequency of relevé points for each of 28 turlough vegetation communities

Hydrological indicators derived as part of this research were also used a by O'Rourke, investigating the effect of flooding disturbance on the diversity of plant communities in turloughs (O'Rourke, 2009). In this study, vegetation groups were defined for each transect using hierarchical cluster analysis and NMS ordination. Sixteen plant communities or groups were classified thus, with four groups along each transect. Species richness (α-diversity) was used to represent overall plant diversity, with transects in Caranavoodaun showing a greater species diversity than those of Blackrock. Species diversity was also found to vary along the flooding gradient itself.

The effects of the hydrological parameters of flood frequency and duration, and the topographic slope parameter, were investigated using Spearman's rank correlations and multiple linear regressions. An example for Blackrock transect A (BLKA) is given in Table 11.1 (O'Rourke, 2009). In this case, a significant positive correlation was identified between species richness and slope, while mean duration and mean frequency of flooding showed a significant negative correlation with species richness.

	Species richness	Slope	Mean duration	Mean frequency
Species richness	1.000	-	-	-
Slope	0.642	1.000	-	-
Mean duration	-0.770	-0.881	1.000	-
Mean frequency	-0.881	-0.608	0.772	1.000

Table 11.1: Spearman's rank correlations of environmental variables and species richness for Blackrock transect A (O'Rourke, 2009)

A common trend identified across all transects was a decrease in species richness with decreasing elevation within the turlough basin. The highest species diversity was found in the upper reaches of the turlough flooding range, with groups associated with the longest duration of flooding showing the lowest species diversity (Figure 11.8). In Blackrock turlough, the lower reaches of the turlough basin were dominated by annual plant species. The special adaptations of such annual species, such as the avoidance as dormant rhizomes utilised by the silverweed *Potentilla anserina*, allow rapid colonisation of recently exposed, highly disturbed areas following flood recession (Tynan et al., 2007). However, this pattern was not recorded in Caranavoodaun turlough. Here, unlike in Blackrock, annuals became less prevalent further down the turlough basin and instead an increase in amphibious species was identified. One possible explanation for this is the substantial differences in hydrological behaviour and in the characteristic regime of the respective turloughs. In Blackrock turlough, the highly variable hydrological conditions are not suitable for the support of amphibious species and so the lower reaches are dominated by the more adaptable annuals. In contrast, the relatively high flood durations and low frequency experienced at low elevations within Caranavoodaun turlough promote the development of perennial species. Thus this study showed that hydrological factors exhibited a significant effect on species diversity of vegetation communities, despite the inherent limitations of a short sampling and hydrological record. Moreover, the trophic status of both turloughs is significantly different. Eutrophic Blackrock draws water from the more acidic limestones of the Slieve Aughty Mountains, while Caranavoodaun is oligotrophic drawing input mainly from local shallow karst.

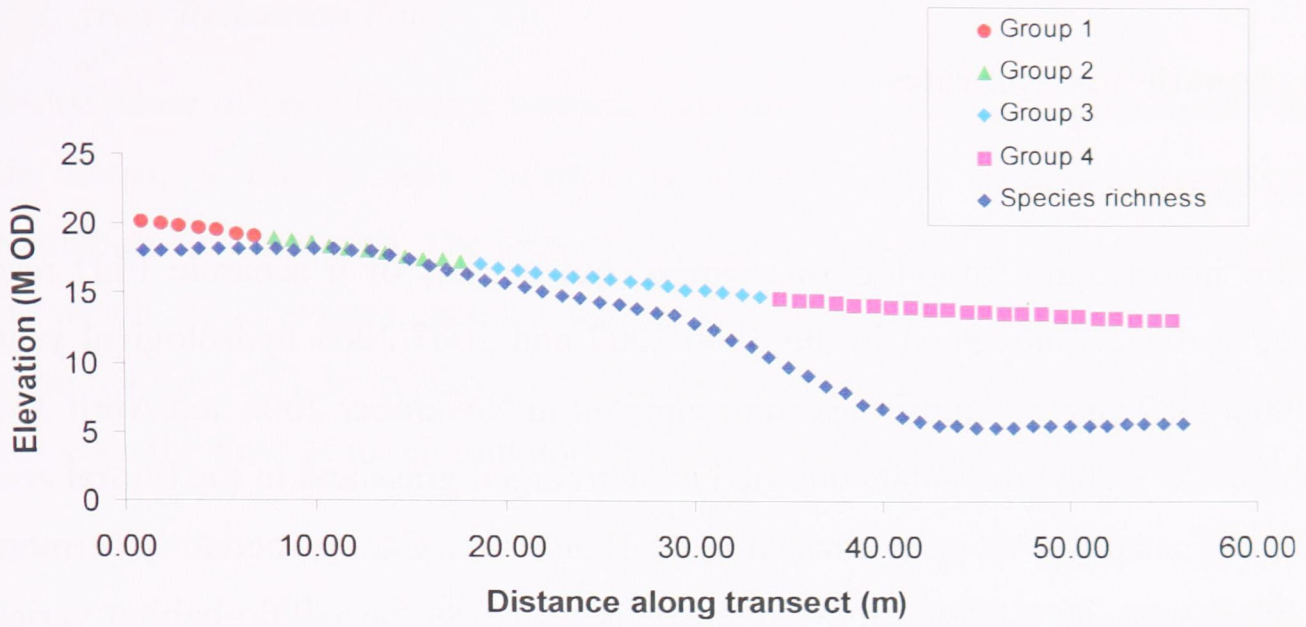


Figure 11.8: The change in vegetation composition and species richness along transect Blackrock transect B (O'Rourke, 2009)

11.4. Aquatic Invertebrates

11.4.1. Introduction

Aquatic invertebrate sampling was carried out as part of a separate PhD research project by Gwendolin Porst in the 2006/2007 and 2007/2008 hydrological years. In the 2006/2007 year all study sites were sampled in November 2006 and April 2007. In each case the sampled habitat consisted of submerged grassland in the littoral zone. In 2007/2008 a subset of sites consisting of Blackrock, Caranavoodaun, Termon and Roo West were investigated more intensively to assess the within-habitat variability of aquatic macroinvertebrate assemblages. The four turloughs were sampled monthly for their macroinvertebrate communities from December 2007 to April 2008. Two additional turloughs, Brierfield and Lisduff, were sampled using two different strategies (multi-habitat sweep net and single-habitat box sampling) in April 2007 to study the between-habitat variability of aquatic macroinvertebrate communities.

11.4.2. Hydroecological Indicators

11.4.2.1. Hydroperiod

In this context hydroperiod as defined as the total number of days a turlough was inundated during one year. Where a unimodal flood regime occurred the hydroperiod represented the total duration of the flood event, whereas with multimodal flooding the hydroperiod was the sum of the durations of the individual flood events. In this context a turlough was defined as dry when either the Diver® recorded zero depth of water or when a minimal amount of water remained, such as would be present in a drainage ditch or swallow hole. Any small permanent water bodies were noted during the topographic surveying work and supplied as side notes to each hydroperiod. The analysis period was chosen as the year from 1st September to 31st August so the full flooding period which began in mid-September 2006 would be taken into account. Turloughs which retained a significant body of water throughout the year were assigned a hydroperiod of 365 days. In the 2007/2008 flooding season the hydroperiod was calculated using the same criteria, where the onset of flooding in November 2007 represented the beginning of. All calculated hydroperiods are given in appendix F.

11.4.2.2. Areal Reduction Rate

As the dry phase of an ephemeral wetland represents an ecological disturbance for its aquatic fauna, a metric was required to quantify this disturbance and allow differentiation between sites. The idea of the areal reduction rate is to characterize the rate at which flood waters receded across the surface of the turlough. The areal reduction rate (dA/dT), in m^2/day, is defined as the average rate of decrease in surface area between the time of maximum and minimum flooded area and is given by:

$$dA/dT = \frac{A_{max} - A_{min}}{\Delta T} \qquad \textit{Equation 11.5}$$

Where:

A_{max} = maximum flood area (m^2)

A_{min} = minimum flood area (m^2)

T = time between occurrence of maximum and minimum flood area (days)

As the flood area reduced at varying rates during the recession depending upon local topography, preliminary collaborative analyses were carried out between aquatic invertebrate data and areal reduction rates calculated over a range of different intervals. Due to the limited invertebrate data available and the range of other factors which affect species populations it was decided to use a general areal reduction rate base upon the maximum and minimum recorded areas during the monitoring periods (Table 11.2). In calculating the areal reduction rate the maximum flood area corresponded to the highest recorded flood level and extent. The minimum flood area was taken as either zero where the turlough fully emptied, or in cases where a permanent water body was present the surface area of the permanent water body.

Site Name	Max Date	Max Area (m^2)	Min Date	dT (Days)	dA (m^2)	dA/dT
Caranavoodaun	10/02/2008	354866	22/05/2008	102	-354866	-3479
Roo West	08/02/2008	410721	28/05/2008	110	-410721	-3734
Termon	16/03/2008	402128	30/07/2008	136	-141710	-1042
Blackrock	07/02/2008	663368	08/04/2008	61	-663368	-10875
Brierfield	14/02/2008	485275	19/06/2008	126	-485275	-3851
Lisduff	08/02/2008	537626	07/06/2008	120	-537626	-4480

Table 11.2: Areal reduction rate information used in aquatic invertebrate analysis

11.4.2.3. Flood Velocity

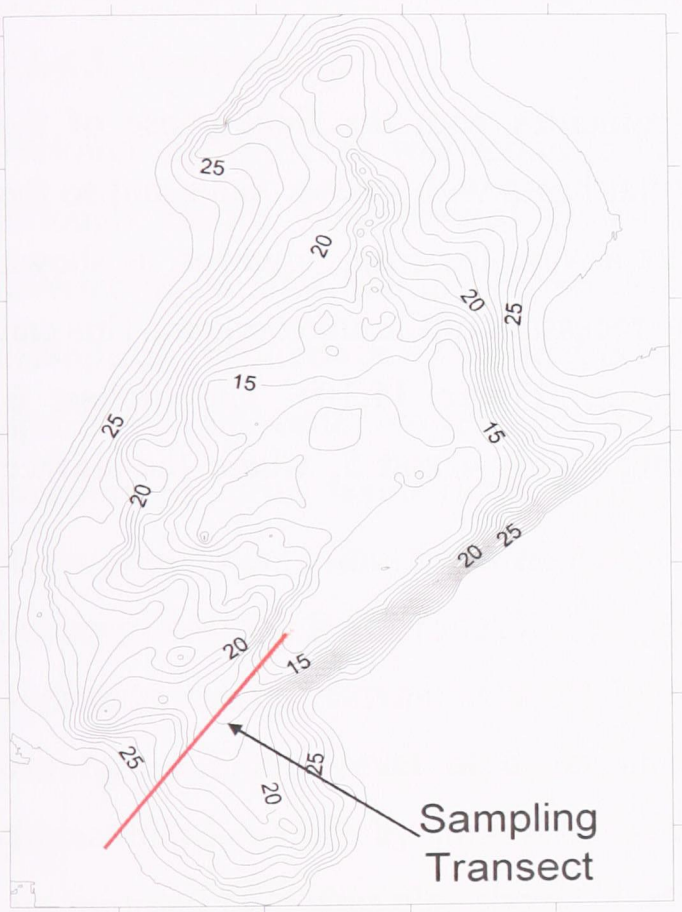
As surface gradient can vary substantially in different parts of the turlough, the exact location of sampling points would be required in order to calculate the velocity of flood recession. While sampling locations were not recorded in the field, the general area of sampling within the turlough was known as well as the date and time at which it occurred. From a combination of the hydrological records and the turlough DTM, the flood level and extent at the time of sampling could be ascertained and thus a good estimate of sampling location coordinates be made. The distance between sampling points (δ) was then calculated from these coordinates using:

$$\delta = \sqrt{(x_2 - x_1)^2 + (y_2 - y_1)^2 + (z_2 - z_1)^2} \qquad \textit{Equation 11.6}$$

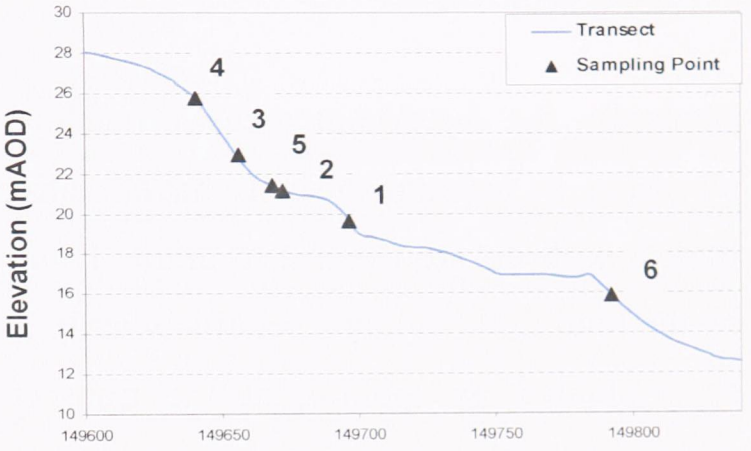
By dividing the distance by the time elapsed between sampling events, the mean floodwater velocity along the sampling transect during the intervening period was determined.

An example of the flood velocity analysis is shown for Blackrock turlough, Co. Galway (Figure 11.9). Figure 11.2 *(a)* shows the sampling transect location within the turlough basin, with the corresponding elevation profile with sample point locations is given in Figure 11.9 *(b)*. The chronological order that the sampling point occurred within the time series is labelled 1 to 6. The highest flood velocity (-7.092 m/day)

over the sampling period occurred during the final phase of recession, between points 5 and 6, which coincided with the flattest section of transect. This pattern is repeated in Roo West and Termon as the highest recession velocities of -5.116 of -0.163 m/day respectively were recorded during the last between the 1/4/2008 and 7/5/2008 (Table 11.2). In Termon, due to the extended duration of flooding the last sampling event took place relatively early in its recession. The average flood velocity further increased in the latter phase of the recession, rising to 0.324 m/day in the month following the 07/05/2008.



(a)



(b)

Date	Distance D (m)	dT (days)	V (m/day)
04/12/2007	-	-	-
19/12/2007	38.45	15	2.563
08/01/2008	25.68	20	1.284
04/02/2008	25.76	27	0.954
04/03/2008	45.03	29	-1.553
01/04/2008	198.57	28	-7.092

(c)

Figure 11.9: (a) Contour map of Blackrock turlough including invertebrate sampling transect, (b) Elevation profile of transect and (c) calculations of flood velocity between sampling events

Date	Flood Velocity (m/day)			
	Blackrock	Caranavoodaun	Roo West	Termon
19/12/2007	2.563	0.335	4.68	0.77
08/01/2008	1.284	0.091	1.324	0.455
04/02/2008	0.954	0.667	1.889	0.52
04/03/2008	-1.553	-0.414	-1.04	0.071
01/04/2008	-7.092	-0.215	-0.81	-0.074
07/05/2008	-	-0.059	-5.116	-0.163

Table 11.3: Flood velocities for aquatic sampling intervals on turlough subset

Generally the maximum recession velocity coincides with the final phase of the recession, as turloughs usually have relatively flat bases with steeper sides and so the flattest sections are the last to drain. This is not always the case, however, as shown by the high flood velocity relatively early in the recession of Caranavoodaun. This can be explained by looking at the transect profile (Figure 11.10). The highest is associated with the recession between sampling points 4 and 5, where the surface gradient is at its least.

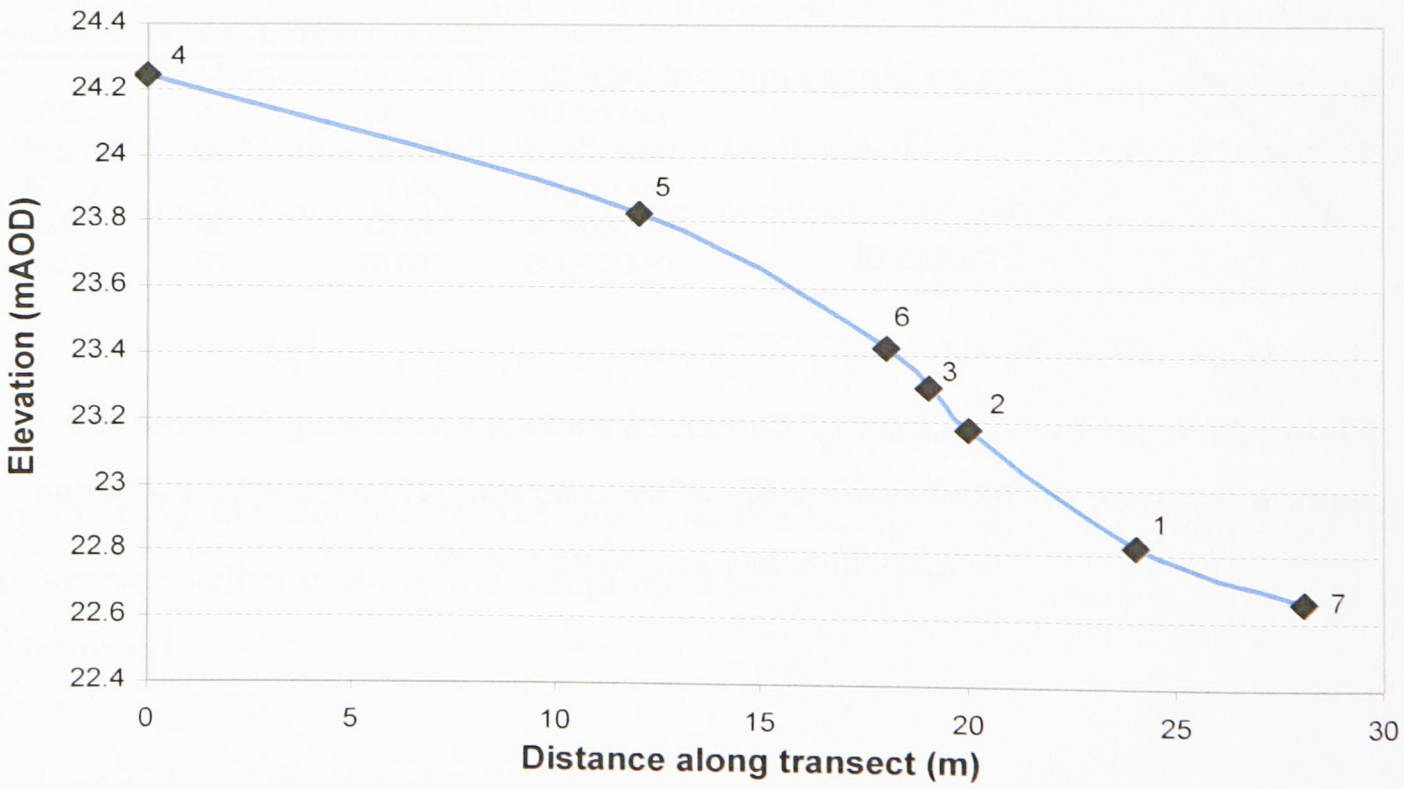


Figure 11.10: Transect elevation profile and aquatic invertebrate sampling locations for Caranavoodaun turlough, Co. Galway

If disturbance is related to the rate of change from an aquatic to a terrestrial environment, this shows that the highest level of disturbance is associated with areas showing a shallow surface gradient. Here, slower moving invertebrates may not have sufficient time to withdraw to aquatic refuges such as drainage ditches or swallow holes as the flood recedes. Thus topographic gradient provides a useful indicator of disturbance for aquatic invertebrates. When combined with hydrological and topographic data, the level of disturbance can be quantified for different regions of the turlough basin and also facilitates detailed inter-site comparisons.

11.4.3. Conclusions

Turlough hydroperiod was found to have severe effects on successional patterns of turlough macro invertebrates (Porst, 2009). In the context of aquatic macro invertebrate studies, the dry phase of a turlough hydrological cycle is considered an ecological disturbance. The hydroperiod hydrological variable was included in Spearman rank-order correlation analyses to compare mean abundance and log-transformed mean taxon richness in a subset of 8 studied turloughs (Porst, 2009). Hydroperiod was found to correlate positively with mean abundance and mean taxon richness ($R=0.88$; $P<0.01$ and $R=0.74$; $P<0.05$ respectively) (Porst and Irvine, 2009a). Turloughs which showed a short hydroperiod and high areal reduction rate, and therefore a higher level of disturbance, displayed a lower biodiversity and were characterised mainly by permanent residents well adapted to the recurring drought conditions. These sites also showed a level of inter annual variability which depended on the prevailing hydrological conditions. After "dry" years, invertebrate communities were dominated by permanent species whereas after "wet" years greater numbers of ephemeral species were detected. This is because the "wet" years represent a more stable environment for ephemeral species not well suited to changes in the environment. Also the requisite habitat conditions (i.e. flooding) are more likely to occur at a time that coincides with the aquatic phase of an ephemeral invertebrate's life stage during wet years.

Variability in taxon richness was found to correlate negatively with increasing habitat permanence. Turloughs with greater habitat persistence, that is a longer hydroperiod, represent a lower disturbance and so sustain more stable communities. The turlough

with the longest hydroperiod in the study, Termon, showed the highest numbers of macro invertebrates and relatively high taxon richness. It also usually had the highest monthly and average seasonal taxon richness. Sites displaying a longer hydroperiod and the presence of permanent water body were also found to support fauna with a life span exceeding 1 year, with small fish found in Termon as it supported a substantial water body throughout the year. The small permanent ponds present in Brierfield, Co. Roscommon, provided suitable conditions for the smooth newt *Triturus vulgaris* as these aquatic habitats allowed the newt tadpoles to metamorphose (Porst, 2009).

In general, taxon richness increased following the onset of flooding. The majority of macro invertebrate species present are permanent residents which are able to rapidly re-colonise during the initial phase of flooding. Thereafter, the turlough is colonised by and so taxon richness increases. Following flood recession, the taxon richness decreases again as the dominant species once again become the permanent residents.

Canonical Correspondence Analysis (CCA) carried out to examine the variability present in the macro invertebrate community suggested that hydroperiod had a low influence on community structures of macro invertebrates relative to effects of season (Porst and Irvine, 2009a). However, turlough hydrology and the turlough habitat are intimately linked with the seasonality of the Irish climate, and the strong identified seasonal effect had likely an overriding effect in the CCA analysis. Despite this, the effect of hydroperiod on community structure was evident as shown by the positive correlation of ephemeral macro invertebrate orders *Heteroptera* and *Trichoptera* with increasing flood duration, thus identifying a direct link between hydroperiod and macro invertebrate life-stages (Porst, 2009).

11.5. Hydrochemistry and Phytoplankton

11.5.1. Introduction

Hydrochemistry and phytoplankton sampling was carried out as part of a separate PhD research project by Helder Pereira in the 2006/2007 and 2007/2008 hydrological years. In the first year, all 22 sites were sampled monthly from October 2006 until emptying, which was taken to occur between April and June 2007. Single samples

were taken from the turlough edge using a weighted 5 L plastic bottle thrown from the shore into an area of open water (Pereira et al., 2009). Measurements of conductivity, temperature and dissolved oxygen were taken in the field at the time of sampling. Laboratory analysis was then carried out to determine the hydro-chemical parameters of total phosphorous (TP), soluble reactive phosphorous (SRP), total nitrogen (TN), total oxidised nitrogen (TON), chlorophyll a (Chl a), pH, alkalinity and colour. In the second year of sampling (2007/2008 flooding season), multiple samples were collected in a subset of turloughs consisting of Blackrock, Caranavoodaun, Termon and Roo West to examine the spatial variation in hydro-chemical parameters within turlough water bodies.

11.5.2. Hydroecological Indicators

11.5.2.1. Topographic Data

Hydrologically active karst features such as springs, swallow holes and estavelles were identified during the topographic surveys and site visits carried out as part of the hydrology research. These features were then used to guide the location of sampling points during the second year of hydro-chemical sampling. Once the sample locations had been decided, the ground elevation at each sampling point was derived using the point GPS coordinates and relevant DTM. This, combined with the stage time series, allowed the depth of water at each point to be ascertained during the sampling events.

11.5.2.2. Hydrological Time Series

Hydrological time series composed of daily averages for stage, volume and area were directly used in the interpretation of water chemistry parameters, with temporal patterns of flooding were compared to turlough nutrient variations over the same period. Summary parameters such as maxima, mean depth (volume / area), and time taken from maximum volume to 25% of maximum were generated from these time series for descriptive purposes. Also, volume and area data which coincided with sampling events were extracted from the relevant time series for use in nutrient mass balance and loading calculations.

11.5.2.3. Hydroperiod

In water chemistry and phytoplankton analysis, hydroperiod is defined as the total number of days a turlough is inundated during the main flooding season. Therefore,

unlike in the earlier definition for invertebrates, smaller flood events during the summer season are not taken into account. Where hydrological records were not available from before the first sampling event in October 2006, the onset of flooding was taken to occur on the 21st September 2006, as this was the time identified from preliminary site visits as the beginning of flooding in the majority of turloughs. Where turloughs completely emptied the cessation of flooding was taken as the final date on which floodwaters were recorded but, in turloughs where flooding persisted throughout the year, the time at which turlough volume receded to 10% of the peak recorded volume was used to define the end of flooding (Pereira, 2010).The hydroperiod was thus calculated for all 22 turloughs (Table 11.4):

Site Name	Hydroperiod (days)	Site Name	Hydroperiod (days)
Ardkill	293	Kilglassaun	223
Ballinderreen	211	Knockaunroe	213
Blackrock	169	Lisduff	234
Brierfield	267	Lough Aleenaun	158
Caherglassaun	200	Lough Coy	187
Caranavoodaun	205	Rathnalulleagh	175
Carrowreagh	186	Roo West*	213
Coolcam	346	Skealoghan	213
Croaghill	348	Termon	304
Garryland	211	Tullynafrankagh	246
Gealain	212	Turloughmore	135

Table 11.4: Hydroperiod for the 2006/2007 flooding season for 22 monitoring sites (*2007/2008 value used due to hydrological data unavailability)

Another variation on the theme of hydroperiod used was the 'Number of days flooded' (at a given sampled day), which is the interval between the onset of flooding until the sampling event; this variable accounts for periods of dryness that could occur in the middle of the main flooding season.

11.5.2.4. Aggregation Period

The aggregation period coefficients derived during the aggregated rainfall modelling process in chapter 9 were used to represent a notional residence time for each turlough (Table 11.5). The aggregation period is an indicator of the memory of the system, or

how long water is retained within the turlough, and so provides an indirect measure of flood duration. A large aggregation period implies long flood duration with a lengthy recession, while a smaller value indicates a hydrological regime with rapid filling and emptying.

Site Name	Aggregation Period (days)	Site Name	Aggregation Period (days)
Ardkill	135	Lisduff	90
Blackrock	38	Lough Aleenaun	10
Brierfield	144	Lough Coy	44
Caherglassaun	66	Lough Gealain	81
Caranavoodaun	80	Rathnalulleagh	85
Carrowreagh	108	Roo West	82
Coolcam	163	Skealoghan	73
Croaghill	120	Termon	176
Garryland	67	Turloughmore	15
Knockaunroe	82		

Table 11.5: Aggregation period for 19 monitored turloughs

11.5.3. Conclusions

Turlough hydrological changes did not appear to be strongly related to the variation in the level of nutrients over a flooding season, with no clear link identified between the temporal variation in hydrological regime and the nutrient level or temporal variation (Pereira, 2010). TP and Chl a displayed an erratic temporal behaviour, with peaks sometimes happening during low water levels at the start and end of the flooding season, but with numerous examples of peaks throughout the duration of flooding (Pereira, 2010).

TN did show some pattern in a number of sites, whereby the concentration of total Nitrogen (TN) increased following the onset of flooding, reached a peak, and then fell during the recession period. However, the timing of the peak did not show a consistent relation to peak water level. In some cases it approximately coincided with peak flood levels, but often before and after. Some consistency was shown in the timing of the TN peaks themselves, with the highest concentrations recorded in the December or January samples for 20 out of the 22 turloughs. Given the monthly

resolution of the sampling data, the exact timing of the peak levels is not definitive and so this distribution across December and January could be closer than it appears.

Mass balance calculations based on recorded volumes and TN concentrations have shown that in order for dilution to be the main mechanism responsible for lowering TN concentrations, an extremely high level of turnover is required during the recession period (Pereira, 2010). This would entail water continuously entering the site in large quantities during the recession, with figures as high as 55% turnover during a month (Table 11.6). These calculations were carried out on the assumption that incoming water had negligible nutrient concentrations and didn't account for mixing during the calculation period, and so realistic values for nutrient loading would push these figures even higher. Were dilution the primary cause for the recorded TN seasonal variation, these figures would clearly point towards the flow-through conceptual model.

Site Name	Calculation Interval	Volume ($*10^3$ m^3)		TN concentration (mg/L)		Required Turnover (%)
		Initial	Final	Initial	Final	
Blackrock	Feb - Mar 2008	3646	1638	1.2	1	15.5
Caranavoodaun	Feb - Mar 2007	278	207	2.4	1.7	32.2
Caranavoodaun	Mar - Apr 2007	207	85	1.7	0.8	54.6
Lisduff	Jan - Feb 2007	761	620	3.1	1.8	40
Lisduff	Mar - Apr 2007	594	405	1.6	1.2	24.5
Roo West	Feb - Mar 2008	983	675	0.8	0.4	46.7
Skealoghan	Jan - Feb 2007	334	178	1.6	0.8	48

Table 11.6: Mass balance calculations of the volume of water (as percentage of total final volume) that would need to enter a turlough as total nitrogen (TN) concentrations and water levels concomitantly decrease (adapted from Pereira 2010)

This was investigated using the inflow and outflow values derived during the reservoir modelling process for Lisduff turlough (chapter 9). A mass balance was carried out at each time step between sampling intervals in order to determine the inflow concentration required to produce the recorded TN levels. It was found that the

average TN concentration needed was 1.35 mg/L between February and March, and 0.45 mg/L between March and April. While the first value seems plausible, the second is at the lower end of TN concentrations recorded across all the study sites throughout the flooding season, let alone in Lisduff which showed the third highest average TN concentration over the sampling period. Also, when this calculation was carried out in the interval between the next sampling events, from April to May, the low inflow levels caused by negligible rainfall failed to explain the drop in TN, irrespective of concentration. This indicates other possible mechanisms, such as the uptake of soluble N by vegetation within the turlough basin, as also affecting the temporal pattern of nutrient levels within turloughs.

However, it is difficult to draw any definitive conclusions from this due to the resolution of the hydrochemistry data, and it is clear that more detailed hydrochemical research is needed to elucidate this issue (Pereira, 2010). More detailed hydrochemical data for a subset of turloughs and the surrounding areas, together with further progress in the study of turlough hydrological operation and modelling, can provide a more comprehensive insight into the operation of turlough hydrological systems as a whole.

11.6. Soil Nutrients

11.6.1. Introduction

Soil nutrient sampling was carried out on eighteen turloughs by Sarah Kimberley, as part of a postdoctoral research project. The main objectives of this research was to examine the relationships between turlough soil nutrient properties and the spatial variability in these properties, as well as to characterise the relative importance of flooding factors, land use and vegetation on turlough soil properties. Six soil samples were collected from each turlough to a maximum depth of 20 cm, with soil sample locations were distributed across the upper, middle and lower elevation zones within each turlough. Soil types were determined using a modified version of soil categories generated by the Irish Forest Soils element of the Forest Inventory Planning System (FIPS-IFS). Samples were analysed for pH, organic matter content (OM), calcium carbonate content ($CaCO_3$), non-calcareous sand/silt/clay fraction (INORG), total nitrogen (TN), total phosphorus (TP).

11.6.2. Hydroecological Indicators

11.6.2.1. Topographic Data

As with the vegetation relevé data, the elevation of soil sampling points had to be derived from individual turlough DTMs. In total, were derived for 128 sample locations across 21 turloughs using the method described in *Section 11.2.1*. During this process four samples were found to lie outside the turlough boundary, as defined by the maximum water level recorded during the monitoring period and so were excluded from the data analysis. Hydrological data limitations lead to samples from a further three turloughs, namely Kilglassaun, Roo West and Ballinderreen, being discarded leaving a final dataset of 104 soil samples.

11.6.2.2. Duration

Duration data was derived for each soil sample point using daily average water levels from the 2007 and 2008 calendar years. First, duration curves were generated for each individual turlough using the method described in *Section 11.2.2*, for the individual 2007 and 2008 years as well as the combined 2007/2008 period. Next, the specific value corresponding to the sample elevation was isolated from the duration curve.

This process was repeated for all soil samples, and was automated within Excel using a custom function written in Visual Basic.

There was substantial inter annual variation in flood duration, with most points experiencing a higher duration in 2008 than in 2007. This variability is shown in Figure 11.11, where a shift towards higher duration can clearly be seen in the distribution of 2008 duration relative to those of 2007. Analysis of the individual durations showed an average decrease of 15.3%, with a point in Lough Gealain showing an increase in duration of over 34% during 2008 compared to that of 2007. As soil nutrients likely respond to long rather than short hydrological patterns, the average duration over the combined 2007/2008 period was used in analyses.

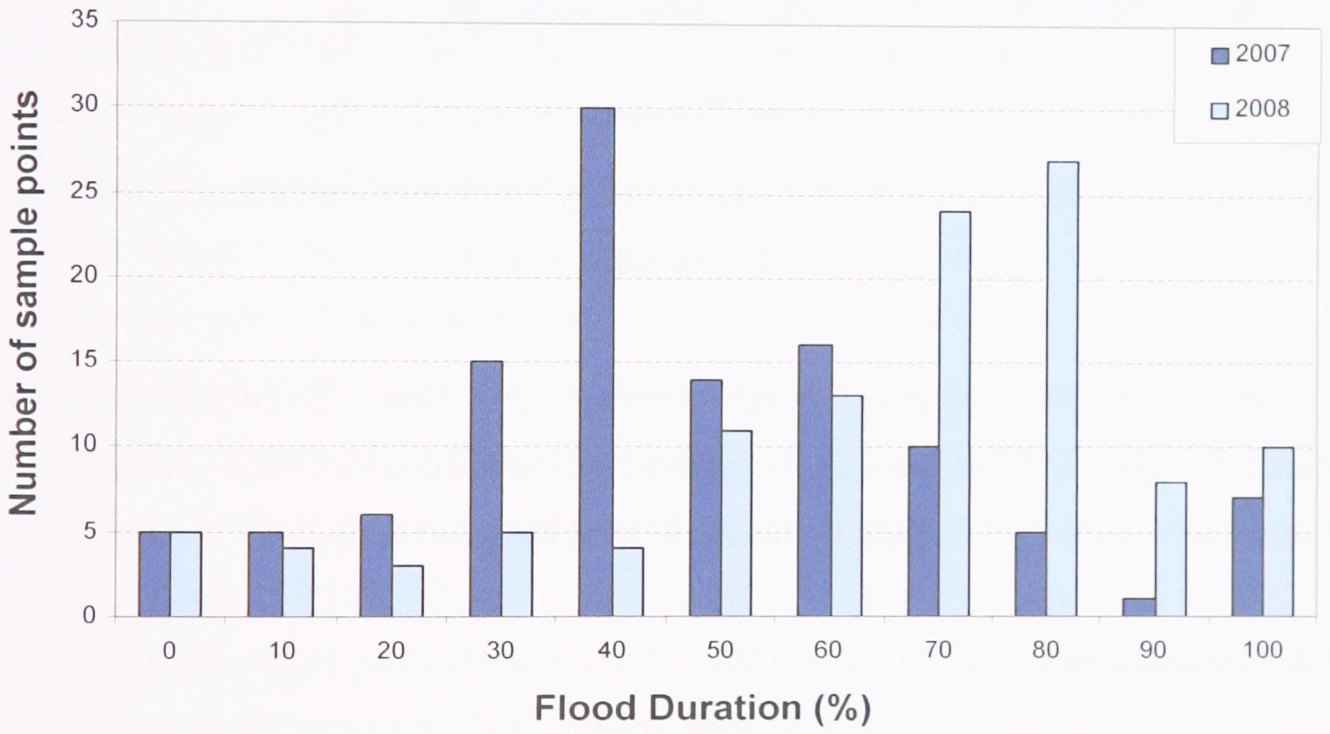


Figure 11.11: Distribution of flood duration of soil sample locations for the 2007 and 2008 calendar years

11.6.2.3. Frequency

As described earlier, flood frequency is defined as the number of times a given water level is equalled or exceeded over a given interval. In this case the intervals were the 2007 and 2008 calendar years and the combined 2007/2008 period. As outlined in *section 11.3.2.3*, flood frequency was calculated for each point by counting the number of times that the sample elevation became inundated during the interval in question. The distribution of flood frequency showed more stability as shown in

Figure 11.12, with the average frequency of flooding increasing by only 0.13 (σ = 1.6) between 2007 and 2008. Again, as with duration, flood frequency used in the soil nutrient analyses were calculated over the combined 2007/2008 period.

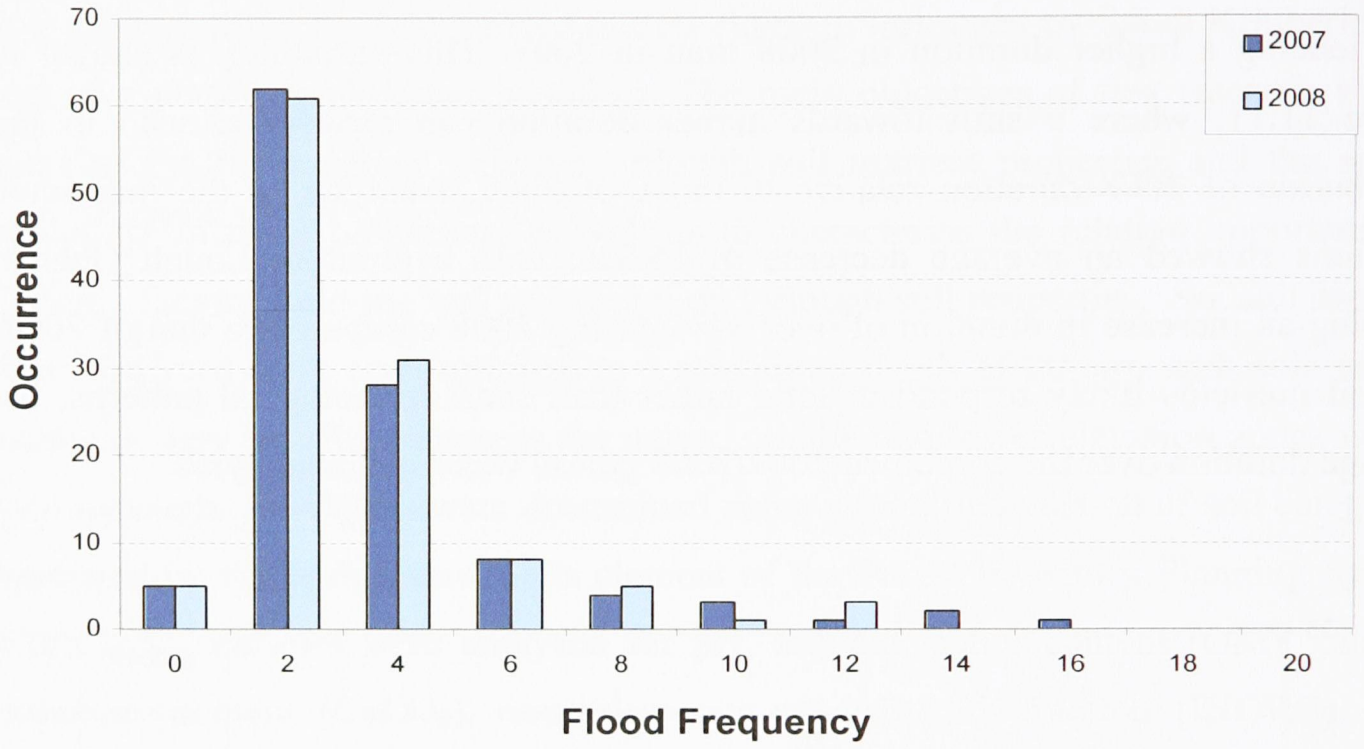


Figure 11.12: Distribution of flood frequencies of soil sample locations for the 2007 and 2008 calendar years

The hydrological indicators of flood duration and flood frequency were also combined to give a third parameter: average flood duration. The average flood duration was defined as the flood duration divided by flood frequency.

11.6.3. Conclusions

Statistical analyses were carried out, by Sarah Kimberley, on the soil parameters of total nitrogen (TN), total phosphorus (TP), pH, organic matter content (OM), calcium carbonate content ($CaCO_3$), non-calcareous sand/silt/clay fraction (INORG) and soil depth, as well as the hydrological parameters of flood duration (FD), flood frequency (FF) and average flood duration (AD). Data normality was checked using the Kolmogorov-Smirnov test for $n > 50$, and the Shapiro Wilks test for $n < 50$. The datasets were found to be non-normally distributed and so Spearman rank-order correlation was used to compare the variables. The parameters which showed a significant correlation with the hydrological parameters of FD, FF and AD are given in Table 11.7:

	TP (mg kg^{-1})	$CaCO_3$	FD (days)	FF	AD (days)
TP (mg kg^{-1})	1				
$CaCO_3$	-0.018	1			
FD (days)	-0.084	**0.445**	1		
FF	**0.351**	-0.078	-0.134	1	
AD (days)	**-0.371**	0.267	**0.615**	**-0.772**	1

Table 11.7: Spearman Rank correlation matrix of R values with highlighted values significant at the $P \leq 0.001$ level

Flooding frequency was identified as an important driver of total phosphorus (TP) variation in turlough soils, with TP showing a significant positive association with flood frequency (FF) ($R = 0.351$; $P \leq 0.001$). A plot of TP against FF shows a general increasing trend (Figure 11.13 *(a)*), indicating that higher TP concentrations are associated with more frequent inundation events. Low TP concentrations (< 500 mg kg^{-1}) were found to be associated with flooding patterns consisting of less than seven inundation events. TP also showed a significant negative association with average duration (AD) ($R = -0.371$; $P \leq 0.001$). A general decreasing trend can be seen from the scatterplot (Figure 11.13 *(b)*), but this association lacked clear form and direction. This lack of clarity is demonstrated by the group of outliers located at an AD of 730 days in Figure 11.13. These points represent sample locations which were permanently inundated throughout the two year period. Despite experiencing the same hydrological conditions they show approximately an order of magnitude difference in TP concentrations, ranging from 250 to 2250 mg kg^{-1}.

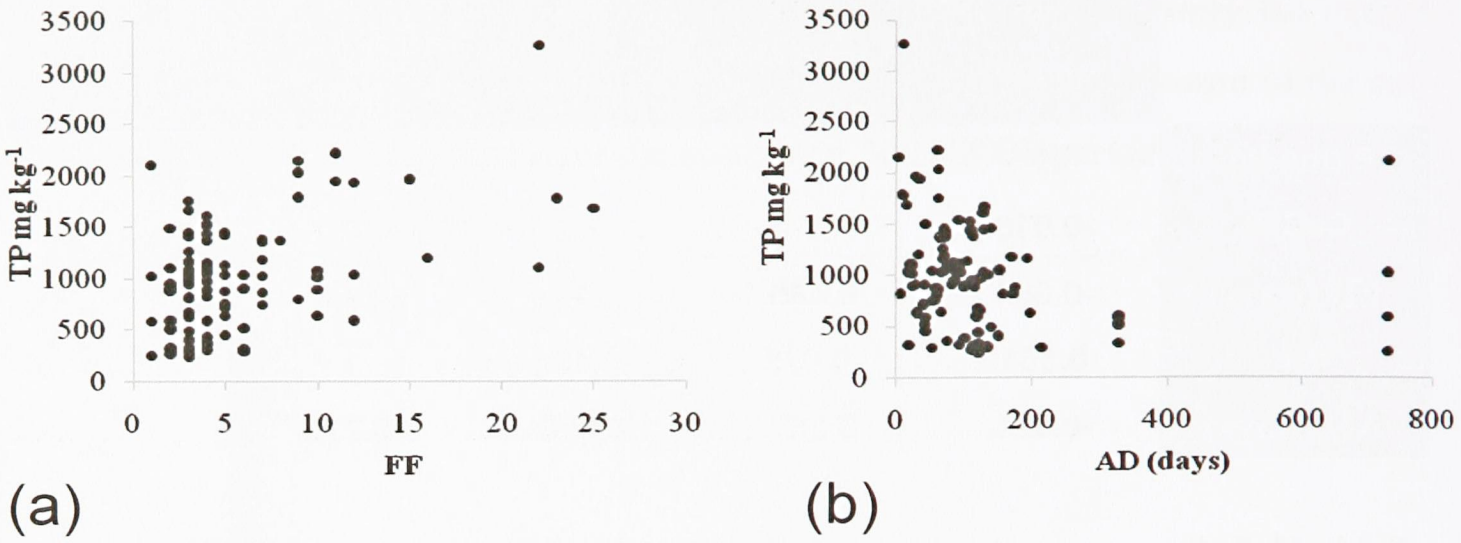


Figure 11.13: Scatterplots of associations between (a) total phosphorus (TP) and flooding frequency (FF) and (b) total phosphorus (TP) and average inundation duration (AD)

A significant positive association ($R = 0.445$; $P \leq 0.001$) was also shown between $CaCO_3$ and flood duration (FD). Samples which comprised of more than 50% $CaCO_3$ associated with FD in excess of 300 days. This supports the view of Coxon (1987), who found that the marl (calcite) deposition was associated with a longer duration of flooding than sand/silt and silt/clay deposits. However, long flood duration did not consistently result in the $CaCO_3$ accumulation implying that other environmental controls, such as floodwater alkalinity, are likely to play an important role in determining the $CaCO_3$ content of turlough soils.

In conclusion, flood frequency and flood duration were found to show significant associations with the total phosphorus and calcium carbonate soil properties respectively. However, given the high level of inter annual variability in turlough flooding regimes, longer term hydrological datasets are required to further elucidate these relationships and evaluate the influences of hydrological indicators on turlough soil property variation. The requirement for such long term records further emphasises the need for continued monitoring of turlough sites, but also the value of hydrological modelling for generating such records.

CHAPTER 12. CONCLUSIONS

12.1. Turlough Hydrodynamics

The primary aim of this study was to characterise the hydrodynamic behaviour and hydrological regime of a broad set of turloughs chosen as representative of turlough geographical distribution and hydrological behaviour. This was achieved through the measurement of relevant hydrological parameters, the mapping of topography within turlough basins, and the analysis and interpretation of extensive hydrological datasets using appropriate hydraulic and time series analysis techniques. Following on from this, two general turlough hydrological models were developed for the prediction of turlough flooding behaviour from rainfall and evapotranspiration records.

Relevant hydrological and topographic data were collected for a set of 22 turloughs chosen to represent the hydrological and ecological diversity of the turlough habitat. Three years of hourly water-level data were collected for the twenty two study sites. Detailed topographic surveys were carried out on the study sites, with over 20000 topographic points across an area of over 1000 hectares using accurate GPS surveying techniques. Digital terrain models were generated for each site from this topographic data and then used to transform water level data into the corresponding volume and area time series. These datasets provided the first quantitative hydrological records upon which to base the characterization of turlough hydrodynamic behaviour, enabled the development of hydraulic models for the prediction of water level response, as well as forming a basis for the derivation of hydroecological indicators that influence biological diversity within and among turloughs.

The hydrological typology of turloughs did not naturally group into distinct types when compared using a variety of hydrological parameters; instead the behaviour was spread across a continuum. However, these techniques did quantify this continuum, and so allow the hydrological functioning of a turlough to be placed in terms of the overall spectrum of turlough hydrodynamics.

This continuum was evident throughout the various analysis methodologies, from the simple descriptors of depth, volume and area through to those derived during time

series analysis techniques. Maximum depth of flooding varied substantially between monitored turloughs, from 2.0 to 15.4 metres with a median of 4.6 metres, reflecting the differences in characteristic flood regime and geomorphology of each site. An order of magnitude difference existed between the largest and smallest sites volumetrically, with a maximum flood volume range from 350,000m^3 to 4 million m^3. While sites showing the greatest depth generally corresponded to the largest turloughs volumetrically, a different set of sites showed the greatest flooded area. The maximum extent of flooding of the study sites (13.7 to 78.8 ha) was a reflection of turlough basin topography and geomorphology, with the highest areas shown by those turloughs located in shallow expansive basins. The annual temporal variability of these hydrological descriptors was compared using the ratio of highest to lowest yearly maxima. Annual maximum depth of flooding was the most stable parameter across the monitoring period, with a mean ratio of 1.2, while volume displayed the greatest annual variability (average ratio of 1.67). The yearly variation did not appear explicitly associated with the nature of the flooding regime. Instead, site specific factors such as surface drains or connections to adjoining depressions were controlling factors in the annual flood extent.

The analysis of net flows entering and exiting a turlough provided an insight into their hydrological operation. The causative relationship between precipitation and rainfall was investigated and quantified. Generally the highest inflows coincided with the greatest magnitude rainfall event, but not always. In some cases, the rainfall–inflow relationship displayed a cumulative effect where high inflow rates were generated by a series of consecutive lower intensity rainfall events. Another factor affecting the association between rainfall and inflow was the preceding flow conditions. The flow response shown by turloughs to similar magnitude rainfall events was less following a recession period than following a prolonged filling period. It was also apparent that the length of the recession had an effect upon the level of inflow, with longer recessions further damping the inflow response. This is indicative of the effect that storage within the turlough catchment area has on turlough flooding. The drainage of the karst aquifer during recession frees up storage and capacity within the bedrock system which can accommodate a component of subsequent rainfall, thus lessening the amount of water passing to storage within the turlough. When this storage is full and so no longer damps the rainfall response, it was found that the relationship

between rainfall and inflow could be represented using a linear approximation. A correlation between cumulative rainfall and volume during the rising limb of the volume hydrograph produced correlation coefficients of between 0.954 and 0.996. While the mechanisms and processes involved are inherently non-linear, the high correlations found show that it can be approximated as such for inflow periods.

Analysis of the recession behaviour of the study sites yielded key information about the nature and capacity of turlough drainage systems. The nature of the relationship between stage and outflow was derived from stage-discharge plots. These plots showed that a stage-discharge curve defining a turlough's maximum drainage capacity as a function of stage could be formed using the maximum outflow values across the flooding range. The stage-discharge curves themselves took an array of forms. Many sites showed a continuous smooth curve across most or all of the flood range, while others had a number of discontinuities in the stage-discharge relationship. These discontinuous curves required distinctive discharge curves within different flood ranges, possibly representing the operation of distinct systems within the turlough basin. A number of sites also showed an apparent maximum outflow capacity, which remained constant in the upper range of flooding. This maximum outflow capacity was found to be associated with turloughs which displayed a long duration, unimodal flooding regime. The stage-discharge curves provided a vital tool for the derivation of one unknown within the turlough water balance equation (the outflow), which formed the basis of the reservoir modelling techniques developed in this thesis. A characteristic recession constant was also derived for each turlough using an approximation of the recession limb of the volume hydrograph. The slope of this linear approximation provided a characteristic drainage capacity for each turlough, with capacities ranging from 0.070 to 1.152m^3/s, with a median value of 0.154 m^3/s. This recession constant provided a useful indicator of the drainage capacity of the karst flow network underlying each turlough.

Simple correlation analysis of turlough water levels showed the diversity in hydrological regimes and the continuum of hydrological behaviour that exists. A number of turloughs showed comparable hydrological regimes, as shown by extremely high correlation values of over 0.99 in many cases. These sites were often in close geographical proximity, indicating potential hydraulic connections or similar

modus operandi. Other sites, such as Termon Lough near the Clare border in south Co. Galway and Coolcam on the Roscommon border in north Co. Galway, were geographically distant but still showed a high level of similarity (R=0.990) , and so geographical location was not the determining factor in turlough regime. This correlation analysis also identified end members of the turlough hydrological continuum (Figure 12.1).

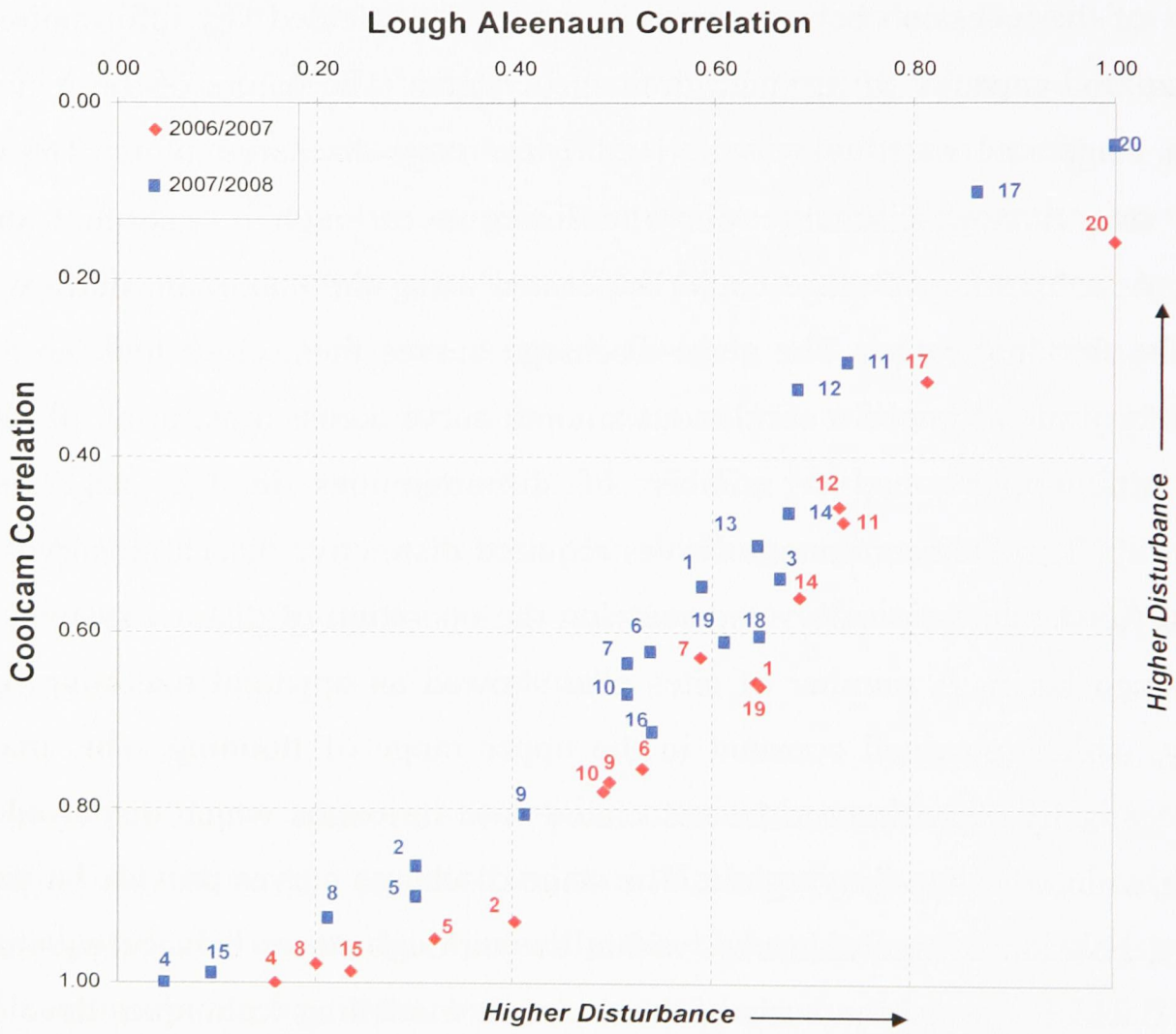


Figure 12.1: A plot of correlation with Lough Aleenaun versus the corresponding correlation with Coolcam for each turlough for the 2006/2007 and 2007/2008 hydrological years

At one end are turloughs with a strongly seasonal characteristic regime composed of single long duration flood events with gentle rising and recession hydrograph limbs. At the other end lie turloughs which display a multimodal flooding regime characterised by rapid responses to rainfall events and highly fluctuating water levels throughout the year. Autocorrelation of turlough water level revealed the seasonality of turlough flooding associated with the annual recharge cycle of the aquifer. Again, a continuum of behaviour was identified from metrics based upon the stage

correlogram, with decorrelation lag times ranging from 3 to 61 days. Smoother correlograms, with high decorrelation lag times, were found to be indicative of a long duration, low frequency flooding regime. More responsive turloughs showed far more variability in autocorrelation slope, with corresponding lower decorrelation lag times. The memory effect in the system in response to rainfall events was quantified using autocorrelation of the net flow time series and cross correlation with precipitation records. Frequency analysis of turlough water level time series again showed the continuum of turlough hydrological behaviour. The dominant frequency in turloughs characterised by unimodal flooding regimes was that of the annual flooding pattern. In contrast, turloughs showing multimodal flooding regimes had a more even distribution of energy across the frequency spectrum, with clearly defined peaked of comparable magnitude.

12.2. Hydrological Modelling

Two hydrological modelling methodologies were successfully developed for predicting turlough water levels, flood duration and extent from historic rainfall and evapotranspiration records. The first model, the aggregated rainfall model, used linear regression to predict turlough volume from aggregated (summed) rainfall over a defined interval. This model showed that between 49.3 and 93.4% of the variability in daily turlough volume could be predicted from rainfall data when soil moisture deficit effects were included (mean 81.6%, median 87.7%). This technique produced three characteristic hydrological parameters for each turlough which allowed the comparison of turlough hydrological behaviour based on quantitative recorded data rather than qualitative descriptions. The aggregation period $\boldsymbol{T}$ provided an indicator of the memory of the system, and so an indirect measure of flood duration. Aggregation periods ranged from a low of only 10 days to 176 days, again showing the continuum present in turlough hydrological behaviour. The storage capacity $\boldsymbol{S}$ defined the volume of water required to have built up in the karst flow system before flooding occurs in the turlough basin. This parameter was indicative of the storage within the karst aquifer; values ranging from around 6000 m^3 to almost 700000m^3 were identified. The final parameter, the contributing area $\boldsymbol{\alpha}$, defined the minimum magnitude of the zone of contribution and so provides a lower limit for the required

catchment area. This is the minimum topographic area required to supply the recorded water volume within the turlough, and varied from 0.77 to 13km^2.

The second modelling methodology used a refined version of the reservoir modelling technique to predict volume using rainfall and evapotranspiration as input. This approach again conceptualised the turlough as a reservoir with the same physical characteristics as the turlough being modelled (stage-volume-area relationships). However, this method used a set of characteristic hydraulic equations governing turlough flow to calculate daily changes in water volume. This method was used for a subset of 8 turlough sites spread across the continuum of turlough hydrological regimes. Daily inflow was defined as a function of rainfall, a notional contributing area and an inflow hydrograph. The notional catchment areas used in the reservoir models were on average 2.6 times greater than their equivalents in the aggregated rainfall model, and varied from 2.1km^2 to 6.4km^2. Outflow was defined using the characteristic stage-discharge curve identified earlier in this thesis. The model outputs well represented the recorded water levels, showing an average efficiency of 91%, an increase over the aggregated rainfall method of 4%.

12.3. Conceptual Model

The interpretation of the inflow and outflow time series used in the reservoir modelling procedure is dependent upon the hydrological functioning of the turlough. This functioning can be described using two conceptual models: the flow – through model and the surcharged tank model. In the first scenario, the flow time series represent the actual flows which occur within the turlough at each time step. In the second scenario, rather than representing actual movement of groundwater through the turlough, the flow time series indirectly represent the relative heads within both the turlough and the underlying and surrounding karst flow system.

12.3.1. Flow-Through Model

The simplest interpretation of this reservoir model configuration is that of a flow-through system, with both inflow and outflow occurring simultaneously within the turlough basin (Figure 12.2). In this case, groundwater inflow and outflow would

occur independently at distinct points within the turlough basin. Hence there is no continuous conduit shown passing beneath the turlough which would enable potential inflow to bypass the turlough. Inflow could be derived from a number of sources: direct rainfall, surface runoff, epikarst flow, conduit driven inflow or a combination of some or all of these. Some sources of inflow would act independently of the water level within the turlough, such as direct rainfall and overland flow. Others would be a function of turlough water level, such as shallow groundwater flow entering the turlough from the epikarst. At low water levels a gradient would exist into the turlough thus producing inflow. As the turlough water level rises, sections of the epikarst would become inundated and potentially cease its contribution. It is feasible that the gradient could potentially reverse with floodwater entering the storage within the epikarst, similar to bank storage within rivers. Also, the discharge rate from a conduit system terminating within the turlough basin would vary depending upon the head driving it as well as the head within the turlough. In this conceptual model the inflow time series represents the cumulative effect of all systems supplying floodwater to the turlough.

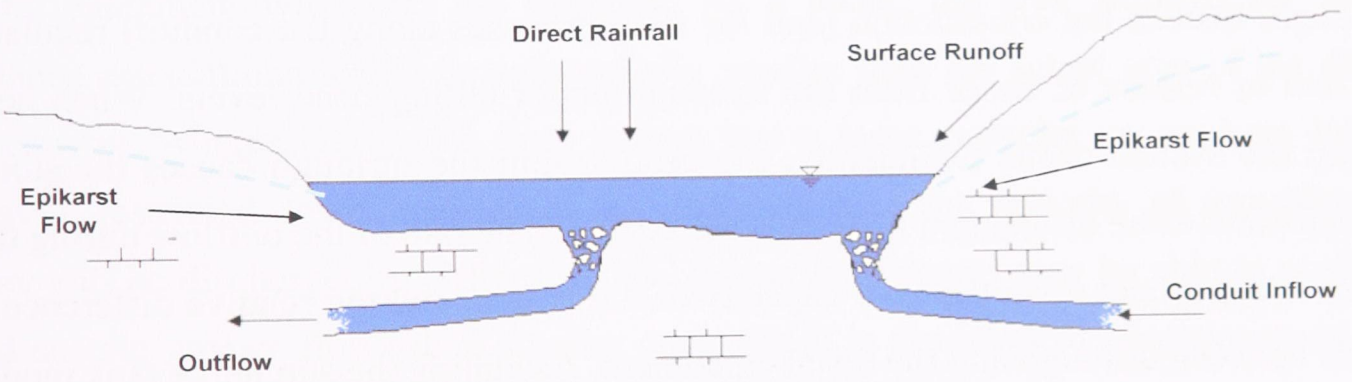


Figure 12.2: Conceptual model for the flow-through turlough system

Turlough discharge occurs in isolation from the inflow points, and may take the form of conduits, fractures or a combination of both. In this case, the outflow time series as defined by the stage - discharge curve, quantifies the cumulative capacity of all modes of outflow. It follows that in such a system there would be a constant flow of groundwater through the turlough, with a lower residence time than that of the surcharged tank model.

12.3.2. Surcharged Tank

The second conceptual model would be that of a surcharged tank, analogous to a tank in a plumbing system, where the volume response in the turlough is dependent upon the relative heads in the turlough and underlying karst flow system (Figure 12.3). In this model the turlough acts as overflow storage for the underlying karst flow network, essentially accumulating excess groundwater that cannot be accommodated due to insufficient capacity. The single conduit shown in Figure 12.3 may represent an actual conduit, a conduit system or an area of interconnected fractures. Two catchments are defined in the model. The first is the distal catchment area, which drains via the conduit system beneath the turlough. The interaction between this system and the turlough is a function of the relative heads within both. The second is the local topographic catchment of the turlough itself, which supplies water to the turlough via direct rainfall, surface runoff and shallow groundwater flow independent of the turlough water level. Rainfall on the distal catchment enters the turlough via the conduit flow system, the capacity of which is controlled by the restriction.

During normal recession periods, flow through the conduit system does not enter the turlough. Instead the constriction (and /or friction losses along the conduit) regulates the rate of release of water from the turlough under falling head levels. When head within the system drops sufficiently, the head within the turlough causes the stored groundwater to be discharged back into the system. The rate of the outflow during this phase is dependent upon the flow capacity of the system and the relative difference in heads between turlough and the distal catchment. Assuming the surcharge tank model, there is no outflow from the turlough during filling periods, and little inflow into the turlough during recession periods. There will still be inflow into the turlough due to direct rainfall, surface runoff and diffuse shallow groundwater flow from the areas immediately surrounding the turlough but in this scenario the net flow approximates actual turlough flow.

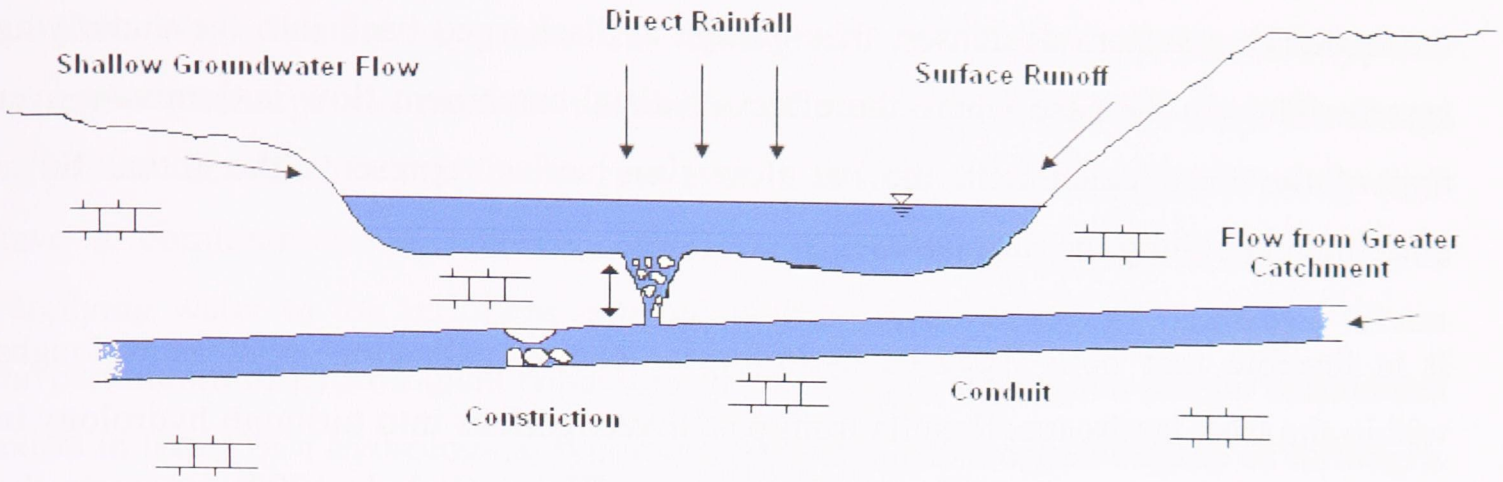


Figure 12.3: Conceptual model for turlough operation as a surcharged tank

Under this model, the proportion of distal catchment recharge entering the turlough depends upon the flow configuration and capacity of the system. The groundwater flow generated from the distal catchment is divided between that which enters the turlough and that which bypasses it. If the distal catchment is large but has a relatively unrestricted flow system, then only a small fraction of the recharge generated from the distal catchment will enter the turlough. As a result, the area required for water balance calculations would be substantially smaller than the actual area of the distal catchment. Alternatively, if a flow system has a large capacity up gradient but is heavily restricted down gradient of the turlough, then the majority of groundwater flow will be discharged into the turlough. Larger catchments may be able to produce and sustain greater flows than smaller ones, but it is the level of constriction in the system and the nature of the hydraulic connections with the turlough that governs the effect this has upon a turlough's hydrological regime. Thus, (outflow) constriction is a determining factor in the hydrological behaviour of turloughs. The constriction itself could be due to a localised narrowing of the conduit or an effective constriction as a result of longer conduit head losses.

With regard to the notional inflow and outflow time series, the outflow is signified by the head within the turlough in terms of the outflow that would occur during full recession given the water level. The inflow time series characterises changes in head within the underlying system as well as the contribution of direct sources of recharge. The balance between hypothetical inflow and outflow controls the rate of filling and

emptying. When there is a gradient into the turlough, i.e. inflow is greater than outflow, the volume stored within the turlough basin increases. When the head within the underlying system decreases, this storage is discharged back into the underlying system. Thus in the case where the effect of distal catchment flow is dominant over that of the local catchment, the net flow time series represents the actual flows entering and exiting the turlough.

It is feasible that both types of hydrological conceptualisation exist as turloughs within the Irish landscape. Results from past investigations into turlough hydrology in the Gort lowlands area (Gill, 2010; Southern Water Global, 1998) supports the surcharge tank model. These studies concluded that the system in this area operated on the basis of a significant conduit system with surcharged tanks, and pipe network modelling based on this idea gave a good simulation of turlough hydrological behaviour. Physical evidence for the surcharge tank model can be seen in turloughs such as Lough Coy, where large estevelles have been witnessed operating in response to the conditions present in the underlying conduit system.

However, the Gort-Kinvarra system consists of exceptionally well-developed conduit systems and large catchment areas in comparison to the majority of other Irish karst systems. Instead, most turloughs form part of much smaller karst flow systems. Evidence for the flow-through conceptual model has been identified during this research. In Lough Aleenaun, groundwater has been observed simultaneously rising and sinking at separate points within the turlough basin, suggesting a flow through system. In this case, the capacity of mechanisms supplying water to the turlough basin exceed those the drain it, and so flooding occurs. Another potential flow-through system was identified in Lough Gealain turlough where a large spring flowed into the northeast corner of the turlough basin. The source of this spring lay above the high water mark of the turlough and so the turlough water level had no influence on the inflow rate.

The sites named above may represent the pure, 'type' examples of each system model, but it is equally likely that many turloughs are a complex combination of both modes of functioning. Obvious evidence of groundwater simultaneously entering and exiting the turlough was not found at other study sites, but that is not to say that it is

not occurring. However, it is difficult to envisage the hydraulic conditions required to support a purely diffuse, phreatic flow-through groundwater system within the epikarst. While water may enter the turlough in this manner, it is unlikely that turloughs discharge via phreatic pathways, given the nature of the stage-discharge behaviour identified in this thesis. However, it is likely that a number of study sites have a combination of relatively shallow pathways (phreatic and/or confined) supplying water to the turloughs coupled with confined discharge pathways. Given the continuum of hydrological behaviour, the results indicate that a similar continuum exists in terms of a hydrological typology. Thus the hydrological regime of turloughs should be considered in light of this continuum rather than in relation to discrete groupings.

In order to determine the precise hydrological operation of individual turloughs, further research is required which could help to elucidate this aspect of turlough hydrology, such as the indirect estimation of flows within turlough basins, detailed hydrochemical investigations and/or tracing into turloughs during both the filling period and recession phase.

12.4. Hydroecology

Turloughs are groundwater features as well as wetlands and as such are classified as Groundwater Dependent Terrestrial Ecosystems (GWDTEs) under the Water Framework Directive (2000/60/EC), and as a Priority Habitat in Annex 1 of the EU Habitats Directive (92/43/EEC). Both EU directives necessitate the monitoring and management of these habitats to ensure that favourable conservation and groundwater status is achieved. This requirement led the National Parks and Wildlife Service (NPWS) to commission a multidisciplinary project entitled "Assessing the Conservation Status of Turloughs". The purpose of this project was to provide a greater understanding of the structures and functions of turloughs as GWDTEs, and to define and quantify linkages between hydrology and the characteristic ecology, and so provide a more comprehensive understanding of the pressures on these ecosystems. Characterising the intrinsic behaviour of turloughs both hydrologically and ecologically and identifying linkages between various hydrological and ecological parameters will allow the risks posed to these protected habitats to be evaluated.

The behaviour of a turlough as a wetland is fundamentally driven by its hydrology, with the hydrological regime resulting in a characteristic ecology associated with the pattern of groundwater inundation. The secondary aim of the research described in this thesis was to apply this new found understanding of turlough hydrodynamics and hydrology, through the development of hydroecological indicators, in order to explain aspects of this characteristic ecology associated with turlough flooding.

The "Assessing the Conservation Status of Turloughs" multidisciplinary project generated four ecological datasets: vegetation, aquatic invertebrates, hydrochemistry and phytoplankton, and soil nutrients. The nature and resolution of each ecological dataset was assessed to enable the identification of novel hydrological indicators representing the various aspects of turlough hydrological behaviour. A range of indicators were derived from water level, volume and area time series, while others emerged from the digital terrain and hydrological modelling processes. The undifferentiated continuum of hydrological behaviour was reflected in an equally undifferentiated range of hydrological indicator values, such as the range of flood durations within and between turloughs. The use of the hydrological indicators developed in this thesis provided an important tool with which to interpret the characteristic ecology associated with the turlough habitat. The continuum of hydrological behaviour is reflected in the continuum of ecological indicators, and the non-uniqueness of the turlough ecology, hence the difficulty in determining discrete ecological typologies for turloughs and corresponding risk assessment strategies.

12.5. Recommendations

12.5.1. Further Investigations

The primary objective of this thesis was the characterization of turlough hydrodynamics and hydrological regime across a broad set of turlough sites. As a reconnaissance study, there were limitations to the level of investigation outside of pure hydrology that could be applied. More focused studies of individual sites using a broad range of investigation techniques, such as tracing, geophysics and exploratory boreholes, could confirm the nature of the conceptual model proposed here. Further measurements of groundwater levels in the areas surrounding turloughs could clarify the nature of the contribution made by the topographic area, and possibly differentiate the contribution of topographic (proximal) catchment from the larger (distal) catchment. Detailed correlation with appropriate hydrochemical data could similarly serve to identify the sources of inflow into the turlough basin, and potentially used in mass balances or mixing models to validate a conceptual model of operation.

12.5.2. Flood Risk Assessment

Turloughs in Ireland have been a focus of continuing research mainly due to the unique flora and fauna in this type of aquatic environment, but also from a more anthropogenic point of view, due to the risks of localised flooding. This flooding can pose significant risk to human health, the environment and economic activity. While the primary focus of the model developed during this study was the generation of hydrological indicators linked to ecological risk criteria, it could be adapted and expanded for use in defining flood risk.

The existing model is constructed from topographic and water-level data from which relationships between water level, volume, area and associated flows are derived. While specific GPS surveys of turloughs have been undertaken to date, the precision of newly available DTM data may be sufficient as a model input – and could be assessed accordingly. As there is insufficient water-level time series to allow direct flood-risk assessment to be made using time-series analysis, existing longer-term rainfall records could be used in combination with the turlough response model already developed. Furthermore, in the absence of monitoring data, relationships

derived between flood indicator species and hydrological regime could be used to classify the nature and extent of flooding at un-gauged sites.

12.5.3. Continued Hydrological Monitoring

It is critical to the development of further understanding of Irish karst systems that the monitoring of turlough sites be continued. The importance of this research is twofold. First, longer-term records at existing monitoring sites could be used to further validate and refine the hydrological models developed during this research, thus improving their predictive quality. By expanding the monitoring to un-gauged sites, the modelling procedure could be applied to a broader set of turloughs and thus to a greater understanding of their distinctive behaviour. Secondly, additional data may help to define the role that subcutaneous or epikarst zone plays in defining a turlough's characteristic flooding regime.

12.5.4. Indirect Flow Measurement

The understanding of turlough temporal flow behaviour could be greatly improved through the use of indirect flow-measurement techniques such as thermal imaging, continuous water-temperature measurements and stable isotope analyses. Thermal imaging, or thermography, could potentially identify both the locations and periods of operation of inflow points within a turlough basin. Carried out on a large scale, thermography could also identify areas of interaction between surface and groundwater in turlough catchment areas. This information would provide invaluable guidance for future research, such as tracing experiments to define turlough zones of contribution. On a local scale, intensive spatial temperature monitoring together with stable isotope analyses would provide a valuable insight into turlough operation and potentially bring clarity to the issue of turlough hydrological operation.

References

Al-fares, W., Bakalowicz, M., Guerin, R., Dukhan, M., 2002. Analysis of the karst aquifer structure of the Lamalou area (Herault, France) with ground penetrating radar. Journal of Applied Geophysics, 51: 97-106.

Allott, N., 1976. An Ecological Study of *Cinclidotus fontinaloides* (Hedw.) P. Beauv. . B.A., (Ed.), (Mod.) Thesis, Trinity College, Dublin.

Atkinson, T.C., 1977. Diffuse flow and conduit flow in limestone terrain in the Mendip Hills, Somerset (Great Britian). Journal of Hydrology, 35: 93-110.

Atkinson, T.C., Smith, D.I., Lavis, J.J., Whitaker, R.J., 1973. Experiments in tracing underground waters in limestones. Journal of Hydrology, 19: 323-349.

Avdagic, I., 1976. Determination of flow through flooded karst poljes by use of poljes and piezometric borehole water levels. In: Yevjevich, V. (Ed.), Karst Hydrology and Water Resources: Vol. 1 Karst Hydrology. Water Resources Publications, Colorado, pp. 341-354.

Baedke, S.J., Krothe, N.C., 2000. Quantitative tracer test of the Beech Creek aquifer at the Ammunition Burning Grounds, Naval Surface Warfare Centre, Crane, Indiana. In: Sasowsky, I.D., Wicks, C.M. (Eds.), Groundwater Flow and Contaminant Transport in Carbonate Aquifers. A.A. Balkema, Rotterdam, pp. 15 - 30.

Baertschi, P., 1976. Absolute 18O content of Standard Mean Ocean Water. Earth and Planetary Science Letters, 31(3): 341-344.

Bailly-Comte, V., Jourde, H., Roesch, A., Pistre, S., Batiot-Guilhe, C., 2008. Time series analyses for Karst/River interactions assessment: Case of the Coulazou river (Southern France). Journal of Hydrology, 349: 98-114.

Bakalowicz, M., 2005. Karst groundwater: a challenge for new resources. Hydrogeology Journal, 13: 148 - 160.

Banks, D., Davies, C., Davies, W., 1996. The Chalk as a karstic aquifer: evidence from a tracer test at Stanford Dingley, Berkshire, UK. Quarterly Journal of Engineering Geology, 28: S31 - S38.

Bechtel, T.D., Bosch, F.P., Gurk, M., 2007. Geophysical methods. In: Goldscheider, N., Drew, D. (Eds.), Methods in Karst Hydrogeology. Taylor & Francis, pp. 171-200.

Benischke, R., Goldscheider, N., Smart, C., 2007. Tracer techniques. In: Goldscheider, N., Drew, D. (Eds.), Methods in karst hydrogeology. Taylor & Francis, pp. 147-170.

Beven, K.J., 2000. Rainfall-runoff modelling - The primer. John Wiley and Sons, Chichester.

Birk, S., Liedl, R., Sauter, M., 2004. Identification of localised recharge and conduit flow by combined analysis of hydraulic and physico-chemical spring responses (Urenbrunnen, SW-Germany). Journal of Hydrology, 286: 179-193.

Black, T.J., 1997. Evaporite karst of the northern lower peninsula of Michigan. Carbonates and Evaporites, 12: 81-83.

Blackstock, T.H., Duigan, C.A., Stevens, D.P., Yeo, M.J.M., 1993. Vegetation zonation and invertebrate fauna in Pant-y-Llyn, an unusual seasonal lake in South Wales, U.K. Aquatic Conservation: Marine and Freshwater Ecosystems, 3: 253-268.

Bogle, F.R., Loy, K., 1995. The application of thermal infrared photography in the identification of submerged springs in Chickamaugua Reservoir, Hamilton County, Tennessee. In: Beck, B.F. (Ed.), Fifth Multidisciplinary Conference on Sinkholes and the Engineering and Environmental Impacts of Karst, Gatlinburg, Tennessee, pp. 415-424.

Boland, H., Crowe, O., Walsh, A., 2008. Irish Wetland Bird Survey: Results of waterbird monitoring in Ireland in 2006/07. Irish Birds, 8: 341-350.

Bonacci, O., 1982. Specific hydrometry of karst regions, Advances in Hydrometry. IAHS publication 134, Exeter, pp. 321-333.

Bonacci, O., 1987. Karst hydrology: with special reference to the Dinaric karst. Springer-Verlag, Berlin.

Bonacci, O., 1993. Karst spring hydrographs as indicators of karst aquifers. Hydrological Sciences, 38(1): 51-62.

Bonacci, O., Bojanic, D., 1991. Rhythmic karst springs. Hydrological Sciences Journal, 36(1): 35-47.

Bond, K.G.M., 1997. Insect survey Lepidoptera. In: Southern Water Global and Jennings O'Donovan and Partners, Editor, An Investigation of the Flooding Problems in the Gort–Ardrahan Area of South Galway, Ecology Baseline Study Vol. II, The Office of Public Works, Dublin.

Boussinesq, J., 1904. Recherches theoretiques sur l'ecoulement des nappes d'eau infiltrees dans le sol et sur le debit des sources. Journal de Mathematiques Pures et Appliquees, 10: 5-78.

Box, G.E.P., Jenkins, G.M., Reinsel, G.C., 2008. Time Series Analysis: Forecasting and Control. Wiley.

Briggs, I.C., 1974. Machine contouring using minimum curvature. Geophysics, 39(1): 39-48.

Butscher, C., Huggenberger, P., 2007. Implications for karst hydrology from 3D geological modeling using the aquifer base gradient approach. Journal of Hydrology, 342(1-2): 184-198.

Byrne, R.A., Reynolds, J.D., 1982. Preliminary notes on a doline in Lough Gealain, the Burren, Co. Clare. Irish Naturalists` Journal, 20: 375-377.

Casanova, M.T., Brock, M.A., 2000. How do depth, duration and frequency of flooding influence the establishment of wetland plant communities? Plant Ecology, 147(237 - 250).

Chatfield, C., 1989. The Analysis of Time Series. Chapman and Hall London.

Cheng, J.M., Chen, C.X., 2005. An integrated linear/non-linear flow model for the conduit-fissure-pore media in the karst triple void system. Environmental Geology, 47: 163-174.

Clark, I., Fritz, P., 1997. Environmental Isotopes in Hydrogeology. Lewis Publishers, Boca Raton.

Cooley, J.W., Tukey, J.W., 1965. An Algorithm for the Machine Computation of the Complex Fourier Series. Mathematics of Computation, 19: 297-301.

Coxon, C.E., 1986. A Study of the hydrology and geomorphology of turloughs. Ph.D. (unpublished) Thesis, Department of Geography, Trinity College Dublin.

Coxon, C.E., 1987. The spatial distribution of turloughs. Irish Geography, 20 11-23.

Coxon, C.E., 1987b. An examination of the characteristics of turloughs using multivariate statistical techniques. Irish Geography, 20: 24-42.

Coxon, C.E., Coxon, P., 1994. Carbonate deposition in turloughs (seasonal lakes) on the western limestone lowlands of Ireland. II: The sedimentary record. Irish Geography, 27(1): 28-35.

Coxon, C.E., Drew, D.P., 1986. Groundwater flow in the lowland limestone aquifer of eastern Co. Galway and eastern Co. Mayo western Ireland. In: Paterson, K., Sweeting, M.M. (Eds.), New Directions in Karst. Geo Books, Norwich, United Kingdom, pp. 259-279.

Coxon, C.E., Drew, D.P., 1998. Interaction of surface water and groundwater in Irish karst areas: implications for water resource management In: Brahana, J.V., Eckstein, Y., Ongley, L.K., Schneider, R., Moore, J.E. (Eds.), Gambling with Groundwater - Physical, Chemical and Biological Aspects of Aquifer-Stream Relations. American Institute of Hydrology, St. Paul, Minnesota, pp. 161-168.

Coxon, C.E., Drew, D.P., 2000. Interdependence of groundwater and surface water in lowland karst areas of western Ireland: management issues arising from water and contaminant transfers. . In: Robins, N.S., Misstear, B.D. (Eds.), Groundwater in the celtic regions: Studies in Hard Rock and Quaternary Hydrology. The Geological Society of London, London, United Kingdom, pp. 81-88.

Coxon, P., McMorrow, S., Coxon, C., Nolan, T., 2005. Pollnahallia: A Tertiary palaeosurface and a glimpse of Ireland's pre-Pleistocene landscape. In: Coxon, P. (Ed.), The Quaternary of Central Western Ireland: Field Guide. Quaternary Research Association, London, pp. 79-100.

Craig, H., 1961. Isotopic variations in meteoric waters. Science, 133: 1702-1703.

Cressie, N.A.C., 1991. Statistics for Spatial Data. John Wiley & Sons, New York.

D'Arcy, G.H., 1983. Post-drainage Assessments of Impacts on a Part of the River Clare Catchment, County Galway. M.Sc. Thesis, Trinity College, Dublin.

Davis, F.W., 1990. Modeling vegetation pattern using digital terrain data. Landscape Ecology, 4(1): 69 - 80.

Deakin, J., 2000. Groundwater protection zone delineation at a large karst spring in western Ireland. In: Robins, N.S., Misstear, B. (Eds.), Groundwater in the Celtic Regions: Studies in Hard Rock and Quaternary Hydrogeology. British Geological Society, London, pp. 89-98.

Denic-Jukic, V., Jukic, D., 2003. Composite transfer functions for karst aquifers. Journal of Hydrology, 274(1-4): 80-94.

Diefendorf, A.F., Patterson, W.P., 2005. Survey of Stable Isotope values in Irish surface waters. Journal of Paleolimnology, 34: 257 - 269.

Draper, N., Smith, H., 1981. Applied Regression Analysis. Wiley-Interscience.

Dreiss, S.J., 1982. Linear Kernels for karst aquifers. Water Resources Research, 18(4): 865-876.

Dreiss, S.J., 1989. Regional Scale Transport in a Karst Aquifer 2, Linear Systems and Time Moment Analysis. Water Resources Research, 25(1): 126-134.

Drew, D., 1990. The Hydrology of the Burren, Co. Clare. Irish Geography, 23(2): 69-89.

Drew, D., 2008. Hydrogeology of lowland karst in Ireland. Quarterly Journal of Engineering Geology and Hydrogeology, 41: 61 - 72.

Drew, D., Burke, A.M., Daly, D., 1996. Assessing the extent and degree of karstification in Ireland. In: Rozkowski, A. (Ed.), International Conference on Karst Fractured Aquifers - Vulnerability and Sustainability, University of Silesia, Katowice-Ustron, Poland, pp. 37-47.

Drew, D., Chance, H., 2007. The Hydrogeology of Karst Springs in the Republic of Ireland. Irish Groundwater Newsletter, 46: 13-14.

Drew, D., Daly, D., 1993. Groundwater and Karstification in Mid-Galway, South Mayo and North Clare, RS 93/3 (groundwater). Geological Survey of Ireland, Dublin, Republic of Ireland.

Drew, D., Hotzl, H. (Eds.), 1999. The management of karst environments. Karst Hydrogeology and Human Activities, Impacts, Consequences and Implications. International Association of Hydrogeologists, Balkema, Rotterdam.

Drew, D., Jones, G.L., 2000. Post-Carboniferous pre-Quaternary karstification in Ireland. Proceedings of the Geologists Association, 111: 345-353.

Drew, D.P., 1976. Hydrology of the north Co. Galway - south Co. Mayo lowland karst area, western Ireland, Proceedings of the 6th International Conference of Speleology, Prague, pp. 57-61.

Drew, D.P., Coxon, C.E., 1988. The effects of land drainage on groundwater resources in karstic areas of Ireland. In: Yuan Daoxian, Editor, Proceedings of the 21st I.A.H. Congress, Geological Publishing House, Beijing, China, pp. 204–209.

Dreybrodt, W., 1990. The role of dissolution kinetics in the development of karst aquifers in limestone: a model simulation of karst evolution. Journal of Geology, 98: 639-655.

Dreybrodt, W., 1992. Dynamics of karstification: a model applied to hydraulic structures in karst terranes. Applied Hydrogeology, 3: 20-32.

Dreybrodt, W., 1996. Principles of Early Development of Karst Conduits Under Natural and Man-Made Conditions Revealed by Mathematical Analysis of Numerical Models. Water Resources Research, 32(9): 2923-2935.

Drogue, C., 1972. Statistical Analysis of Hydrographs of Karst Springs. Journal of Hydrology, 15: 49-68.

Duigan, C.A., Frey, D.G., 1987. Eurycercus glacialis, a chydorid cladoceran new to Ireland. Irish Naturalists' Journal 22(5): 180-183.

Einsiedl, F., 2005. Flow system dynamics and water storage of a fissured-porous karst aquifer characterized by artificial and environmental tracers. Journal of Hydrology, 312(1-4): 312-321.

Eisenlohr, L., Kiraly, L., Bouzelboudjen, M., Rossier, Y., 1997. Numerical simulation as a tool for checking the interpretation of karst spring hydrographs. Journal of Hydrology, 193: 306-315.

Feeney, R., 2007. Mapping Turlough Vegetation, Msc. Thesis, Trinity College Dublin.

Fetter, C.W., 2001. Applied Hydrogeology. Prentice Hall.

Field, M.S., 1993. Karst Hydrology and chemical contamination. Journal of Environmental Systems, 22: 1-26.

Filipponi, M., Jeannin, P.Y., Tacher, L., 2009. Evidence of inception horizons in karst conduit networks. Geomorphology, 106: 86-99.

Fleury, P., Bakalowicz, M., de Marsily, G., 2007a. Submarine springs and coastal karst aquifers: A review. Journal of Hydrology, 339(1-2): 79-92.

Fleury, P., Plagnes, V., Bakalowicz, M., 2007b. Modelling of the functioning of karst aquifers with a reservoir model: Application to Fontaine de Vaucluse (South of France). Journal of Hydrology, 435: 38-49.

Ford, D., 1997. Principal features of evaporite karst in Canada. Carbonates and Evaporites, 12(1): 15-23.

Ford, D., Williams, P., 2007. Karst Hydrogeology and Geomorphology. Wiley & Sons, Chichester, England.
Fossitt, J.A., 2000. A guide to habitats in Ireland. The Heritage Council, Kilkenny.
Gale, S.J., 1984. The hydraulics of conduit flow in carbonate aquifers. Journal of Hydrology, 70: 309-327.
Gat, J.R., 1995. Stable isotopes of fresh and saline lakes. In: Lerman, A., Imboden, D.M., Gat, J.R. (Eds.), Physics and Chemistry of Lakes. Springer, Berlin, pp. 139-165.
Gill, L., 2010. Modelling a network of turloughs. PhD Thesis, Trinity College Dublin.
Golden Software Inc, 2002. Surfer 8 User Guide: contouring and surface mapping for scientists and engineers. Golden Software Inc., Colorado.
Goldscheider, N., Andreo, B., 2007. The geological and geomorphological framework. In: Goldscheider, N., Drew, D. (Eds.), Methods in karst hydrogeology. IAH international contributions to hydrogeology Taylor & Francis, pp. 9-24.
Goldscheider, N., Bechtel, T.D., 2009. Editors message: The housing crisis from underground - damage to a historic town by geothermal drillings through anhydrite, Staufen, Germany. Hydrogeology Journal, 17(3): 491-293.
Goldscheider, N., Drew, D. (Eds.), 2007. Methods in karst hydrogeology. International contibutions to hydrogeology, 26. Taylor & Francis.
Gonfiantini, R., 1986. Environmental isotopes in lake studies. In: Fritz, P., Fontes, J.C. (Eds.), Handbook of environmental isotope geochemistry, Volume 2: The Terrestrial Environment. Elsevier, Amsterdam, pp. 113-168.
Good, J.A., 1997. Soil/Ecotonal Invertebrates. In: Partners, S.W.G.a.J.O.D.a. (Ed.), An Investigation of the Flooding Problems in the Gort-Ardrahan Area of South Galway. Ecology Baseline Study, Vol. I. The Office of Public Works, Dublin, pp. 221-249.
Goodwillie, R., 1992. Turloughs over 10 hectares: Vegetation survey and evaluation, Unpublished report for the National Parks and Wildlife Services, Office of Public Works, Dublin.
Goodwillie, R., 2001. Materials for an Action Plan for the priority habitat Turloughs. Draft Report for National Parks and Wildlife, Duchas, Dublin.
Goodwillie, R., 2003. Vegetation of turloughs. In: Otte, M.L. (Ed.), Wetlands of Ireland, Distribution, ecology, uses and economic value. University College Dublin Press, Dublin, pp. 135-144.
Goodwillie, R., Reynolds, J.D., 2003. Turloughs. In: Otte, M.L. (Ed.), Wetlands of Ireland: Distribution, ecology, uses and economic value. University College Dublin Press, Dublin, pp. 130-134.
Grasso, D.A., Jeannin, P.-Y., Zwahlen, F., 2003. A deterministic approach to the coupled analysis of karst springs' hydrographs and chemographs. Journal of Hydrology, 271(1-4): 65-76.
Groves, C.G., 2007. Hydrological Methods. In: Goldscheider, N., Drew, D. (Eds.), Methods in Karst Hydrogeology. IAH international contributions to hydrogeology Taylor & Francis, pp. 45-64.
Groves, C.G., Howard, A.D., 1994. Early development of karst systems: 1. Preferential flow path enlargement under laminar flow. Water Resources Research, 30(10): 2837-2846.
GSI, 2011. Karst Database. Geological Survey of Ireland.

Guion, P.D., Gutteridge, P., Davies, S.J., 2000. Carboniferous sedimentation and volcanism on the Laurussian margin. In: Woodcock, N., Strachan, R. (Eds.), Geological history of Britain and Ireland, Blackwell Science, pp. 227-270.

Gunn, J., 1983. Point-recharge of limestone aquifers - a model from New Zealand karst. Journal of Hydrology, 61: 19-29.

Gunn, J., 1986. Solute processes and karst landforms. In: Trudgill, S.T. (Ed.), Solute Processes. Wiley & Sons, pp. 363-403.

Gunn, J., 2010. Is the term 'Karst Aquifer' misleading? In: Andreo, B., Carrasco, F., Duran, J.J., LaMoreaux, J.W. (Eds.), Advances in research in karst media. Springer, pp. 57-62.

Habib, E., Krajewski, W.F., Kruger, A., 2001. Sampling errors of tipping-bucket rain gauge measurements. Journal of Hydrologic Engineering, 6(2): 159-166.

Halihan, T., Sharp, J.M., Mace, R.E., 2000. Flow in the San Antonio segment of the Edwards aquifer: matrix, fractures or conduits? In: Sasowsky, I.D., Wicks, C.M. (Eds.), Groundwater Flow and Contaminant Transport in Carbonate Aquifers. A.A. Balkema, Rotterdam, pp. 129-146.

Halihan, T., Wicks, C.M., 1998. Modeling of storm responses in conduit flow aquifers with reservoirs. Journal of Hydrology, 208: 82-91.

Hardwick, P., Gunn, J., 1995. Landform - groundwater interactions in the Gwenlais karst, South Wales. In: Brown, A.G. (Ed.), Geomorphology and Groundwater. John Wiley, New York, pp. 75-91.

Hardy, R.L., 1990. Theory and applications of the Multiquadratic-Biharmonic Method. Computers and Mathematics with Applications, 19(8/9): 163 - 208.

Heesom, D., Mahdjoubi, M., 2001. Effect of Grid Resolution and Terrain Characteristics on Data from DTM. Journal of Computing in Civil Engineering, 15(2): 137-143.

Hickey, C., 2003. Recent Developments in Mapping of Karst systems using Microgravity, Geological Survey of Ireland Groundwater Newsletter, pp. 22-25.

Hickey, C., 2009. An understanding of the workings of lowland karst Hydrogeology in Ireland using Roscommon as an example. PhD Thesis, Trinity College Dublin.

Jannsen, P.H.M., Heuberger, P.S.C., 1995. Calibration process-oriented models. Ecological Modelling, 83: 55-66.

Jeannin, P.Y., 2001. Modeling flow in phreatic and epiphreatic karst conduits in the Holloch cave (Muotatal, Switzerland). Water Resources Research, 37: 191-200.

Jeannin, P.Y., Groves, C.G., Hauselmann, P., 2007. Speleological investigations. In: Goldscheider, N., Drew, D. (Eds.), Methods in karst hydrogeology. IAH international contributions to hydrogeology Taylor & Francis.

Jocque, M., Riddoch, B.J., Brendonck, L., 2007. Successional phases and species replacements in freshwater rock pools: towards a biological definition of ephemeral systems. Freshwater Biology, 52: 1734-1744.

Johnston, P.M., Peach, D., 1999. Hydrological modelling of the flows in the karst limestones of the Gort Lowlands, Proceedings of the Annual Irish Association of Hydrogeologists Symposium, Tullamore, Co. Offaly, Ireland.

Jukic, D., Denic-Jukic, V., 2005. Nonlinear kernel functions for karst aquifers. Journal of Hydrology, 328: 360-374.

Karst Working Group, 2000. The Karst of Ireland, Limestone Landscapes, Caves and Groundwater Drainage Systems. Geological Survey of Ireland, Dublin.

Kavanagh, B.F., 2009. Surveying: principles and applications. Pearson Prentice Hall, London.

Kennie, T.J.M., Petrie, G., 1990. Introduction to terrain modelling - application fields and terminology. In: Kennie, T.J.M., G.Petrie (Eds.), Terrain modelling in surveying and civil engineering. Whittles Publishing, Latheronwheel, Caithness, pp. 1-3.

Kilroy, G., Coxon, C., Allott, N., Rybaczuk, K., 2001. The contribution of groundwater phosphorus to surface water eutrophication in Ireland. In: Griebler, C., Danielpol, L., Gibert, J., Nachtnebel, M.P., Notenboom, J. (Eds.), A Tool for Management of Water Resources. Office of Official Publications of the European Communities, Luxembourg, pp. 343-349.

Kimberley, S., 2007a. Habitats Directive Conservation Assessment Report, Trinity College Dublin.

Kimberley, S., 2007b. Spatial and temporal fluxes of plant nutrients in turlough soils. PhD Thesis, Department of Botany, Trinity College, Dublin.

Klimchouk, A.B., 1992. Large gypsum caves in the Ukraine and their genesis. Cave Science, 19: 3-13.

Kovacic, G., 2010. An attempt towards an assessment of the Cerknica polje water balance. Acta Carsologica, 39(1): 39-50.

Kovacs, A., Perrochet, P., Kiraly, L., Jeannin, P.Y., 2005. A quantitative method for the characterisation of karst aquifers based on spring hydrograph analysis. Journal of Hydrology, 303: 152-164.

Kovacs, A., Sauter, M., 2007. Modelling karst hydrodynamics. In: Goldscheider, N., Drew, D. (Eds.), Methods in karst hydrogeology. IAH international contributions to hydrogeology 26. Taylor & Francis, pp. 201-222.

Krause, P., Boyle, D.P., Base, F., 2005. Comparison of different efficiency criteria for hydrological model assessment. Advances in Geosciences, 5: 89-97.

Kresic, N., 2007. Hydraulic methods. In: Goldscheider, N., Drew, D. (Eds.), Methods in Karst Hydrogeology. IAH international contributions to hydrogeology 26. Taylor & Francis, pp. 65-92.

Kresic, N., Bonacci, O., 2009. Spring Discharge Hydrograph. In: Kresic, N., Stevanovic, Z. (Eds.), Groundwater Hydrology of Springs: Engineering, Theory, Management and Sustainability. Butterworth-Heinemann, pp. 129-163.

Labat, D., Ababou, R., Mangin, A., 2000a. Rainfall-runoff relations for karstic springs. Part I: convolution and spectral analyses. Journal of Hydrology, 238(3-4): 123-148.

Labat, D., Ababou, R., Mangin, A., 2000b. Rainfall-runoff relations for karstic springs. Part II: continuous wavelet and discrete orthogonal multiresolution analyses. Journal of Hydrology, 238(3-4): 149-178.

Labat, D., Mangin, A., Ababou, R., 2002. Rainfall-runoff relations for karstic springs: multifractal analyses. Journal of Hydrology, 256(3-4): 176-195.

Larocque, M., Mangin, A., Razack, M., Banton, O., 1998. Contribution of correlation and spectral analyses to the regional study of a large karst aquifer (Charente, France). Journal of Hydrology, 205: 217-231.

Lee, J.Y., Lee, K.K., 2000. Use of hydrologic time series data for the identification of recharge mechanism in a fractured bedrock aquifer system. Journal of Hydrology, 229: 190-201.

Li, Z., 1992. Variation of the accuracy of digital terrain modelling with sampling interval. Photogrammetric Record, 14: 113-128.

Lloyd, C.D., Atkinson, P.M., 2001. Assessing uncertainty in estimates with ordinary and indicator kriging. Computers & Geosciences, 27: 929 - 937.

Long, A.J., Derickson, R.G., 1999. Linear systems analysis in a karst aquifer. Journal of Hydrology, 219(3-4): 206-217.

Lopez-Chicano, M., Calvache, M.L., Martin-Rosales, W., Gisbert, J., 2002. Conditioning factors in flooding of karstic poljes - the case of the Zafarraya polje (South Spain). Catena, 49: 331-352.

Lott, D.A., Foster, G.N., 1990. Records of terrestrial coleoptera from wetland sites in 1987, including Stenus glabellus Thomson (Staphylinidae) new to the British Isles. Irish Naturalists' Journal, 23: 280-282.

Lowe, D., 2000. Role of stratigraphic elements in speleogenesis: the speleoinception concept. In: Klimchouk, A.B., Ford, D., Palmer, A.N., Dreybrodt, W. (Eds.), Speleogenesis: evolution of karst aquifers. National Speleological Society, Huntsville, Alabama, pp. 65-76.

Lynn, D.E., Waldren, S., 2001. Morphological variation in populations of *Ranunculus repens* L. (creeping buttercup) from the temporary limestone lakes (turloughs) in the west of Ireland. Annals of Botany, 87: 9-17.

Lynn, D.E., Waldren, S., 2003. The turlough form of *Ranunculus repens*. In: Otte, M.L. (Ed.), Wetlands of Ireland. Distribution, ecology, uses and economic value. University College Dublin Press, Dublin, pp. 157-159.

MacGowran, B., 1985. Phytosociological and ecological studies on turloughs in the west of Ireland. PhD Thesis, Department of Botany, University College, Galway.

Madden, B., Heery, S., 1996. Breeding Waterfowl in South Galway Area. In: Southern Water Global and Jennings O'Donovan and Partners (Eds.), An investigation into the Flooding Problems in the Gort–Ardrahan area of South Galway. Interim Factual Report September 1996. Report to the Office of Public Works, Dublin., Section 11, pp. 48–50.

Madden, B., Heery, S., 1997. Wintering Waterfowl in South Galway Area. In: Southern Water Global and Jennings O'Donovan and partners (Eds.), An investigation into the Flooding Problems in the Gort–Ardrahan area of South Galway. Ecology Baseline, Vol. I. The Office of Public Works, Dublin, pp. 132–208.

Maillet, E., 1905. Essais d'hydraulique souterraine et fluviale.

Maini, A.K., Agrawal, V., 2007. Satellite technology: principles and applications. John Wiley, Chichester.

Marnell, F., 1998. The distribution of the smooth newt Triturus vulgaris L., in Ireland. Bulletin of the Irish Biogeographical Society, 22: 84-96.

Marnell, F., 1999. The distribution of the common frog, Rana temporaria L. in Ireland. Bulletin of the Irish Biogeographical Society, 23: 60-70.

Mayr, C., Lucke, A., Stichler, W., Trimborn, P., Ercolano, B., Oliva, G., Ohlendorf, C., Soto, J., Fey, M., Haberzettl, T., Jannsen, S., Schabitz, F., Schleser, G.H., Wille, M., Zolitschka, B., 2007. Precipitation origin and evaporation of lakes in semi-arid Patagonia (Argentina) inferred from stable isotopes ($d^{18}O$, $d^{2}H$). Journal of Hydrology, 334: 53-63.

McCormac, J.C., 2004. Surveying. John Wiley & Sons, New York, Chichester.

McGrath, R.J., Styles, P., Thomas, E., Neale, S., 2002. Integrated high-resolution geophysical investigations as potential tools for water resource investigations in karst terrain. Environmental Geology, 42: 552-557.

Mitchell, G.F., Ryan, M., 1998. Reading the Irish Landscape. Town House, Dublin.

Mochales, T., Casas, A.M., Pueyo, E.L., Pueyo, O., Roman, M.T., Pocovi, A., Soriano, M.A., Anson, D., 2008. Detection of underground cavities by combining gravity, magnetic and ground penetrating radar surveys: a case study from the Zaragoza area, NE Spain. Environmental Geology, 53: 1067-1077.

Mook, W.G., 2000. Environmental isotopes in the hydrological cycle - principles and applications: Volume 1, Volume 1. UNESCO. International Hydrological Programme (UNESCO-IHP).

Moore, I.D., Grayson, R.B., Ladson, A.R., 1991. Digital terrain modelling: a review of hydrological, geomorphological, and biological applications. Hydrological Processes, 5: 3 - 30.

Morales, T., Fdez. de Valderrama, I., Uriarte, J.A., Antiguedad, I., Olazar, M., 2007. Predicting travel times and transport characterization in karst conduits by analyzing tracer-breakthrough curves. Journal of Hydrology, 334(1-2): 183-198.

Moran, J., Kelly, S., Sheehy Skeffington, M., Gormally, M., 2008. The use of GIS techniques to quantify the hydrological regime of a karst wetland (Skealoghan turlough) in Ireland. Applied Vegetation Science, 11(1): 25 - 36.

Nash, J.E., 1959. Systematic determination of unit hydrograph parameters. Journal of Geophysical Research, 64: 111-115.

Neuman, S.P., De Marsily, G., 1976. Identification of linear systems response by parametric programming. Water Resources Research, 12(2): 253-262.

Ní Bhriain, B., Gormally, M., Sheehy Skeffington, M., 2003. Changes in land use practices at two turloughs, on the east Burren limestones, Co. Galway, with reference to nature conservation Biology and Environment Proceedings of the Royal Irish Academy, 103B(3): 169-176.

Ni Bhriain, B., Sheehy Skeffington, M., Gormally, M., 2002. Conservation implications of land use practices on the plant and carabid beetle communities of two turloughs in Co. Galway, Ireland. Biological Conservation, 105: 81-92.

Nier, A.O., 1950. A redetermination of the relative abundances of the isotopes of carbon, nitrogen, oxygen, argon and potassium. Physical Review, 77: 789-793.

O'Rourke, A., 2009. Effects of flooding disturbance on the diversity of plant communities in turloughs. MSc. Thesis, Trinity College Dublin, Dublin.

O'Mahony, C., 1998. Bat activity and abundance in Coole–Garryland Nature Reserve, Co. Galway. Diploma Thesis, University College Cork, Ireland.

Padilla, A., Pulido-Bosch, A., 1995. Study of hydrographs of karstic aquifers by means of correlation and cross-spectral analysis. Journal of Hydrology, 168: 73-89.

Padilla, A., Pulido-Bosch, A., 2008. Simple procedure to simulate karstic aquifers. Hydrological Processes, 22(12): 1876-1884.

Palmer, A.N., 1991. Origin and morphology of limestone caves. Geological Society of America Bulletin, 103: 1-21.

Panagopoulos, G., Lambrakis, N., 2006. The contribution of time series analysis to the study of the hydrodynamic characteristics of the karst systems: Application on two typical karst aquifers of Greece (Trifilia, Almyros Crete). Journal of Hydrology, 329: 368-376.

Peach, D., Watson, S., Carpenter, C., 1997. Flooding problems in the Gort - Ardrahan area of south Galway: Conceptual model of the hydrogeological regime, (unpublished internal report). Southern Water Global.

Penman, H.L., 1950. Evaporation over the British Isles. Quarterly Journal of of the Royal Meteorological Society, LXXVI(330): 372 - 383.

Pereira, H., 2010. Hydrochemistry and Algal Communities of Turloughs (Karstic Seasonal Lakes). PhD Thesis, Trinity College Dublin.

Pereira, H., Coxon, C., Allott, N., 2009. Turlough water quality and implications for groundwater management, 29th Annual Groundwater Conference - International Association of Hydrogeologists (IAH) Irish Group. International Association of Hydrogeologists, Tullamore.

Plummer, L.N., Busenburg, E., 1982. The solubilities of calcite, aragonite and vaterite in CO_2-H_2O solutions between 0 and 90°C and an evaluation of the aqueous model for the system $CaCO_3$-CO_2-H_2O. Geochimica et Cosmochimica Acta, 46: 1011-1040.

Porst, G., 2009. The Effects of Season, Habitat, Hydroperiod and Water Chemistry on the Distribution of Turlough Aquatic Invertebrate Communities. PhD Thesis, Trinity College Dublin, Dublin.

Porst, G., Irvine, K., 2009a. Distinctiveness of macroinvertebrate communities in turloughs (temporary ponds) and their response to environmental variables. Aquatic Conservation: Marine and Freshwater Systems, 19(4): 456 - 465.

Porst, G., Naughton, O., Gill, L., Johnston, P.M., Irvine, K., 2009. The importance of disturbance for seasonal and inter-annual succession of macroinvertebrates in turloughs.

Pracht, M., Lees, A., Leake, B., Feely, M., Long, B., Morris, J., McConnell, B., 2004. Geology of Galway Bay: a geological description to accompany the Bedrock Geology 1:100,000 Scale Map Series, Sheet 14, Galway Bay. Geological Survey of Ireland.

Praeger, R.L., 1932. The flora of the turloughs: a preliminary note. Proceedings of the Royal Irish Academy, 41(B): 37-45.

Quinlan, J.F., 1989. Groundwater monitoring in karst terranes: recommended protocols, regulatory problems, and implicit assumptions, U.S. Environmental Protection Agency Draft Report, Las Vegas.

Quinlan, J.F., Smart, C., Schindel, G.M., Alexander Jr., E.C., Edwards, K.J., Smith, A.R., 1991. Recommended administrative/regulatory definition of karst aquifer, principles of classificatino of carbonate aquifers, practical evaluation of vulnerability of karst aquifers, and determination of optimum sampling frequency at springs, Proceedings of the Third Conference on Hydrogeology, Ecology, Monitoring, and Management of Groundwater in Karst Terranes, pp. 573-635.

Ray, J.A., 1997. Overflow conduit systems in Kentucky: a consequence of limited underflow capacity. In: Becks, F.B., Stephenson, J.B. (Eds.), The Engineering Geology and Hydrogeology of Karst Terranes. A.A. Balkema, Rotterdam, pp. 69-76.

Regan, E., Sheehy Skeffington, M., Gormally, M., 2007. Wetland plant communities of turloughs in southeast Galway/north Clare, Ireland in relation to environmental factors. Aquatic Botany, 87: 22 - 30.

Reynolds, J.D., 1996b. An investigation of the flooding problems in the Gort–Ardrahan area of South Galway Interim Factual Report September 1996. Report to the Office of Public Works, Dublin. Section 11-4 Invertebrates, pp. 50–59.

Reynolds, J.D., 1997. Invertebrate surveys of S.E. Galway turloughs. Baseline Report. In: Southern Water Global and Jennings O'Donovan and Partners (Eds.), An

Investigation of the Flooding Problems in the Gort–Ardrahan Area of South Galway. Ecology Baseline Study Vol. II. The Office of Public Works, Dublin. pp. 126–141.

Reynolds, J.D., 2003. Fauna of turloughs and other wetlands. In: Otte, M.L. (Ed.), Wetlands of Ireland, Distribution, ecology, uses and economic value. University College Dublin Press, Dublin, pp. 145-156.

Reynolds, J.D., Duignan, C., Marnell, F., O'Connor, A., 1998. Extreme and ephemeral water bodies in Ireland. In: Giller, P.S. (Ed.), Studies in Irish Limnology. Marine Institute, Dublin, pp. 67-99.

Reynolds, J.D., Murphy, M., Connor, A.O., 2004. Early season cladoceran diversity of Atlantic temporary ponds (turloughs). Archives des Sciences, 57: 97-104.

Rodriguez, R., 1995. Mapping karst solution features by the integrated geophysical method. In: Beck, B.F. (Ed.), Karst geohazards. Balkema, Rotterdam, pp. 443-449.

Ryder, J., Moran, R., McDonnell, R.J., Gormally, M., 2005. Conservation implications of grazing practices on the plant and dipteran communities of a turlough in Co. Mayo, Ireland. Biodiversity and Conservation, 14: 186-187.

Sasowsky, I.D., 2000. Carbonate aquifers: a review of thoughts and methods. In: Sasowsky, I.D., Wicks, C.M. (Eds.), Groundwater flow and Contaminant Transport in Carbonate Aquifers. A.A. Balkema, Rotterdam, pp. 1-14.

Sauter, M., 1991. Assessment of hydraulic conductivity in a karst aquifer at local and regional scale, 3rd Conference on Hydrogeology, Monitoring and MAnagement of Ground Water in Karst Terranes, Nashville, pp. 39-56.

Sauter, M., 1992. Quantification and forecasting of regional groundwater flow and transport in a karst aquifer (Gallusquelle, Malm, SW. Germany). Tubinger Geowissenschaftlichen Abhandlungen, Reihe C.13, 150 pp.

Sauter, M., Liedl, R., 2000. Modelling karst aquifer genesis using a coupled continuum-pipe flow model. In: Klimchouk, A.B. (Ed.), Speleogenesis - evolution of karst aquifers. National Speleological Society, Alabama, pp. 212-219.

Scanlon, B.R., Mace, R.E., Barrett, M.E., Smith, B., 2003. Can we simulate regional groundwater flow in a karst system using equivalent porous media models? Case study, Barton Springs, Edward Aquifer, USA. Journal of Hydrology, 276(137-158).

Sevastopulo, G.D., Wyse Jackson, P.N., 2001. Carboniferous (Dinantian). In: Hepworth Holland, C. (Ed.), The Geology of Ireland. Dunedin Academic Press, Edinburgh.

Shaw, E.M., 1994. Hydrology in Practise. Chapman and Hall, London.

Sheehy Skeffington, M., Gormally, M., 2007. Turloughs: A mosaic of biodiversity and management systems unique to Ireland. Acta Carsologica, 36(2): 217 - 222.

Sheehy Skeffington, M., Moran, J., O Connor, A., Regan, E., Coxon, C.E., Scott, N.E., Gormally, M., 2006. Turloughs - Ireland's unique wetland habitat. Biological Conservation, 133(3): 265-290.

Sheehy Skeffington, M., Scott, N.E., 2008. Do turloughs occur in Slovenia? Acta Carsologica, 37: 291-236.

Sheppard, R., 1993. Ireland's Wetland Wealth. The birdlife of the estuaries, lakes, coasts, rivers, bogs and turloughs of Ireland. The Report of the Winter Wetlands Survey 1984/1985 and 1986/1987. Irish Wildbird Conservancy, Dublin.

Sibson, R., 1980. A vector identity for the Drichlet tesselation. Math. Proc. Cambridge Phil. Soc, 87: 151 - 155.

Sibson, R., 1981. A Brief Description of Natural Neighbour Interpolation. In: Barnett, V. (Ed.), Interpreting Multivariate Data. John Wiley and Sons, New York, pp. 21 - 36.

Smith, W.H.F., Wessel, P., 1990. Gridding with continuous curvature splines in tension. Geophysics, 55(n): 293 - 305.

Southern Water Global, 1998. An investigation of the flooding problems in the Gort-Ardrahan area of South Galway. Final Report, April 1998. Produced by Southern Water Global and Jennings O`Donovan and Partners for the Office of Public Works, Dublin.

Speight, M.C.D., 1977. Notes on three ground beetles (Coleoptera: Carbidae) Dyschirius luedersi new to Ireland, Badister peltatus and Chlaenius tristis reinstated as Irish. Irish Naturalists' Journal 19(4): 116-118.

Springer, S., 2002. The impact of Land Use Changes on the Habitat Requirement of the Otter (Lutra lutra) in the West of Ireland. MSc Thesis, NUI, Galway.

Svenson, U., Dreybrodt, W., 1992. Dissolution kinetics of natural calcite minerals in CO2 - water systems approaching calcite equilibrium. Chemical Geology, 100: 129-145.

Thompson, J.A., Bell, J.C., Butler, C.A., 2001. Digital elevation model resolution: effects on terrain attribute calculation and quantitative soil-landscape modeling. Geoderma, 100(1-2): 67-89.

Tynan, S., Gill, M., Johnston, P.M., 2007. Development of a Methodology for the Characterisation of a Karstic Groundwater Body with Particular Emphasis on the Linkage with Associated Ecosystems such as Turlough Ecosystems. Final Research Report to the Environmental Protection Agency (Project No. 2002-W-DS-08-M1). EPA, Johnstown Castle Estate, Wexford, Ireland.

Uren, J., Price, W.F., 2006. Surveying for engineers. Palgrave Macmillan.

Valdes, D., Dupont, J.-P., Laignel, B., Ogier, S., Leboulanger, T., Mahler, B.J., 2007. A spatial analysis of structural controls on Karst groundwater geochemistry at a regional scale. Journal of Hydrology, 340(3-4): 244-255.

Van Everdingen, R.O., 1981. Morphology, hydrology and hydrochemistry of karst in permafrost near Great Bear Lake, Northwest Territories. Paper 11, National Hydrological Research Institute of Canada.

Visser, M., Regan, E., Moran, J., Gormally, M., Sheehy Skeffington, M., 2006. The rise and fall of turlough typologies: a call for a continuum concept. . Wetlands, 26(3): 745-764.

White, P., 1984. The Effect of Submergence on Plants from a Turlough and a Non-Turlough Population of Ranunculus repens, L. B.Sc. Thesis, Department of Botany, NUI, Galway.

White, P.S., Pickett, S.T.A., 1985. Natural disturbance and patch dynamics: an introduction. In: Pickett, S.T.A., White, P.S. (Eds.), The Ecology of Natural Disturbance and Patch Dynamics. Academic Press, Orlando, pp. 3-14.

White, W.B., 1988. Geomorphology and Hydrology of Karst Terrains. Oxford University Press.

White, W.B., 2002. Karst hydrology: recent developments and open questions. Engineering Geology, 65(2-3): 85-105.

White, W.B., White, E.L., 2005. Ground water flux distribution between matrix, fractures, and conduits: constraints on modeling / Speleogenesis and Evolution of Karst Aquifers 3 (2), www.speleogenesis.info, 6 pages.

Williams, C., Doherty, O., Gormally, M., 2006. Gasterosteus aculeatus L. and Pungitius pungitius(L.) - two species of stickleback from turloughs in Co. Mayo and Roscommon. Irish Naturalists Journal, 28(7): 276-279.

Williams, D.D., 2006. The biology of temporary waters. Oxford University Press, Oxford.

Williams, P.W., 1964. Aspects of the Limestone Physiography of Parts of Counties Clare and Galway, Western Ireland, Unpublished PhD Thesis. University of Cambridge.

Williams, P.W., 1970. Limestone morphology in Ireland. In: Stephens, N., Glasscock, R.E. (Eds.), Irish Geographical Studies. Queen's University, Belfast, pp. 105-124.

Williams, P.W., 1983. The role of the subcutaneous zone in karst hydrology. Journal of Hydrology, 61: 45-67.

Working Group on Groundwater, 2004. Guidance on the assessment of pressures and impacts on groundwater dependent terrestrial ecosystems, Risk Assessment Sheet GWDTERA2a – Risk to Turloughs from Phosphate. Water Framework Directive Pressures and Impacts Assessment Methodology, Guidance Document no. GW9. Working Group on Groundwater, Sub-committee on Turloughs. Environment Protection Agency, Dublin.

Working Group on Groundwater, 2005. Approach to Delineation of Groundwater Bodies, Guidance document no. GW2 . Working Group on Groundwater, . Environment Protection Agency, Dublin.

Worthington, S.R.H., 2003. A comprehensive strategy for understanding flow in carbonate aquifers. In: Palmer, A.N., Palmer, M.V., Sasowsky, I.D. (Eds.), Karst Modeling: Special Publication 5. The Karst Water Institute, Charles Town, West Virginia, pp. 30-37.

Worthington, S.R.H., Ford, D., 2009. Self-organized Pemeability in Carbonate Aquifers. Ground Water, 47(3): 326-336.

Worthington, S.R.H., Ford, D.C., Davies, G.J., 2000. Matrix, fracture and channel components of storage and flow in a Paleozoic limestone aquifer. In: Sasowsky, I.D., Wicks, C.M. (Eds.), Groundwater Flow and Contaminant Transport in Carbonate Aquifers, pp. 113-128.

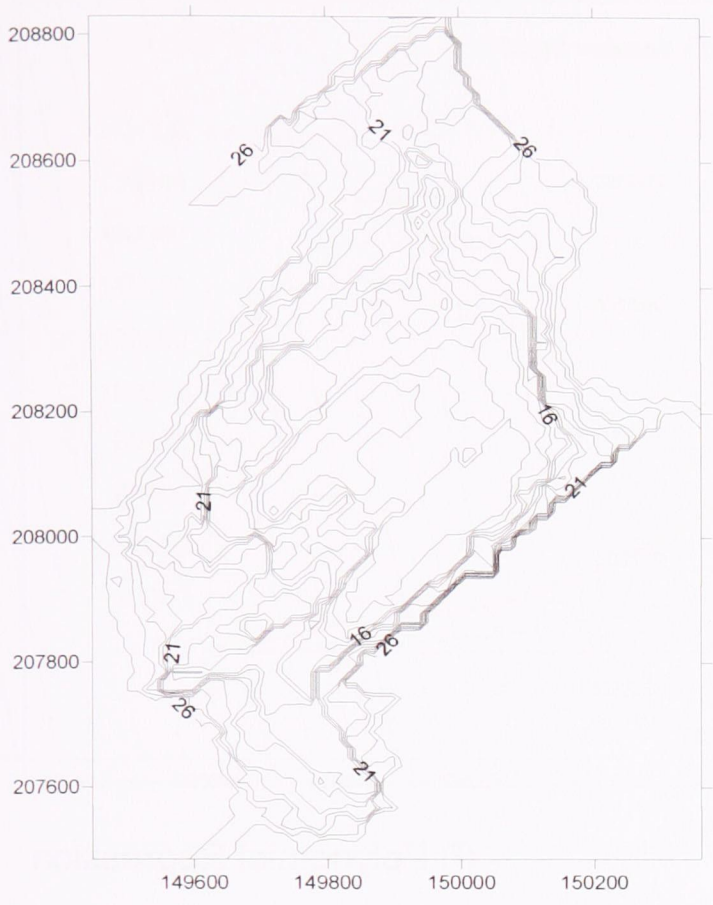
Yanalak, M., 2003. Effect of Gridding Method on Digital Terain Model Profile Data Based on Scattered Data. Journal of Computing in Civil Engineering, 17(1): 51-67.

Yanalak, M., Baykal, O., 2003. Digital Elevation Model Based Volume Calculations Using Topographic Data. Journal of Surveying Engineering: 56-64.

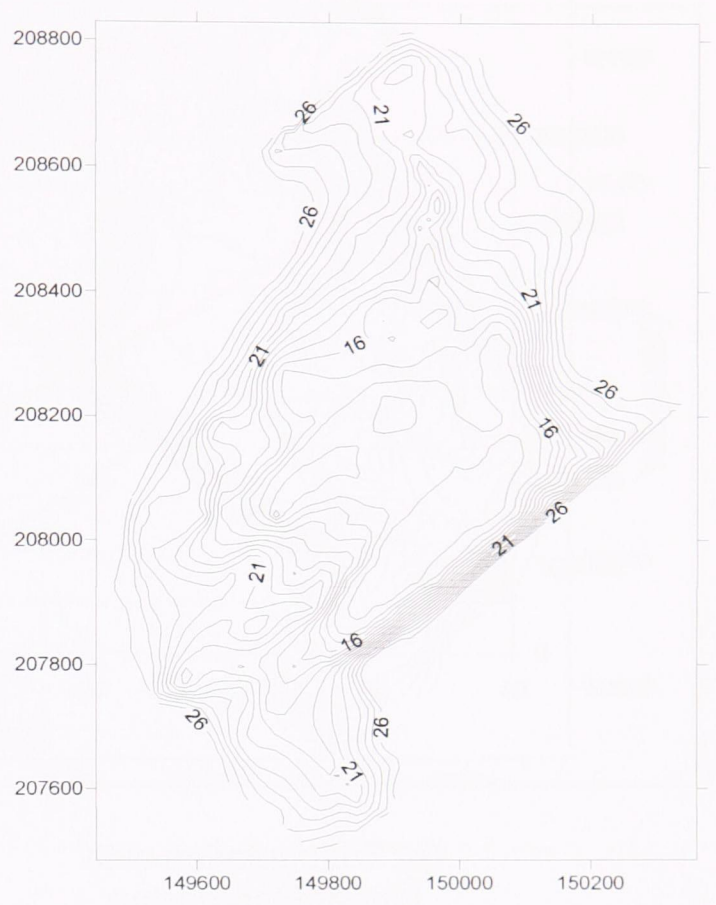
Zhou, W., 2007. Drainage and flooding in karst terrains. Environmental Geology, 51: 963-973.

Zibret, Z., Simunic, Z., 1976. A rapid method for determining water budget of enclosed and flooded karst plains. In: Yevjevich, V. (Ed.), Karst Hydrology and Water Resources: Vol. 1 Karst Hydrology. Water Resources Publications, Colorado, pp. 319-339.

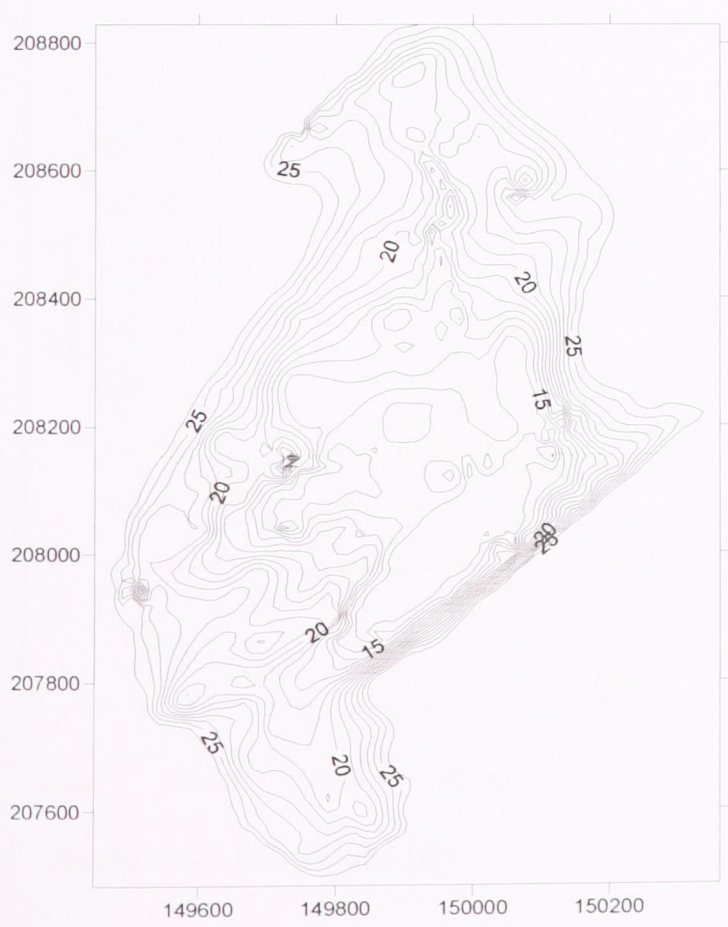
Appendix A: Surveying



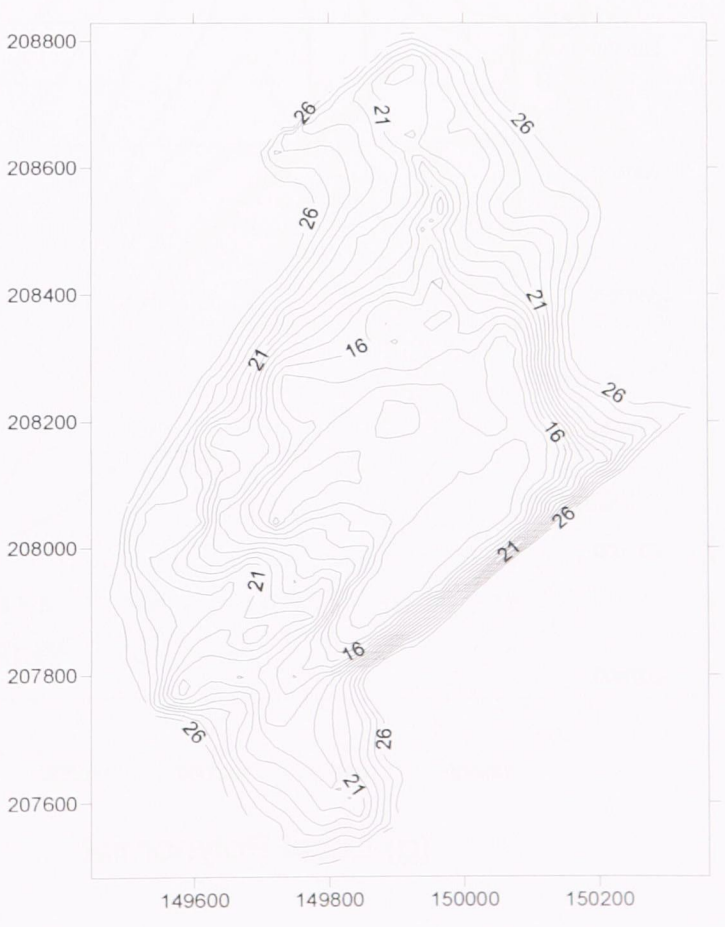
(a) Nearest Neighbour



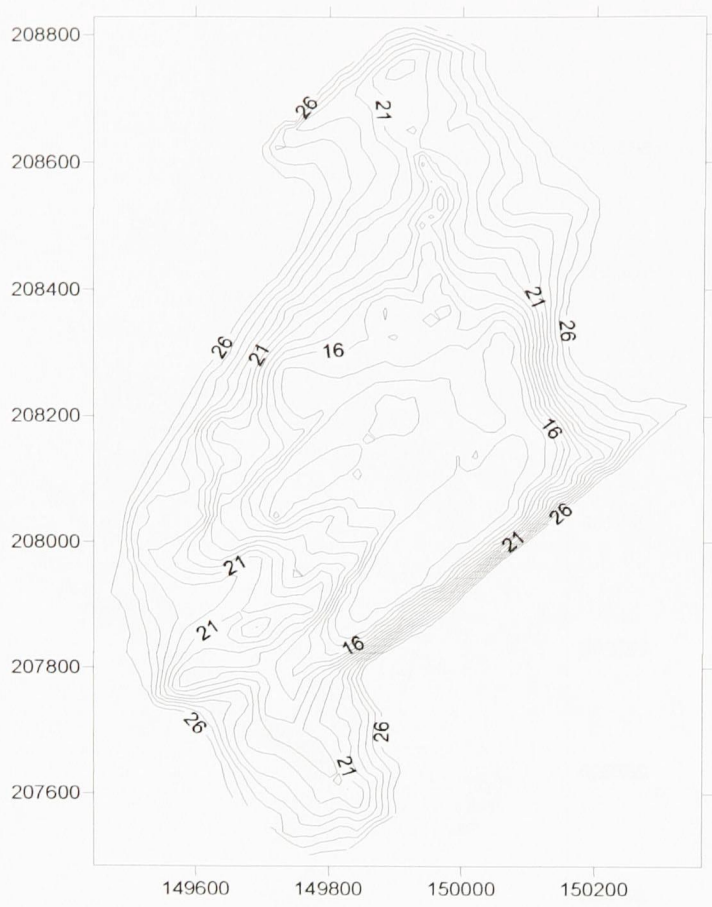
(b) Natural Neighbour



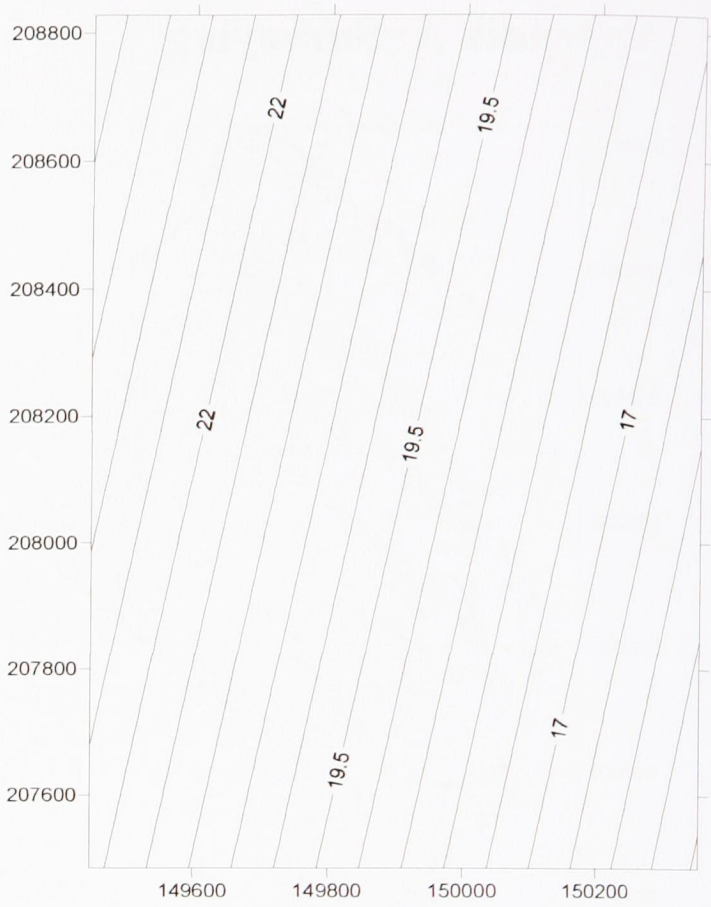
(c) Kriging



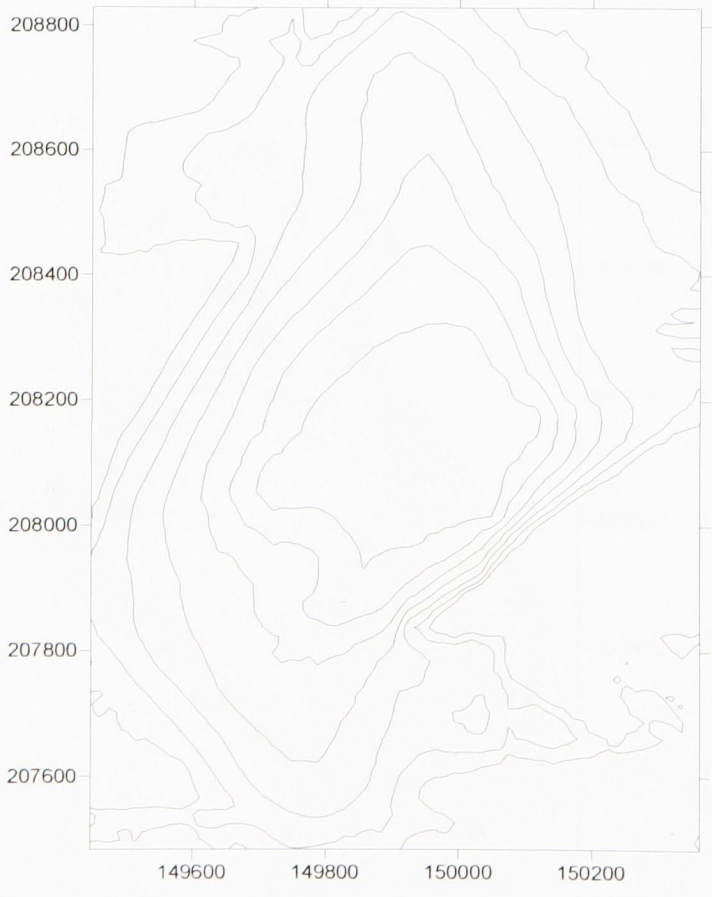
(d) Multiquadric



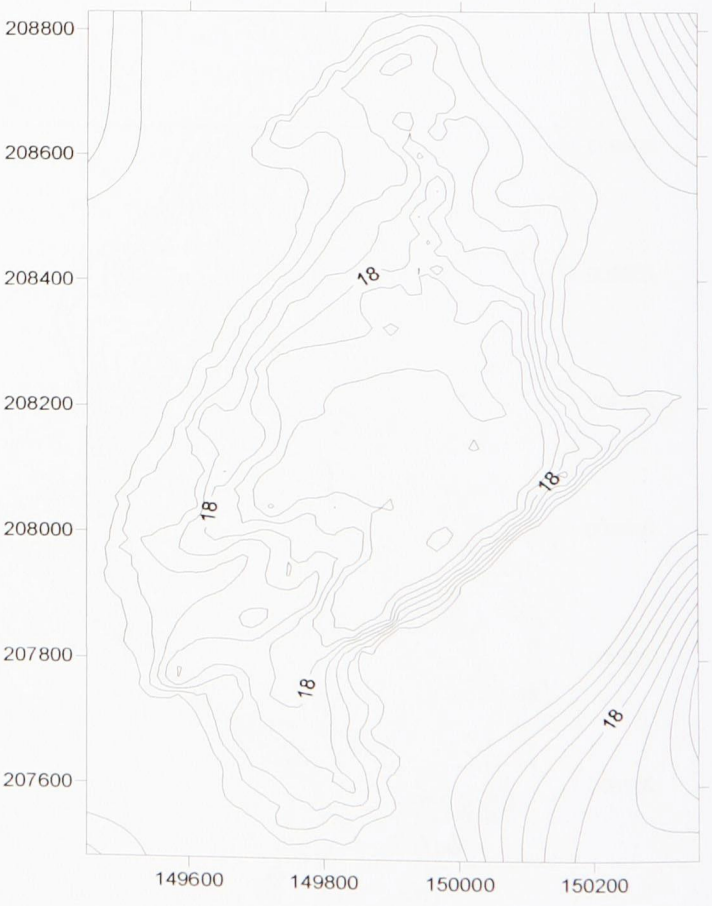
(e) Triangulation with Linear Regression



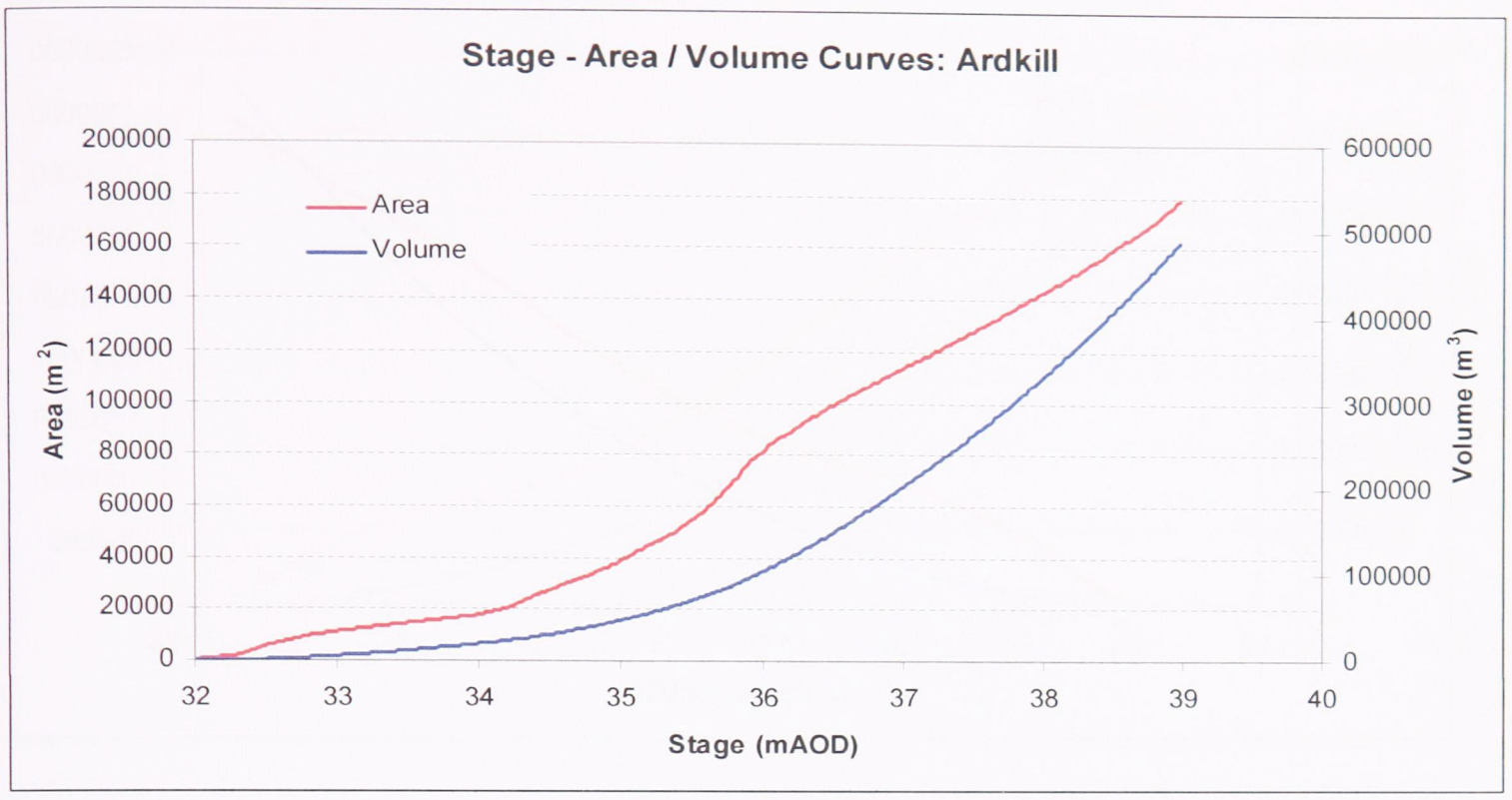
(f) Polynomial Regression

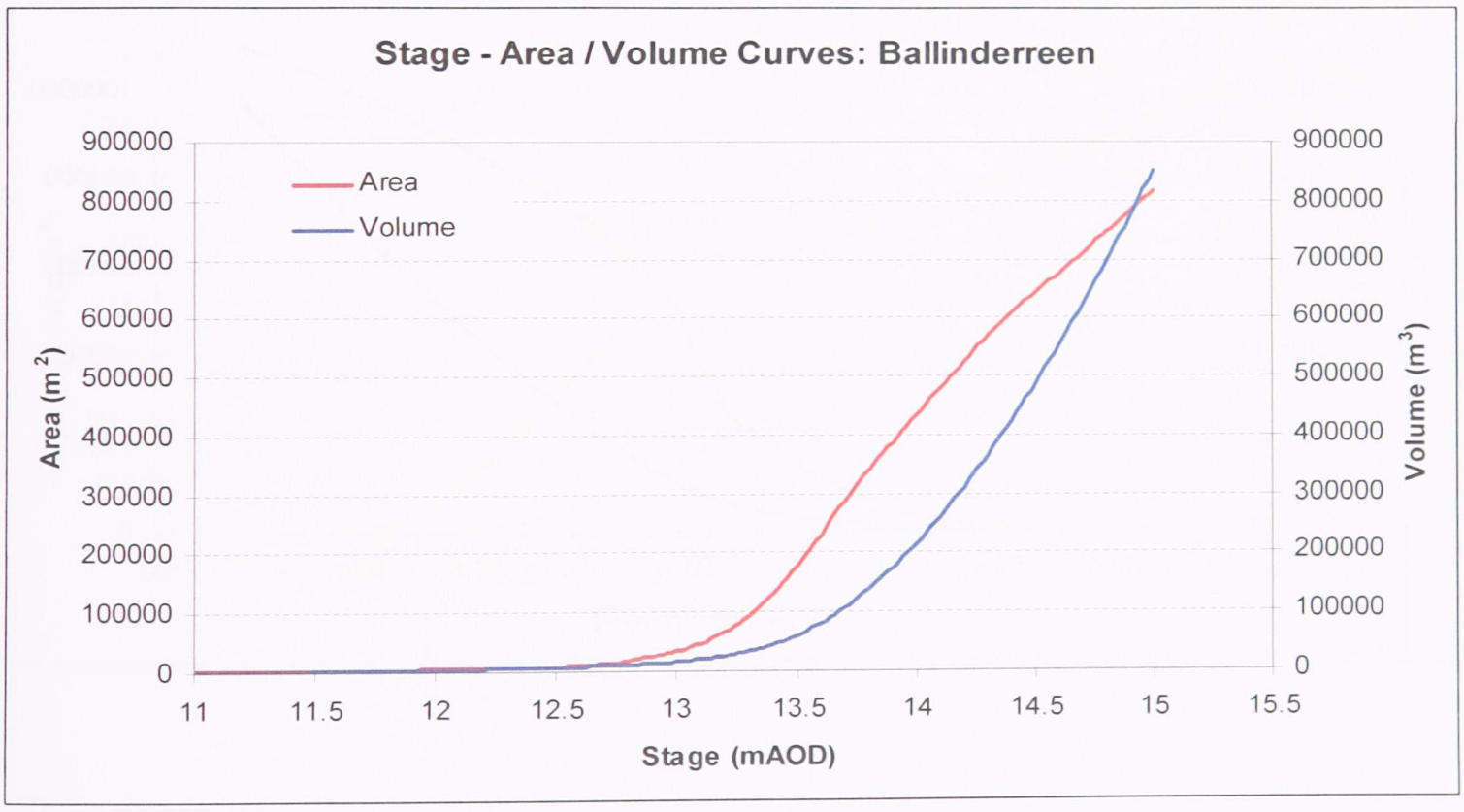


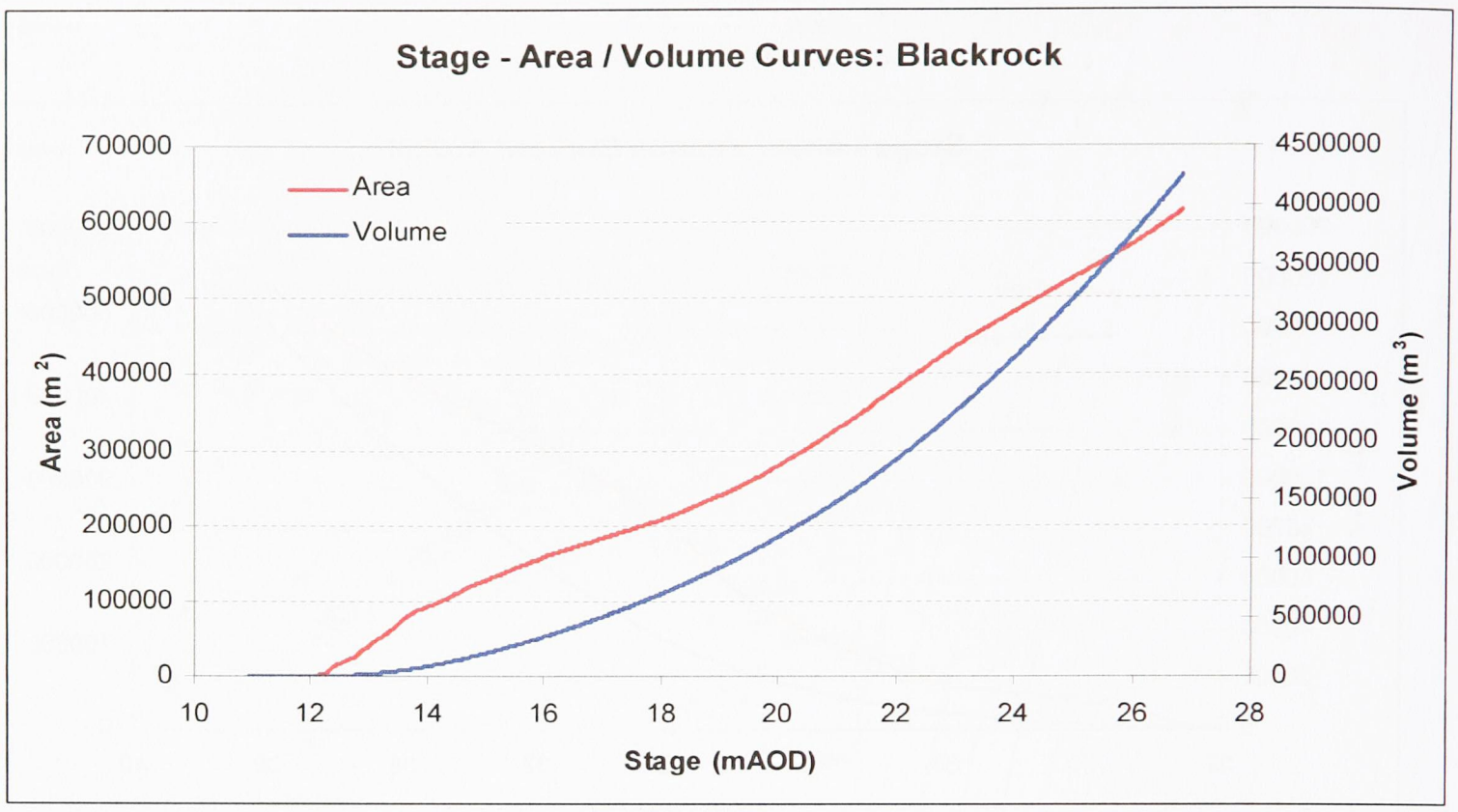
(g) Local Polynomial

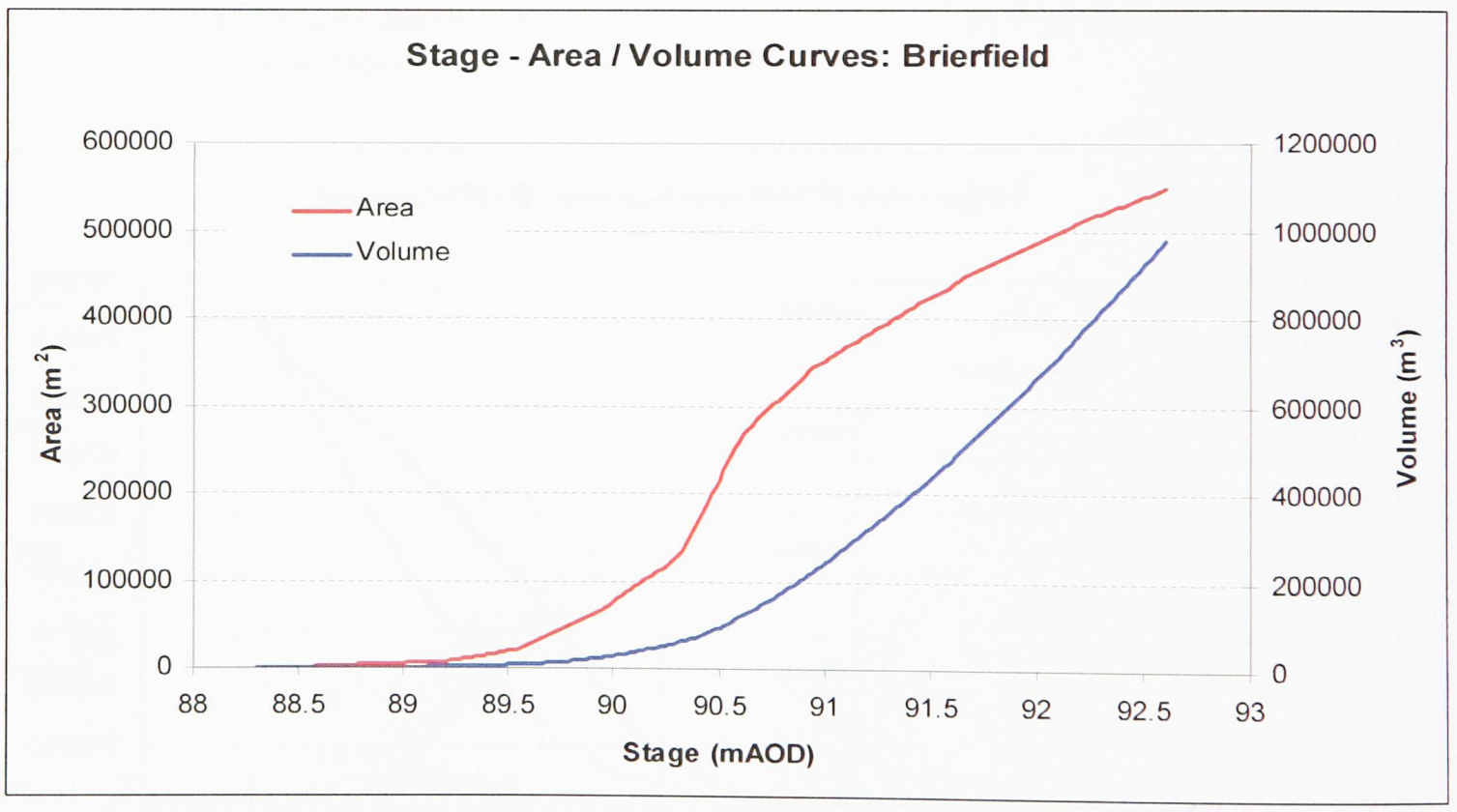


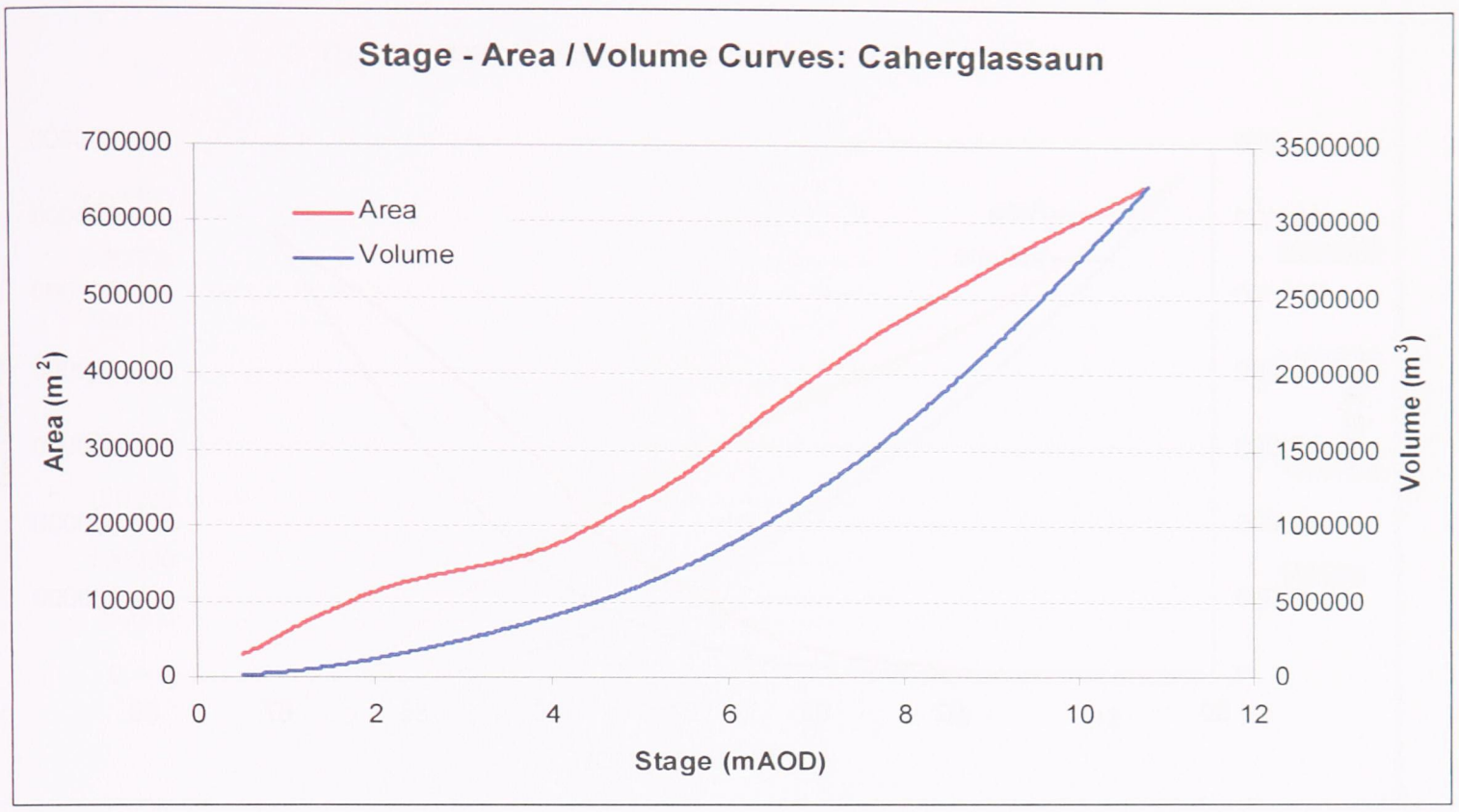
(h) Minimum Curvature

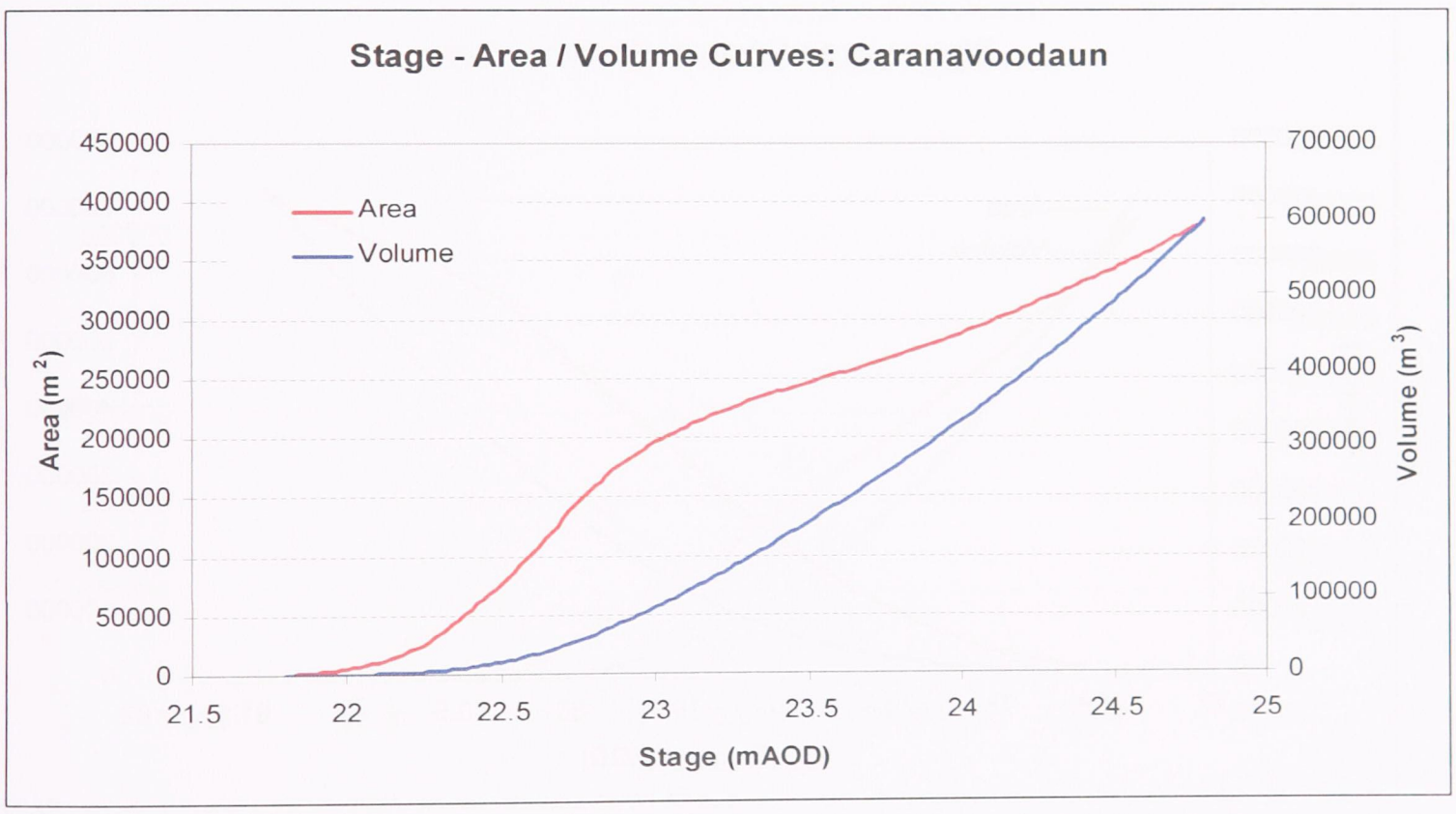

Stage - Area / Volume Curves: Ardkill
Area
Volume
Area (m 2)
Volume (m3)
Stage (mAOD)
200000
180000
160000
140000
120000
100000
80000
60000
40000
20000
0
600000
500000
400000
300000
200000
100000
0
32
33
34
35
36
37
38
39
40

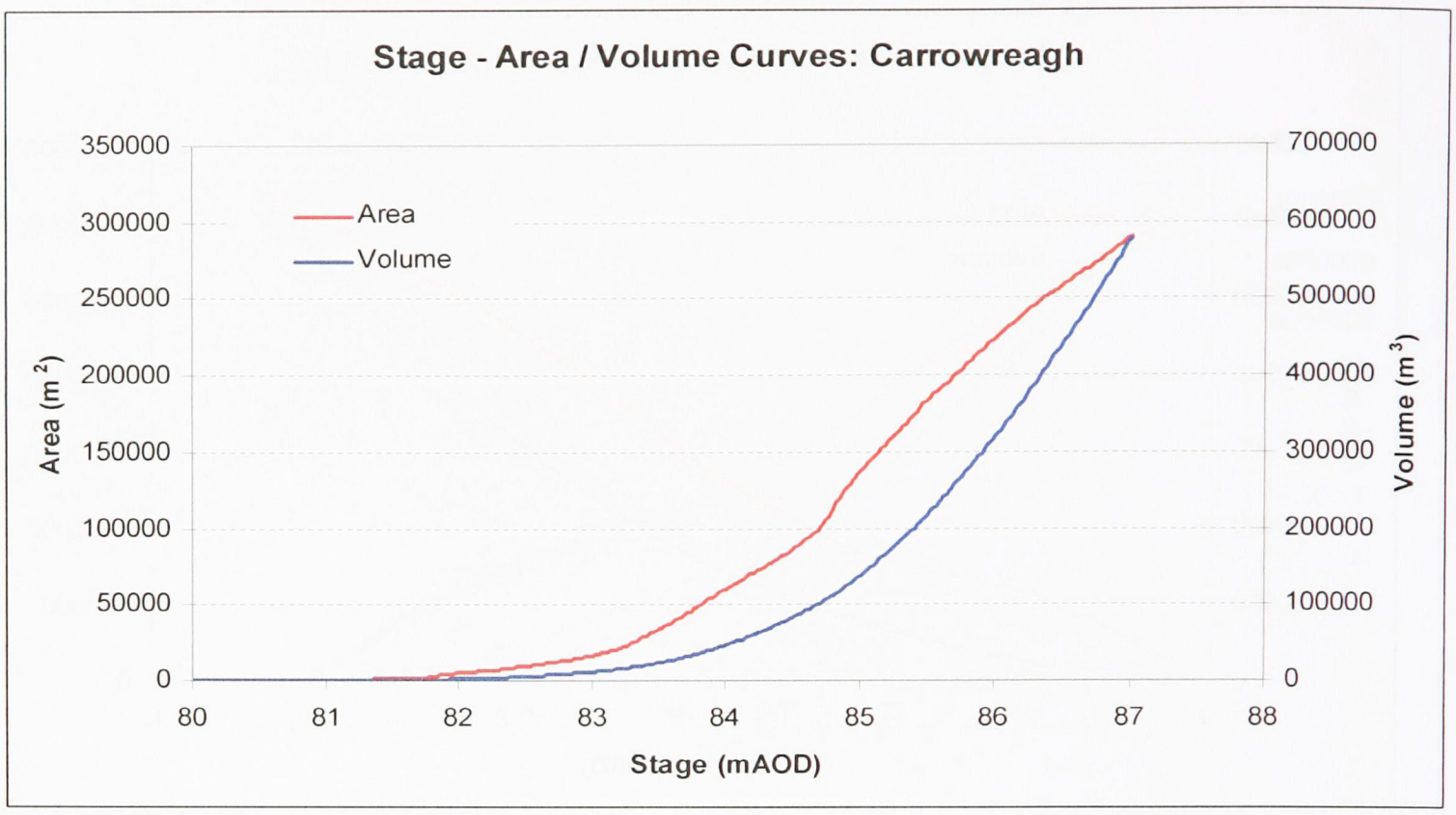

Stage - Area / Volume Curves: Ballinderreen
Area
Volume
Area (m 2)
Volume (m3)
Stage (mAOD)
900000
800000
700000
600000
500000
400000
300000
200000
100000
0
11
11.5
12
12.5
13
13.5
14
14.5
15
15.5

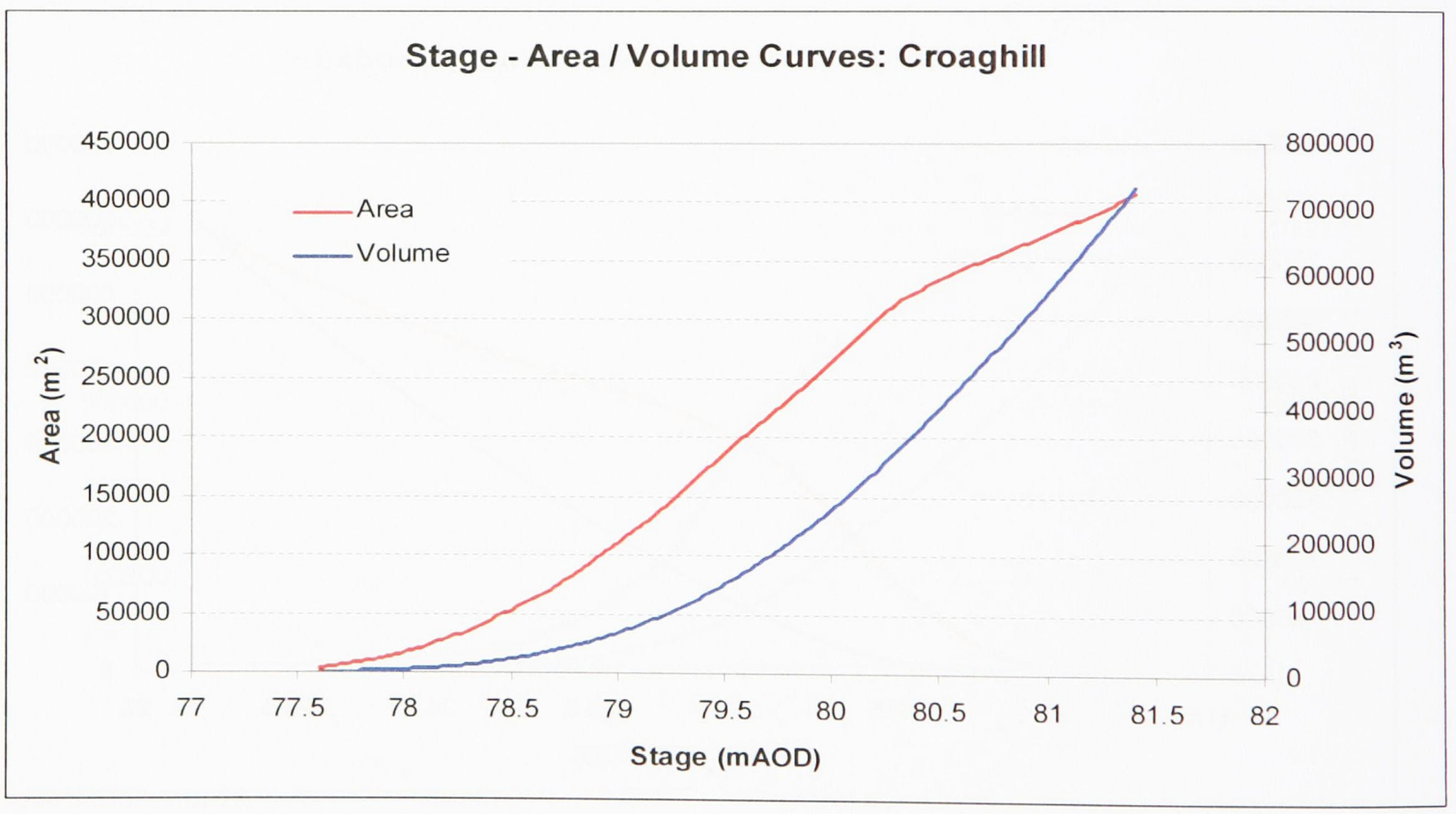

Stage - Area / Volume Curves: Blackrock
Area
Volume
Area (m 2)
Volume (m3)
Stage (mAOD)
700000
600000
500000
400000
300000
200000
100000
0
4500000
4000000
3500000
3000000
2500000
2000000
1500000
1000000
500000
0
10
12
14
16
18
20
22
24
26
28

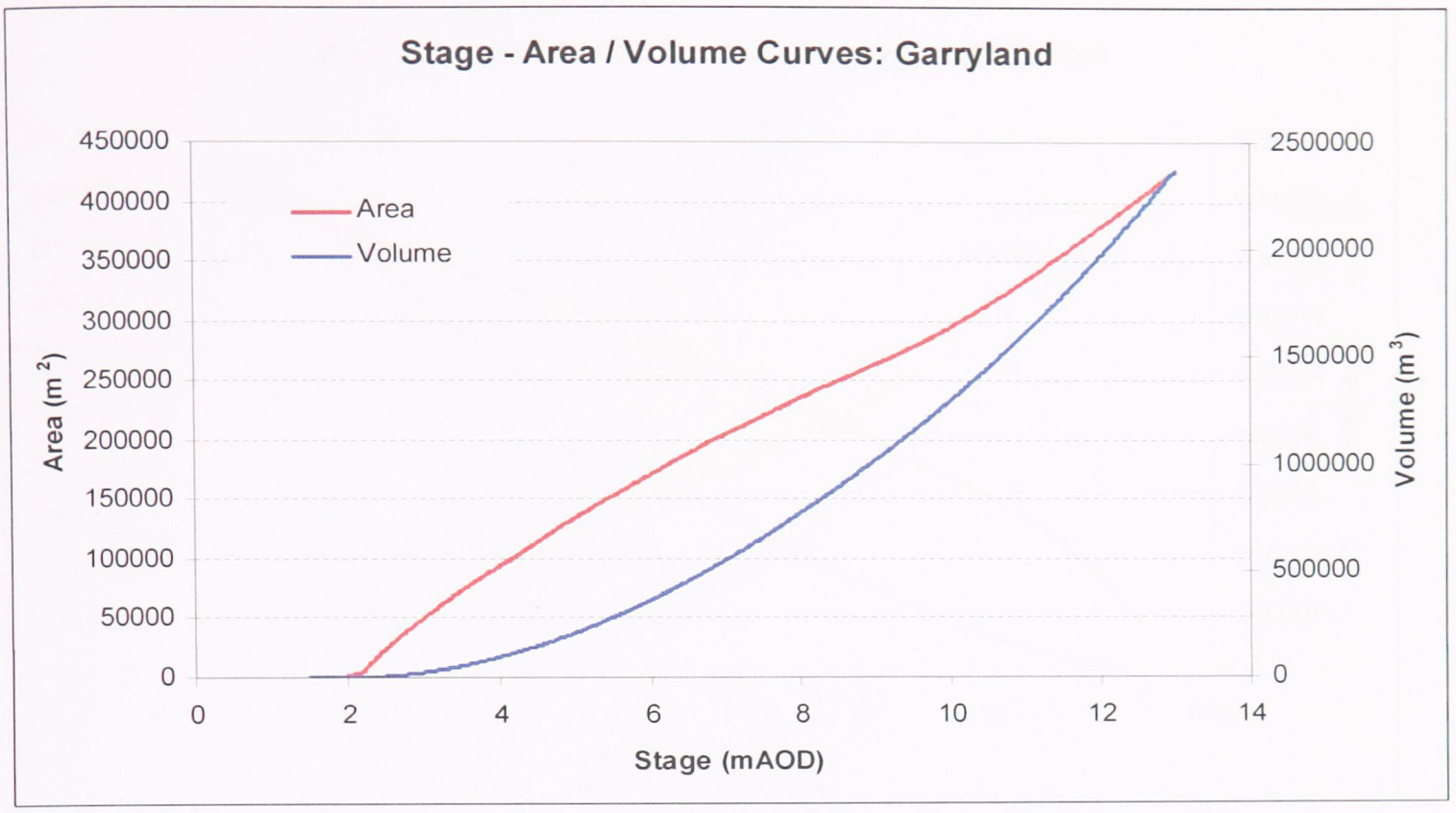

Stage - Area / Volume Curves: Brierfield
Area
Volume
Area (m 2)
Volume (m3)
Stage (mAOD)
600000
500000
400000
300000
200000
100000
0
1200000
1000000
800000
600000
400000
200000
0
88
88.5
89
89.5
90
90.5
91
91.5
92
92.5
93

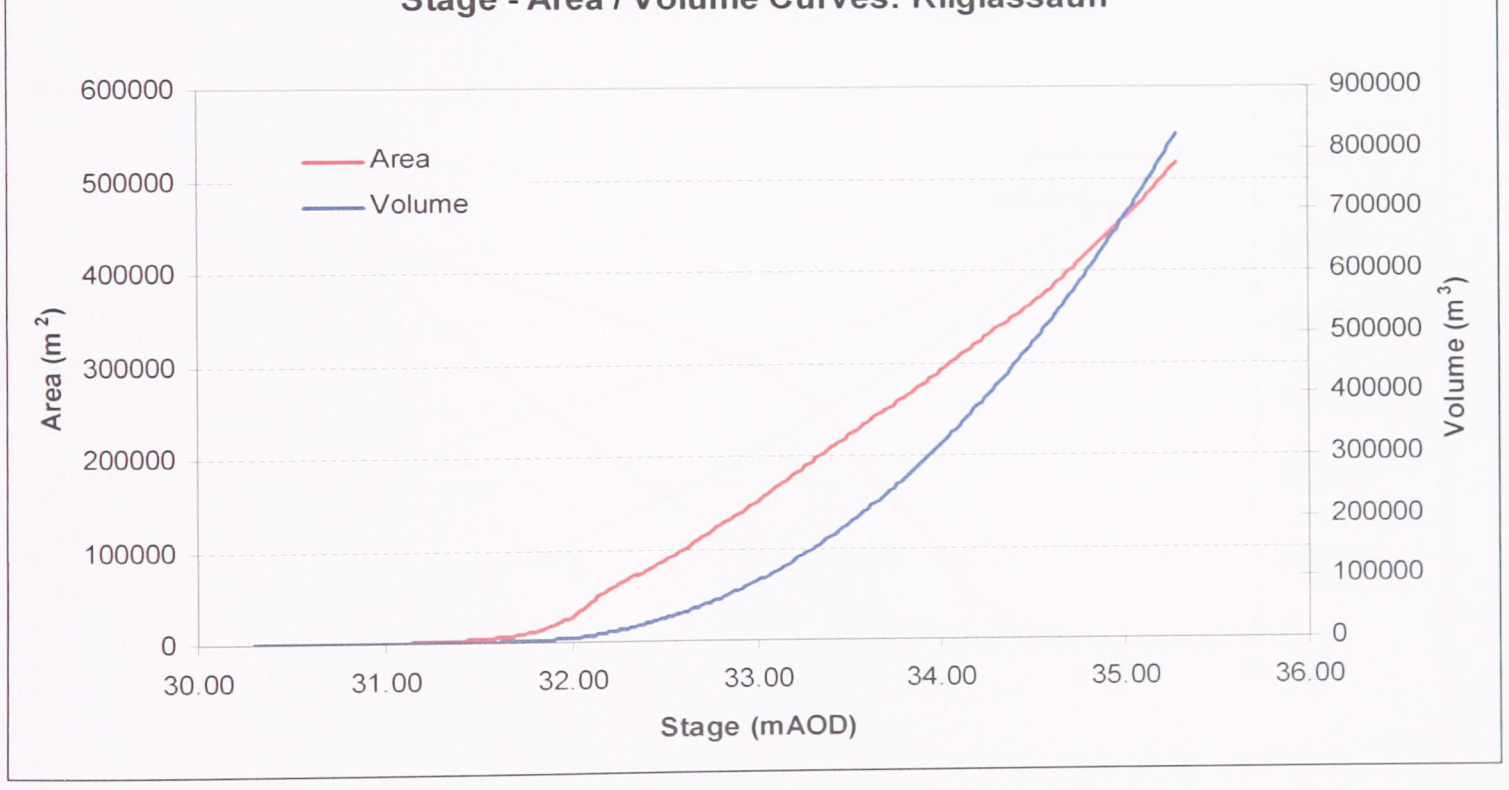

Stage - Area / Volume Curves: Caherglassaun
Area
Volume
Area (m 2)
Volume (m 3)
Stage (mAOD)
700000
600000
500000
400000
300000
200000
100000
0
3500000
3000000
2500000
2000000
1500000
1000000
500000
0
0
2
4
6
8
10
12

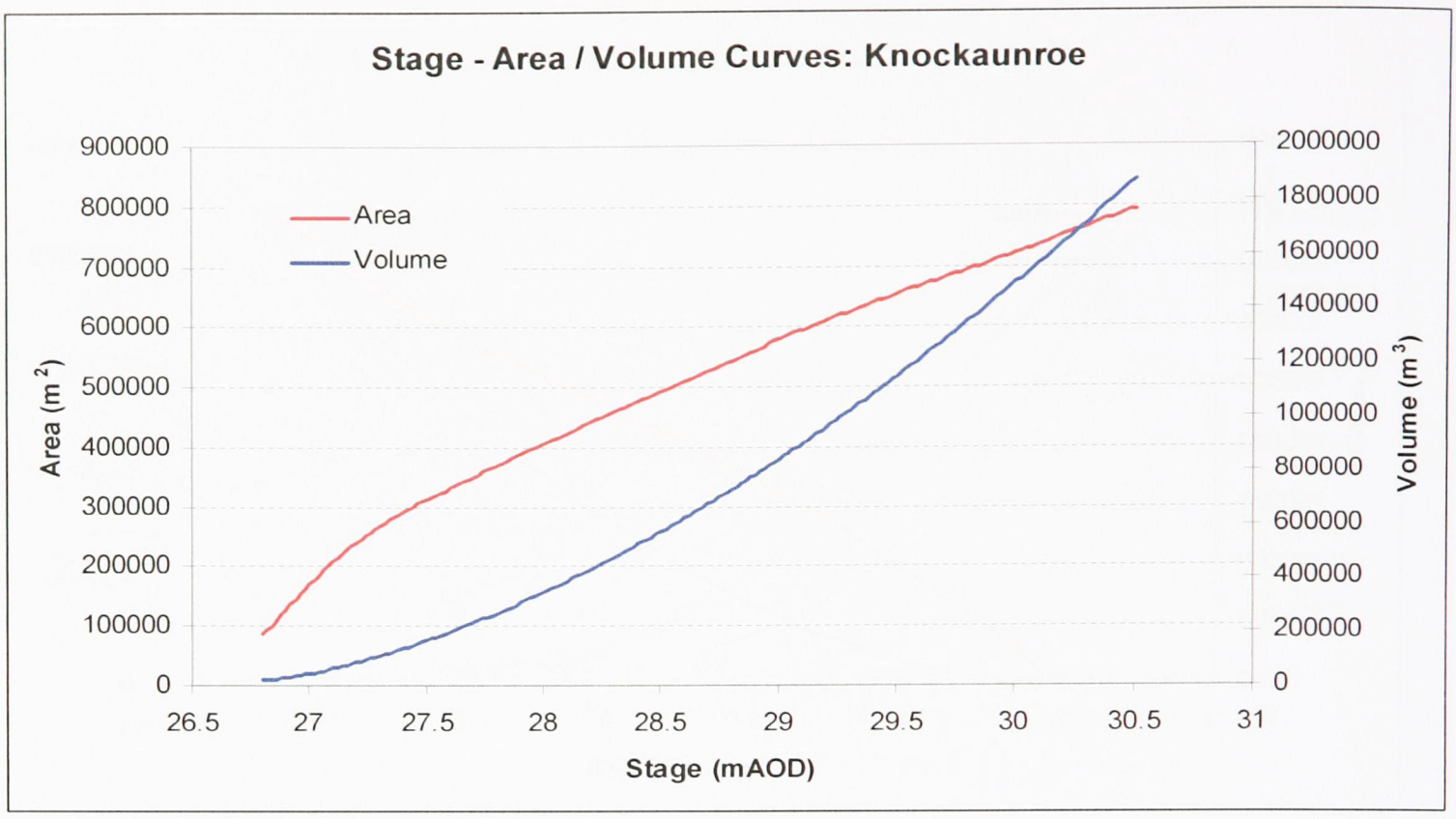

Stage - Area / Volume Curves: Caranavoodaun
Area
Volume
Area (m 2)
Volume (m 3)
Stage (mAOD)
450000
400000
350000
300000
250000
200000
150000
100000
50000
0
700000
600000
500000
400000
300000
200000
100000
0
21.5
22
22.5
23
23.5
24
24.5
25

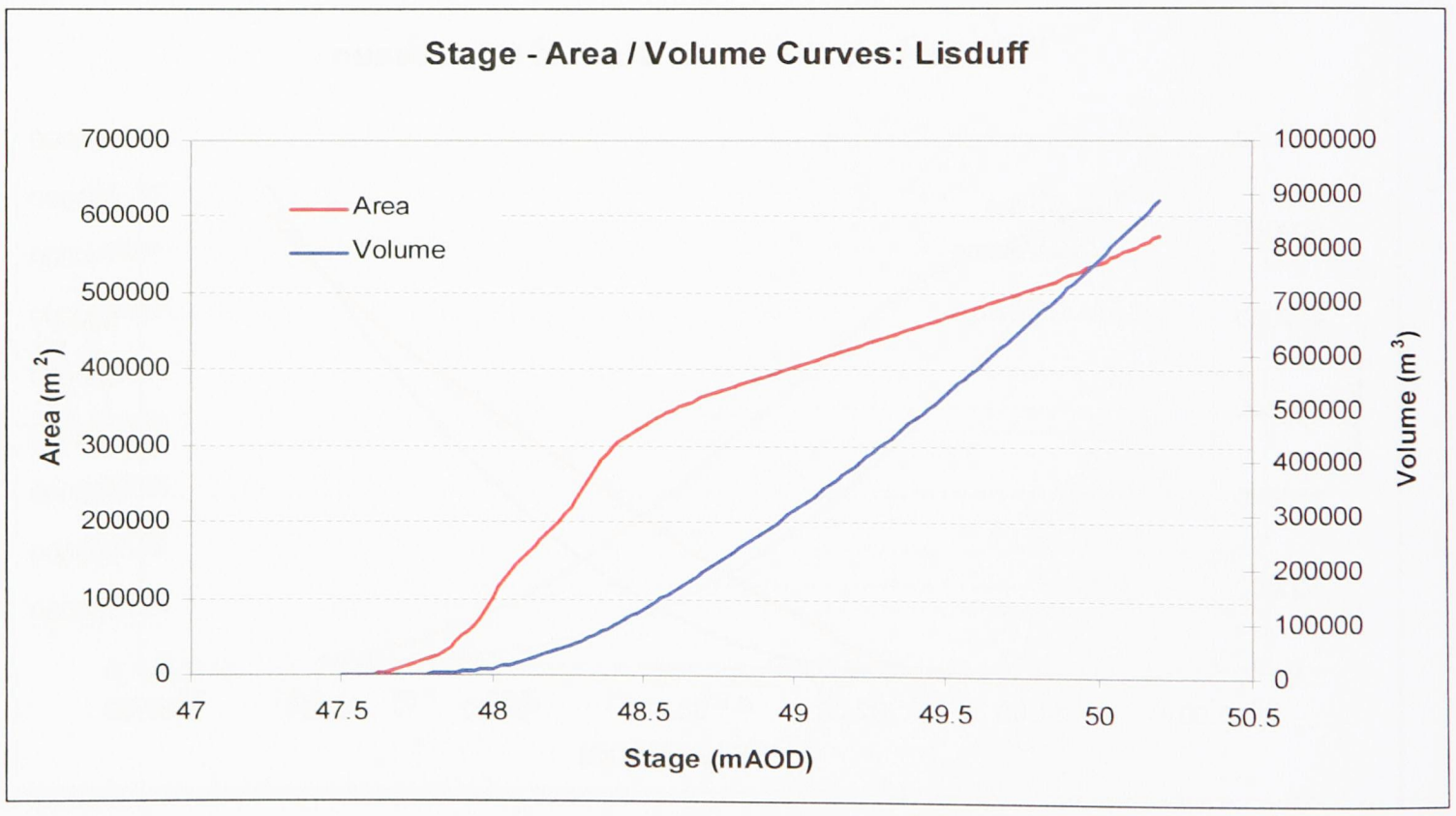

Stage - Area / Volume Curves: Carrowreagh
Area
Volume
Area (m 2)
Volume (m 3)
Stage (mAOD)
350000
300000
250000
200000
150000
100000
50000
0
700000
600000
500000
400000
300000
200000
100000
0
80
81
82
83
84
85
86
87
88

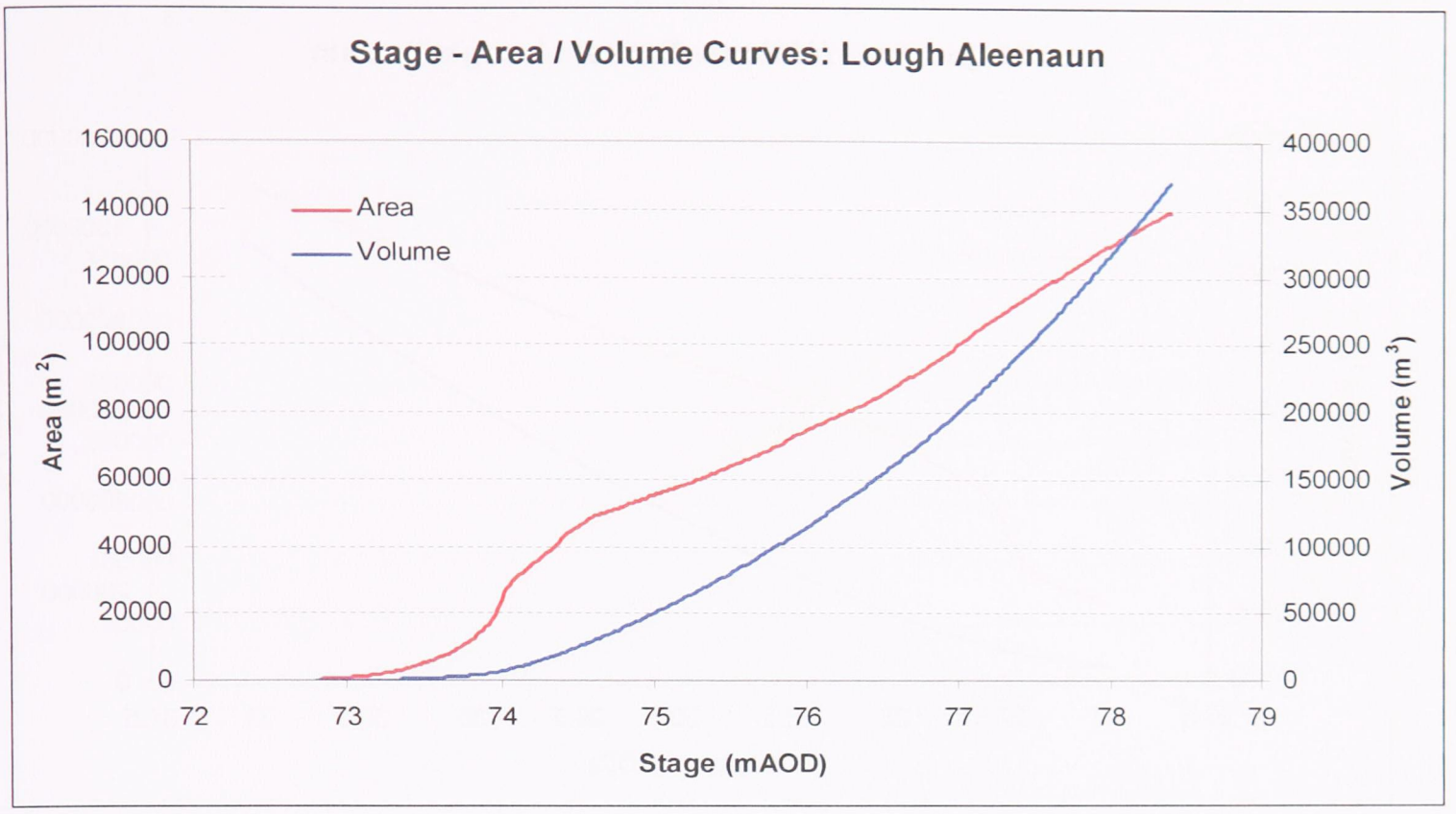

Stage - Area / Volume Curves: Croaghill
Area
Volume
Area (m 2)
Volume (m 3)
Stage (mAOD)
450000
400000
350000
300000
250000
200000
150000
100000
50000
0
800000
700000
600000
500000
400000
300000
200000
100000
0
77
77.5
78
78.5
79
79.5
80
80.5
81
81.5
82

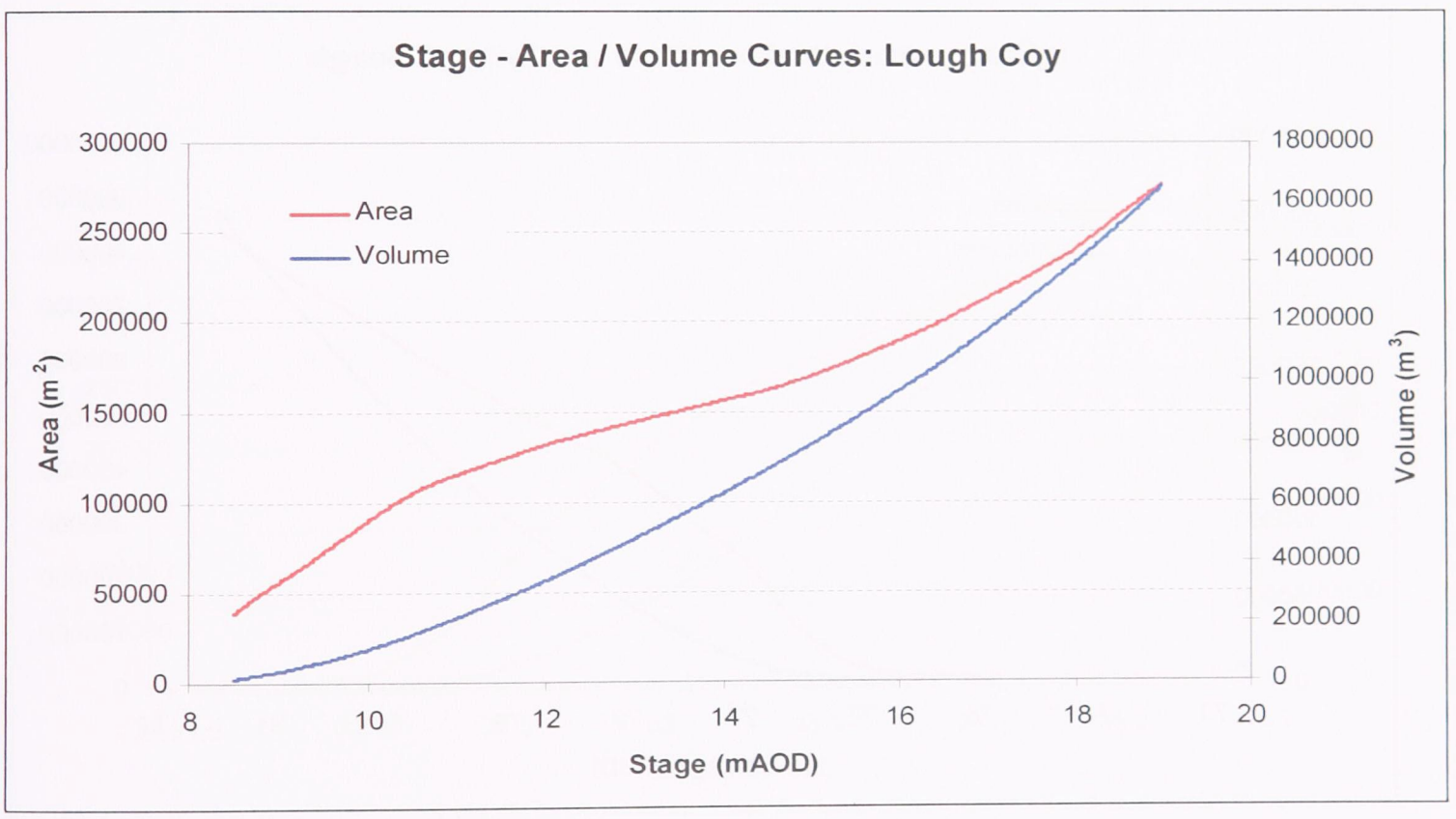

Stage - Area / Volume Curves: Garryland
Area
Volume
Area (m 2)
Volume (m 3)
Stage (mAOD)
450000
400000
350000
300000
250000
200000
150000
100000
50000
0
2500000
2000000
1500000
1000000
500000
0
0
2
4
6
8
10
12
14

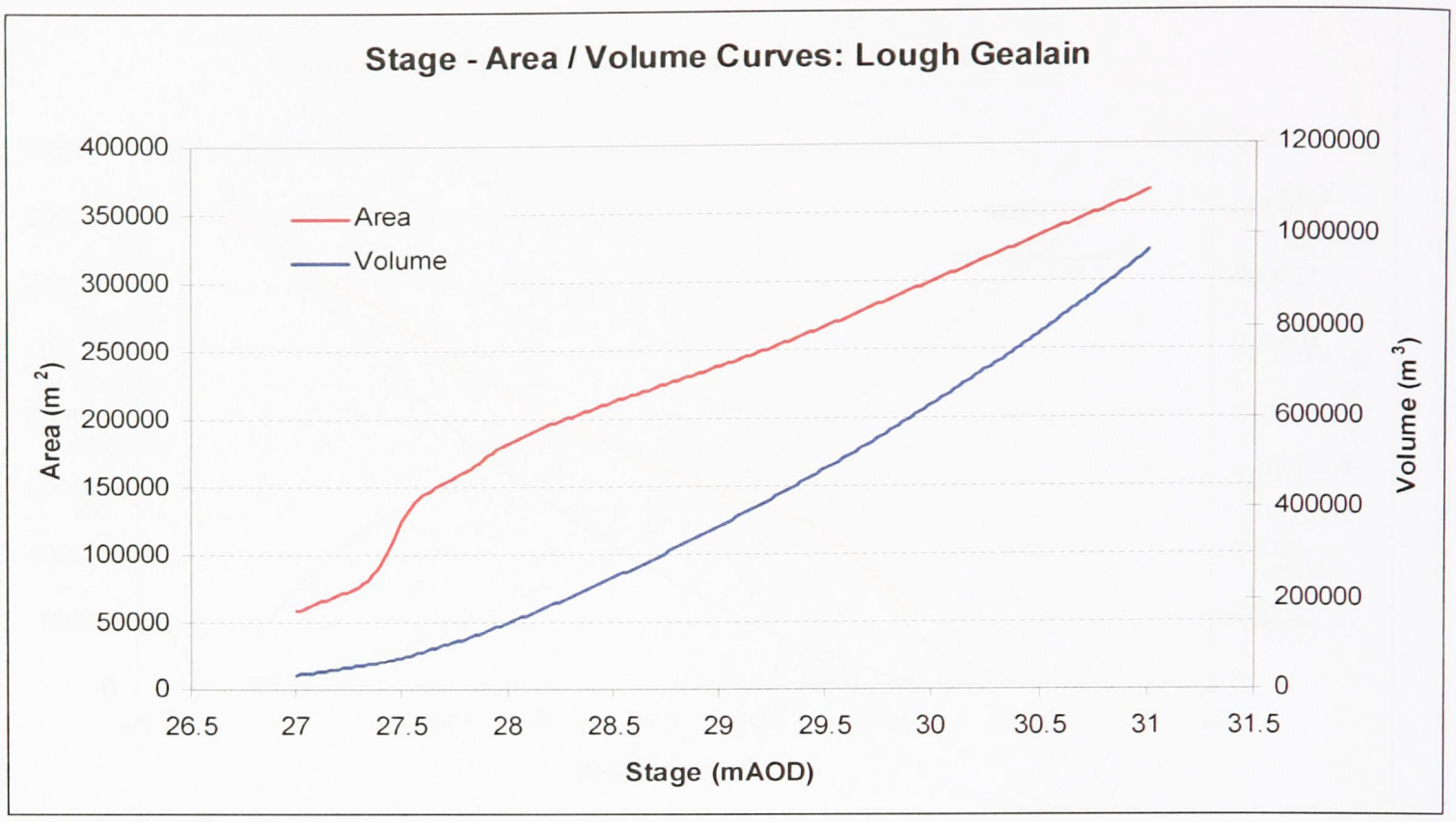

Stage - Area / Volume Curves: Kilglassaun
Area
Volume
Area (m 2)
Volume (m 3)
Stage (mAOD)
600000
500000
400000
300000
200000
100000
0
900000
800000
700000
600000
500000
400000
300000
200000
100000
0
30.00
31.00
32.00
33.00
34.00
35.00
36.00

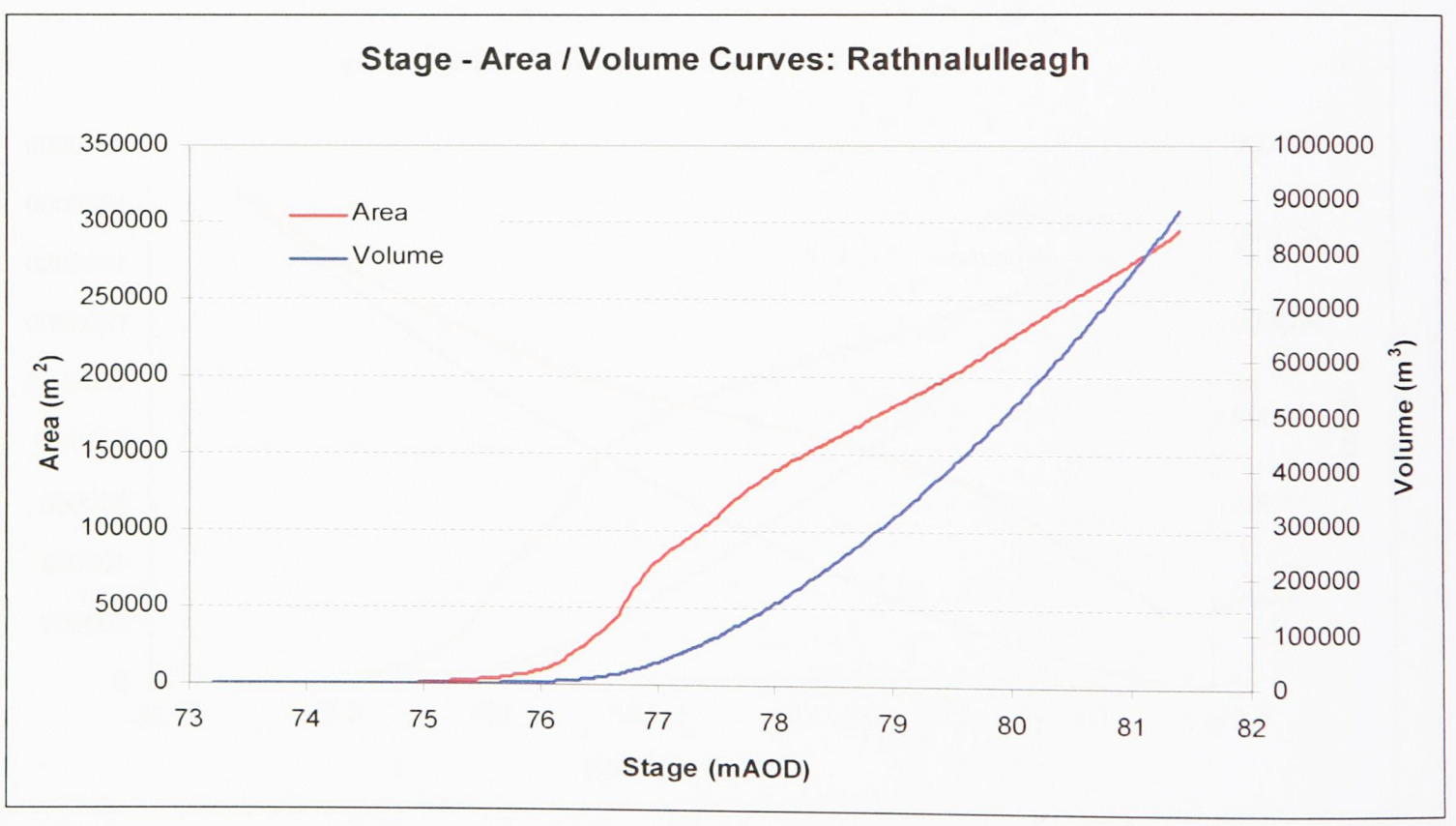

Stage - Area / Volume Curves: Knockaunroe
900000
800000
700000
600000
500000
400000
300000
200000
100000
0
Area (m 2)
2000000
1800000
1600000
1400000
1200000
1000000
800000
600000
400000
200000
0
Volume (m 3)
Area
Volume
26.5
27
27.5
28
28.5
29
29.5
30
30.5
31
Stage (mAOD)

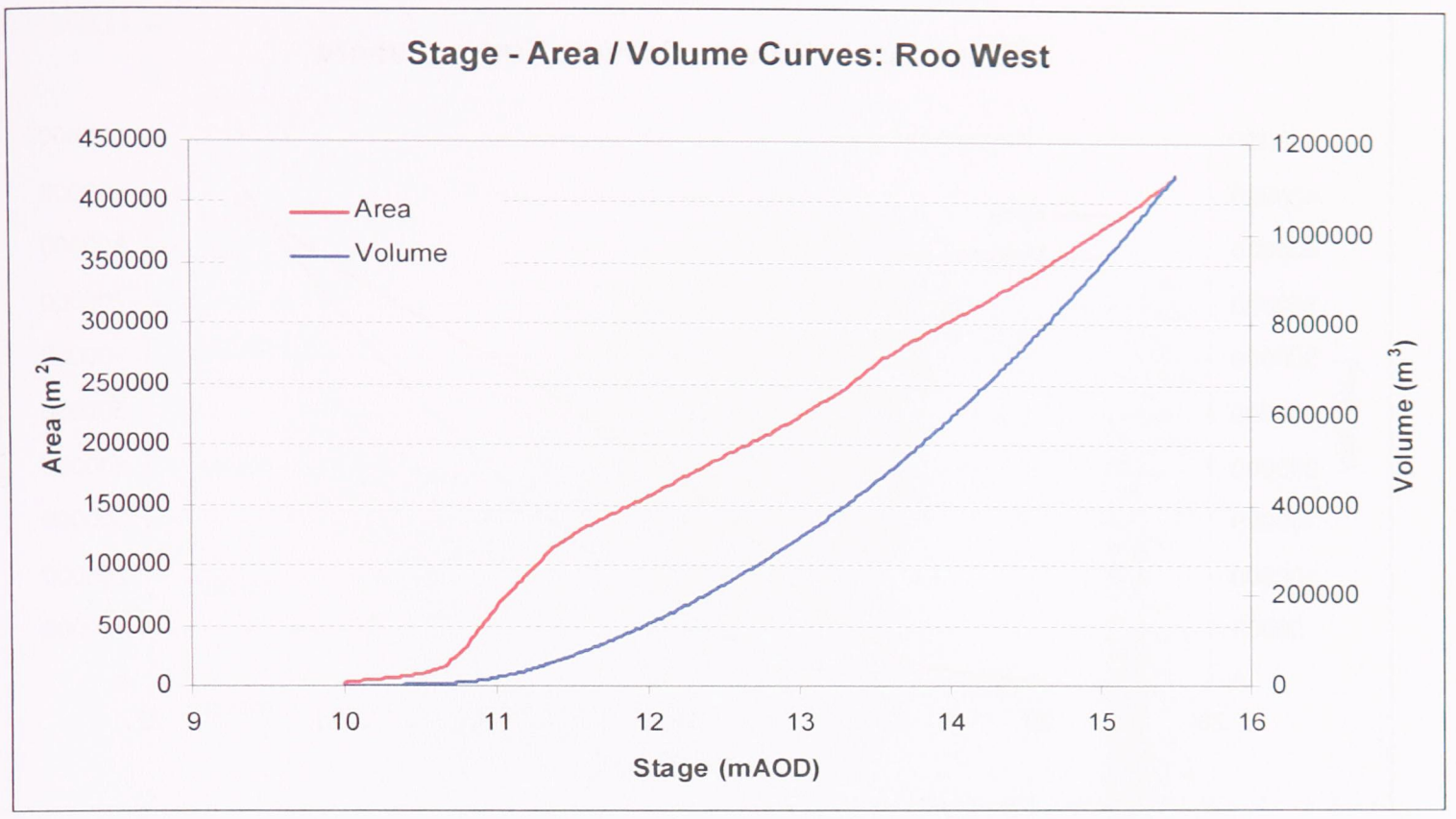

Stage - Area / Volume Curves: Lisduff
700000
600000
500000
400000
300000
200000
100000
0
Area (m 2)
1000000
900000
800000
700000
600000
500000
400000
300000
200000
100000
0
Volume (m 3)
Area
Volume
47
47.5
48
48.5
49
49.5
50
50.5
Stage (mAOD)

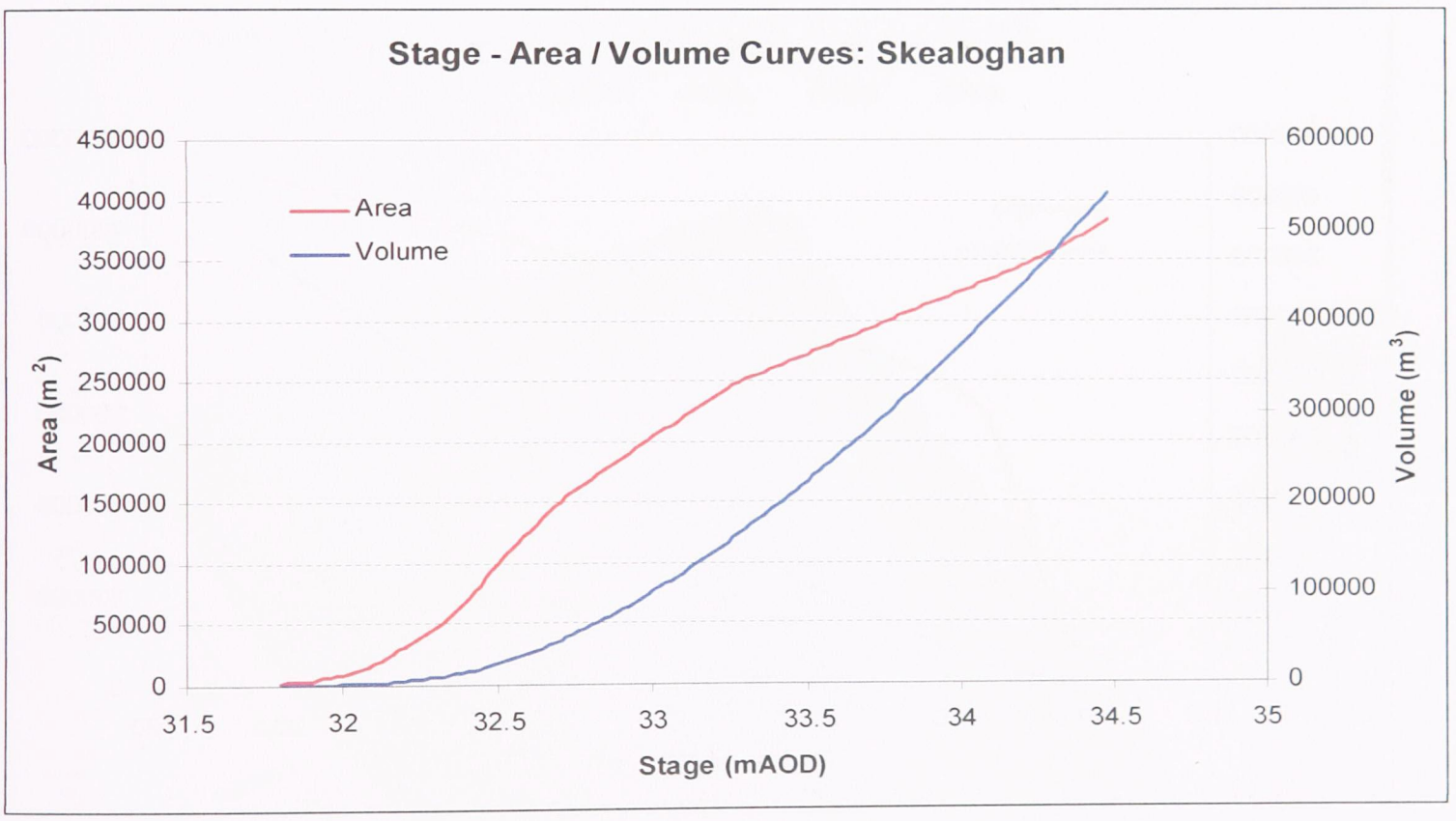

Stage - Area / Volume Curves: Lough Aleenaun
160000
140000
120000
100000
80000
60000
40000
20000
0
Area (m 2)
400000
350000
300000
250000
200000
150000
100000
50000
0
Volume (m 3)
Area
Volume
72
73
74
75
76
77
78
79
Stage (mAOD)

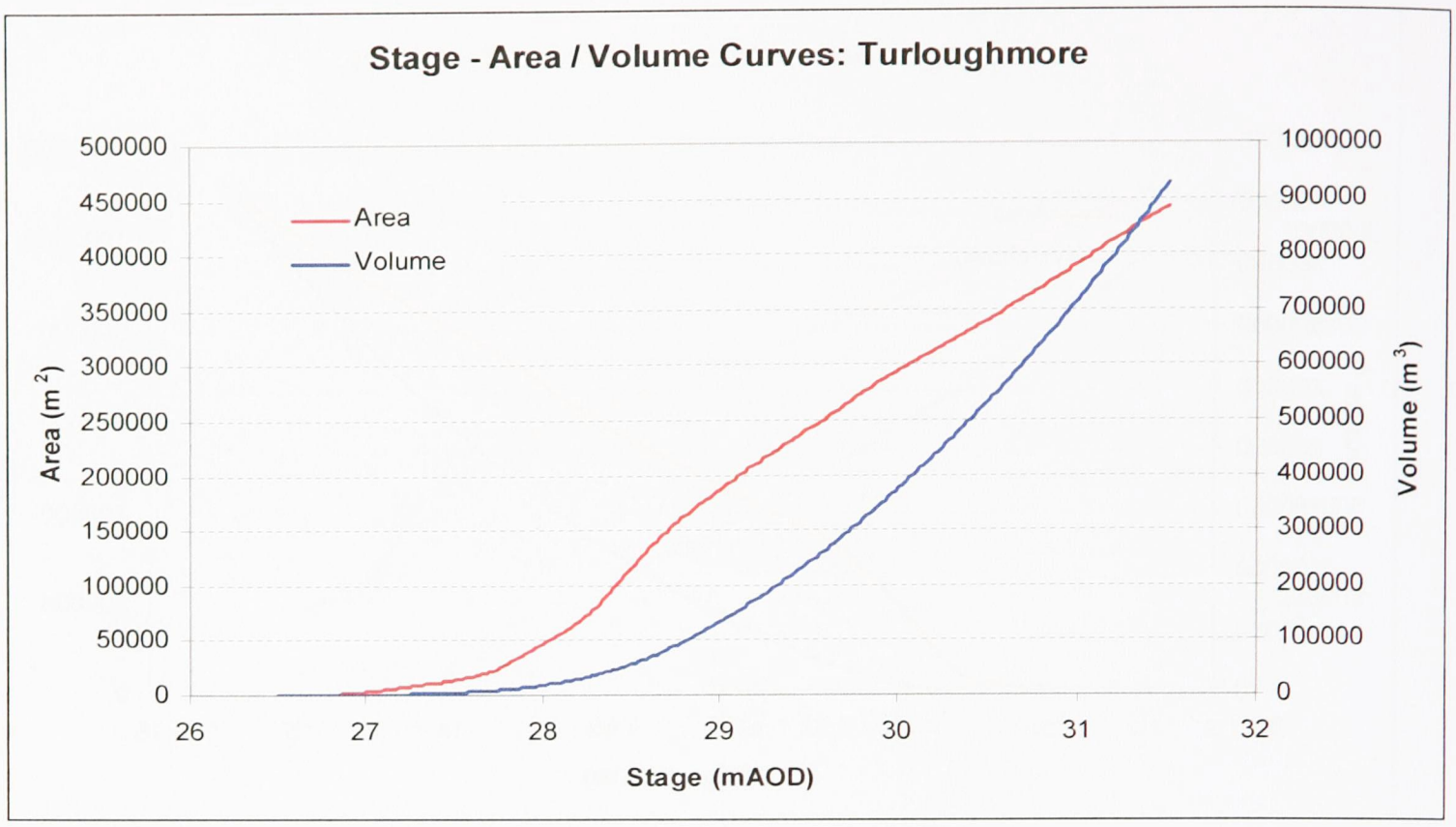

Stage - Area / Volume Curves: Lough Coy
300000
250000
200000
150000
100000
50000
0
Area (m 2)
1800000
1600000
1400000
1200000
1000000
800000
600000
400000
200000
0
Volume (m 3)
Area
Volume
8
10
12
14
16
18
20
Stage (mAOD)

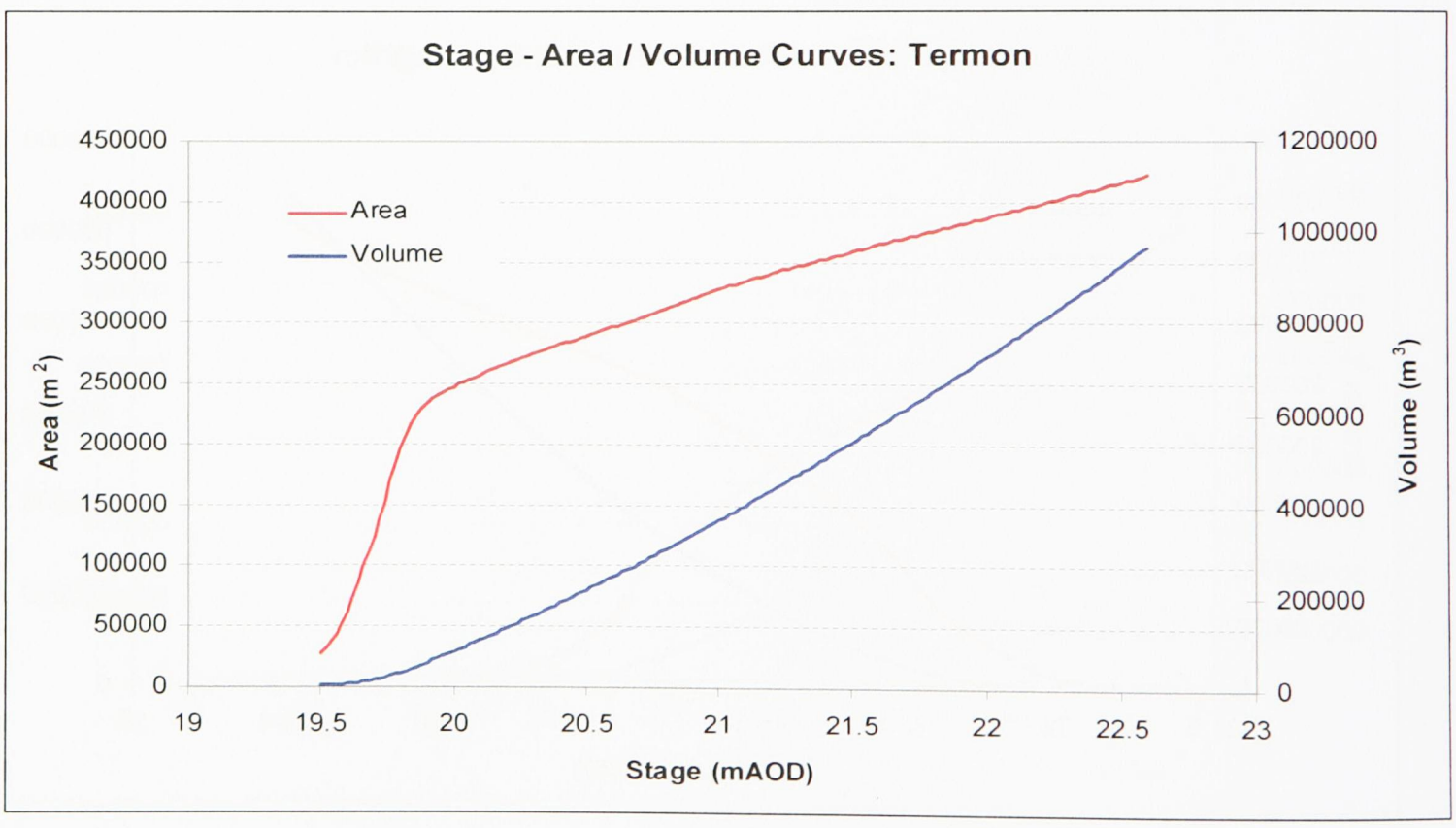

Stage - Area / Volume Curves: Lough Gealain
Area
Volume
Area (m 2)
Volume (m 3)
Stage (mAOD)
400000
350000
300000
250000
200000
150000
100000
50000
0
1200000
1000000
800000
600000
400000
200000
0
26.5
27
27.5
28
28.5
29
29.5
30
30.5
31
31.5


Stage - Area / Volume Curves: Rathnalulleagh
Area
Volume
Area (m 2)
Volume (m 3)
Stage (mAOD)
350000
300000
250000
200000
150000
100000
50000
0
1000000
900000
800000
700000
600000
500000
400000
300000
200000
100000
0
73
74
75
76
77
78
79
80
81
82

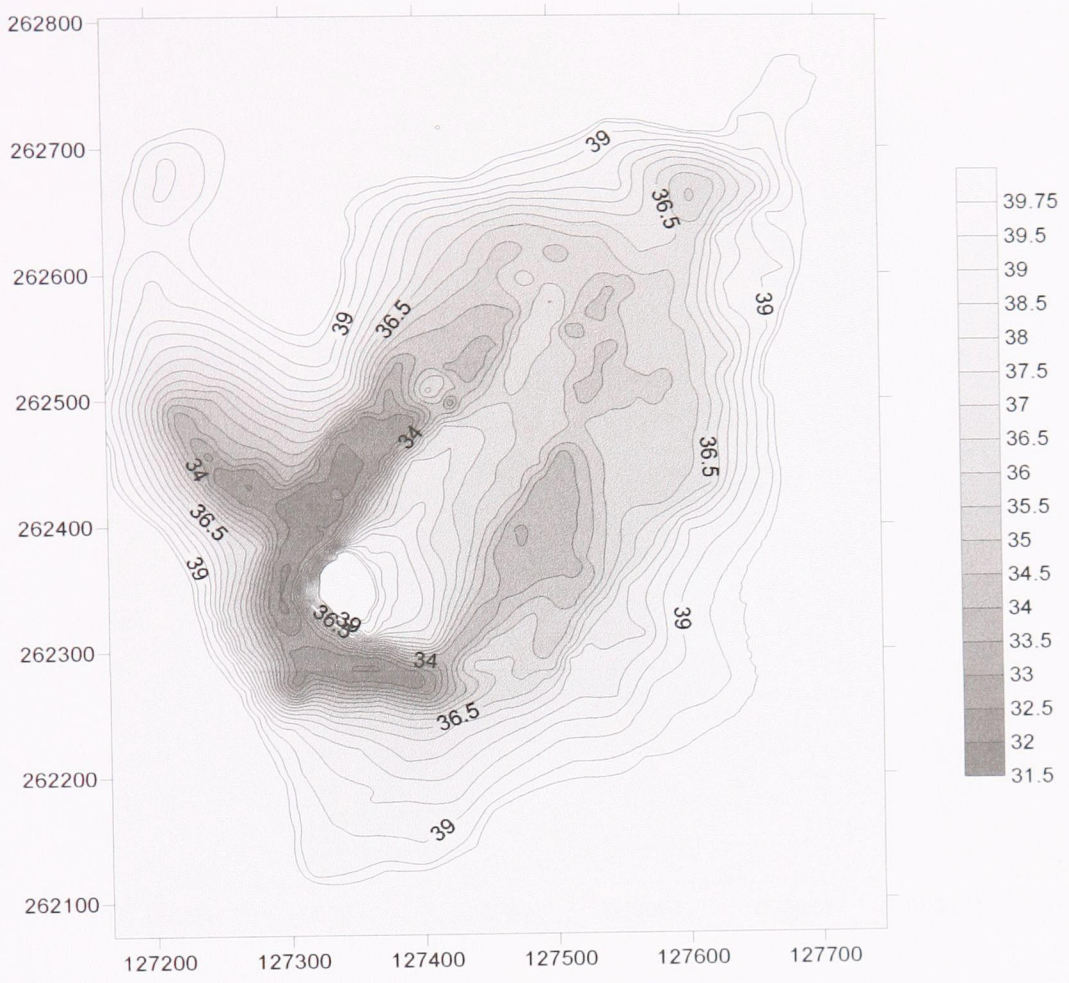

Stage - Area / Volume Curves: Roo West
Area
Volume
Area (m 2)
Volume (m 3)
Stage (mAOD)
450000
400000
350000
300000
250000
200000
150000
100000
50000
0
1200000
1000000
800000
600000
400000
200000
0
9
10
11
12
13
14
15
16

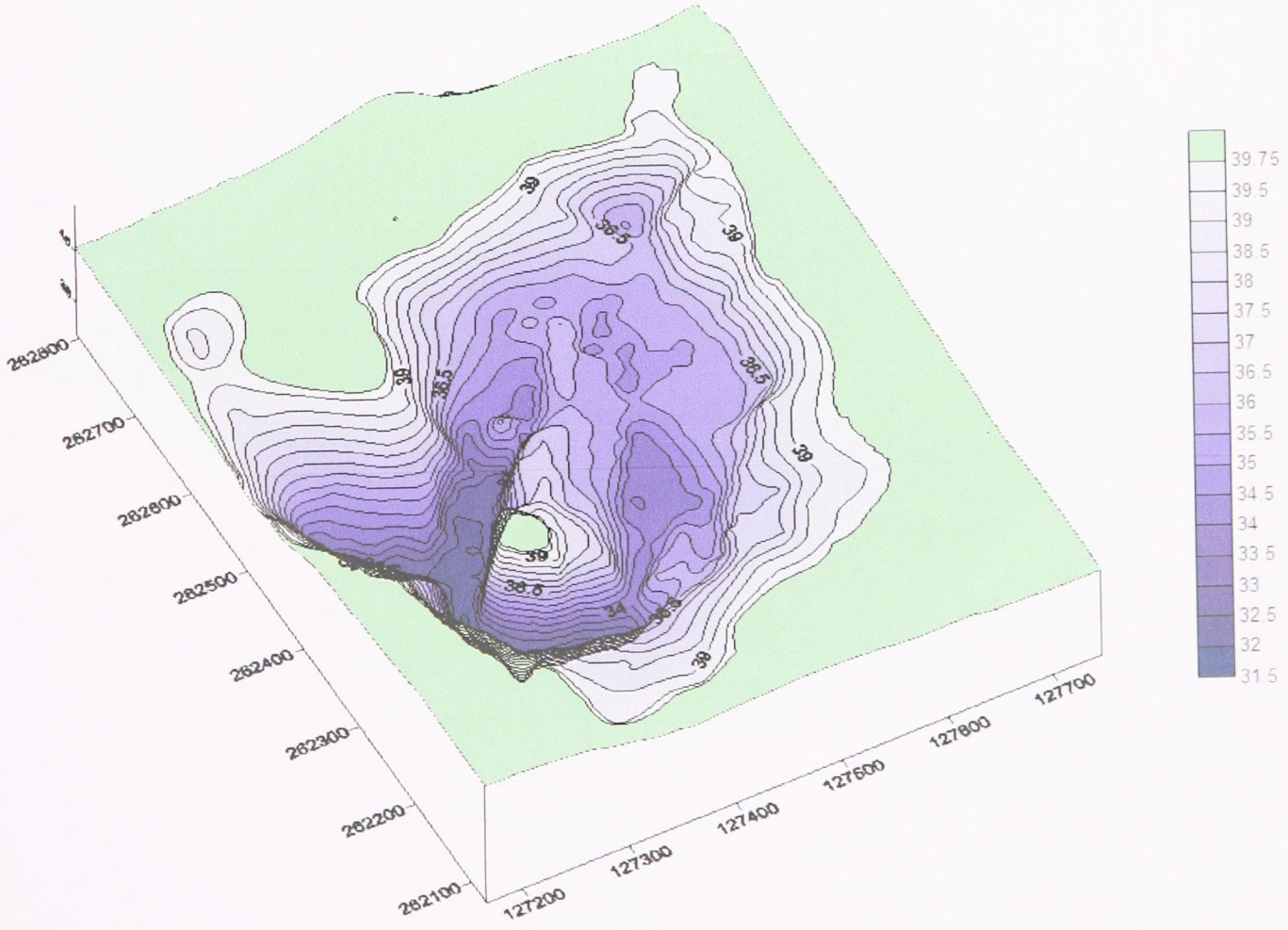

Stage - Area / Volume Curves: Skealoghan
Area
Volume
Area (m 2)
Volume (m 3)
Stage (mAOD)
450000
400000
350000
300000
250000
200000
150000
100000
50000
0
600000
500000
400000
300000
200000
100000
0
31.5
32
32.5
33
33.5
34
34.5
35


Stage - Area / Volume Curves: Turloughmore
Area
Volume
Area (m 2)
Volume (m 3)
Stage (mAOD)
500000
450000
400000
350000
300000
250000
200000
150000
100000
50000
0
1000000
900000
800000
700000
600000
500000
400000
300000
200000
100000
0
26
27
28
29
30
31
32


Stage - Area / Volume Curves: Termon
Area
Volume
Area (m 2)
Volume (m 3)
Stage (mAOD)
450000
400000
350000
300000
250000
200000
150000
100000
50000
0
1200000
1000000
800000
600000
400000
200000
0
19
19.5
20
20.5
21
21.5
22
22.5
23

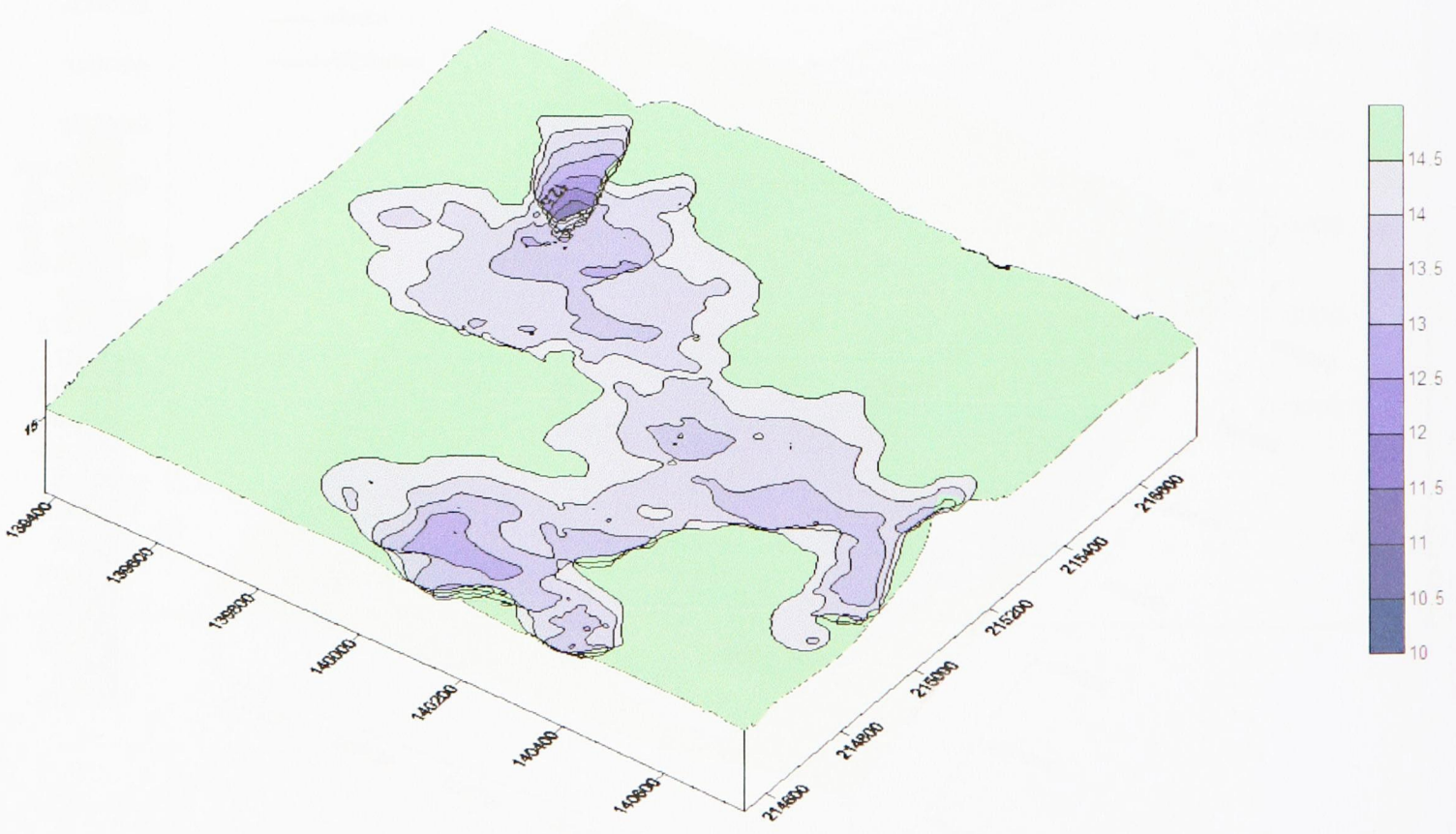
ARDKILL


262800
262700
262600
262500
262400
262300
262200
262100
127200
127300
127400
127500
127600
127700
39
36.5
34
39.75
39.5
39
38.5
38
37.5
37
36.5
36
35.5
35
34.5
34
33.5
33
32.5
32
31.5

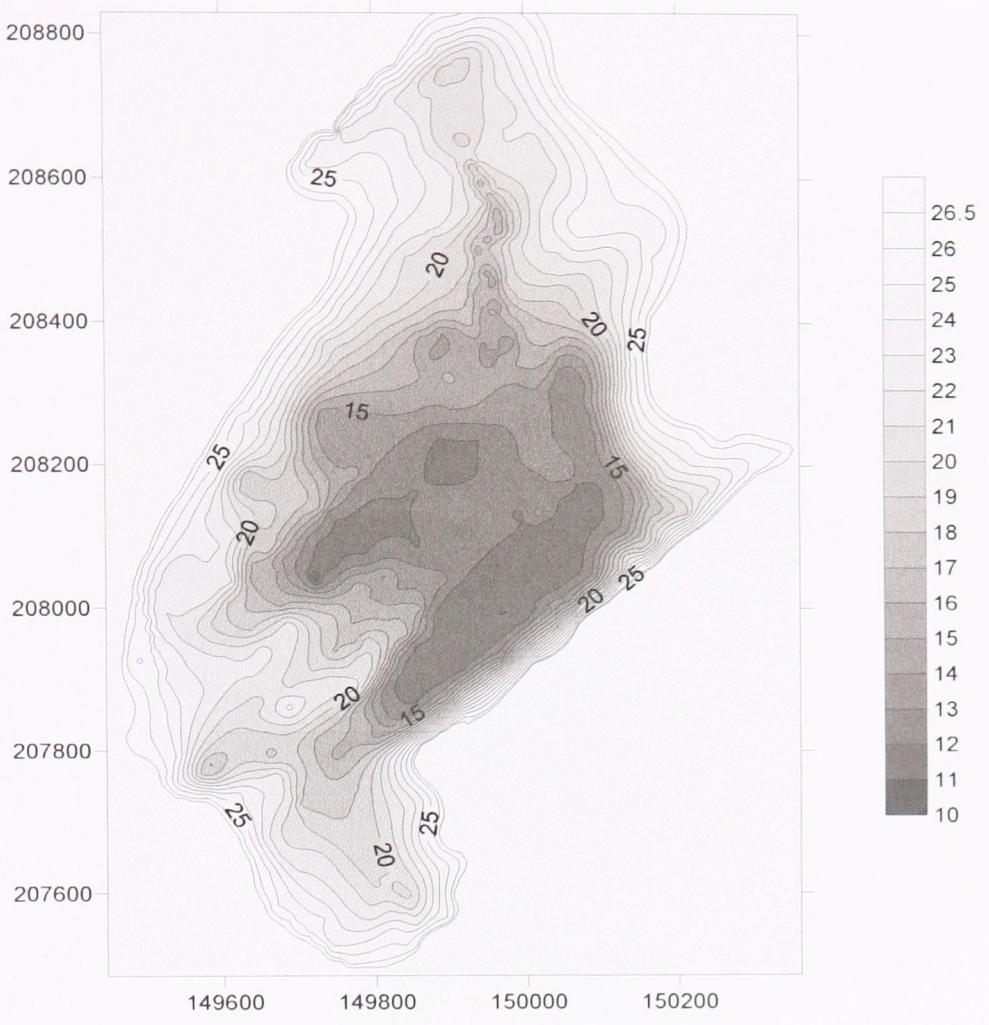

262800
262700
262600
262500
262400
262300
262200
262100
127200
127300
127400
127600
127800
127700
39
36.5
34
39.75
39.5
39
38.5
38
37.5
37
36.5
36
35.5
35
34.5
34
33.5
33
32.5
32
31.5

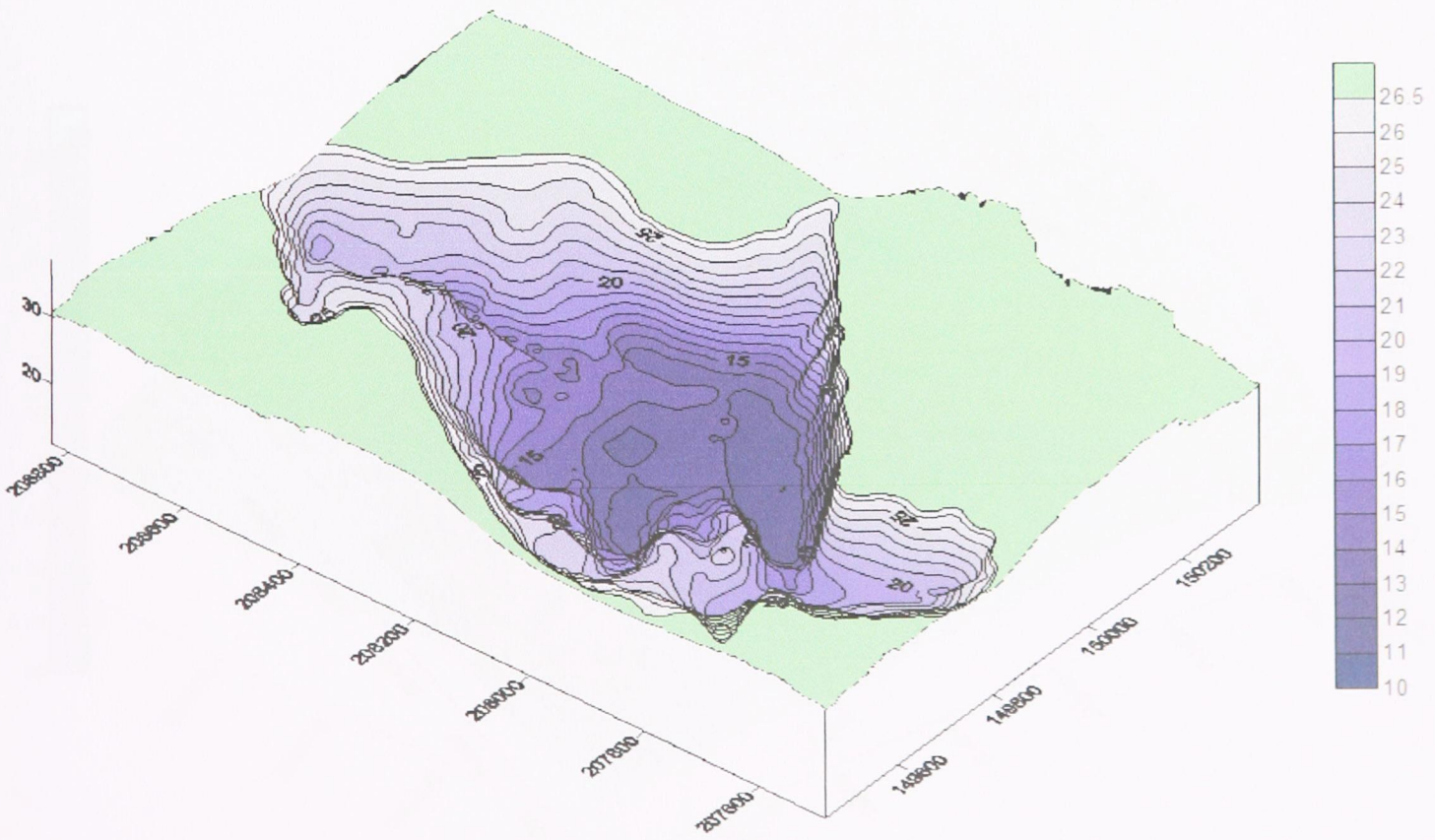
BALLINDERREEN



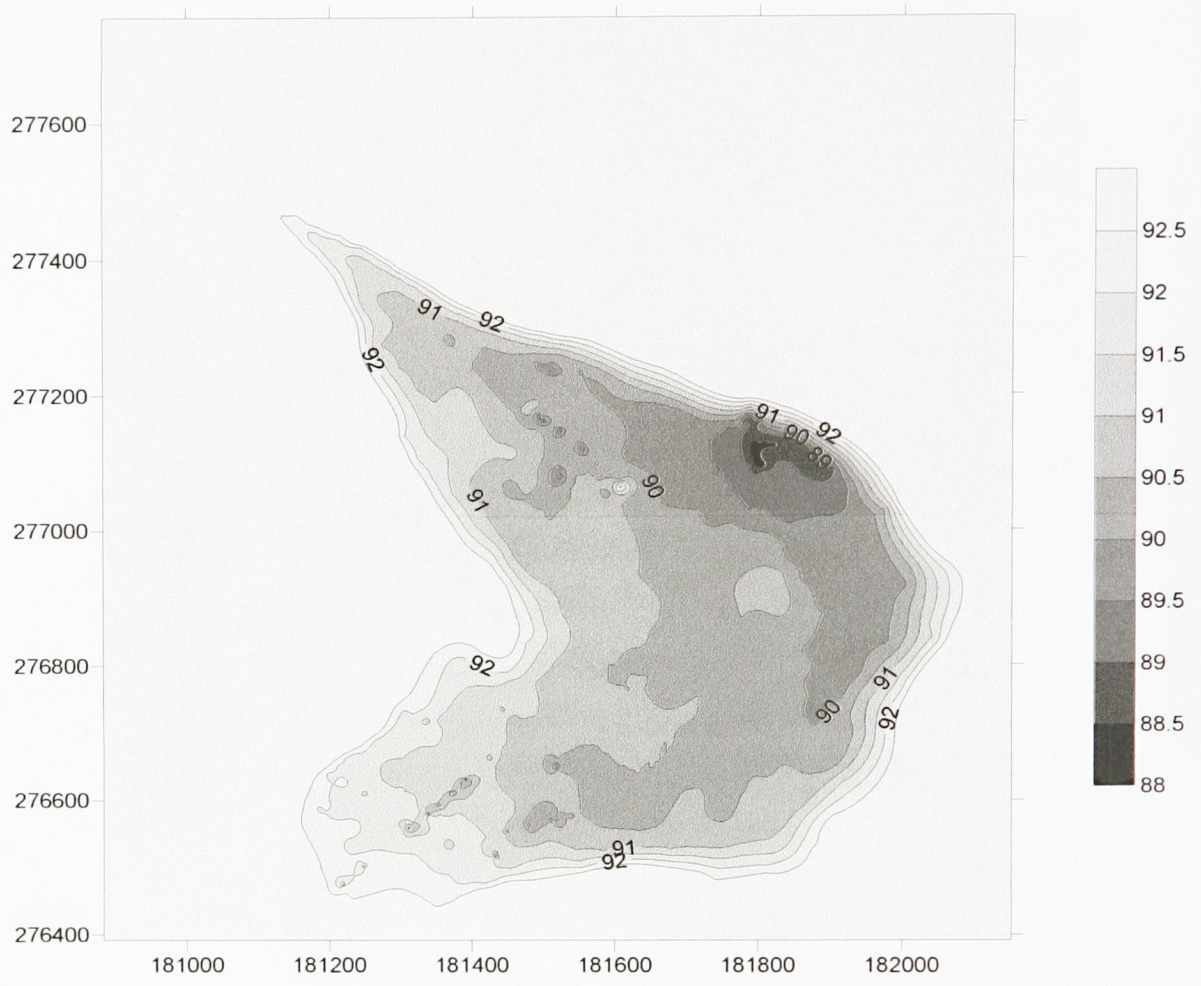


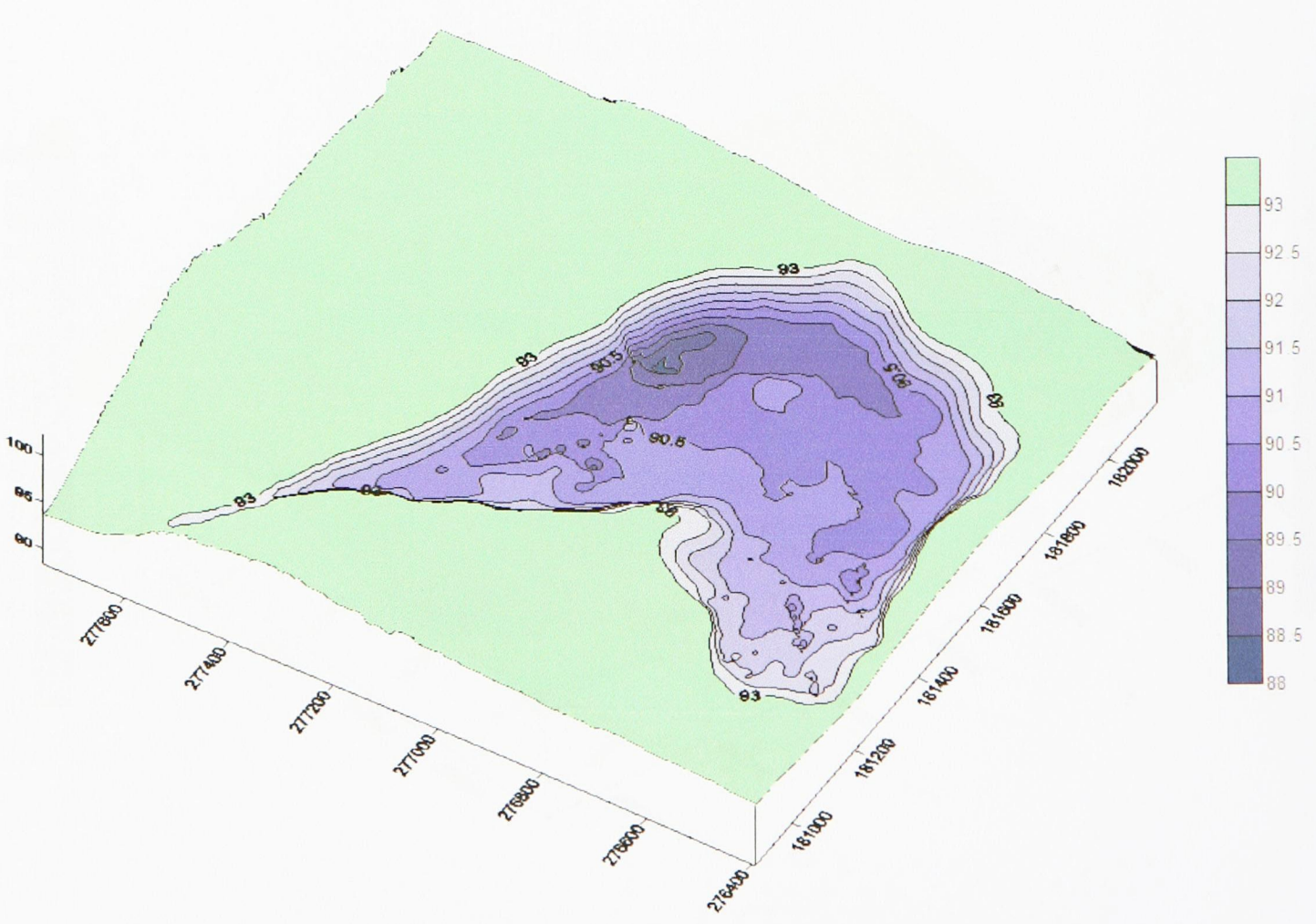
BLACKROCK


208800
208600
208400
208200
208000
207800
207600
149600
149800
150000
150200
26.5
26
25
24
23
22
21
20
19
18
17
16
15
14
13
12
11
10

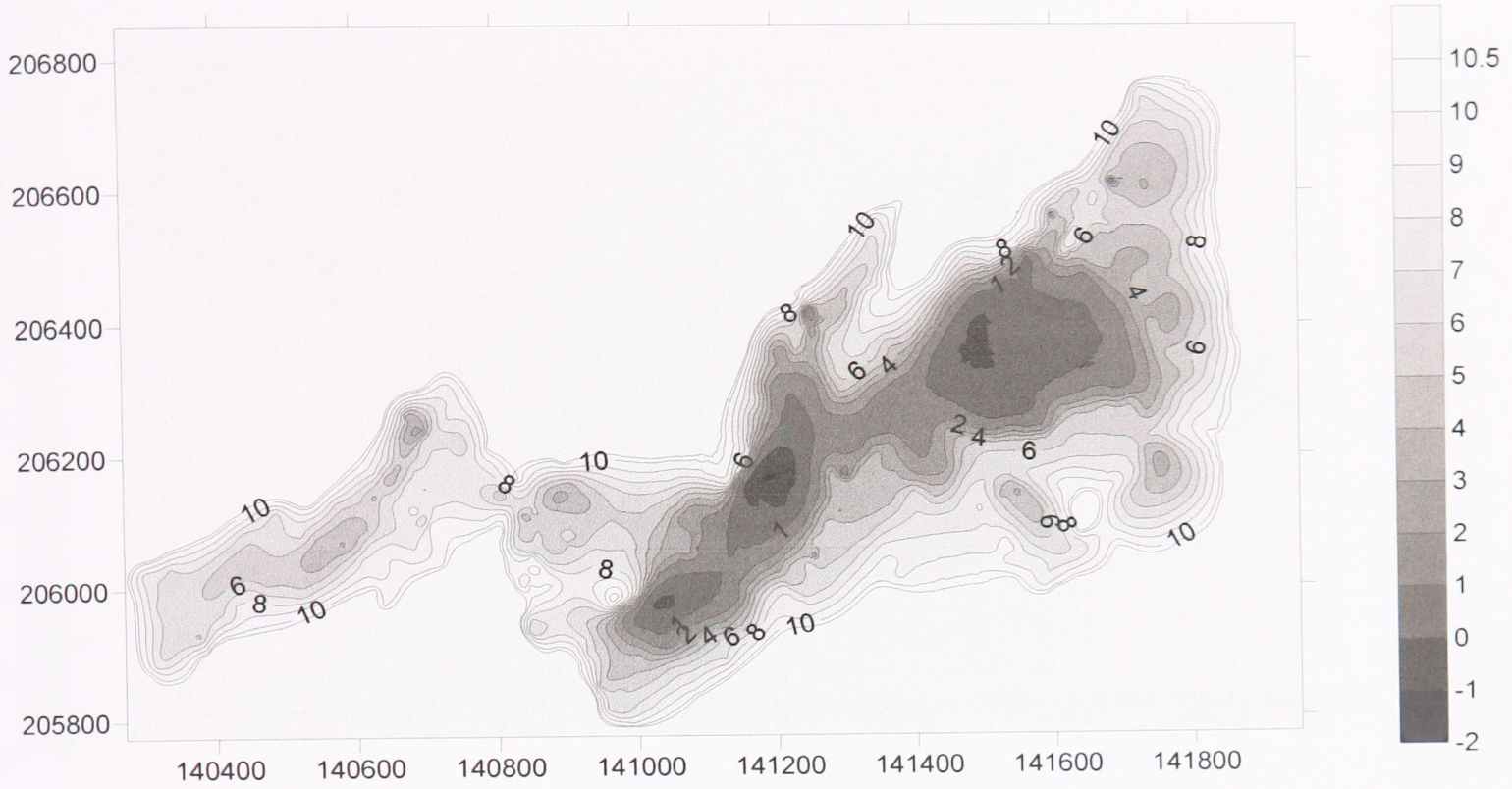

26.5
26
25
24
23
22
21
20
19
18
17
16
15
14
13
12
11
10

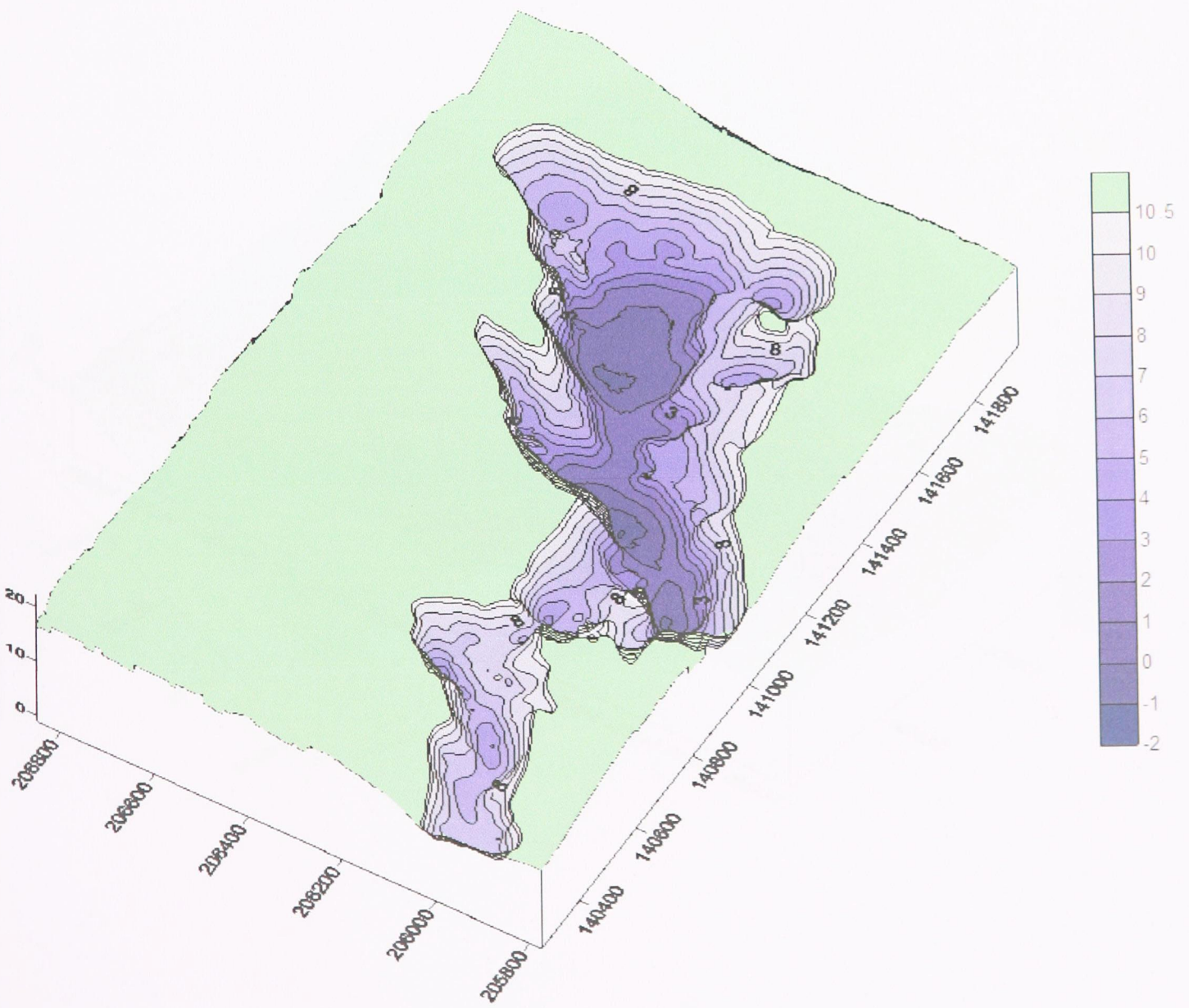
BRIERFIELD


277600
277400
277200
277000
276800
276600
276400
181000
181200
181400
181600
181800
182000
91
92
90
89
92.5
91.5
90.5
89.5
88.5
88

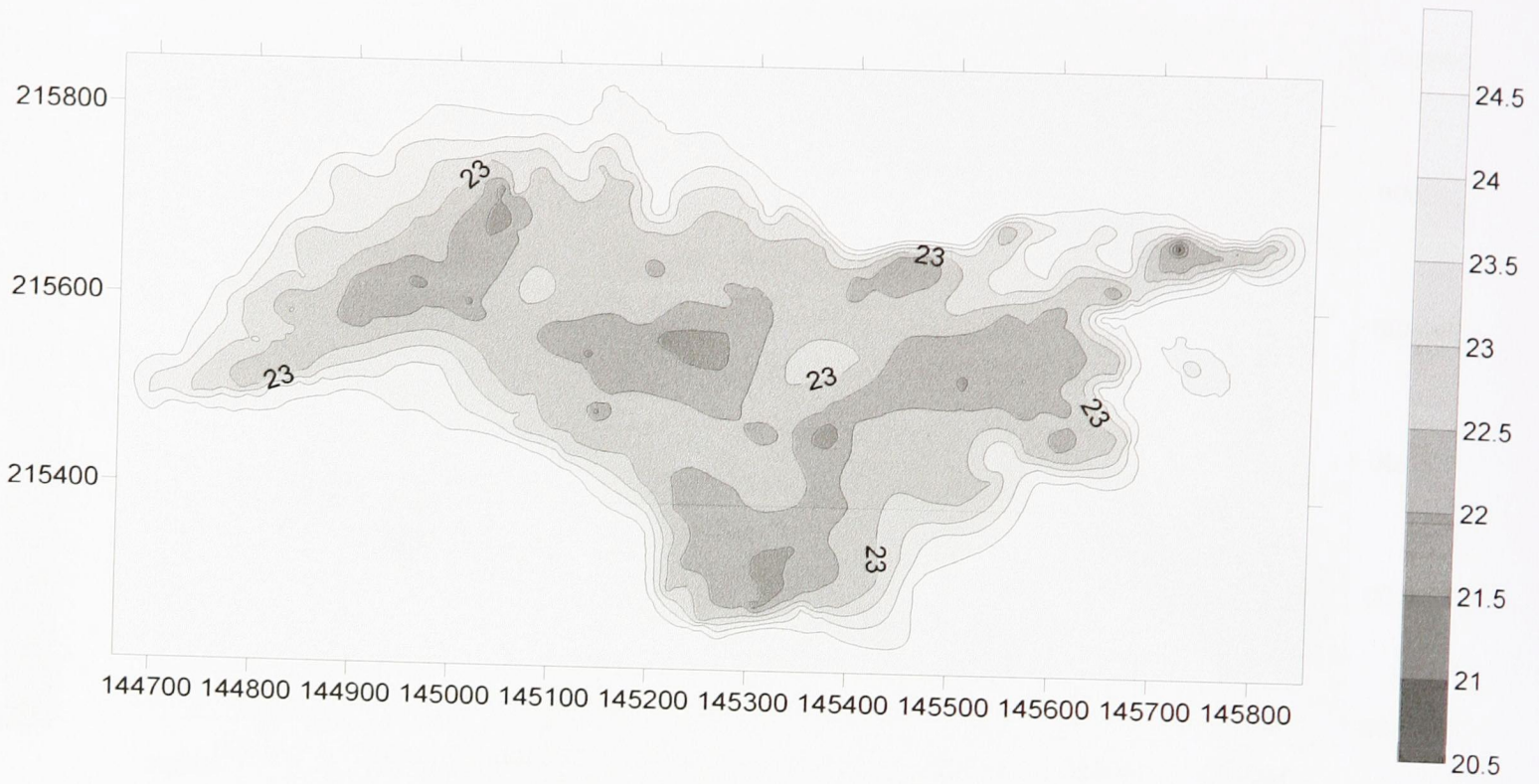

93
92.5
92
91.5
91
90.5
90
89.5
89
88.5
88
277800
277600
277400
277200
277000
276800
276600
276400
181000
181200
181400
181600
181800
182000

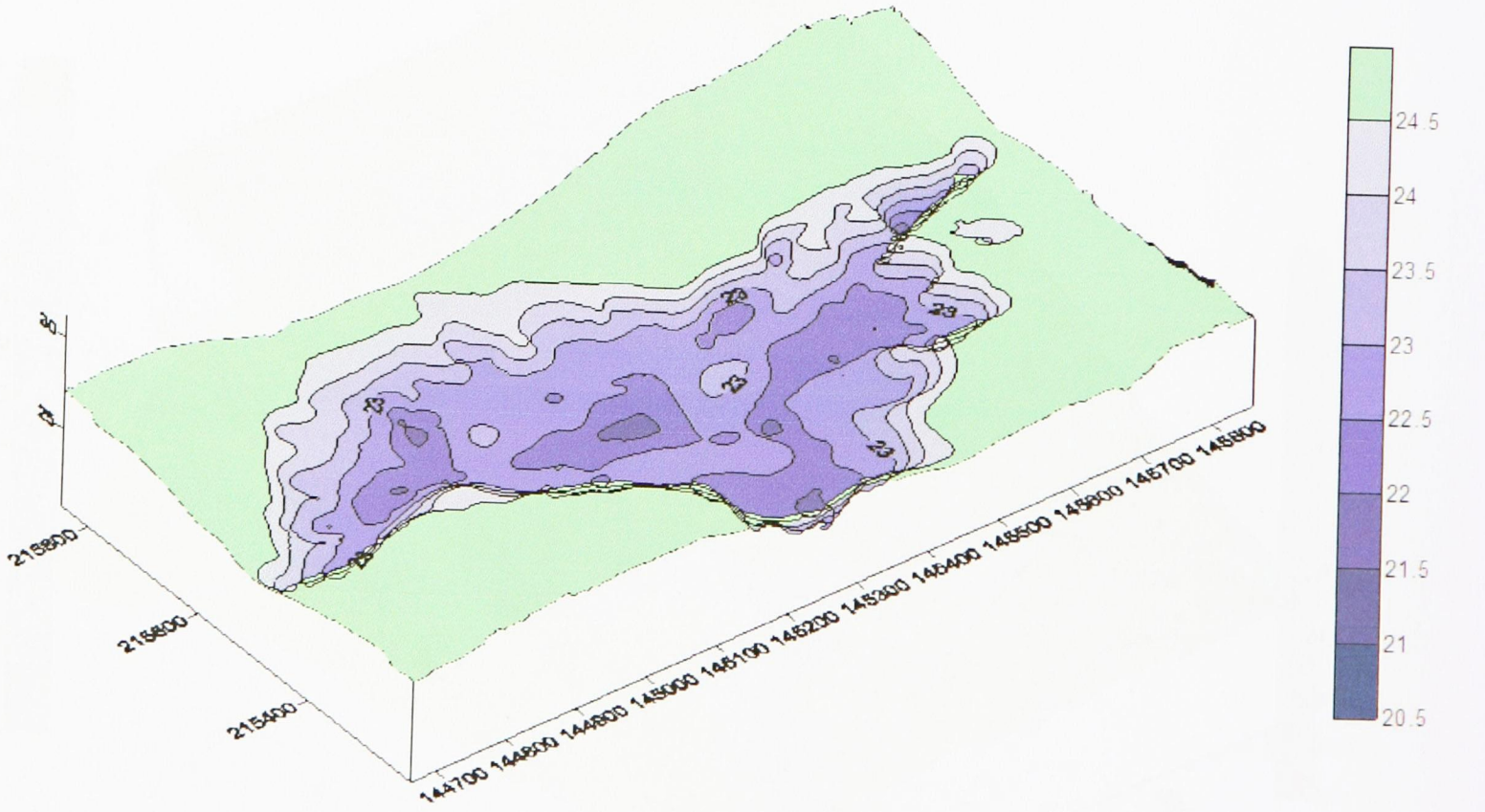
CAHERGLASSAUN



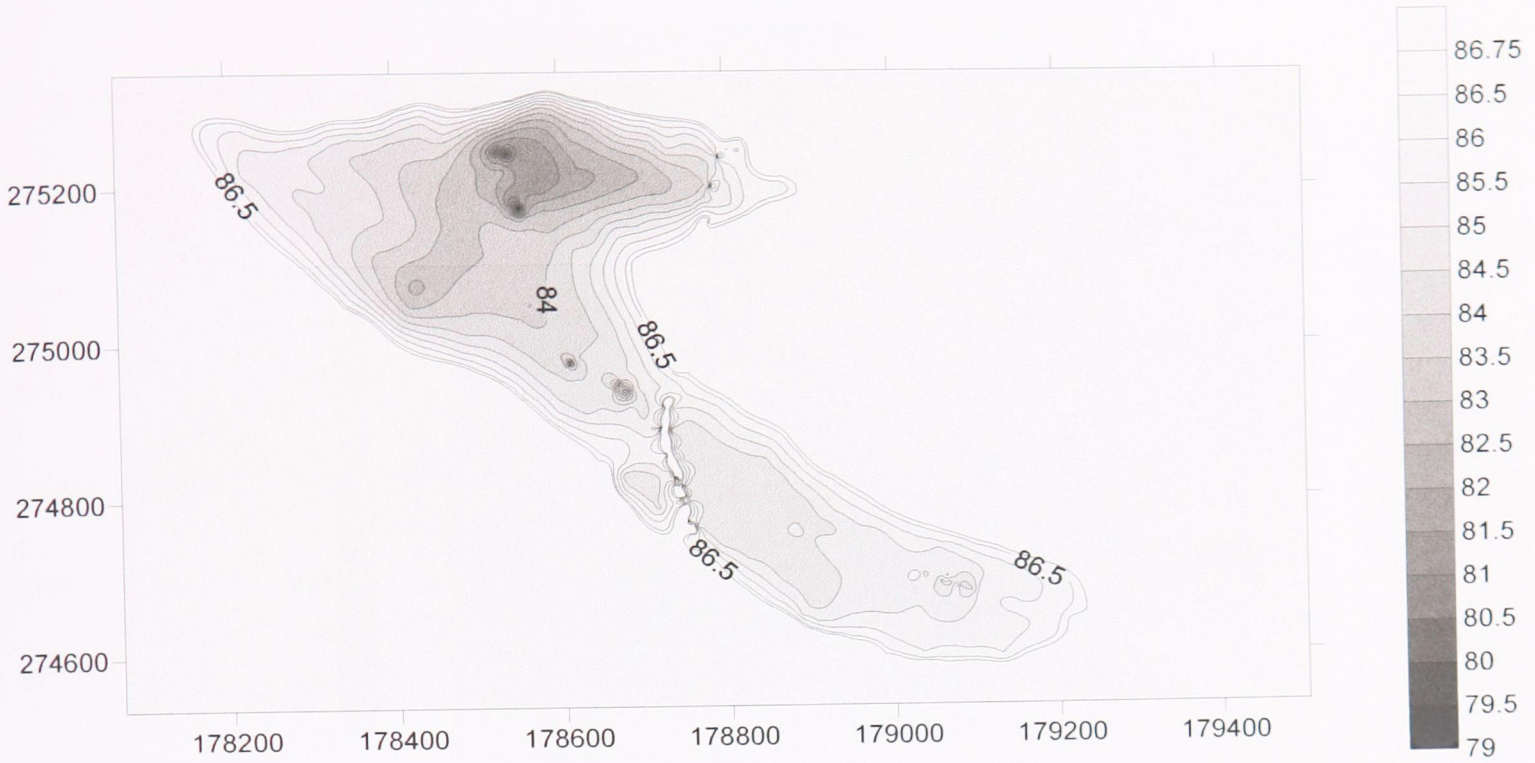


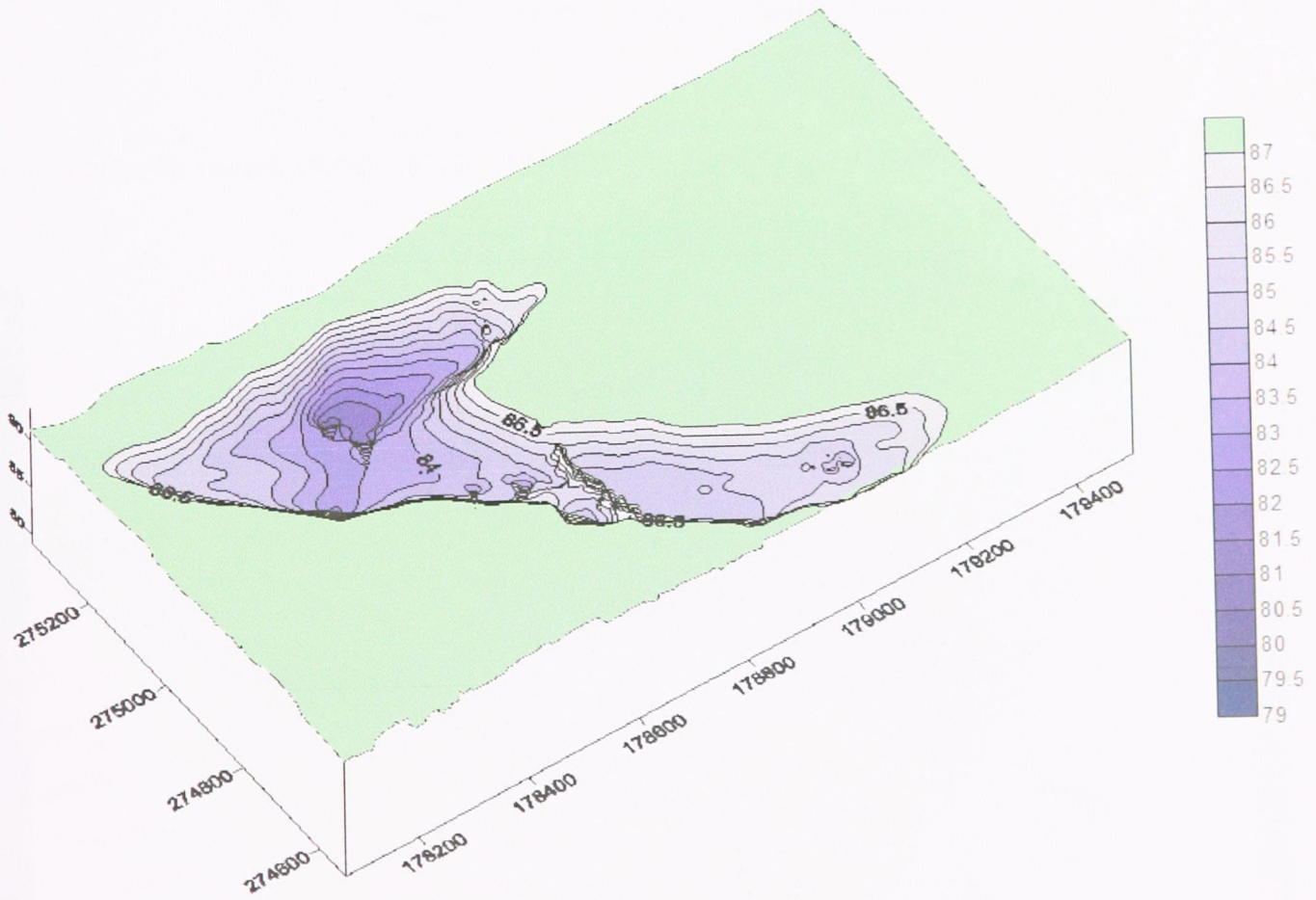
CARANAVOODAUN



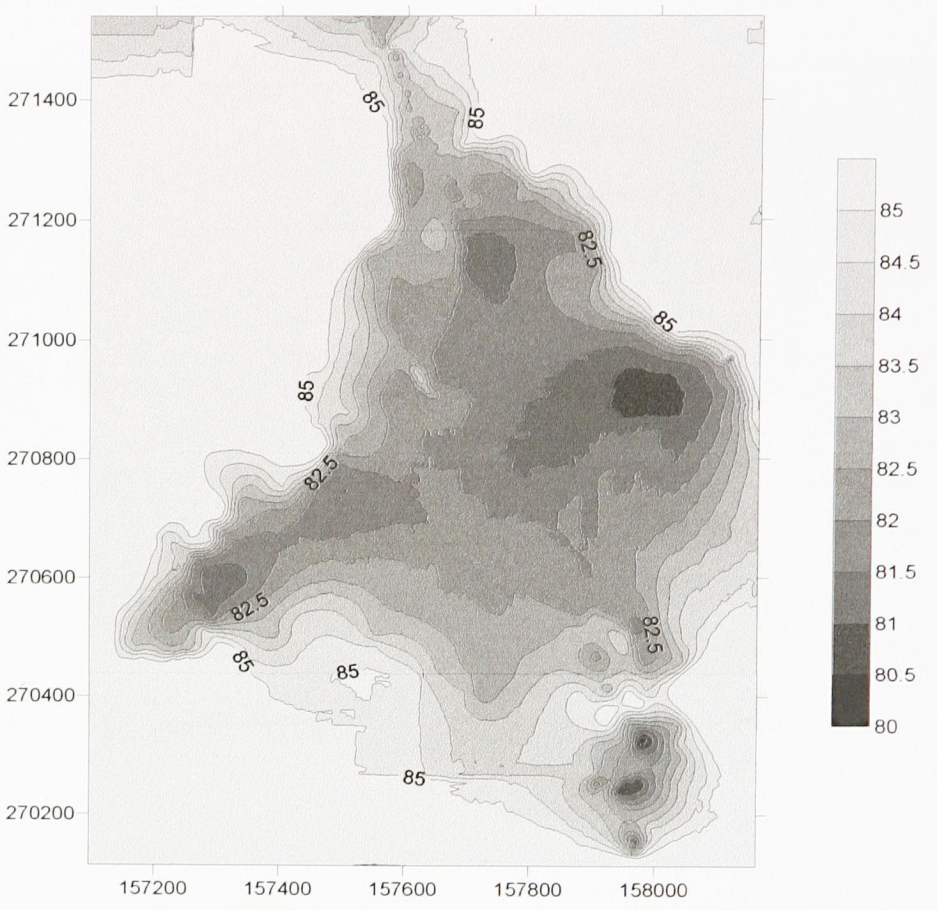


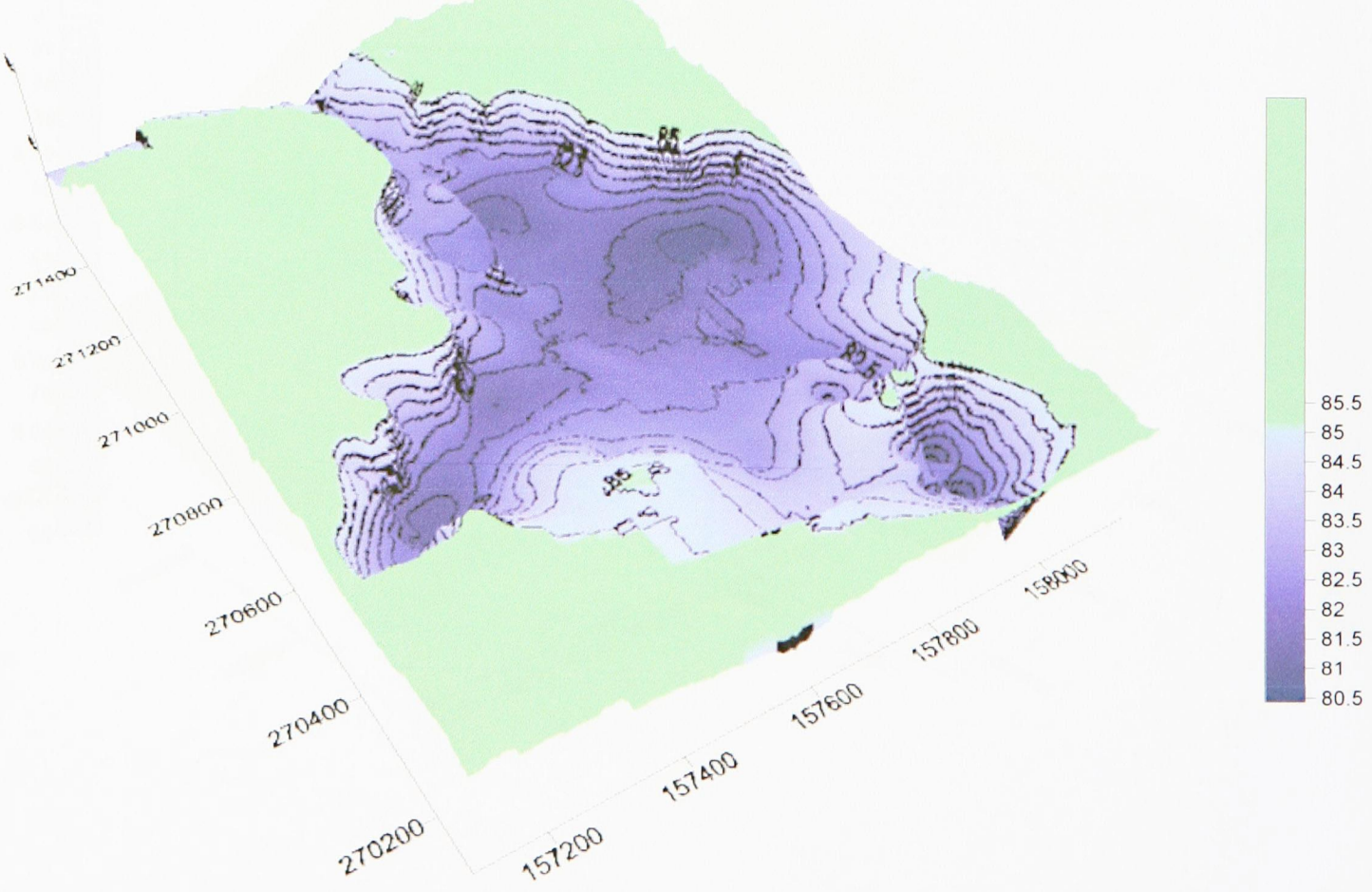
CARROWREAGH



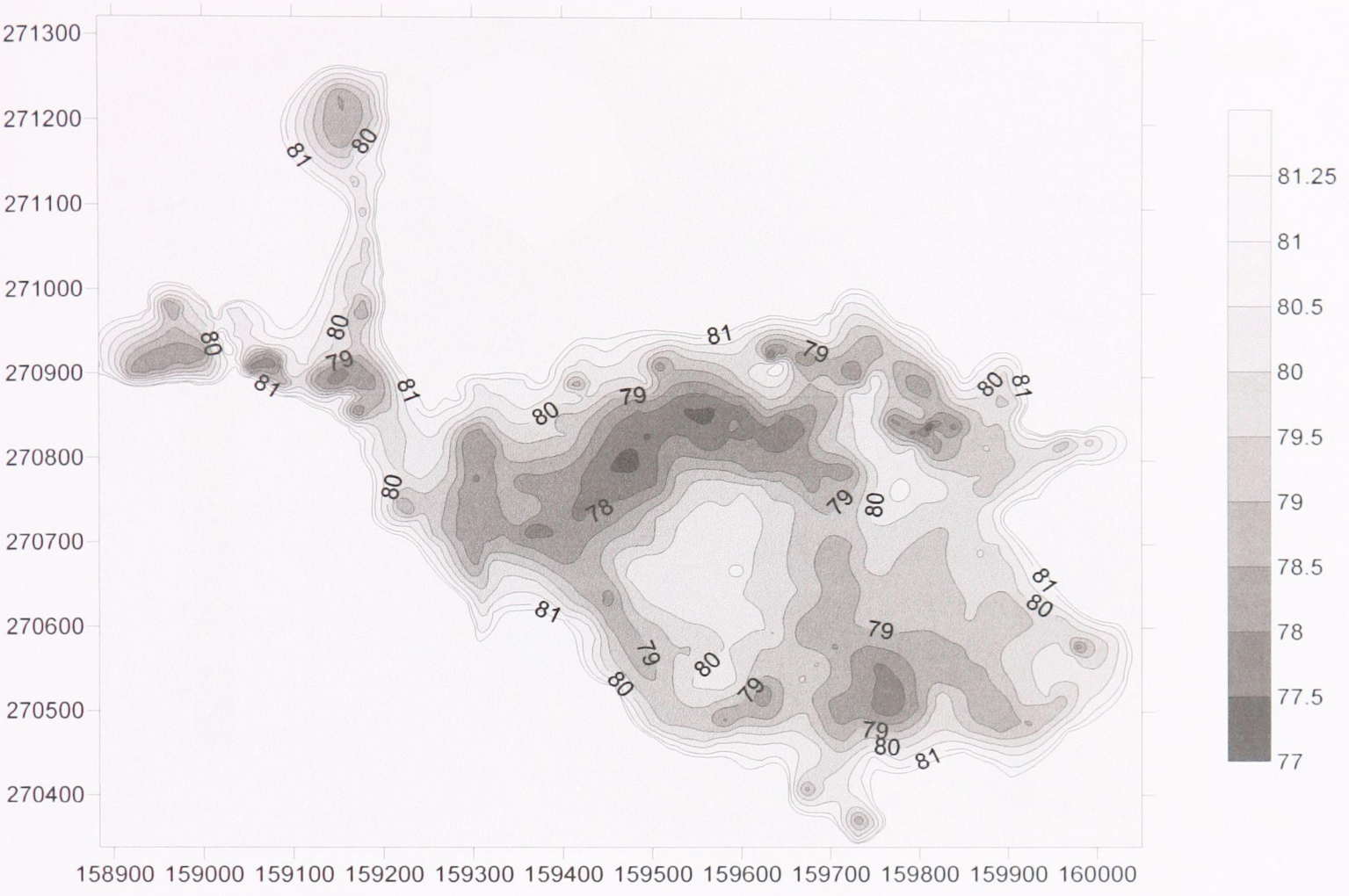


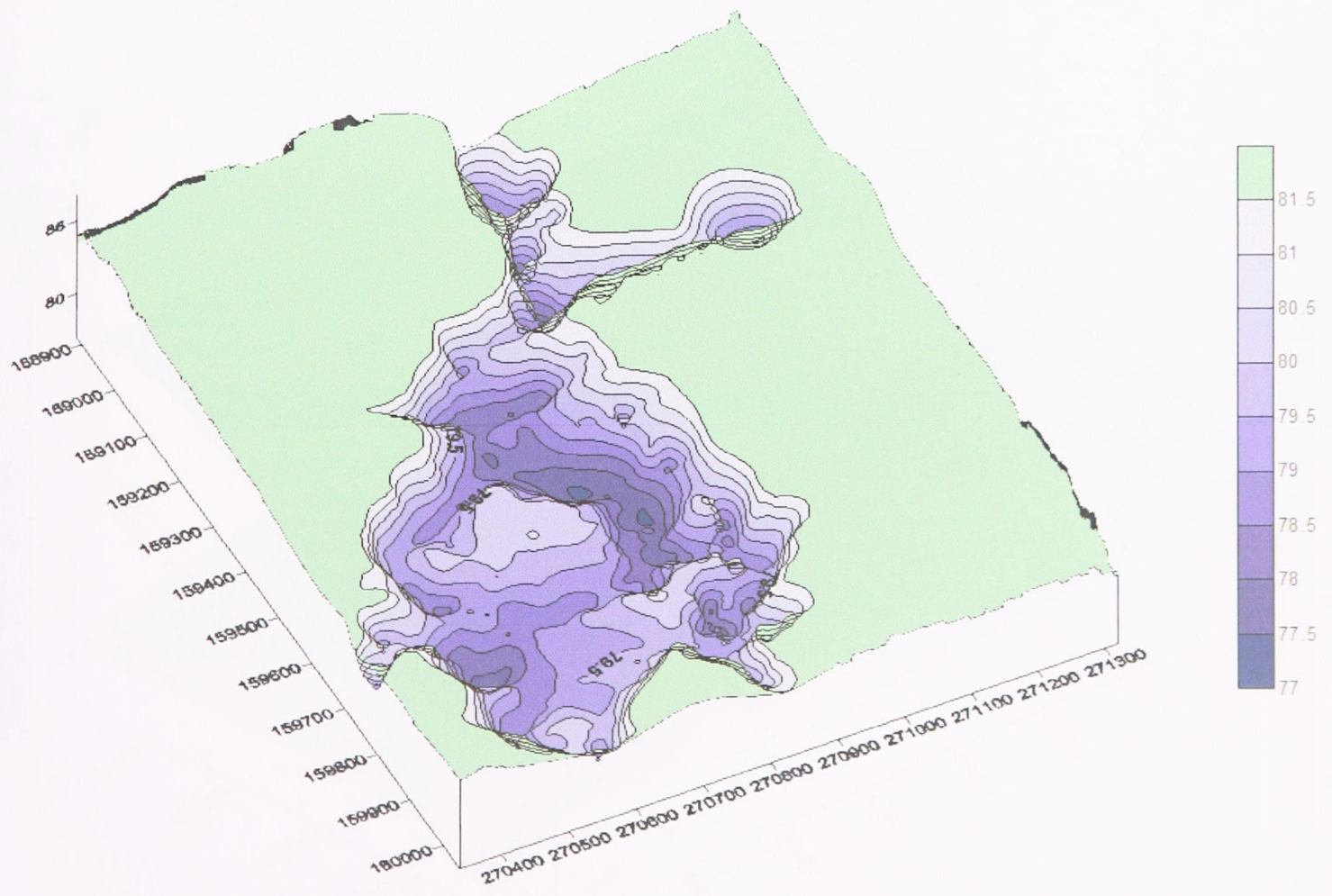
COOLCAM


271400
271200
271000
270800
270600
270400
270200
157200
157400
157600
157800
158000
85
82.5
85
84.5
84
83.5
83
82.5
82
81.5
81
80.5
80

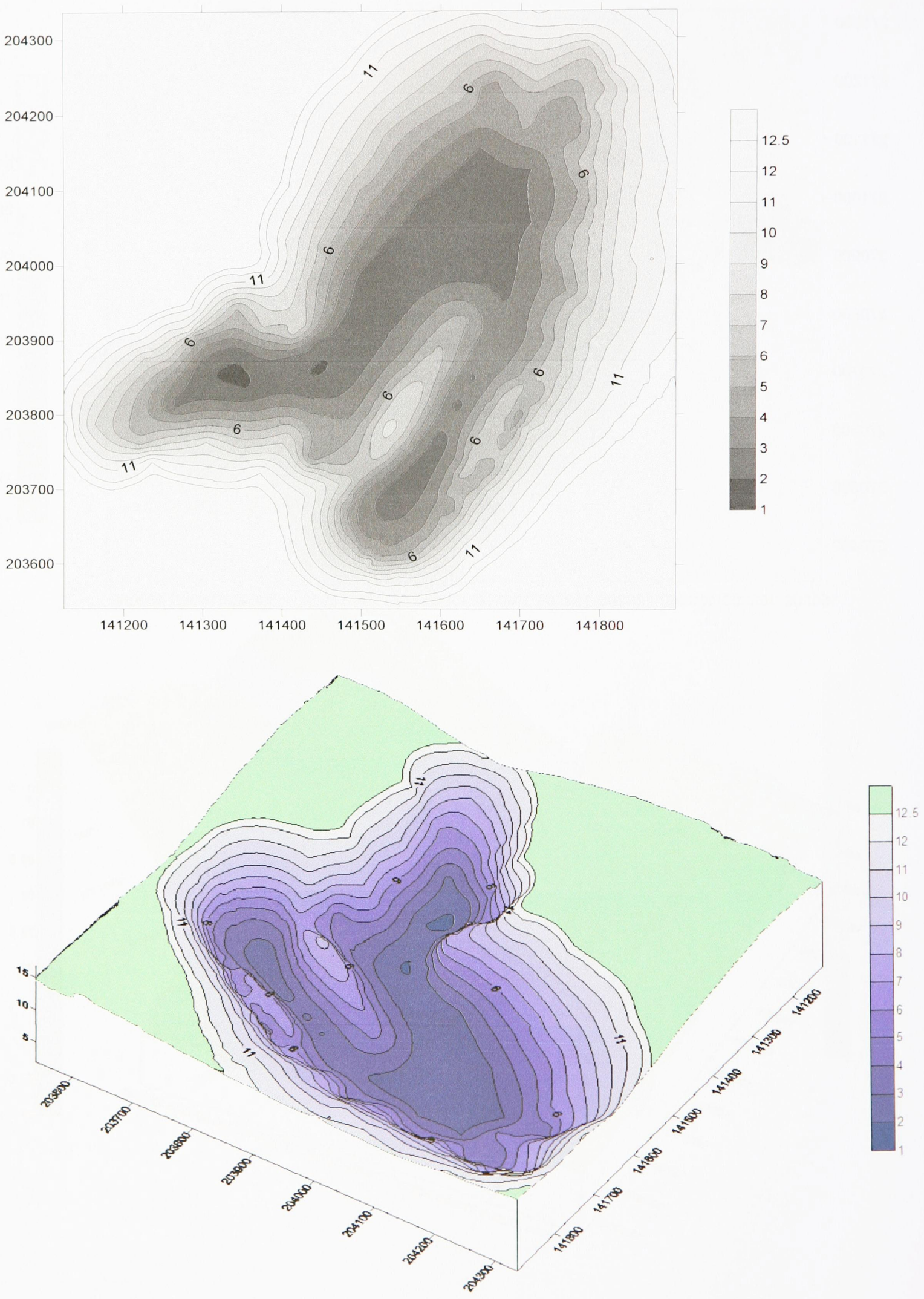

271400
271200
271000
270800
270600
270400
270200
157200
157400
157600
157800
158000
85.5
85
84.5
84
83.5
83
82.5
82
81.5
81
80.5

CROAGHILL

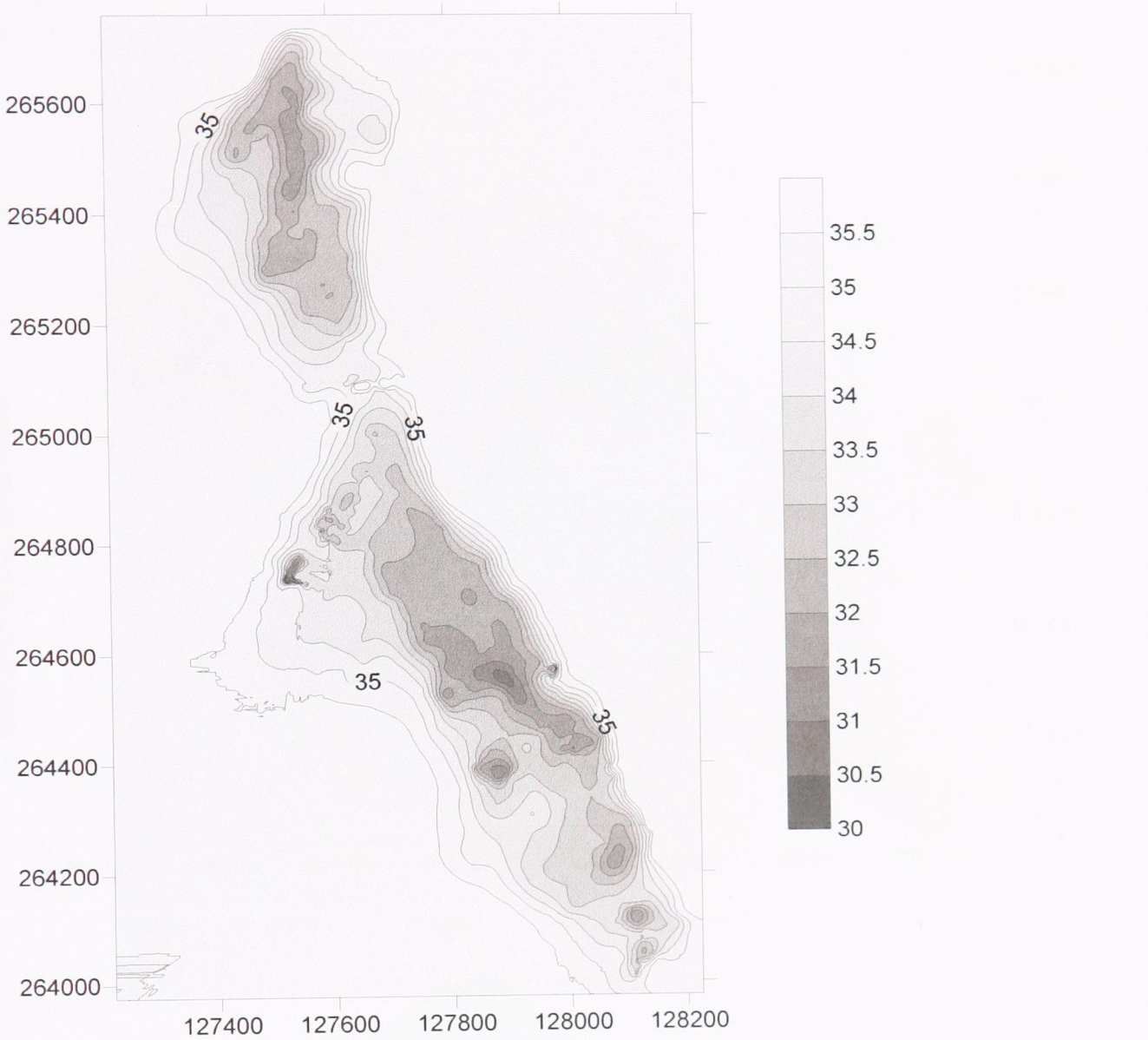

271300
271200
271100
271000
270900
270800
270700
270600
270500
270400
158900 159000 159100 159200 159300 159400 159500 159600 159700 159800 159900 160000
81.25
81
80.5
80
79.5
79
78.5
78
77.5
77

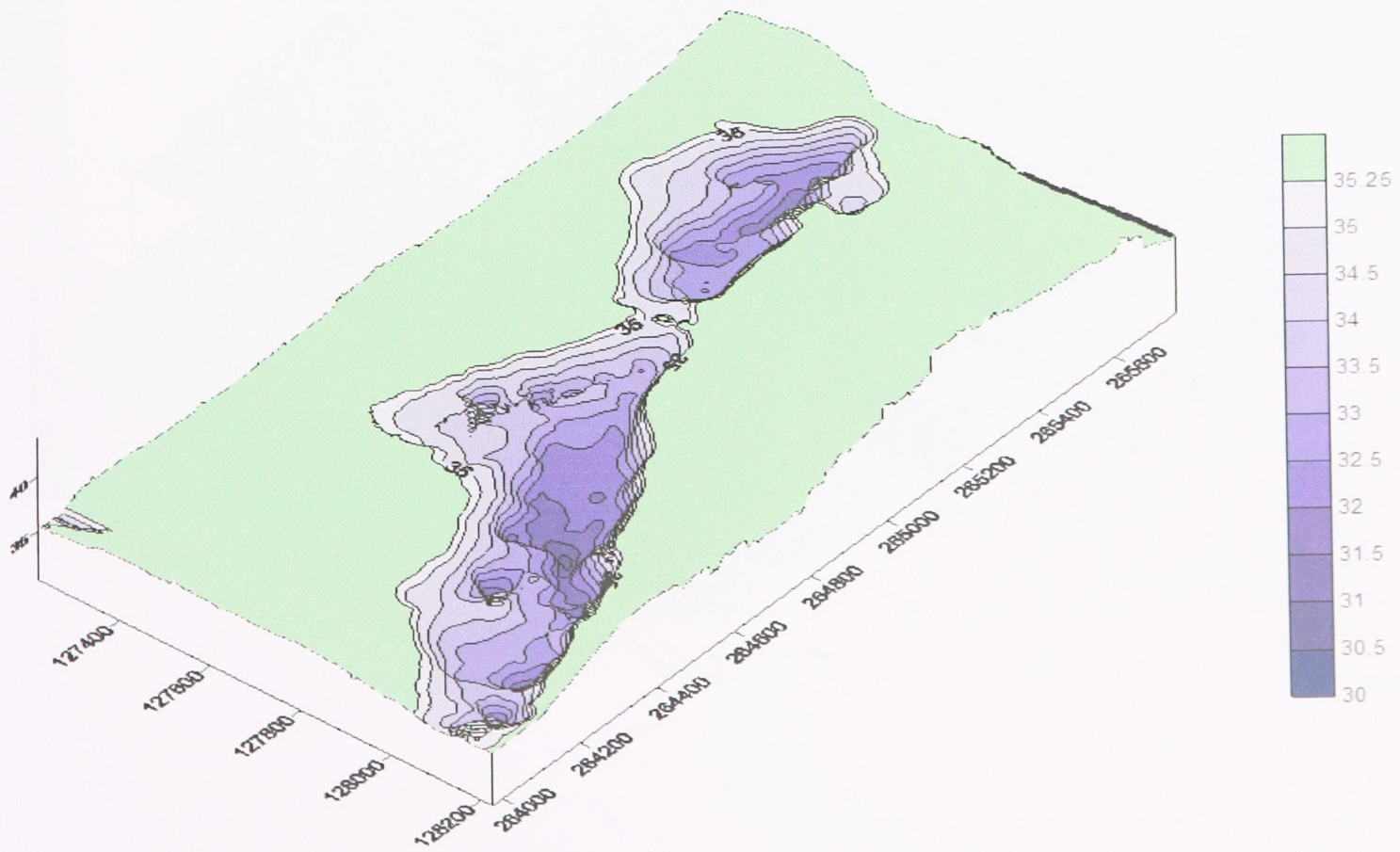

86
80
158900
159000
159100
159200
159300
159400
159500
159600
159700
159800
159900
160000
270400 270500 270600 270700 270800 270900 271000 271100 271200 271300
81.5
81
80.5
80
79.5
79
78.5
78
77.5
77

GARRYLAND

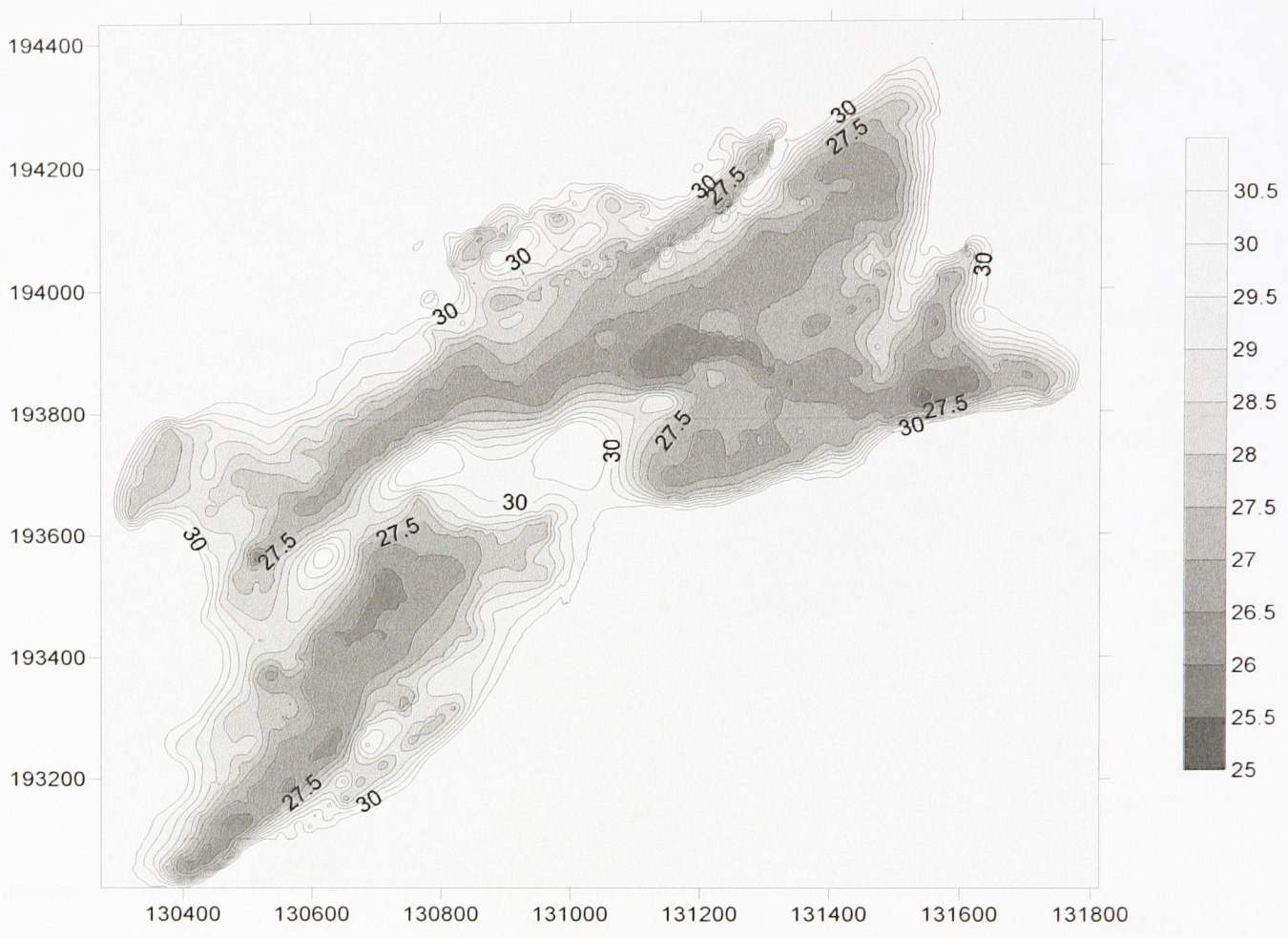

204300
204200
204100
204000
203900
203800
203700
203600
141200
141300
141400
141500
141600
141700
141800
12.5
12
11
10
9
8
7
6
5
4
3
2
1

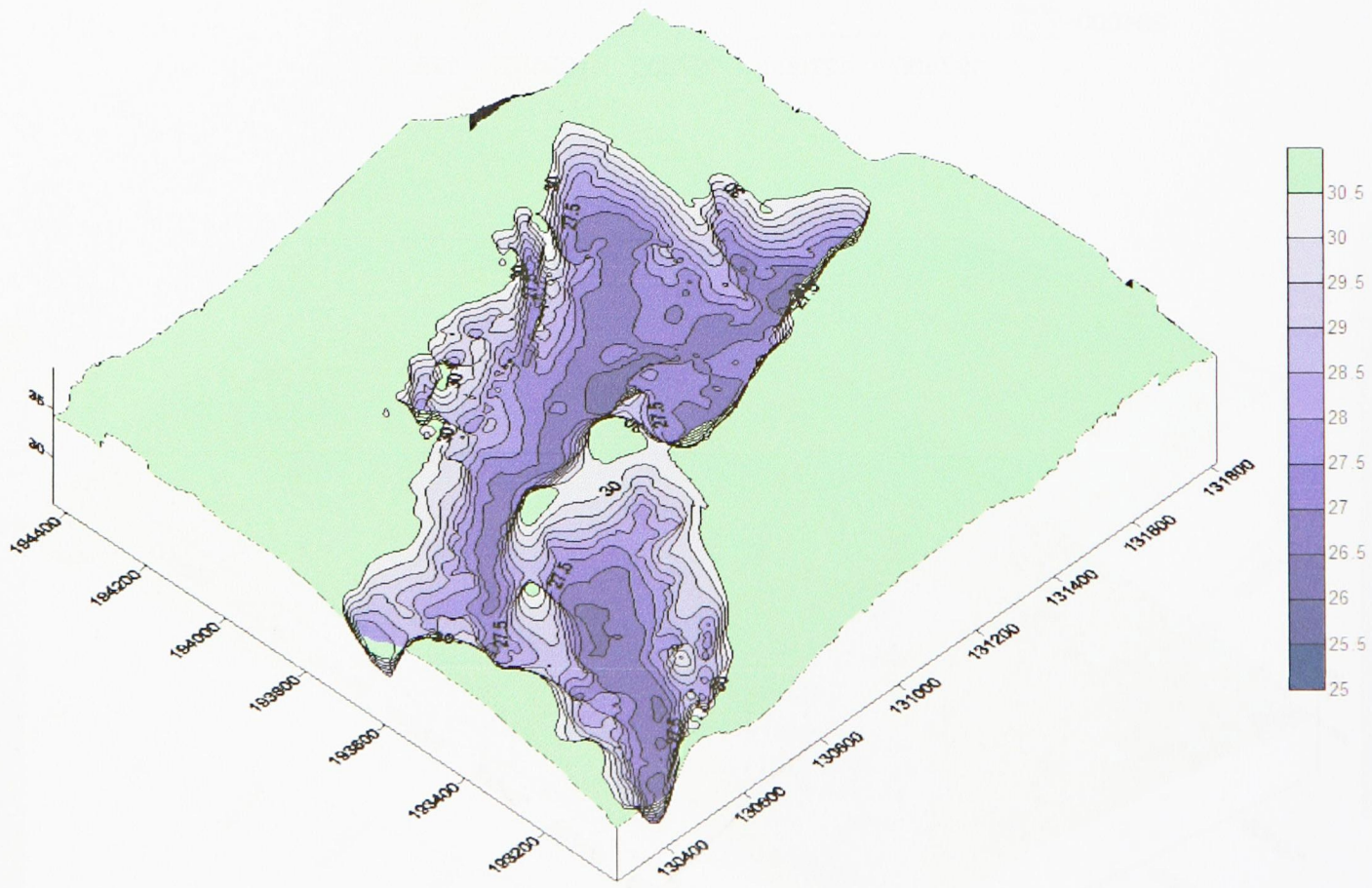
KILGLASSAUN



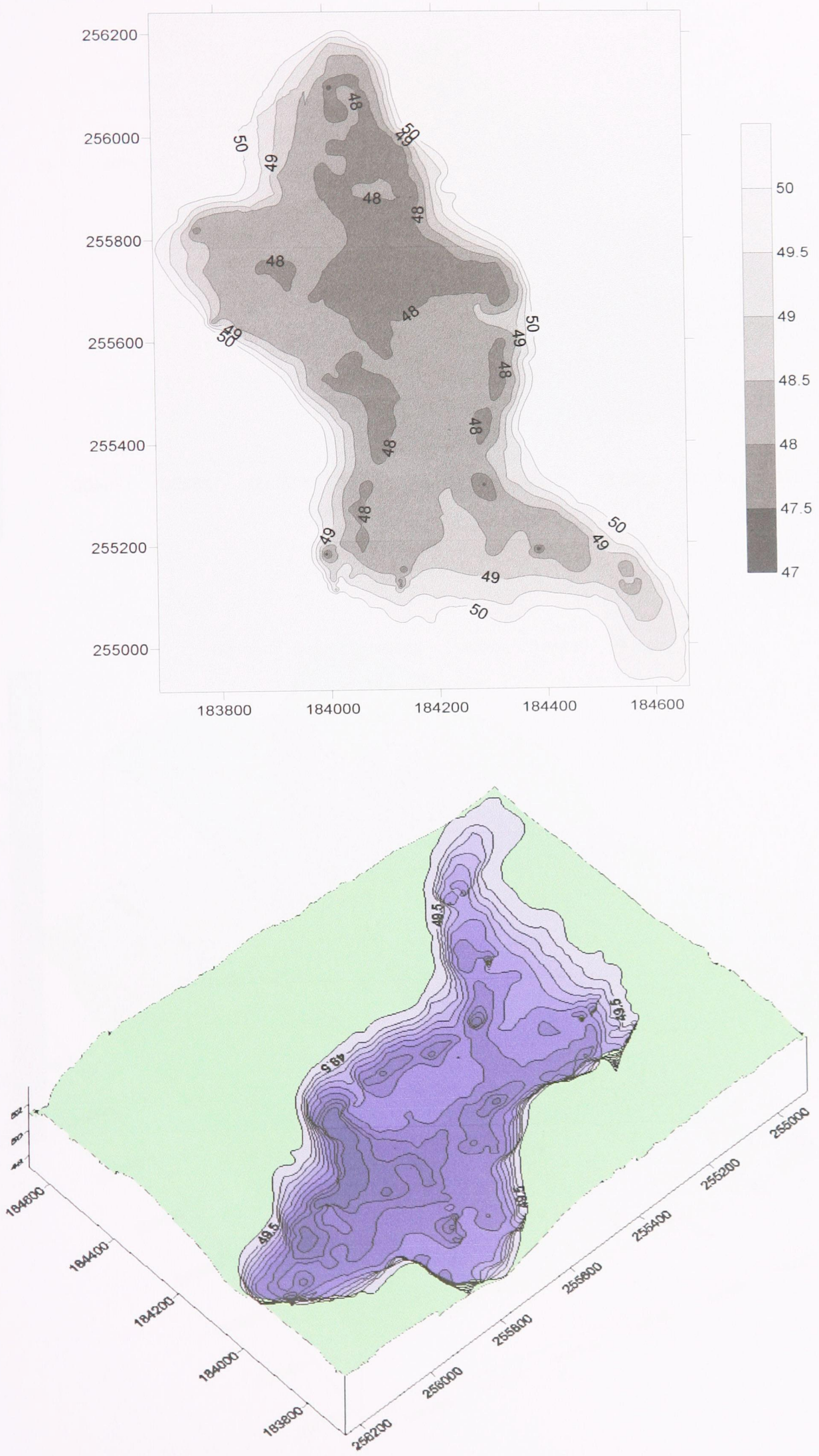


KNOCKAUNROE

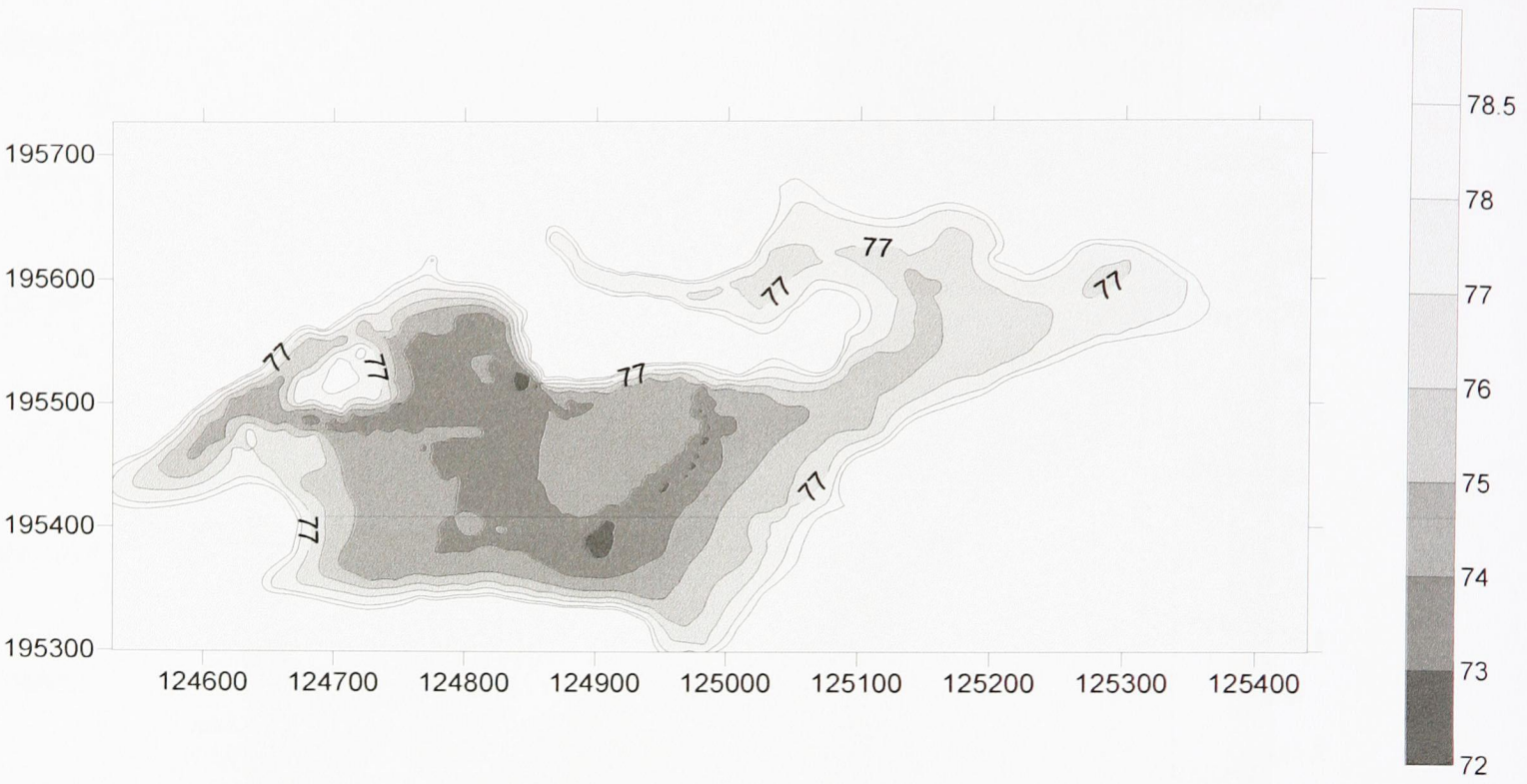


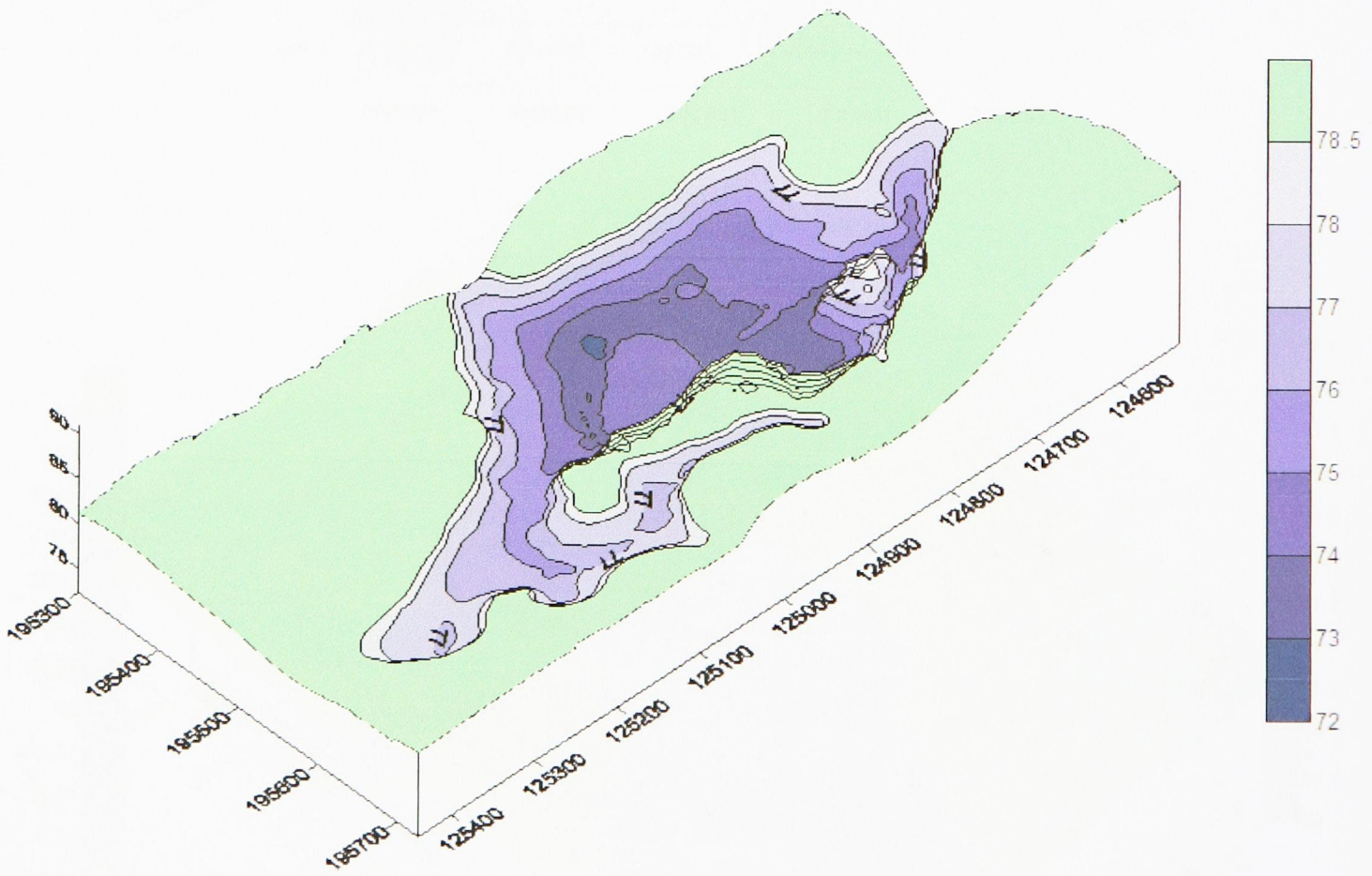


LISDUFF

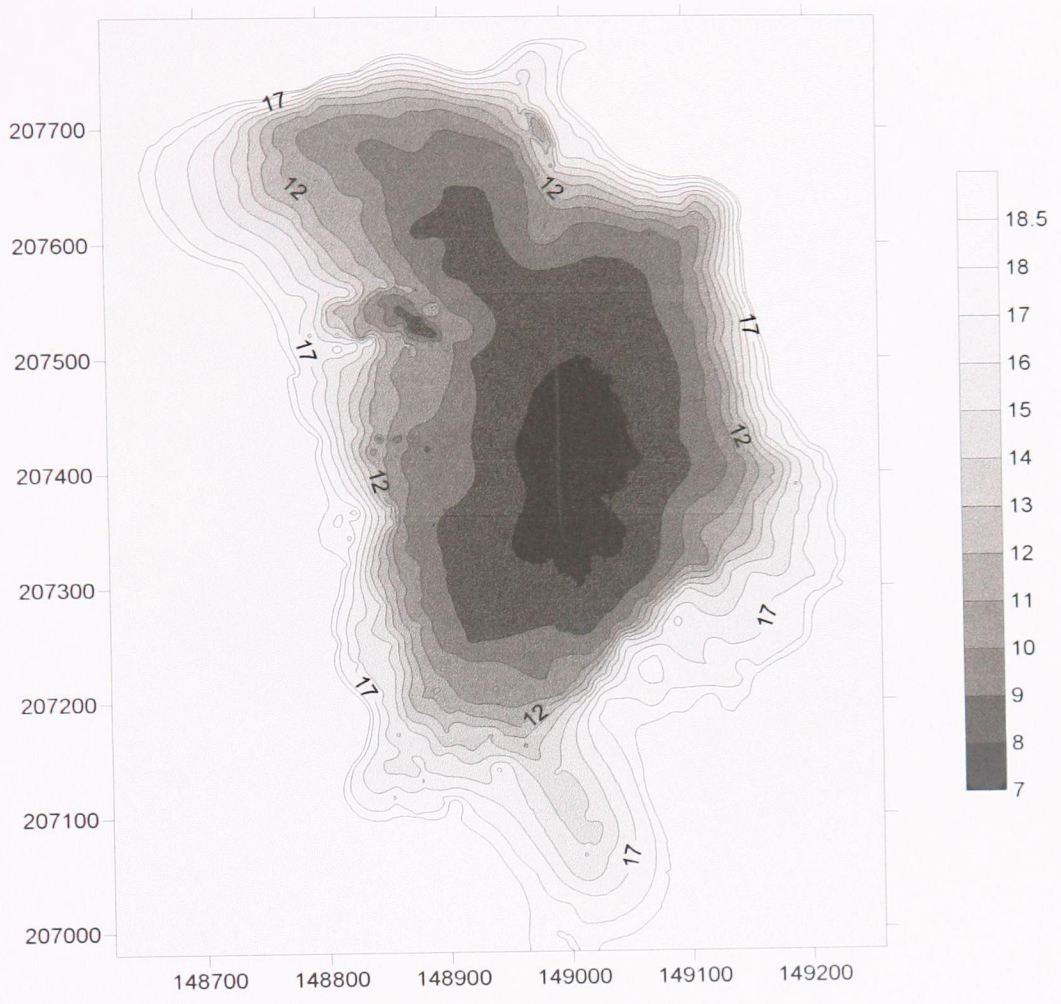

256200
256000
255800
255600
255400
255200
255000
183800
184000
184200
184400
184600
50
49.5
49
48.5
48
47.5
47
49.5
49.25
48.75
48.25
47.875
47.75
47.25

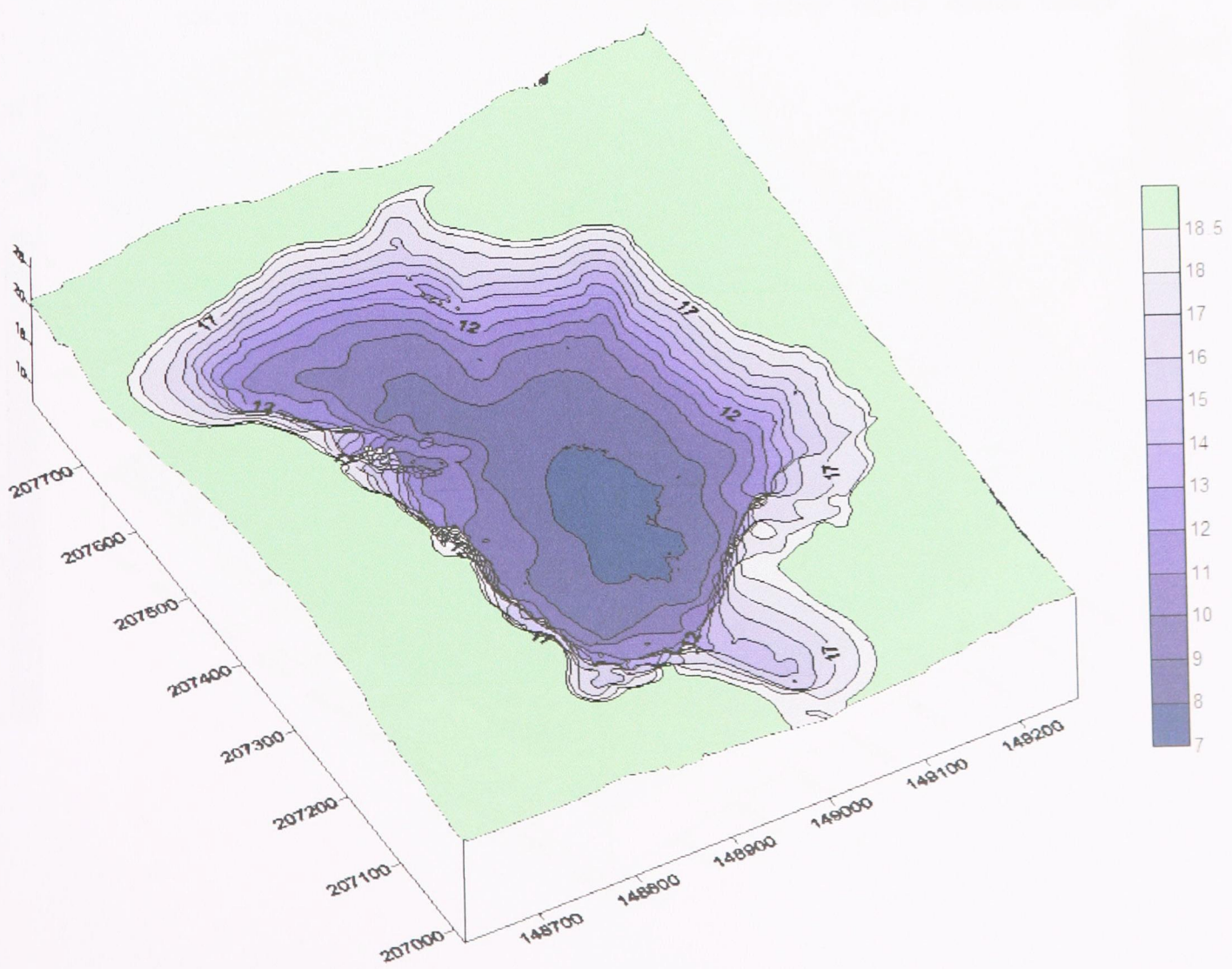
LOUGH ALEENAUN



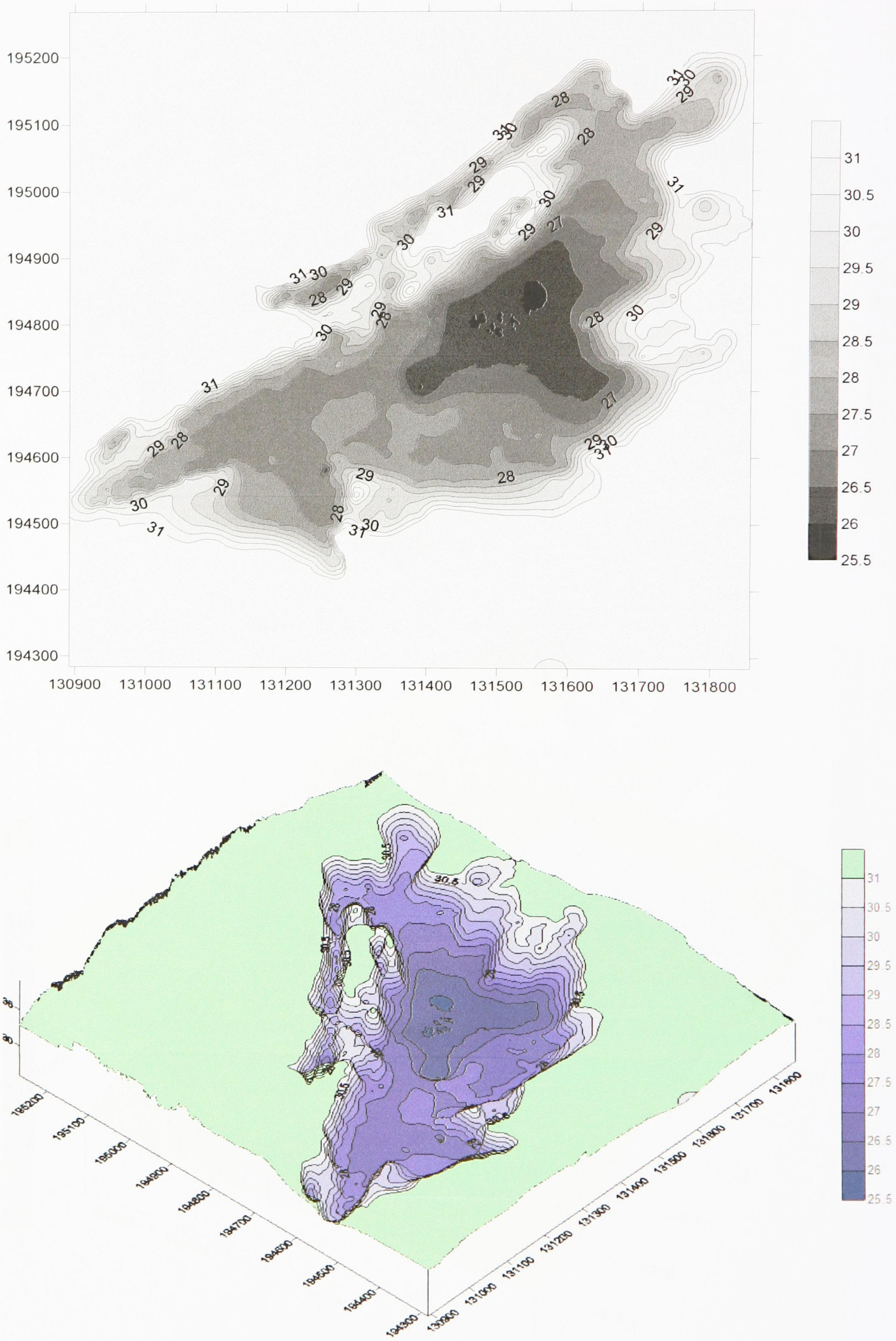


LOUGH COY

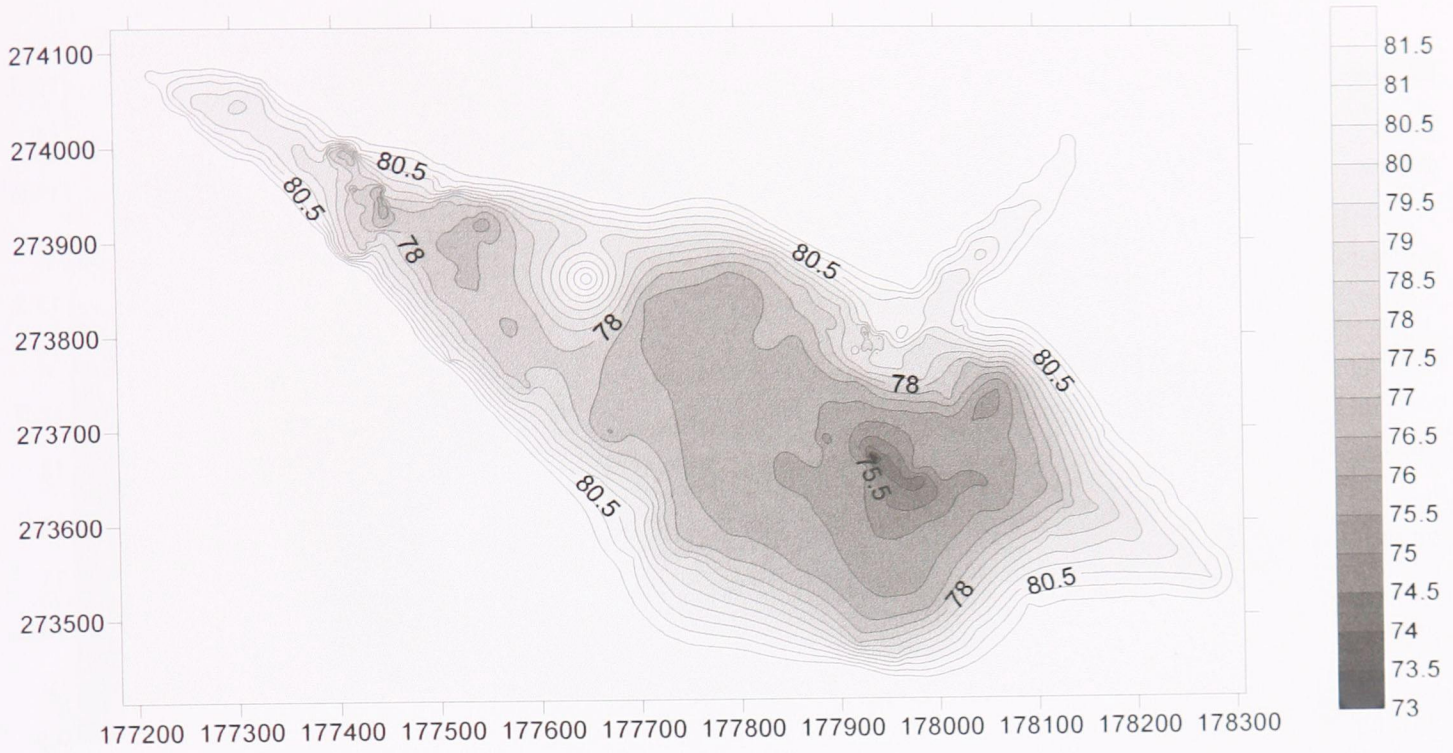

207700
207600
207500
207400
207300
207200
207100
207000
148700
148800
148900
149000
149100
149200
17
12
18.5
18
17
16
15
14
13
12
11
10
9
8
7

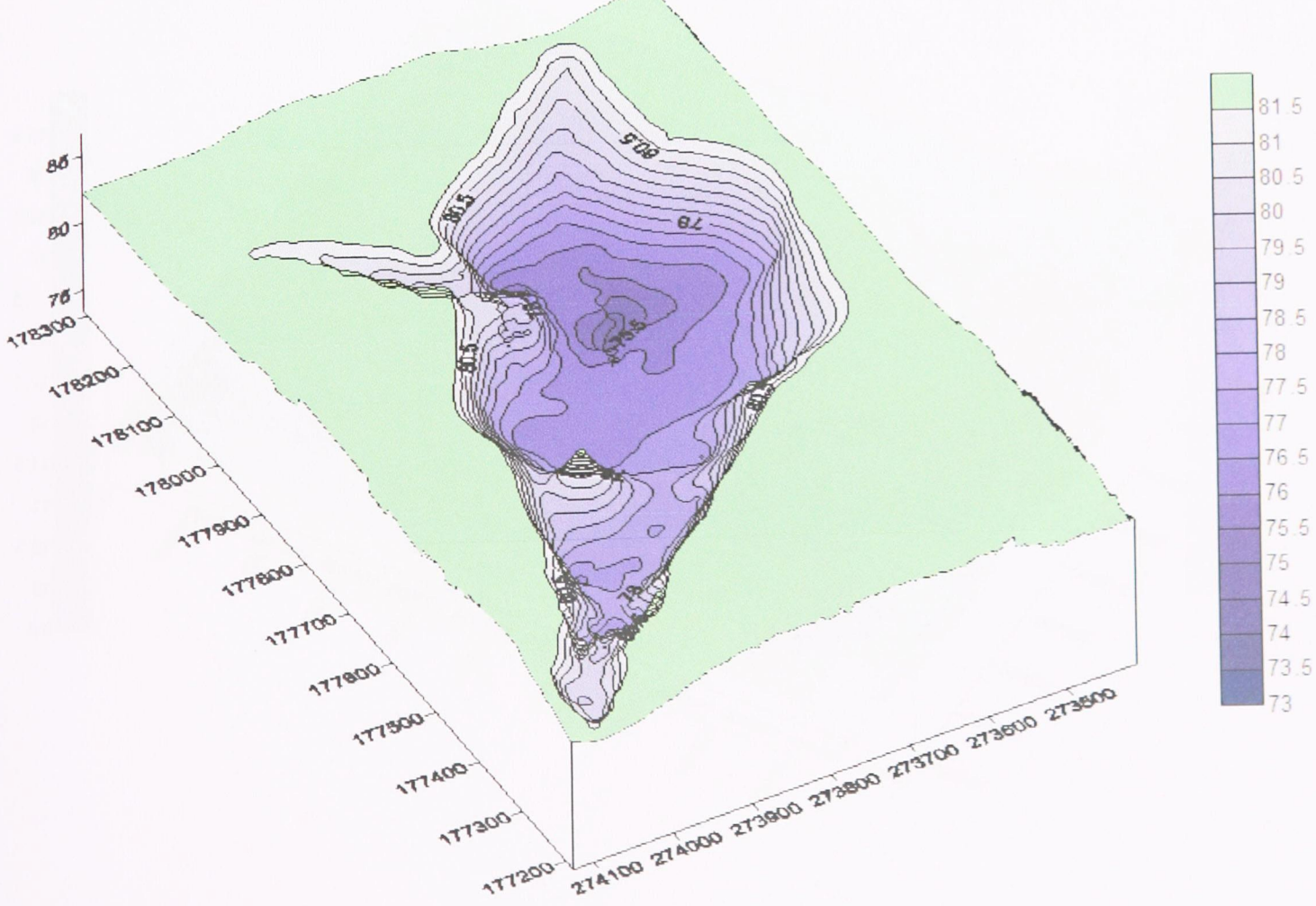

207700
207600
207500
207400
207300
207200
207100
207000
148700
148800
148900
149000
149100
149200
17
12
18.5
18
17
16
15
14
13
12
11
10
9
8
7

LOUGH GEALAIN

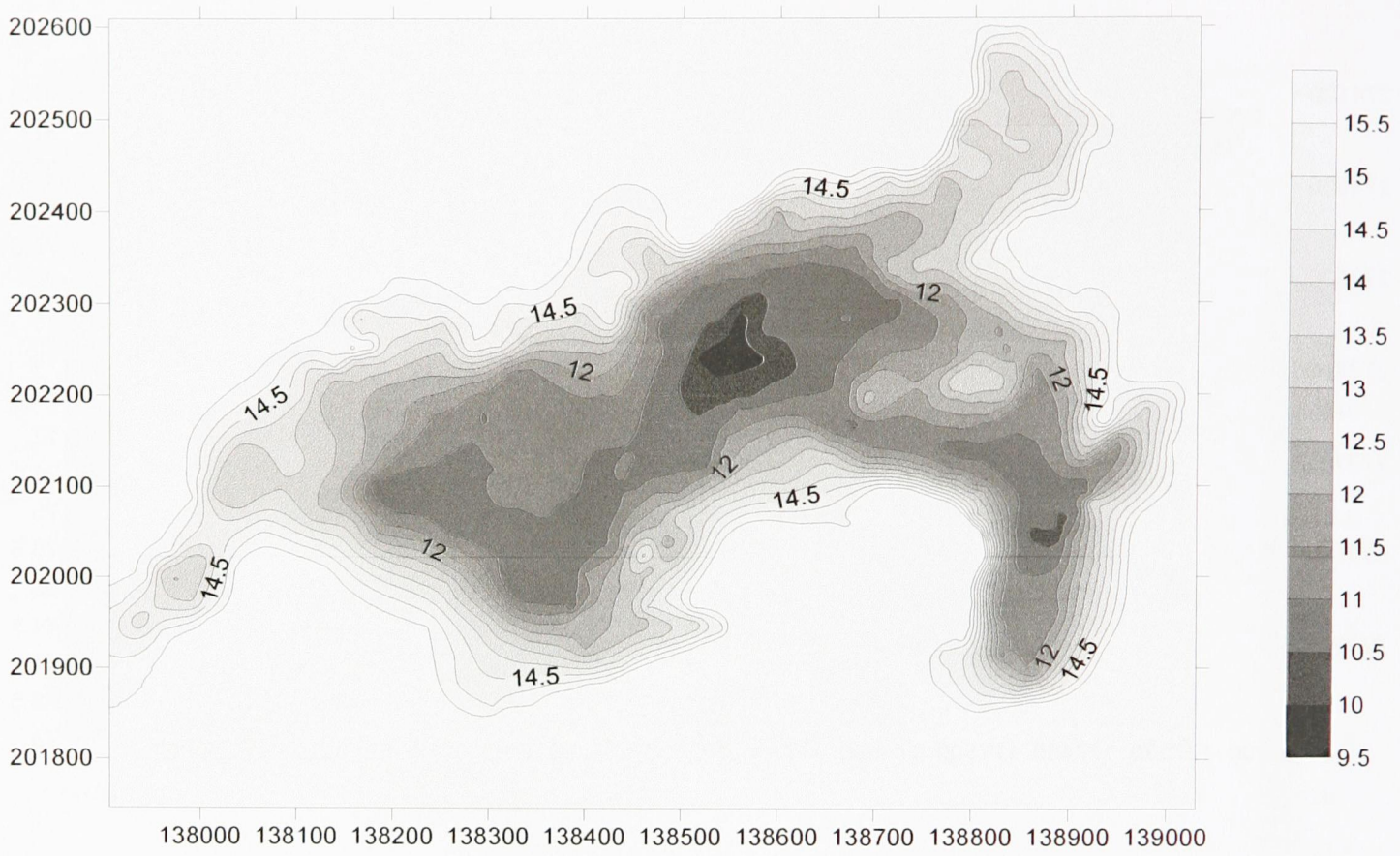


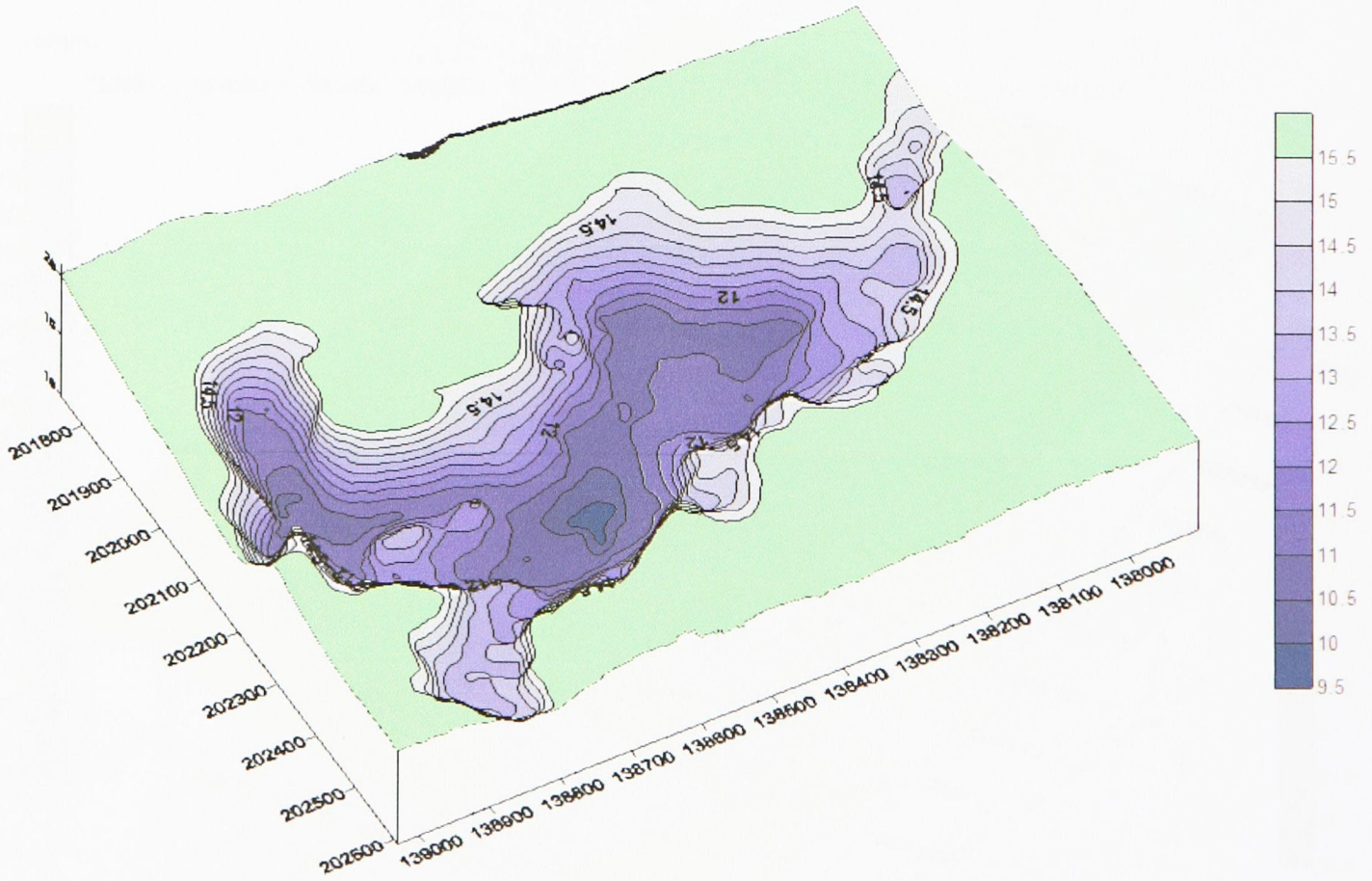
RATHNALULLEAGH



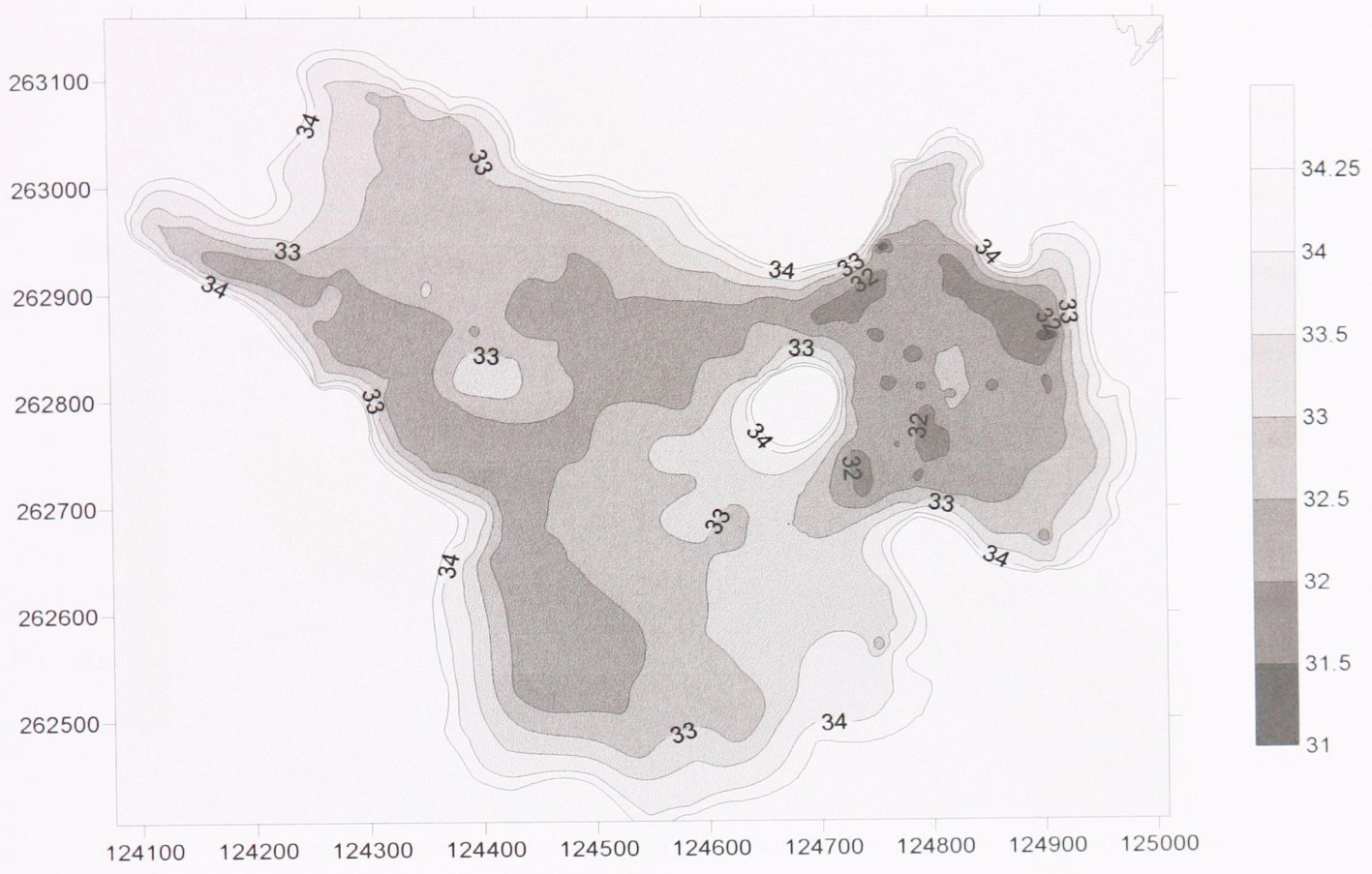


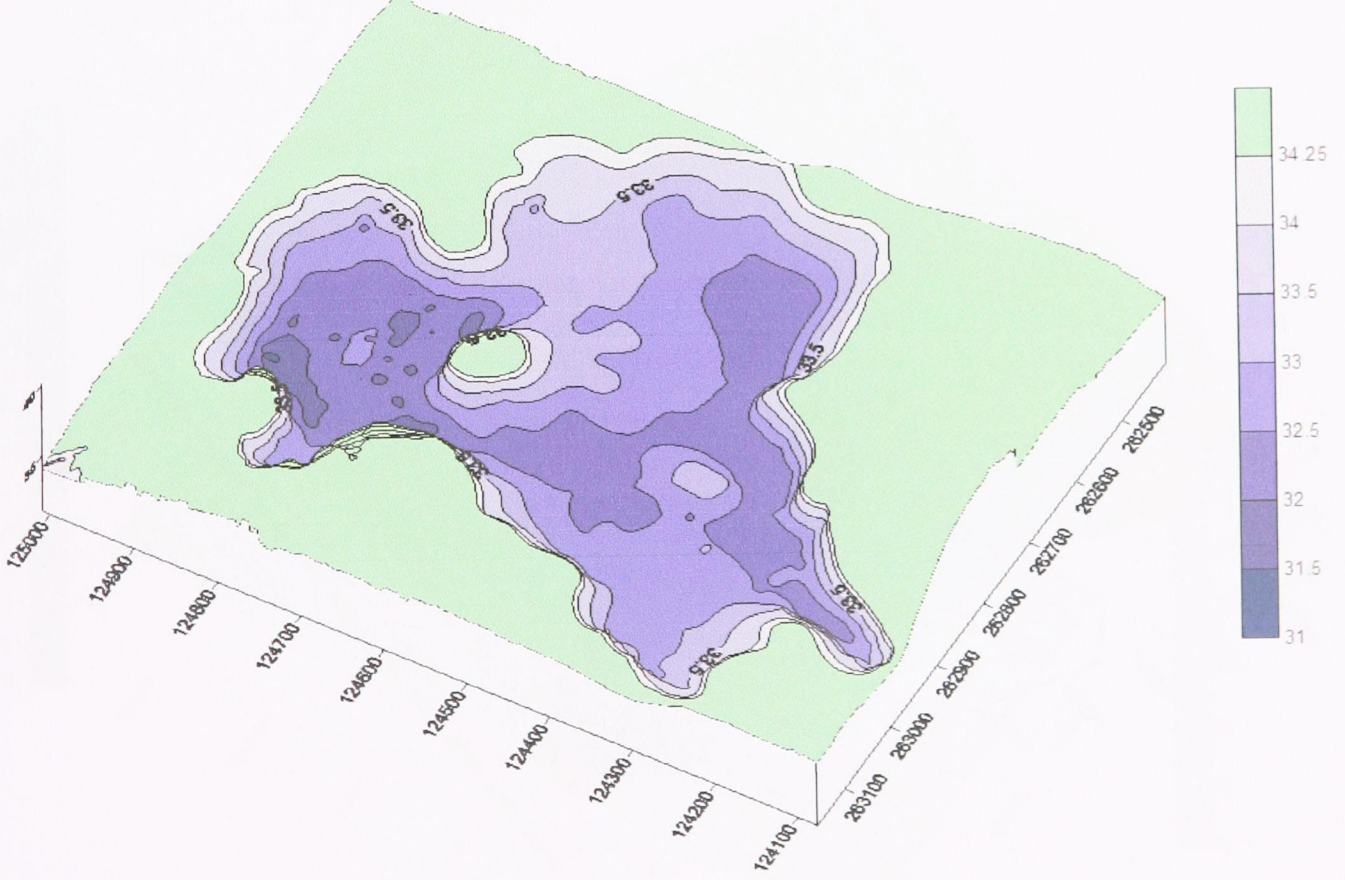
ROO WEST


202600
202500
202400
202300
202200
202100
202000
201900
201800
138000 138100 138200 138300 138400 138500 138600 138700 138800 138900 139000
14.5
12
15.5
15
14.5
14
13.5
13
12.5
12
11.5
11
10.5
10
9.5

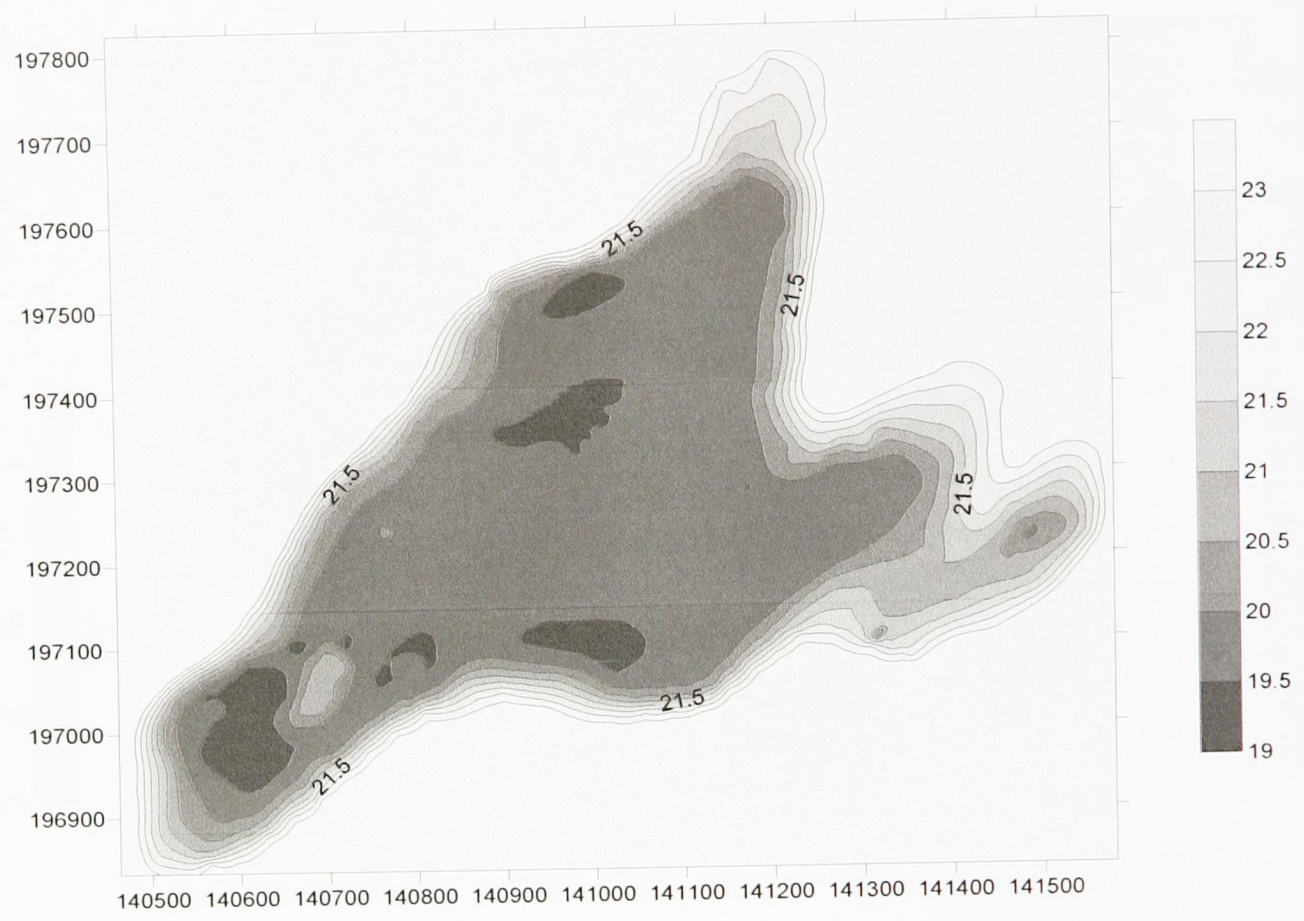

201800
201900
202000
202100
202200
202300
202400
202500
202500
138900 138900 138600 138700 138800 138500 138400 138300 138200 138100 138000
14.5
12
15.5
15
14.5
14
13.5
13
12.5
12
11.5
11
10.5
10
9.5

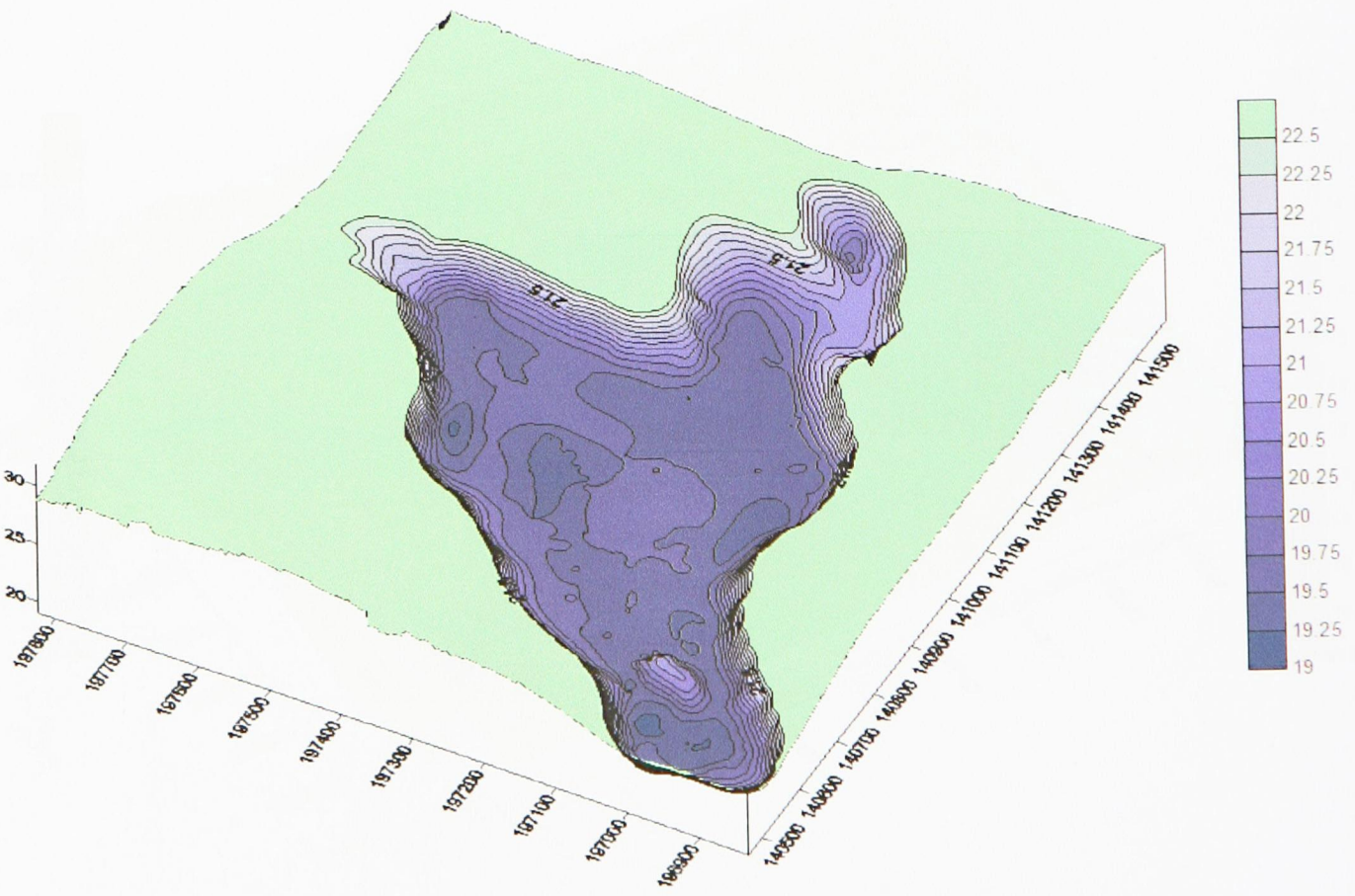
SKEALOGHAN


263100
263000
262900
262800
262700
262600
262500
124100
124200
124300
124400
124500
124600
124700
124800
124900
125000
34.25
34
33.5
33
32.5
32
31.5
31

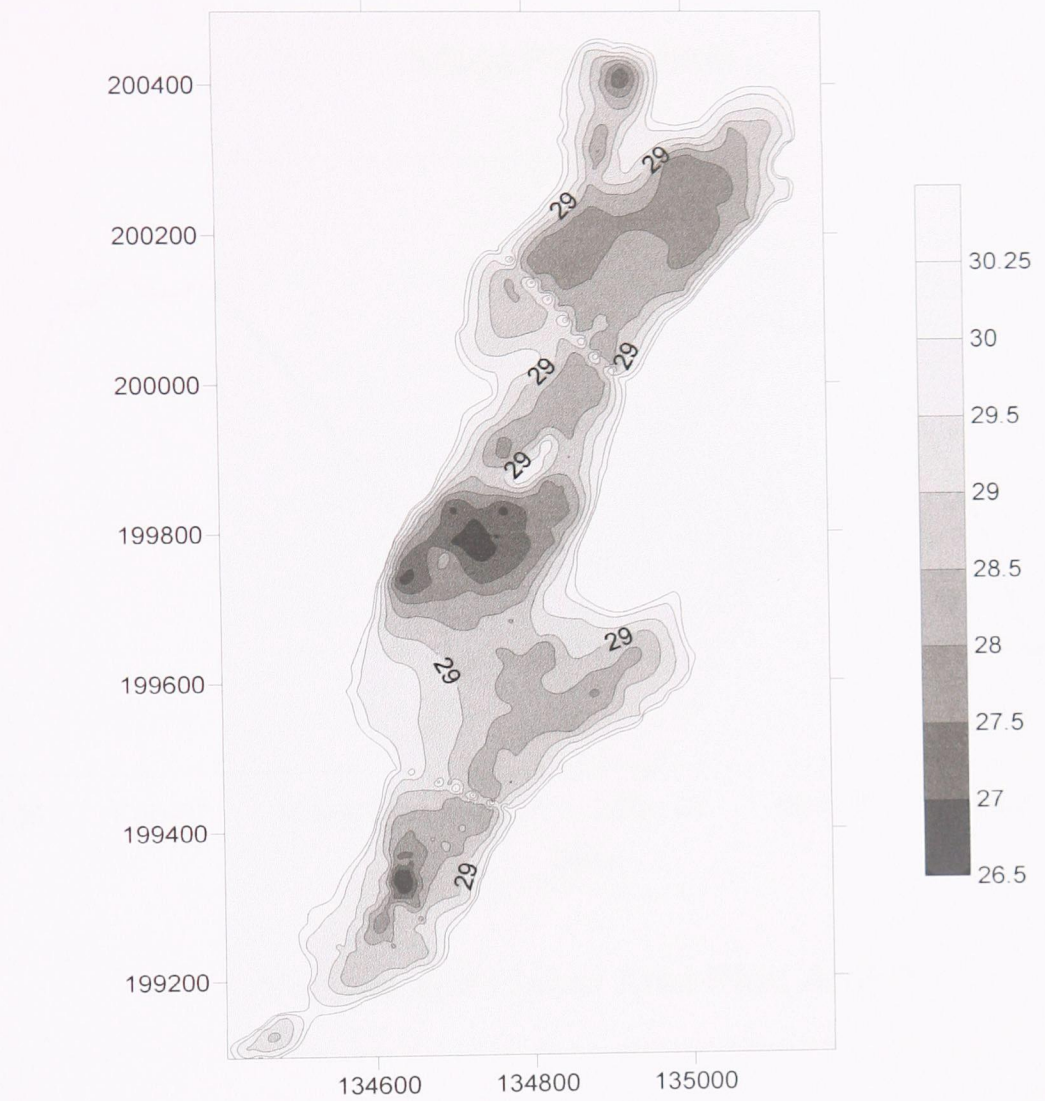

34.25
34
33.5
33
32.5
32
31.5
31

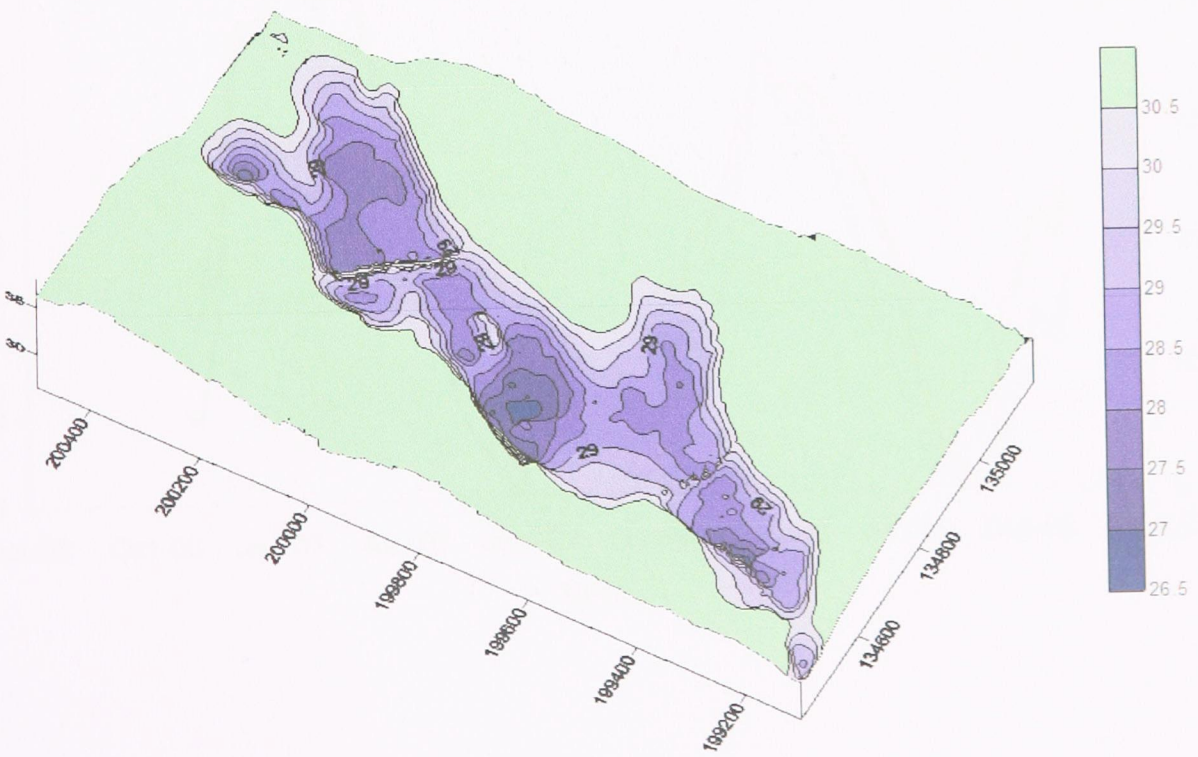
TERMON


197800
197700
197600
197500
197400
197300
197200
197100
197000
196900
140500 140600 140700 140800 140900 141000 141100 141200 141300 141400 141500
21.5
21.5
21.5
21.5
21.5
23
22.5
22
21.5
21
20.5
20
19.5
19

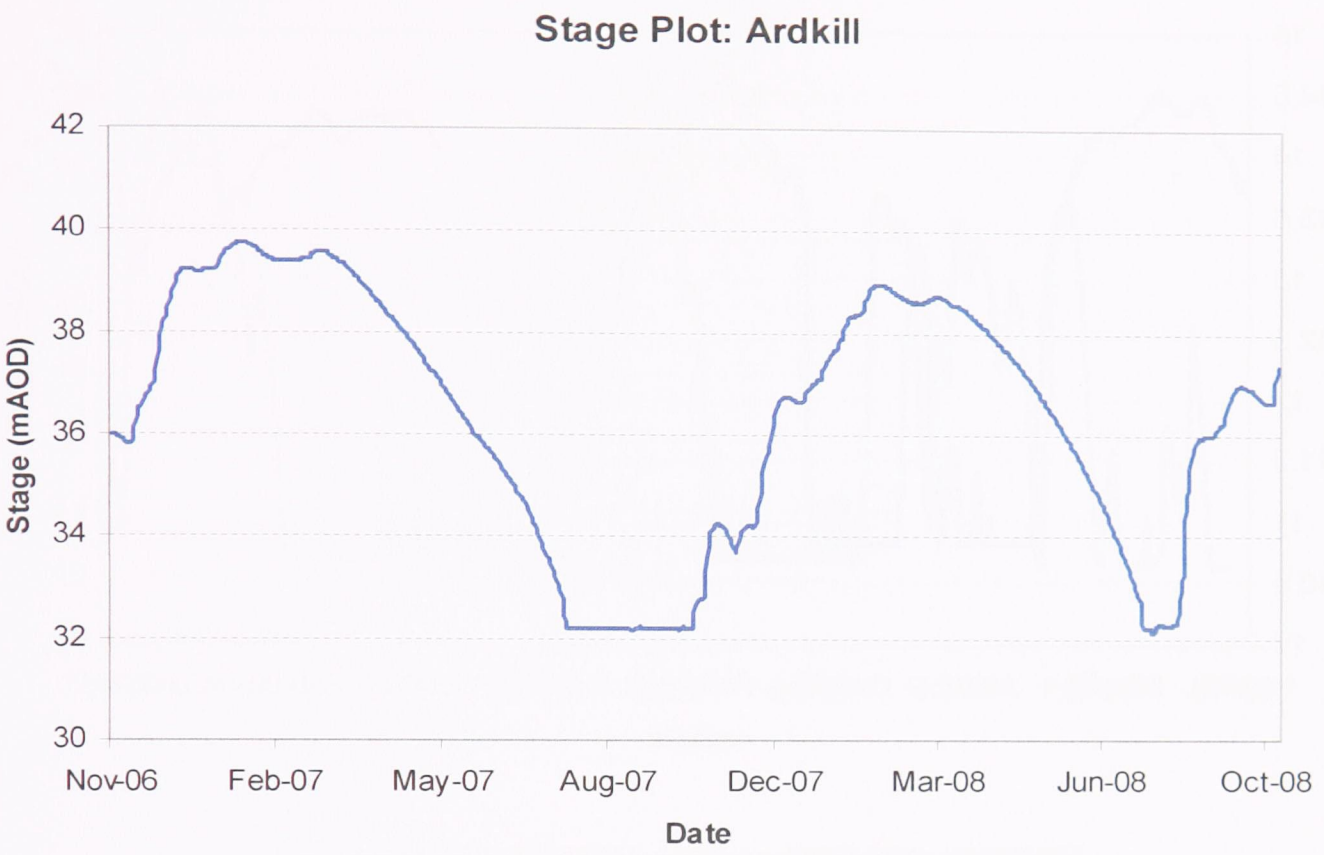

22.5
22.25
22
21.75
21.5
21.25
21
20.75
20.5
20.25
20
19.75
19.5
19.25
19

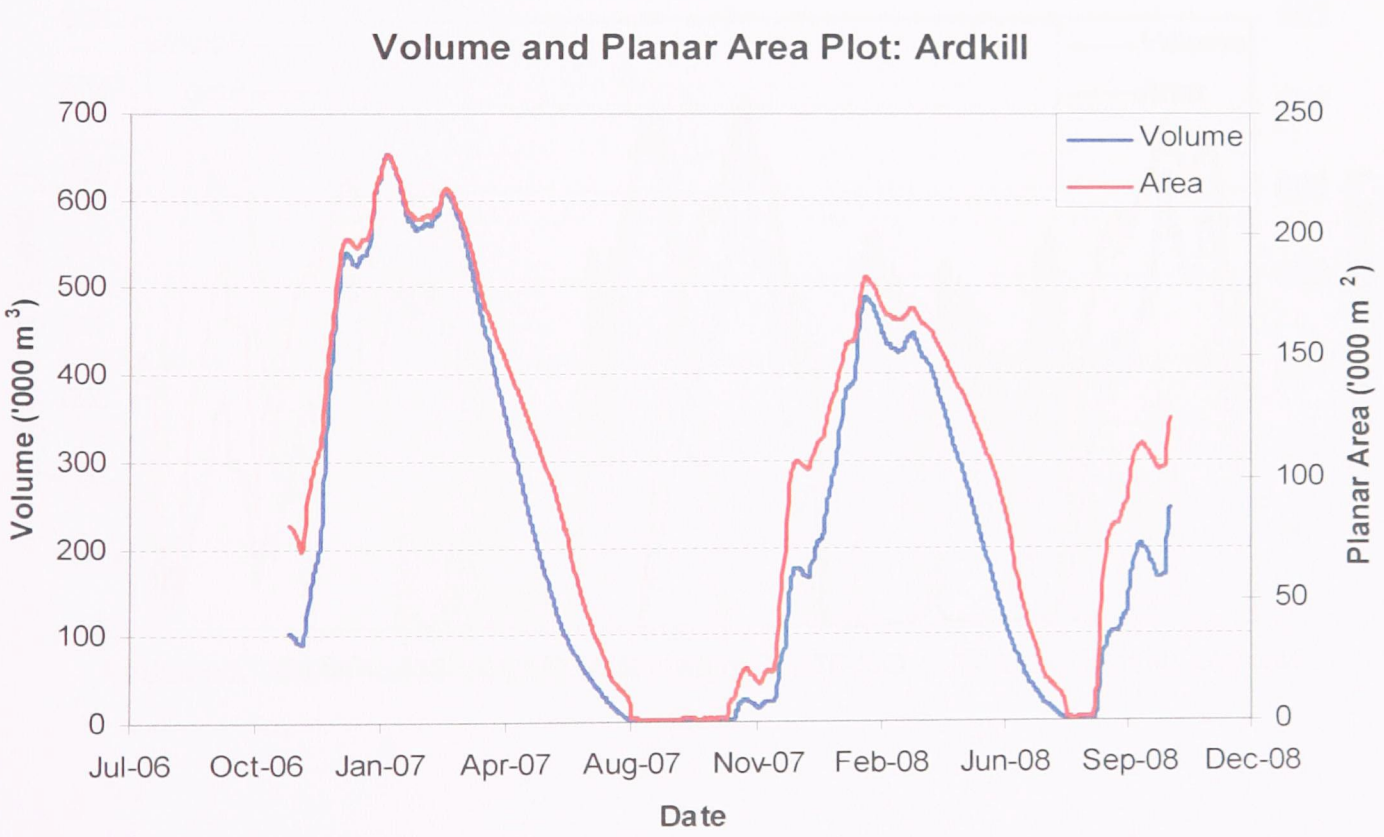
TURLOUGHMORE



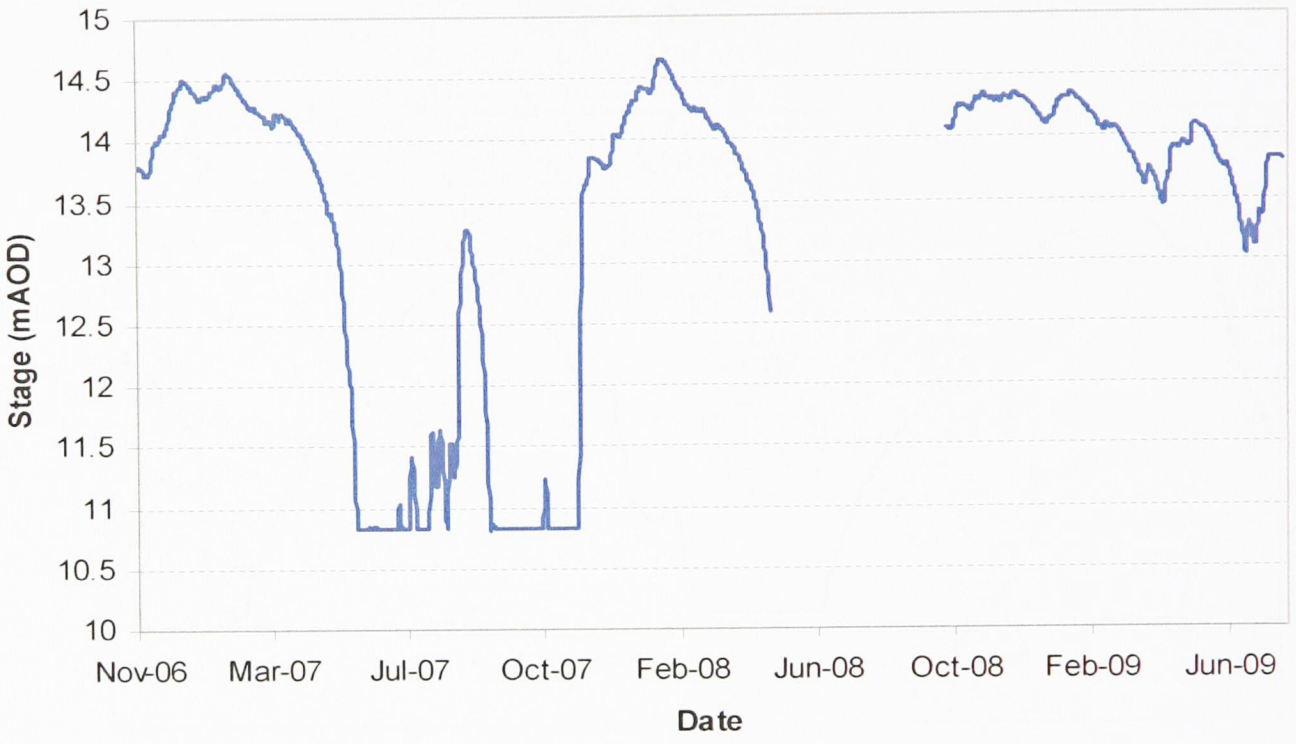


Appendix B: Hydrological Plots

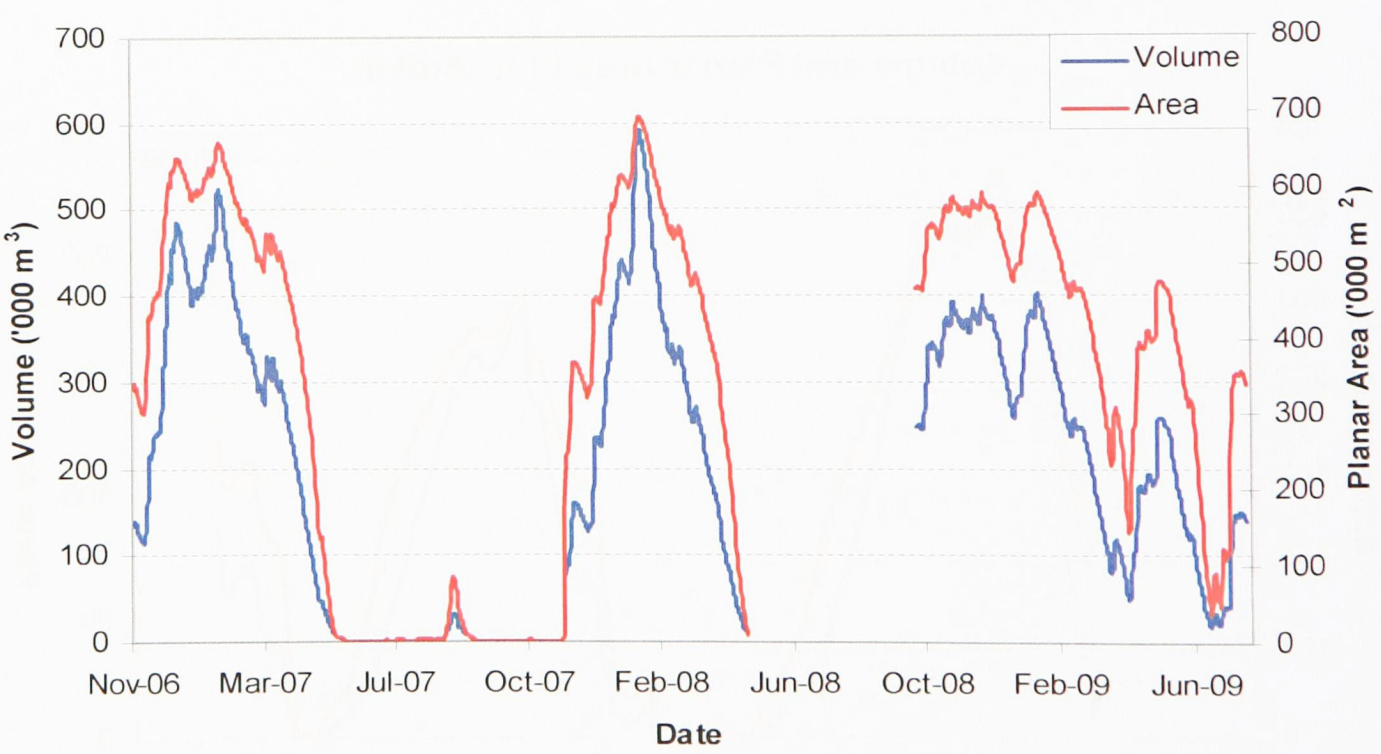




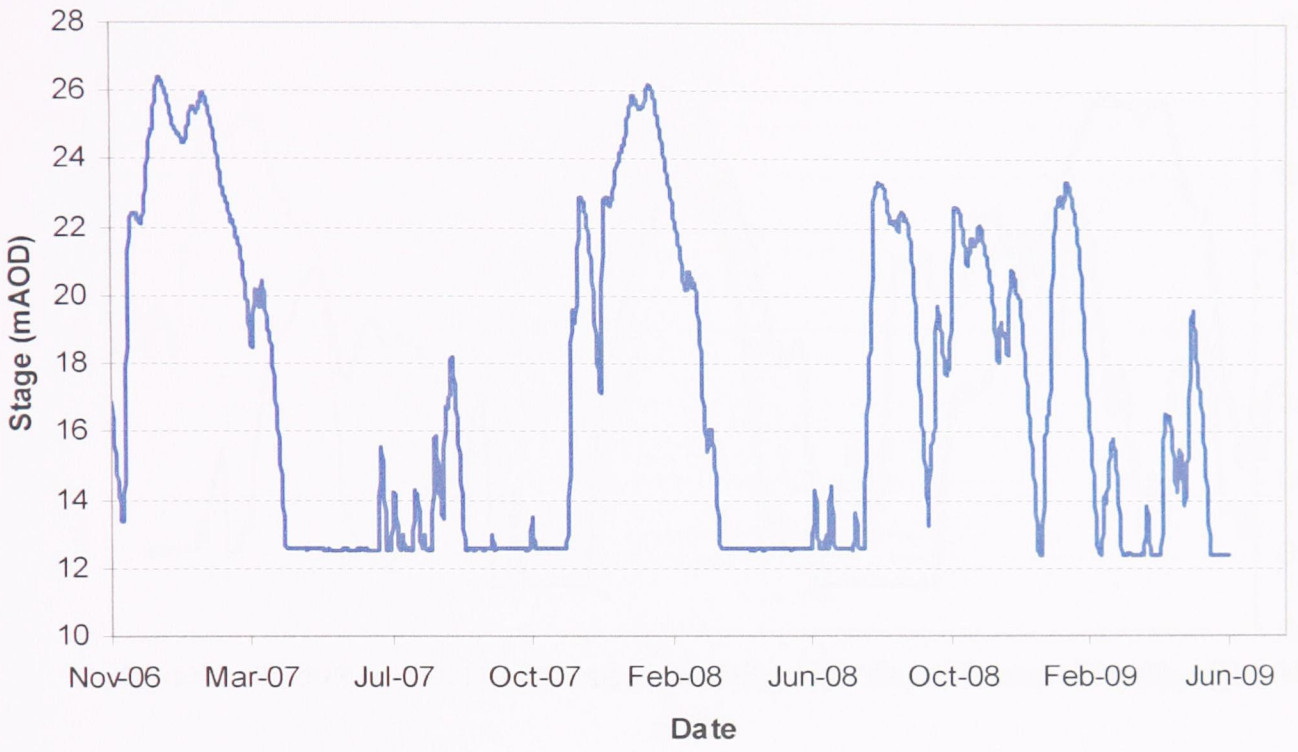
Stage Plot: Ballinderreen



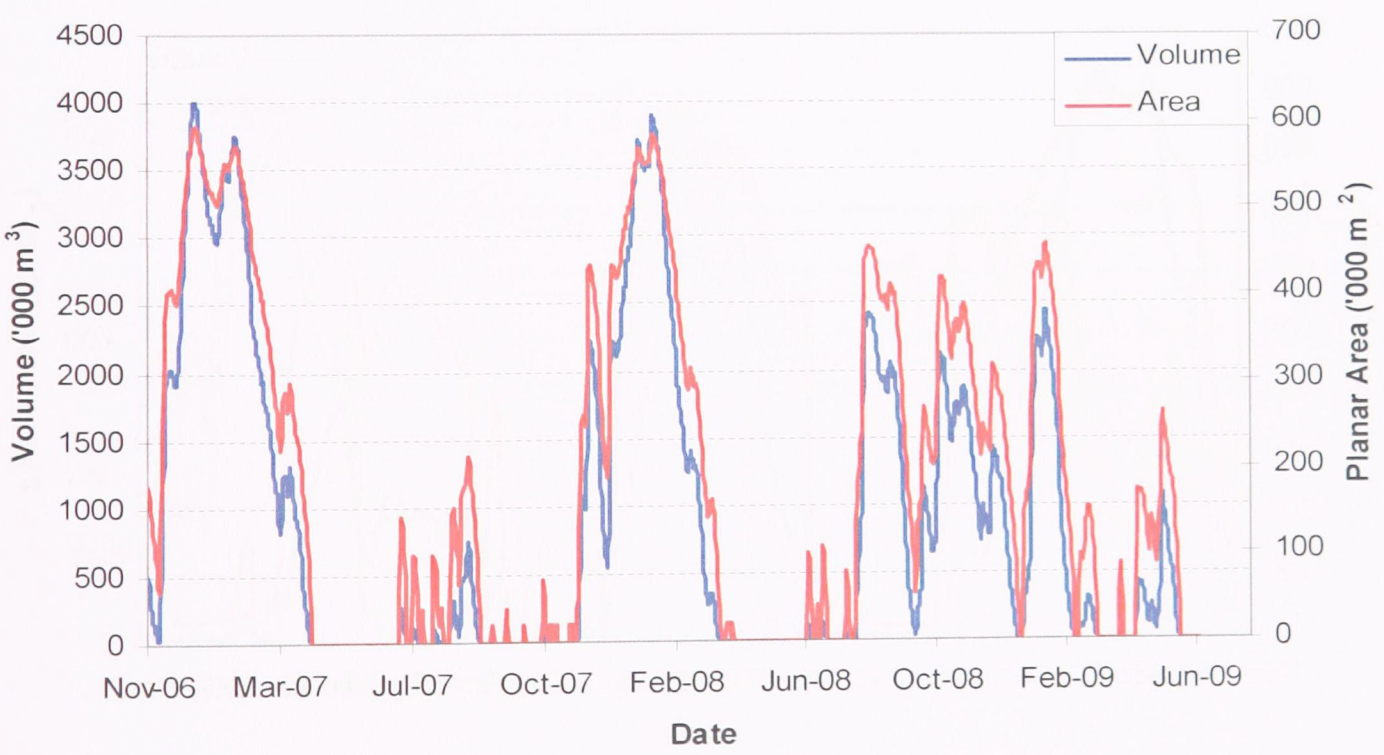
Volume and Planar Area Plot: Ballinderreen



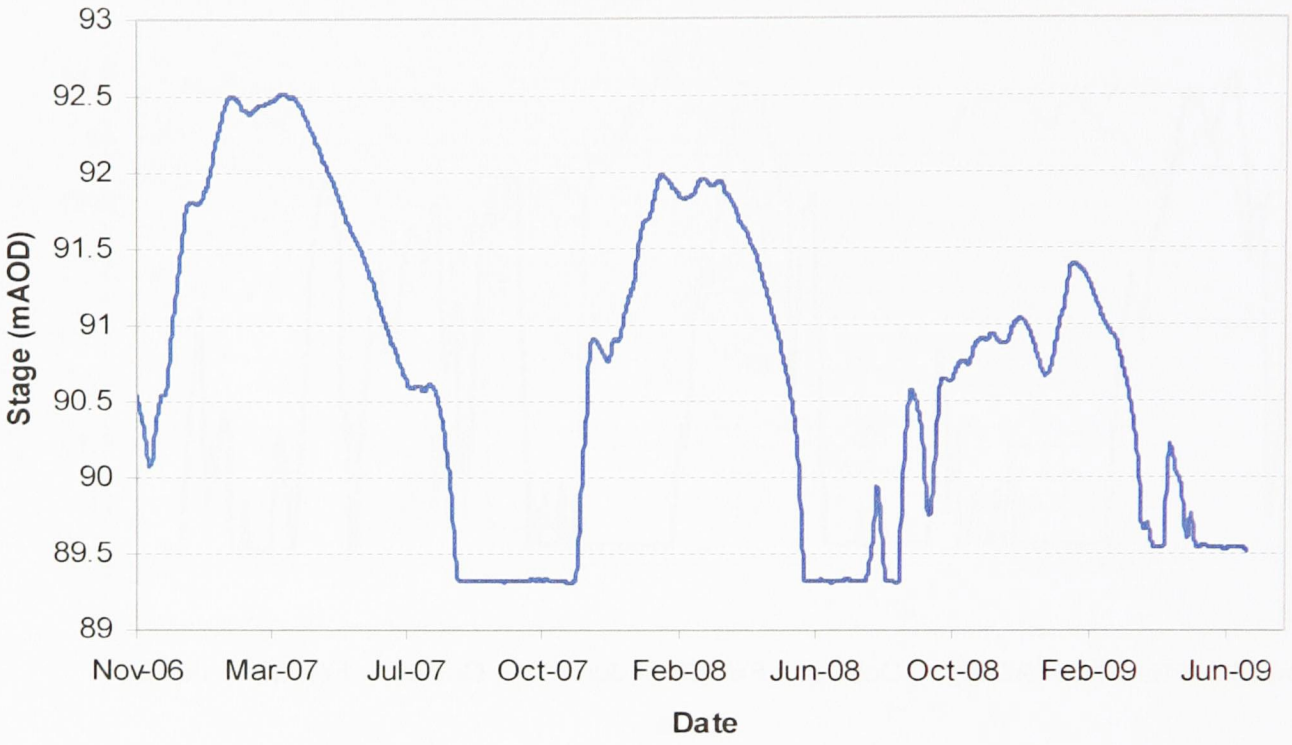
Stage Plot: Blackrock



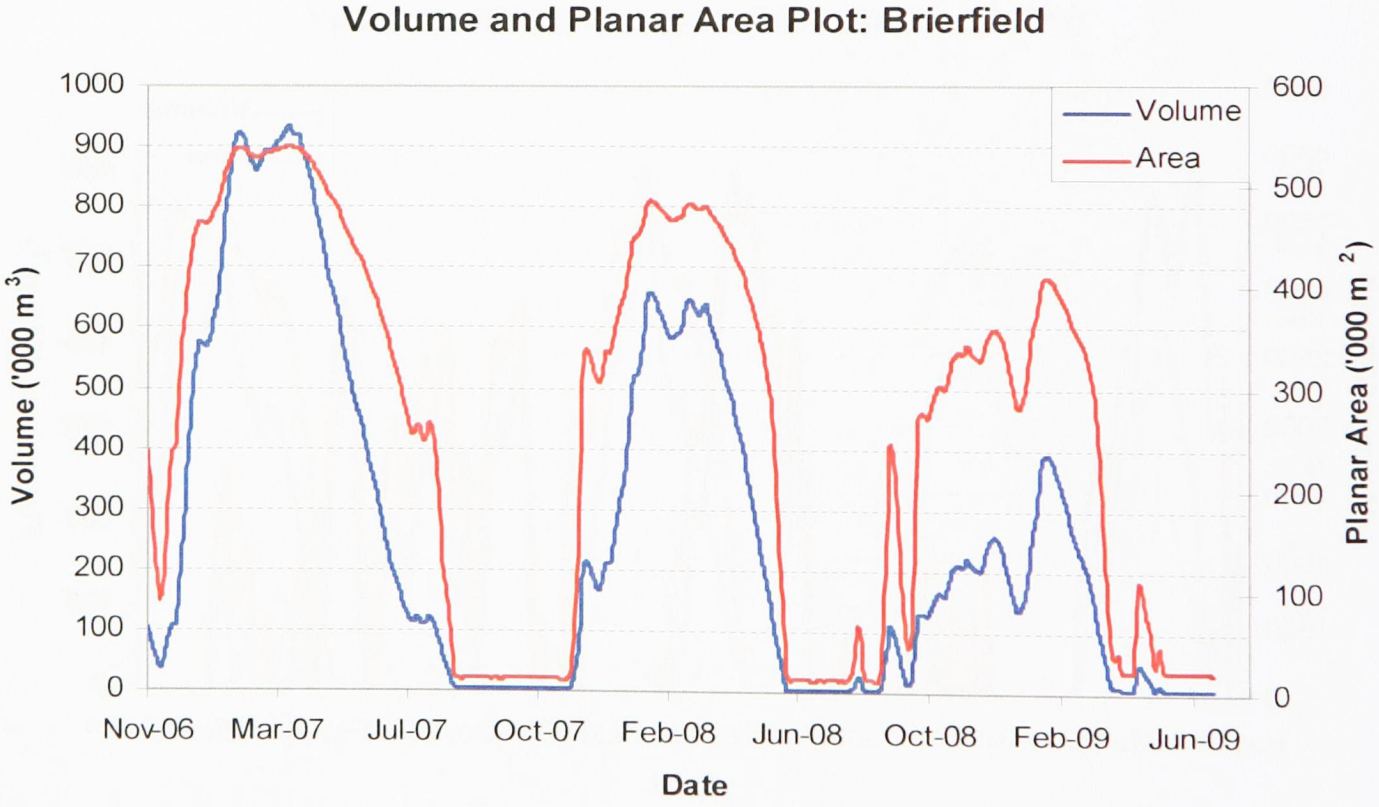
Volume and Planar Area Plot: Blackrock



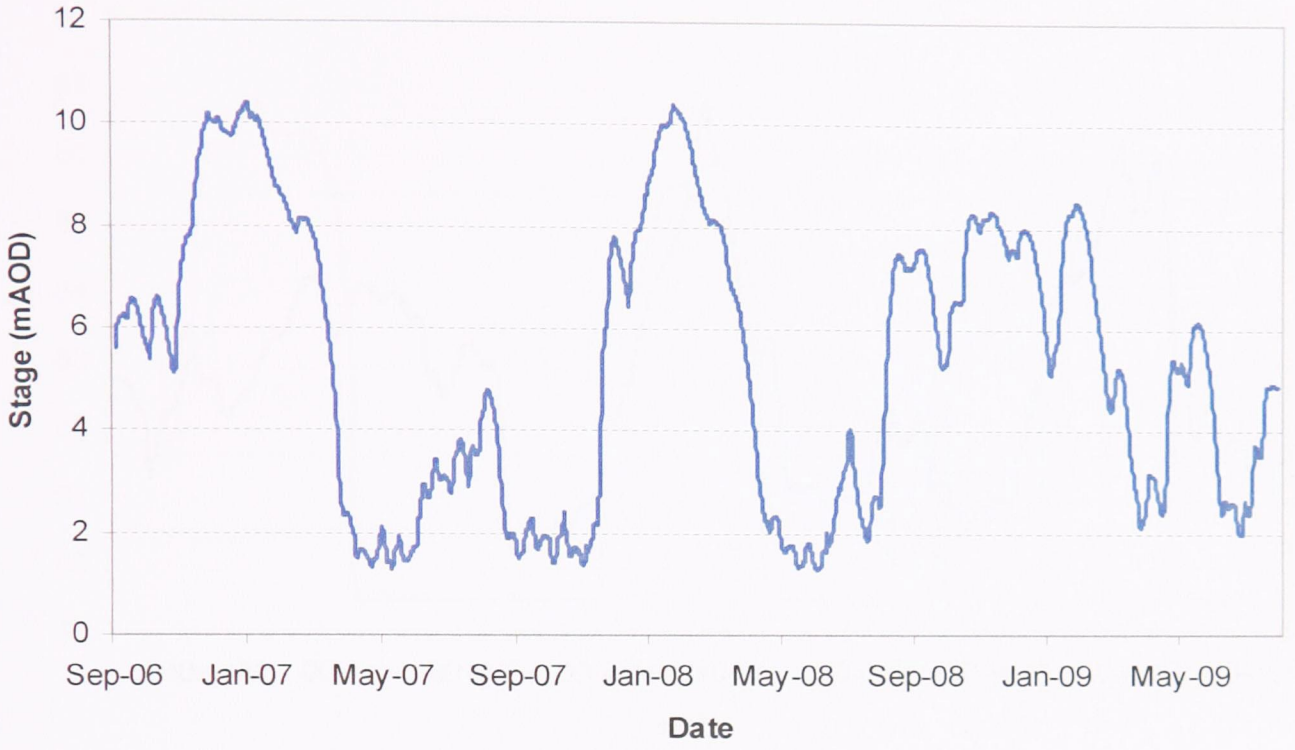
Stage Plot: Brierfield



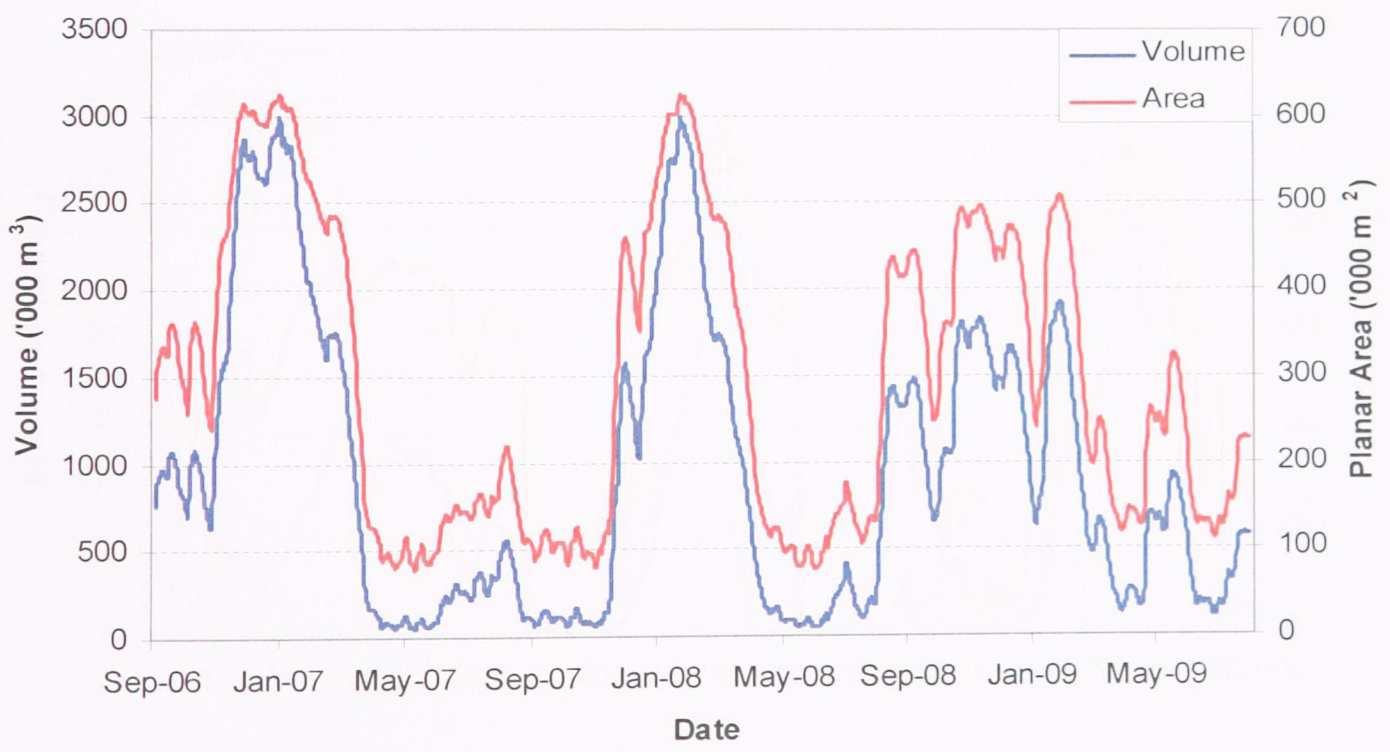
Volume and Planar Area Plot: Brierfield



Stage Plot: Caherglassaun



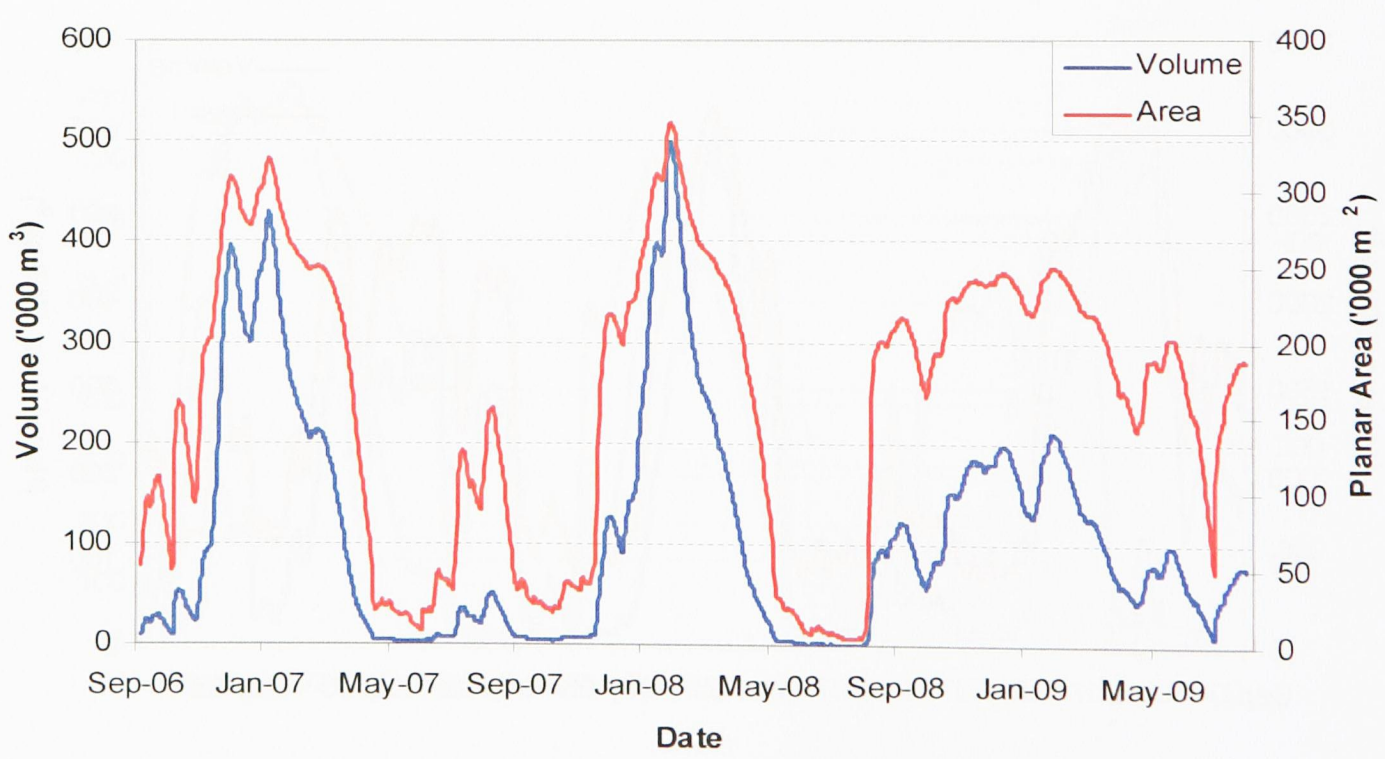
Volume and Planar Area Plot: Caherglassaun



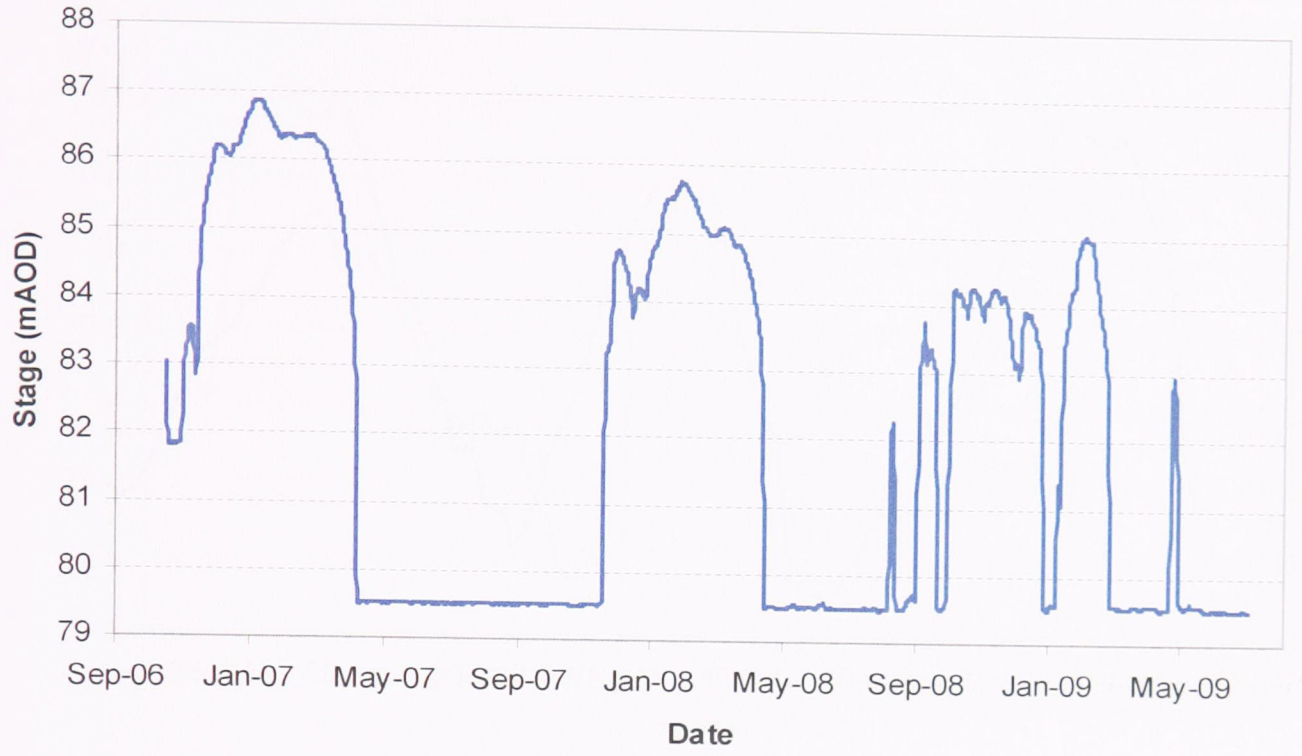
Stage Plot: Caranavoodaun



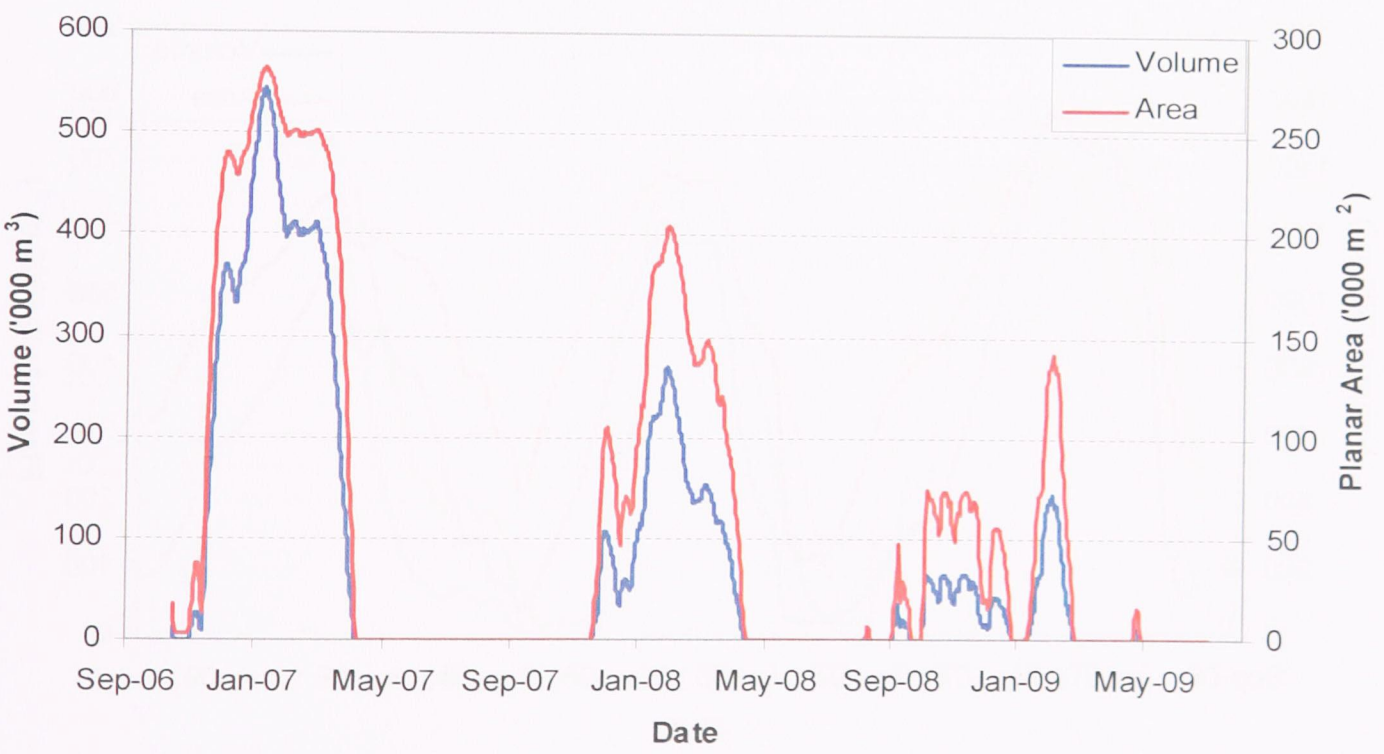
Volume and Planar Area Plot: Caranavoodaun



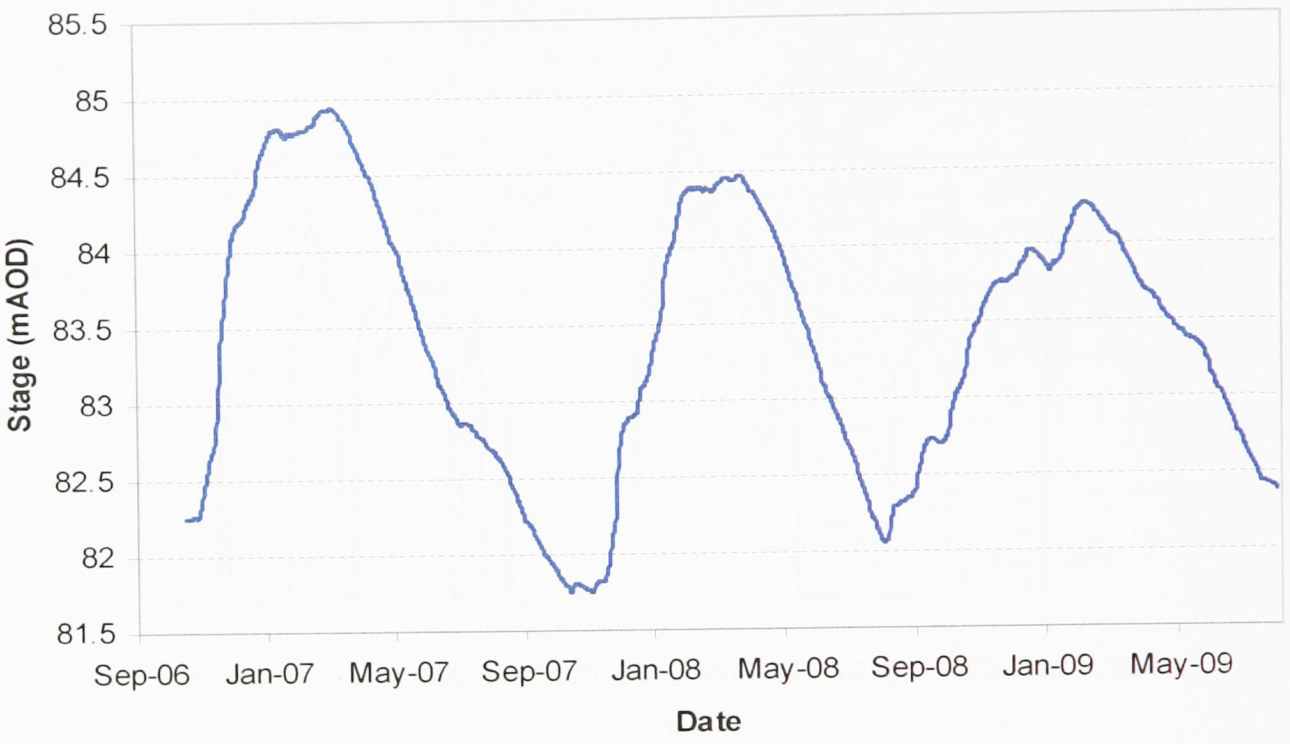
Stage Plot: Carrowreagh



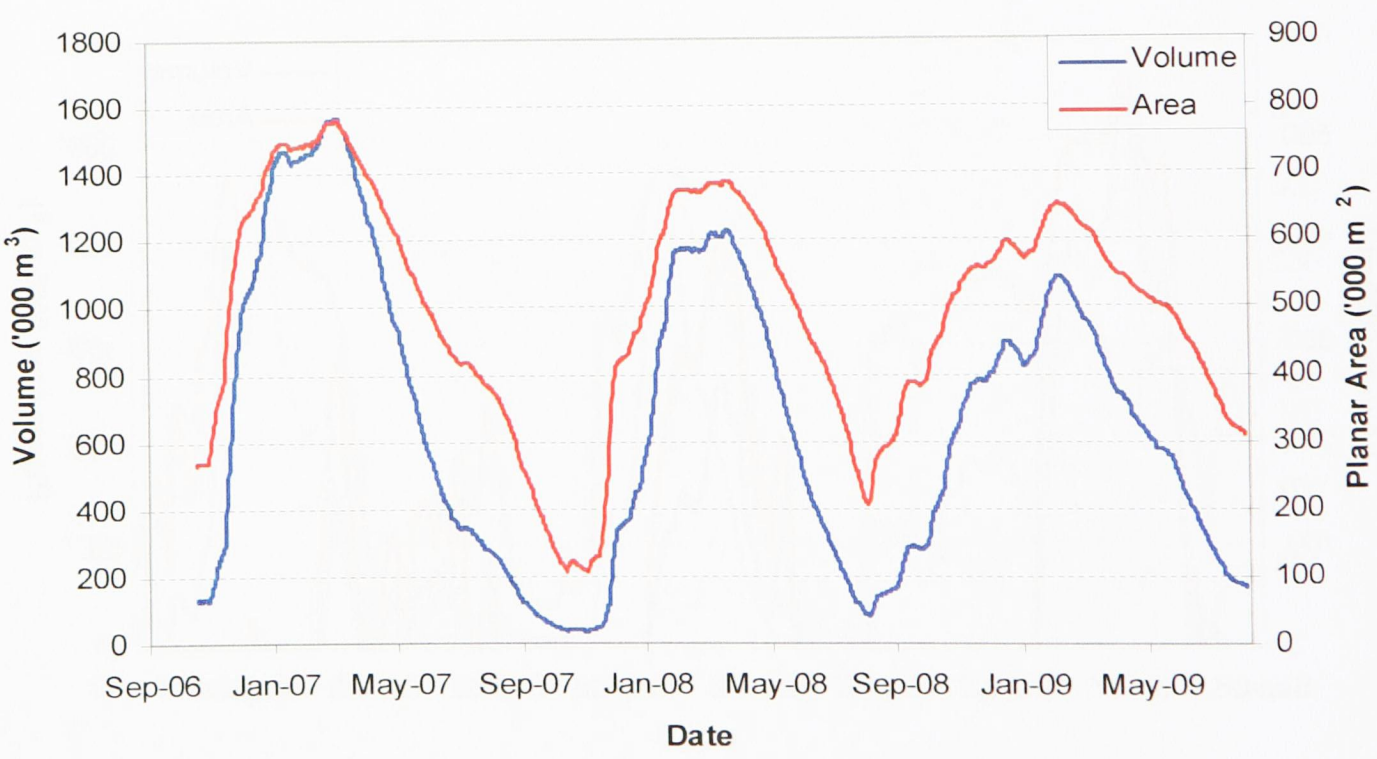
Volume and Planar Area Plot: Carrowreagh



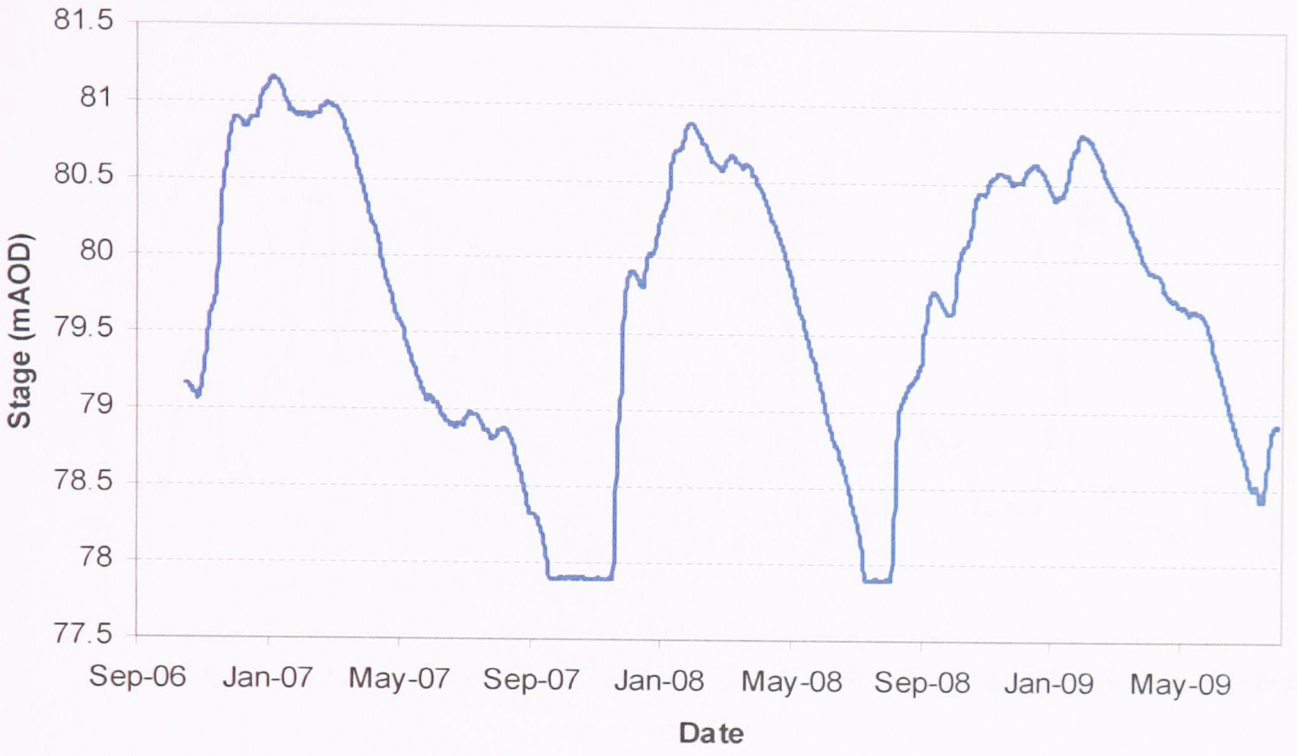
Stage Plot: Coolcam



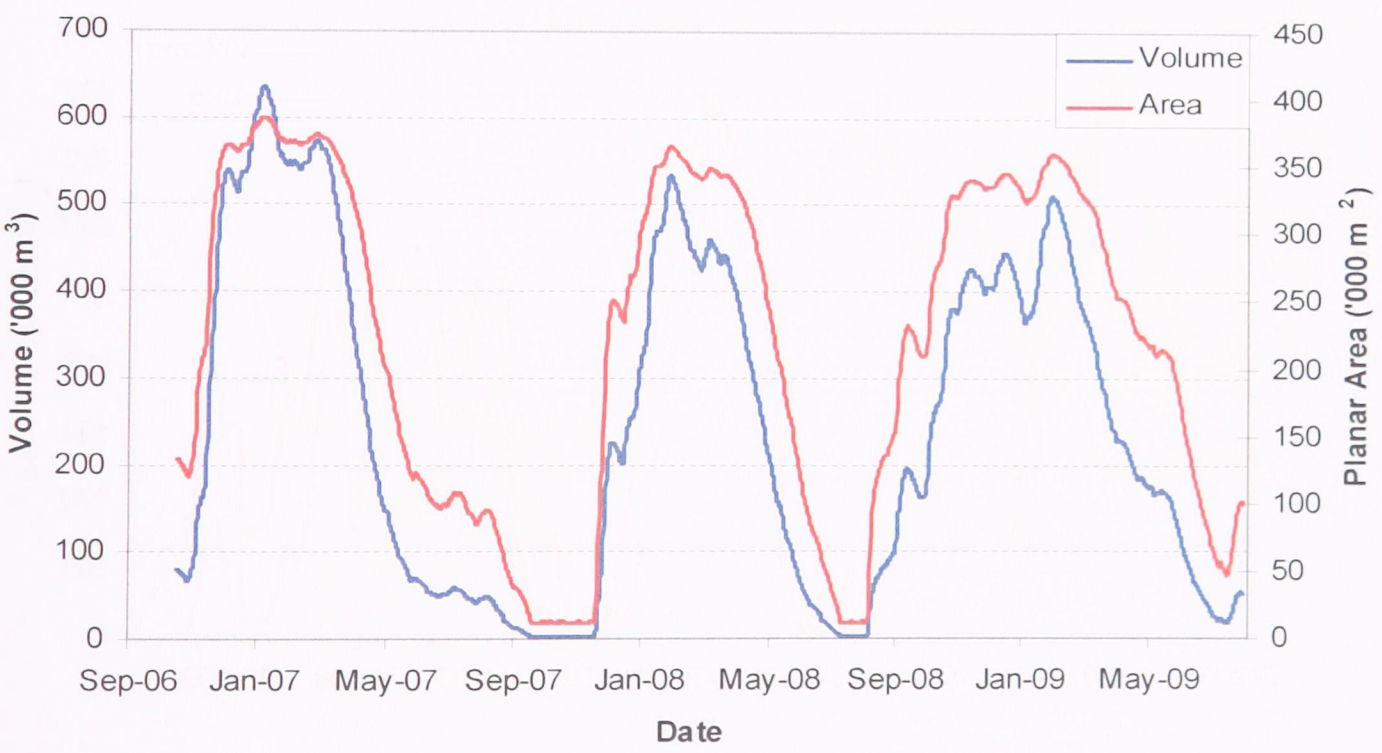
Volume and Planar Area Plot: Coolcam

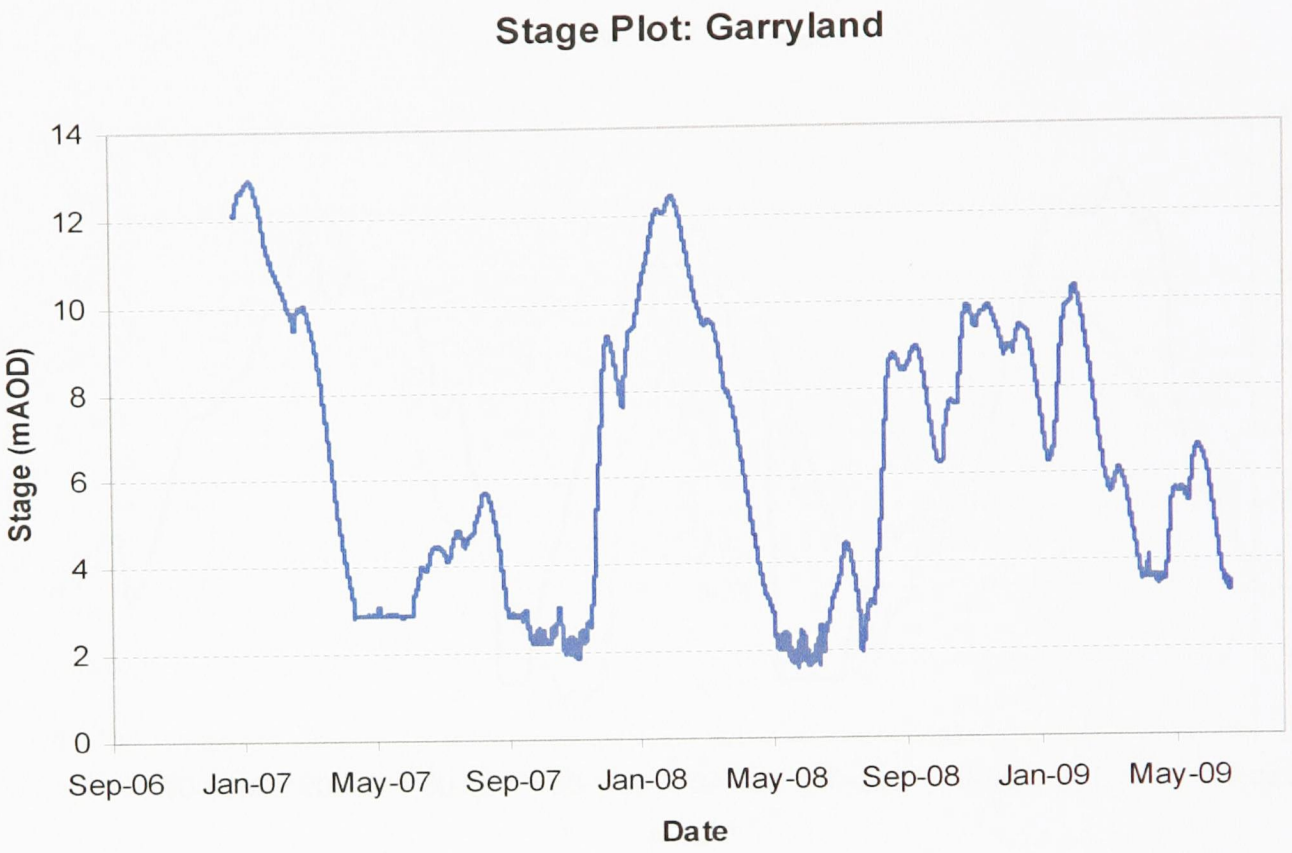


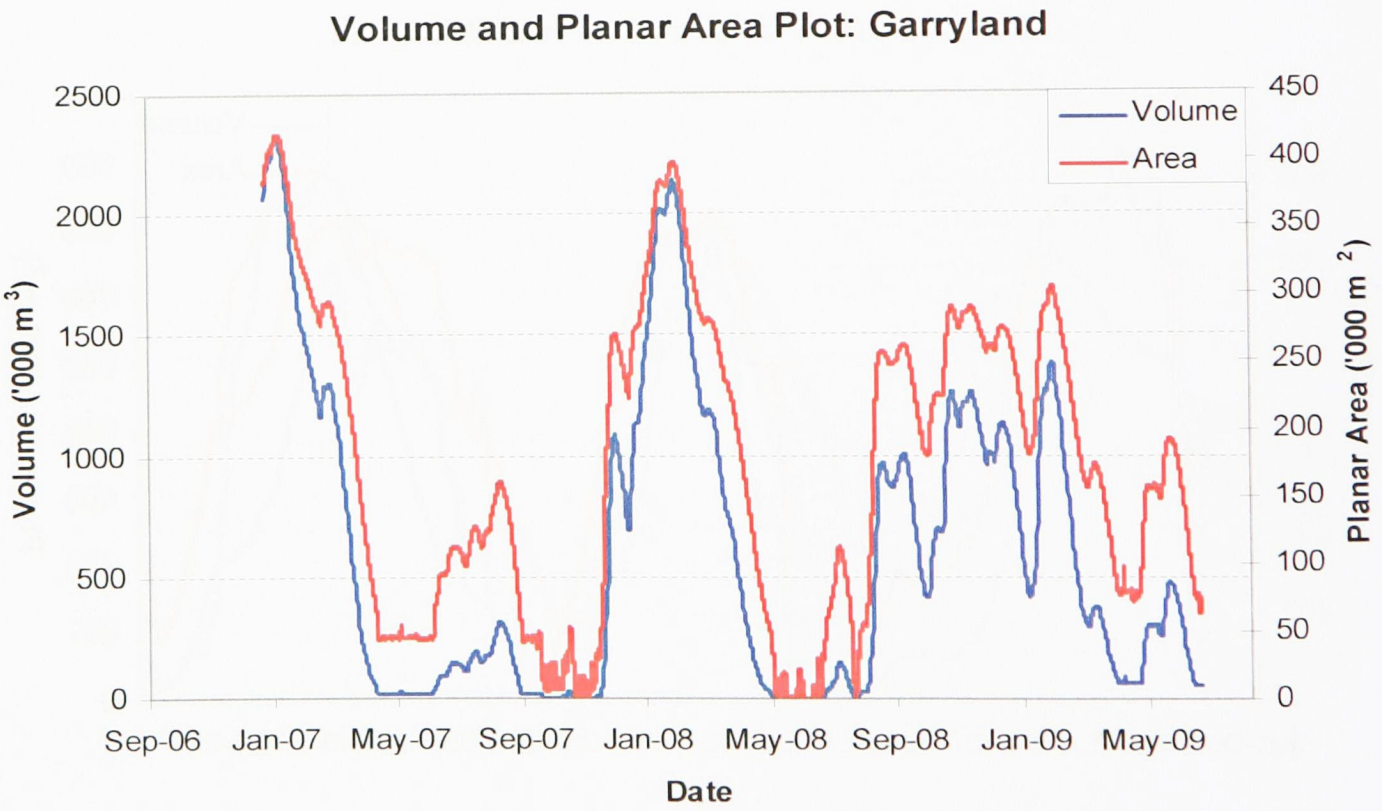
Stage Plot: Croaghill



Volume and Planar Area Plot: Croaghill




Stage Plot: Garryland
Stage (mAOD)
14
12
10
8
6
4
2
0
Sep-06
Jan-07
May-07
Sep-07
Jan-08
May-08
Sep-08
Jan-09
May-09
Date


Volume and Planar Area Plot: Garryland
Volume ('000 m 3)
Planar Area ('000 m 2)
Volume
Area
2500
2000
1500
1000
500
0
450
400
350
300
250
200
150
100
50
0
Sep-06
Jan-07
May-07
Sep-07
Jan-08
May-08
Sep-08
Jan-09
May-09
Date

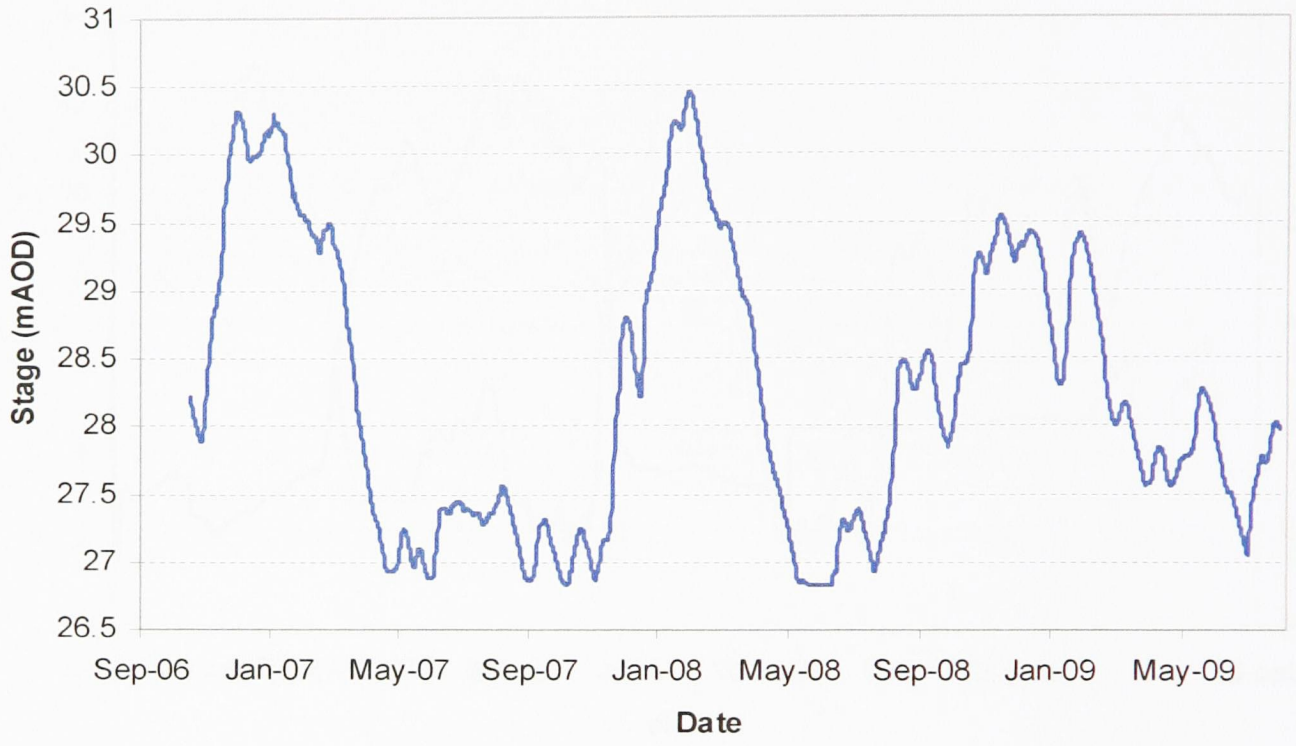
Stage Plot: Kilglassaun



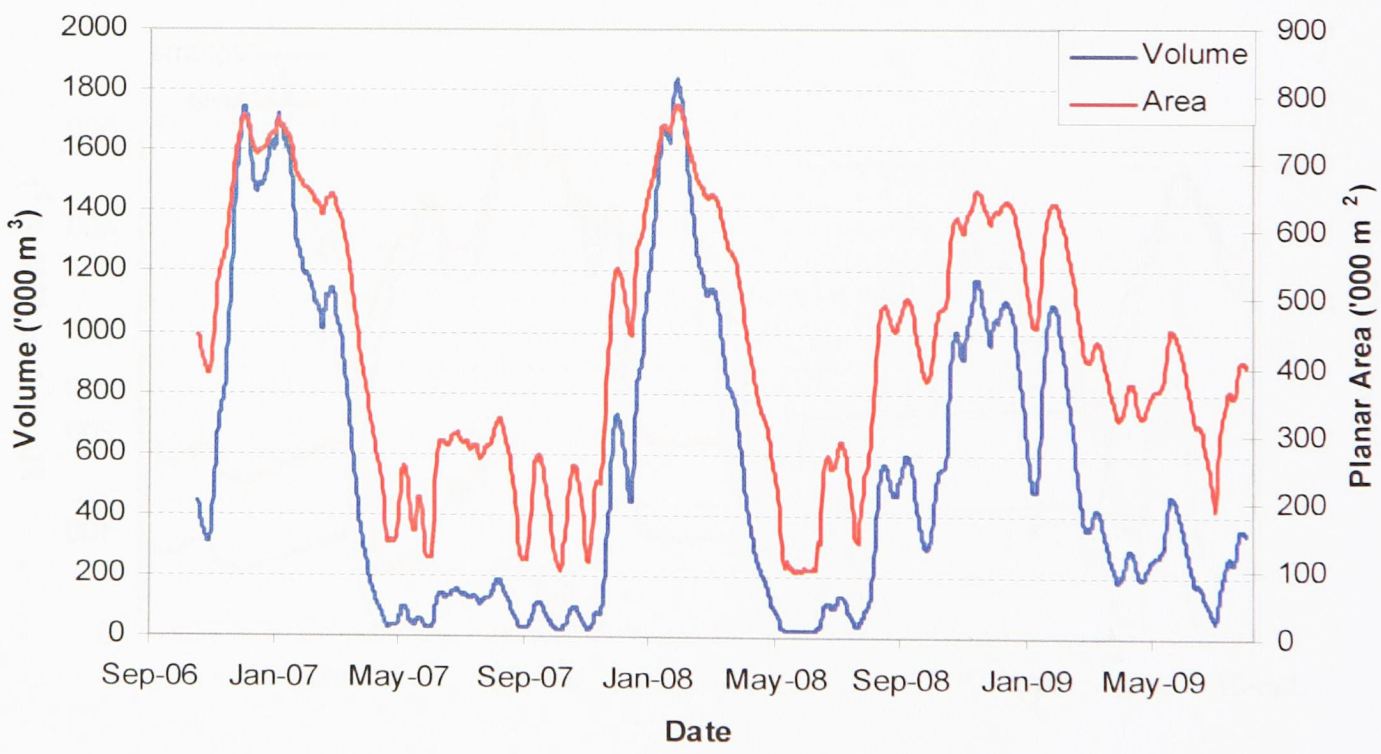
Volume and Planar Area Plot: Kilglassaun

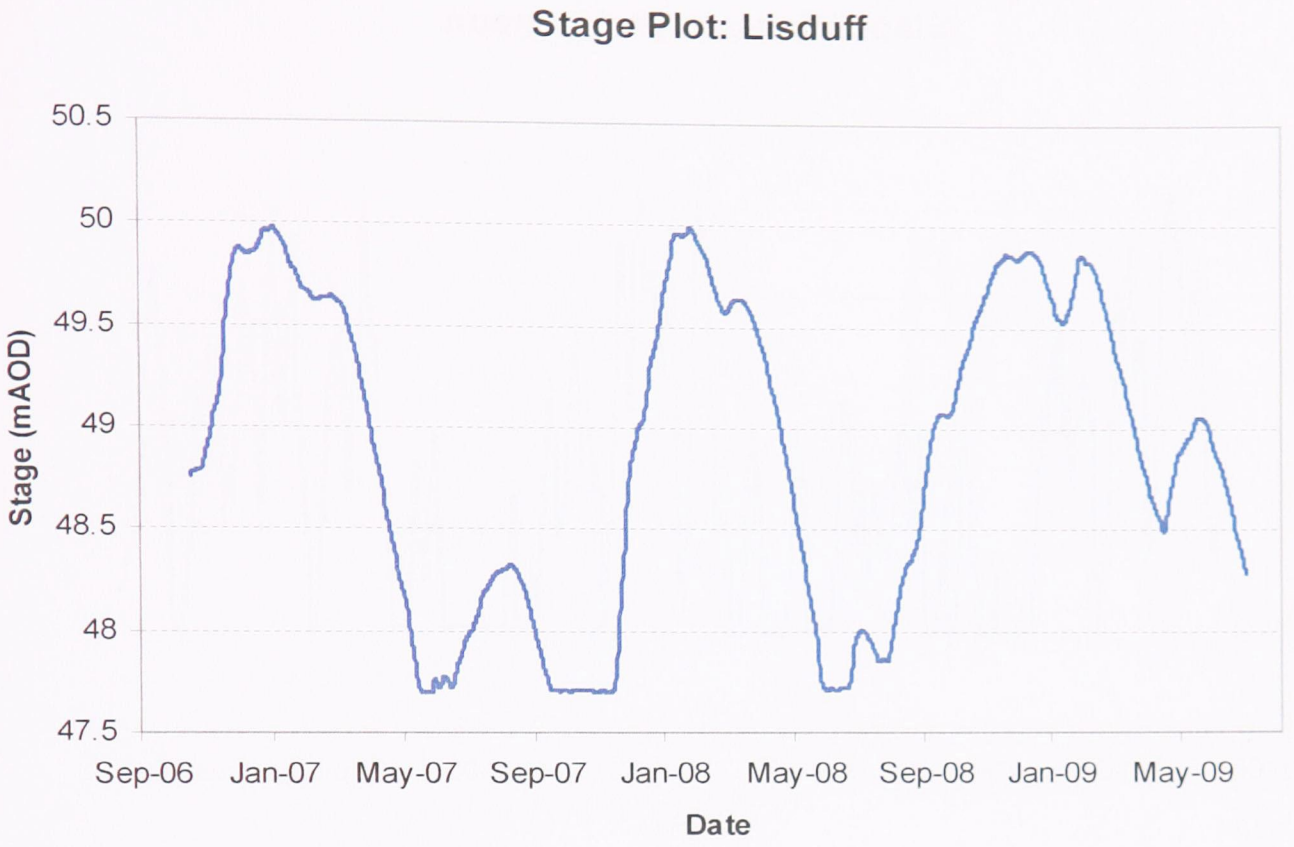


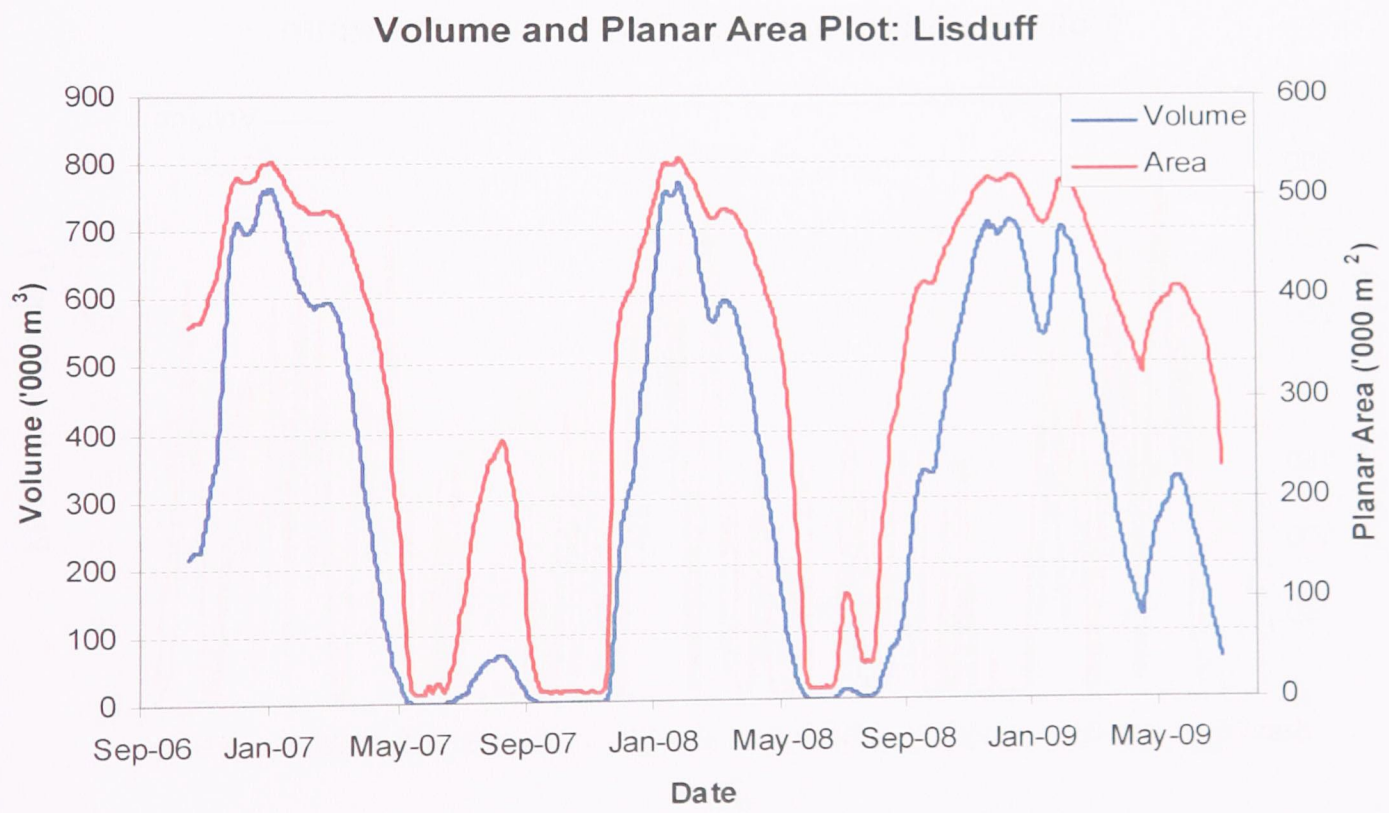
Stage Plot: Knockaunroe



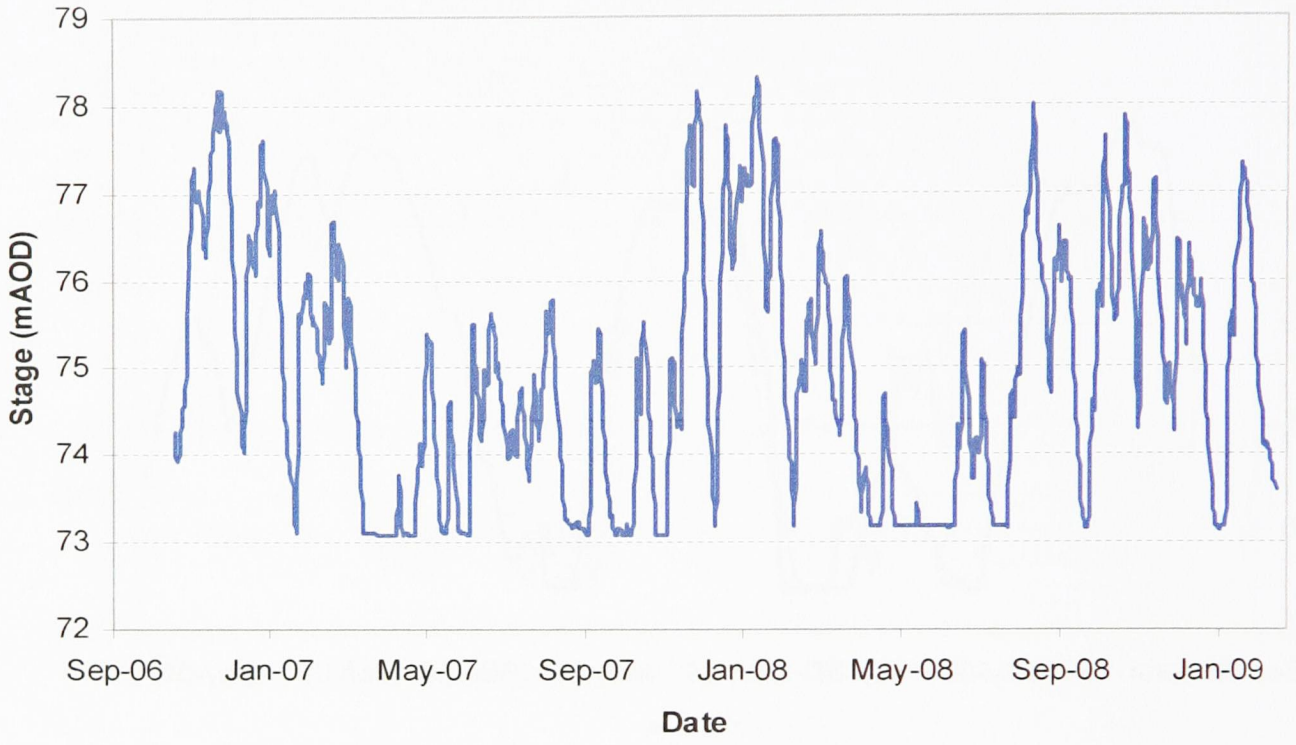
Volume and Planar Area Plot: Knockaunroe



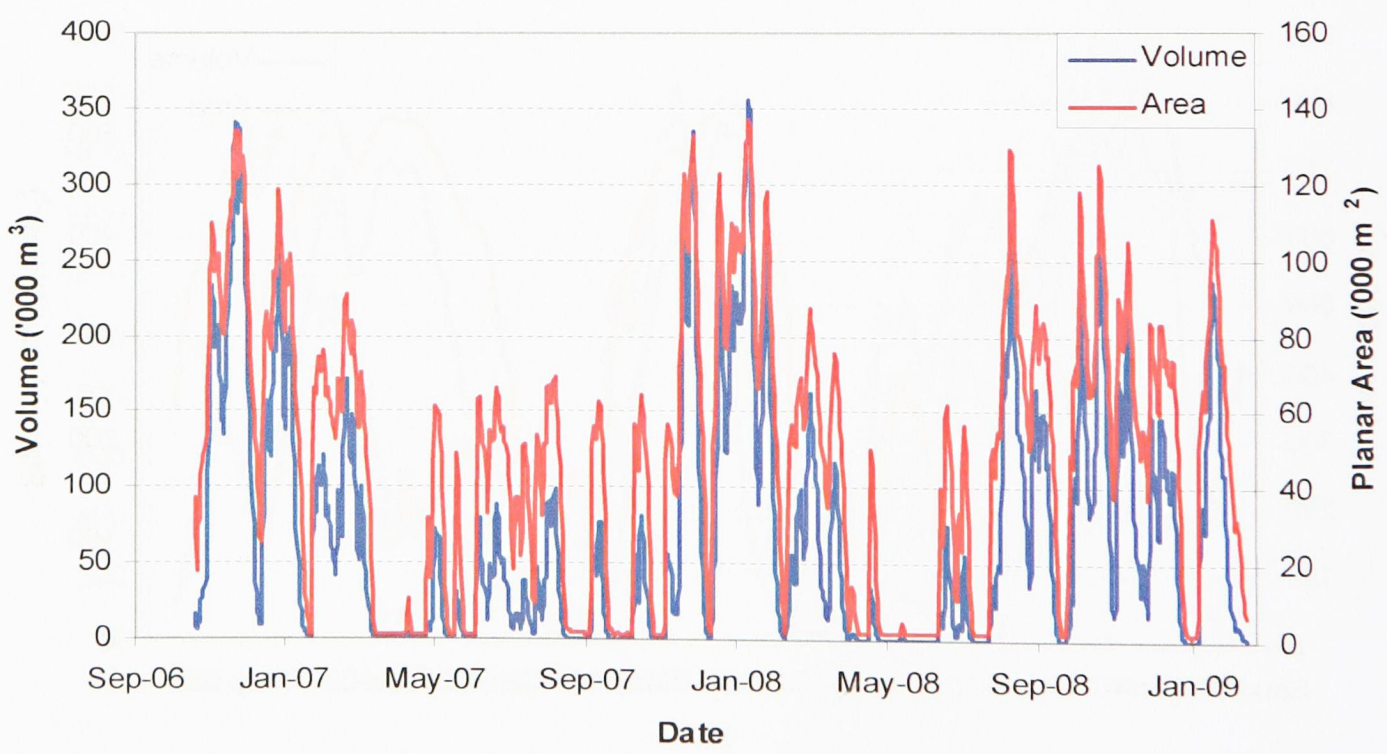

Stage Plot: Lisduff
50.5
50
49.5
49
48.5
48
47.5
Stage (mAOD)
Sep-06
Jan-07
May-07
Sep-07
Jan-08
May-08
Sep-08
Jan-09
May-09
Date


Volume and Planar Area Plot: Lisduff
900
800
700
600
500
400
300
200
100
0
Volume ('000 m 3)
600
500
400
300
200
100
0
Planar Area ('000 m 2)
Volume
Area
Sep-06
Jan-07
May-07
Sep-07
Jan-08
May-08
Sep-08
Jan-09
May-09
Date

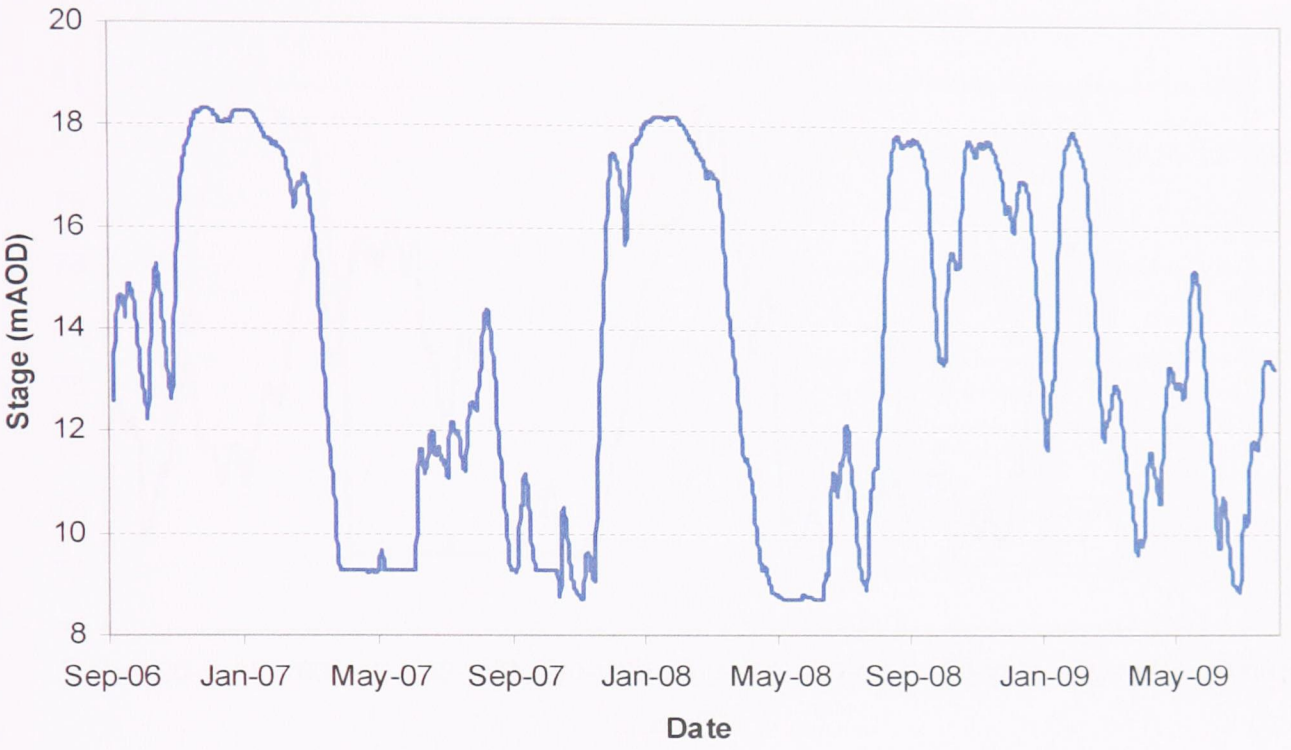
Stage Plot: Lough Aleenaun



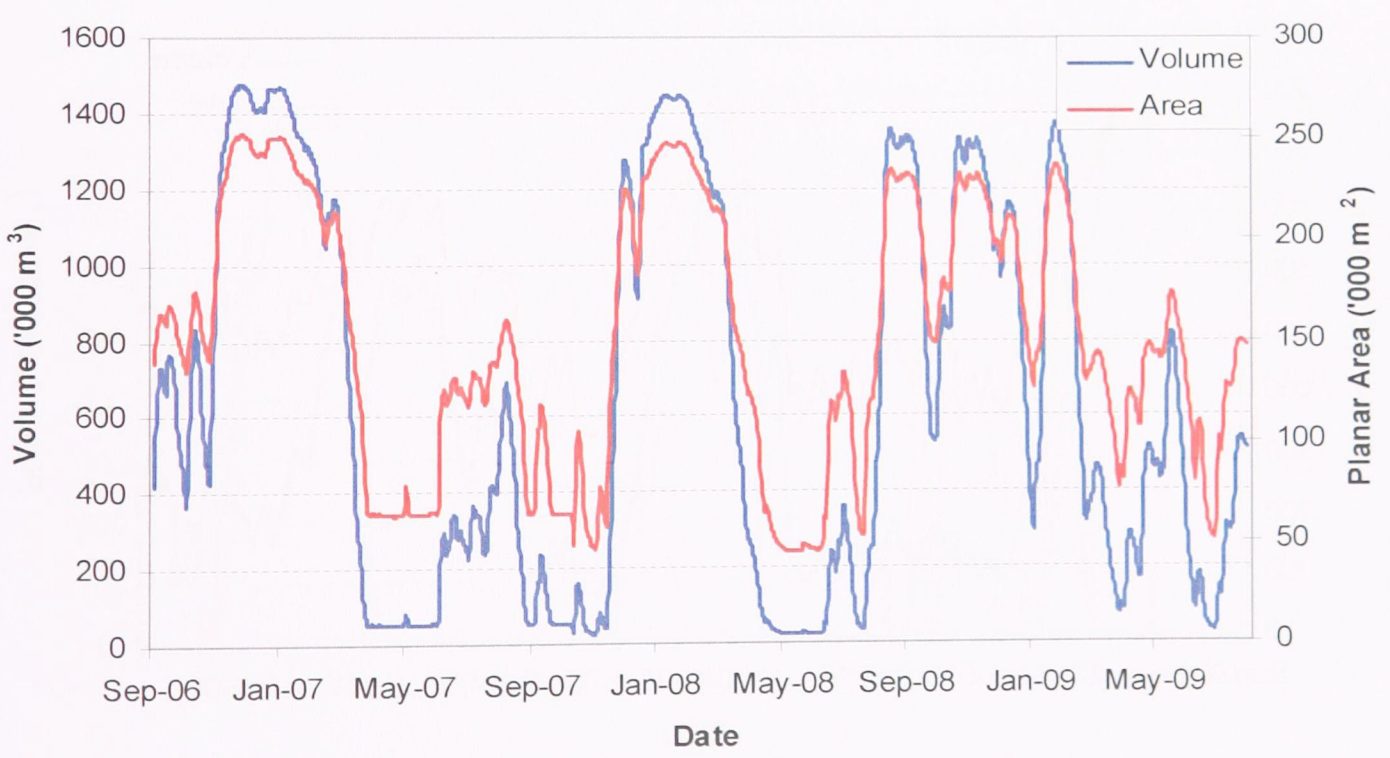
Volume and Planar Area Plot: Lough Aleenaun



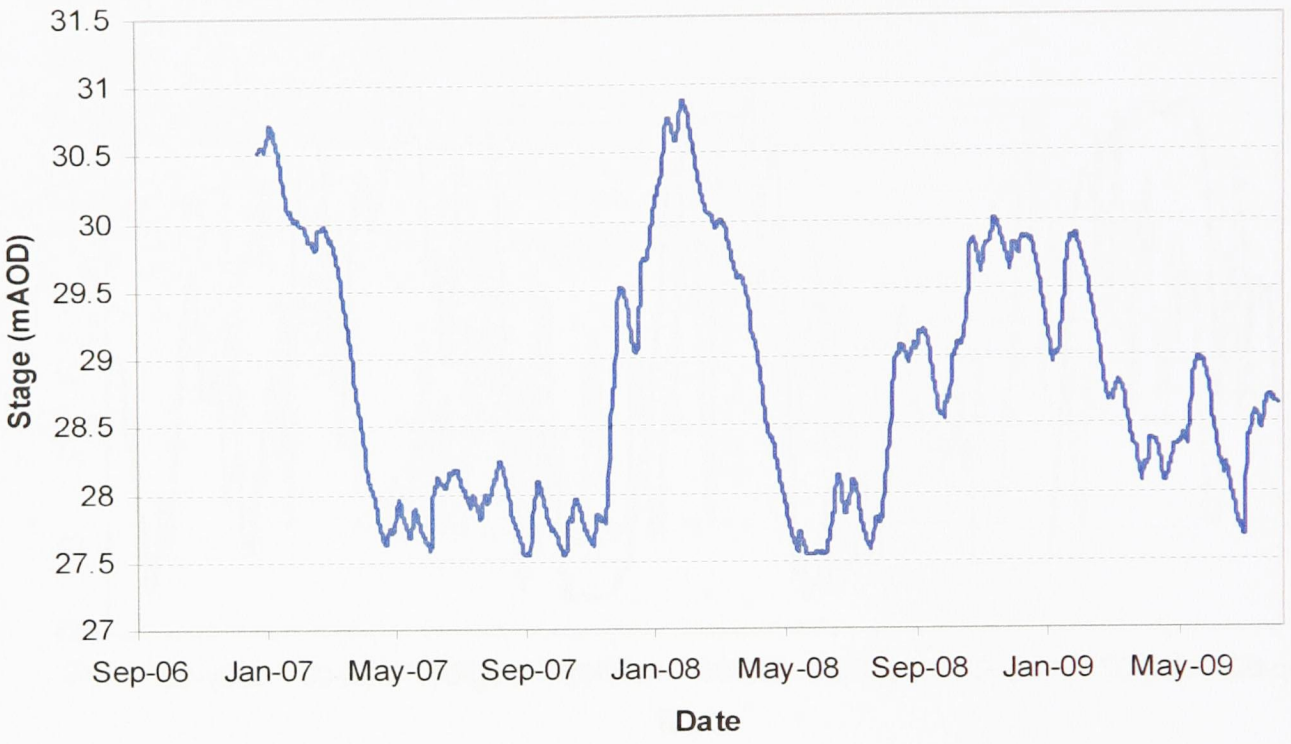
Stage Plot: Lough Coy



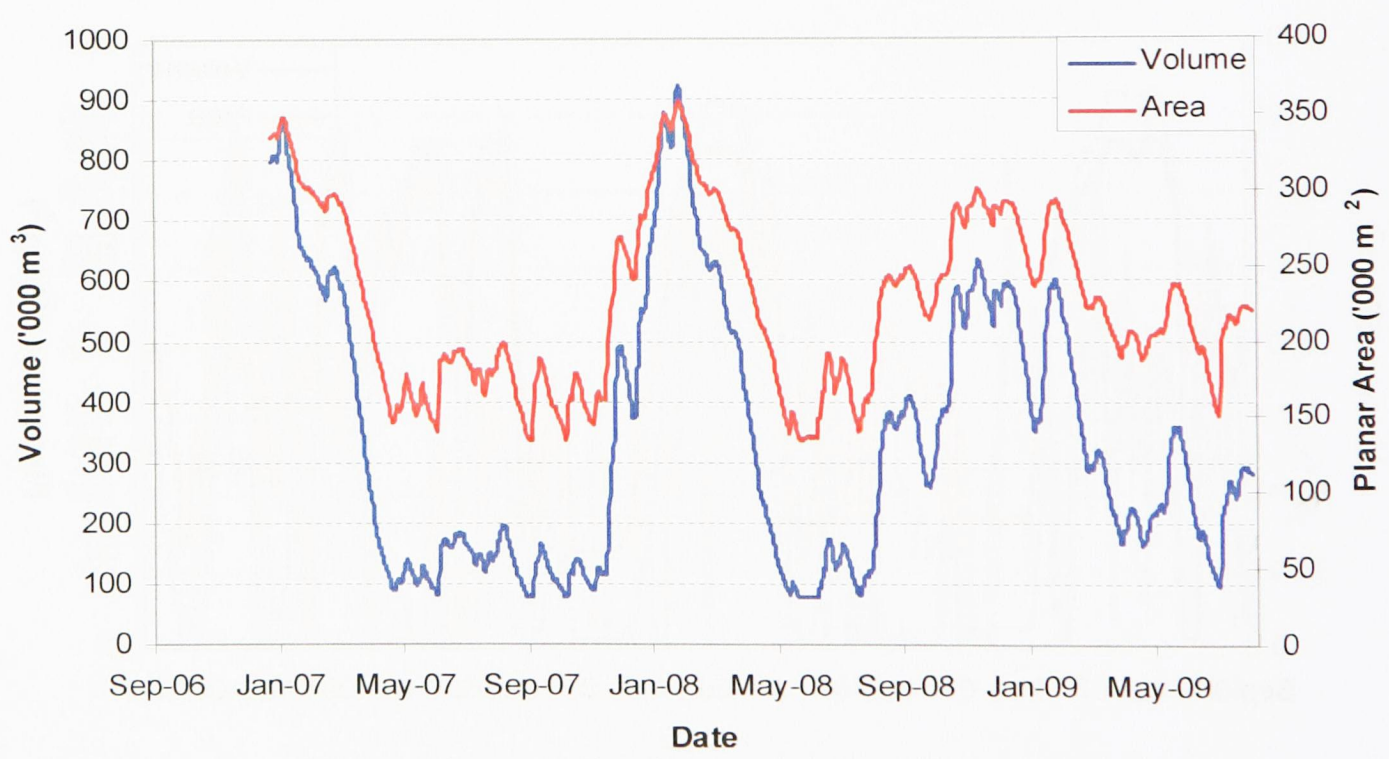
Volume and Planar Area Plot: Lough Coy



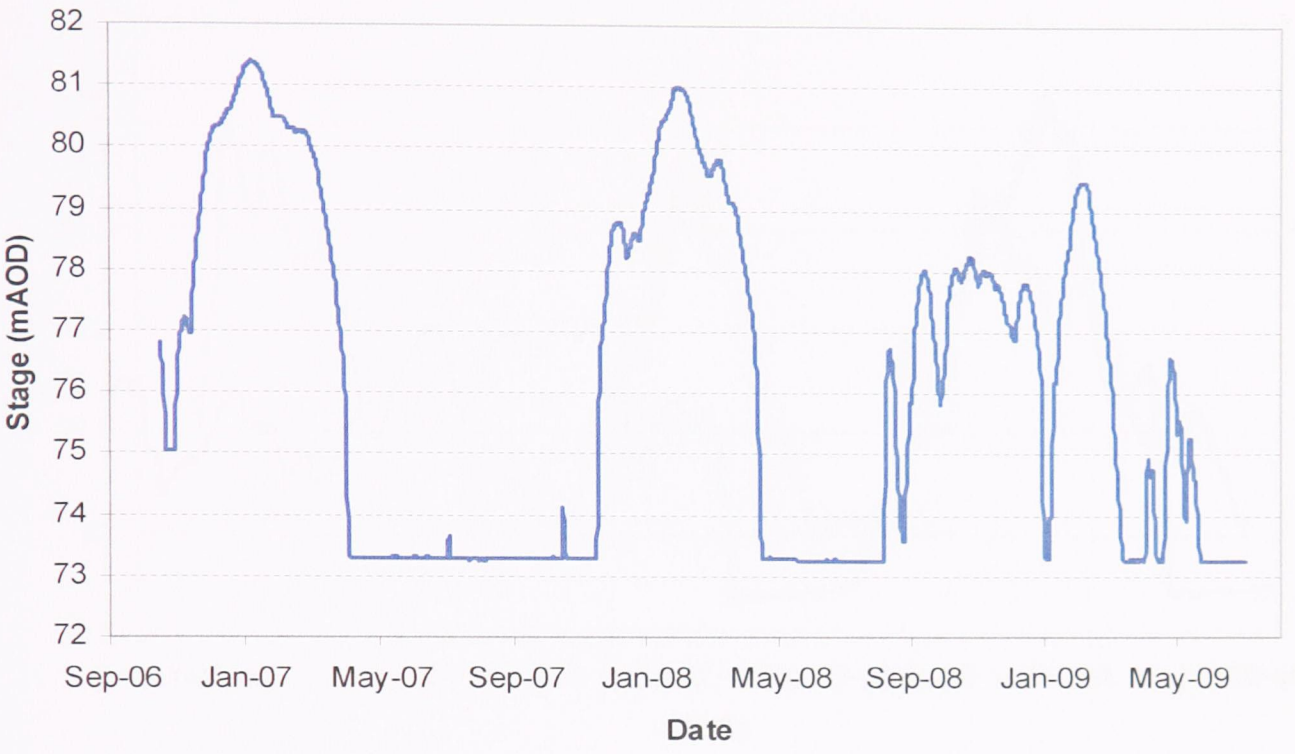
Stage Plot: Lough Gealain



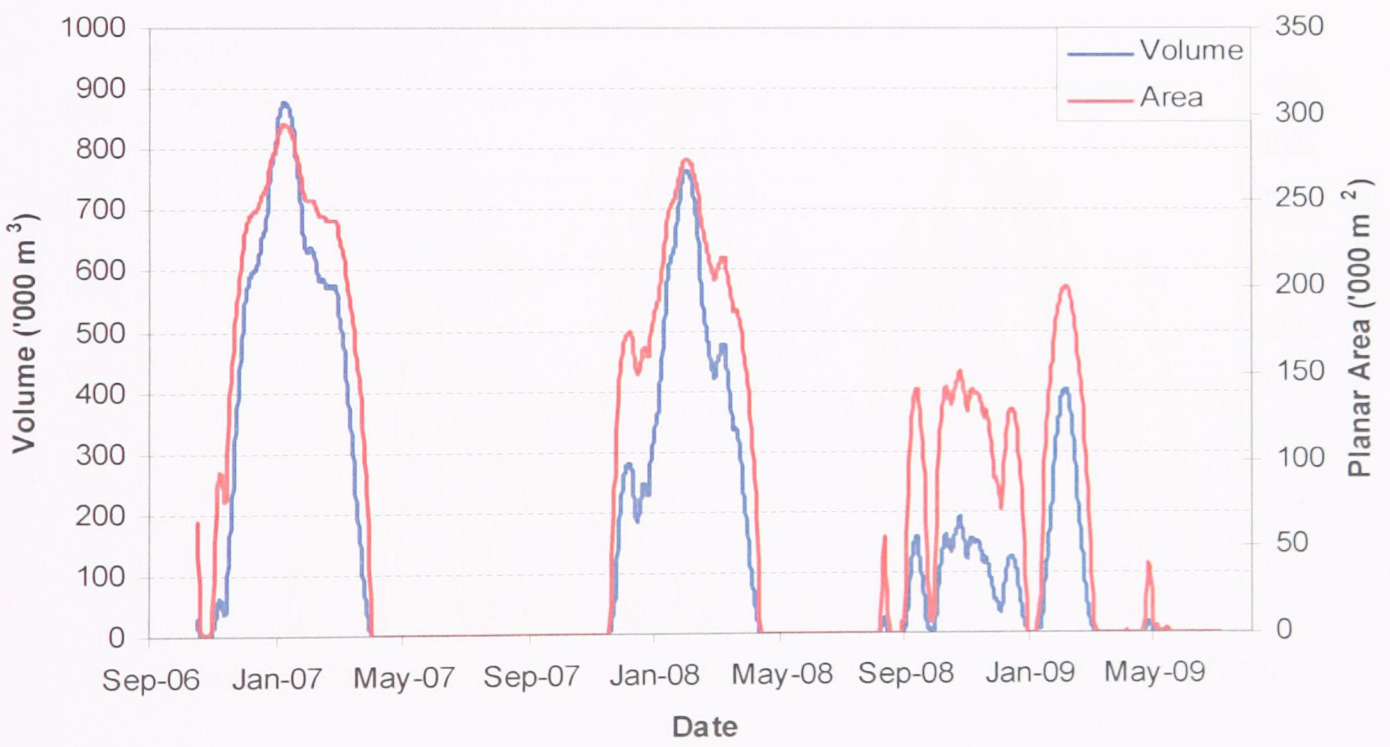
Volume and Planar Area Plot: Lough Gealain



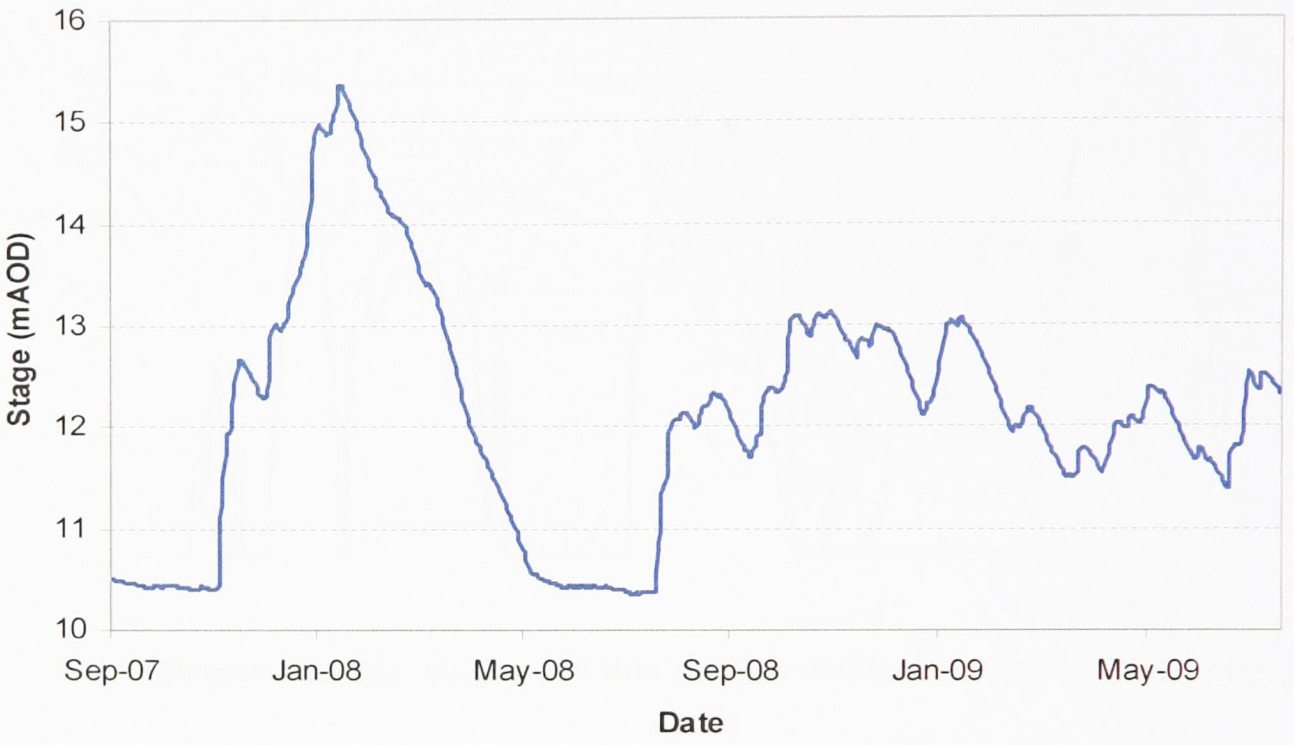
Stage Plot: Rathnalulleagh



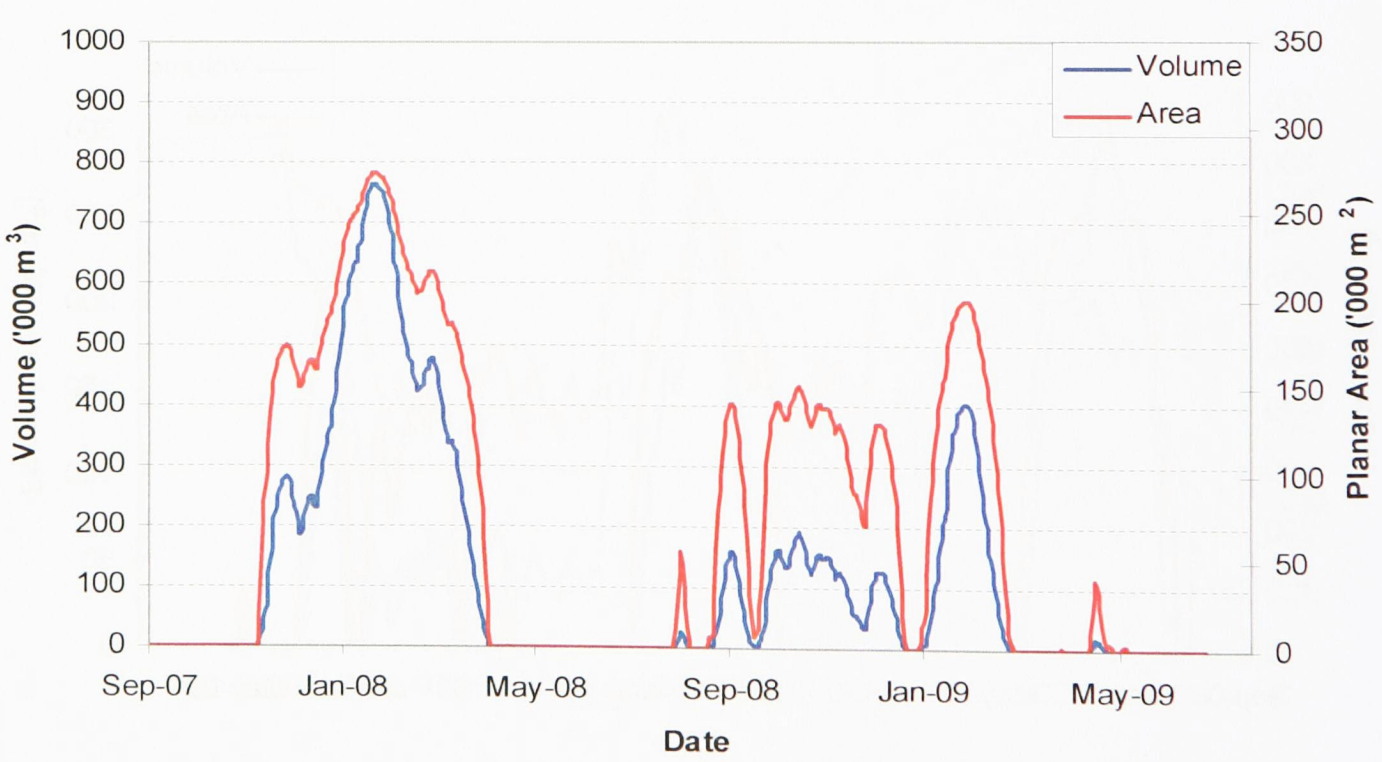
Volume and Planar Area Plot: Rathnalulleagh



Stage Plot: Roo West



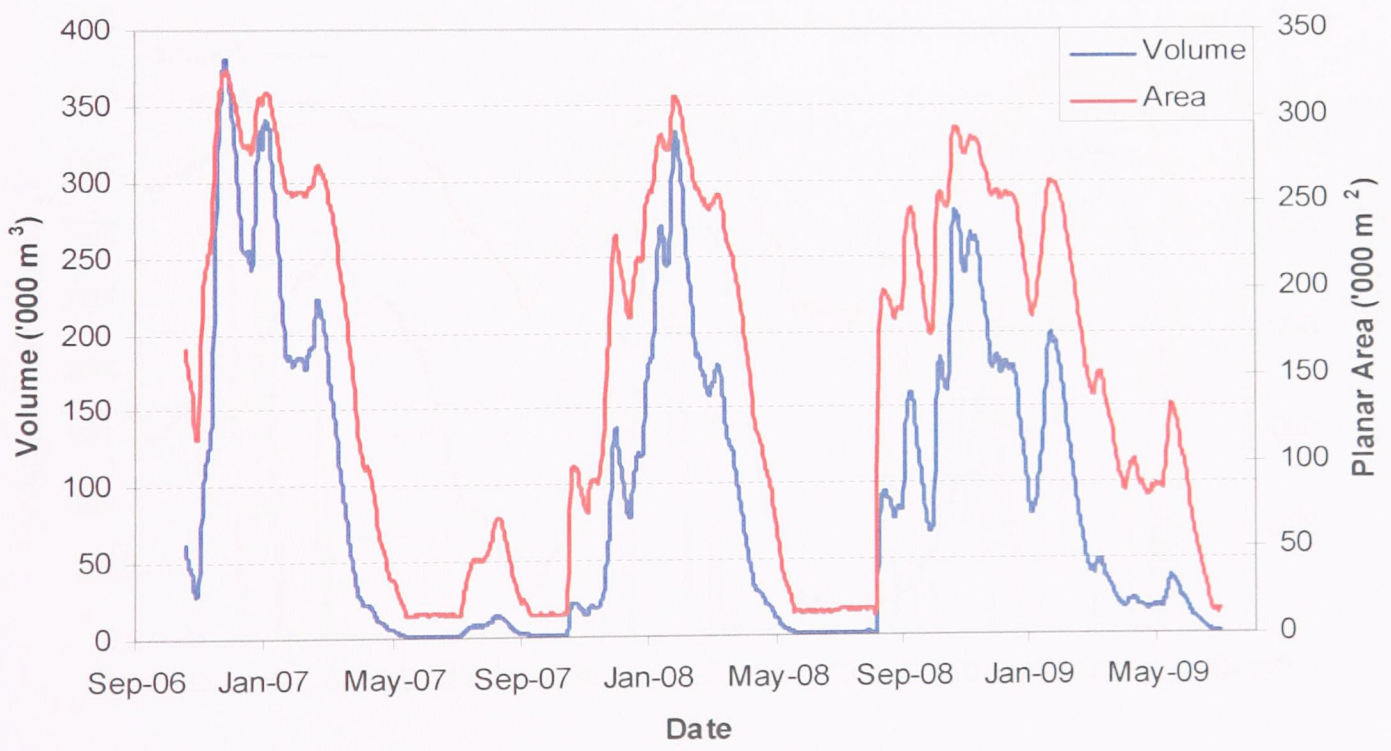
Volume and Planar Area Plot: Roo West

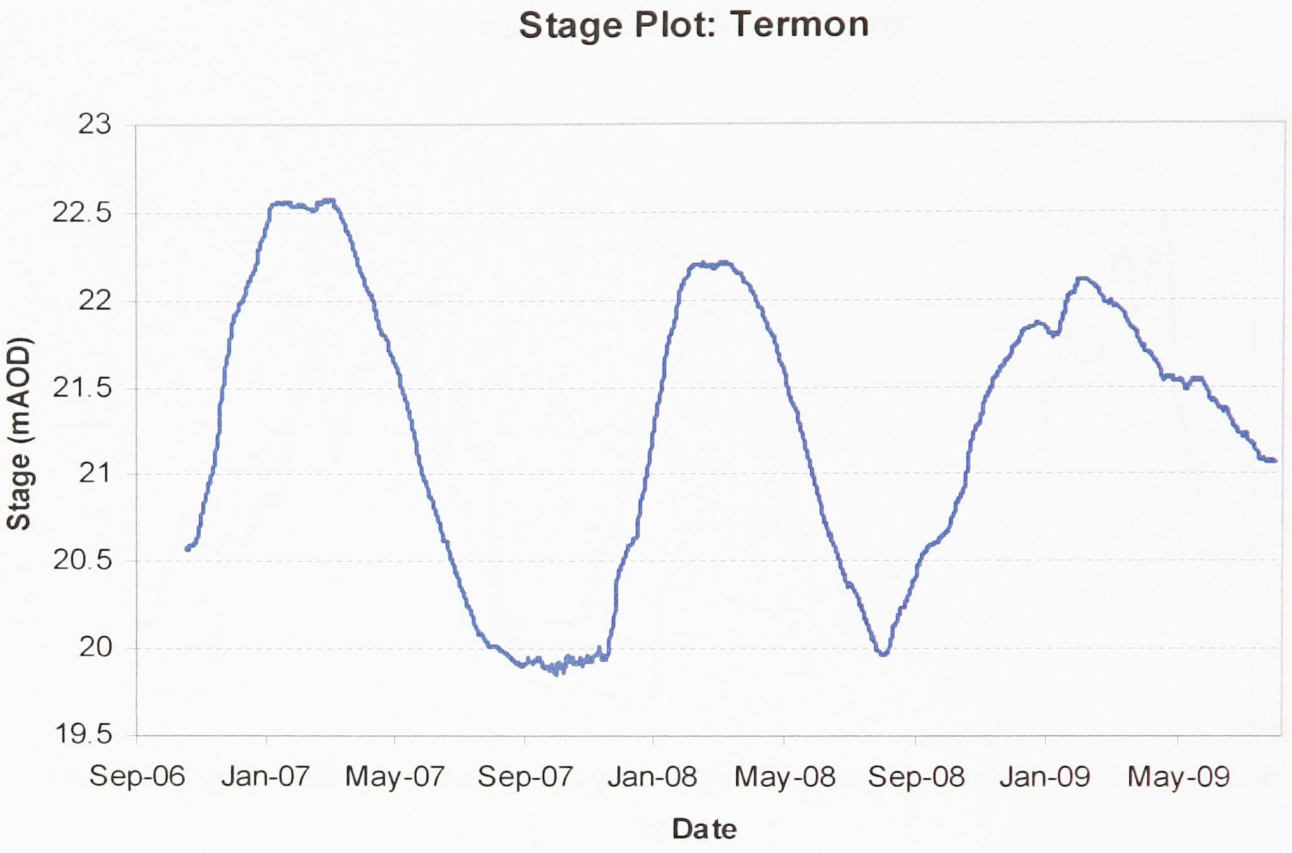


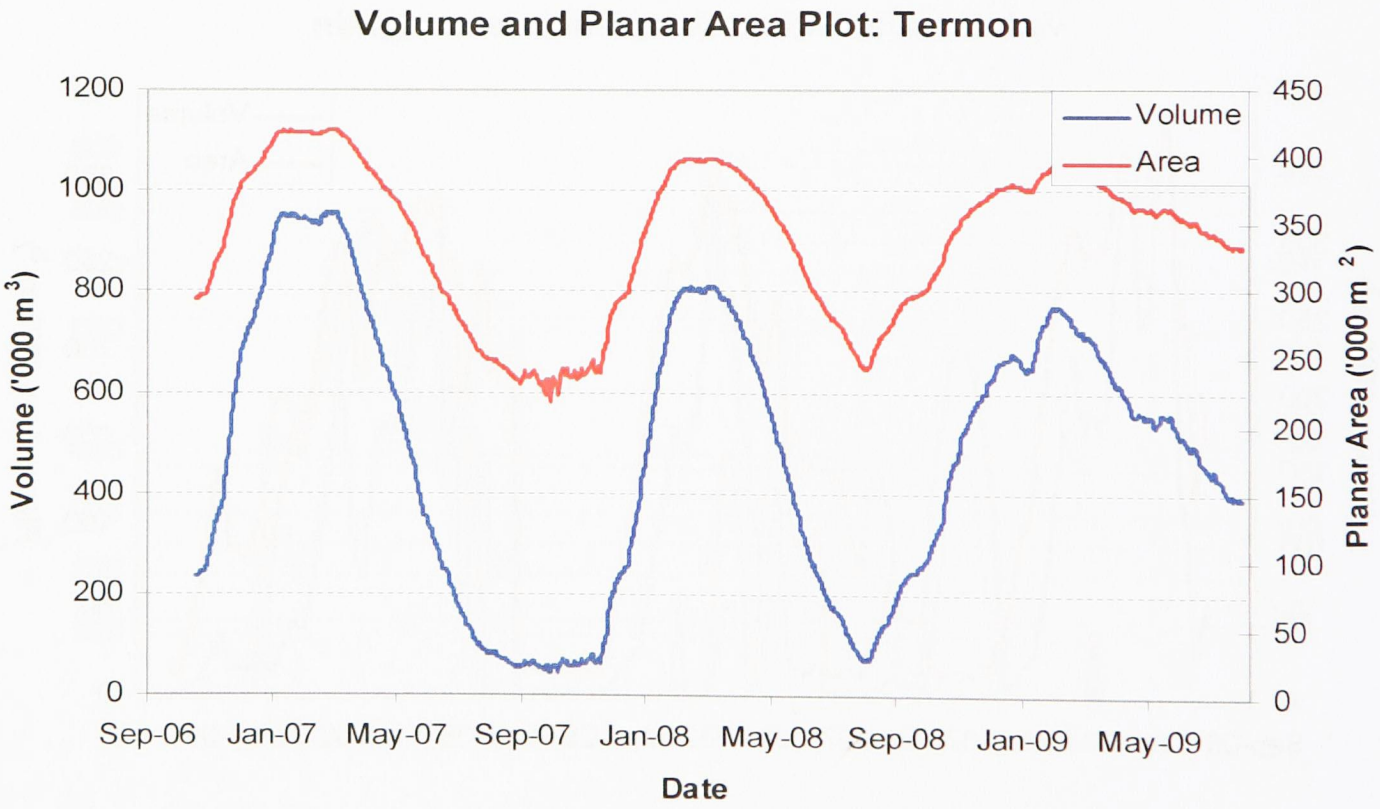
Stage Plot: Skealoghan



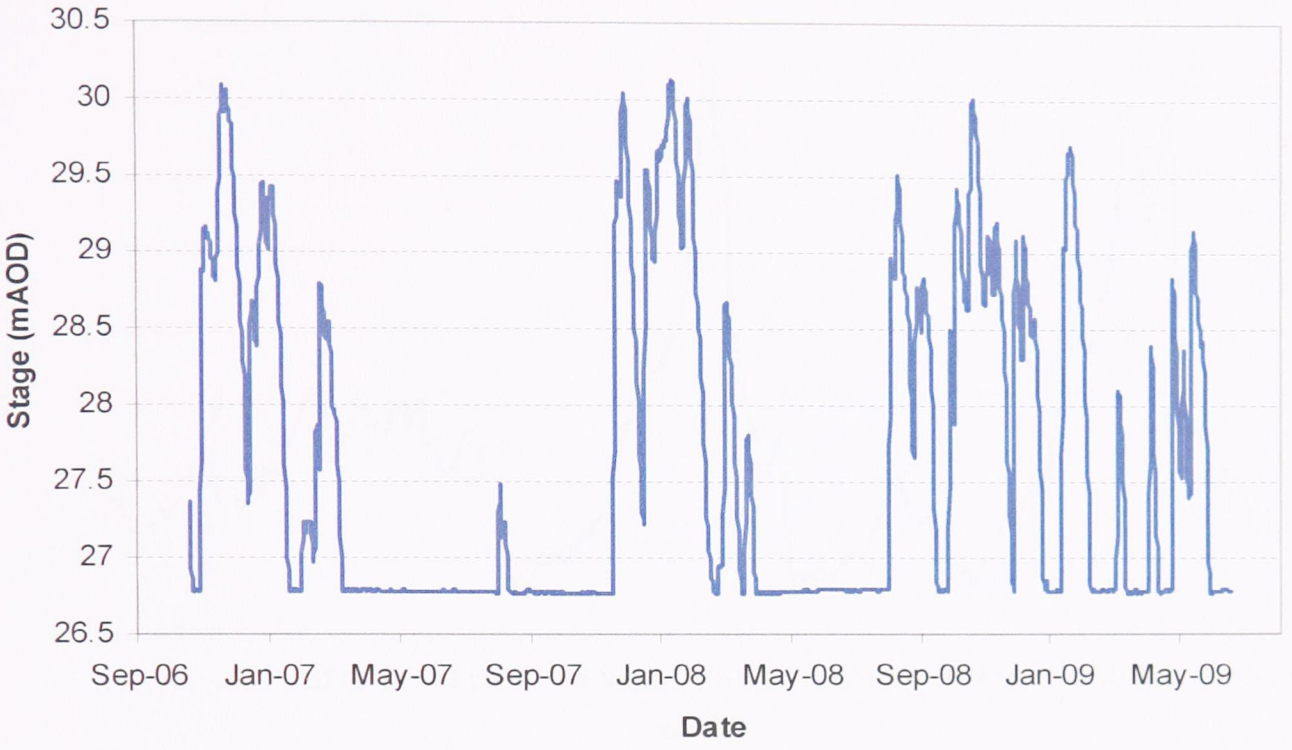
Volume and Planar Area Plot: Skealoghan



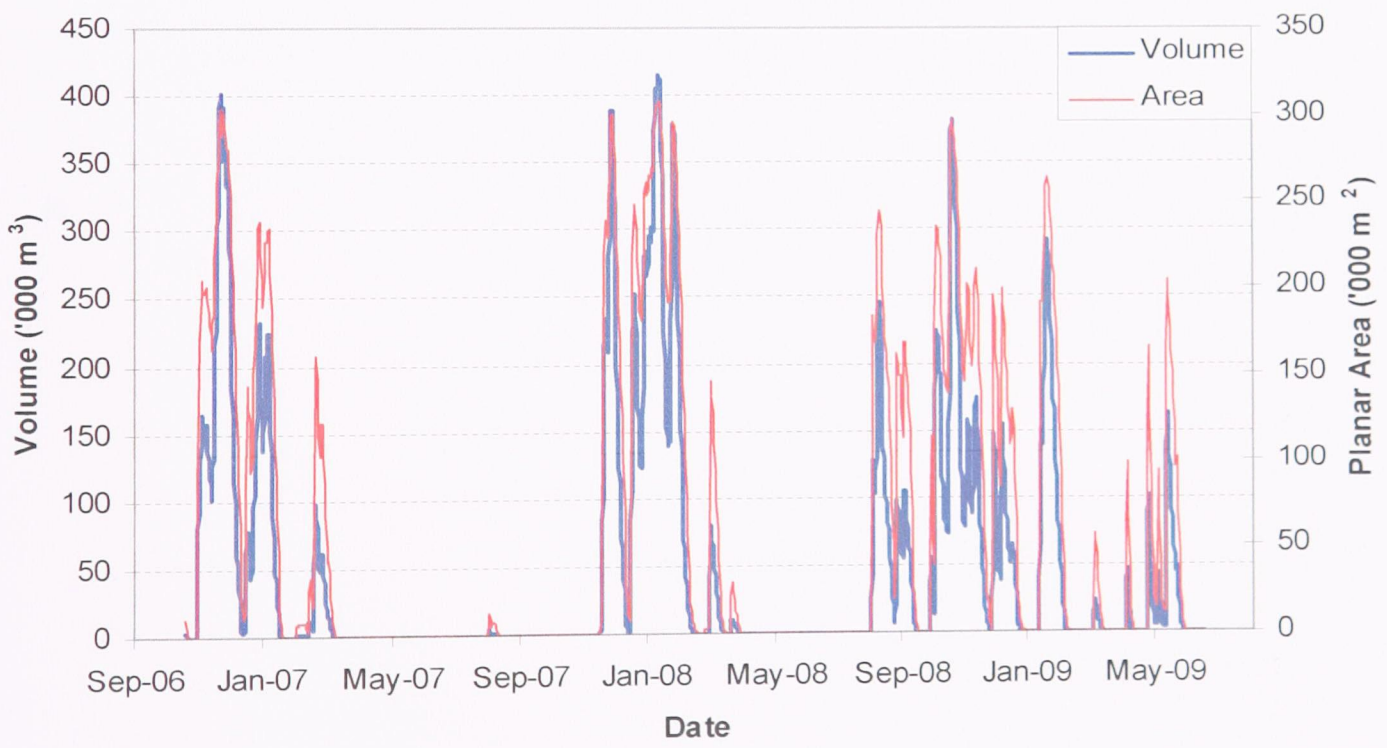

Stage Plot: Termon
Stage (mAOD)
23
22.5
22
21.5
21
20.5
20
19.5
Sep-06
Jan-07
May-07
Sep-07
Jan-08
May-08
Sep-08
Jan-09
May-09
Date

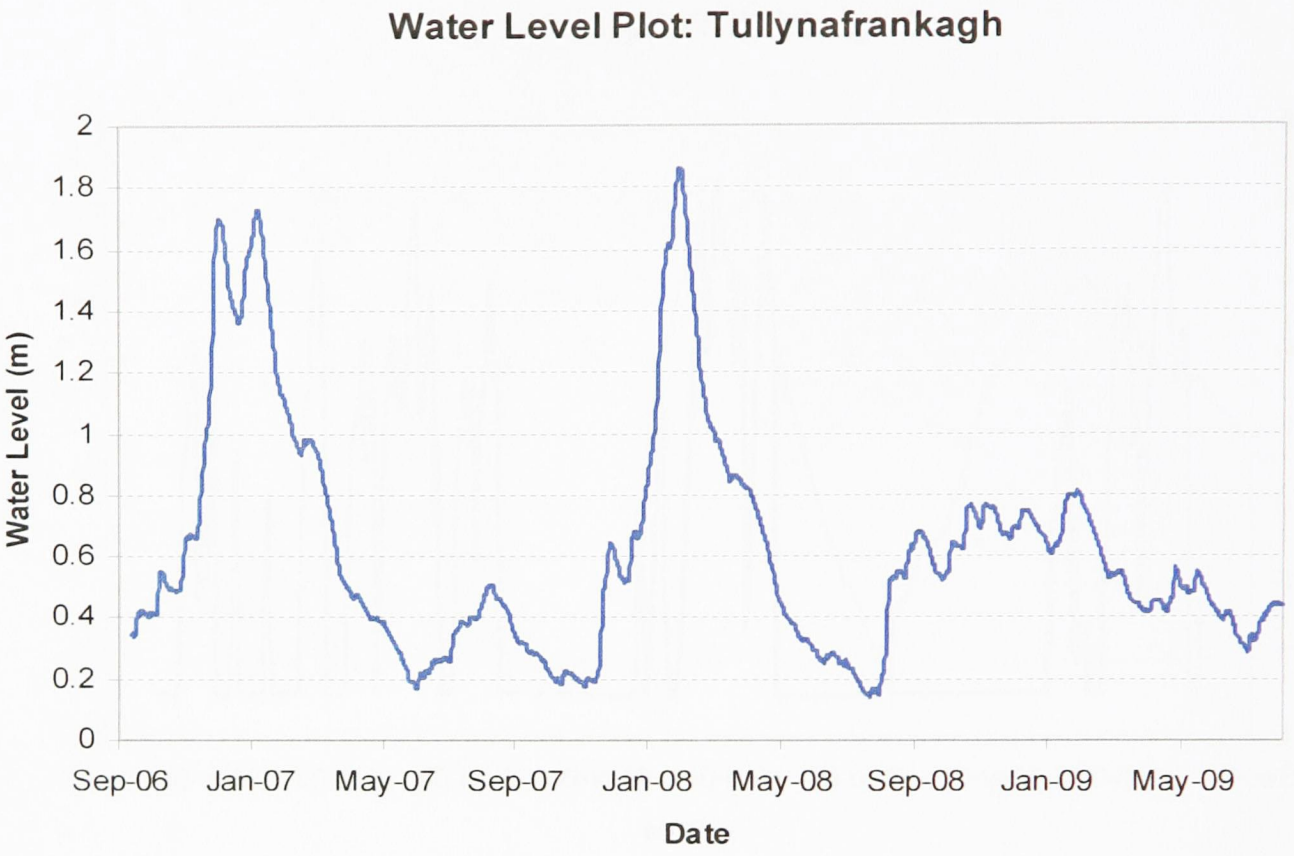

Volume and Planar Area Plot: Termon
Volume ('000 m 3)
Planar Area ('000 m 2)
Volume
Area
1200
1000
800
600
400
200
0
450
400
350
300
250
200
150
100
50
0
Sep-06
Jan-07
May-07
Sep-07
Jan-08
May-08
Sep-08
Jan-09
May-09
Date

Stage Plot: Turloughmore



Volume and Planar Area Plot: Turloughmore

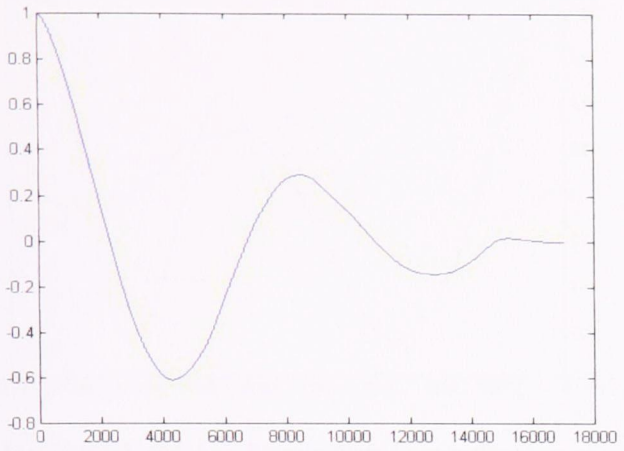



Water Level Plot: Tullynafrankagh
Water Level (m)
2
1.8
1.6
1.4
1.2
1
0.8
0.6
0.4
0.2
0
Sep-06
Jan-07
May-07
Sep-07
Jan-08
May-08
Sep-08
Jan-09
May-09
Date

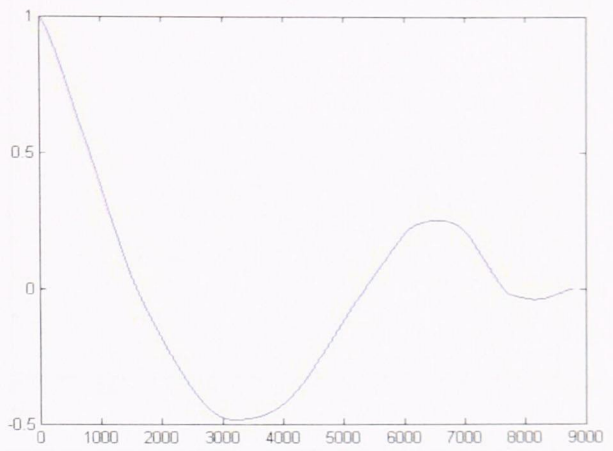
Appendix C: Correlation Analyses

	Blackrock	Lough Coy	Garryland	Caherglassaun	Coolcam	Croaghill	Rathnalulleagh	Carrowreagh	Brierfield	Skealoghan	Ardkill	Kilglassaun	Lough Gealain	Knockaunroe	Lisduff	Caranavoodaun	Roo West	Termon	Turloughmore	Lough Aleenaun
Blackrock	1.00																			
Lough Coy	0.95	1.00																		
Garryland	0.94	0.96	1.00																	
Caherglassaun	0.94	0.97	1.00	1.00																
Coolcam	0.29	0.32	0.50	0.46	1.00															
Croaghill	0.61	0.64	0.76	0.73	0.90	1.00														
Rathnalulleagh	0.81	0.85	0.93	0.92	0.62	0.83	1.00													
Carrowreagh	0.74	0.78	0.88	0.87	0.63	0.81	0.98	1.00												
Brierfield	0.45	0.47	0.64	0.61	0.92	0.95	0.78	0.79	1.00											
Skealoghan	0.88	0.89	0.96	0.94	0.55	0.80	0.94	0.89	0.72	1.00										
Ardkill	0.58	0.61	0.72	0.70	0.87	0.98	0.79	0.77	0.92	0.81	1.00									
Kilglassaun	0.89	0.94	0.95	0.95	0.54	0.75	0.94	0.92	0.71	0.92	0.71	1.00								
Lough Gealain	0.89	0.90	0.98	0.97	0.60	0.82	0.96	0.92	0.74	0.96	0.78	0.94	1.00							
Knockaunroe	0.88	0.89	0.97	0.96	0.61	0.81	0.95	0.91	0.74	0.96	0.77	0.93	1.00	1.00						
Lisduff	0.70	0.74	0.87	0.84	0.81	0.94	0.91	0.90	0.91	0.89	0.90	0.87	0.92	0.92	1.00					
Caranavoodaun	0.84	0.83	0.94	0.92	0.67	0.86	0.94	0.90	0.80	0.97	0.85	0.90	0.97	0.97	0.94	1.00				
Roo West	0.83	0.83	0.94	0.92	0.71	0.88	0.95	0.92	0.83	0.95	0.85	0.91	0.98	0.98	0.95	0.99	1.00			
Termon	0.35	0.37	0.55	0.52	0.99	0.91	0.67	0.68	0.94	0.62	0.89	0.59	0.66	0.67	0.85	0.73	0.77	1.00		
Turloughmore	0.85	0.76	0.74	0.76	0.10	0.41	0.62	0.59	0.30	0.68	0.38	0.75	0.71	0.68	0.50	0.61	0.62	0.14	1.00	
Lough Aleenaun	0.74	0.69	0.66	0.68	0.05	0.30	0.54	0.52	0.21	0.59	0.30	0.67	0.65	0.61	0.41	0.52	0.54	0.10	0.86	1.00
Minimum	0.29	0.32	0.50	0.46	0.05	0.30	0.54	0.52	0.21	0.55	0.30	0.54	0.60	0.61	0.41	0.52	0.54	0.10	0.10	0.05
Maximum	0.95	0.97	1.00	1.00	0.99	0.98	0.98	0.98	0.95	0.97	0.98	0.95	0.99	0.99	0.95	0.99	0.99	0.99	0.86	0.86
Difference	0.66	0.65	0.49	0.53	0.94	0.67	0.44	0.46	0.73	0.42	0.67	0.41	0.39	0.39	0.54	0.47	0.45	0.89	0.76	0.81

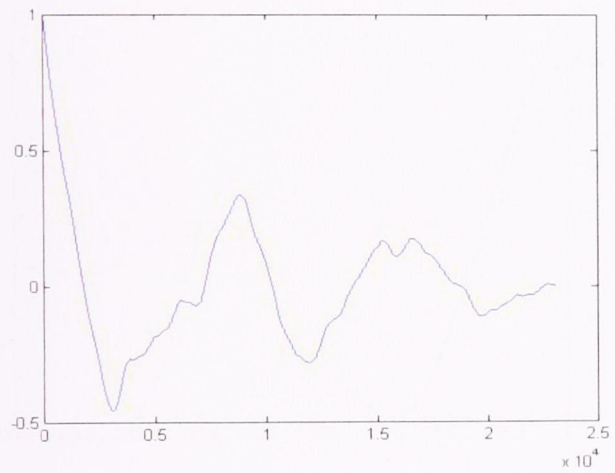
AUTOCORRELATION RESULTS: HOURLY STAGE DATA



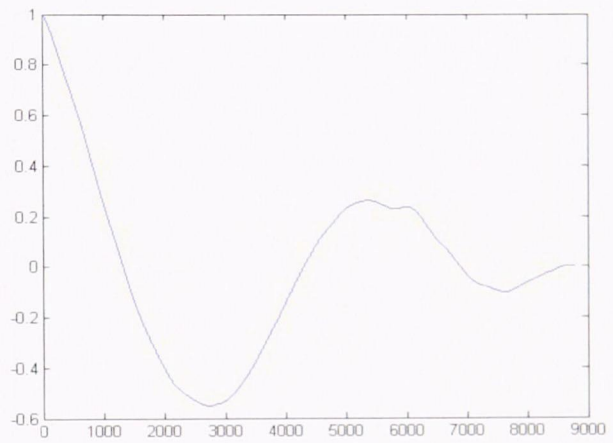
Ardkill – Monitoring period



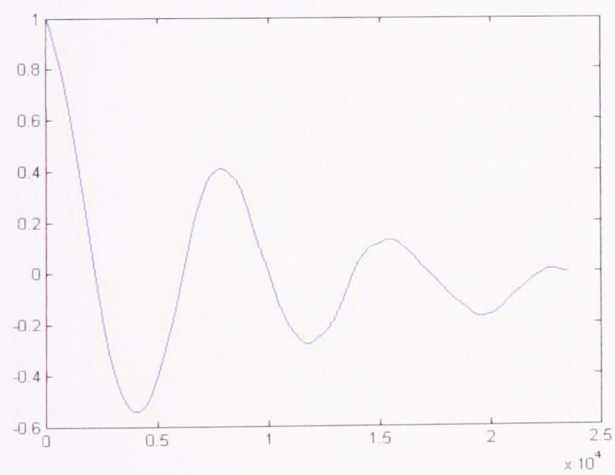
Ardkill - 2007/2008



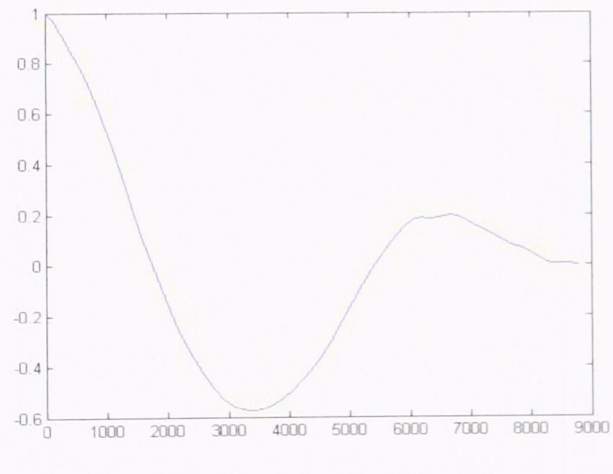
Blackrock – Monitoring period



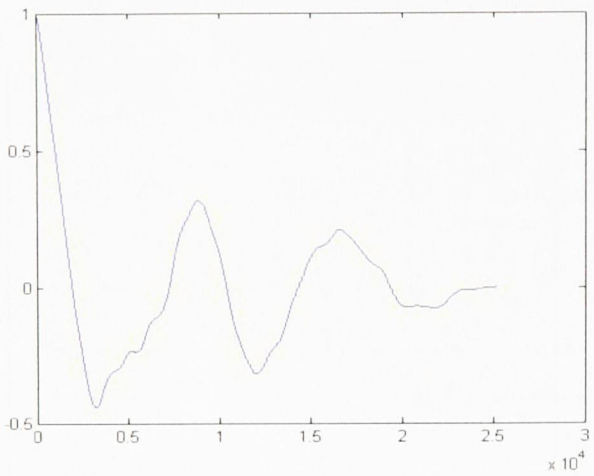
Blackrock – 2007/2008



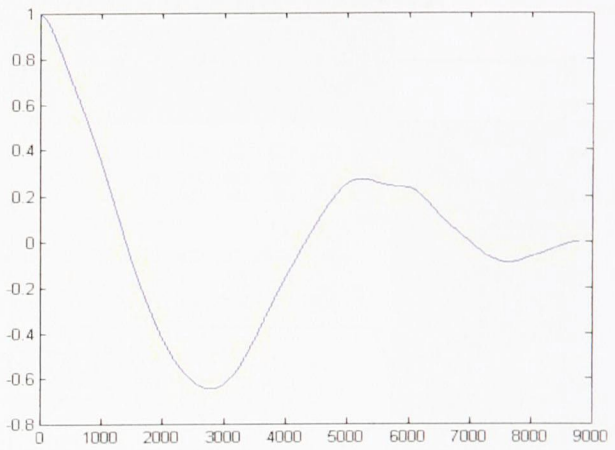
Brierfield – Monitoring period



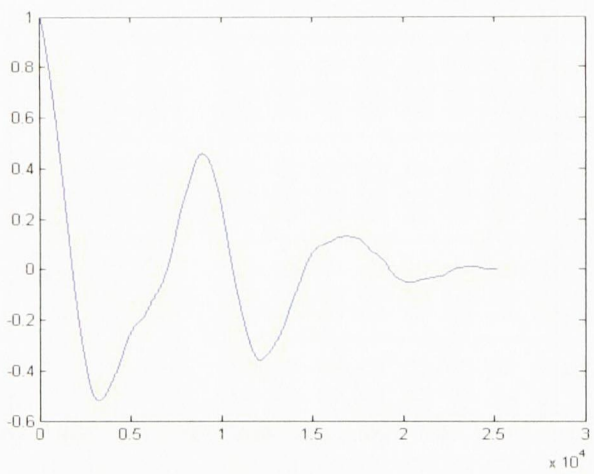
Brierfield – 2007/2008



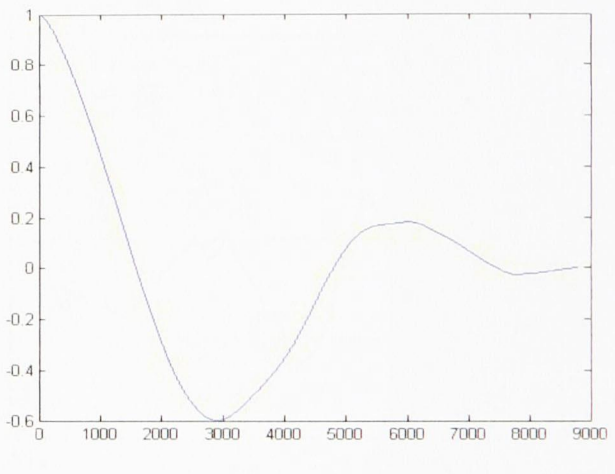
Caherglassaun – Monitoring period



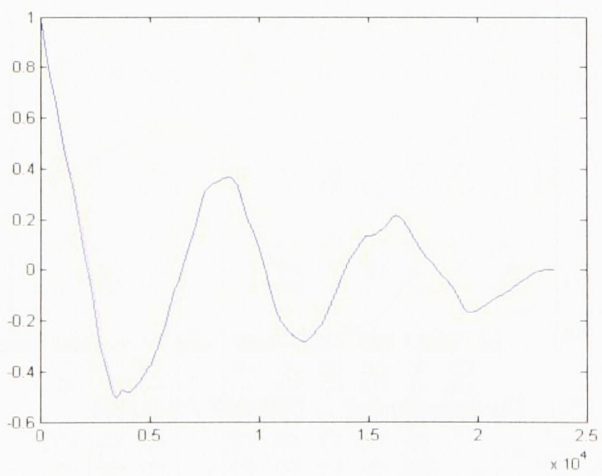
Caherglassaun – 2007/2008



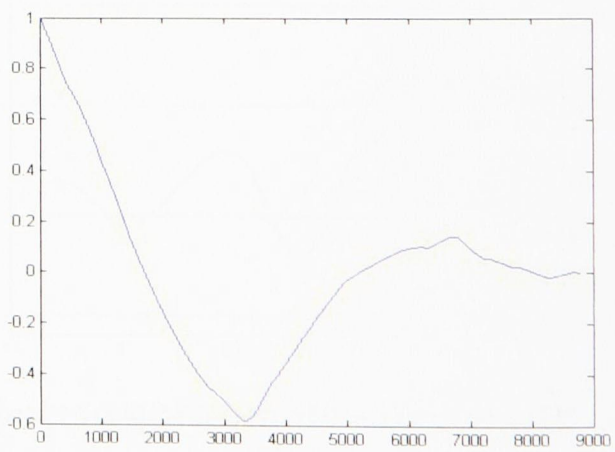
Caranavoodaun – Monitoring period



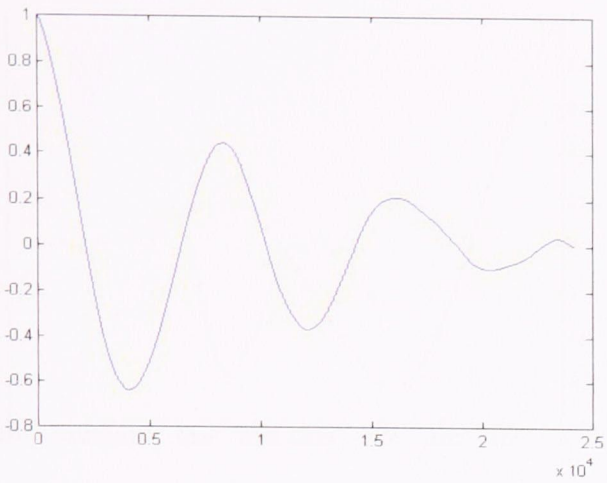
Caranavoodaun – 2007/2008



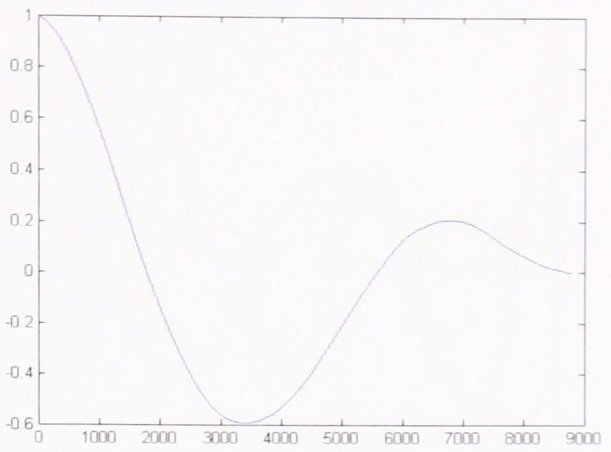
Carrowreagh – Monitoring period



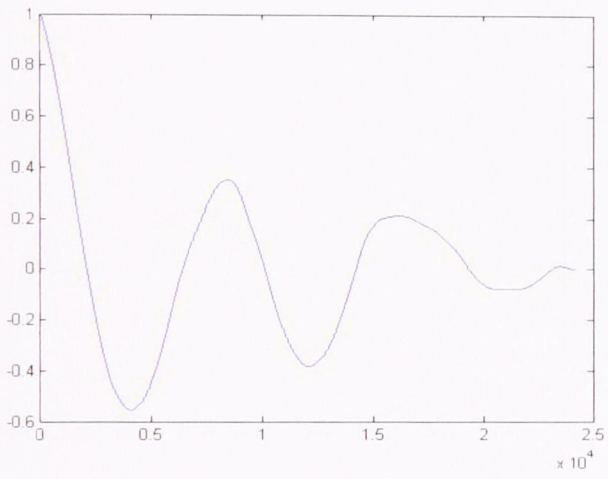
Carrowreagh – 2007/2008



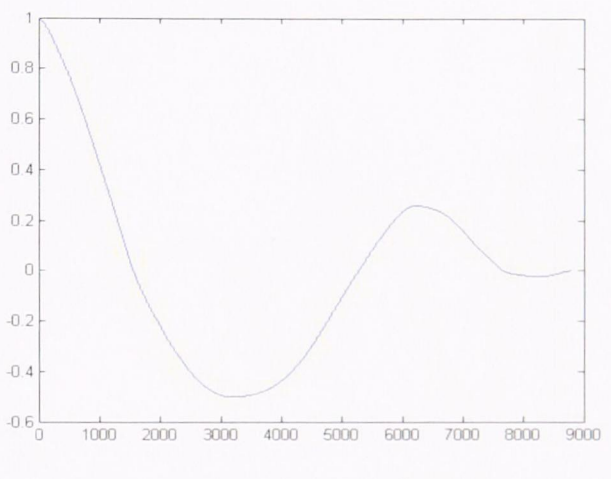
Coolcam – Monitoring period



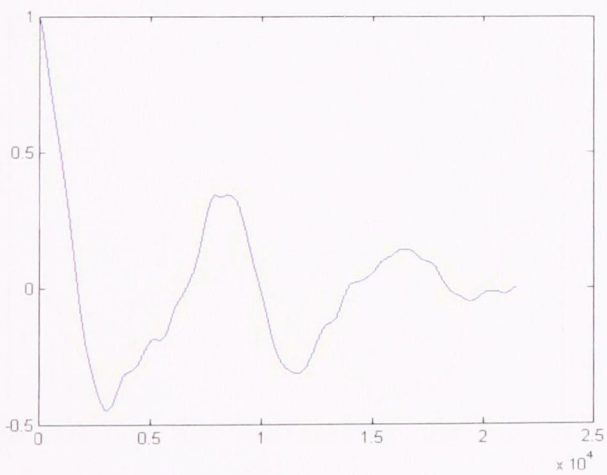
Coolcam – 2007/2008



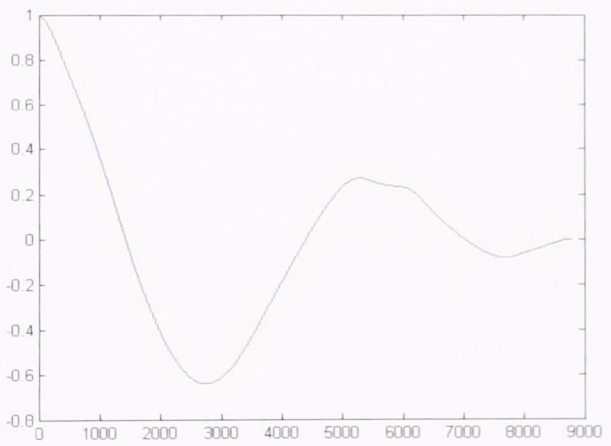
Croaghill – Monitoring period



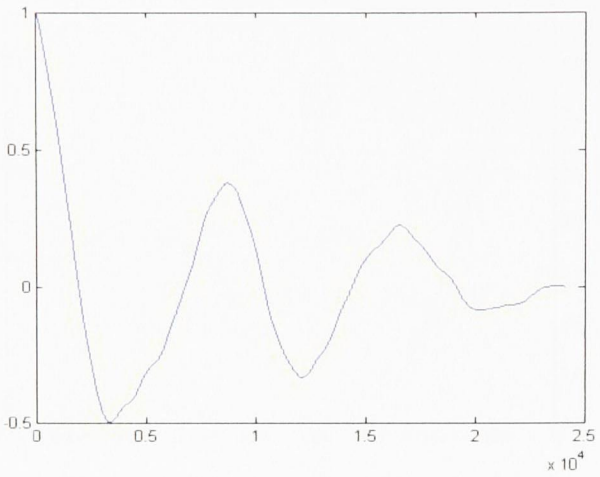
Croaghill – 2007/2008



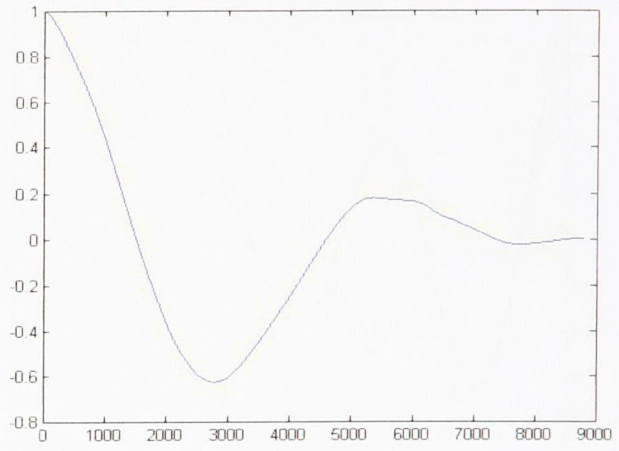
Garryland – Monitoring period



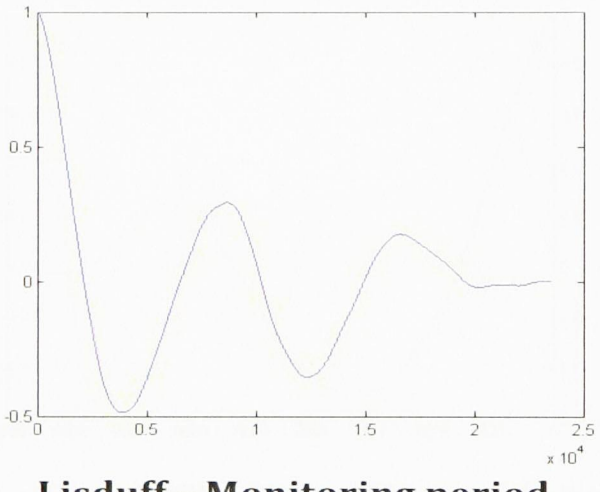
Garryland – 2007/2008



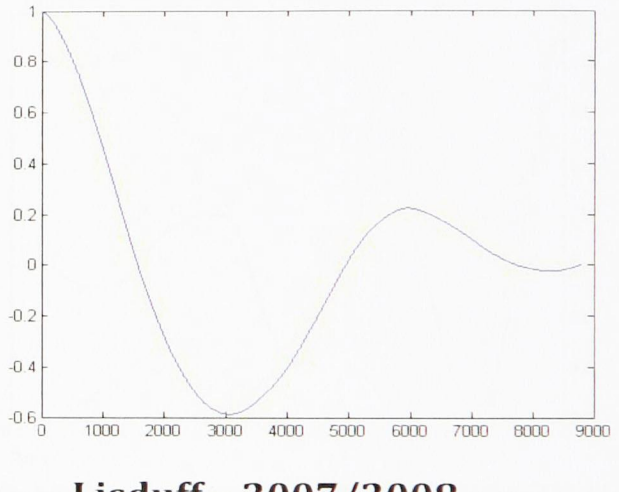
Knockaunroe – Monitoring period



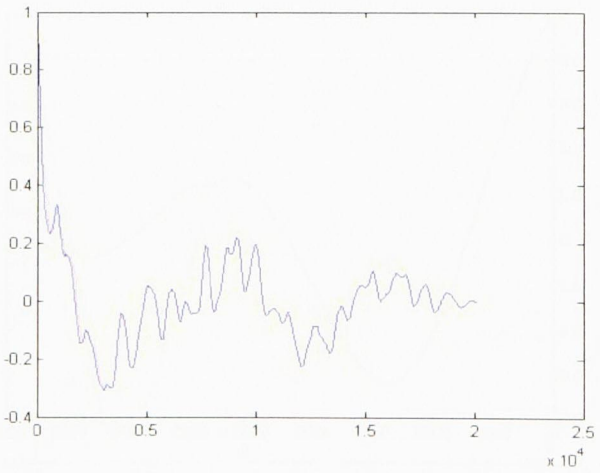
Knockaunroe – 2007/2008



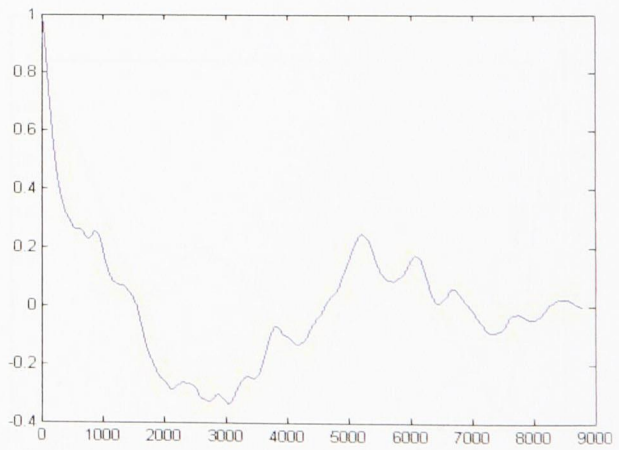
Lisduff – Monitoring period



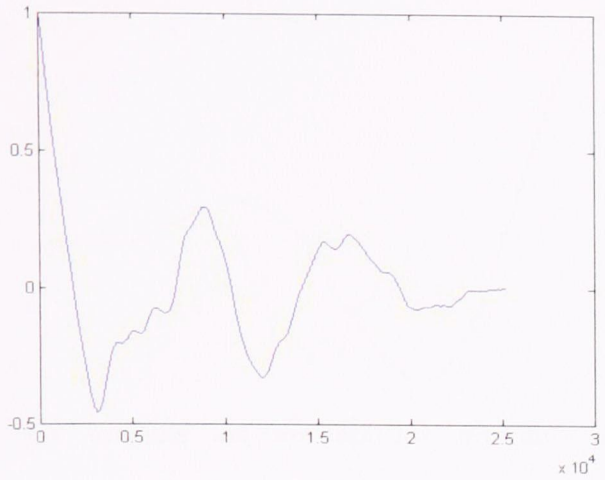
Lisduff – 2007/2008



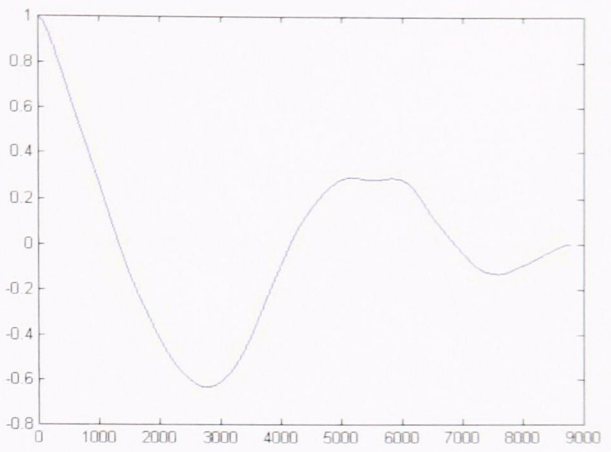
Lough Aleenaun – Monitoring period



Lough Aleenaun – 2007/2008



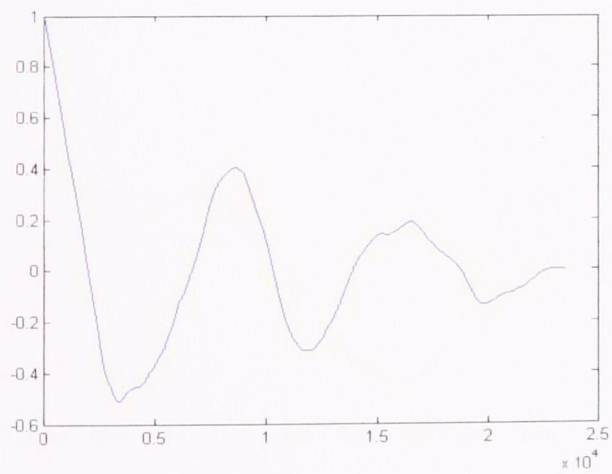
Lough Coy – Monitoring period



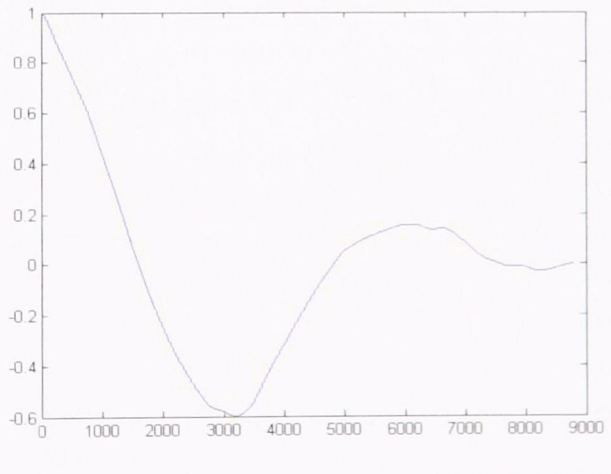
Lough Coy – 2007/2008

Lough Gealain – Monitoring period

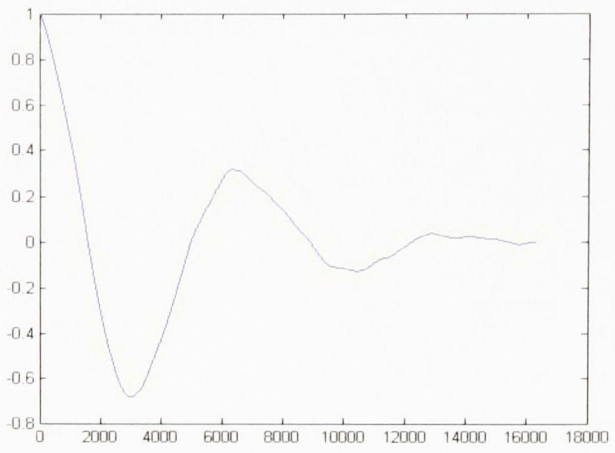
Lough Gealain – 2007/2008



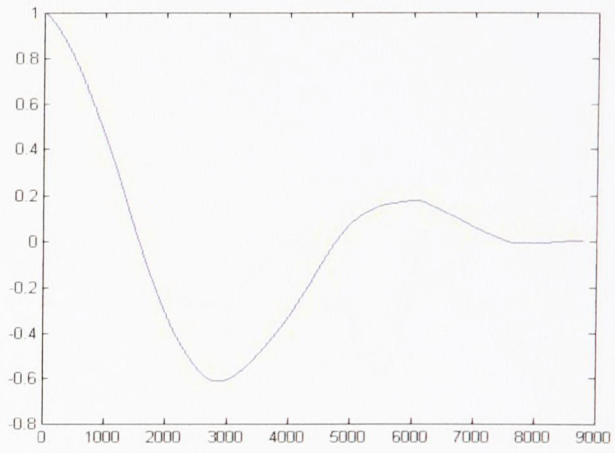
Rathnalulleagh – Monitoring period



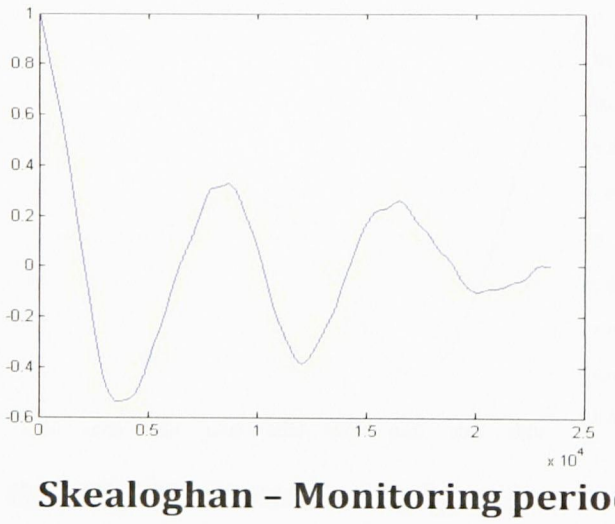
Rathnalulleagh – 2007/2008



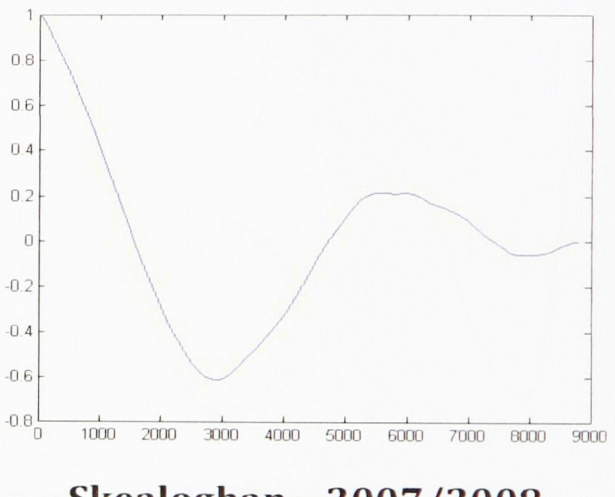
Roo West – Monitoring period



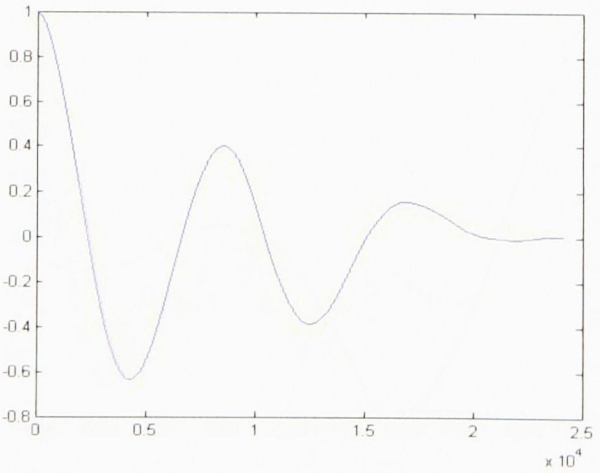
Roo West – 2007/2008



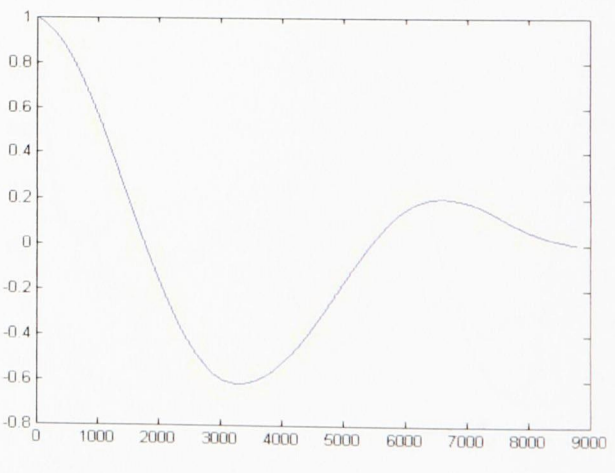
Skealoghan – Monitoring period



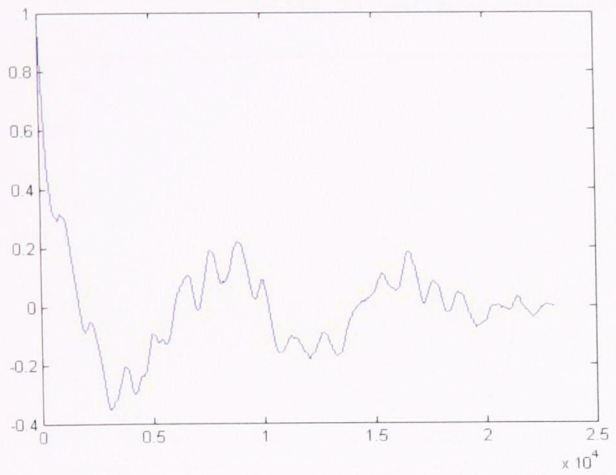
Skealoghan – 2007/2008



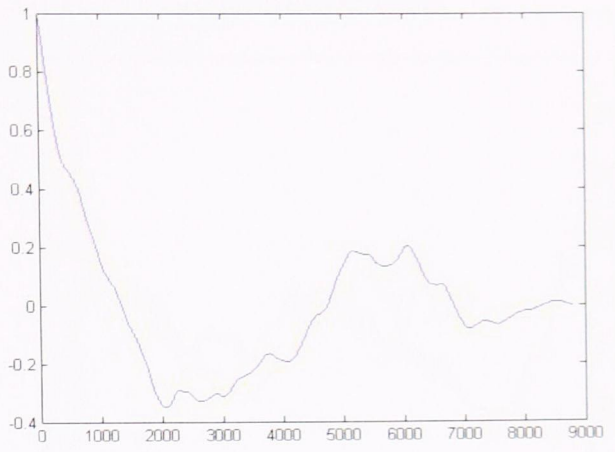
Termon – Monitoring period



Termon – 2007/2008

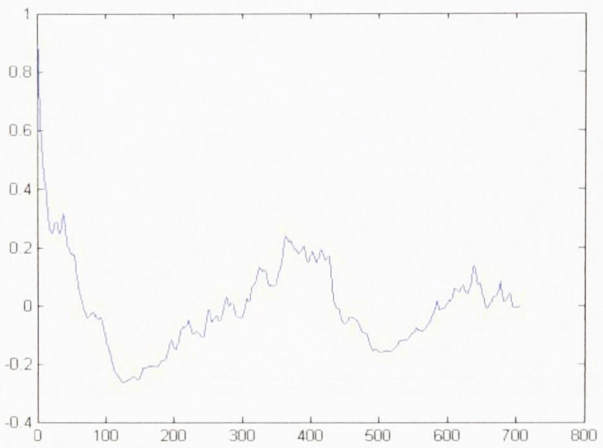


Turloughmore – Monitoring period

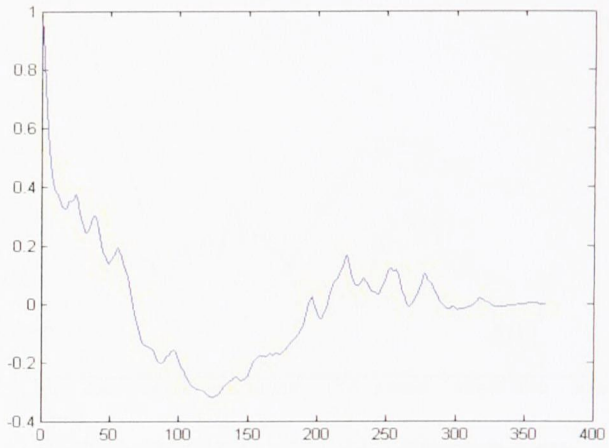


Turloughmore – 2007/2008

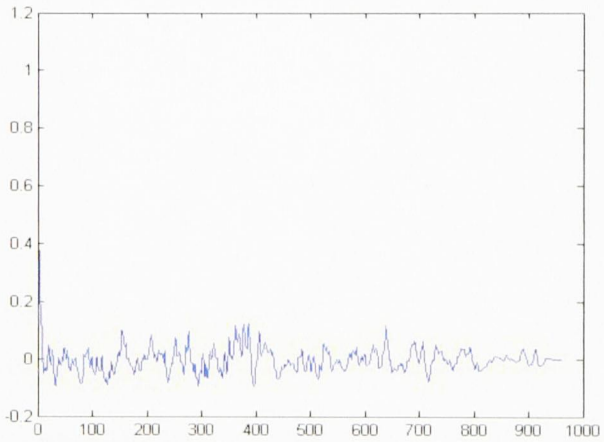
AUTOCORRELATION RESULTS: DAILY FLOW DATA



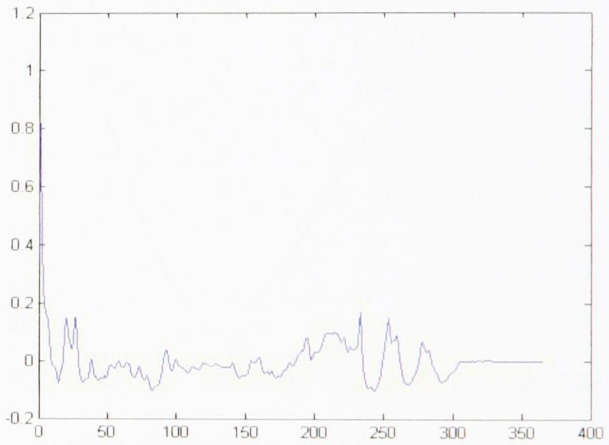
Ardkill – Monitoring period



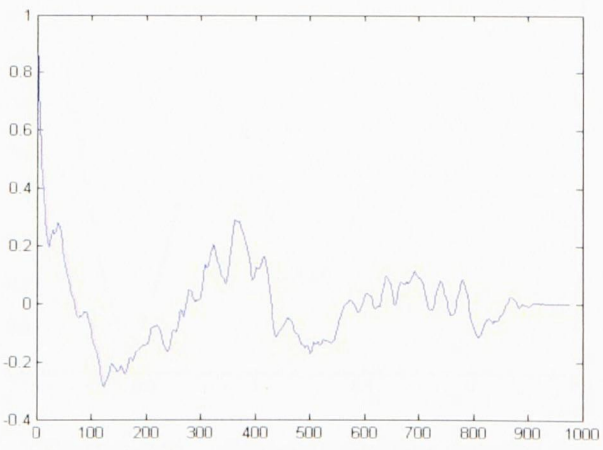
Ardkill - 2007/2008



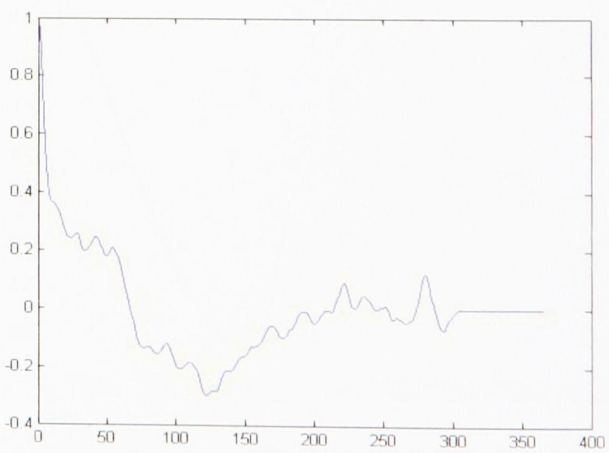
Blackrock – Monitoring period



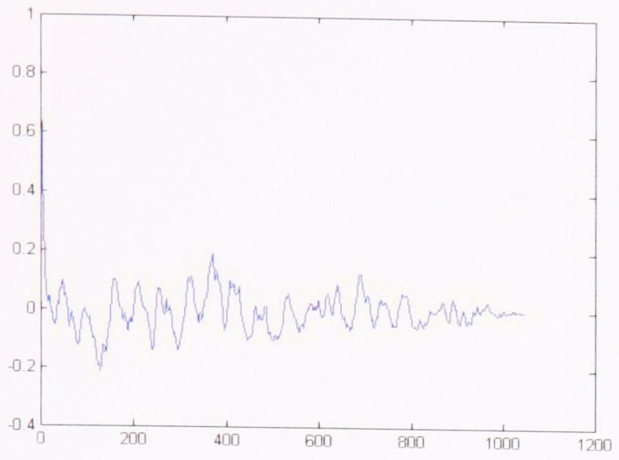
Blackrock – 2007/2008



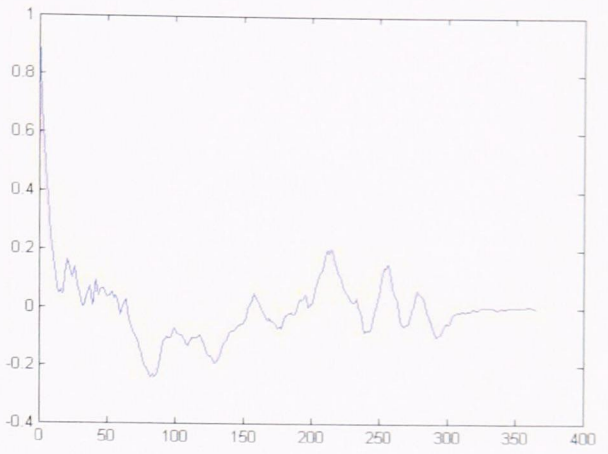
Brierfield – Monitoring period



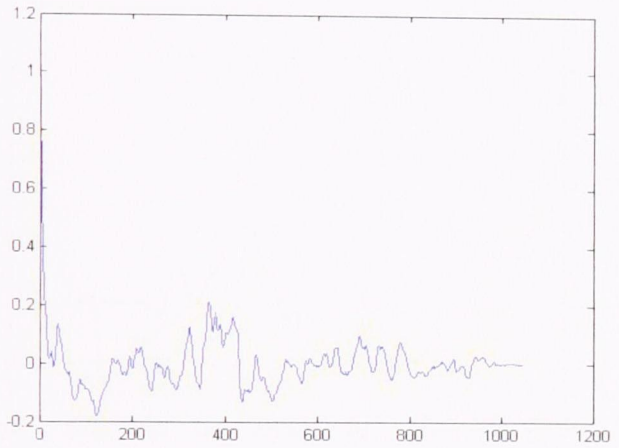
Brierfield – 2007/2008



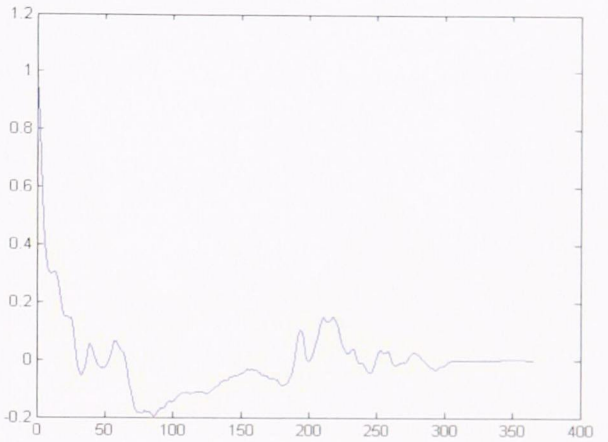
Caherglassaun – Monitoring period



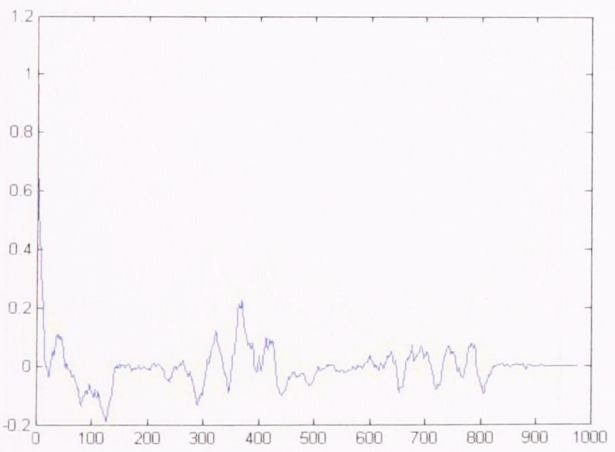
Caherglassaun – 2007/2008



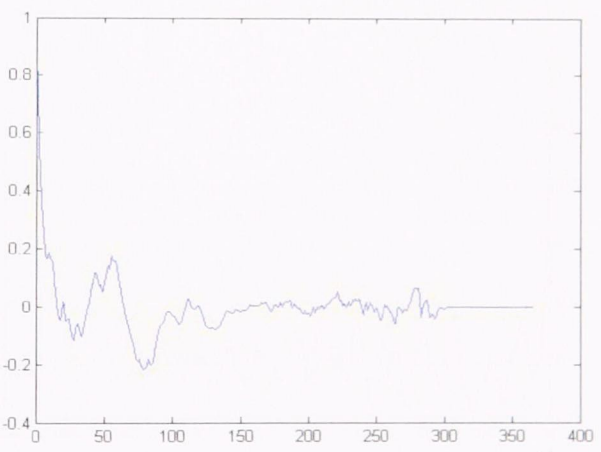
Caranavoodaun – Monitoring period



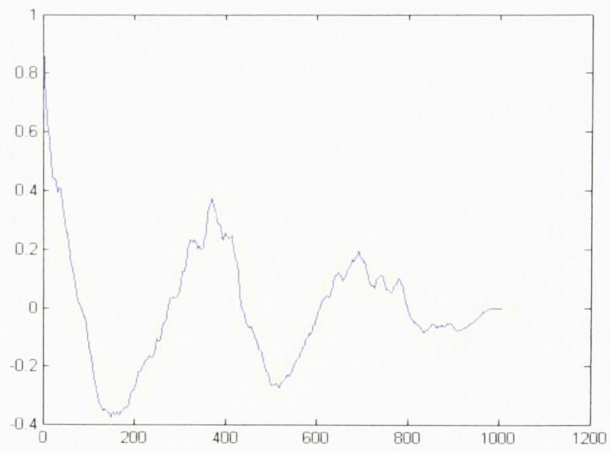
Caranavoodaun – 2007/2008



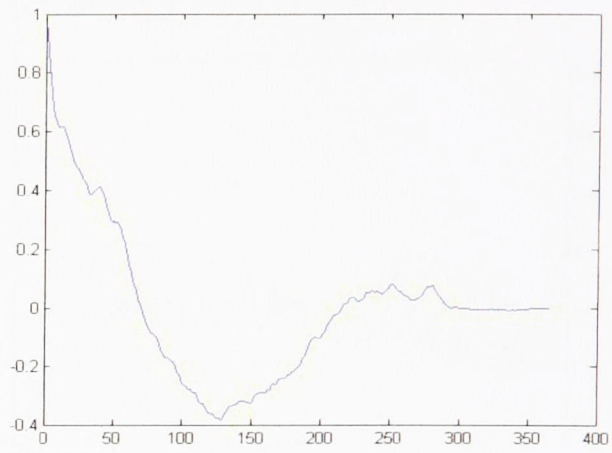
Carrowreagh – Monitoring period



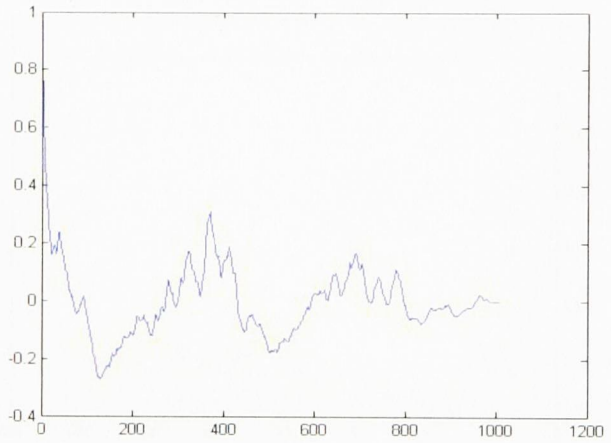
Carrowreagh – 2007/2008



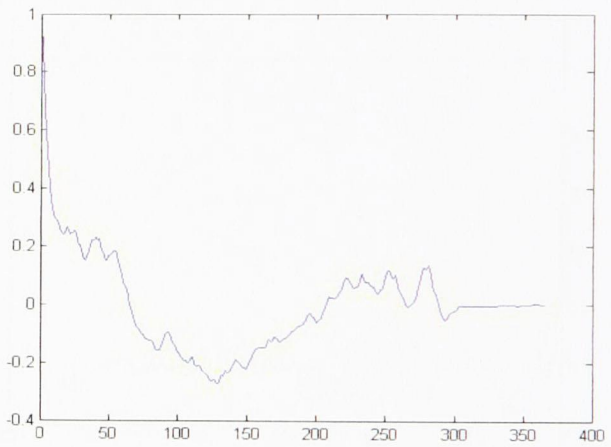
Coolcam – Monitoring period



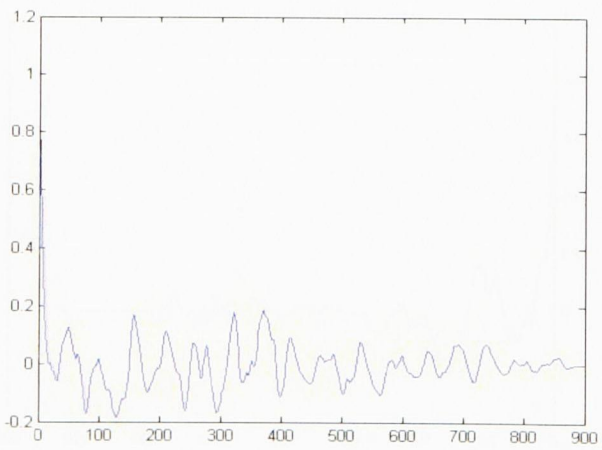
Coolcam – 2007/2008



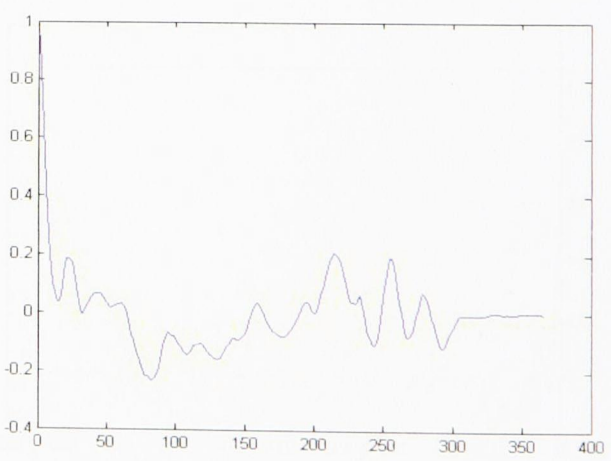
Croaghill – Monitoring period



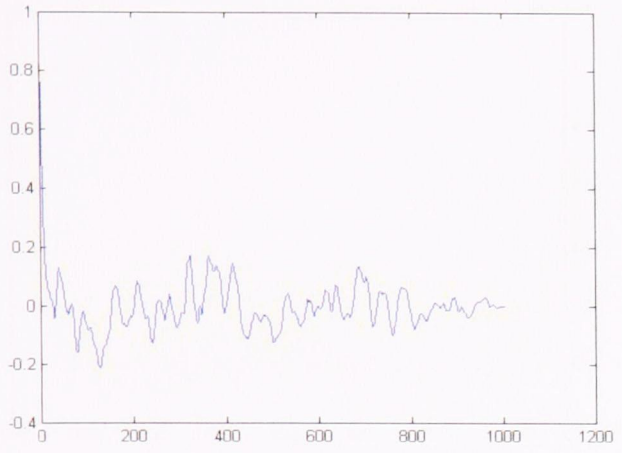
Croaghill – 2007/2008



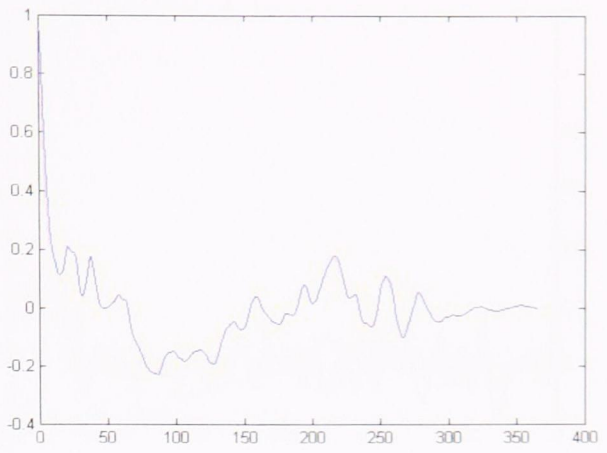
Garryland – Monitoring period



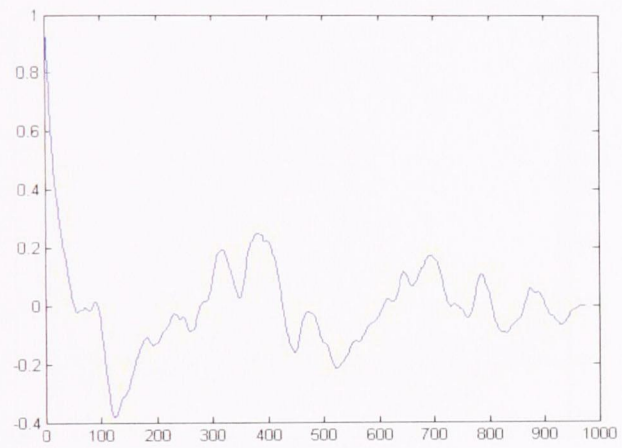
Garryland – 2007/2008



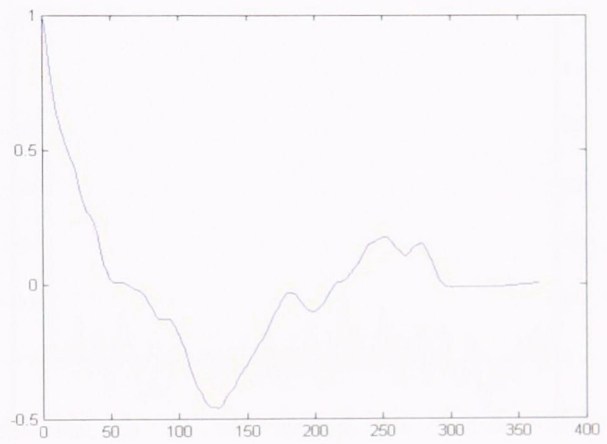
Knockaunroe – Monitoring period



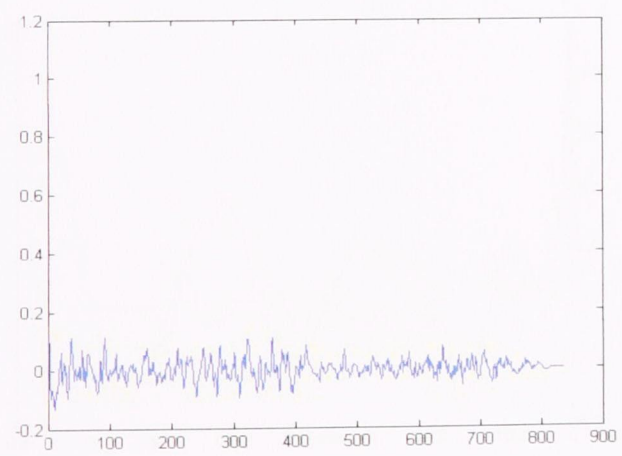
Knockaunroe – 2007/2008



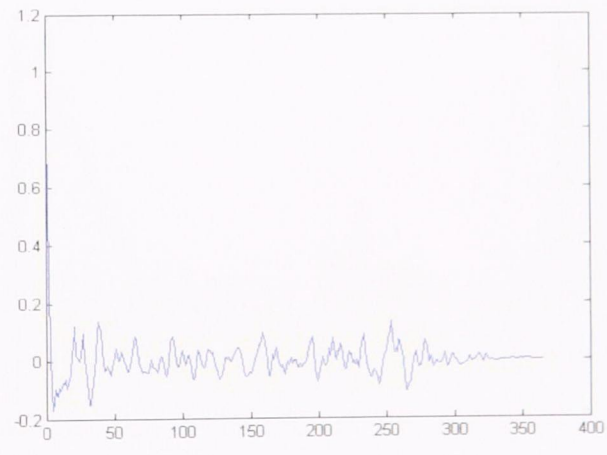
Lisduff – Monitoring period



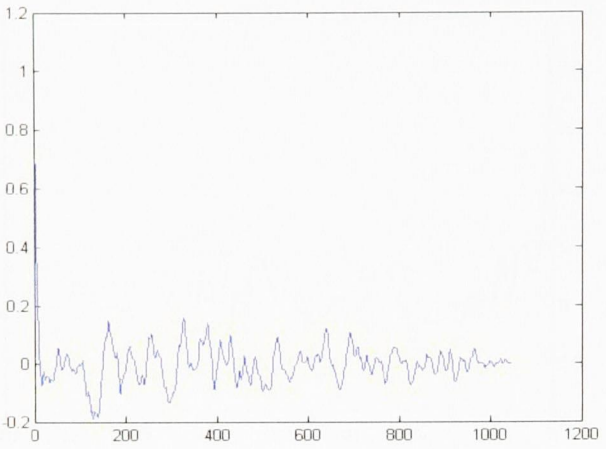
Lisduff – 2007/2008



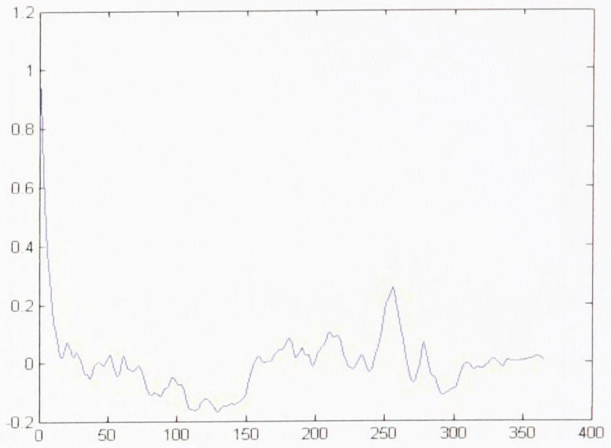
Lough Aleenaun – Monitoring period



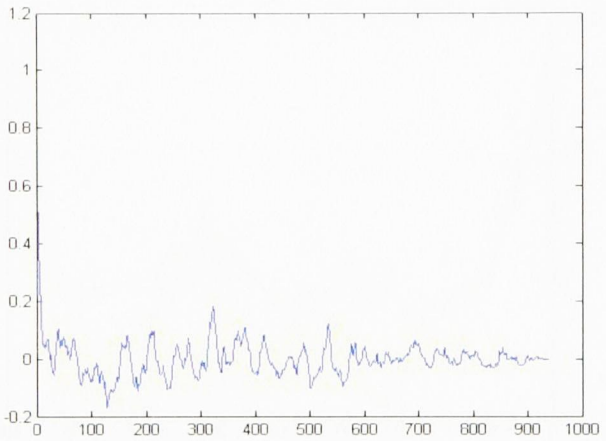
Lough Aleenaun – 2007/2008



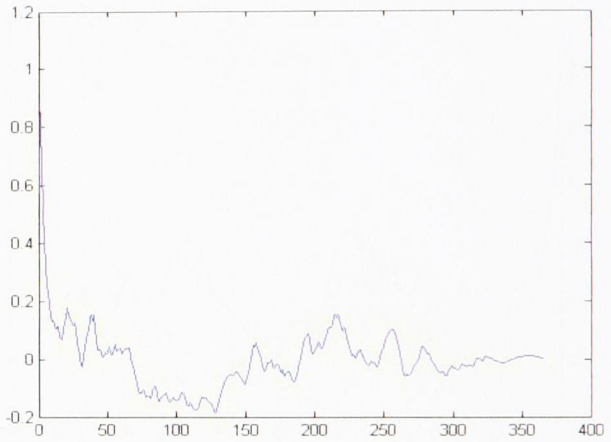
Lough Coy – Monitoring period



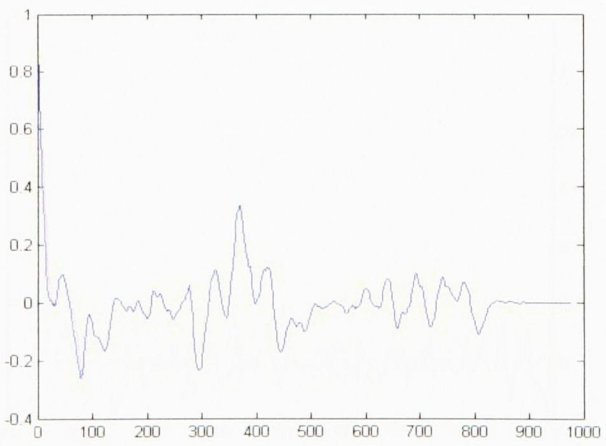
Lough Coy – 2007/2008



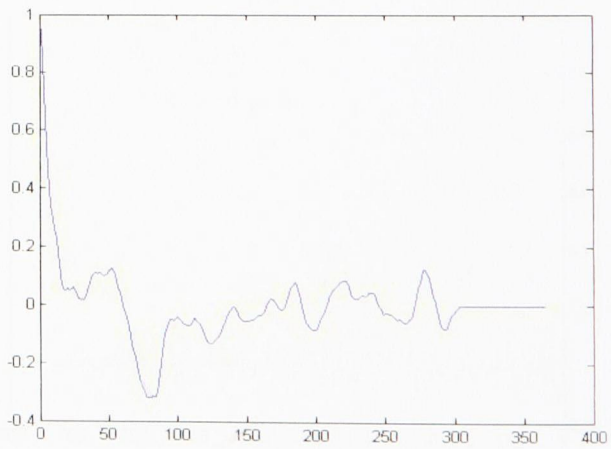
Lough Gealain – Monitoring period



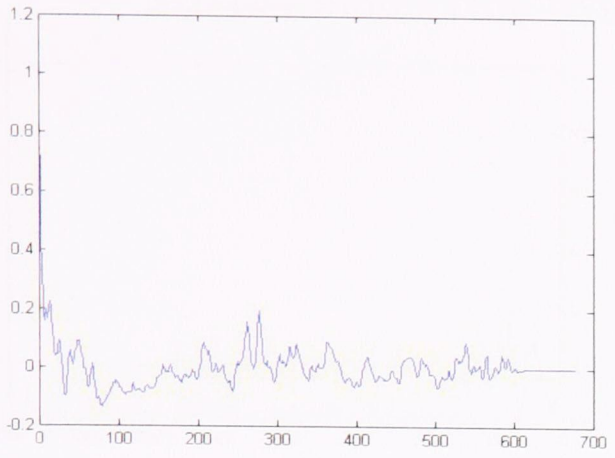
Lough Gealain – 2007/2008



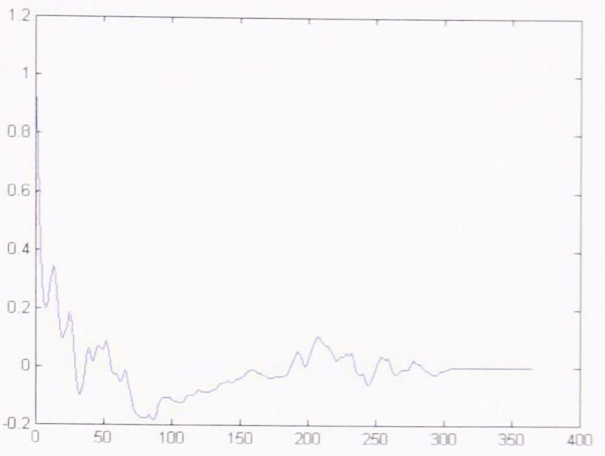
Rathnalulleagh – Monitoring period



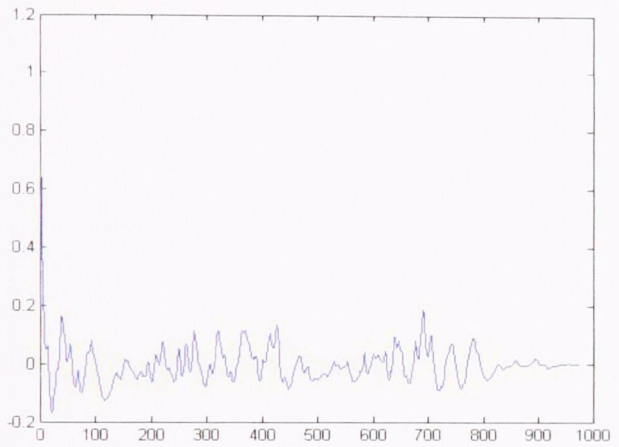
Rathnalulleagh – 2007/2008



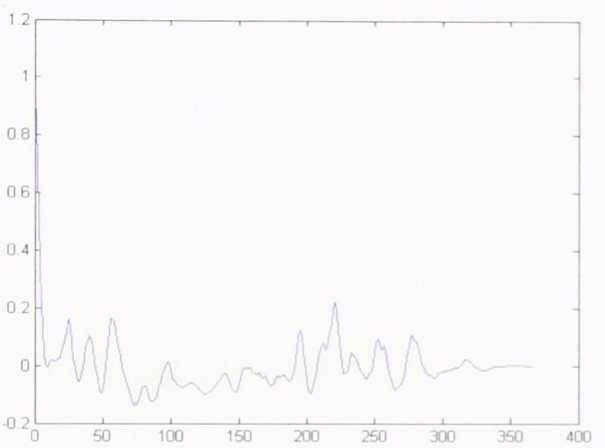
Roo West – Monitoring period



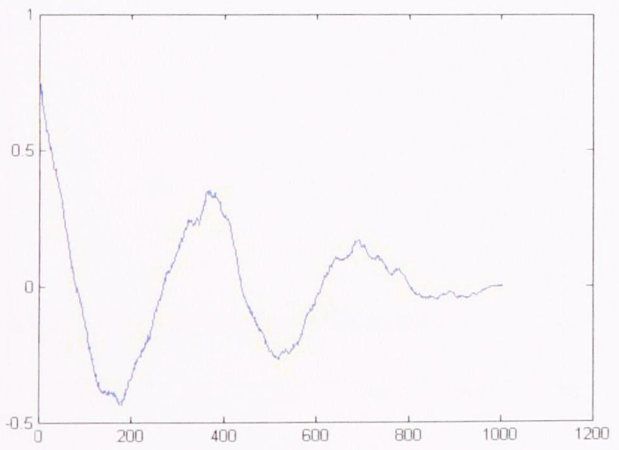
Roo West – 2007/2008



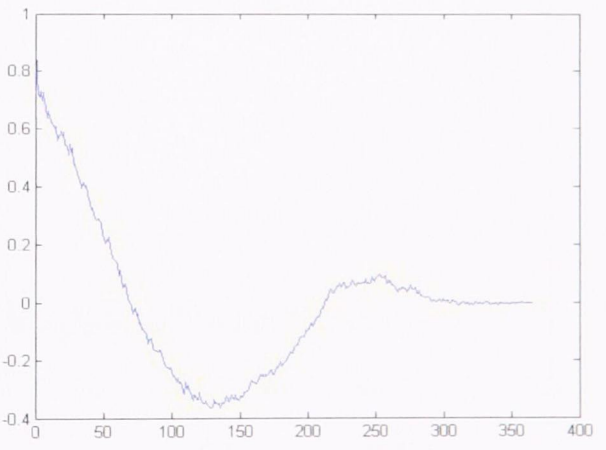
Skealoghan – Monitoring period



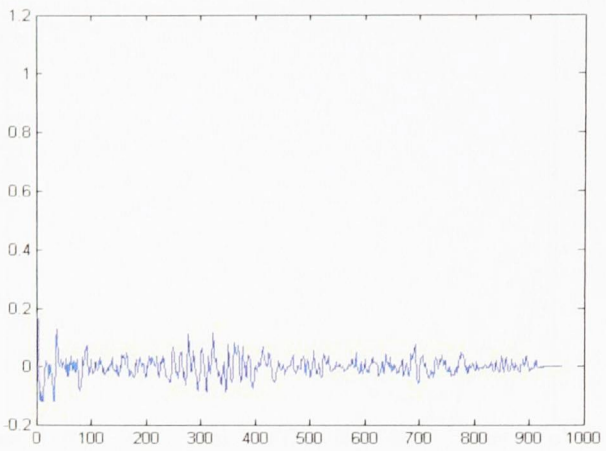
Skealoghan – 2007/2008



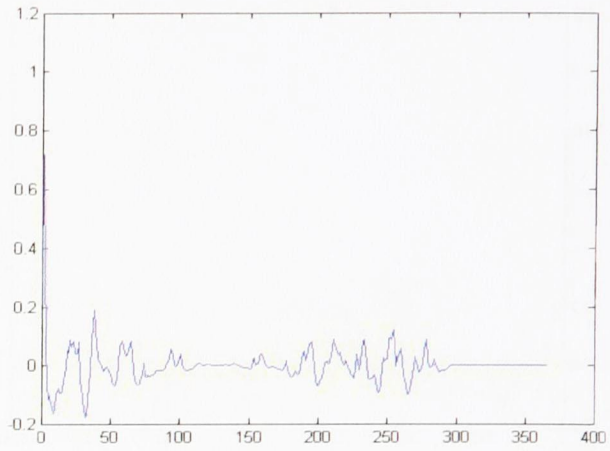
Termon – Monitoring period



Termon – 2007/2008

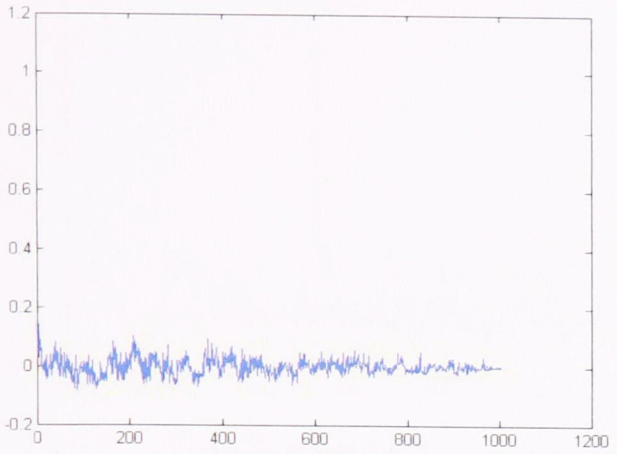


Turloughmore – Monitoring period

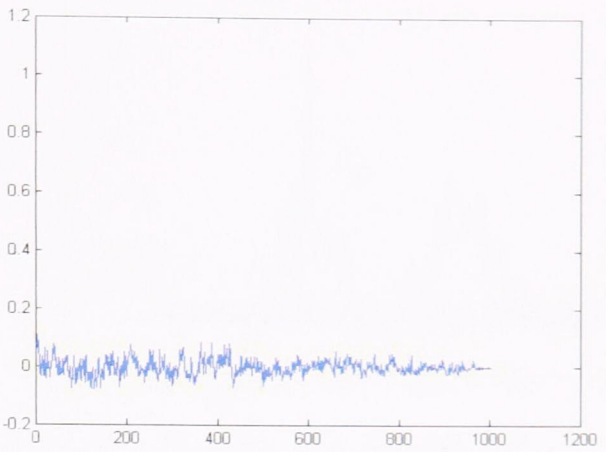


Turloughmore – 2007/2008

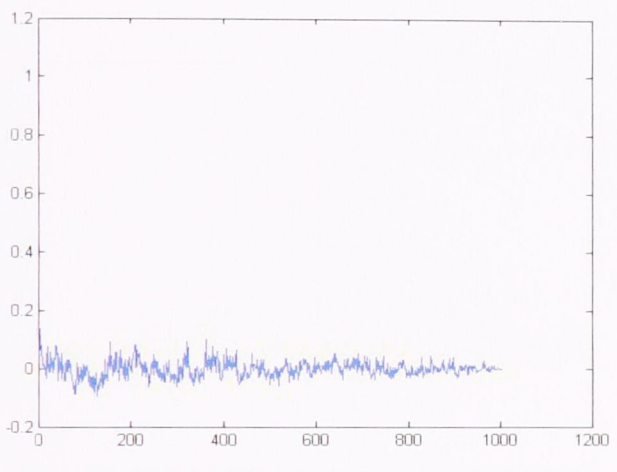
AUTOCORRELATION RESULTS: DAILY RAINFALL DATA



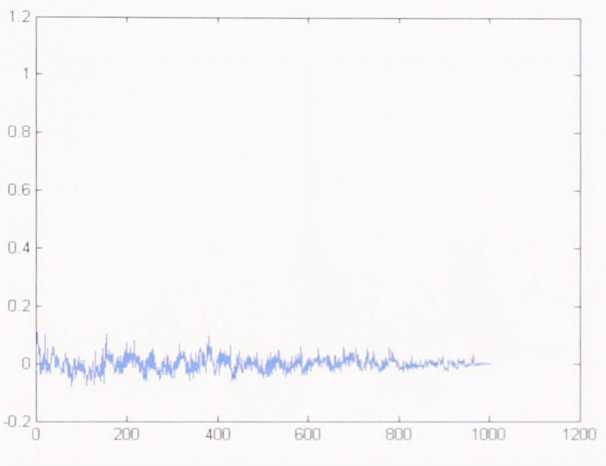
Ballinagare



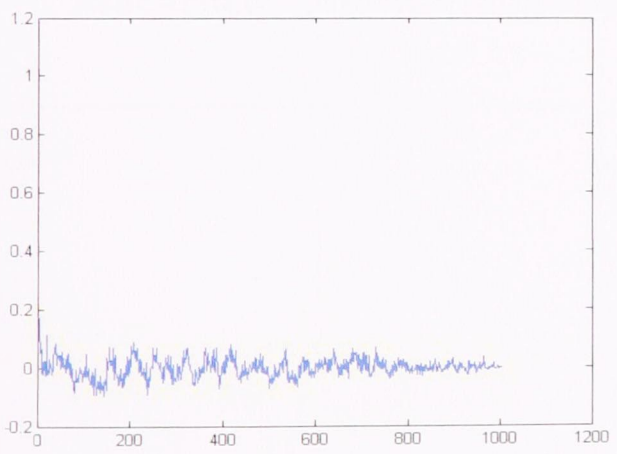
Ballygar



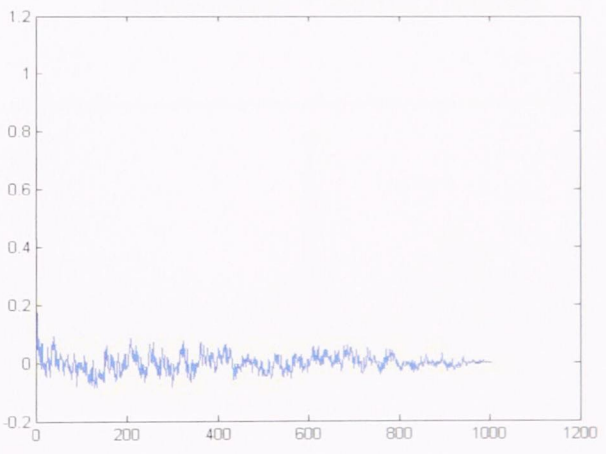
Carheeny Beg



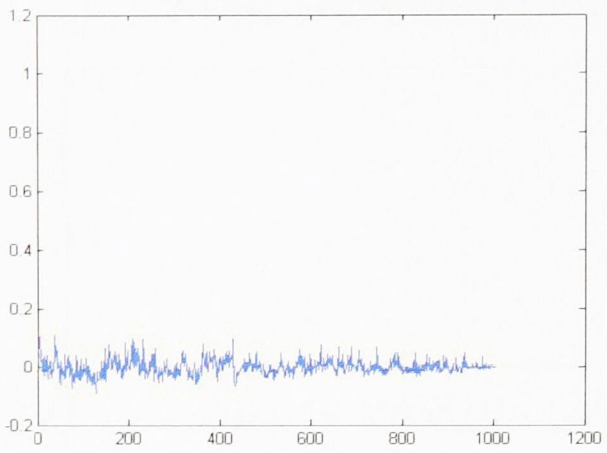
Carron



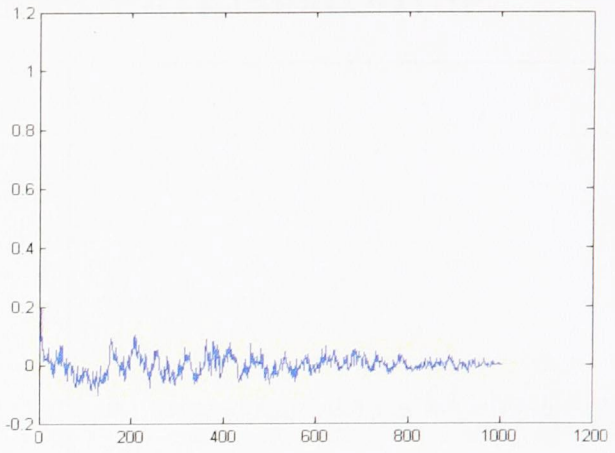
Claremorris



Glenamaddy

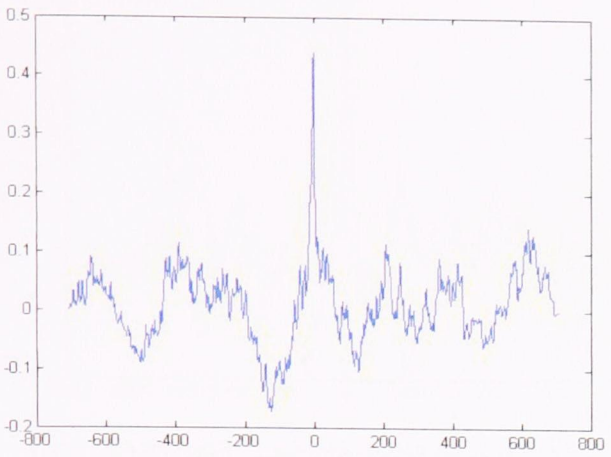


Gort

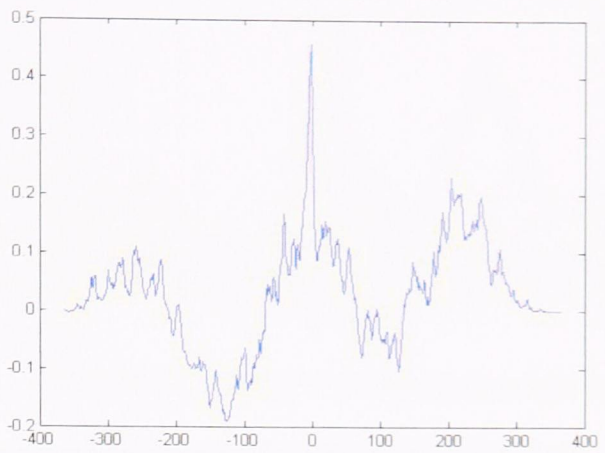


Roscommon

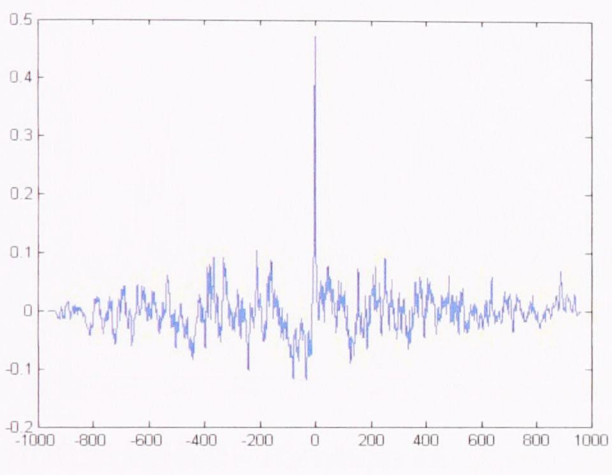
CROSS CORRELATION RESULTS: DAILY FLOW-RAINFALL DATA



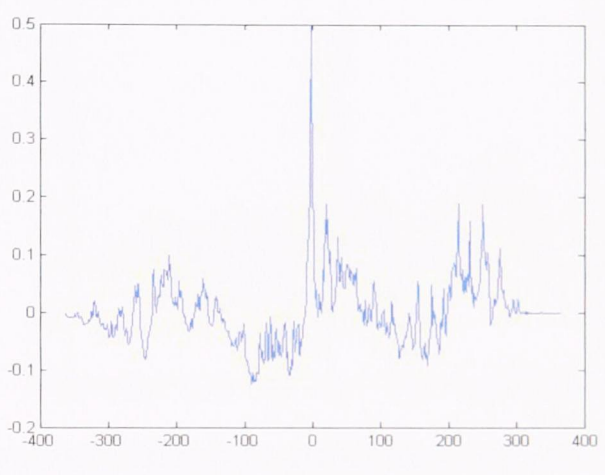
Ardkill – Monitoring period



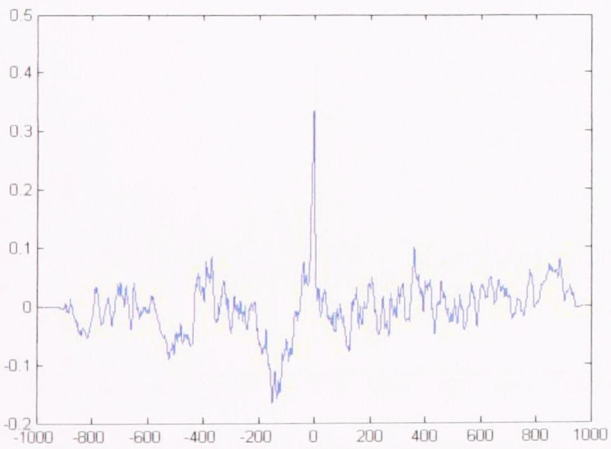
Ardkill - 2007/2008



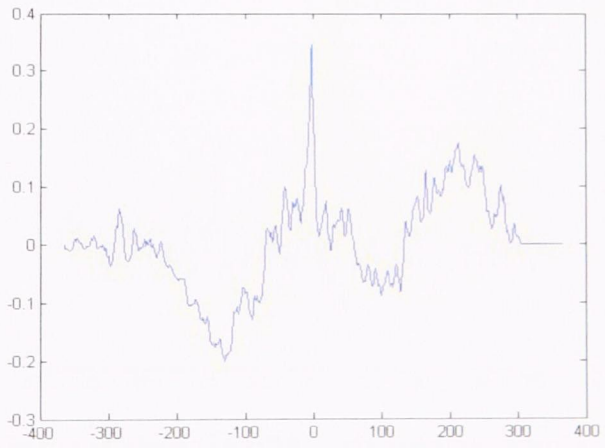
Blackrock – Monitoring period



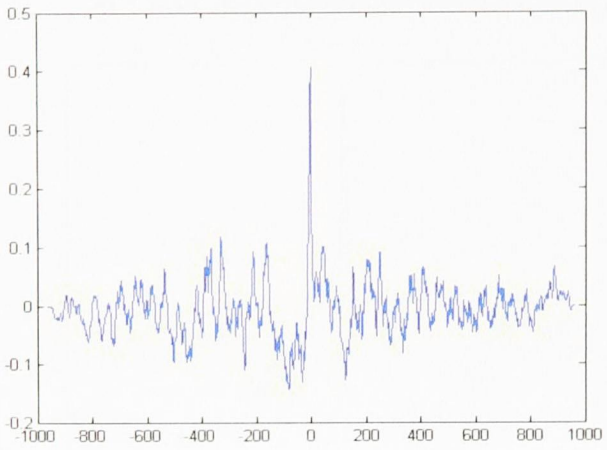
Blackrock – 2007/2008



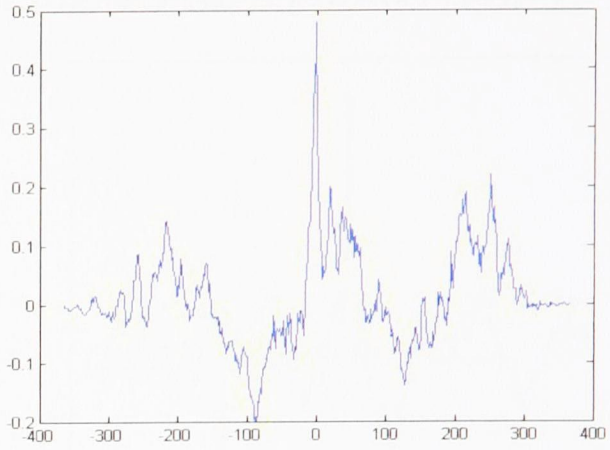
Brierfield – Monitoring period



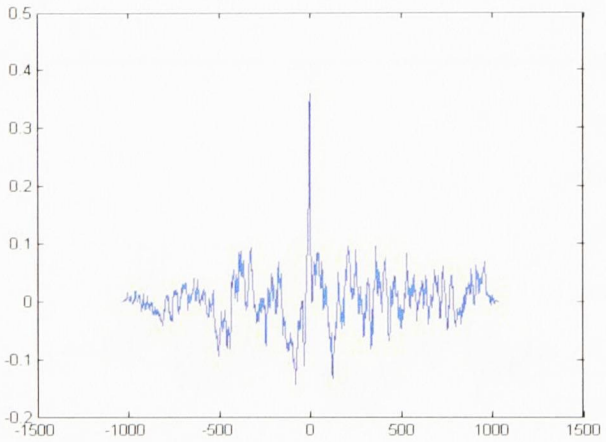
Brierfield – 2007/2008



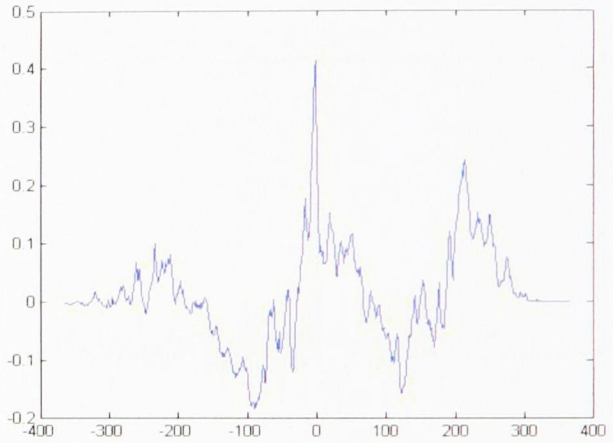
Caherglassaun – Monitoring period



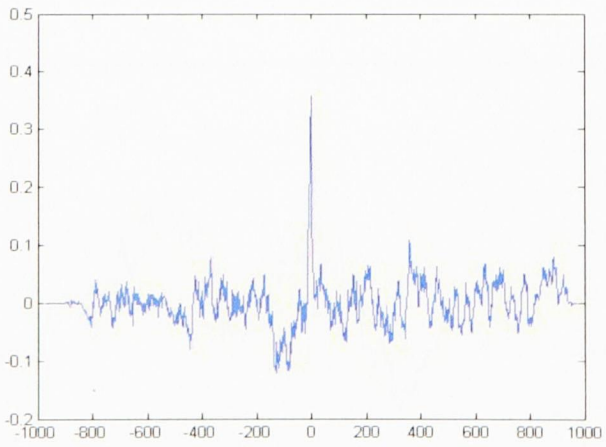
Caherglassaun – 2007/2008



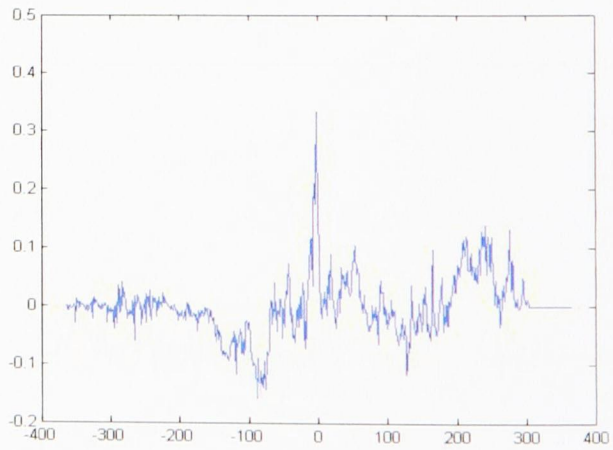
Caranavoodaun – Monitoring period



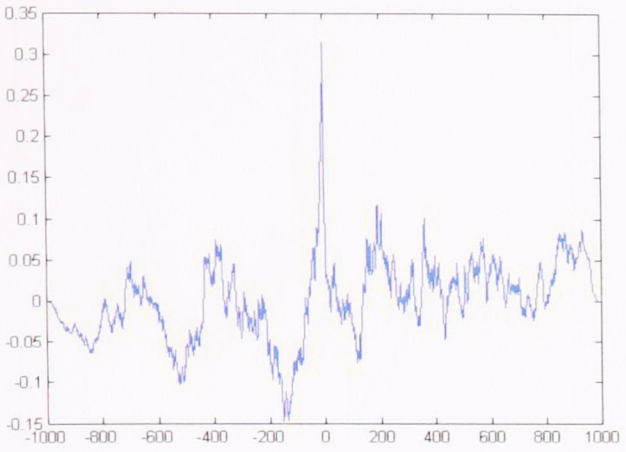
Caranavoodaun – 2007/2008



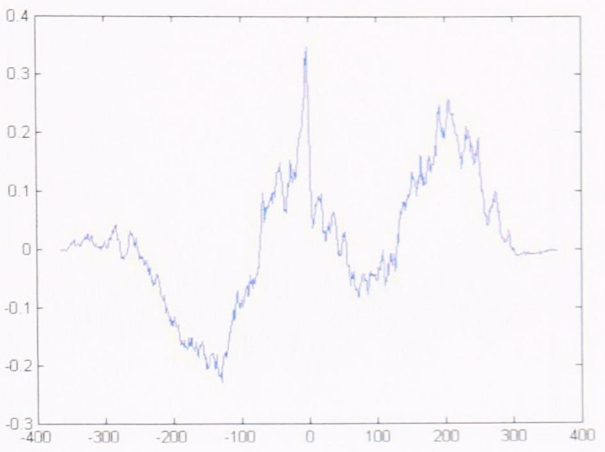
Carrowreagh – Monitoring period



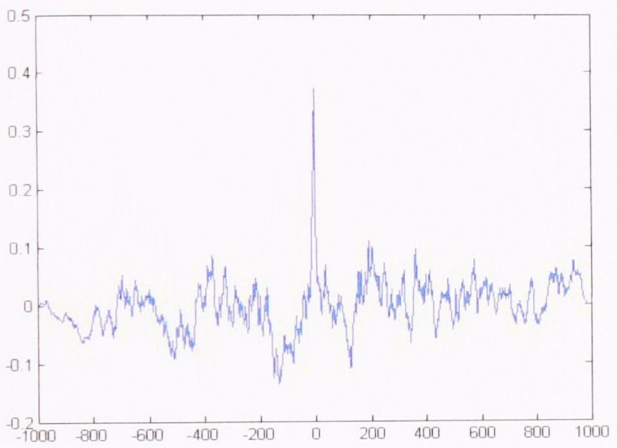
Carrowreagh – 2007/2008



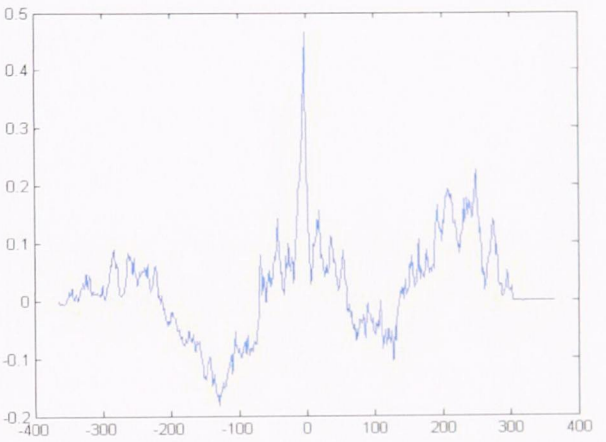
Coolcam – Monitoring period



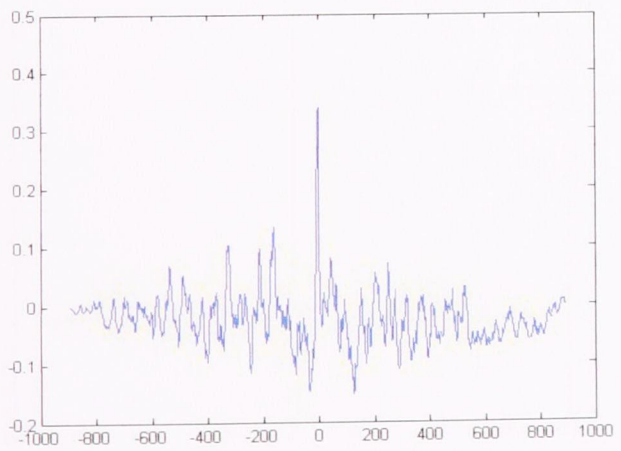
Coolcam – 2007/2008



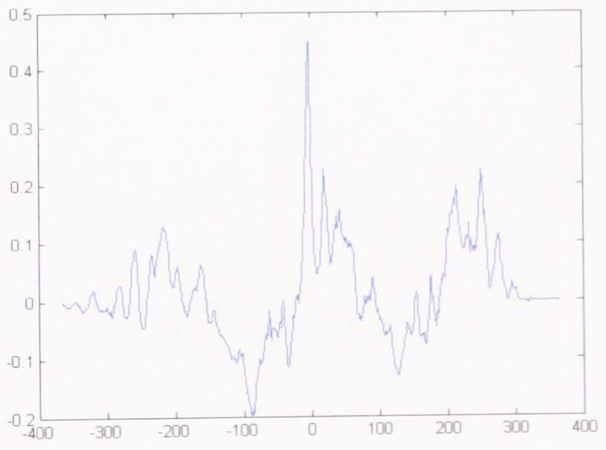
Croaghill – Monitoring period



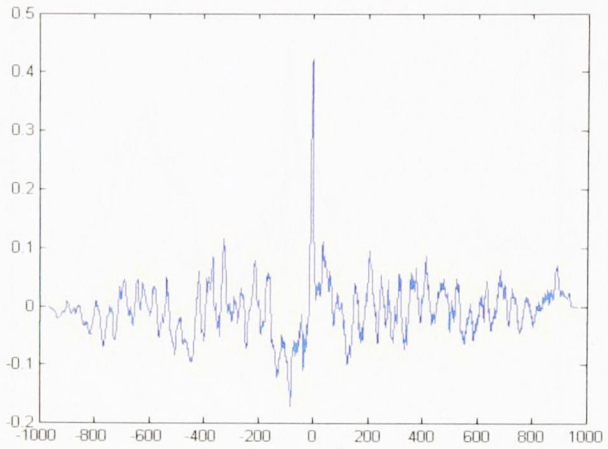
Croaghill – 2007/2008



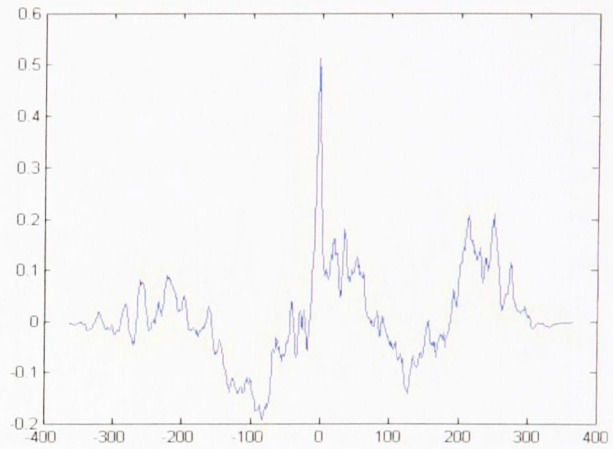
Garryland – Monitoring period



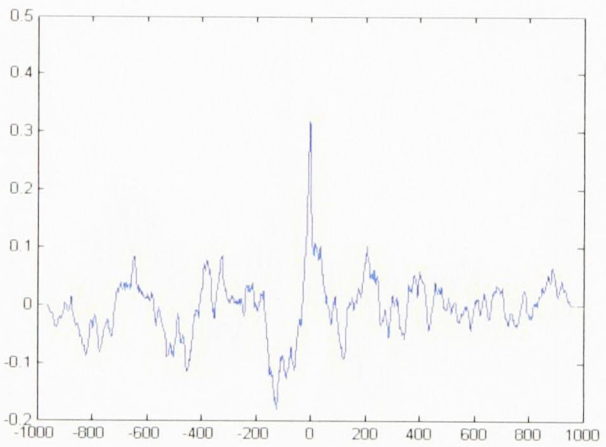
Garryland – 2007/2008



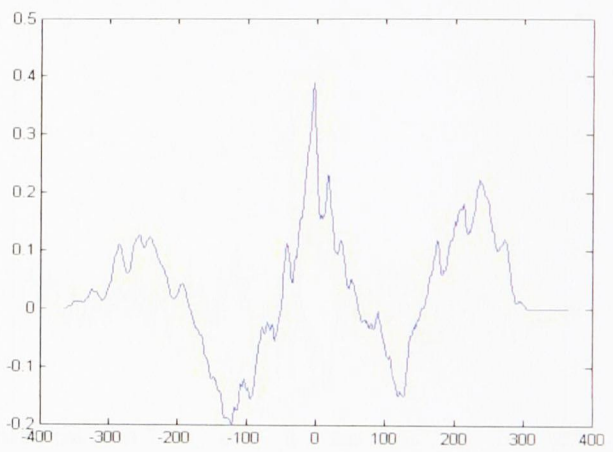
Knockaunroe – Monitoring period



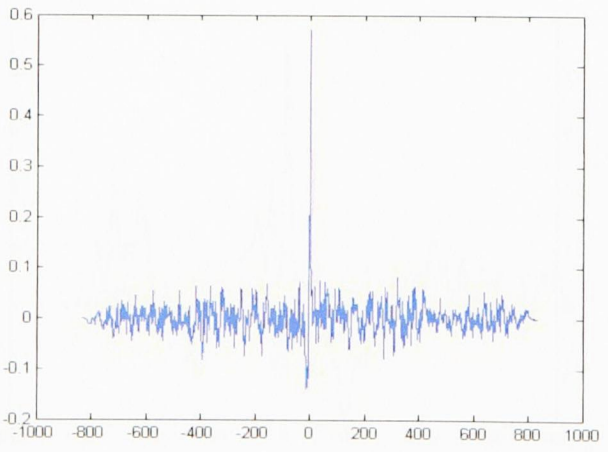
Knockaunroe – 2007/2008



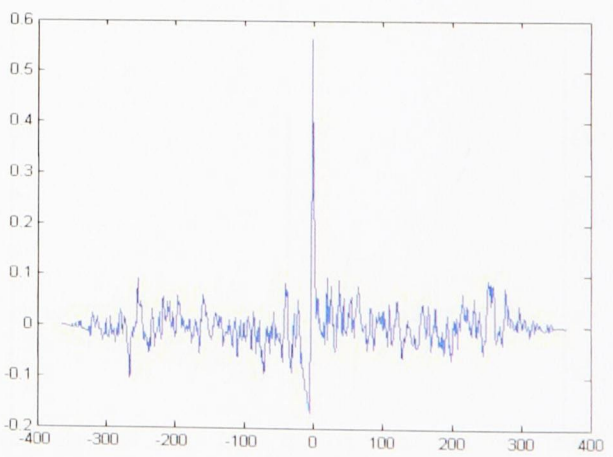
Lisduff – Monitoring period



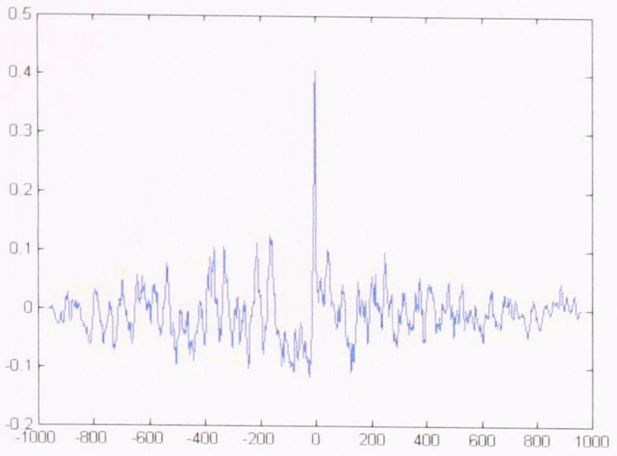
Lisduff – 2007/2008



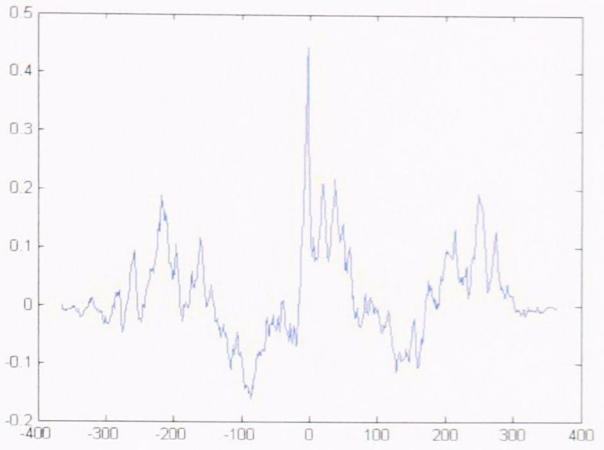
Lough Aleenaun – Monitoring period



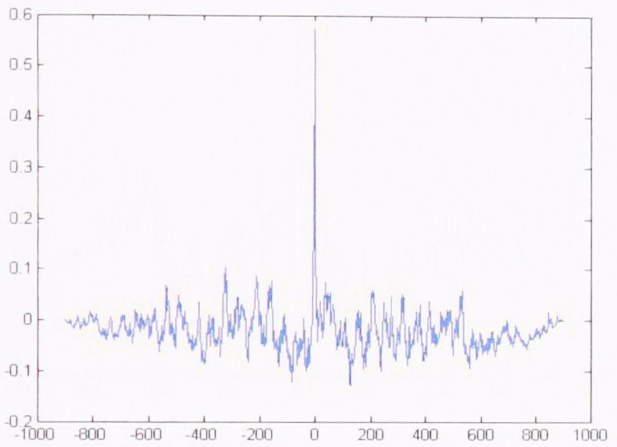
Lough Aleenaun – 2007/2008



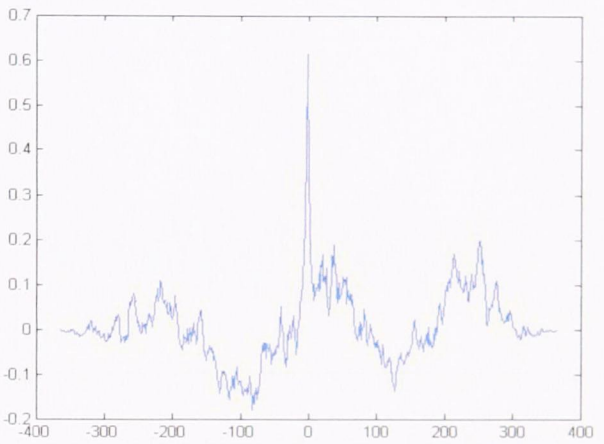
Lough Coy – Monitoring period



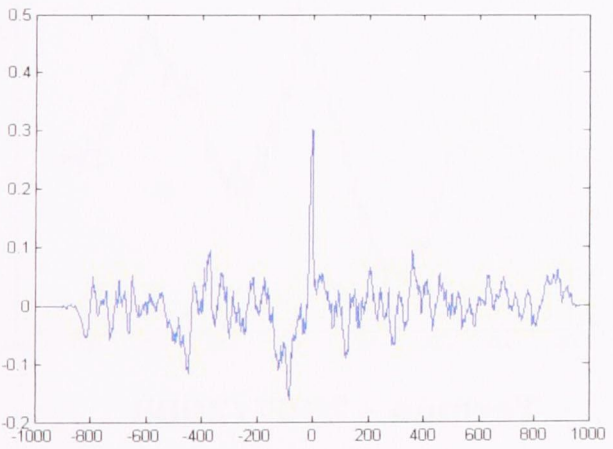
Lough Coy – 2007/2008



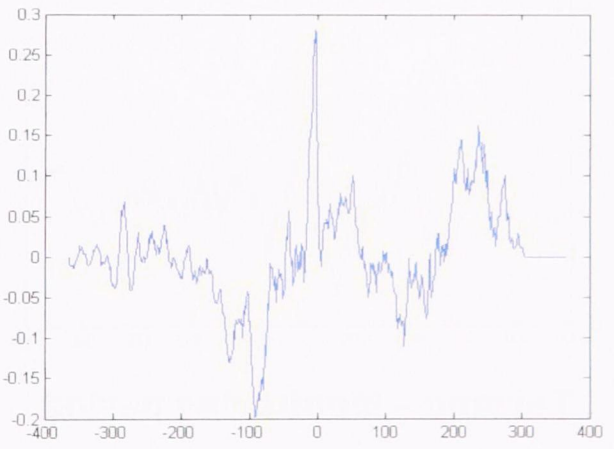
Lough Gealain – Monitoring period



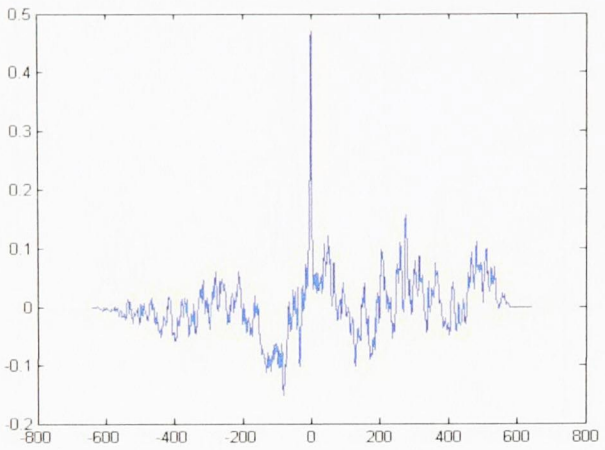
Lough Gealain – 2007/2008



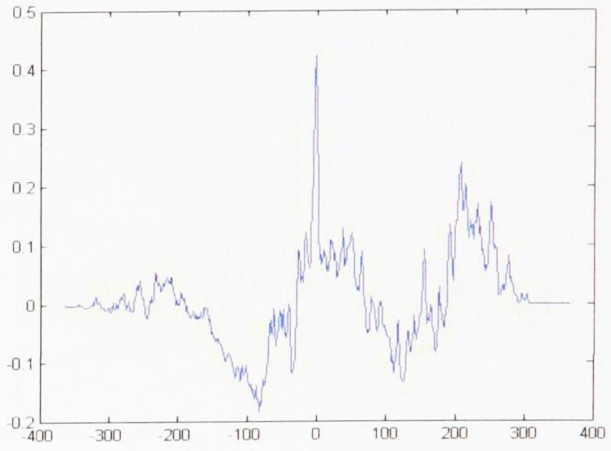
Rathnalulleagh – Monitoring period



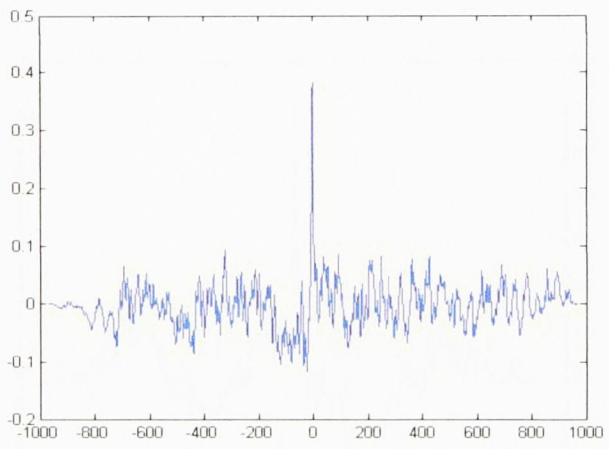
Rathnalulleagh – 2007/2008



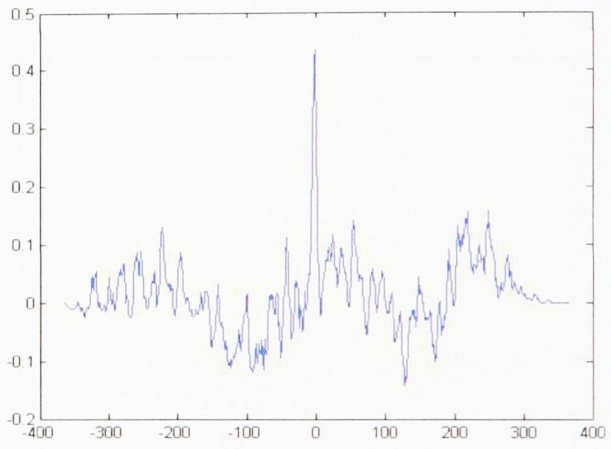
Roo West – Monitoring period



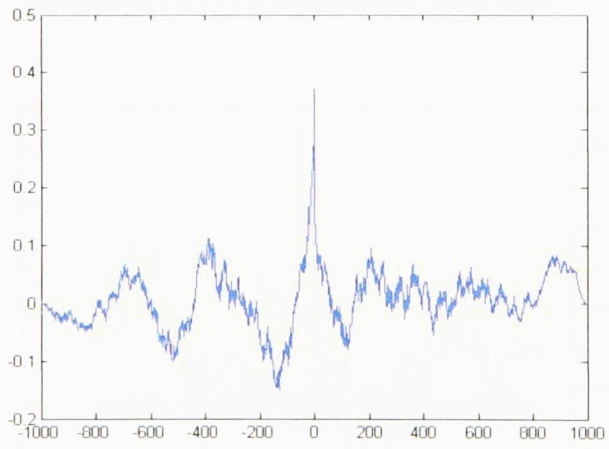
Roo West – 2007/2008



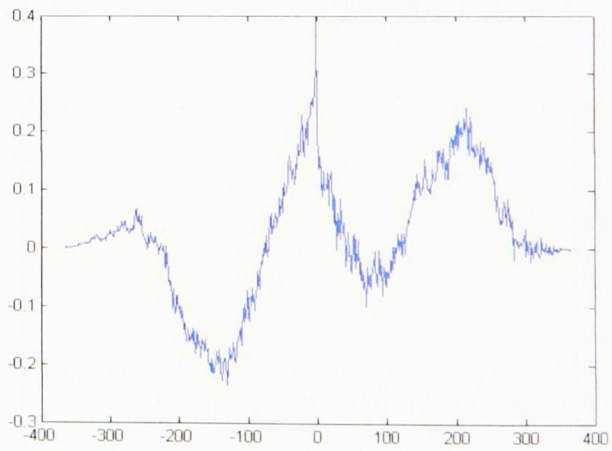
Skealoghan – Monitoring period



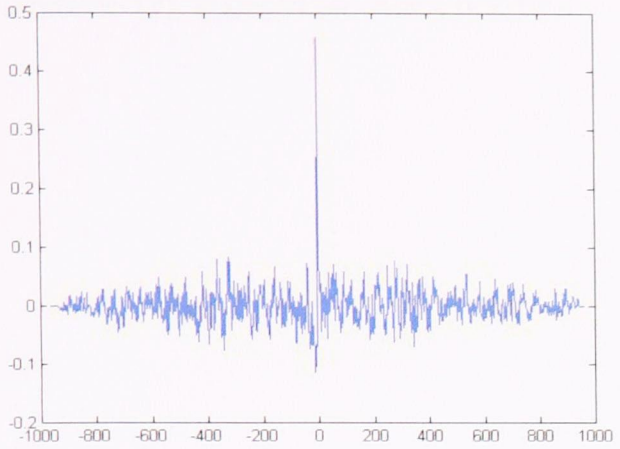
Skealoghan – 2007/2008



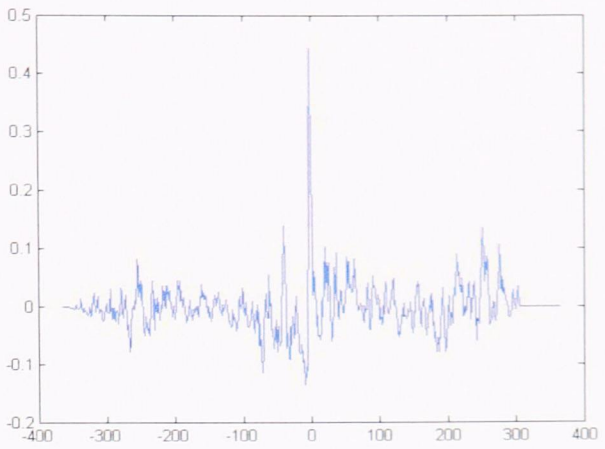
Termon – Monitoring period



Termon – 2007/2008



Turloughmore – Monitoring period



Turloughmore – 2007/2008

Appendix D: Fourier Analyses

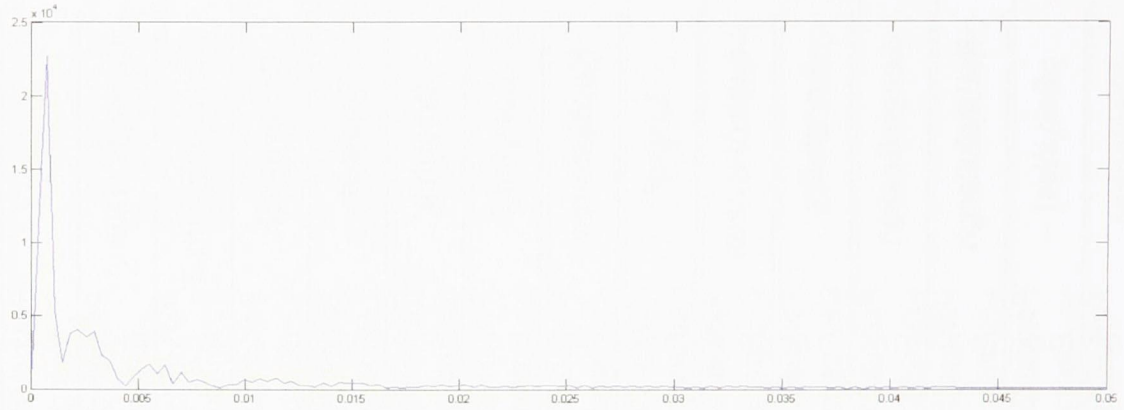
FAST FOURIER TRANSFORM (FFT) RESULTS: FULL MONITORING PERIOD

Site Name		Order of Energy									
		1	2	3	4	5	6	7	8	9	10
Ardkill	*Period (days)*	354.6	118.2	88.6	47.3	41.7	37.3	24.5	33.8	26.3	28.4
	Energy	22704.3	4049.2	3954.6	1697.2	1631.8	1168.6	716.6	654.4	631.5	322.4
Blackrock	*Period (days)*	320.6	192.3	961.7	87.4	53.4	120.2	64.1	45.8	38.5	35.6
	Energy	48213.5	32022.1	21097.5	16452.6	13381.5	10720.2	7048.0	5424.2	5019.1	4005.2
Brierfield	*Period (days)*	326.0	195.6	97.8	46.6	139.7	51.5	69.9	31.5	34.9	42.5
	Energy	13368.3	2516.8	1899.6	1225.0	1197.6	948.8	902.8	626.8	604.5	422.2
Caherglassaun	*Period (days)*	349.0	209.4	1047.0	87.3	52.4	65.4	130.9	41.9	36.1	31.7
	Energy	34884.8	18627.7	14619.2	8547.2	6429.4	3900.5	3123.8	2841.8	2272.8	1834.4
Caranavoodaun	*Period (days)*	348.9	209.3	130.8	52.3	87.2	104.7	65.4	45.5	36.1	38.8
	Energy	8243.9	4632.3	1083.1	1070.6	1016.0	976.3	758.8	496.7	397.8	211.9
Carrowreagh	*Period (days)*	326.0	195.6	97.8	61.1	75.2	51.5	31.5	46.6	40.8	28.8
	Energy	32430.7	11087.0	7274.6	5445.5	4299.4	3966.4	3815.3	2775.4	2571.5	776.8
Coolcam	*Period (days)*	335.9	1007.8	201.6	126.0	77.5	53.0	45.8	63.0	42.0	37.3
	Energy	12838.8	4292.6	3412.7	1628.2	742.9	732.5	454.4	399.4	278.5	197.8
Croaghill	*Period (days)*	335.6	1006.8	201.4	125.9	53.0	91.5	67.1	45.8	40.3	36.0
	Energy	13245.8	5789.2	4655.6	2739.1	1021.5	905.5	691.8	669.3	446.4	435.0
Garryland	*Period (days)*	298.3	179.0	52.6	74.6	63.9	35.8	40.7	32.0	111.9	28.0
	Energy	30390.6	22199.4	8125.0	5327.2	4865.1	3291.2	3258.6	3107.4	2120.5	1758.1
Knockaunroe	*Period (days)*	335.0	201.0	1004.9	52.9	100.5	77.3	67.0	41.9	35.9	45.7
	Energy	13295.0	6252.1	5270.2	2184.0	1925.7	1776.2	1176.2	937.7	754.0	662.8
Lisduff	*Period (days)*	325.7	977.0	195.4	97.7	81.4	54.3	65.1	36.2	46.5	42.5
	Energy	9607.3	4867.7	3464.3	1535.9	1054.2	558.8	430.2	334.5	316.0	252.4
Lough Aleenaun	*Period (days)*	209.2	418.5	52.3	32.2	76.1	41.8	34.9	46.5	104.6	38.0
	Energy	8192.9	8147.0	6629.4	5257.0	3967.5	3370.7	3056.2	2669.8	2403.2	1819.6
Lough Coy	*Period (days)*	349.0	209.4	1046.9	87.2	52.3	65.4	130.9	41.9	104.7	45.5
	Energy	39748.5	24433.8	15866.6	12544.5	7797.9	5354.8	5150.6	4491.8	3415.2	1956.1
Lough Gealain	*Period (days)*	312.7	187.6	85.3	67.0	52.1	40.8	32.3	36.1	27.6	29.3
	Energy	10916.7	5374.5	1966.4	1579.6	1459.1	1273.2	744.4	709.2	493.0	461.6
Rathnalulleagh	*Period (days)*	326.0	195.6	97.8	69.9	61.1	51.5	31.6	40.8	34.9	46.6
	Energy	34638.2	16477.8	6226.8	3795.5	3608.6	3222.4	2986.1	2421.2	2136.8	1875.2
Roo West	*Period (days)*	339.5	52.2	84.9	67.9	45.3	30.9	26.1	28.3	37.7	34.0
	Energy	9745.9	1670.4	1662.5	1521.6	993.4	627.4	542.8	478.6	454.0	380.7
Skealoghan	*Period (days)*	325.3	975.9	195.2	88.7	108.4	54.2	69.7	46.5	40.7	36.1
	Energy	7301.9	3258.5	2750.4	1176.3	904.4	788.8	699.8	660.3	439.8	386.5
Termon	*Period (days)*	335.0	1004.9	201.0	125.6	100.5	77.3	52.9	45.7	59.1	41.9
	Energy	11315.6	5847.9	2542.2	1345.1	807.7	567.9	540.9	243.5	215.6	204.9
Turloughmore	*Period (days)*	320.6	53.4	961.8	87.4	45.8	120.2	38.5	35.6	68.7	32.1
	Energy	9761.9	5250.1	3706.7	3351.9	2934.0	2546.2	2034.2	2002.7	1988.9	1862.1

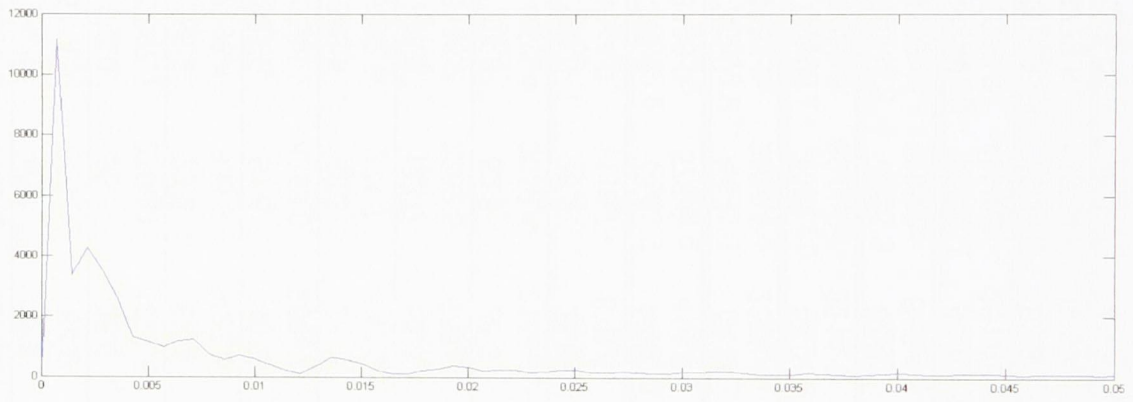
FAST FOURIER TRANSFORM (FFT) RESULTS: 2007/2008 HYDROLOGICAL YEAR

Site Name		Order of Energy									
		1	2	3	4	5	6	7	8	9	10
Ardkill	*Period (days)*	365.9	122.0	36.6	28.1	19.3	13.6	10.8	12.2	8.3	9.6
	Energy	11157.7	4253.7	1223.4	706.2	620.6	356.1	240.4	237.7	203.8	172.4
Blackrock	*Period (days)*	183.0	52.3	36.6	28.1	19.3	14.1	13.1	15.9	21.5	12.2
	Energy	20627.0	4143.2	3276.9	2758.6	1364.2	1288.6	1151.4	814.1	623.3	534.4
Brierfield	*Period (days)*	365.9	40.7	73.2	52.3	28.1	13.6	18.3	12.2	22.9	10.8
	Energy	5714.2	686.3	564.9	531.8	466.3	150.5	137.6	116.3	85.4	43.3
Caherglassaun	*Period (days)*	183.0	52.3	36.6	28.1	22.9	19.3	17.4	13.6	15.2	12.2
	Energy	12897.7	2763.1	1927.5	893.2	556.3	477.6	378.1	301.8	232.2	122.3
Caranavoodaun	*Period (days)*	365.9	73.2	52.3	36.6	28.1	19.3	17.4	13.6	12.2	15.2
	Energy	2996.1	866.9	427.0	338.2	275.3	170.5	134.1	124.5	71.9	55.0
Carrowreagh	*Period (days)*	365.9	91.5	40.7	52.3	30.5	26.1	13.6	17.4	19.3	21.5
	Energy	10544.2	4350.0	2868.6	2154.4	1671.6	1363.2	753.7	561.5	534.6	400.8
Coolcam	*Period (days)*	365.9	52.3	28.1	19.3	13.1	10.5	14.6	15.9	12.2	9.6
	Energy	5562.8	271.7	147.2	81.2	43.5	30.4	25.7	25.3	24.7	20.6
Croaghill	*Period (days)*	365.9	122.0	52.3	40.7	28.1	19.3	13.1	12.2	9.6	10.8
	Energy	5476.7	2282.5	578.9	523.2	449.8	224.6	138.9	108.4	89.2	79.9
Garryland	*Period (days)*	183.0	52.3	36.6	28.1	17.4	19.3	15.9	21.5	14.1	11.8
	Energy	14673.4	3032.4	2156.4	1256.8	597.5	579.3	446.0	432.8	419.0	197.6
Knockaunroe	*Period (days)*	183.0	73.2	36.6	52.3	28.1	19.3	17.4	21.5	13.6	14.6
	Energy	4644.0	1116.7	678.6	648.4	342.9	200.7	164.2	160.5	131.5	64.5
Lisduff	*Period (days)*	365.9	73.2	52.3	40.7	30.5	19.3	16.6	13.6	15.2	11.8
	Energy	3890.0	579.8	414.8	386.7	256.8	158.7	106.1	102.7	86.5	81.7
Lough Aleenaun	*Period (days)*	183.0	52.3	73.2	36.6	30.5	22.9	19.3	17.4	14.1	15.2
	Energy	4937.0	2634.6	2378.4	2026.5	1424.3	1253.1	1094.4	895.5	584.8	583.9
Lough Coy	*Period (days)*	183.0	91.5	52.3	40.7	26.1	30.5	17.4	21.5	13.6	14.6
	Energy	16006.5	6941.9	3211.5	2518.6	1245.4	986.1	886.1	603.9	397.6	381.2
Lough Gealain	*Period (days)*	183.0	73.2	52.3	40.7	28.1	19.3	17.4	21.5	24.4	15.2
	Energy	4153.4	1105.2	617.4	571.6	343.2	213.4	196.2	175.8	157.1	82.0
Rathnalulleagh	*Period (days)*	365.9	91.5	40.7	52.3	30.5	26.1	17.4	13.6	12.2	11.4
	Energy	11859.8	4598.5	2617.6	2232.5	1601.8	1383.9	1125.1	525.6	386.4	309.7
Roo West	*Period (days)*	365.9	73.2	52.3	28.1	13.6	19.3	17.4	10.8	11.8	15.2
	Energy	6779.5	1307.4	886.4	434.8	269.9	265.3	234.7	148.9	122.0	111.4
Skealoghan	*Period (days)*	365.9	73.2	45.7	36.6	28.1	19.3	17.4	13.1	12.2	14.6
	Energy	2171.8	782.5	380.5	348.1	288.2	208.2	116.7	111.0	99.8	53.1
Termon	*Period (days)*	365.9	73.2	52.3	28.1	19.3	15.2	13.1	9.4	11.8	10.8
	Energy	4904.4	355.7	217.5	140.2	65.4	44.4	37.1	36.5	32.3	30.7
Turloughmore	*Period (days)*	183.0	52.3	73.2	30.5	36.6	22.9	19.3	17.4	13.6	15.2
	Energy	3909.1	1647.9	1341.1	1193.6	1152.7	947.1	582.5	438.3	344.7	302.5

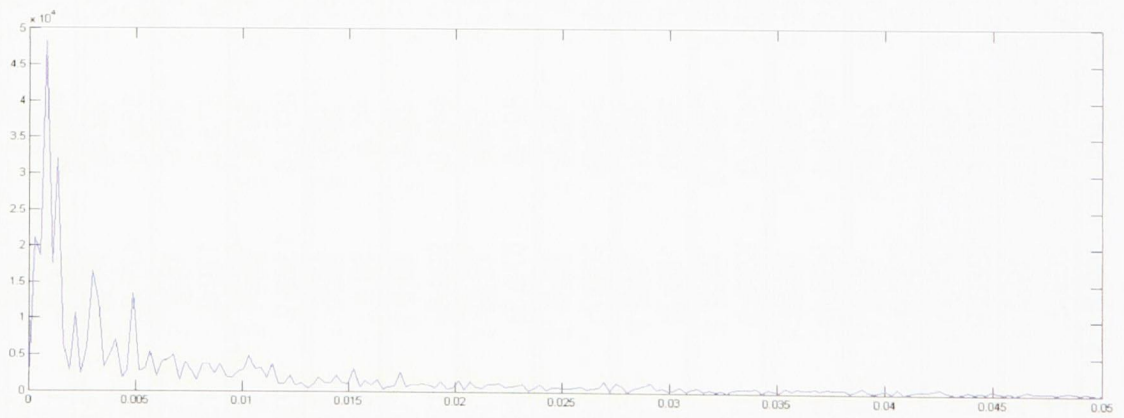
FAST FOURIER TRANSFORMS (FFT) RESULTS: HOURLY STAGE DATA



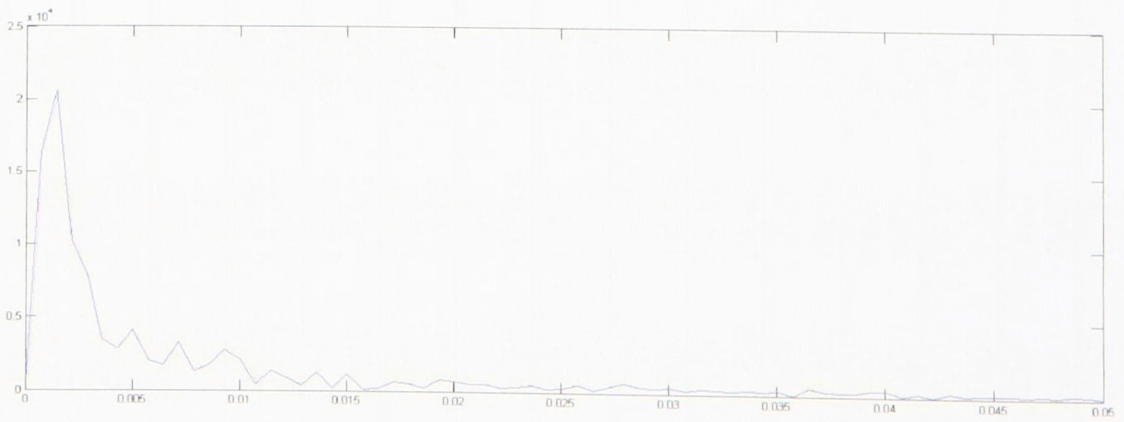
Ardkill – Monitoring period



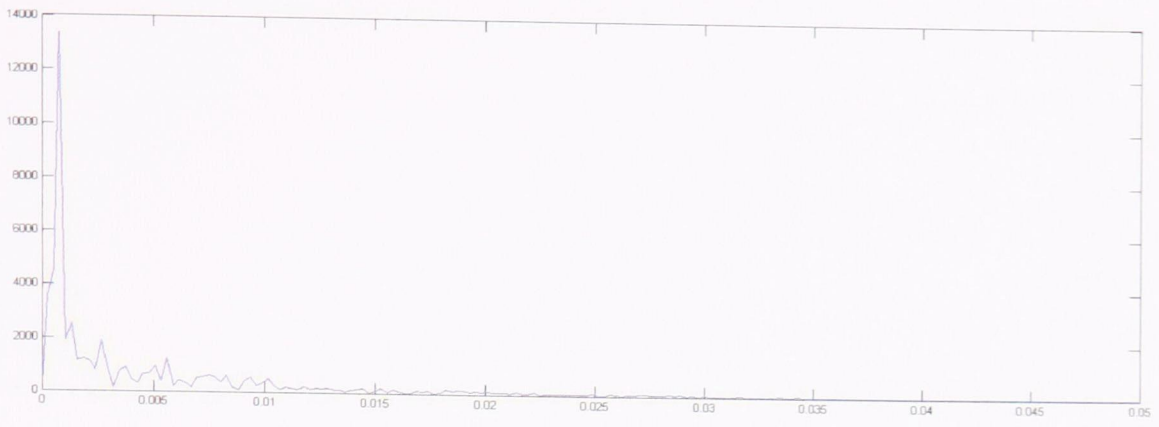
Ardkill – 2007/2008



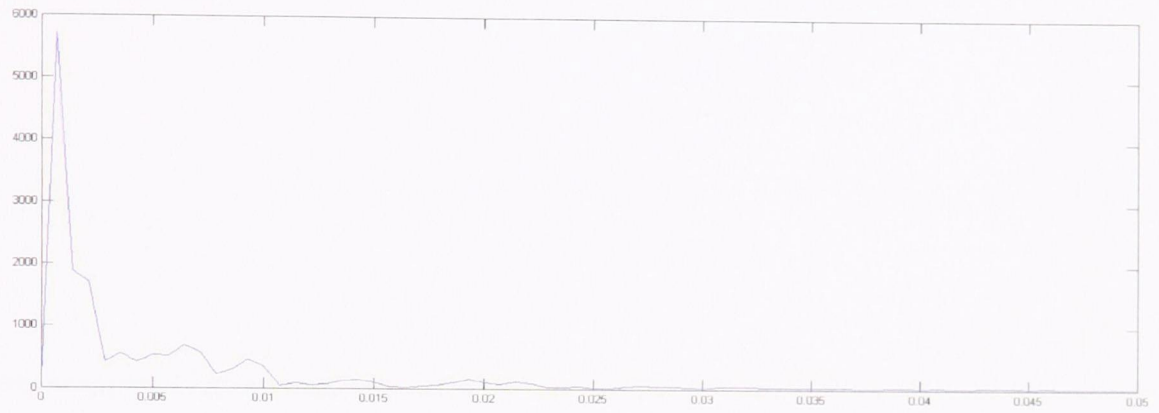
Blackrock – Monitoring period



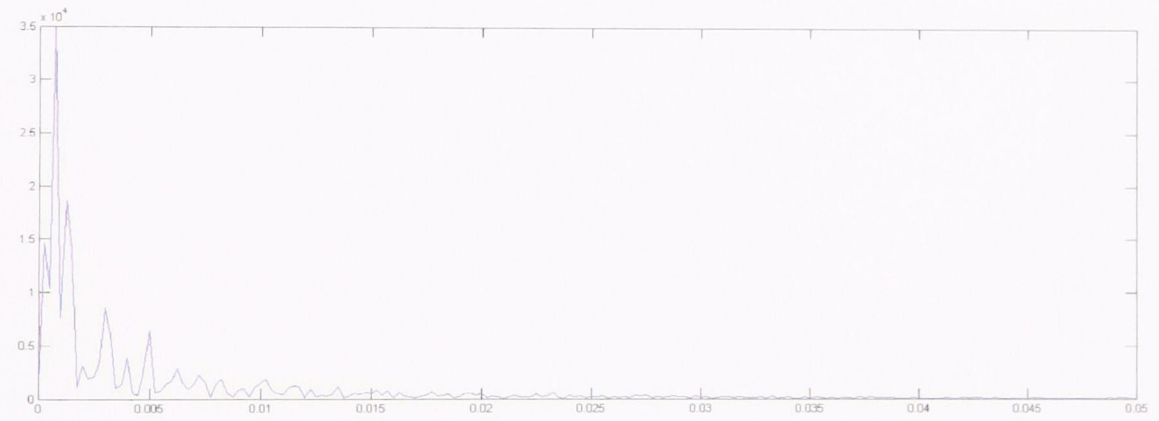
Blackrock – 2007/2008



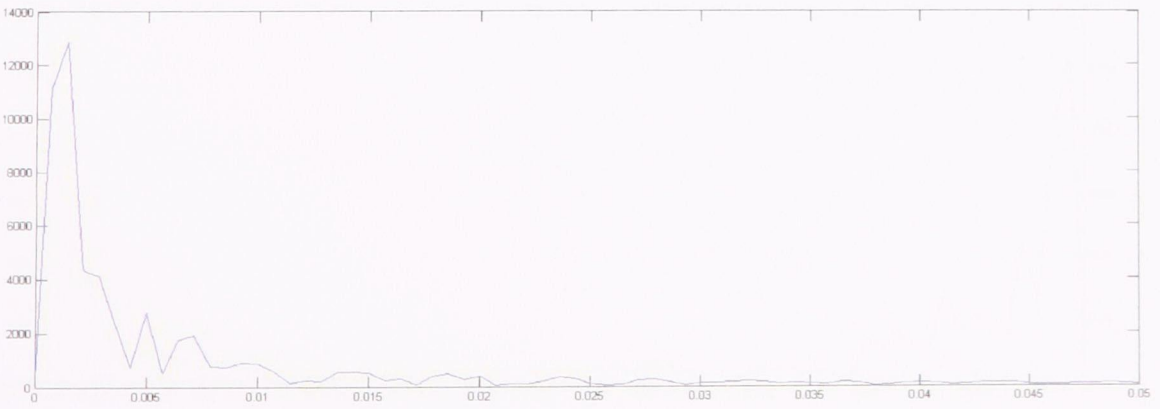
Brierfield – Monitoring period



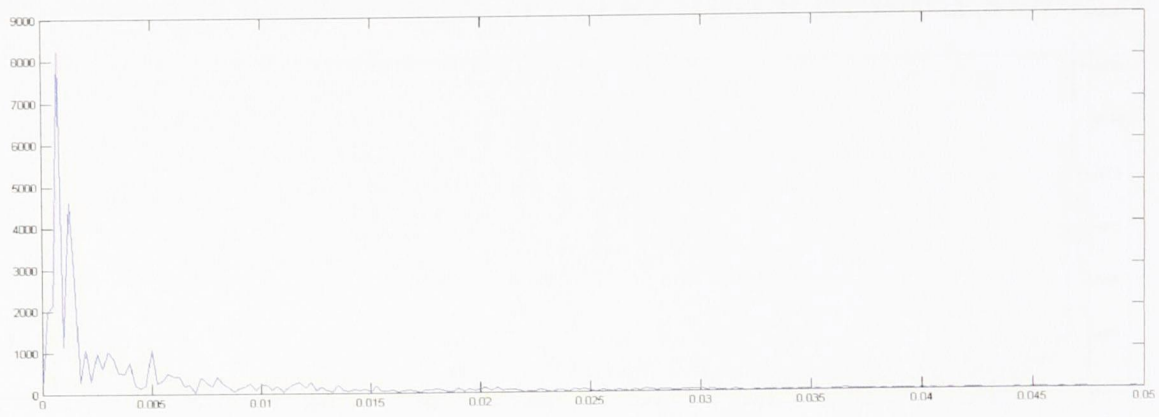
Brierfield – 2007/2008



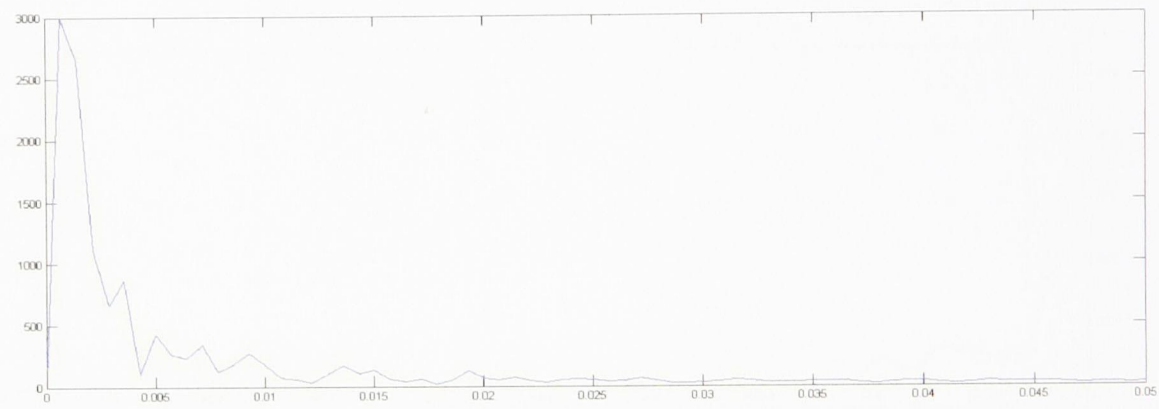
Caherglassaun – Monitoring period



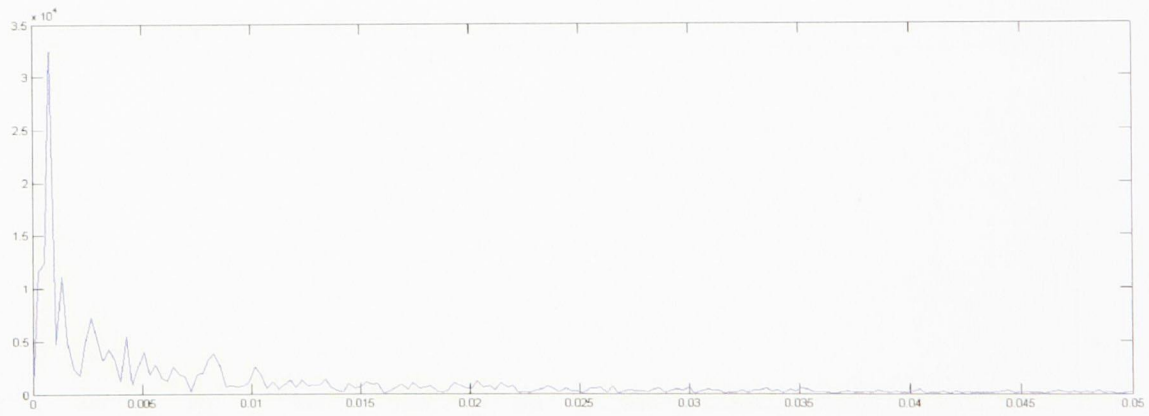
Caherglassaun – 2007/2008



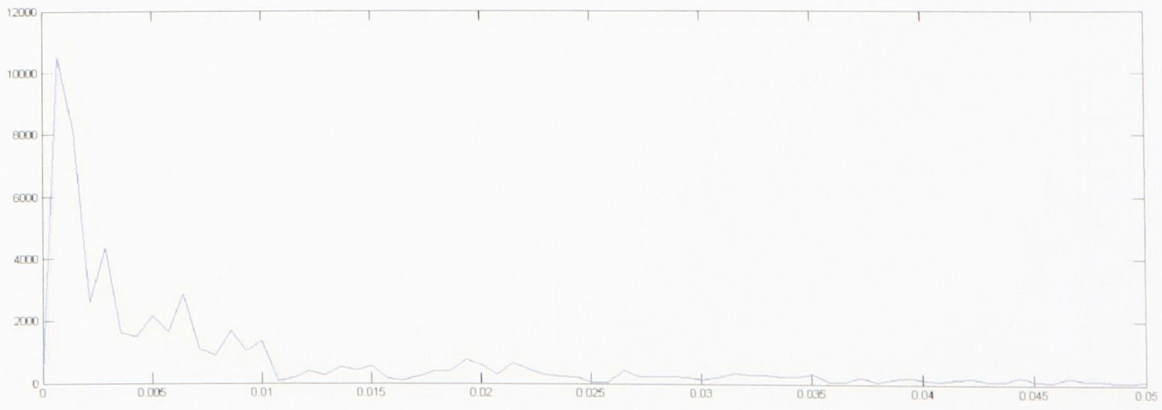
Caranavoodaun – Monitoring period



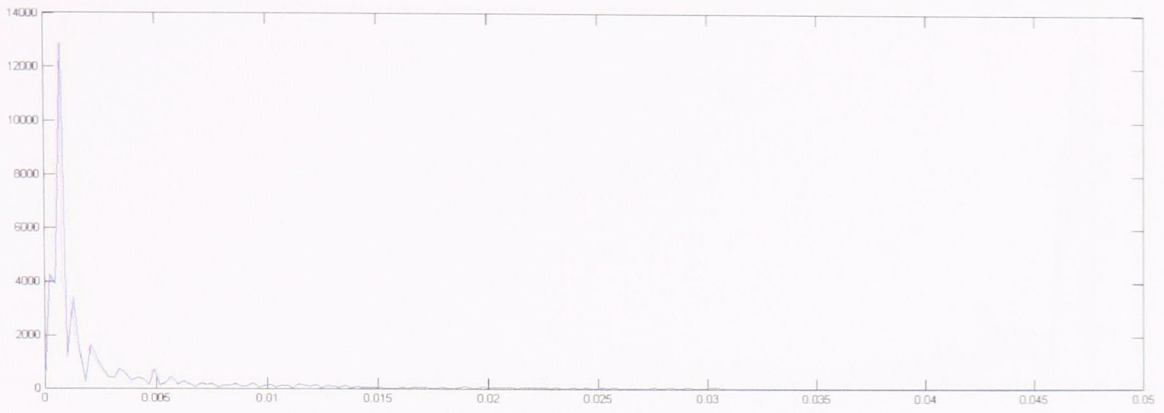
Caranavoodaun – 2007/2008



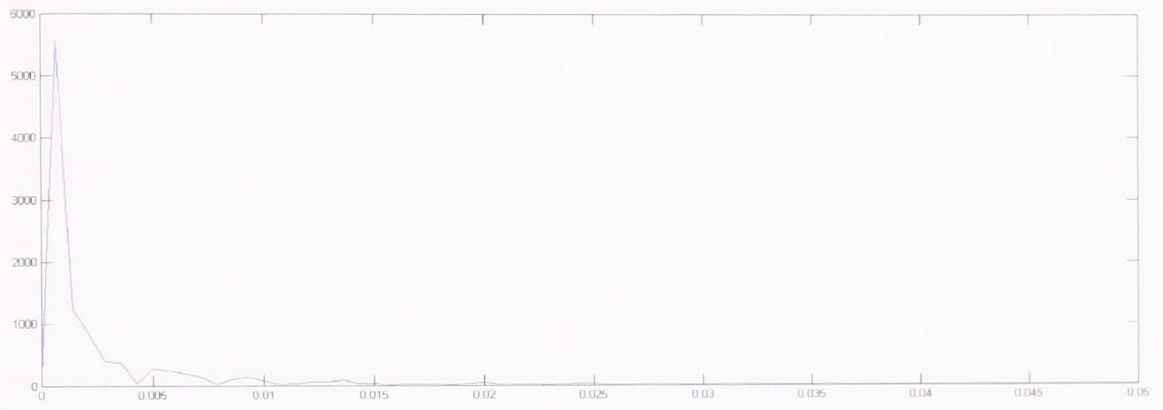
Carrowreagh – Monitoring period



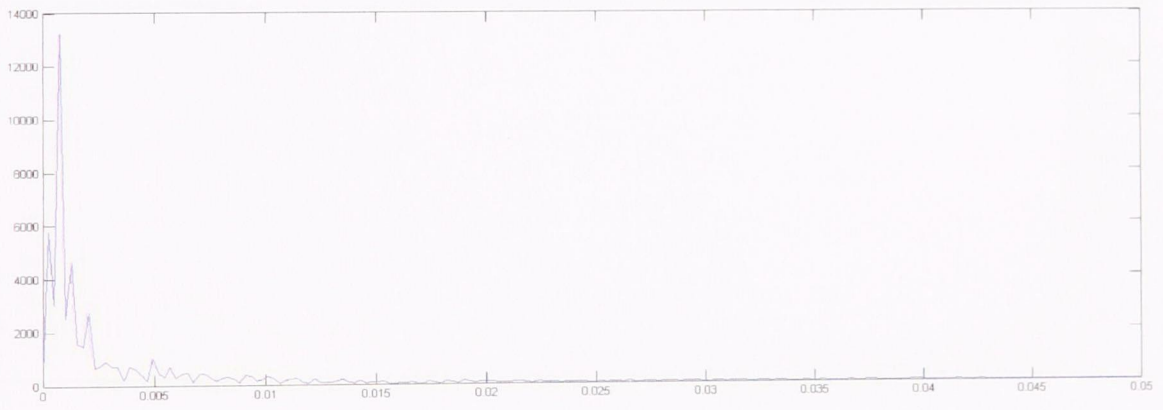
Carrowreagh – 2007/2008



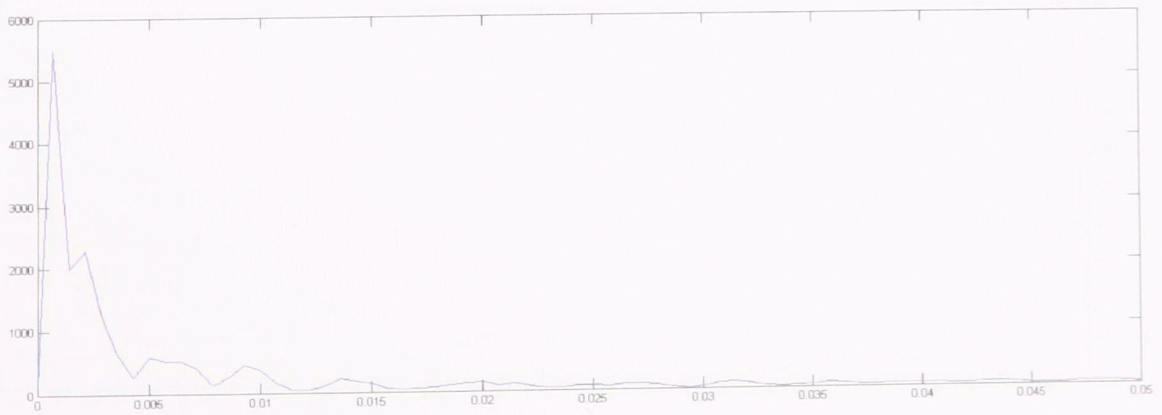
Coolcam – Monitoring period



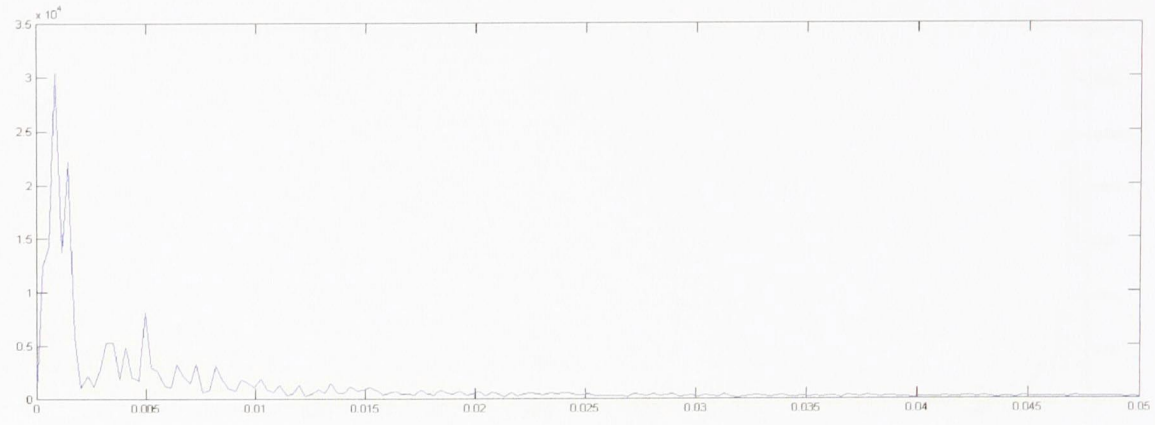
Coolcam – 2007/2008



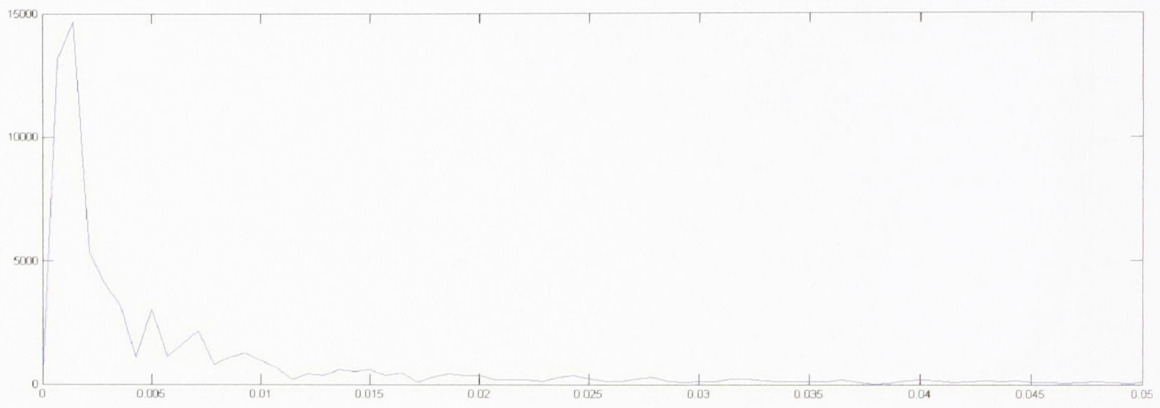
Croaghill – Monitoring period



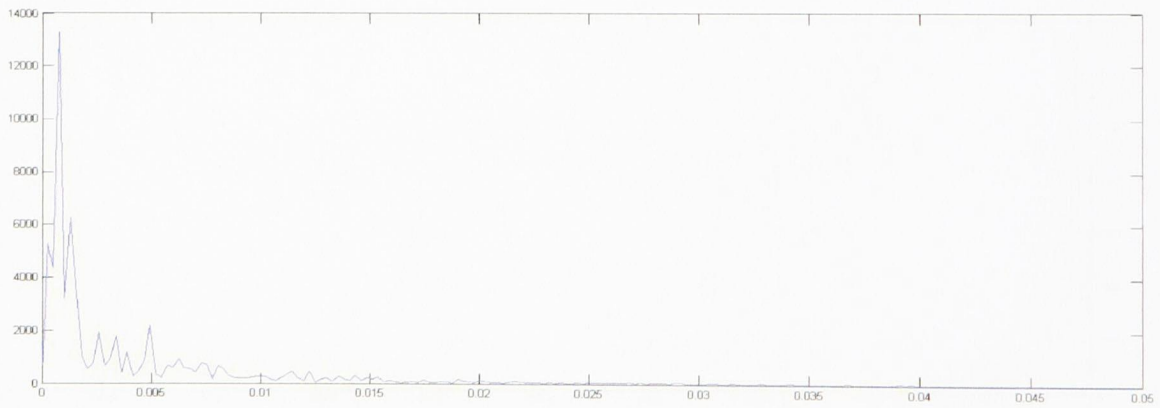
Croaghill – 2007/2008



Garryland – Monitoring period



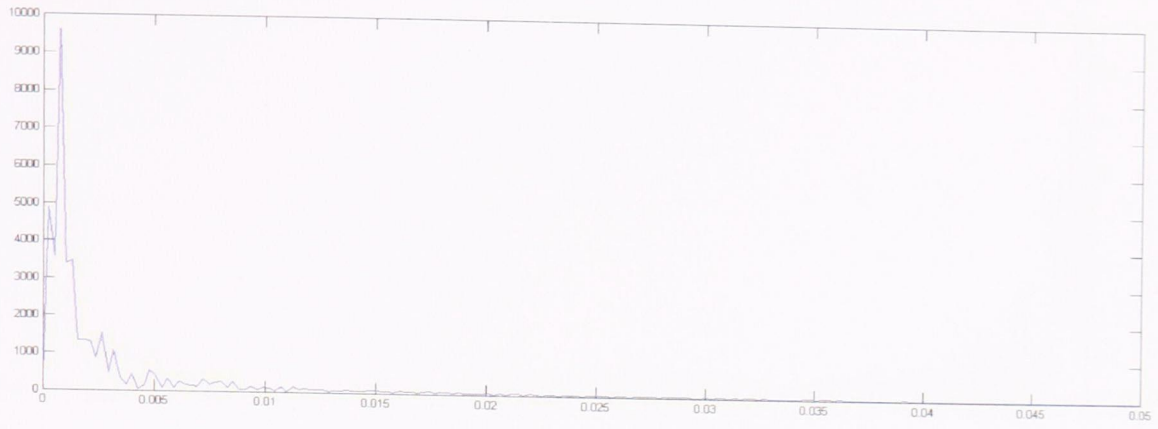
Garryland – 2007/2008



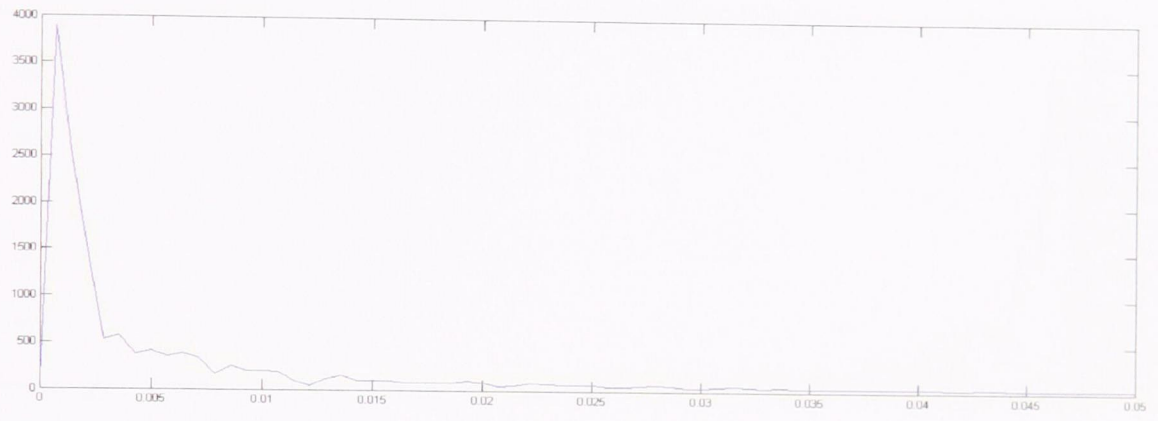
Knockaunroe – Monitoring period



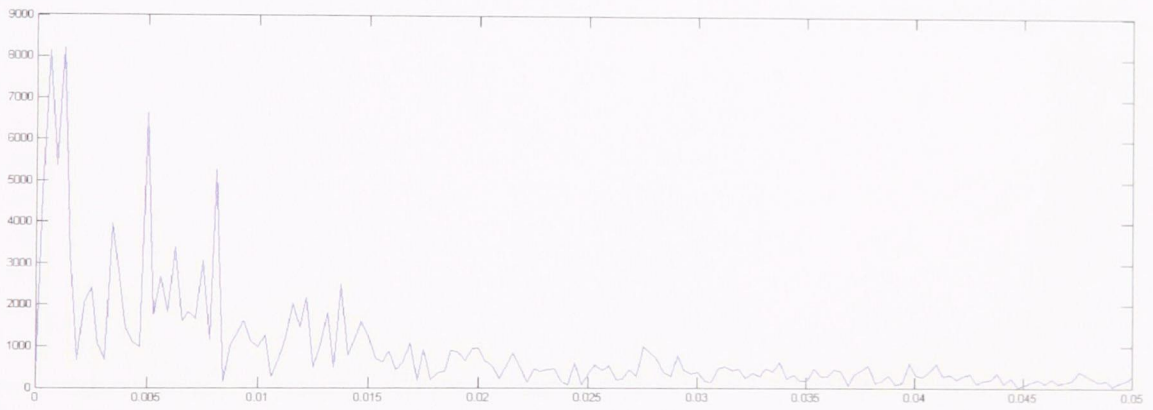
Knockaunroe – 2007/2008



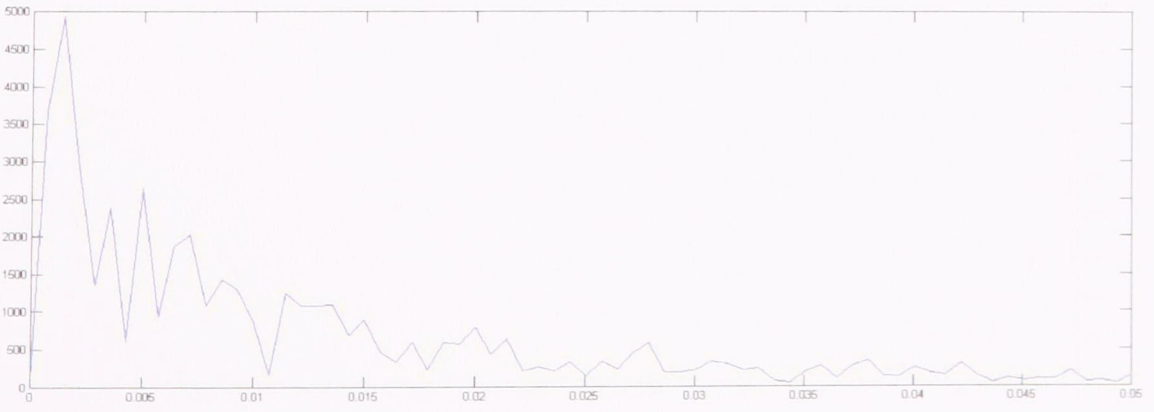
Lisduff – Monitoring period



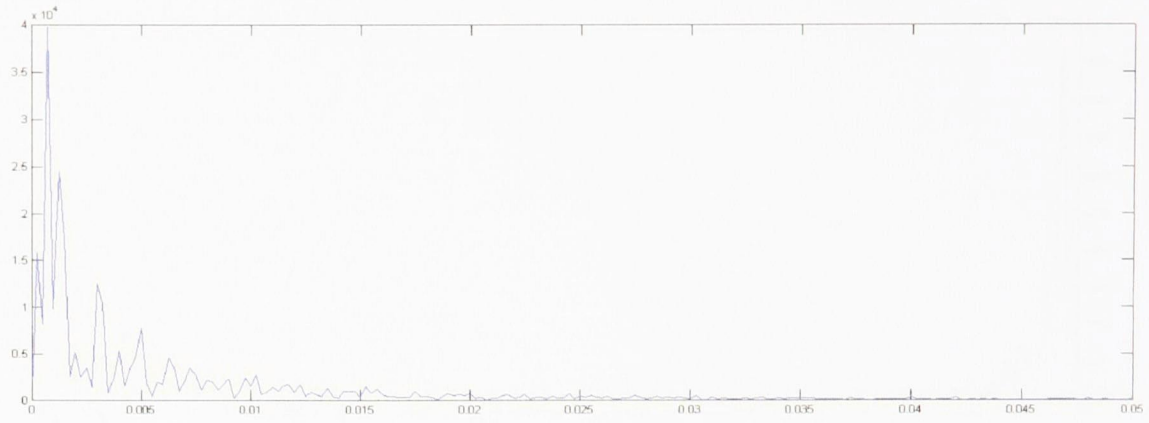
Lisduff – 2007/2008



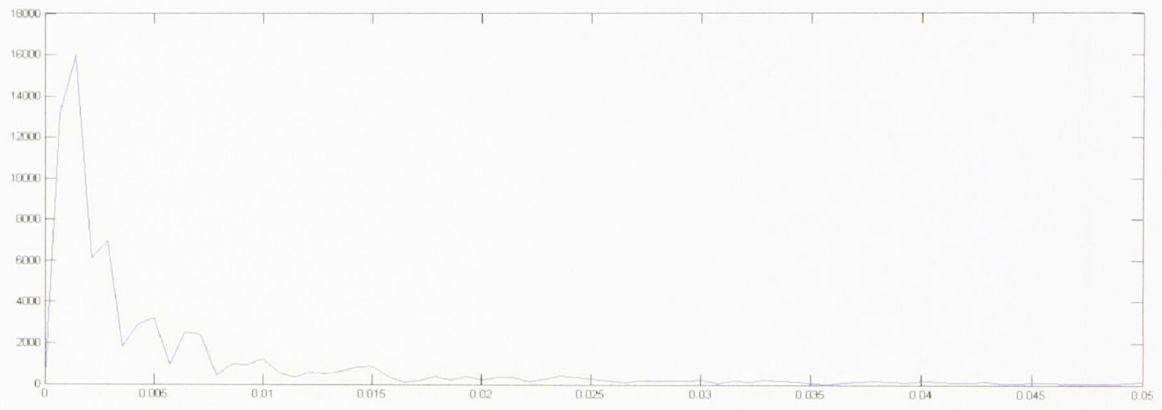
Lough Aleenaun – Monitoring period



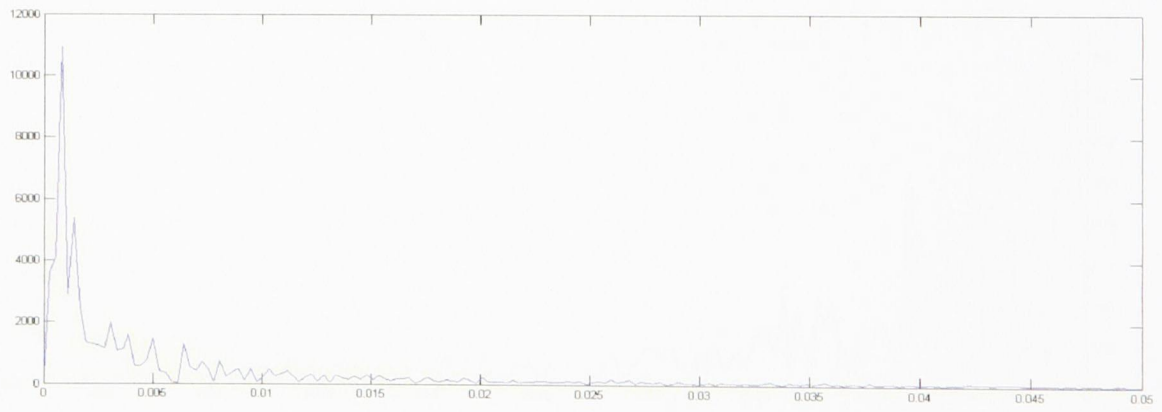
Lough Aleenaun – 2007/2008



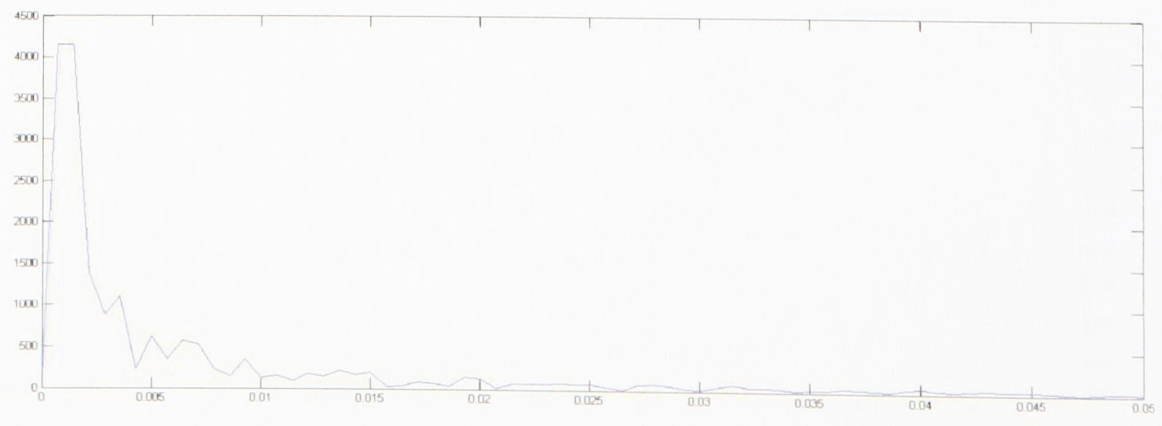
Lough Coy – Monitoring period



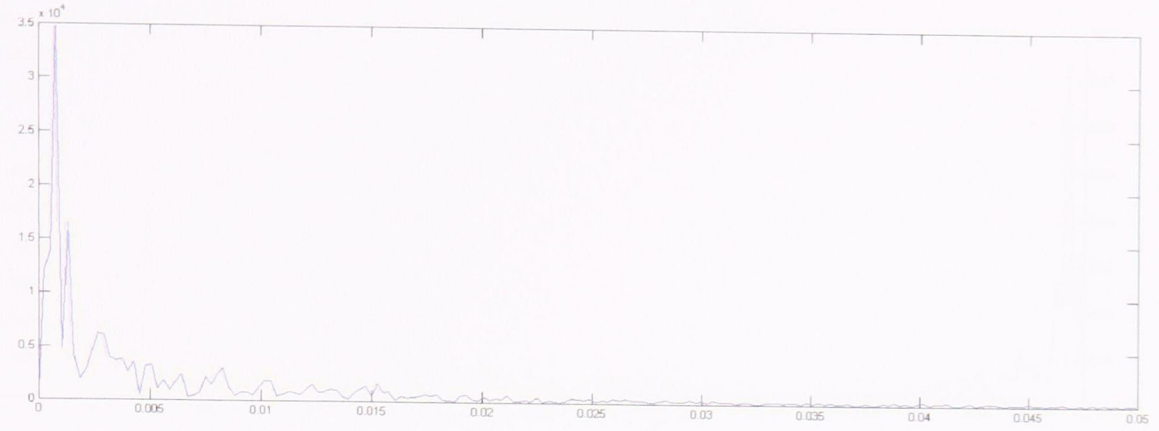
Lough Coy – 2007/2008



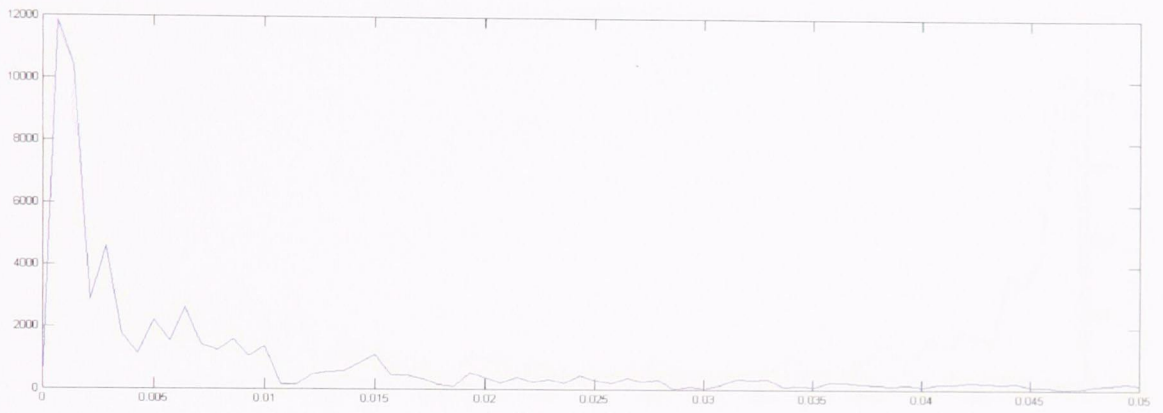
Lough Gealain – Monitoring period



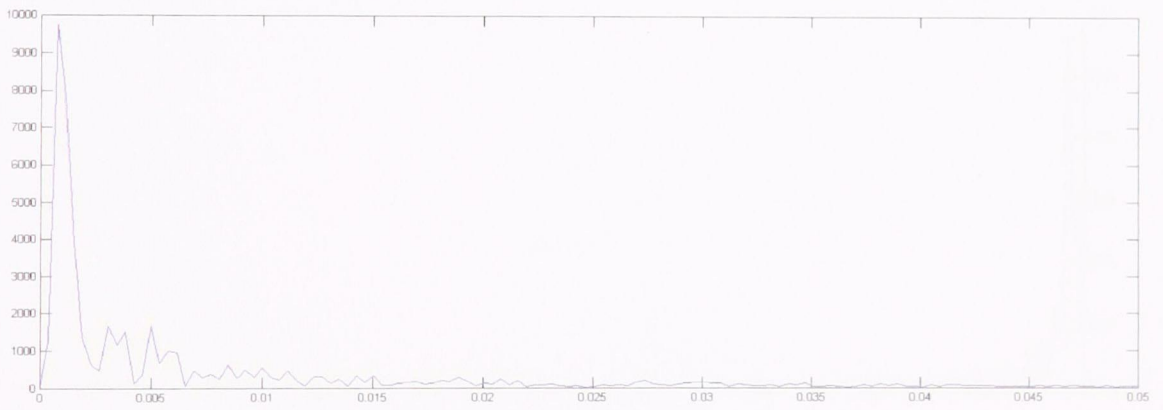
Lough Gealain – 2007/2008



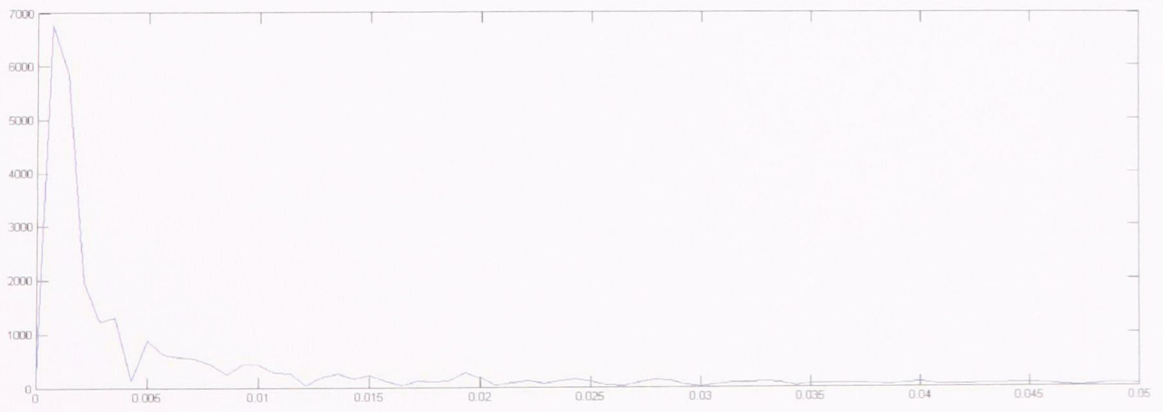
Rathnalulleagh – Monitoring period



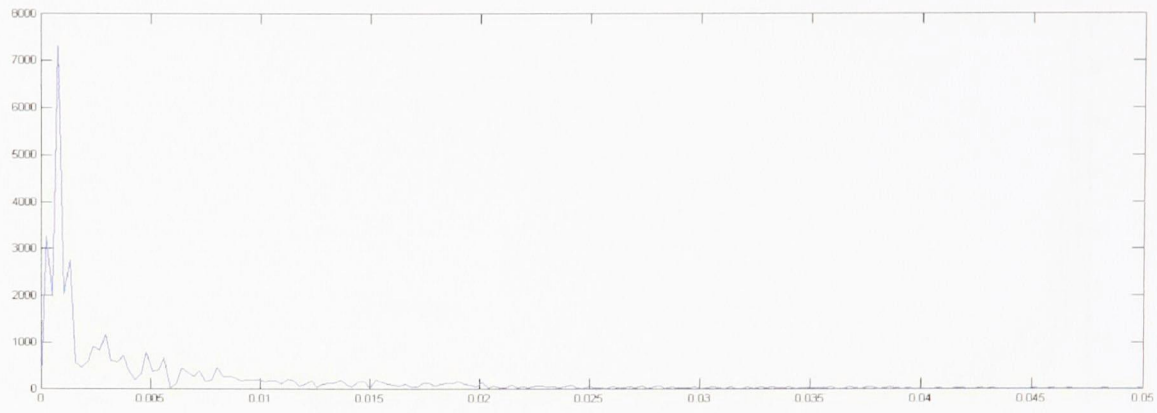
Rathnalulleagh – 2007/2008



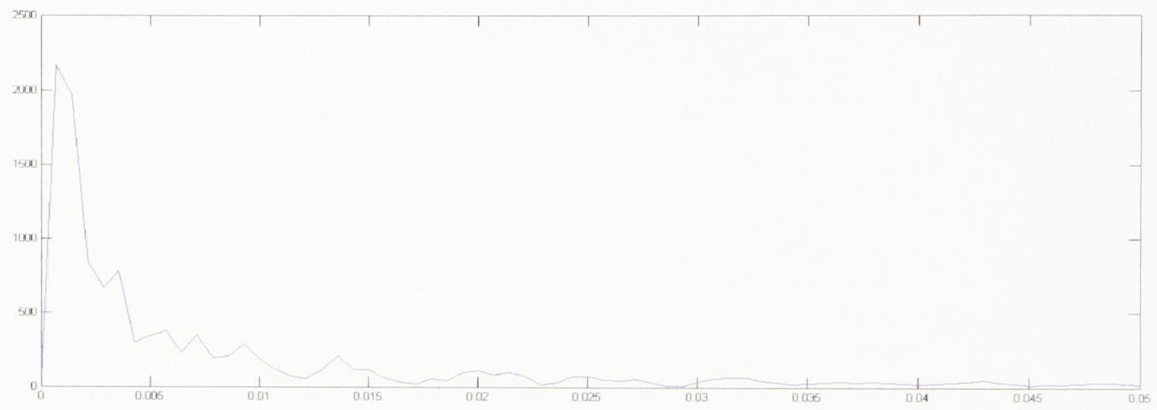
Roo West – Monitoring period



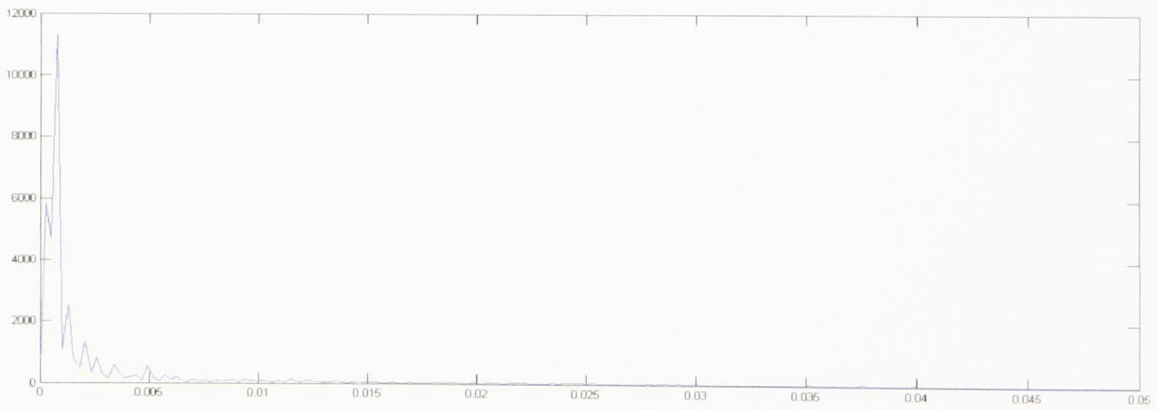
Roo West – 2007/2008



Skealoghan – Monitoring period



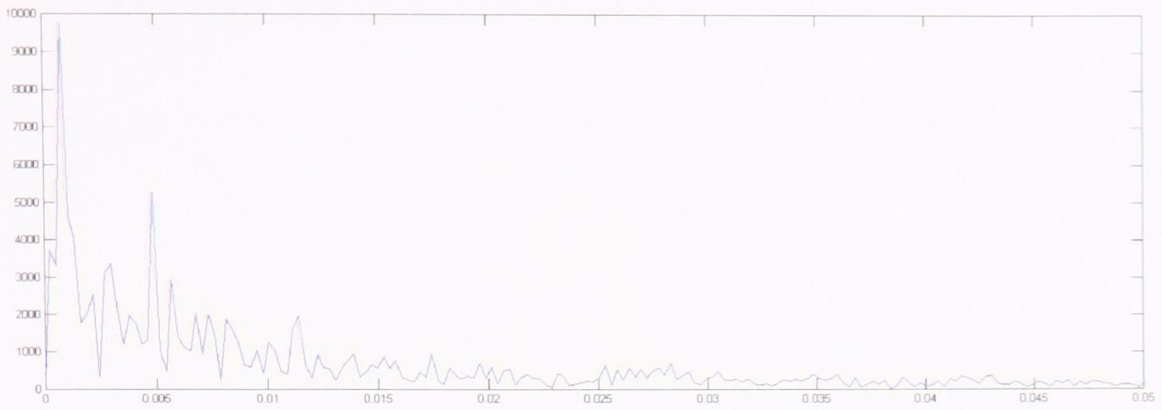
Skealoghan – 2007/2008



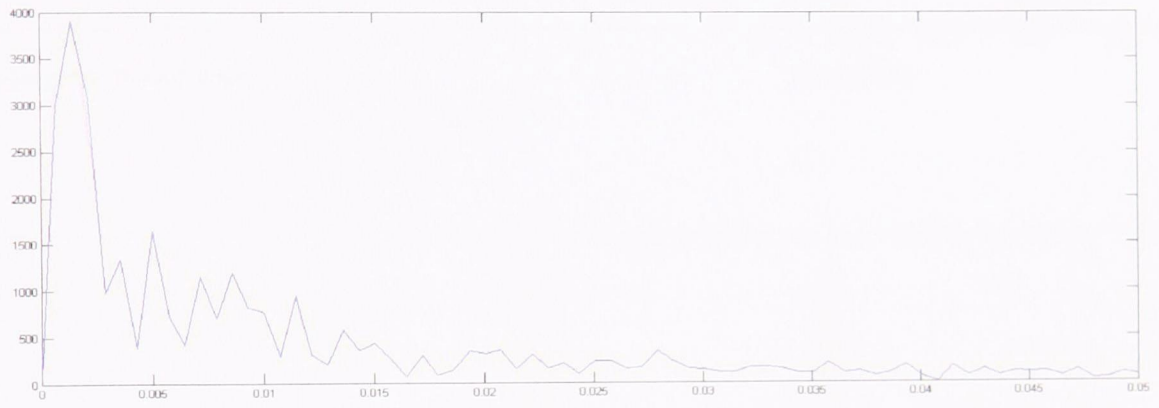
Termon – Monitoring period



Termon – 2007/2008

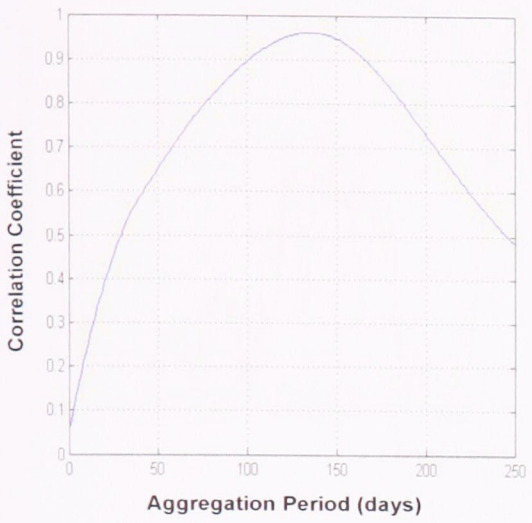


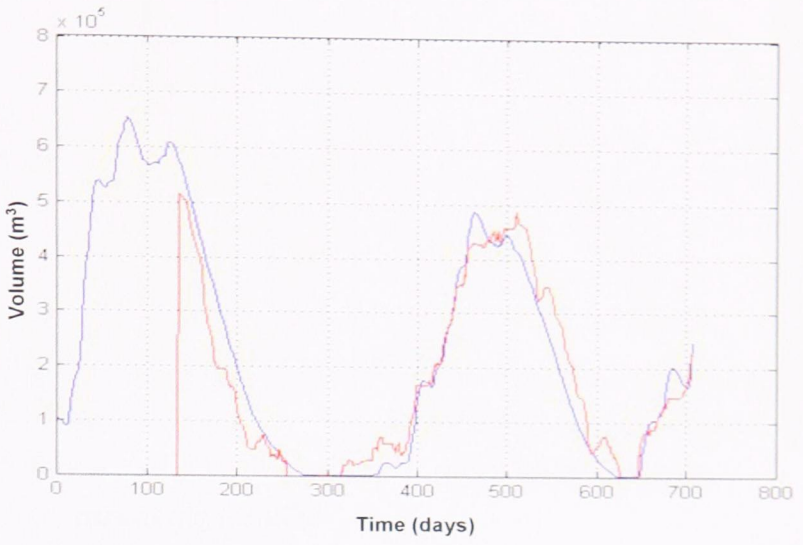
Turloughmore – Monitoring period



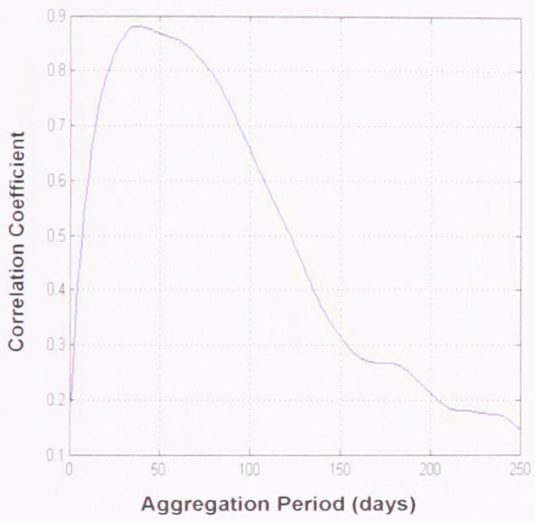
Turloughmore – 2007/2008

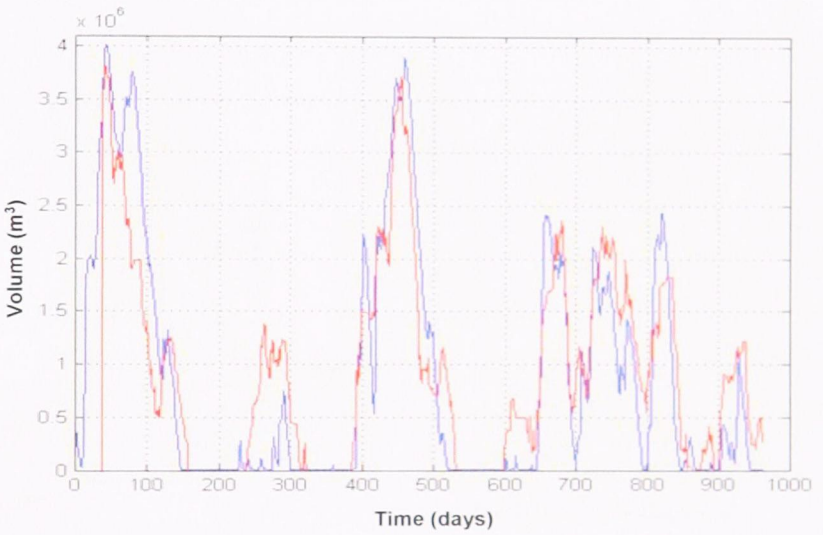
Appendix E: Aggregated Rainfall Model



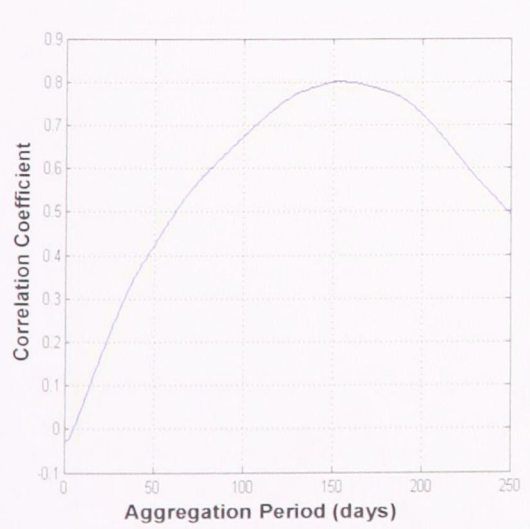


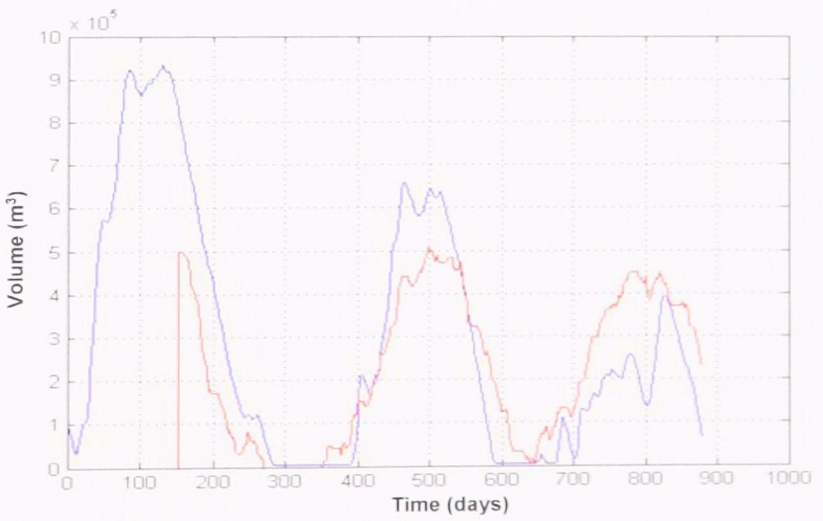
Ardkill



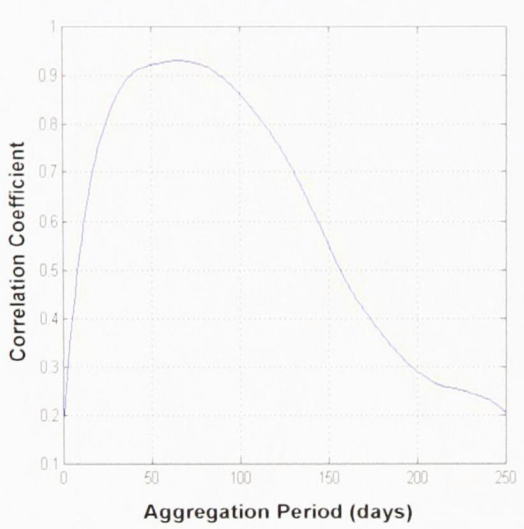


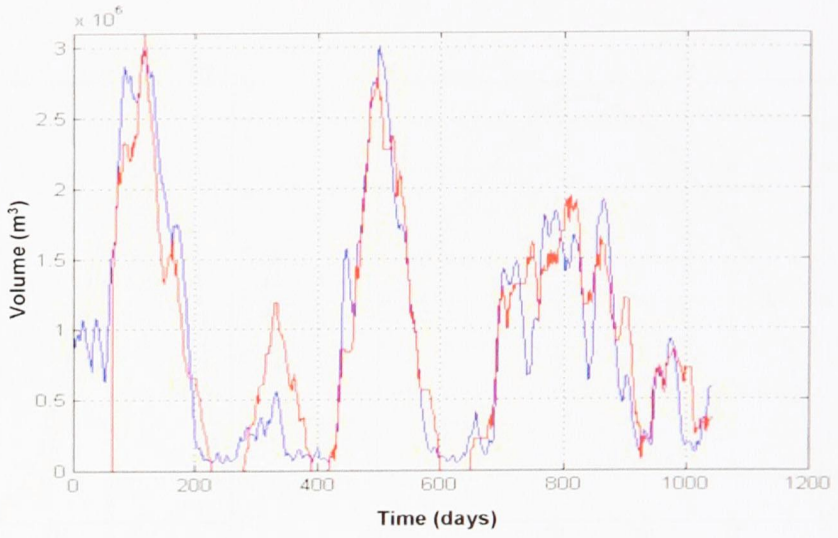
Blackrock



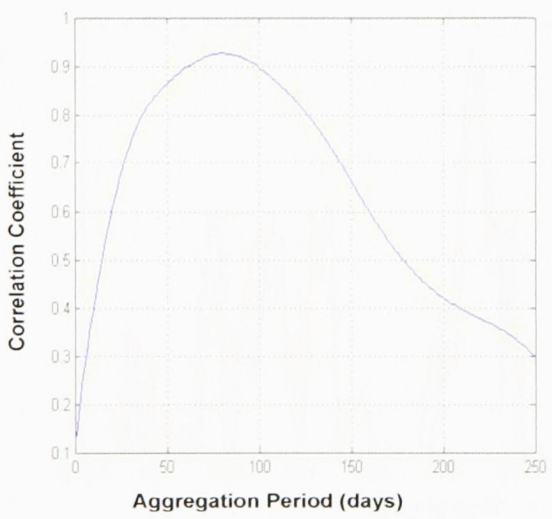


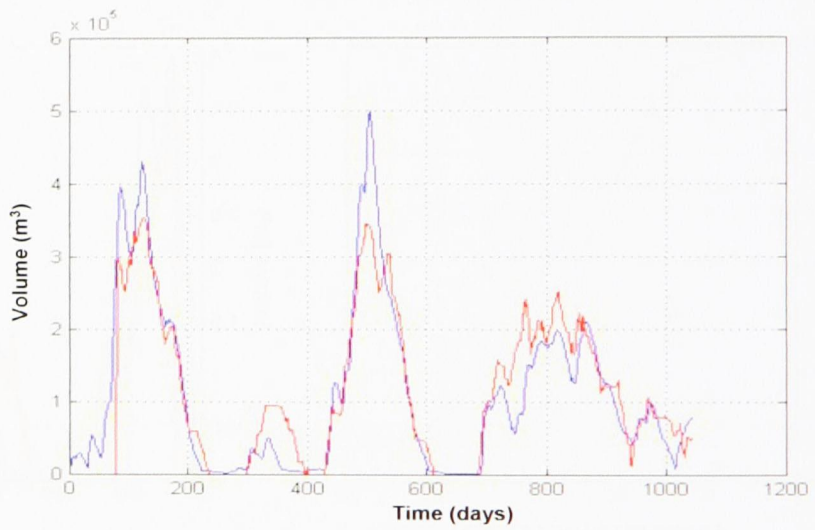
Brierfield



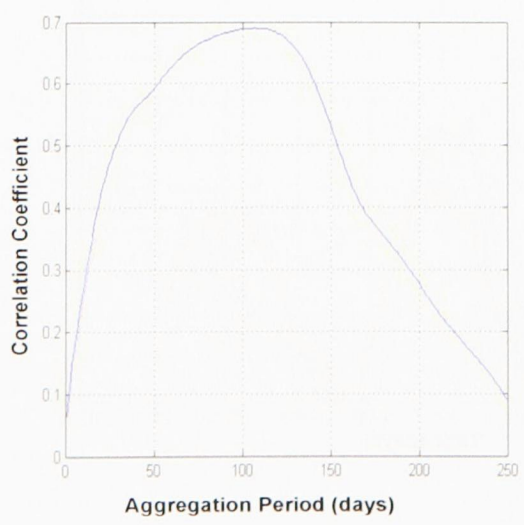


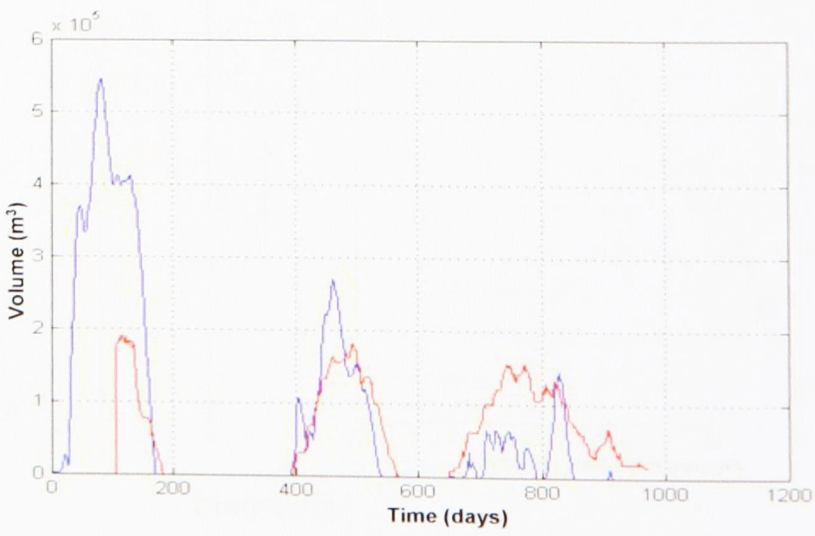
Caherglassaun



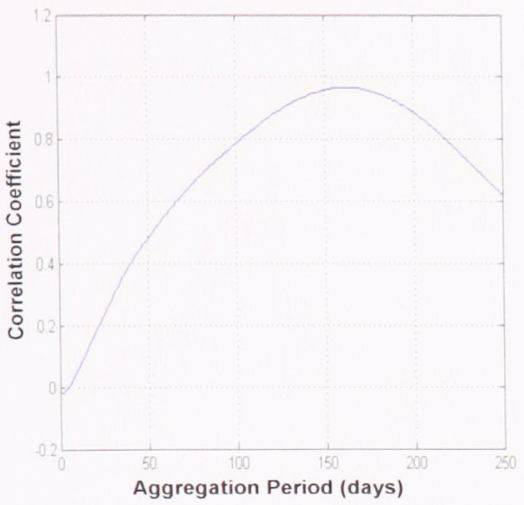


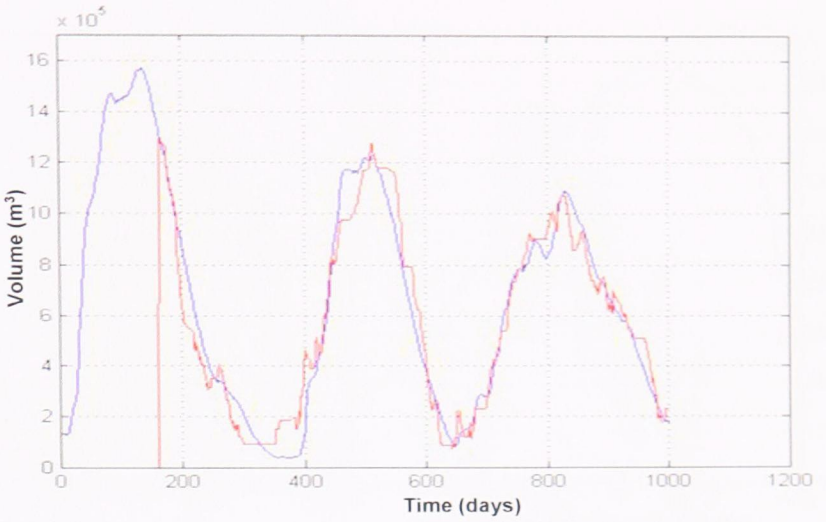
Caranavoodaun



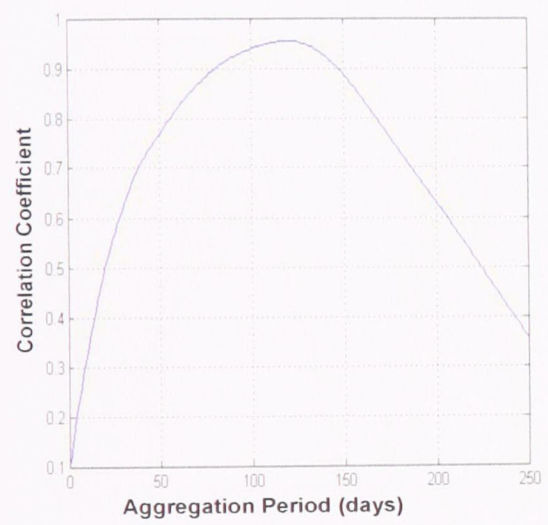


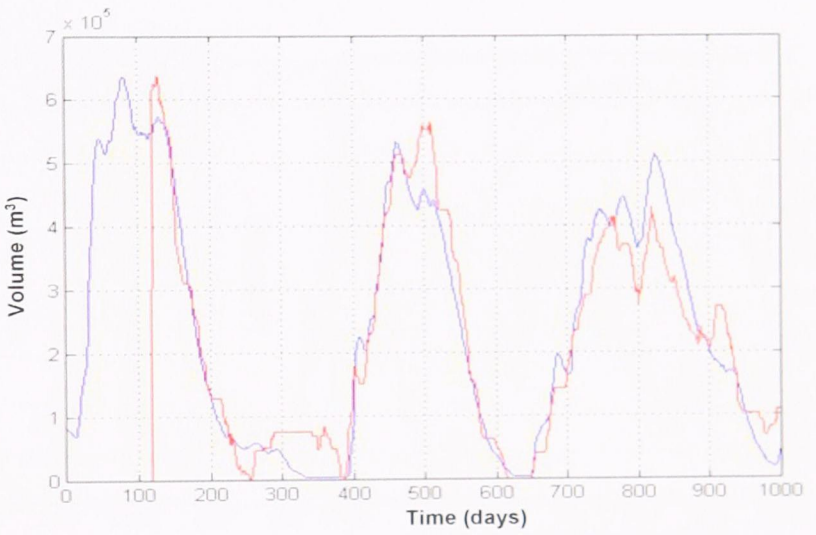
Carrowreagh



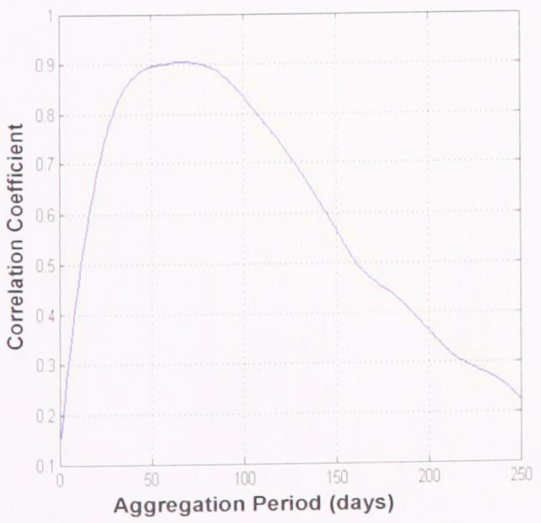


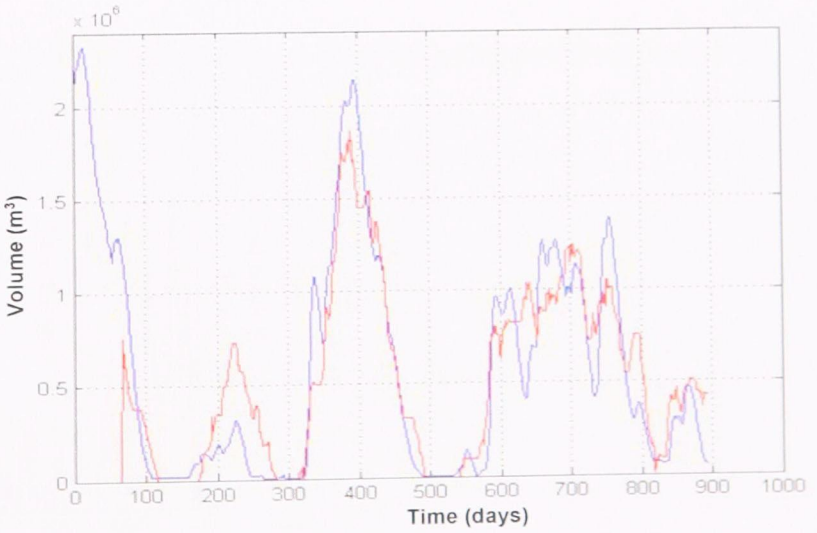
Coolcam



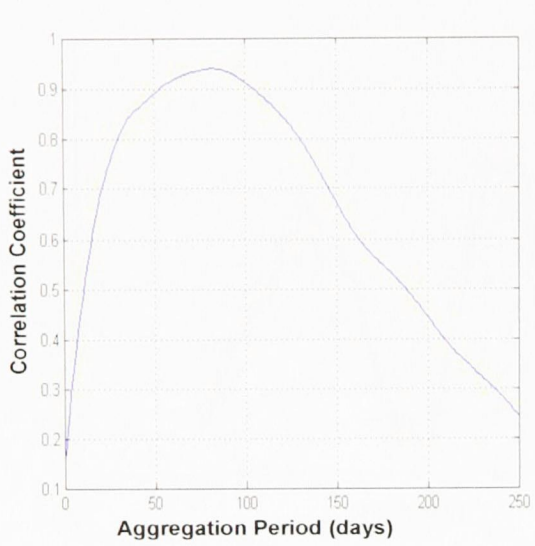


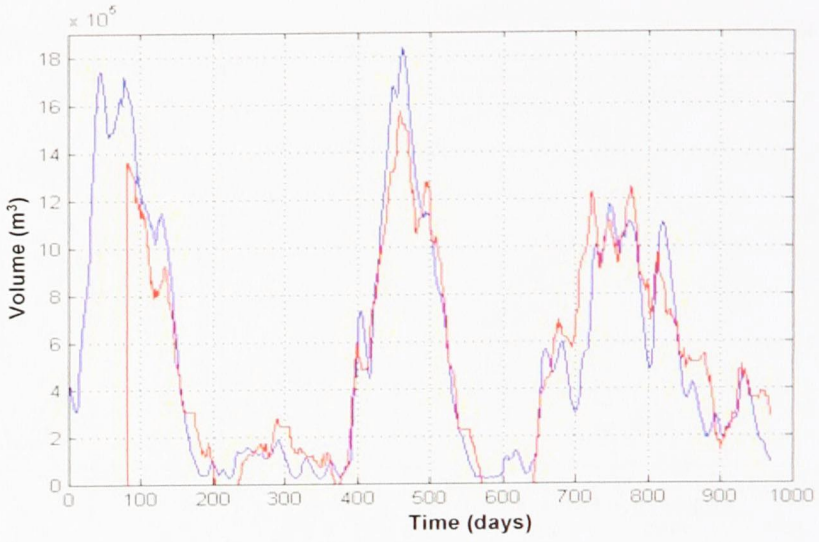
Croaghill



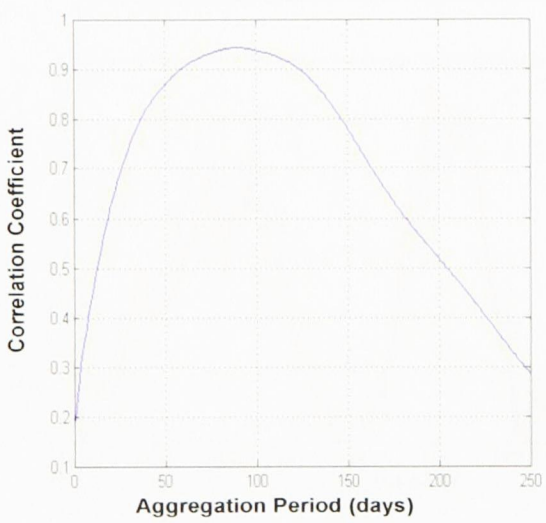


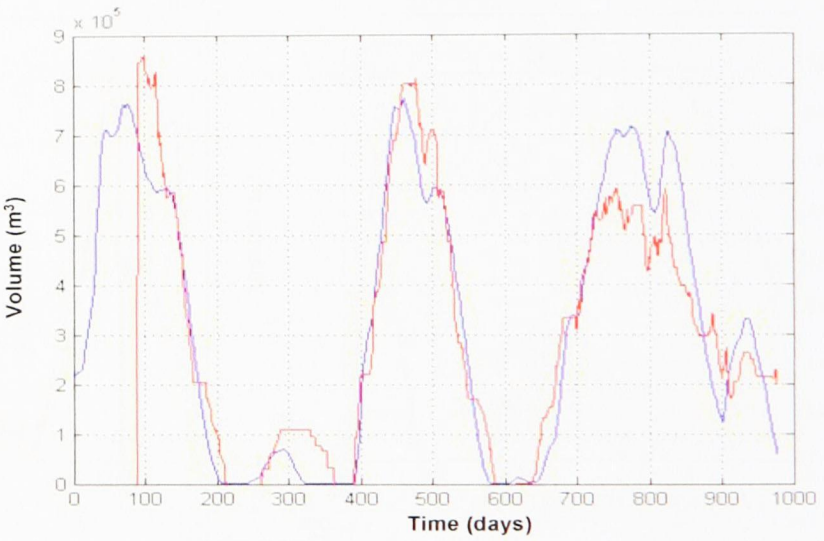
Garryland



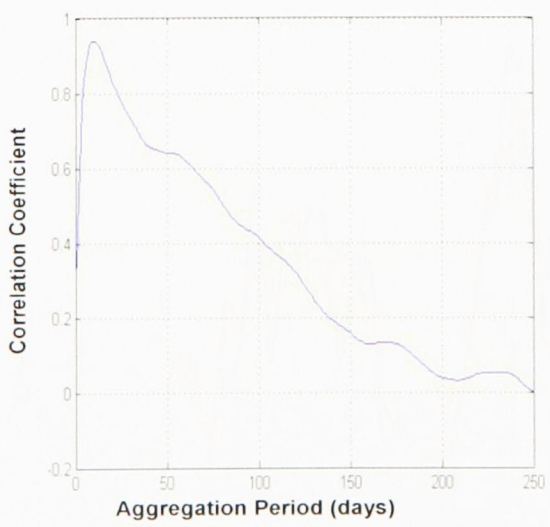


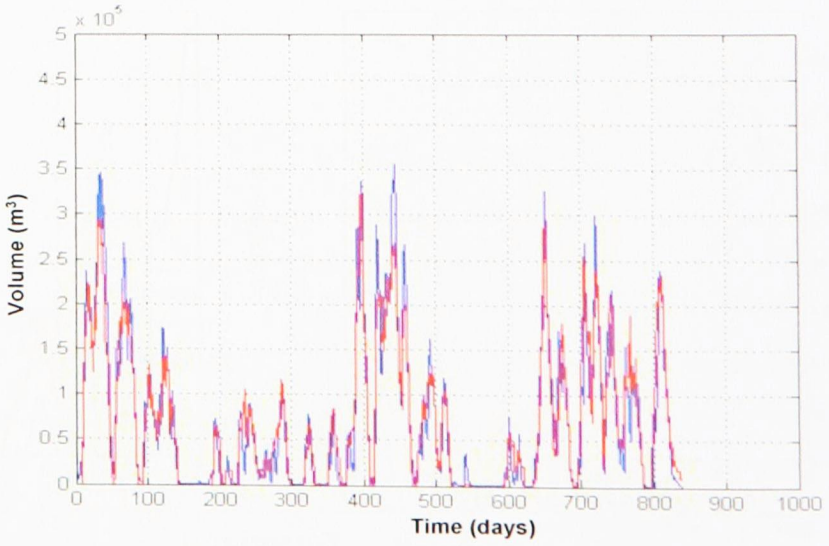
Knockaunroe



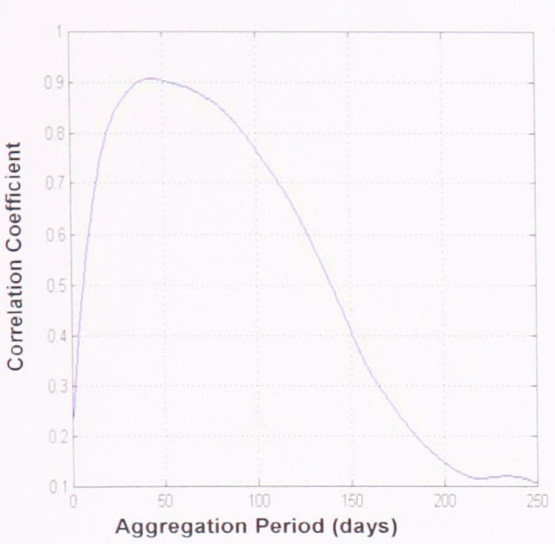


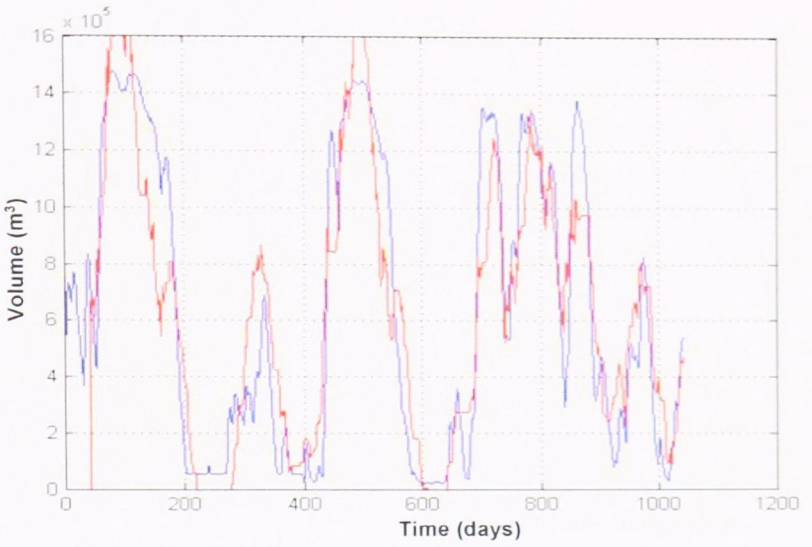
Lisduff



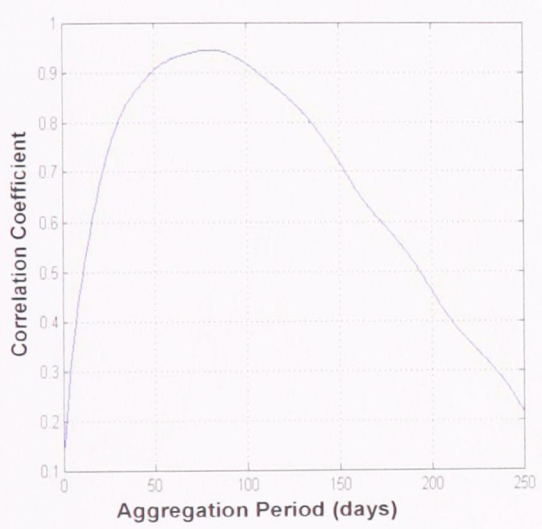


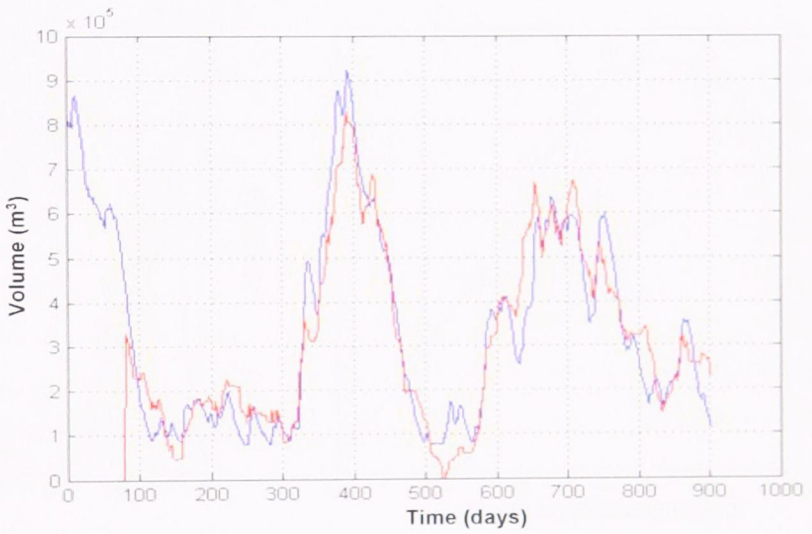
Lough Aleenaun



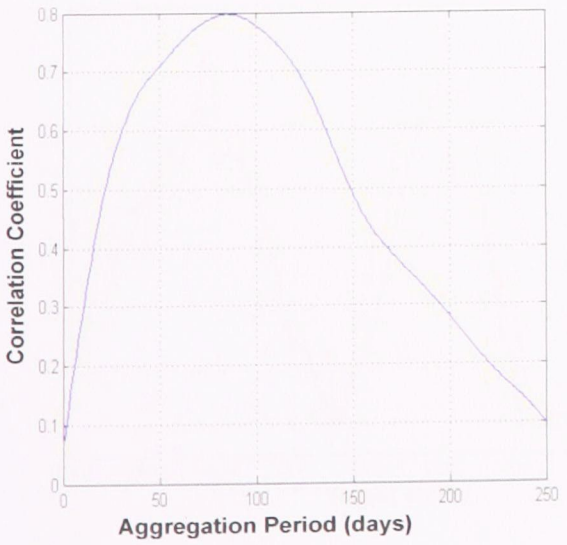


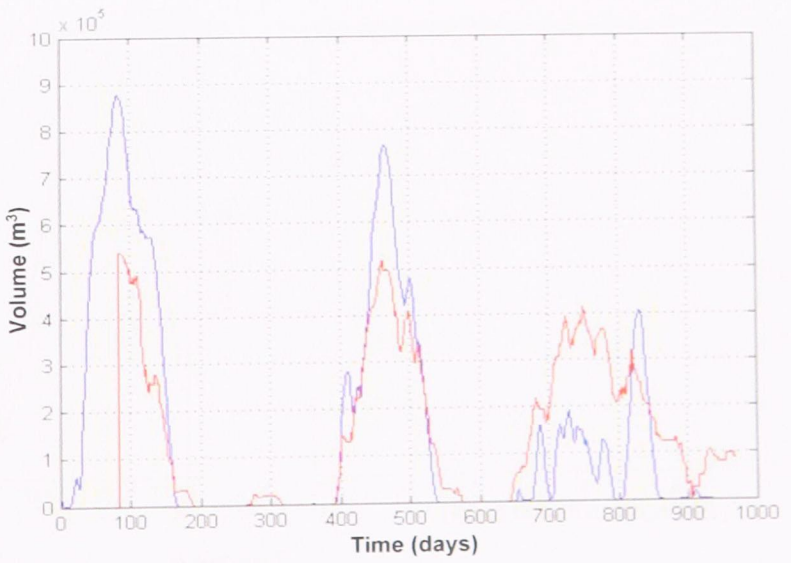
Lough Coy



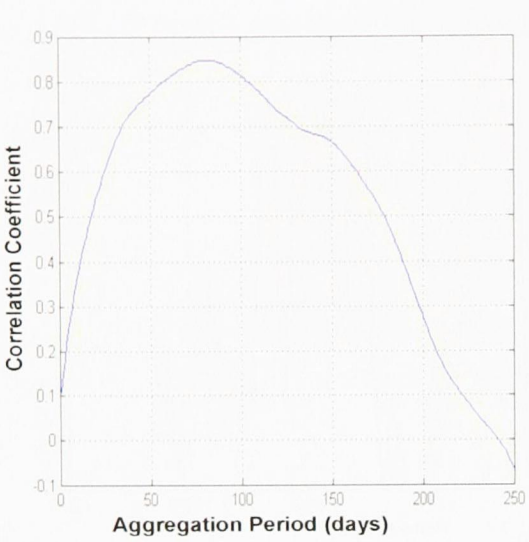


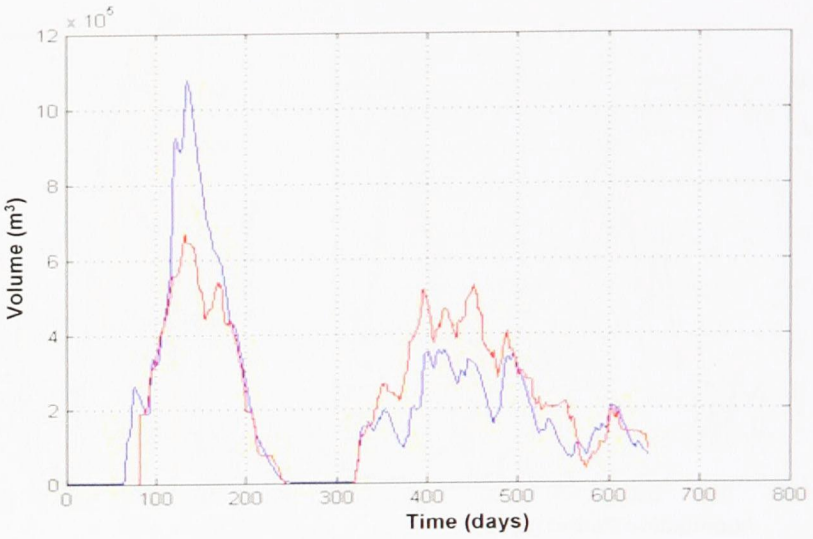
Lough Gealain



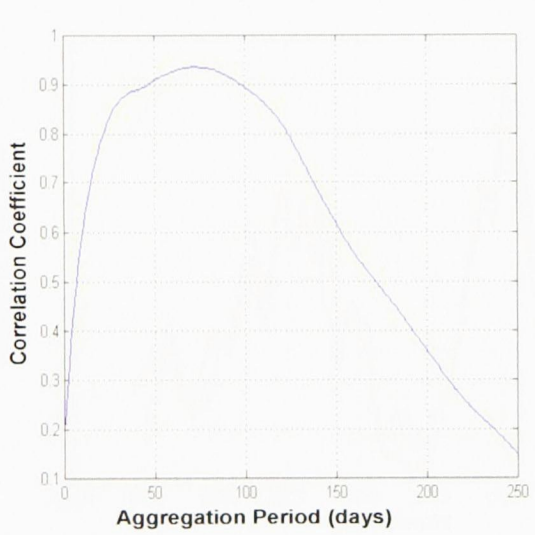


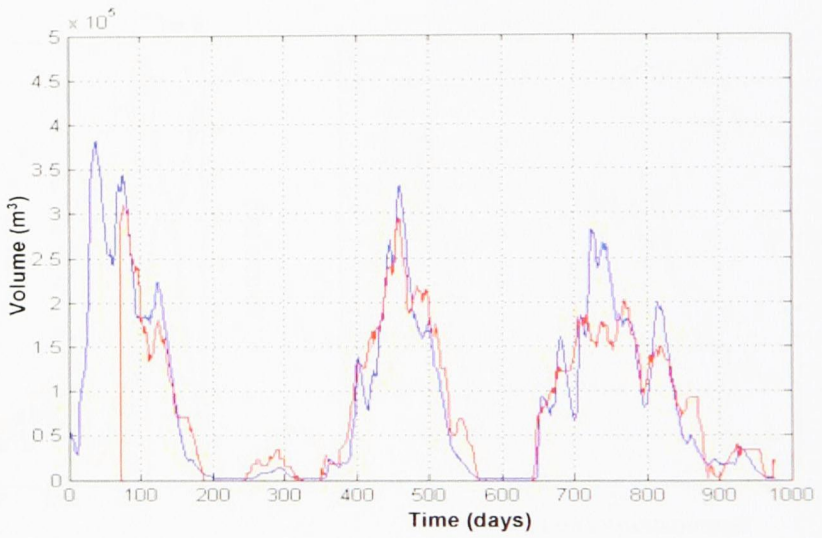
Rathnalulleagh



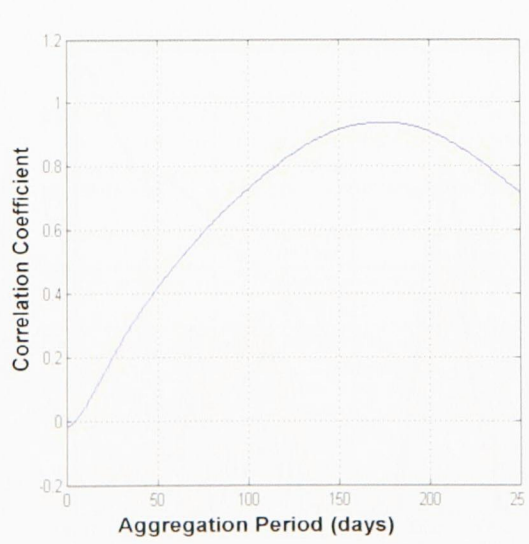


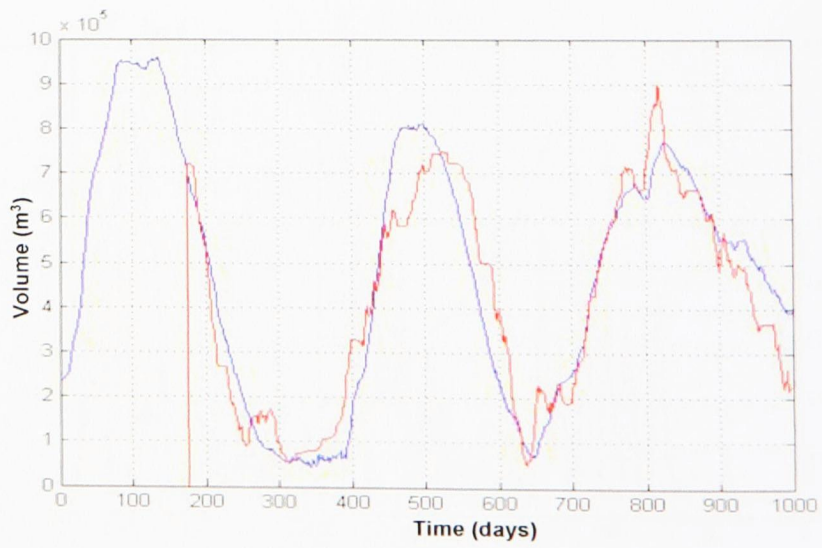
Roo West



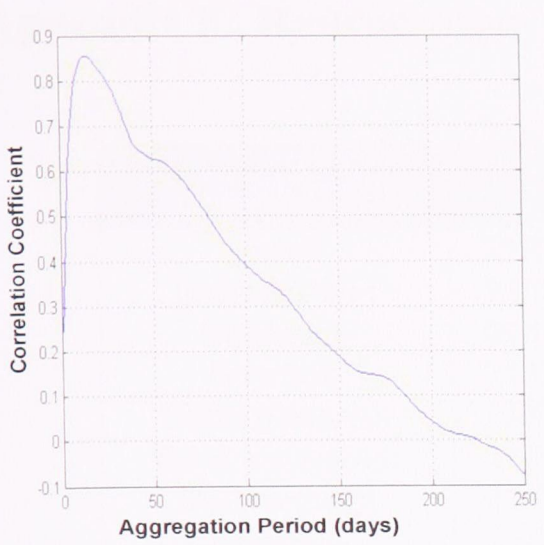


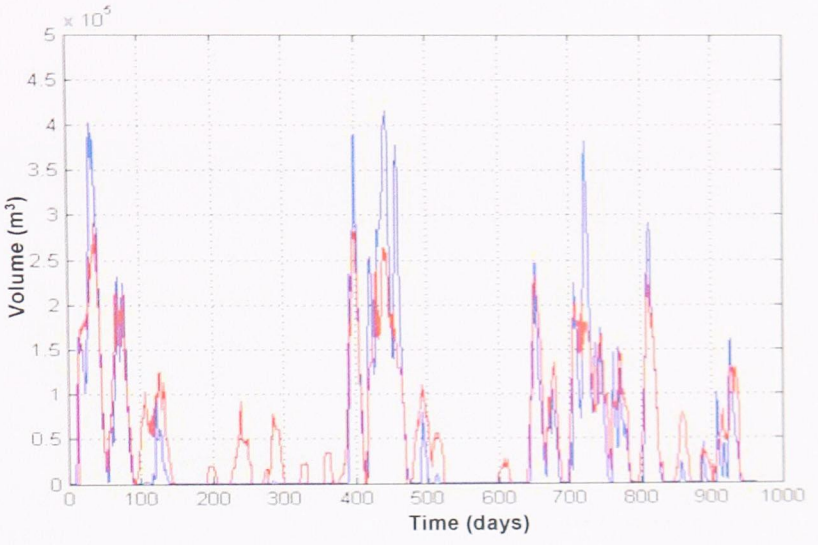
Skealoghan





Termon





Turloughmore

Appendix F: Hydroecology

Site Name	Start	Finish	Inundation (Days)	Inundation (Weeks)
Ardkill	21/09/2006	14/07/2007	296	42.3
Ballinderreen	21/09/2006	18/05/2007	239	34.1
Blackrock	21/09/2006	05/04/2007	196	28
Brierfield	21/09/2006	18/08/2007	331	47.3
Caherglassaun	21/09/2006		Year	52
Caranavoodaun	21/09/2006	07/05/2007	228	32.6
Carrowreagh	21/09/2006	29/04/2007	220	31.4
Coolcam	21/09/2006		Year	52
Croaghill	21/09/2006		Year	52
Garryland	21/09/2006	30/04/2007	221	31.6
Kilglassaun	21/09/2006	25/04/2007	216	30.9
Knockaunroe	21/09/2006	10/05/2007	231	33
Lisduff	21/09/2006	04/06/2007	256	36.6
Lough Aleenaun	21/09/2006	03/04/2007	194	27.7
Lough Coy	21/09/2006	19/04/2007	Year	52
Lough Gealain	21/09/2006	09/05/2007	230	32.9
Rathnalulleagh	21/09/2006	23/04/2007	214	30.6
Skealoghan	21/09/2006	31/05/2007	252	36
Termon South	21/09/2006		Year	52
Tullynafrankagh	21/09/2006		Year	52
Turloughmore	21/09/2006	07/02/2007	139	19.9
Roo West	N/A	N/A	N/A	N/A

Name	Group Number	Constant Species
Lolium perenne - Trifolium repens	10	*Lolium perenne, Trifolium repens, Agrostis stolonifera, Bellis perennis, Cardamine pratensis, Festuca rubra, Scorzoneroides autumnalis, Prunella vulgaris*
Lolium perenne - Trifolium repens - Agrostis stolonifera	15	*Agrostis stolonifera, Trifolium repens, Lolium perenne*
Filipendula ulmaria - Vicia cracca	12	*Filipendula ulmaria, Agrostis stolonifera, Potentilla anserina, Vicia cracca*
Carex nigra - Carex panicea	8	*Carex nigra, Hydrocotyle vulgaris, Carex panicea, Filipendula ulmaria, Molinia caerulea, Potentilla erecta*
Limestone grassland	5	*Festuca rubra, Lotus corniculatus, Plantago lanceolata, Potentilla erecta, Carex flacca, Carex panicea, Succisa pratensis, Trifolium repens*
Poa annua-Plantago major	1	*Plantago major, Polygonum aviculare, Agrostis stolonifera, Matricaria discoidea, Poa annua*
Agrostis stoloniferia - Potentilla anserina - Festuca rubra	4	*Agrostis stolonifera, Scorzoneroides autumnalis, Filipendula ulmaria, Lotus corniculatus, Potentilla anserina, Ranunculus repens, Trifolium repens*
Schoenus nigricans fen	21	*Molinia caerulea, Potentilla erecta, Schoenus nigricans, Succisa pratensis*
Agrostis stoloniferia - Ranunculus repens	3	*Agrostis stolonifera, Potentilla anserina, Ranunculus repens, Carex hirta, Carex nigra, Filipendula ulmaria, Galium palustre, Scorzoneroides autumnalis, Trifolium repens*
Filipendula ulmaria - Potentilla erecta - Viola	20	*Filipendula ulmaria, Lotus corniculatus, Potentilla anserina, Potentilla erecta, Viola species, Carex nigra, Galium palustre, Plantago media, Rumex acetosa*
Flooded pavement	28	*Viola species, Festuca rubra, Potentilla fruticosa, Succisa pratensis*
Potentilla anserina - Potentilla reptans	19	*Agrostis stolonifera, Potentilla anserina, Potentilla reptans, Ranunculus repens*
Agrostis stolonifera - Glyceris fluitans	18	*Agrostis stolonifera, Glyceria fluitans*
Phalaris arundinace - Potentilla anserina	9	*Phalaris arundinacea, Potentilla anserina*
Potentilla anserina - Carex nigra	13	*Potentilla anserina, Agrostis stolonifera, Carex nigra*
Molinia caerulea - Carex panicea	22	*Carex panicea, Molinia caerulea, Carex hostiana, Mentha aquatica*
Carex nigra - Leontodon autumnalis	23	*Scorzoneroides autumnalis, Agrostis stolonifera, Carex nigra, Filipendula ulmaria, Hydrocotyle vulgaris, Phalaris arundinacea, Potentilla anserina*
Equisetum fluviatile swamp	16	*Equisetum fluviatile, Menyanthes trifoliata, Agrostis stolonifera*
Eleocharis palustris - Phalaris arundinacea	7	*Eleocharis palustris, Phalaris arundinacea, Galium palustre*
Eleocharis acicularis	26	*Agrostis stolonifera, Eleocharis acicularis, Callitriche species, Lythrum portula, Ranunculus trichophyllus, Rorippa islandica*
Persicaria amphibia - Elocharis palustris	2	*Agrostis stolonifera, Eleocharis palustris, Galium palustre, Persicaria amphibia, Potentilla anserina, Ranunculus repens*
Carex nigra - Carex viridula	25	*Carex nigra, Carex viridula agg., Molinia caerulea, Ranunculus flammula, Schoenus nigricans*
Carex nigra - Ranunculus flammula	17	*Hydrocotyle vulgaris, Mentha aquatica, Potentilla anserina, Agrostis stolonifera, Carex nigra, Galium palustre, Ranunculus flammula*
Carex nigra - Equisetum fluviatile	27	*Carex nigra, Equisetum fluviatile*
Eleocharis palustris - Ranunculus flammula	6	*Eleocharis palustris, Mentha aquatica, Ranunculus flammula*
Persicaria amphibia - Mentha aquatica	11	*Persicaria amphibia, Mentha aquatica*
Potamogeton natans - Glyceria fluitans	24	*Potamogeton natans, Glyceria fluitans*
Reedbed	14	*Mentha aquatica, Schoenoplectus lacustris*

Turlough Vegetation Communities (source Nova Sharkey, Botany Dept., Trinity College Dublin)